ANTIVIRAL IMMUNE RESPONSE IN FISH AND SHELLFISH, 2nd Edition

EDITED BY: Verónica Chico Gras, Maria Del Mar Ortega-Villaizan and Luis Mercado

PUBLISHED IN: Frontiers in Immunology

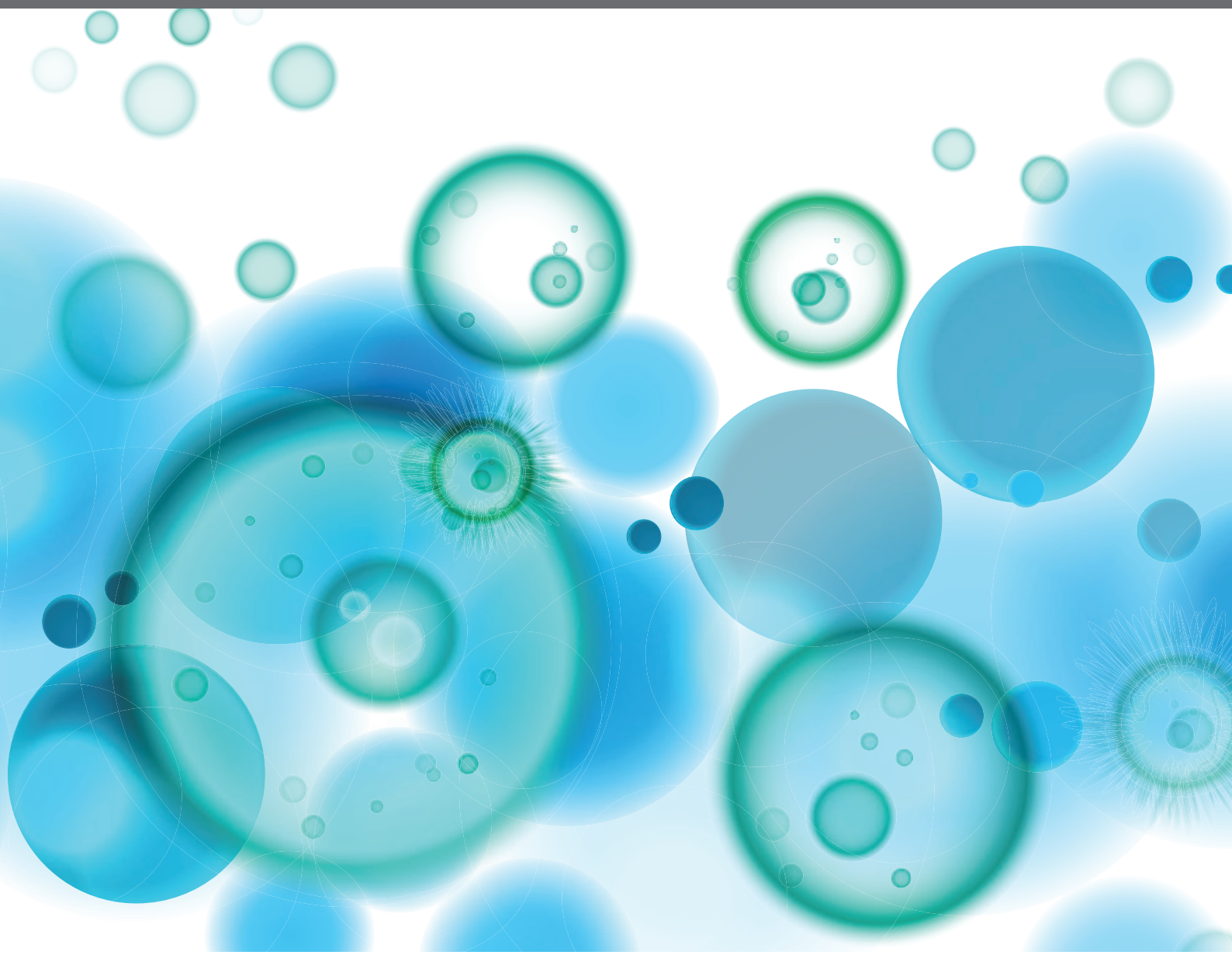

frontiers Research Topics

ISSN 1664-8714
ISBN 978-2-83252-141-0
DOI 10.3389/978-2-83252-141-0

About Frontiers

Frontiers is more than just an open-access publisher of scholarly articles: it is a pioneering approach to the world of academia, radically improving the way scholarly research is managed. The grand vision of Frontiers is a world where all people have an equal opportunity to seek, share and generate knowledge. Frontiers provides immediate and permanent online open access to all its publications, but this alone is not enough to realize our grand goals.

Frontiers Journal Series

The Frontiers Journal Series is a multi-tier and interdisciplinary set of open-access, online journals, promising a paradigm shift from the current review, selection and dissemination processes in academic publishing. All Frontiers journals are driven by researchers for researchers; therefore, they constitute a service to the scholarly community. At the same time, the Frontiers Journal Series operates on a revolutionary invention, the tiered publishing system, initially addressing specific communities of scholars, and gradually climbing up to broader public understanding, thus serving the interests of the lay society, too.

Dedication to Quality

Each Frontiers article is a landmark of the highest quality, thanks to genuinely collaborative interactions between authors and review editors, who include some of the world's best academicians. Research must be certified by peers before entering a stream of knowledge that may eventually reach the public - and shape society; therefore, Frontiers only applies the most rigorous and unbiased reviews.
Frontiers revolutionizes research publishing by freely delivering the most outstanding research, evaluated with no bias from both the academic and social point of view. By applying the most advanced information technologies, Frontiers is catapulting scholarly publishing into a new generation.

What are Frontiers Research Topics?

Frontiers Research Topics are very popular trademarks of the Frontiers Journals Series: they are collections of at least ten articles, all centered on a particular subject. With their unique mix of varied contributions from Original Research to Review Articles, Frontiers Research Topics unify the most influential researchers, the latest key findings and historical advances in a hot research area! Find out more on how to host your own Frontiers Research Topic or contribute to one as an author by contacting the Frontiers Editorial Office: frontiersin.org/about/contact

ANTIVIRAL IMMUNE RESPONSE IN FISH AND SHELLFISH, 2nd Edition

Topic Editors:
Verónica Chico Gras, Universidad Miguel Hernández de Elche, Spain
Maria Del Mar Ortega-Villaizan, Miguel Hernández University of Elche, Spain
Luis Mercado, Pontifical Catholic University of Valparaíso, Chile

Publisher's note: In this 2nd edition, the following article has been updated: Ortega-Villaizan M, Mercado L and Chico V (2023) Editorial: Antiviral immune response in fish and shellfish. *Front. Immunol*. 14:1155538. doi: 10.3389/fimmu.2023.1155538

Citation: Gras, V. C., Del Mar Ortega-Villaizan, M., Mercado, L., eds. (2023). Antiviral Immune Response in Fish and Shellfish, 2nd Edition. Lausanne: Frontiers Media SA. doi: 10.3389/978-2-83252-141-0

Table of Contents

frontiers | Frontiers in Immunology

TYPE Editorial
PUBLISHED 28 March 2023
DOI 10.3389/fimmu.2023.1155538

OPEN ACCESS

EDITED BY
Gyri T. Haugland,
University of Bergen, Norway

REVIEWED BY
Roy Ambli Dalmo,
UiT The Arctic University of Norway, Norway

*CORRESPONDENCE
V. Chico
vchico@umh.es

SPECIALTY SECTION
This article was submitted to Comparative Immunology, a section of the journal Frontiers in Immunology

RECEIVED 31 January 2023
ACCEPTED 20 March 2023
PUBLISHED 28 March 2023

CITATION
Ortega-Villaizan M, Mercado L and Chico V (2023) Editorial: Antiviral immune response in fish and shellfish.
Front. Immunol. 14:1155538.
doi: 10.3389/fimmu.2023.1155538

Editorial: Antiviral immune response in fish and shellfish

M. Ortega-Villaizan[1], L. Mercado[2] and V. Chico[1]*

[1]Instituto de Investigación, Desarrollo e Innovación en Biotecnología Sanitaria de Elche (IDiBE), Universidad Miguel Hernández (IDiBE-UMH), Elche, Spain, [2]Instituto de Biología, Pontificia Universidad Católica de Valparaíso, Valparaíso, Chile

KEYWORDS

fish, shellfish, antiviral, immune response, virus, bacteria, innate immunity

Editorial on the Research Topic
Antiviral immune response in fish and shellfish

Innate immunity constitutes the main defense mechanism in fish and shellfish, which is the most antique and efficient system to protect organisms against microbial infections. In addition, lower vertebrates have less evolved adaptive immune responses compared to higher vertebrates, and therefore, rely on innate immune defenses for the control of pathogens (1). Nonetheless, it is worth noting that the contribution of both innate and adaptive immune responses leads to global protection against pathogens in the organism.

The objective of this Research Topic is to reflect the significant advances in the study of the immune response against viral infections in fish. This topic contributes to identifying new mechanisms of response to infections and new effector molecules against viral pathogens. In addition, these studies provide a further understanding of the resistance of lower vertebrates to pathogens infection as well as to the prevention of exacerbated immune responses.

The contributing articles collected in this Research Topic are grouped into the following proposed sections related to the antiviral defense in fish:

1 Antiviral mechanisms involved in innate immunity and cellular response to viral infections in fish

The first mechanism of response to infection is the innate immune response which comprises a set of cells and molecules that are involved in the body's defense against infections.

In this section, we can find the advances in the understanding of the defense strategies in the Atlantic salmon against viral infections through a meta-analysis based on microarray transcriptomic analysis. Krasnov et al. were able to distinguish between pathogen-specific responses from stress and general inflammation. They found that viral responsive genes were similar to different stressors such as DNA or RNA viruses, to the injection of bacterial DNA (plasmid), and the exposure to PAMPs (CpG and gardiquimod), but they responded to inflammation and bacteria with quite a low sensitivity.

Vallejos-Vidal et al. revised the immune response mechanisms of one of the most pathogenic viruses, which affects farmed Atlantic salmon, the piscine orthoreovirus (PRV).

They revised how an experimental infection of PRV triggers the antiviral immune response in salmonid RBCs. In addition, they showed how PRV elicited a Th1-type response and a positive regulatory effect on the CTL-mediated immune responses. The immune mechanisms related to the phenotype of permanently PRV-infected fish and their effects on the progression of secondary infection were also reviewed.

Malik et al. showed the problem around melanized focal changes "black spots" in the white skeletal muscle of farmed Atlantic salmons infected with PRV-1. The first symptoms observed, which were the "red spots", were featured by hemorrhages and acute inflammation that progressed into chronic inflammation developing the "black spots" in the muscle of salmons. Although the etiology of the spots is unknown, in this study, the authors found in both the red and black spots the presence of macrophages and melano-macrophages associated with abundant PRV-1. Here the authors studied the polarization status of the macrophages and cell-mediated immune responses in both PRV-1-infected and non-infected fish. Altogether, in this study, the authors suggested that PRV-1 could contribute to the pro-inflammatory environment that is essential for the pathogenesis of the spots.

Finally, in this section, Jia et al. shed light on the mechanisms related to the immune response involved in both sensitivity and resistance against cyprinid herpesvirus-3 (CyHV3) in common carp. The authors demonstrated, with a transcriptomic analysis, that specific innate immune mechanisms which included phagocytosis, autophagy, cytotoxicity, and virus blockage by lectins and mucins like mucin 3 (MUC3) were the cause of a marked resistance to CyHV-3 infection in a breeding carp strain.

2 Antiviral determinants and molecules responsible for defense mechanisms

Pathogens are able to trigger the immune response in the host through the activation of a huge variety of determinants or molecules responsible for the defense mechanisms. In this section, the authors identified two antiviral molecules and studied their role in the immune response of fish.

Mou et al. identified different antiviral mechanisms for two viperin homologs (Cgviperin-A and Cgviperin-B) in the auto-allo-hexaploid gibel carp strain against crucian carp (*Carasius auratus*) herpesvirus (CaHV). The C-terminal domain of CgViperin-A and CgViperin-B were found to interact with a negative herpesvirus regulator of host interferon (IFN) production, the CaHV open reading frame 46 right (ORF46R) protein, and to develop the proteasomal degradation of ORF46R *via* reducing K63-linked ubiquitination. CgViperin-B was also found to mediate ORF46R degradation through autophagosomes. Their findings also clarified the different antiviral mechanisms of the duplicated viperin homologs in polyploid fish, which elucidated the evolution of teleost duplicated genes.

Liu et al. showed how the toll-interleukin receptor (TIR)-domain-containing adapter-inducing interferon-β (TRIF), an essential adaptor downstream of Toll-like receptor signaling, played an important role in the innate immune response. The authors showed how common carp TRIF inhibited the replication of spring viremia carp virus (SVCV) in epithelioma papulosum cyprini (EPC) cells. In addition, the authors showed that TRIF increased under *Aeromonas hydrophila* and poly (I:C) stimulation *in vivo* and under poly (I:C), lipopolysaccharide, flagellin, peptidoglycan, and Pam3CSK4 stimulation *in vitro*. In summary, this study indicated that TRIF plays an important role in the innate immune responses of common carp against viral and bacterial infections.

3 Molecular regulation of innate immune responses upon viral infection

A balanced immune response can protect the organism from pathogens, but an exacerbated response can impair the immune homeostasis, leading to uncontrolled inflammation or pathogen invasion. In this section, the molecular regulation of some innate immune responses against viral infection was reviewed.

MicroRNAs (miRNAs) are molecules that are extensively involved in the regulatory systems of inflammation and immune responses in mammals. However, the regulatory pathway of miRNA-mediated immune responses is not well understood in lower vertebrates. In this section, the authors showed that different miRNAs could play an adverse role in the *Miiuy croaker* antimicrobial immunity. Gao et al. showed that pathogens such as rhabdovirus and bacteria up-regulated the expression of miRNAs, showing that an up-regulation of miR-2187 was able to reduce the production of antiviral genes and inflammatory factors through targeting TNF receptor-associated factor 6 (TRAF6), therefore, avoiding an extreme inflammatory response. On the other hand, Sun et al. showed that miR-181b-2 and miR-21-1 modulated antiviral and antibacterial immunity by means of the TRIF-mediated nuclear factor-κB (NF-κB) and interferon regulatory factor 3 (IRF3) signaling pathways.

In the same way, Li et al. described the role of miR-124 in the cellular immune response of *Epinephelus coioides* by Singapore grouper iridovirus (SGIV) infection (entry and replication). The authors showed a significant up-regulation of the miR-124 expression after SGIV infection. Their results suggested that *E. coioides* miR-124 increased viral replication and negatively modulated the host immune response by targeting Jun N-terminal kinases 3 (JNK3)/p38α MAPKinasa. Their results broaden the knowledge of the host immune interactions with viruses.

Metabolites are also known to regulate the immune response and the susceptibility to pathogen infections. He et al. performed metabolome studies of Grass carp infected with GCRV and showed that, after viral infection, most metabolites increased in three-year-old fish and decreased in five-month-old fish. In addition, those differentially expressed metabolites presented antiviral effects both *in vivo* and *in vitro*. In summary, the authors concluded that the

age-dependent viral susceptibility in grass carp depended on the immune system and metabolism of the host.

In summary, this Research Topic compiles recent developments and research in relation to the importance of innate immunity in antiviral defense in fish. Our objective was to increase the interest of research communities in these areas of research and direct this knowledge into new perspectives and strategies related to antiviral defense across aquatic organisms.

Author contributions

VC and MO-V wrote the manuscript with contributions from other authors. VC, MO-V and LM contributed to conception of the Research Topic. All authors contributed to the article and approved the submitted version.

Reference

1. Smith NC, Rise ML, Christian SL. A comparison of the innate and adaptive immune systems in cartilaginous fish, ray-finned fish, and lobe-finned fish. *Front Immunol* (2019) 10.

Conflict of interest

The authors declare that the research was conducted in the absence of any commercial or financial relationships that could be construed as a potential conflict of interest.

Publisher's note

frontiers in Immunology

ORIGINAL RESEARCH
published: 15 February 2021
doi: 10.3389/fimmu.2021.647202

MicroRNA-2187 Modulates the NF-κB and IRF3 Pathway in Teleost Fish by Targeting TRAF6

Wenya Gao[1], *Renjie Chang*[1], *Yuena Sun*[1,2,3]* *and Tianjun Xu*[1,2,3,4]*

[1] *Laboratory of Fish Molecular Immunology, College of Fisheries and Life Science, Shanghai Ocean University, Shanghai, China,* [2] *Laboratory of Marine Biology and Biotechnology, Qingdao National Laboratory for Marine Science and Technology, Qingdao, China,* [3] *Key Laboratory of Exploration and Utilization of Aquatic Genetic Resources (Shanghai Ocean University), Ministry of Education, Shanghai, China,* [4] *National Pathogen Collection Center for Aquatic Animals, Shanghai Ocean University, Shanghai, China*

The innate immune organs and cells detect the invasion of pathogenic microorganisms, which trigger the innate immune response. A proper immune response can protect the organisms from pathogen invasion. However, excessive immunity can destroy immune homeostasis, leading to uncontrolled inflammation or pathogen transmission. Evidence shows that the miRNA-mediated immune regulatory network in mammals has had a significant impact, but the antibacterial and antiviral responses involved in miRNAs need to be further studied in lower vertebrates. Here, we report that miR-2187 as a negative regulator playing a critical role in the antiviral and antibacterial response of miiuy croaker. We find that pathogens such as *Vibrio anguillarum* and *Siniperca chuatsi* rhabdovirus (SCRV) can up-regulate the expression of miR-2187. Elevated miR-2187 is capable of reducing the production of inflammatory factors and antiviral genes by targeting TRAF6, thereby avoiding excessive inflammatory response. Furthermore, we proved that miR-2187 modulates innate immunity through TRAF6-mediated NF-κB and IRF3 signaling pathways. The above results indicate that miR-2187 acts as an immune inhibitor involved in host antibacterial and antiviral responses, thus enriching the immune regulatory network of the interaction between host and pathogen in lower vertebrates.

Keywords: miR-2187, TRAF6, immune response, negative regulation, fish

OPEN ACCESS

Edited by:
Maria Del Mar Ortega-Villaizan, Miguel Hernández University of Elche, Spain

Reviewed by:
Ningqiu Li, Chinese Academy of Fishery Sciences (CAFS), China
Jaime Eugenio Figueroa, Austral University of Chile, Chile

***Correspondence:**
Yuena Sun
yuenasun@163.com
Tianjun Xu
tianjunxu@163.com

Specialty section:
This article was submitted to Comparative Immunology, a section of the journal Frontiers in Immunology

Received: *29 December 2020*
Accepted: *22 January 2021*
Published: *15 February 2021*

Citation:
Gao W, Chang R, Sun Y and Xu T (2021) MicroRNA-2187 Modulates the NF-κB and IRF3 Pathway in Teleost Fish by Targeting TRAF6 Front. Immunol. 12:647202. doi: 10.3389/fimmu.2021.647202

INTRODUCTION

Innate immunity and acquired immunity are important ways for the body to protect itself from pathogenic microorganisms (1). Invading pathogens are effectively identified by various extracellular or intracellular pattern-recognition receptors (PRRs) which can recognize conserved signature molecular structures termed as pathogen-associated molecular patterns (PAMPs) (2). PRRs rapidly initiate a series of immune responses by inducing the production of inflammatory cytokines, chemokines, and type I interferon (IFNs) after ligand binding (3). PRRs are a kind of evolutionarily conserved host sensor, including Toll-like receptors (TLRs), RIG-I-like receptors (RLRs), NOD-like receptors (NLRs), and C-type lectin receptors. Among them, TLRs and RLRs are the most studied receptors in the immune responses (4, 5).

TLRs are recognized as the main sensors of pathogens involved in the regulation of innate and adaptive immune system. Once TLRs recognize the molecular structure of pathogens,

TLRs will activate the NF-κB transcription factor through activating the myeloid differentiation factor 88 (MyD88) and tumor necrosis factor receptor related factor 6 (TRAF6). Upon TRAF6 activated, it could co-catalyze the synthesis of Lys63-linked polyubiquitin chains with a dimeric ubiquitin conjugating enzyme complex Ubc13-Uev1A thereby activating the protein kinase complex containing TAK1, TAB1, and TAB2, leading to activation and nuclear translocation of transcription factor NF-κB (6, 7). Then, such the inflammatory cytokines including IL-1β, IL-8, and TNF-α were transcribed subsequently. And at the same time, IRF family is also activated by IKK kinase family. Unlike TLRs-mediated antiviral response, RLRs are used as sensors of cytoplasmic to detect viruses. After effective identification of virus intrusion, both RIG-I and MDA5 will interact with the CARD-containing mitochondrial antiviral signal protein (MAVS) which contains multiple TRAF-interacting motifs (TIMs) and can then interact with TRAF family members to signal the transcription of type I IFN and inflammatory cytokines (8). Similar to TLR signaling, TRAF6 also plays an indispensable role in RLR-mediated NF-κB signaling pathway and IRF3 is directly activated by TBK1. It is worth noting that NF-κB activation is an important common event in both TLR and RLR signaling pathways.

TRAF6, an important intracellular multifunctional signaling molecule, was the most widely studied member of TRAF family. TRAF6 contains a highly conserved C-terminal TRAF domain and a helical coiled structure N-terminal activation domain (9). Presently, accumulating evidences have reported that TRAF6 could be activated under VSV infection, bacterial lipopolysaccharide (LPS), and poly(I:C) stimulation (10, 11), which indicated that TRAF6 is critical for both antibacterial and antiviral innate immunity. TRAF6 not only acts as a signal transducer in the NF-κB pathway but activates inhibitor of IκB kinase (IKK) in response to pro-inflammatory cytokines (12). Besides, TRAF6 acts as an E3 ubiquitin ligase to catalyze the K63 polyubiquitination of TAK1, which in turn leads to the activation of IKK and activates downstream signaling molecules, thereby inducing the activation of IRF3, IRF7, and NF-κB (13). The latest report demonstrated that the deletion of TRAF6 promoted the replication of Newcastle disease virus in mouse embryonic fibroblasts (MEF cells) (14). With the increasing importance of TRAF6 in immune regulation, its role in fish has gradually received attention. However, the functions and mechanisms of TRAF6 in fish are poorly understood when compared with mammalian TRAF6.

MicroRNAs are non-coding RNAs consisting of 19–23 nucleotides, which can regulate gene expression by binding to the 3′untranslated region (3′-UTR) of target genes. miRNAs can regulate mRNA expression at the post-transcriptional level mainly by inhibiting the translation of mRNA or promoting the degradation of mRNA (15, 16). According to reports, more than 60% of mRNA is regulated by miRNAs to some extent (17), so miRNAs have become an important transcription factor that controls cell protein content. At present, a number of studies on miRNAs extensively involved in the regulation of TLR and RIG-I pathways at different levels in response to pathogen invasion have been reported (18). For example, the adaptor protein MyD88 associated with TLR has been studied, which can be regulated by miR-3570 and miR-214, thereby regulating the innate immune response (19, 20). And the RIG-I-induced cytokines and antiviral genes also could be strictly constrained by miiuy croaker miR-3570 through targeting MAVS to avoid excess immunity (21). miR-146a, a critical miRNA, inhibits the TLR signaling pathway by targeting IRAK1 and TRAF6 (22). Miiuy croaker miR-203 and miR-21 have been studied in regulating the innate immune response of bacterial infections by inhibiting IRAK4-mediated NF-κB signaling (23, 24). Additionally, a recent study showed that the signaling molecule TAK1 has been regulated by miR-217, and miR-217 also plays important roles in regulating TAK1-induced NF-κB and IRF3 signals (25). Overall, these studies show that miRNAs act as an essential fine-tuning regulator in fish PRRs signaling transduction.

Miiuy croaker (*Miichthys miiuy*) has important medicinal value and is an important economic marine fish. Presently, this species has been used as a model for studying the fish immunology, because extensive researches on its transcriptome, whole genome, functional genes and immune pathway regulation have been reported (26–28). Due to the diversity of the water environment, fish is constantly threatened by bacteria and viruses, among which Gram-negative bacteria and rhabdovirus are important groups. *V. anguillarum* is a Gram-negative pathogen, while SCRV is a member of rhabdovirus, a kind of fish RNA virus. Both of these pathogens can cause severe hemorrhagic septicemia according to reports (29). Therefore, the regulation mechanism of *V. anguillarum* and SCRV infection in teleost is the focus of our research.

In the present study, we report a new regulatory mechanism of miRNA in response to innate immunity. We have explored the expression of miR-2187 and the relationship between miR-2187 and TRAF6 under the stimulation of Gram-negative bacteria or *Siniperca chuatsi* rhabdovirus (SCRV), a typical fish RNA rhabdovirus. Importantly, we found that miiuy croaker miR-2187 could be rapidly upregulated after *V. anguillarum*, LPS, SCRV, and poly(I:C) treatment. Further analysis showed that up-regulated miR-2187 can inhibit the expression of TARF6, and inhibit inflammatory cytokine genes and IFN-stimulating genes (ISG) through TRAF6-mediated NF-κB and IRF3 signaling pathways, thereby avoiding excessive inflammation. This tight negative regulation mechanism plays an important role in attenuating inflammatory response and avoiding excessive inflammation. These data not only provide more theoretical basis for studying miRNA as a negative feedback regulator involved in the antibacterial and antiviral immune response in fish, but enriched miRNA-mediated networks of host-pathogen interactions.

MATERIALS AND METHODS

Sample and Challenge

Healthy Miiuy croakers (weight, ∼50 g) come from the Fisheries Research Institute of Zhoushan, Zhejiang Province, China. Before the experiment, the fish was conditioned for at least 6 weeks in an air-filled seawater tanks at 25°C. Bacterial and SCRV challenge were performed as described previously (25, 30). In

short, healthy miiuy croakers were challenge with 100 μl of *V. anguillarum* (1.5×10^8 CFU/ml), LPS (InvivoGen, 1mg/ml), poly(I:C) (InvivoGen, 1mg/ml), or SCRV at a multiplicity of infection (MOI) of 5 through intraperitoneal route, and individual challenged with 100 μl of physiological saline as a comparison group. After that, the fish were killed at different time points and the spleen tissues were collected for RNA extraction. All animal experimental procedures were carried out in accordance with the National Institutes of Health's Guide for the Care and Use of Laboratory Animals, and the experimental protocols were approved by the Research Ethics Committee of Shanghai Ocean University.

Cell Culture and Transfection

Epithelioma papulosum cyprinid (EPC) cells were cultured in medium 199 (Invitrogen) supplemented containing 10% FBS, 1% Penicillin-Streptomycin Solution (100×) under condition with 5% CO_2 at 26°C. Cells with no stimulation were collected as the control, and each experiment have three biological replicates. Miiuy croaker macrophages were aseptically isolated from the head kidney samples as described (30). The cells were cultured in L-15 (Hyclone) medium supplemented with 15% FBS (Life Technologies) and 1% Penicillin-Streptomycin Solution (100×). Miiuy croaker kidney cell lines (MKC) were cultured in incubator at 26°C. Cells were divided into 24-well or 48-well plates before they were transferred until 80% of cell density.

Prior to transient transfection, cells were seeded into each well of a 24-well or 48-well plate and incubated overnight. Subsequently, EPC cells were transfected with the plasmid using X-tremeGENE HP DNA Transfection Reagent (Roche) according to the manufacturer's protocol. RNA oligoribonucleotides were transfected into MKC cells by using Lipofectamine RNAiMAX (Invitrogen). Washing the macrophages and infecting them with LPS, poly(I:C) or SCRV with MOI of 5, and incubate at different times as indicated.

Plasmid Construction

In order to construct the TRAF6 expression plasmid, the full-length coding sequence (CDS) region and 3′-untranslated regions (3′UTR) of the miiuy croaker TRAF6 gene were amplified by specific primer pairs and restricted endonuclease sites *Hind* III and *EcoR* I, and then inserted into pcDNA3.1 vector (Invitrogen) with a Flag tag. To construct a TRAF6 3′-UTR plasmid, the full-length TRAF6 3′-UTR region of *M. miiuy*, *L. crocea,* or *S. ocellatus* were cloned into pmir-GLO luciferase reporter vector to construct the wild type TRAF6-3′UTR plasmid. The mutant-types of the TRAF6 3′-UTR reporter vector were conducted by using Mut Express II Fast Mutagenesis Kit V2 (Vazyme) with mutant primers. Additionally, the wild type of miiuy croaker TRAF6 3′-UTR or the mutant-type was cloned into the mVenus-C1 vector (Invitrogen) which contained the sequence of enhanced GFP. In addition, to construct the pre-miRNA vector, the pre-miR-2187 sequences were amplified by PCR and then cloned into pcDNA3.1 vector (Invitrogen). Correct construction of the plasmids was verified by Sanger sequencing and extracted using endotoxin-free plasmid DNA miniprep kit (Tiangen), before transient transfection, and the expression of protein was confirmed by Western blot analysis. The sequences of all primers are listed in **Supplementary Table 1**.

miR-2187 Target Prediction

We used two calculation methods with TargetScan (31), miRanda (32) to predict the targets of miR-2187. Predictions were ranked based on the predicted efficacy of targeting as calculated using the context and scores of the sites.

Mimics and Inhibitors

miR-2187 mimics (dsRNA oligonucleotides), and control oligo nucleotides were commercially synthesized by GenePharma (Shanghai, China). Their sequences are as follows: miR-2187 mimics were 5′-UUACAGGCUAUGCUAAUCUGU-3′(sense), 5′-AGAUUAGCAUAGCCUGUAAUU-3′(antisense); negative control mimics were 5′-UUCUCCGAACGUGUCACGUTT-3′(sense), 5′-ACGUGACACGUUCGGAGAATT-3′ (antisense); miR-2187 inhibitor (ssRNA oligonucleotides chemically modified by 2′-Ome) were 5′-ACAGAUUAGCAUAGCCUGUAA-3′; inhibitors control were 5′-CAGUACUUUUGUGUAGUACAA-3′.

RNA Interference

The TRAF6-specific siRNA (si-TRAF6) were 5′-GUGUCACGUAUCUUCAUTT-3′ (sense), 5′-GAUGAAGAUACCGUGACACTT-3′ (antisense). The scrambled control RNA sequences were 5′-UUCUCCGAACGUGUCACGUTT-3′ (sense) and 5′-ACGUGACACGUUCGGAGAATT-3′ (antisense).

Evaluation of mRNA Levels

Extract viral RNA from intracellular by using the Body Fluid Viral DNA/RNA Miniprep Kit (Axygen). Total RNA which was extracted by TRIzol Reagent (Invitrogen) according to the requirements of manufacturer and cDNA is reverse-transcribed from extracted RNA using the FastQuant RT Kit (Tiangen Biotech), which includes DNase treatment of RNA genome pollution. The expression patterns were performed by using SYBR Premix Ex Taq™ (Takara). Use miRcute miRNA qPCR detection kit for miR-2187 expression analysis (Tiangen). Real-time PCR was performed in an Applied Biosystems® QuantStudio 3 (Thermo Fisher Scientific). β-actin and 5.8S rRNA were employed as internal controls for mRNA and miRNA, respectively as described (33). Primer sequences are displayed in **Supplementary Table 1**.

Dual-Luciferase Reporter Assays

For miRNA target identification, EPC cells were co-transfected with wild-type or mutant-type TRAF6 3′-UTR luciferase reporter plasmids, along with miR-2187 mimics, miR-2187 inhibitors, controls or pre-miR-2187 plasmid for 24 h. Additionally, EPC cells were co-transfected with luciferase reporter genes, phRL-TK *Renilla* luciferase plasmid, TRAF6 expression plasmid, along with either miR-2187 mimics or controls. Reporter luciferase activities were measured using the Dual-Luciferase reporter assay system (Promega) (34). After 24 h transfection, they were treated with LPS or poly(I:C) for 6 or 12 h, respectively, then the cells were collected and assayed for reporter activity by using the dual-luciferase reporter assay system. Finally, the relative luciferase

activities were determined by calculating the ratio of *Renilla* luciferase activities over firefly luciferase activities. For each experiment, three independent experiments were performed, and each experiment was performed in three times.

Western Blotting

Total EPC cellular or macrophages lysates were generated by using 1×SDS-PAGE loading buffer, respectively. Proteins were extracted from cells and were measured with the BCA Protein Assay Kit (Vazyme) and then subjected to SDS-PAGE (10%) gel and transferred to polyvinylidence fluoride (Millipore, USA) membranes by semidry manner (Bio-Rad Trans Blot Turbo System) (35). The membranes were blocked for 1 h with 5% BSA. Then the membranes were incubated at 4°C overnight with anti-flag mouse mAb. Protein was blotted with different antibodies (Abs). The antibody against TRAF6 was diluted at 1: 400 (ProteinTech), anti-Flag and anti-Tubulin monoclonal antibody were diluted at 1:2,000 (Sigma), and HRP-conjugated anti-rabbit IgG or anti-mouse IgG (Abbkine) was diluted at 1:5,000. The results were representative of three independent experiments. The immunoreactive proteins were detected by using WesternBright^{TM} ECL (Advansta). The digital imaging was performed with a cold charge-coupled-device camera.

Virus Yield Quantification

MKC cells were transfected with RNA oligonucleotides and then infected with SCRV (MOI = 5) as indicated. A volume of 0.1 ml of the cultural supernatant was then serially diluted on the monolayer of EPC cells, and EPC cells were seeded into 96-well plates 1 day before measurement. The 50% tissue culture infectious dose ($TCID_{50}$) was measured after 3 days.

Statistical Analysis

All experiments were performed with at least three times independently, with three replicates for each experiment. The relative gene expression data was acquired using the $2^{-\Delta\Delta CT}$ method, and comparisons between groups were analyzed by one-way analysis of variance (ANOVA) followed by Duncan's multiple comparison tests (36, 37). All data are presented as the mean ± SE; a value of $p < 0.05$ was considered significant.

RESULTS

RNA Virus and Gram-Negative Bacteria Infection Enhanced miR-2187 Expression

In order to explore the influence of pathogen infection on the miRNA profile, the miRNA profile in *V. anguillarum* or LPS-stimulated miiuy croaker liver tissues was investigated firstly. As shown in **Figures 1A,B**, the level of miR-2187 can be significantly enhanced after the *V. anguillarum* or LPS treatment, and reaches its peak at 24 h, respectively. Furthermore, the expression pattern of miR-2187 was further verified in miiuy croaker spleen tissues following SCRV or poly(I:C) treatment. Similar to the results of LPS stimulation significantly upregulated the expression of miR-2187 at the individual level (**Figures 1C,D**). These results demonstrated that miR-2187 could be regulated in miiuy croaker in response to Gram-negative bacterial and SCRV infection.

miR-2187 Depresses the Expression of Inflammatory Cytokines and Antiviral Genes

Given that miR-2187 can be upregulated upon bacterial and virus infection, then we explored whether miR-2187 could participate in both bacterial- and virus-induced immune response. First, the effect of synthetic miR-2187 mimics and inhibitors on the expression of miR-2187 was assessed in MKC cells. miR-2187 mimics are synthetic double-stranded RNAs (dsRNAs) that simulate naturally occurring mature miRNAs, whereas miR-2187 inhibitors are chemically modified antisense ssRNAs that sequester and inhibit intracellular miRNAs. The results are consistent with expectations, the transfection of miR-2187 mimics sharply enhanced miR-2187 expression whereas miR-2187 inhibitors significantly decreased the expression of miR-2187 (**Figure 2A**). To confirm the role of miR-2187 in the inflammatory response, we investigated miR-2187 on the regulation of inflammatory cytokine production in LPS-treated macrophages. As shown in **Figure 2B**, the results implied that the overexpression of miR-2187 mimics could inhibit the expression levels of LPS-induced TNFα, IL-8, and IL-1β. In contrast to the above results, the inhibition of endogenous miR-2187 significantly increased the expression of the indicated inflammatory cytokines compared with the inhibitory control.

To determine whether miR-2187 could regulate inflammatory cytokine and antiviral genes production upon virus infection, the MKC cells were transfected with NC, miR-2187 mimics, NC-i, or miR-2187 inhibitors, then treated with poly(I:C) and the levels of inflammatory cytokines and antiviral genes were tested. As shown in **Figure 2C**, the expression levels of MX1, Viperin, TNFα, and IL-8 are significantly decreased when MKC were transfected with miR-2187 mimics, while miR-2187 inhibitors upregulated the expression levels of the indicated genes. To further study the function of miR-2187 in regulating RNA virus-induced antiviral immune response, MKC cells were treated with SCRV, then the expression of antiviral genes were detected. As shown in **Figure 2D**, miR-2187 mimics significantly suppressed the expression levels of MX1, Viperin, TNFα, and IL-8 in SCRV-stimulated MKC cells. Contrary to the above results, miR-2187 inhibitors increased the expression of the corresponding gene. Summarizing the above data shows that miR-2187 acts as a negative regulator to regulate antibacterial and antiviral immune response in miiuy croaker.

miR-2187 Target TRAF6

In order to identify a possible target, bioinformatics software was used to search for potential miR-2187 targets. After prediction and analysis, we found the 3′-UTR of TRAF6 has a standard sequence for miR-2187 binding. To confirm that TRAF6 is the direct target of miR-2187, TRAF6 3′-UTR luciferase reporter plasmids with the putative target sites for miR-2187 and the mutant type that mutated of miR-2187 targeting sequences were constructed (**Figure 3A**). Given that miRNA processing system is conserved in vertebrates from mammals to fish, we constructed the pre-miR-2187 sequence plasmid and then transfected it into EPC cells for *in vitro* expression (**Figure 3B**).

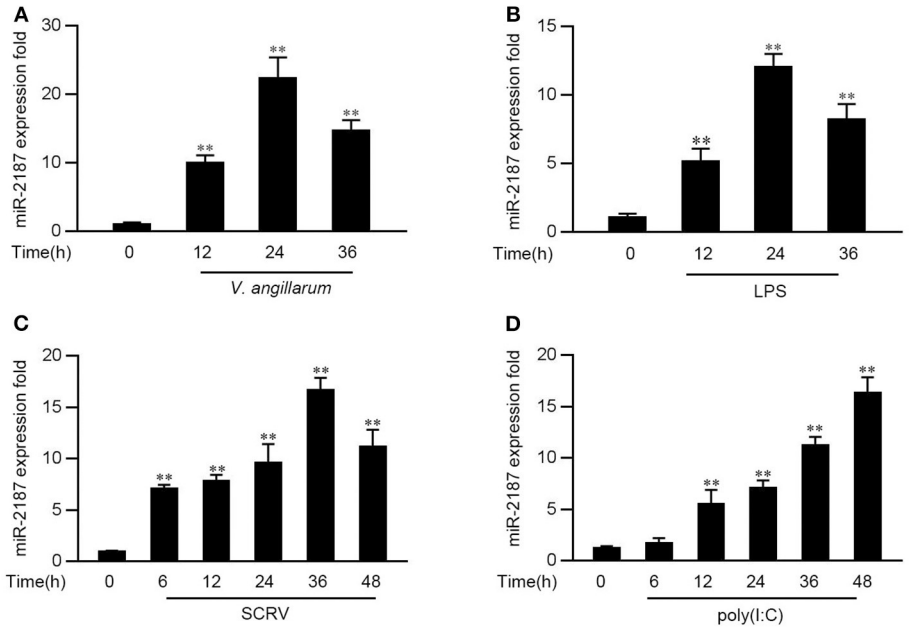

FIGURE 1 | The expression profiles of miR-2187 following Gram-negative bacteria and RNA viral treatment. **(A)** The expression profile of miR-2187 in miiuy croker liver tissues of different time points after infection of the *V. anguillarum* was detected by qRT-PCR. **(B)** The expression profiles of miR-2187 in LPS-stimulated miiuy croaker liver samples. **(C,D)** The expression profiles of miR-2187 in miiuy croaker spleen tissues were measured by qRT-PCR at indicated time after poly(I:C) **(C)** or SCRV **(D)** stimulation. The miR-2187 expression levels were all measured by qRT-PCR and normalized to 5.8S rRNA. Results are standardized to 1 in control samples. All data represented the mean ± SE from three independent triplicated experiments. $^{**}p < 0.01$ vs. the controls.

Then TRAF6 3′UTR together with miR-2187 mimics or NC were transfected into EPC cells. miR-2187 mimics induces a significant decrease in luciferase activity only in wild-type TRAF6 3′UTR (**Figure 3C**). Furthermore, as shown in **Figure 3D**, using miR-2187 mimics and inhibitors to further verify its down-regulation mechanism, and the results revealed that the inhibition of luciferase activity by miR-2187 was weaken after co-transfection with the miR-2187 inhibitors. We also found that the down-regulation mechanism of miR-2187 mimics was time dependent in EPC cells (**Figure 3E**).

Consistent with the result of miR-2187, when the pre-miR-2187 plasmid and the wild type of TRAF6 3′UTR or the mutant 3′-UTR were co-transfected into the EPC cells, we found that pre-miR-2187 decreased the luciferase activity of the wild-type plasmid but did not reduce the mutant plasmid luciferase activity (**Figure 3F**). When the luciferase reporter plasmids were co-transfected with the pre-miR-2187 plasmid and miR-2187 inhibitors, we observed that pre-miR-2187 plasmid significantly reduced luciferase activity of the wild-type plasmid, whereas the inhibition effect was weakened by miR-2187 inhibitors (**Figure 3G**). Pre-miR-2187-triggered time gradient experiment was performed and the result was similar to transfection of miR-2187 (**Figure 3H**). For further validation, the results revealed that miR-2187 or pre-miR-2187 plasmid could significantly inhibit GFP gene expression, whereas no effect on fluorescence intensity was observed in cells transfected with the mutant form (**Figures 3I,J**). In summary, these results fully demonstrated that miR-2187 directly targets the 3′UTR of TRAF6.

miR-2187 Depresses TRAF6 Expression at the Posttranscriptional Level

MicroRNAs regulate target genes by binding to their 3′-UTR, and then we next determined whether miR-2187 is involved in the regulation of TRAF6 expression. First, we constructed TRAF6 expression plasmid that includes the full-length CDS region and 3′-UTR of miiuy croaker TRAF6, and then co-transfected with miR-2187 mimics into EPC cells. As shown in **Figure 4A**, the overexpression of miR-2187 exerted a potent inhibitory effect in dose-dependent manner on the expression of TRAF6 whether at mRNA level or at the protein level. Consistent with above results, the mRNA expression levels of TRAF6 were consistent with the protein expression levels indicating that pre-miR-2187 depresses TRAF6 expression at the posttranscriptional level (**Figure 4B**). To investigate the regulation of miR-2187 on endogenous TRAF6, we detected the effect of miR-2187 on TRAF6 gene after transfection of MKC cells. Overexpression of miR-2187 significantly inhibited endogenous TRAF6 at protein and mRNA expression level (**Figure 4C**). In contrast, miR-2187 inhibitors distinctly enhanced TARF6 expression compared with control inhibitors (**Figure 4D**). In addition, in order to detect whether miR-2187 will inhibit the expression of TRAF6 during viral infection and LPS stimulation. We transfected the miR-2187 into the MKC cells for 48 h, and then stimulated the cells with LPS, SCRV, or poly(I:C). The result (**Figure 4E**) indicated that the expression of TRAF6 could be significantly enhanced after LPS, SCRV or poly(I:C) treatment, and overexpressed miR-2187 inhibits TRAF6 expression in MKC cells. In contrast to the

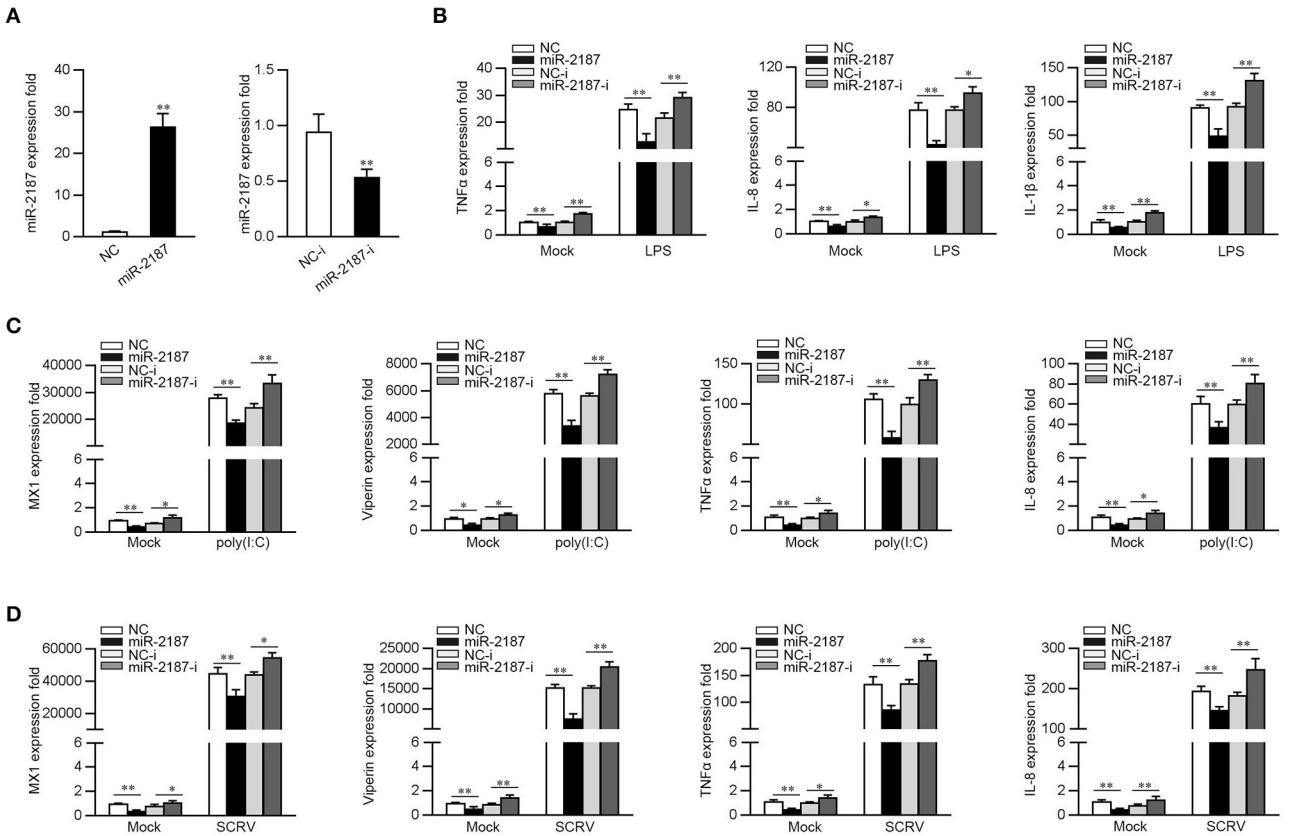

FIGURE 2 | miR-2187 inhibits the expression of inflammatory factors and antiviral genes. **(A)** MKC cells were transfected with control mimics (NC) or miR-2187 mimics (left panel) and negative control mimics (NC-i) or miR-2187 (right panel) for 48 h, the expression of miR-2187 was determined by qRT-PCR and standardized to 5.8S rRNA. **(B)** MKC cells were transfected with NC, miR-2187, NC-i, miR-2187-i for 48 h. Then, the macrophages were treated with LPS for 6 h and the expression of TNF-α, IL-1β, IL-8, and were tested by qRT-PCR and standardized to β-actin. **(C,D)** MKC cells were transfected with NC, miR-2187 mimics, NC-i or miR-2187-i for 48 h, which was stimulated with poly(I:C) or SCRV, and the mRNA level of MX1, Viperin, TNFα, and IL-8 were determined by qRT-PCR normalized to β-actin. All data are presented as the means ± SE from three independent triplicated experiments. $^{**}p < 0.01$; $^{*}p < 0.05$ vs. the controls.

transfection of miR-2187, miR-2187 inhibitor can significantly enhance the expression of TRAF6 after LPS, SCRV, or poly(I:C) treatment (**Figure 4F**). Overall, these results indicated that miR-2187 inhibits the expression of TRAF6 gene at posttranscriptional levels, and miR-2187 can also inhibit TRAF6 expression during LPS stimulation or RNA virus infection.

miR-2187 Depresses TRAF6-Mediated NF-κB and IRF3 Signaling Pathway

Studies have shown that TRAF6 activates the canonical IKK complex, leading to the activation of NF-κB, and can regulate the expression of inflammatory cytokines. Given that miR-2187 can inhibit the production of inflammatory factors and antiviral genes, we explore the underlying regulation mechanism of miR-2187 on TRAF6-induced NF-κB and IRF3 signaling pathway. First, miiuy croaker TRAF6 expression plasmid and NF-κB, IL-1β, IL-8, IRF3, or ISRE reporter genes were co-transfected into EPC cells for 24 h. The results of dual-luciferase reporter assays indicting overexpression of TRAF6 can activate NF-κB and IRF3 luciferase reporter genes, as well as IL-8, IL-1β, and ISRE luciferase reporter genes (**Figure 5A**). The above results indicated that miR-2187 targets and regulates the TRAF6, we then examined whether overexpression of miR-2187 inhibits the activation of NF-κB, IRF3, and ISRE luciferase reporters by targeting TRAF6. To this end, we transfected with miiuy croaker TRAF6 expression plasmid, together with miR-2187 mimics or negative control mimics into EPC cells. The results showed in **Figure 5B**, miR-2187 mimics significantly inhibits the activation of NF-κB, IL-1β, IL-8, IRF3, and ISRE induced by the overexpression of TRAF6.

Given that miR-2187 regulates the expression of inflammatory cytokines and antiviral genes, then we tested whether miR-2187 regulates the activity of the indicated luciferase reporter gene under different stimulations. As shown in **Figure 5C**, although overexpression of TRFA6 markedly up-regulated the luciferase activity of NF-κB, IL-8, and IL-1β reporter genes compared with controls, the activating effects were more significant after stimulation with LPS. Except for LPS stimulation, poly(I:C) stimulation was also used to determine

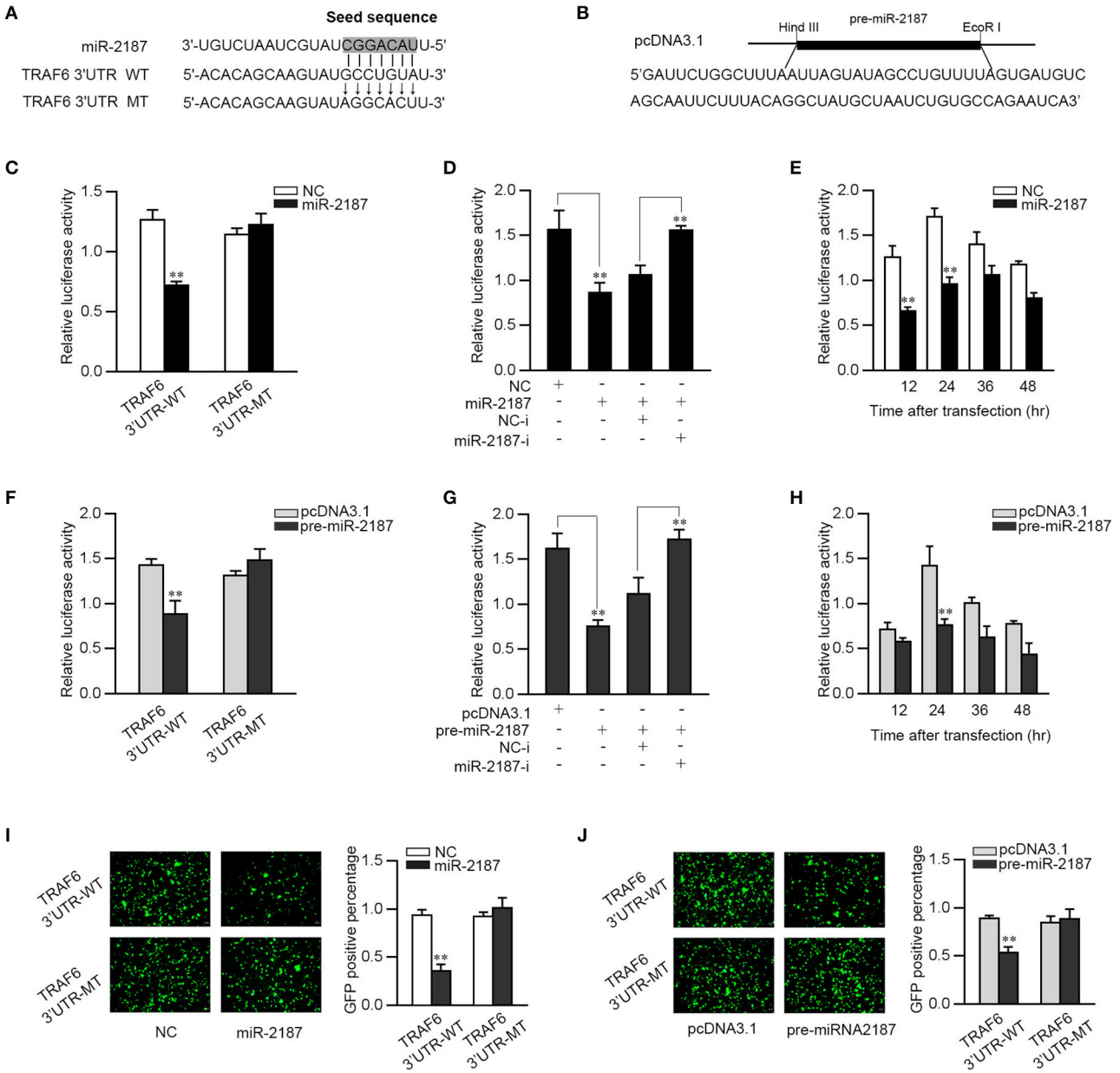

FIGURE 3 | miR-2187 targets miiuy croaker TRAF6 gene. **(A)** Sequence alignment of miR-2187 and its binding site in the 3′-UTR of TRAF6. **(B)** The pre-miR-2187 sequence and the construction of the plasmid. **(C)** EPC cells were transfected with NC or miR-2187 along with wild-type TRAF6-3′UTR (TRAF6-3′UTR-WT) or the mutant type of TRAF6 3′-UTR (TRAF6 3′UTR-MT) for 24 h, the luciferase activity was evaluated. **(D)** EPC cells were co-transfected with TRAF6 3′-UTR-WT, together with NC, miR-2187, NC-i or miR-2187-i 24 h. For each transfection, the total amount of oligonucleotides was controlled and normalized. **(E)** The time gradient experiments were conducted for miR-2187 transfection. **(F)** EPC cells were transfected with pcDNA3.1 or pre-miR-2187 along with TRAF6-3′UTR-WT or the TRAF6 3′-UTR-MT. **(G)** EPC cells were co-transfected with TRAF6 3′-UTR-WT, together with pcDNA3.1, pre-miR-2187, NC-i or miR-2187-i for 24 h. **(H)** The time gradient experiments were conducted for pre-miR-2187 transfection. The wild type or mutant type of TRAF6 3′-UTR was cloned into mVenus-C1 vector. EPC cells were co-transfected with the wild type or mutant type of mVenus-TRAF6 3′-UTR, together with NC or miR-2187 **(I)** and pcDNA3.1 or pre-miR-2187 **(J)**. At 48 h post-transfection, the fluorescence intensity was measured by enzyme-labeled instrument. Scale bar, 20 μm; original magnification × 10. All the luciferase activity was normalized to *Renilla* luciferase activity. All data are presented as the means ± SE from at least three independent triplicated experiments. $^{**}p < 0.01$ vs. the controls.

the luciferase activity of antiviral signaling induced by TRAF6. The results showed that the activation trend of IRF3 signal pathway is more obvious than that of the unstimulated control group under overexpression of TRFA6 (**Figure 5D**). Moreover, the gradient experiment induced by pre-miR-2187 plasmid further verified the indicated results. Pre-miR-2187 showed obviously inhibitory effect on NF-κB, IL-8, IL-1β, IRF3, and ISRE reporter genes during LPS or poly(I:C) infection

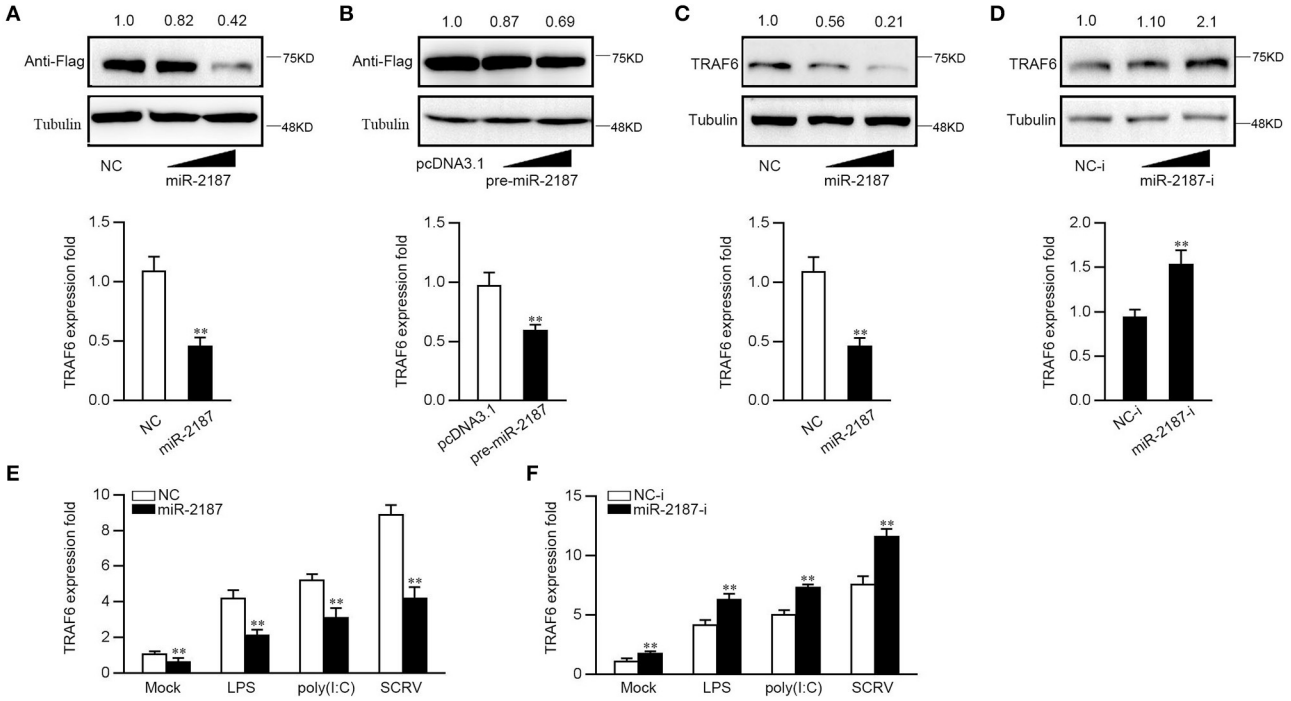

FIGURE 4 | miR-2187 inhibits the expression of TRAF6. **(A,B)** EPC cells were co-transfected with TRAF6 expression plasmid, pcDNA3.1 or pre-miR-2187 along with NC or miR-2187 **(A)** and pcDNA3.1 or pre-miR-2187 **(B)**. After 48 h, western blotting (upper panel) or qRT-PCR (lower panel) was used to determine the expression of TRAF6, respectively. **(C,D)** MKC cells were transfected with NC or miR-2187 **(C)** and NC-i or miR-2187-i **(D)**. After 48 h post-transfection, the protein and mRNA expression of TRAF6 were detected by western blotting (upper panel) or qRT-PCR (lower panel), respectively. **(E,F)** After transfection of NC or miR-2187 **(E)** and NC-i or miR-2187-i **(F)** for 48 h, MKC cells were treated with LPS, poly(I:C) or SCRV, respectively. The mRNA expression of TRAF6 was analyzed by qRT-PCR and normalized to β-actin. All data are presented as the means ± SE from three independent triplicated experiments. $^{**}p < 0.01$ vs. the controls.

(**Figures 5E,F**). Collectively, these data sufficiently demonstrated that miR-2187 could negatively regulate TRAF6-mediated NF-κB and IRF3 signaling pathway upon LPS or poly(I:C) stimulation, respectively.

Knockdown of TRAF6 Attenuated Antibacterial and Antiviral Immune Response

To further investigate the contribution of TRAF6 to the antiviral and antibacterial response, we silenced TRAF6 to determine the expression of inflammatory cytokines and ISGs upon LPS, poly(I:C) or SCRV treatment. TRAF6-specific small interfering RNA (si-TRAF6) was transfected into MKC cells, the expression levels of endogenous TRFA6 in protein and mRNA were significantly inhibited (**Figure 6A**). We knocked down TRAF6 and checked the expression of TRAF6 upon the macrophages were treated with LPS, poly(I:C), or SCRV. As shown in **Figure 6B**, si-TRAF6 effectively suppressed the expression level of TRAF6 in MKC cells after LPS, poly(I:C), or SCRV treatment. Afterwards, MKC cells were transfected with TRAF6-specific siRNA and then stimulated with LPS. As shown in **Figure 6C**, knockdown of TRAF6 significantly decreased the expression of TNF-α and IL-8 in MKC cells stimulated with LPS. Similar downregulation trends were also detected in MKC cells treated with poly(I:C) or SCRV treatment. As shown in **Figures 6D,E**, silenced TRAF6 in MKC cells obviously reduces the expression of TNF-α, IL-8, MX1, Viperin, and ISG15. The above results confirmed that miiuy croaker TRAF6 is involved in regulation of antibacterial and antiviral immune responses, and silenced TRFA6 and miR-2187 overexpression have similar effects on TRAF6.

miR-2187 Feedback Promotes Virus Replication

To further study the biological significance of the upregulation miR-2187 induced by SCRV, we examined the effect of miR-2187 on SCRV replication in EPC cells. By measuring the SCRV 50% tissue culture infectious dose ($TCID_{50}$) levels in the supernatant from the infected MKC cells, we found that replication of SCRV is facilitated by the overexpression of miR-2187, while inhibition of miR-2187 decreased SCRV replication (**Figure 7A**). Consistent with these results, overexpression of miR-2187 promotes SCRV replication, while inhibition of miR-2187 attenuated SCRV replication in infected MKC cells (**Figure 7B**). These results revealed that host miR-2187 can enhance SCRV replication.

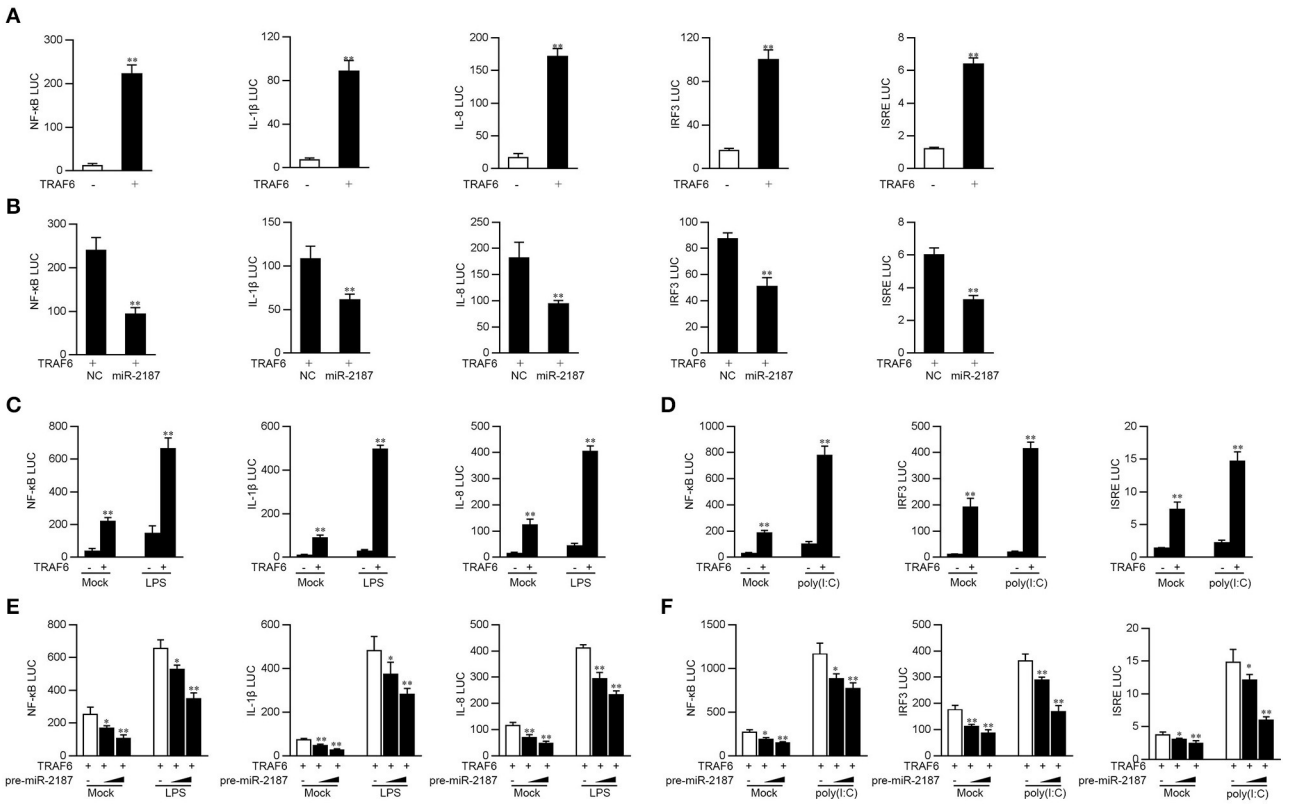

FIGURE 5 | Overexpressed miR-2187 depresses TRAF6-mediated NF-κB and IRF3 signaling. **(A)** Co-transfect EPC cells with TRAF6 expression plasmid, phRL-TK *Renilla* luciferase plasmid and NF-κB, IL-1β, IL-8, IRF3, or ISRE luciferase reporter gene for 24 h, and then measure luciferase activity. **(B)** Luciferase test showed that co-transfection of TRAF6 expression plasmid and NC or miR-2187 with EPC reduced luciferase activity. Co-transfect EPC cells with TRAF6 expression plasmid and stimulated with LPS (1 mg/ml) **(C)** for another 6 h or poly(I:C) (1 mg/ml) for 12 h **(D)**. **(E)** EPC cells were transfected with miR-2187 in a concentration gradient manner, together with luciferase reporter gene for 24 h and stimulated with LPS (1 mg/ml) for another 6 h or poly(I:C) (1 mg/ml) for 12 h **(F)**. Afterward, the luciferase activity was measured. All the luciferase activity was normalized to *Renilla* luciferase activity. All data are presented as the means ± SE from three independent triplicated experiments. $^{**}p < 0.01$; $^{*}p < 0.05$ vs. the controls.

miR-2187 Regulation of TRAF6 Is Widely Found in Teleost Fish

To confirm the universality that miR-2187 targets TRAF6, we explored the mechanism in other fish including *L. crocea* and *S. ocellatus*. In this respect, we generated the luciferase reporter constructs by cloning the TRAF6 3′-UTR of *L. crocea* into the pmir-GLO vector within the mutation at the miR-2187 binding site as a control (**Figure 8A**). miR-2187 mimics significantly suppressed luciferase activity when co-transfected with the *L. crocea* TRAF6-3′UTR reporter plasmid, whereas miR-2187 mimics showed no effect on luciferase activity in cells transfected with mutant types (**Figure 8B**). We also demonstrated that miR-2187 inhibits luciferase activity in a dose-dependent manner. Meanwhile, we found that miR-2187 has a similar inhibitory effects on luciferase activity when co-transfected with the TRAF6 3′-UTR of *S. ocellatus* (**Figures 8C,D**). These results indicate that miR-2187 can target the TRAF6 gene in other teleost fish, verifying that the functions of miR-2187 are conserved to some extent. To summarize the above results, these results showed that Gram-negative bacterial or RNA virus infection can enhance the expression of miR-2187. Up-regulated miR-2187 inhibits the production of inflammatory cytokines and antiviral genes by targeting TRAF6 and subsequently inhibiting NF-κB and IRF3 signaling, thereby avoiding excessive inflammation (**Figure 9**).

DISCUSSION

Aquaculture has developed rapidly over the past three decades to become an efficient protein producer. However, its development has been hampered by pathogenic infections. Rhabdoviruses are a group of enveloped, single-stranded, negative RNA viruses such as SCRV that can cause severe hemorrhagic septicemia in freshwater and marine fish (29, 38). In addition, *V. anguillarum* is a kind of Gram-negative bacterium of curved rod type, which causes high mortality and severe epidemic vibriosis in many marine animals, accompanied by symptoms of hemorrhagic sepsis (39, 40). Hence, it is urgent matter to explore potential immunomodulatory mechanism of teleost. Teleost use PRRs to identify the invasion of pathogenic microorganisms. Similar to mammals, the PRRs of teleost initiate immune response by

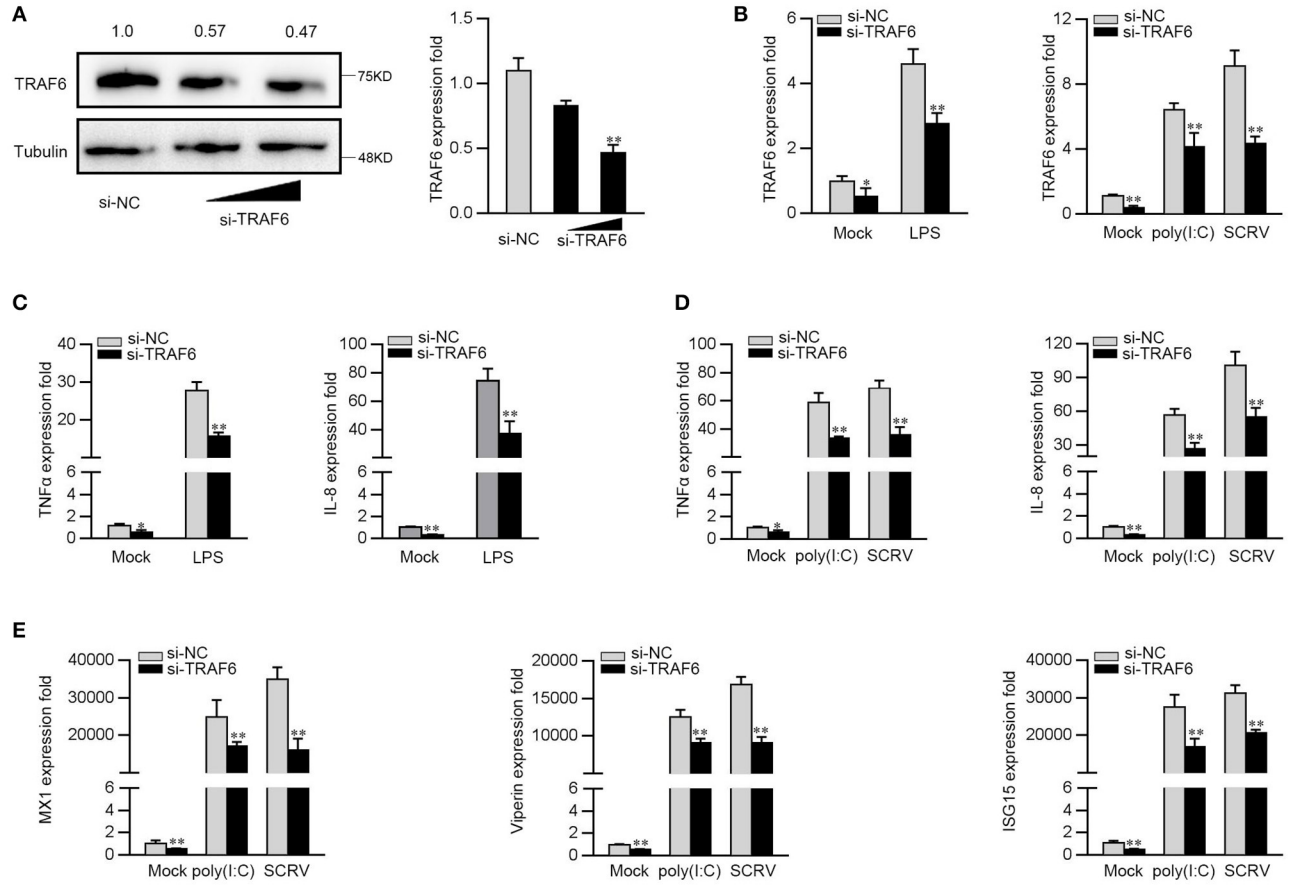

FIGURE 6 | Knockdown of TRAF6 depress the expression of inflammatory factor and antiviral genes. **(A)** MKC were transfected with control siRNA (si-NC) or si-TRAF6 for 48 h, then TRAF6 protein (left panel) and mRNA (right panel) level were determined by western blot and qRT-PCR, respectively. **(B)** MKC were transfected with contrl siRNA (si-NC) or si-TRAF6 for 48 h, the macrophages (MKC) were treated with LPS (left panel), poly(I:C) or SCRV (right panel), respectively. The expression levels of TRAF6 by qRT-PCR. **(C)** MKC cells were transfected with si-NC or si-TRFA6 for 48 h, and treated with LPS for 6 h. The expression levels of TNFα and IL-8 were determined by qRT-PCR. **(D,E)** After transfection of si-NC or si-TRAF6, MKC cells were treated with poly (I:C) or SCRV for another 12 h or 18 h, respectively. The expression levels of TNF-α, IL-8 **(D)**, MX1, Viperin, and ISG15 **(E)**. All data are presented as the means ± SE from three independent triplicated experiments. $^{**}p < 0.01$; $^{*}p < 0.05$ vs. the controls.

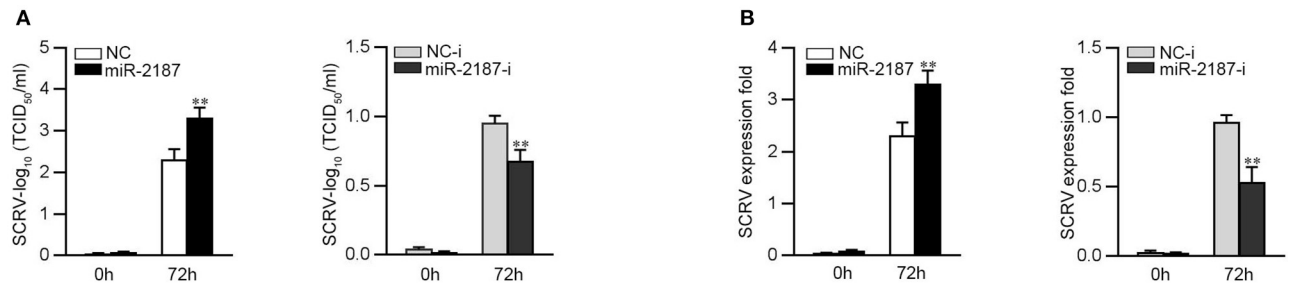

FIGURE 7 | miR-2187 promotes SCRV replication. **(A)** MKC cells were transfected with NC, miR-2187 mimics, NC-i or miR-2187-i, and infected with SCRV at MOI 5 for 1 h and washed and then added with fresh medium. After 72 h, SCRV $TCID_{50}$ in cultural supernatants was measured with EPC cells. **(B)** The qRT-PCR analysis was conducted for intracellular SCRV RNA. All data are presented as the means ± SE from at least three independent triplicated experiments. $^{**}p < 0.01$ vs. the controls.

recognizing the conservative sequence of PAMPs, and then signal the transcription of NF-κB and IRF3/7, leading to the production of inflammatory cytokines and antiviral genes, producing a clearance effect on pathogen invasion (41–43). However, the excessive activation of TLR or RIG-I signals can disrupt the immune balance and cause self-diseases.

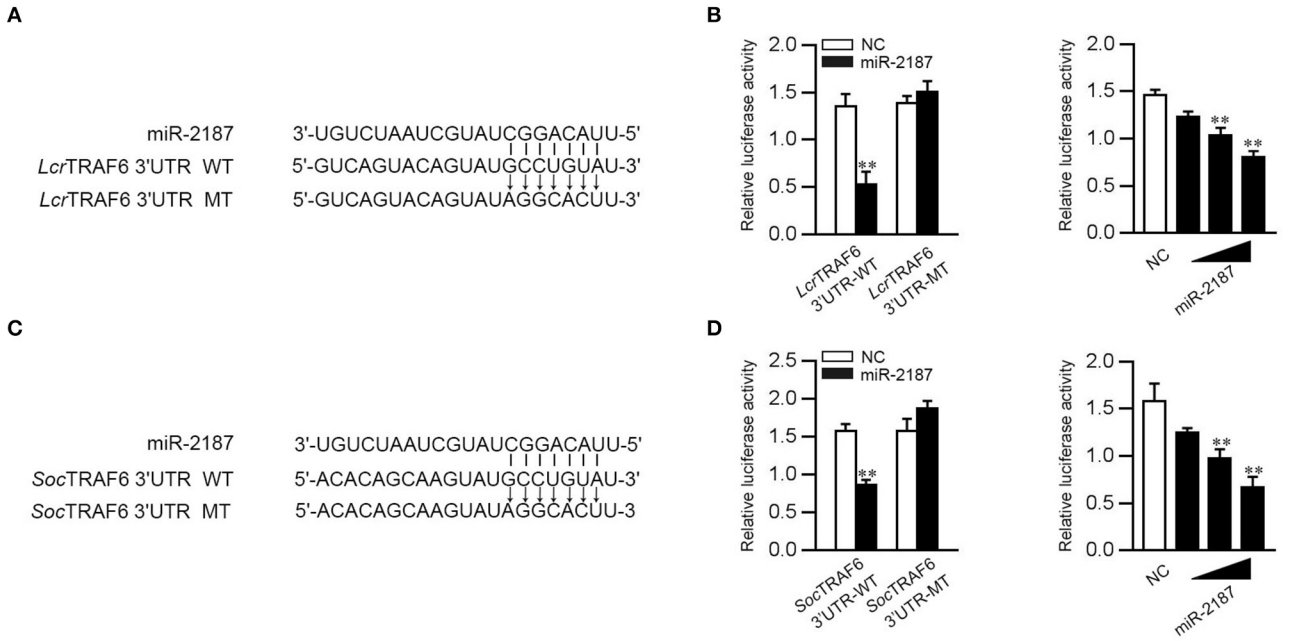

FIGURE 8 | miR-2187 regulation of TRAF6 is widely found in teleost fish. **(A)** Schematic diagram of the predicted target sites of miR-2187 in the 3′UTR of *L. crocea* TRAF6. **(B)** EPC cells were transfected with NC or miR-2187, along with the wild-type or mutant *L. crocea* TRAF6 3′UTR and the luciferase activity was determined (left). The dose gradient experiments were conducted for miR-2187 transfection (right). **(C)** Schematic diagram of the predicted target sites of miR-2187 in 3′-UTR of *S. ocellatus* TRAF6. **(D)** EPC cells were transfected with NC or miR-2187, along with the wild type or the mutant type of *S. ocellatus* TRAF6 3′-UTR and the luciferase activity was determined (left). The dose gradient experiments were conducted for miR-2187 transfection (right). All data are presented as the means ±SE from at least three independent triplicated experiments. $^{**}p < 0.01$ vs. the controls.

As a member of the RLRs family, RIG-I has been widely studied for its role in detecting viral RNA and antiviral immune response. After activated RIG-I, NF-κB /IRF3 will transfer from the cytoplasm to the nucleus, and induce the transcription of multiple innate immune genes. MAVS is a key downstream adaptor of RIG-I which contains multiple TRAF interaction motifs in the proline-rich region, which are related to the TRAF family (44, 45). Specifically, TRAF6 is a member of the TRAF family. TRAF6 signaling activates the IKK complex, leading to the activation of NF-κB and the expression of inflammatory cytokines, thereby eliminating the invasion of the virus (46). At the same time, the IRF family is also directly activated by TBK1/IKKε. In the innate immune response, from invertebrates to mammals, the signal transduction of the TLR pathway is highly conserved. Toll-like receptors detect pathogen-related molecular patterns (PAMPs) and initiate signaling pathways to resist the invasion of pathogens. When the TLR binds to the corresponding ligand, the IL-1 receptor-associated kinase 4 (IRAK4) will recruit MyD88, further activate TRAF6, and ultimately lead to the activation of NF-κB (47). As indispensable upstream mediators of the NF-κB pathway, TRAF6 has been reported to be regulated by many different molecules. For example, the heat shock protein 27 (HSP27) binds to TRAF6 to regulate the signaling pathway induced by IL-1 (48). The deubiquitinating enzymes such as cylindromatosis (CYLD) can inhibit the activation of MyD88 and TRIF-dependent NF-κB by deubiquitinating TRAF6 (49). Further investigations have reported that overexpression of miR-146a attenuates POCD hippocampal-dependent learning and memory impairment by targeting IRAK1 and TRAF6 (50). In this study, we found that TRAF6 enhances inflammatory cytokine production *via* modulating NF-κB signaling in miiuy croaker. Furthermore, we demonstrated that overexpression of fish TRAF6 could induce the activation of IRF3 signaling and several IFN-inducible genes, such as MX1, Viperin, and ISG15, which suggests the significant role of TRAF6 in host antiviral immunity. However, the regulation of NF-κB and IRF3 signaling pathway by miRNA targeting TRAF6 in fish has not been studied in depth.

Due to the pivotal regulatory role of miRNA, research on the mechanism of miRNA regulating immune response has also been paid more and more attention. At present, miRNAs functions as fine-tuning regulators involved in various biological processes of fish has been increasingly clarified. In *Epinephelus tauvina*, miR-1, miR-30b, miR-150, and miR-184 all function as important regulatory factor upon neuronecrosis virus infection (44). Meanwhile, such as miR-146a (51) and miR-98 (52) have been shown to be involved in innate and adaptive immune responses in teleost fish. As a key regulator of immune response, miRNA not only response to microorganism invasion, but also regulates the replication of some pathogens. For example, miR-30c can be upregulated by porcine reproductive and respiratory syndrome virus, and inducible miR-30c inhibits IFN-I signaling by targeting JAK1, thereby promoting viral replication (53). In this study, we

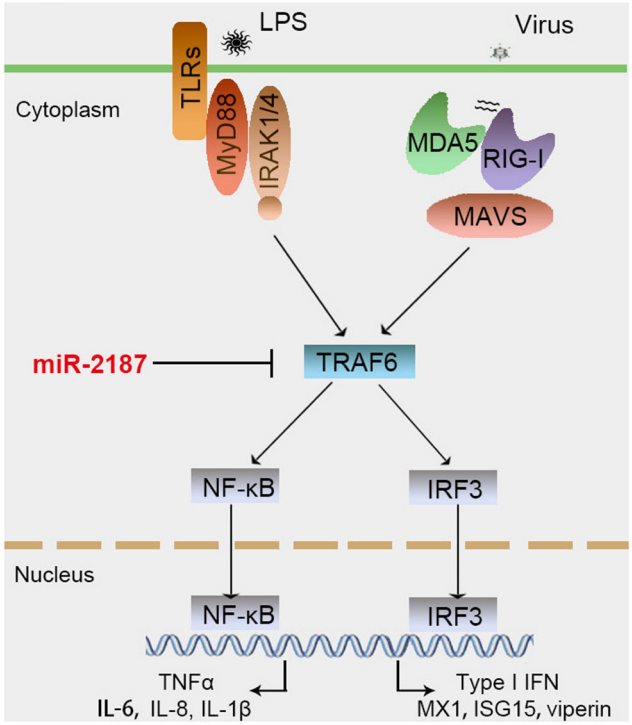

FIGURE 9 | Proposed model for the mechanism by which induced miR-2187 negatively regulates NF-κB and IRF3 signaling expression by targeting TRAF6, thereby avoiding excessive inflammation and immune responses.

found for the first time that the expression of miR-2187 was rapidly upregulated in miiuy croaker after stimulation with Gram-negative bacteria and RNA virus. Upregulated miR-2187 could suppress the production of inflammatory cytokines and antiviral genes. Additionally, overexpression of miR-2187 could promote the publication of SCRV. Overall, these results indicated that inducible miR-2187 decreases the production of inflammatory cytokines and ISGs in LPS- and poly(I:C)-stimulated macrophages through negatively regulating the NF-κB and IRF3 signaling pathway by modulating TRAF6. This could be a novel discovery about the negative regulation of the antibacterial and antiviral immunity, which also enriches the network of miRNAs-induced immune response mechanism in teleost fish.

In conclusion, this study demonstrated that host miR-2187 as a new regulator of TRAF6 plays a negative regulatory role in TRAF6-mediated NF-κB and IRF3 signaling pathways, which provide direct evidence for the role of miR-2187 in antiviral and antibacterial response. In addition, TRAF6 as a new target of miR-2187 has also been confirmed in other teleost fish, proving that miR-2187 targeting TRAF6 is conserved in other fishes. Overall, our research not only enables us to increase our understanding of miR-2187 function, but also provides insight into the regulatory network of miRNA-mediated immune responses against fish pathogen infections.

DATA AVAILABILITY STATEMENT

The original contributions presented in the study are included in the article/**Supplementary Material**, further inquiries can be directed to the corresponding author/s.

ETHICS STATEMENT

The animal study was reviewed and approved by Research Ethics Committee of Shanghai Ocean University.

AUTHOR CONTRIBUTIONS

TX: conceived and designed the experiments. WG and RC: performed the experiments and analyzed the data. YS and TX: contributed reagents, materials, and analysis tools. WG and TX: wrote the paper. All authors contributed to the article and approved the submitted version.

SUPPLEMENTARY MATERIAL

The Supplementary Material for this article can be found online at: https://www.frontiersin.org/articles/10.3389/fimmu.2021.647202/full#supplementary-material

REFERENCES

1. Magnadóttir B. Innate immunity of fish (overview). *Fish Shellfish Immunol.* (2006) 20:137–51. doi: 10.1016/j.fsi.2004.09.006
2. Akira S, Uematsu S, Takeuchi O. Pathogen recognition and innate immunity. *Cell.* (2006) 124:783–801. doi: 10.1016/j.cell.2006.02.015
3. Hyun J, Kanagavelu S, Fukata M. A unique host defense pathway: TRIF mediates both antiviral and antibacterial immune responses. *Microbes Infect.* (2013) 15:1–10. doi: 10.1016/j.micinf.2012.10.011
4. Kawai T, Akira S. The role of pattern-recognition receptors in innate immunity: update on Toll-like receptors. *Nat Immunol.* (2010) 11:373–84. doi: 10.1038/ni.1863
5. Deng L, Wang C, Spencer E, Yang L, Braun A, You J, et al. Activation of the IkappaB kinase complex by TRAF6 requires a dimeric ubiquitin-conjugating enzyme complex and a unique polyubiquitin chain. *Cell.* (2000) 103:351–61. doi: 10.1016/S0092-8674(00)00126-4
6. Skaug B, Jiang X, Chen Z. The role of ubiquitin in NF-kappaB regulatory pathways. *Annu Rev Biochem.* (2009) 78:769–96. doi: 10.1146/annurev.biochem.78.070907.102750
7. Wang C, Deng L, Hong M, Akkaraju G, Inoue J, Chen Z. TAK1 is a ubiquitin-dependent kinase of MKK and IKK. *Nature.* (2001) 412:346–51. doi: 10.1038/35085597
8. Seth R, Sun L, Ea C, Chen Z. Identification and characterization of MAVS, a mitochondrial antiviral signaling protein that activates NF-kappaB and IRF3. *Cell.* (2005) 122:669–82. doi: 10.1016/j.cell.2005.08.012
9. Chung J, Park Y, Ye H, Wu H. All TRAFs are not created equal: common and distinct molecular mechanisms of TRAF-mediated signal transduction. *J Cell Sci.* (2002) 115:679–88.
10. Xu L, Wang Y, Han K, Li L, Zhai Z, Shu H. VISA is an adapter protein required for virus-triggered IFN-beta signaling. *Mol Cell.* (2005) 19:727–40. doi: 10.1016/j.molcel.2005.08.014

11. Konno H, Yamamoto T, Yamazaki K, Gohda J, Akiyama T, Semba K, et al. TRAF6 establishes innate immune responses by activating NF-kappaB and IRF7 upon sensing cytosolic viral RNA and DNA. *PLoS ONE*. (2009) 4:e5674. doi: 10.1371/journal.pone.0005674
12. Scherer D, Brockman J, Chen Z, Maniatis T, Ballard D. Signal-induced degradation of I kappa B alpha requires site-specific ubiquitination. *Proc Natl Acad Sci USA*. (1995) 92:11259–63. doi: 10.1073/pnas.92.24.11259
13. Hayden M, Ghosh S. Shared principles in NF-kappaB signaling. *Cell*. (2008) 132:344–62. doi: 10.1016/j.cell.2008.01.020
14. Naito A, Yoshida H, Nishioka E, Satoh M, Azuma S, Yamamoto T, et al. TRAF6-deficient mice display hypohidrotic ectodermal dysplasia. *PNAS*. (2002) 99:8766–71. doi: 10.1073/pnas.132636999
15. Wienholds E, Plasterk RH. MicroRNA function in animal development. *FEBS Lett*. (2005) 579:5911–22. doi: 10.1016/j.febslet.2005.07.070
16. Hatfield S, Shcherbata H, Fischer K, Nakahara K, Carthew R, Ruohola-Baker H. Stem cell division is regulated by the microRNA pathway. *Nature*. (2005) 435:974–8. doi: 10.1038/nature03816
17. Friedman R, Farh K, Burge C, Bartel D. Most mammalian mRNAs are conserved targets of microRNAs. *Genome Res*. (2009) 19:92–105. doi: 10.1101/gr.082701.108
18. Li Y, Shi X. MicroRNAs in the regulation of TLR and RIG-I pathways. *Cell Mol Immunol*. (2013) 10:65–71. doi: 10.1038/cmi.2012.55
19. Chu Q, Sun Y, Cui J, Xu T. MicroRNA-3570 modulates the NF-κB pathway in teleost fish by targeting MyD88. *J Immunol*. (2017) 198:3274–82. doi: 10.4049/jimmunol.1602064
20. Chu Q, Sun Y, Cui J, Xu T. Inducible microRNA-214 contributes to the suppression of NF-κB–mediated inflammatory response *via* targeting MyD88 gene in fish. *J Biol Chem*. (2017) 292:5282–90. doi: 10.1074/jbc.M117.777078
21. Xu T, Chu Q, Cui J, Bi D. Inducible microRNA-3570 feedback inhibits RIG-I-dependent innate immune response to rhabdovirus in teleost fish by targeting MAVS/IPS-1. *J Virol*. (2018) 92:e01594–17. doi: 10.1128/jvi.01594-17
22. Li S, Yue Y, Xu W, Xiong S. MicroRNA-146a represses mycobacteria-induced inflammatory response and facilitates bacterial replication *via* targeting IRAK-1 and TRAF-6. *PLoS ONE*. (2013) 8:e81438. doi: 10.1371/journal.pone.0081438
23. Xu T, Chu Q, Cui J, Zhao X. The inducible microRNA-203 in fish represses the inflammatory responses to Gram-negative bacteria by targeting IL-1 receptor-associated kinase 4. *J Biol Chem*. (2018) 293:1386–96. doi: 10.1074/jbc.RA117.000158
24. Chu Q, Yan X, Liu L, Xu T. The inducible microRNA-21 negatively modulates the inflammatory response in teleost fish *via* targeting IRAK4. *Front Immunol*. (2019) 10:1623. doi: 10.3389/fimmu.2019.01623
25. Zhang L, Chu Q, Chang R, Xu T. Inducible microRNA-217 inhibits NF-κB and IRF3-driven immune responses in lower vertebrates through targeting TAK1. *J Immunol*. (2020) 205:1620–32. doi: 10.4049/jimmunol.2000341
26. Che R, Wang R, Xu T. Comparative genomic of the teleost cathepsin B and H and involvement in bacterial induced immunity of miiuy croaker. *Fish Shellfish Immunol*. (2014) 41:163–71. doi: 10.1016/j.fsi.2014.08.025
27. Chu Q, Gao Y, Xu G, Wu C, Xu T. Transcriptome comparative analysis revealed poly(I:C) activated RIG-I/MDA5-mediated signaling pathway in miiuy croaker. *Fish Shellfish Immunol*. (2015) 47:168–74. doi: 10.1016/j.fsi.2015.08.032
28. Xu T, Xu G, Che R, Wang R, Wang Y, Li J, et al. The genome of the miiuy croaker reveals well-developed innate immune and sensory systems. *Sci Rep*. (2016) 6:21902. doi: 10.1038/srep21902
29. Zhang Q, Gui J. Virus genomes and virus-host interactions in aquaculture animals. *Sci China Life Sci*. (2015) 58:156–69. doi: 10.1007/s11427-015-4802-y
30. Chu Q, Xu T. miR-192 targeting IL-1R1 regulates the immune response in miiuy croaker after pathogen infection *in vitro* and *in vivo*. *Fish Shellfish Immunol*. (2016) 54:537–43. doi: 10.1016/j.fsi.2016.05.007
31. Lewis B, Shih I, Jones-Rhoades M, Bartel D, Burge C. Prediction of mammalian microRNA targets. *Cell*. (2003) 115:787–98. doi: 10.1016/S0092-8674(03)01018-3
32. John B, Enright AJ, Aravin A, Tuschl T, Sander C, Marks D. Human microRNA targets. *PLoS Biol*. (2004) 2:e363. doi: 10.1371/journal.pbio.0020363
33. Chu Q, Xu T, Zheng W, Chang R, Zhang L. Long non-coding RNA AANCR modulates innate antiviral responses by blocking miR-210-dependent MITA downregulation in teleost fish, *miichthys miiuy*. *Sci China Life Sci*. (2020) 63:1–18. doi: 10.1007/s11427-020-1789-5
34. Xu T, Chu Q, Cui J, Huo R. MicroRNA-216a inhibits NF-κB-mediated inflammatory cytokine production in teleost fish by modulating p65. *Infect Immun*. (2018) 88:e00256–18. doi: 10.1128/IAI.00256-18
35. Laemmli UK. Cleavage of structural proteins during the assembly of the head of bacteriophage T4. *Nature*. (1997) 227:680–5. doi: 10.1038/227680a0
36. Pfaffl M. A new mathematical model for relative quantification in real-time RT-PCR. *Nucl Acids Res*. (2001) 29:45e−45. doi: 10.1093/nar/29.9.e45
37. Livak KJ, Schmittgen TD. Analysis of relative gene expression data using real-time quantitative PCR and the 2−ΔΔCTmethod. *Methods*. (2001) 25:402–8. doi: 10.1006/meth.2001.1262
38. Xu T, Chu Q, Cui J. Rhabdovirus inducible microRNA-210 modulates antiviral innate immune response *via* targeting STING/MITA in fish. *J Immunol*. (2018) 201:982–94. doi: 10.4049/jimmunol.1800377
39. Lokesh J, Fernandes J, Korsnes K, Bergh O, Brinchmann M, Kiron V. Transcriptional regulation of cytokines in the intestine of Atlantic cod fed yeast derived mannan oligosaccharide or β-glucan and challenged with *Vibrio anguillarum*. *Fish Shellfish Immunol*. (2012) 33:626–31. doi: 10.1016/j.fsi.2012.06.017
40. Huang J, Wu Y, Chi S. Dietary supplementation of *Pediococcus pentosaceus* enhances innate immunity, physiological health and resistance to *Vibrio anguillarum* in orange-spotted grouper (*Epinephelus coioides*). *Fish Shellfish Immunol*. (2014) 39:196–205. doi: 10.1016/j.fsi.2014.05.003
41. Zou P, Chang M, Li Y, Xue N, Li J, Chen S, et al. NOD2 in zebrafish functions in antibacterial and also antiviral responses *via* NF-κB, and also MDA5, RIG-I and MAVS. *Fish Shellfish Immunol*. (2016) 55:173–85. doi: 10.1016/j.fsi.2016.05.031
42. Chu Q, Xu T. MicroRNA regulation of Toll-like receptor, RIG-I-like receptor and Nod-like receptor pathways in teleost fish. *Rev Aquac*. (2020) 12:2177–93. doi: 10.1111/raq.12428
43. Chu Q, Xu T, Zheng W, Chang R, Zhang L. Long noncoding RNA MARL regulates antiviral responses through suppression miR-122-dependent MAVS downregulation in lower vertebrates. *PLoS Pathogens*. (2020) 16:e1008670. doi: 10.1371/journal.ppat.1008670
44. Yuan J, Yang Y, Nie H, Li L, Gu W, Lin L, et al. Transcriptome analysis of epithelioma papulosum cyprini cells after SVCV infection. *BMC Genom*. (2014) 15:935. doi: 10.1186/1471-2164-15-935
45. Crill E, Furr-Rogers S, Marriott I. RIG-I is required for VSV-induced cytokine production by murine glia and acts in combination with DAI to initiate responses to HSV-1. *Glia*. (2015) 63:2168–80. doi: 10.1002/glia.22883
46. Zeng H, Zhong Q, Qin Y, Bu Q, Han X, Jia H, et al. Hypoxia-mimetic agents inhibit proliferation and alter the morphology of human umbilical cord-derived mesenchymal stem cells. *BMC Cell Biol*. (2011) 12:32. doi: 10.1186/1471-2121-12-32
47. Rosetto M, Engstrom Y, Baldari C, Telford J, Hultmark D. Signals from the IL-1 receptor homolog, toll, can activate an immune response in a drosophila hemocyte cell line. *Mol Cell Biol Res Commun*. (1995) 209:111–6. doi: 10.1006/bbrc.1995.1477
48. Wu Y, Liu J, Zhang Z, Huang H, Shen J, Zhang S, et al. HSP27 regulates IL-1 stimulated IKK activation through interacting with TRAF6 and affecting its ubiquitination. *Cell Signal*. (2009) 21:143–50. doi: 10.1016/j.cellsig.2008.10.001
49. Kovalenko A, Chable-Bessia C, Cantarella G, Israël A, Wallach D, Courtois G. The tumour suppressor CYLD negatively regulates NF-kappaB signalling by deubiquitination. *Nature*. (2003) 424:801–5. doi: 10.1038/nature01802
50. Chen L, Dong R, Lu Y, Zhou Y, Li K, Zhang Z, et al. MicroRNA-146a protects against cognitive decline induced by surgical trauma by suppressing hippocampal neuroinflammation in mice. *Brain Behav Immun*. (2019) 78:188–201. doi: 10.1016/j.bbi.2019.01.020
51. Hou J, Wang P, Lin L, Liu X, Ma F, An H, et al. MicroRNA-146a feedback inhibits RIG-I-dependent Type I IFN production in macrophages by targeting TRAF6, IRAK1, and IRAK2. *J Immunol*. (2009) 183:2150–8. doi: 10.4049/jimmunol.0900707

52. Hu G, Zhou R, Liu J, Gong A, Chen X. MicroRNA-98 and let-7 regulate expression of suppressor of cytokine signaling 4 in biliary epithelial cells in response to *Cryptosporidium parvum* infection. *J Infect Dis*. (2010) 202:125–35. doi: 10.1086/653212
53. Zhang Q, Huang C, Yang Q, Gao L, Liu H, Tang J, Feng W. MicroRNA-30c modulates type I IFN responses to facilitate porcine reproductive and respiratory syndrome virus infection by targeting JAK1. *J Immunol*. (2016) 196:2272–82. doi: 10.4049/jimmunol.1502006

Conflict of Interest: The authors declare that the research was conducted in the absence of any commercial or financial relationships that could be construed as a potential conflict of interest.

frontiers in Immunology

ORIGINAL RESEARCH
published: 29 April 2021
doi: 10.3389/fimmu.2021.664624

PRV-1 Infected Macrophages in Melanized Focal Changes in White Muscle of Atlantic Salmon (*Salmo salar*) Correlates With a Pro-Inflammatory Environment

Muhammad Salman Malik[1], *Håvard Bjørgen*[2], *Ingvild Berg Nyman*[1], *Øystein Wessel*[1], *Erling Olaf Koppang*[2], *Maria K. Dahle*[3] *and Espen Rimstad*[1]*

[1] Section of Virology, Faculty of Veterinary Medicine, Norwegian University of Life Sciences, Ås, Norway, [2] Section of Anatomy, Faculty of Veterinary Medicine, Norwegian University of Life Sciences, Ås, Norway, [3] Department of Fish Health, Norwegian Veterinary Institute, Oslo, Norway

OPEN ACCESS

Edited by:
Verónica Chico Gras, Universidad Miguel Hernández de Elche, Spain

Reviewed by:
Kim Dawn Thompson, Moredun Research Institute, United Kingdom
Sebastian Boltana, University of Concepcion, Chile

***Correspondence:**
Espen Rimstad
espen.rimstad@nmbu.no

Specialty section:
This article was submitted to Comparative Immunology, a section of the journal Frontiers in Immunology

Received: 05 February 2021
Accepted: 13 April 2021
Published: 29 April 2021

Citation:
Malik MS, Bjørgen H, Nyman IB, Wessel Ø, Koppang EO, Dahle MK and Rimstad E (2021) PRV-1 Infected Macrophages in Melanized Focal Changes in White Muscle of Atlantic Salmon (Salmo salar) Correlates With a Pro-Inflammatory Environment. Front. Immunol. 12:664624. doi: 10.3389/fimmu.2021.664624

Melanized focal changes in white skeletal muscle of farmed Atlantic salmon, "black spots", is a quality problem affecting on average 20% of slaughtered fish. The spots appear initially as "red spots" characterized by hemorrhages and acute inflammation and progress into black spots characterized by chronic inflammation and abundant pigmented cells. *Piscine orthoreovirus* 1 (PRV-1) was previously found to be associated with macrophages and melano-macrophages in red and black spots. Here we have addressed the inflammatory microenvironment of red and black spots by studying the polarization status of the macrophages and cell mediated immune responses in spots, in both PRV-1 infected and non-infected fish. Samples that had been collected at regular intervals through the seawater production phase in a commercial farm were analyzed by multiplex fluorescent *in situ* hybridization (FISH) and RT-qPCR methods. Detection of abundant inducible nitric oxide synthase (iNOS2) expressing M1-polarized macrophages in red spots demonstrated a pro-inflammatory microenvironment. There was an almost perfect co-localization with the iNOS2 expression and PRV-1 infection. Black spots, on the other side, had few iNOS2 expressing cells, but a relatively high number of arginase-2 expressing anti-inflammatory M2-polarized macrophages containing melanin. The numerous M2-polarized melano-macrophages in black spots indicate an ongoing healing phase. Co-localization of PRV-1 and cells expressing $CD8^+$ and MHC-I suggests a targeted immune response taking place in the spots. Altogether, this study indicates that PRV-1 induces a pro-inflammatory environment that is important for the pathogenesis of the spots. We do not have indication that infection of PRV-1 is the initial causative agent of this condition.

Keywords: Atlantic salmon, black spots, macrophage polarization, *Piscine orthoreovirus*, red spots

INTRODUCTION

Melanized focal changes in the white skeletal muscle of farmed Atlantic salmon (*Salmo salar*), "black spots", has emerged as a phenomenon that is found on average in 20% of the Atlantic salmon slaughtered at Norwegian processing plants (1). Fish affected with spots appear clinically healthy, and the condition is therefore regarded as a quality problem rather than associated with a disease state. Most melanized changes locate to the cranio-ventral and mid-ventral parts of the fillet, which could indicate an anatomical and physiological disposition for the condition (2). However, the etiological cause of the focal melanization remains unknown.

The black spots are primarily observed at slaughter of seawater farmed Atlantic salmon (3), and there are no reports that such spots are common in wild fish. Histologically, black spots appear heterogenous. The more severe black spots are classically characterized as chronic inflammatory reactions of granulomatous character, where macrophages are the dominating cell type, and the presence of melano-macrophages gives the black discoloration (3). In a longitudinal study where the presence of spots was followed through the seawater production phase in a commercial farmed salmon population, it was concluded that red spots preceded the formation of black spots (2). The term red spots refer to foci in the white muscle assumed to be intramuscular hemorrhages. The red spots were found to have a stable low prevalence in the production period, while the black spots accumulated over time in the fish population in seawater (2). Histopathological classification of the melanized spots show that they develop over the time the fish population has spent in sea water, and the most serious granulomatous inflammatory changes appear a few months before slaughter and are associated with *Piscine orthoreovirus* 1 (PRV-1) (2). Aggregation of macrophages and other immune cells forming granulomatous structures in the black spots indicate a long-term activation of the immune response (4).

Both immunohistochemistry and *in situ* hybridization methods have demonstrated presence of PRV-1 in melanized foci (2, 4). PRV-1 is a very common infection in farmed Atlantic salmon in the marine phase (5). The presence of PRV-1 in the black spots has been associated with the severity of the spots (2, 4). However, due to the increasing prevalence of PRV-1 infection in farmed Atlantic salmon with time spent in seawater, an alternative hypothesis would be that the presence of melanized changes is coincidental and not caused by PRV-1 infection. In line with this, some macroscopic dark spots are found in fish without detectable PRV-1 infection, but histologically these spots do not show the same chronic inflammatory and granulomatous reactions (2). In black spots with histopathological changes, classified as granulomatous changes, PRV-1 seems to be a consistent finding (2).

PRV virions are naked particles of 70 nm-large icosahedral capsids encompassing the genome of ten double stranded (ds) RNA segments, categorized into long (L1-L3), medium (M1-M3) and small (S1-S4) segments. There are three recognized subtypes of PRV. PRV-1 is mainly found in Atlantic salmon where it may cause heart and skeletal muscle inflammation (HSMI) (6). Following infection of PRV-1 in Atlantic salmon, the virus replicates to high titers in its main target cell, the erythrocyte (7, 8), and subsequently high virulent variants of PRV-1 infect cardiomyocytes leading to the cardiac inflammation observed during heart and skeletal muscle inflammation (HSMI) (9).

Previous studies have indicated that Atlantic salmon does not clear the PRV-1 infection, and the acute infection develops into a persistent, low productive infection (10). In the persistent phase, PRV-1 infection can be found in circulating erythrocytes and renal erythroid progenitor cells, but also in macrophages and melano-macrophages in kidney and spleen (11). In the melanized spots and in the granulomatous reactions of the more severe black spots in particular, PRV-1 is found in macrophage-like cells, melano-macrophages and erythrocytes (2, 12). This could indicate that the infected cells have a role in the pathogenesis of the melanized changes. Melano-macrophages primarily reside in the spleen and head kidney of teleost fish, where they can cluster to form so-called melano-macrophage centers, but they may also migrate to inflamed tissues (13).

Macrophages are often classified according to their polarization rather than their tissue location. The M1 type macrophages are classically activated and polarized by IFN-γ signaling. They produce a pro-inflammatory microenvironment by secreting inflammatory cytokines, and have the capacity to inactivate intracellular pathogens through, among other factors, the action of nitric oxide (NO) and reactive oxygen species (ROS) (14, 15). Presence of M1 macrophages in an area with infection suggests that macrophage polarization have occurred through sensing of danger signals (16, 17). M1 macrophages are a common phenotype of phagocytes during a cell mediated immune response (18).

The M2 macrophages, on the other hand, are anti-inflammatory and are central in wound healing and tissue repair (19, 20). M2 macrophages can be activated by anti-inflammatory cytokines (IL-4 or IL-13) (21) and their main functions are to generate extracellular matrix and polyamines for cell growth and division, in addition to protein synthesis necessary for the healing process (22). There are many indications that the polarized macrophage phenotypes exist also in teleost fish (23, 24), and the presence of inducible nitric oxide synthase (iNOS2) and arginase-2 (Arg2) have been defined as M1 and M2 specific markers, respectively (22).

Interaction between cytotoxic T-lymphocytes (CTLs) and the antigen presenting complex MHC-I on the target cell surface can initiate the killing of target cells by the actions of granzymes and perforins produced by CTLs (25, 26). Involvement of CTLs in the host defense mechanism against PRV-1 infected cells is indicated in HSMI (27) and spots development (12). The specific co-localization pattern of PRV-1 and the targeted response of these immune cells can be exposed through multiplex *in situ* hybridization method.

This study aimed to characterize the polarization of macrophages in red and black spots by multiplex fluorescent *in situ* hybridization (FISH) method and to study the correlation of markers of macrophage polarization, MHC-I and CD8 expressing cells with PRV-1 infection. The reduction of the relative number of PRV-1 infected cells through the spots' stages indicated an elimination of PRV-1 infected cells in the melanized focal spots

in Atlantic salmon. Transformation of red spots into black spots is associated with the emergence of melano-macrophages of M2 phenotype in the white skeletal muscle.

MATERIAL AND METHODS

Samples From Field Trial

Atlantic salmon smolts with an average weight of 110 g were transferred to sea in a commercial setting at Svåsand, Hardanger, Norway, as earlier described (2). The fish were sampled regularly throughout the seawater period and screened visually for presence of red and black spots in the white muscle (2). Formalin fixed samples of red and black spots had been categorized and graded based on macroscopic appearance and the PRV-1 infection status of the population had been monitored by RT-qPCR of gill, spleen and muscle samples by PatoGen Analyse, Ålesund, Norway as earlier described (2). The population was PRV negative upon transfer to sea and the first PRV positive fish were detected at 23 weeks post transfer. At 48 weeks post transfer about 98% of the sampled fish were PRV-1 positive. The samples used in the present study were collected at 4 and 52 weeks post sea transfer, i.e. prior to PRV-1 infection and after the population was near completely infected with PRV-1, in this context referred to as PRV negative and positive, respectively. The seawater temperature was 11-11.5°C at samplings.

The samples were collected from white muscle of the cranio-ventral part of the fillet and were no spots (normal tissue), macroscopic red spots and black spots (**Table 1**). Macroscopically the spots were graded 1-3 where grade 1 was very faint discoloration, 2 was a distinct but not severe discoloration and 3 was a prominent and severe discoloration (2).

RNA Extraction and RT-qPCR

Total RNA was extracted from a 25 mg sample of the tissues from all fish from each group as shown in **Table 1** using 0.65 ml QIAzol Lysis reagent (Qiagen, Hilden, Germany). Tissues were homogenized using 5 mm steel beads in a TissueLyzer II (Qiagen) for 2 x 5 min at 25 Hz. Chloroform was added and the aqueous phase collected for automatic RNA isolation using a RNeasy Mini QIAcube Kit (Qiagen), eluting RNA in 50 µl RNase free water. RNA concentrations were determined in a Nanodrop ND-100 spectrophotometer (Thermo Fisher Scientific, Waltham, MA, USA). Thereafter, RNA was stored at -80°C until further use.

TABLE 1 | Samples selected from red and black spots.

Category	PRV status	Grading	Sampling time (weeks after transfer to sea)
Black spot	Positive (n = 6)	Grade 1-3 black spots	52
	Negative (n = 6)	Grade 1-2 black spots	4
Red spot	Positive (n = 5)	Grade 1-3 red spots	52
	Negative (n = 6)	Grade 1-3 red spots	4
No spot	Positive (n = 6)	No macroscopic lesion	52
	Negative (n = 4)	No macroscopic lesion	4

cDNA was synthesized from 1 µg total RNA by using Quantitect Reverse Transcription Kit (Qiagen) according to the manufacturer's guidelines. In short, the procedure included elimination of genomic DNA and incubation at 42°C for 30 min with RT mastermix including reverse transcriptase enzyme and RNAse inhibitor. Quantitative PCR was performed in duplicates in 96-well plates, using a reaction volume of 12 µl with 15 ng cDNA input per well, and the Maxima SYBR Green/ROX qPCR Master Mix-2x (Thermo Fisher Scientific). Thermal conditions were set for an initial denaturation at 10 min/95°C and 40 cycles of amplification at 15 sec/95°C, 30 sec/60°C and 30 sec/72°C. Melting curve analysis were included to ensure assay specificity. Elongation factor (EF1ab) was used as reference gene (28). No-template control (NTC) were run on the same plate as negative control. The cut off value was set to Ct 35, and fold induction of genes of interest was determined against the reference gene and control samples (29). Primers (**Table 2**) were designed using Vector NTI Advance™ 11 software (Thermo Fisher Scientific), and AlignX application (Vector NTI Advance™ 11 Package, Invitrogen Dynal AS) was used for sequence alignments. (**Table 2**)

Statistical Analysis

Fold change (2- ΔΔCt formula) medians for genes of interest were compared in all groups, using non-parametric Mann-Whitney test due to small sample number, to display differences among the groups. GraphPad Prism version 9.0 (GraphPad Software Inc., La Jolla, CA, USA) was used for statistical analysis and graphical layouts. $p \leq 0.05$ was considered as significantly different.

Histology

Samples for histological examination were selected from PRV-1 infected and uninfected fish populations with or without macroscopic red and black spots (**Table 1**). Selection criteria for the uninfected population with red and black spots was spot grade level 2 (n = 1) because no uninfected fish had grade 3 level black spots. Samples from PRV-1 infected fish with red and black spots had grade 3 (n = 2). Samples from uninfected fish without macroscopic lesion were selected randomly and used as negative control, whereas samples from infected fish without spot were selected based on highest PRV-1 level (**Table S1**). Formalin fixed paraffin embedded (FFPE) tissue section (2 µm thickness) was dehydrated by gradual ethanol baths followed by xylene washing for paraffin clearance. Rehydration of the sections were performed for subsequent staining with hematoxylin and eosin (H&E staining). Standard procedures were followed (32). Bright field microscopy (Carl Zeiss Light Microscopy System with Axio Imager 2 - Carl Zeiss AG, Oberkochen, Germany) was performed for imaging.

Fluorescent *In Situ* Hybridization (FISH)

Sample Pretreatment

FFPE sections were sliced with 5 µm thickness from tissue samples and mounted on Superfrost plus (Thermo Fisher Scientific) slides. Slides were baked at 60°C for 2 h in a HybEZ™ II oven (Advanced Cell Diagnostics, catalog #321720)

TABLE 2 | List of specific primers for genes of interest.

Genes	Primer	Conc.	Sequence (5'-3')	Amplicon (bp)	Accession No.
iNOS2*	F	400 nM	CATCGGCAGGATTCAGTGGTCCAAT	135	XM_014214975.1
	R		GGTAATCGCAGACCTTAGGTTTCCTC		
Arg2*	F	400 nM	CCTGAAGGACTTGGGTGTCCAGTA	109	XM_014190234.1
	R		CCGCTGCTTCCTTGACAAGAGGT		
MHC Class I (30)	F	400 nM	CTGCATTGAGTGGCTGAAGA	175	AF504022
	R		GGTGATCTTGTCCGTCTTTC		
CD8α (31)	F	400 nM	CACTGAGAGAGACGGAAGACG	174	AY693393
	R		TTCAAAAACCTGCCATAAAGC		
Granzyme A (31)	F	400 nM	GACATCATGCTGCTGAAGTTG	81	BT048013
	R		TGCCACAGGGACAGGTAACG		
EF1αb (28)	F	500 nM	TGCCCCTCCAGGATGTCTAC	57	BG933897
	R		CACGGCCCACAGGTACTG		

**Amplification efficiency (E) of newly designed primers were calculated for iNOS2 (E = 0.98) and Arg2 (E = 1.02).*

followed by deparaffinization with 100% ethanol and fresh xylene baths. Samples were pretreated with hydrogen peroxide for 10 min at RT, boiled with RNAscope antigen retrieval reagent (Advanced Cell Diagnostics, catalog #322000) for 15 min at 99°C, and then incubated with RNAscope protease plus reagent for 15 min at 40°C in the HybEZ™ II oven. Hydrophobic barrier was made around the tissue section using Immedge hydrophobic barrier pen (Vector Laboratories, Burlingame, CA).

Multiplex *In Situ* Probe Hybridization

RNAscope® Multiplex fluorescent V2 assay kit (Advanced Cell Diagnostics catalog #323100) was used for simultaneous detection of up to three different RNA targets. Probes (**Table 3**) were designed against; PRV-1 L3 segment (Advanced Cell Diagnostics catalog #537451) iNOS2 (Advanced Cell Diagnostics catalog #548391); Arg2 (Advanced Cell Diagnostics catalog #548381) CD8α (Advanced Cell Diagnostics catalog #836821); Granzyme A (Advanced Cell Diagnostics catalog #836841) and MHC-I (Advanced Cell Diagnostics catalog #836831). Probes against Peptidylpropyl Isomerase B (PPIB) (Advanced Cell Diagnostics, catalog #494421) was used as reference gene for RNA integrity of the target samples. Dihydrodipicolinate reductase (DapB), a bacterial gene from *Bacillus subtilis* (Advanced Cell Diagnostics catalog #310043) was used as negative control gene to assess cross-reactivity and background noise. Probes were mixed and hybridized for 2 hrs at 40°C in the HybEZ™ II oven. Amplification steps (Amp1-Amp3) were performed according to the manufacturer's protocol. Opal fluorophores (**Table 2**) (Akoya Biosciences, CA, United States) were prepared and diluted (1:1500) using tyramide signal amplification (TSA) buffer (Advanced Cell Diagnostics catalog #322809) provided in the kit. Each probe was assigned a fluorophore, having a different emission and excitation range to distinguish each output signal (**Table 3**). Also, every probe was developed, labeled, and blocked separately by incubating with RNAscope® multiplex Fluorescent Detection Reagents v2 (catalog #323110) and diluted Opal fluorophores in a sequential order as per manufacturer recommendations. Each section was counter stained by adding DAPI (fluorescent DNA stain) for 30 sec at room temperature. Mounting was performed by adding 1-2 drops of Prolong Gold antifade mounting reagent (Thermo Fisher Scientific). Imaging was performed in a TCS SP8 gSTED confocal microscope (Leica microsystems GmbH, Mannheim, Germany).

RESULTS

Histology of Red and Black Focal Changes

In samples from white muscle from non-infected fish without visible spots, unaltered and intact myocytes were seen (**Figure 1A**). In samples of non-spot tissue from PRV-1 infected fish, mild myocyte degeneration was observed to some extent along with presence of infiltrating leukocytes (**Figure 1B**).

In red spots the white skeletal muscle tissue showed moderate to severe bleedings, and mild degeneration to moderate myocyte necrosis was observed in uninfected and infected fish, respectively (**Figures 1C, D**). The red spots from PRV-1

TABLE 3 | List of probes and corresponding fluorophores used in FISH.

	Probe	Target Region (bp)	Fluorophores	Emission/Excitation Wavelength (nm)	Channel*
Target	PRV-L3	415–1379	Opal 520 (FP1487001KT)	494/525	C1
	iNOS2	2–949	Opal 620 (FP1495001KT)	588/616	C2
	Arg2	1332–2053	Opal 690 (FP1497001KT)	676/694	C3
	CD8α	8-1033	Opal 620 (FP1495001KT)	588/616	C2
	GzmA	3-1088	Opal 690 (FP1497001KT)	676/694	C3
	MHC-I	2-2321	Opal 620 (FP1495001KT)	588/616	C2
Control	PPIB	20–934	Opal 520 (FP1487001KT)	494/525	C1
	DapB	414–862	Opal 520 (FP1487001KT)	494/525	C1

**Channels signify the specific labeling of each fluorophore separately for their excitation and emission properties.*
Accession numbers; PRV-L3- KY429945; PPIB- NM_001140870; DapB- EF191515, for the other genes the acc. nos. are listed in ***Table 2****.*

infected fish differed from the noninfected fish by infiltration of leukocytes and scattered appearance of adipocytes. In black spots, melanin was found in both groups (**Figures 1E, F**), however, the presence of macrophage-like cells with histologically observable melanin content, referred to as a melano-macrophages, in the samples of the infected fish were more prominent and widespread. Moreover, granulomatous changes in the black spots were observed in PRV-1 positive fish (**Figure 1F**) and never in the uninfected fish.

In Situ Localization of Differentiated, Polarized Macrophages and PRV-1 in Focal Changes

a. Uninfected fish

The positive and negative controls, i.e. using the PPIB and DapB probes, are shown in **Figures S1**, **S2**, respectively. Tissues with macroscopic appearance of red focal changes from uninfected fish showed no iNOS2 specific staining, but some Arg2 positive

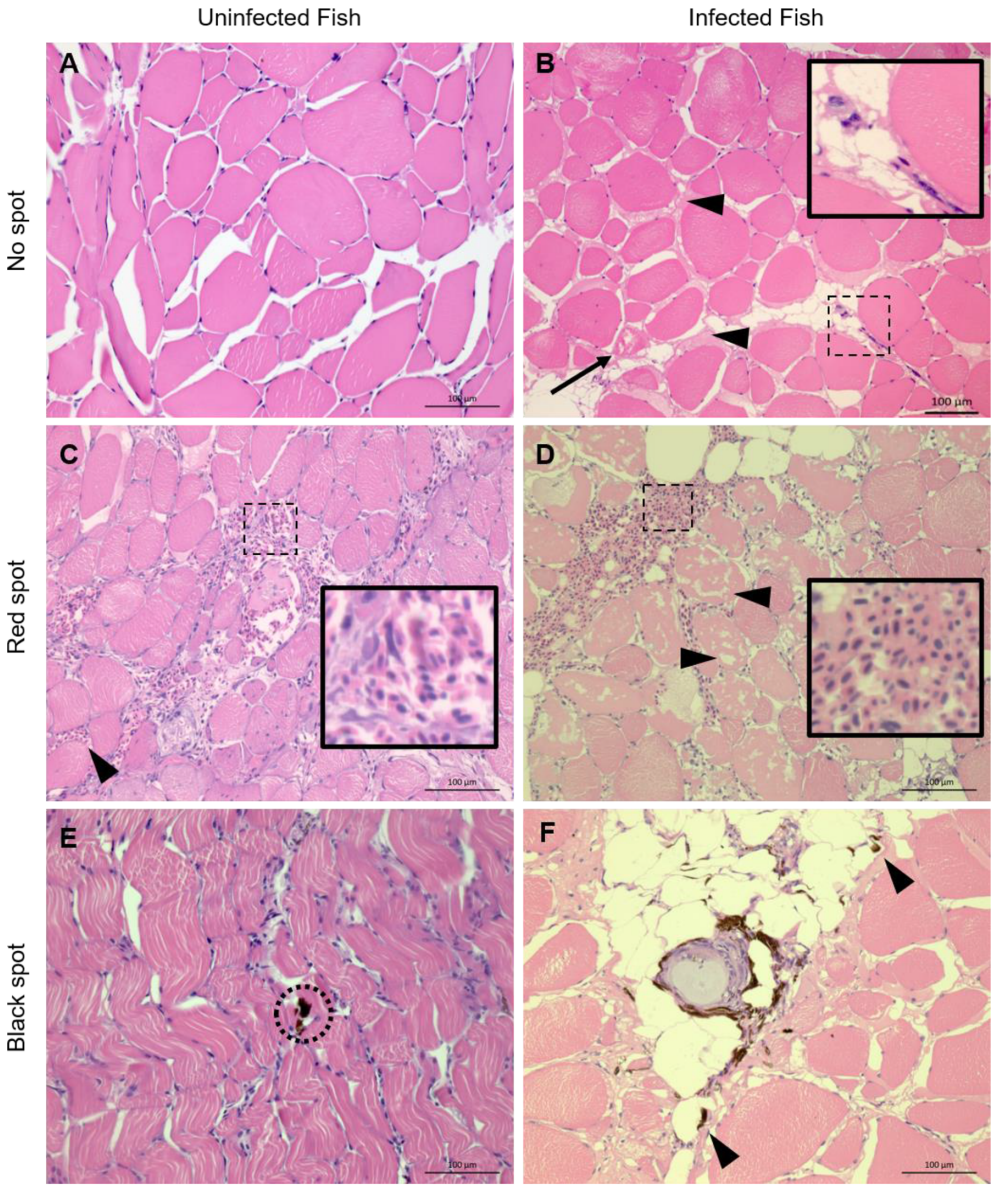

FIGURE 1 | Representative histological sections from white skeletal muscle of noninfected and PRV-1 infected Atlantic salmon HE stained. **(A)** Myocytes with no observable changes. **(B)** Myocytes with mild degeneration (arrow) and presence of inter-myocytial fluid (arrowheads) and few infiltrating leukocytes (inset). **(C)** Uninfected fish, red focal change shows areas with moderate (inset) and minor (arrowhead) hemorrhages. Note minor degeneration in some myocytes with infiltrating macrophages. **(D)** Red focal change in PRV-1 infected fish with large hemorrhage (inset) and massive myocyte necrosis (arrowheads). **(E)** Black spot in uninfected fish. Sporadic occurrence of melano-macrophages (black) in seemingly otherwise non-affected tissue (dotted circle). **(F)** Black spot in infected fish with a typical granulomatous change surrounded with melano-macrophages (black). Arrowheads point to scattered melano-macrophages. Scale bar = 100 µm.

cells (**Figure S3**). Similarly, sections with the macroscopic appearance of black spots from uninfected fish showed low number of iNOS2 or Arg2 positive cells (**Figure S4**). No staining was seen in areas without spots from uninfected fish (**Figure S5**). No PRV-1 signal was detected from noninfected fish groups having spots or no spots (**Figures S3**–**S5**).

b. Red spot. Early phase. PRV-1 infected.

In red focal changes there were hemorrhages (**Figure 2A**) containing a large number of nucleated cells (**Figure 2B**). Hemorrhages analyzed by FISH showed PRV-1 in a few erythrocytes (**Figure 2C**). Numerous iNOS2 positive macrophages, i.e. M1 type polarized macrophages, were surrounding the hemorrhage (**Figure 2D**), but co-localization of PRV-1 and iNOS2 were not seen (**Figure 2E**). There was no staining for Arg2, i.e. M2 type polarized macrophages (**Figure 2F**). Due to the low presence of M1 activated macrophages and lack of organization of the hemorrhages, this appearance was assessed as being an early phase of the red spots.

c. Red spot. Intermediate phase. PRV-1 infected.

In red focal changes from infected fish, where the changes were assessed as more advanced and infiltrating cells were seen between the myocytes (**Figure 3A**). The large number of extravasal erythrocytes of the early phase was not present (**Figure 3B**). Co-localization of PRV-1 and iNOS2 was observed among infiltrating cells found between myocytes (**Figures 3C, D**). There was no staining with Arg2 (**Figure 3F**). Due to the high presence of M1 activated macrophages and the organized appearance of the hemorrhages, but lack of melano-macrophages, this was assessed as being an intermediate phase of the red spots.

d. Red spot. Late phase (transition between red and black spots). PRV-1 infected.

In another region from the same red spot sample, as displayed in **Figure 3**, there were some scattered deposits of melanin (**Figure 4A**). In these areas, there was a modest number of PRV-1 positive cells (**Figure 4B**.) Here, Arg2 specific transcripts were detected (**Figure 4C**), with co-localized PRV-1 staining (**Figure 4D**). Detection of Arg2 was only observed in melano-macrophages found in the sporadic melanin deposits (**Figure 4E**). The commencement of M2 type melano-macrophage detection was assessed as an indication of transition from red to black spots.

e. Black spots. PRV-1 infected

In macroscopic black spots, larger deposits of melanin were seen (**Figure 5A**), and there was a moderate density of cells (**Figure 5B**). PRV-1 stained cells were mainly seen in the area of melanization (**Figures 5C, D**). Scattered areas of iNOS2 positive cell populations were detected in the melanized focal changes (**Figure 5E**), but these only partly co-localized with PRV-1 staining (**Figure 5F**). Arg2 positive cells were also seen in the PRV-1 infected area together with melanin presence (**Figure 5G**), showing some co-localization of PRV-1 and Arg2 (**Figure 5H**). A number of melano-macrophages with PRV-1 were detected. Arg2 positive transcripts were primarily detected in melano-macrophages, but were also present in non-melanized M2 macrophages (**Figure 5I**).

f. No focal changes, PRV-1 infected

In PRV-1 infected fish, samples from areas in white muscle without spots showed co-localization of iNOS2 and PRV-1 (**Figures 6A–D**), while Arg2 and PRV-1 only partly overlapped (**Figures 6E, F**). The staining of iNOS2 and Arg2 did not overlap.

Presence of CD8$^+$ and MHC-1 Positive Cells

a. Red Focal Changes, PRV-1 infected

In situ labeling revealed a mild influx of CD8$^+$ cytotoxic T lymphocytes (CTLs) in the bleeding area of red focal changes in PRV-1 infected fish (**Figure 7A**). Some of the CD8+ cells were also positive for PRV-1 staining, whereas

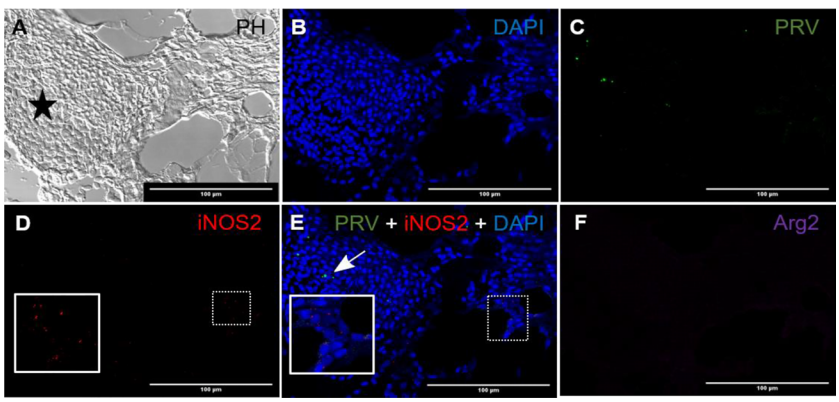

FIGURE 2 | *Fluorescent in situ hybridization of PRV-1, iNOS2 and Arg2 in red focal changes (early phase).* **(A)** Phase contrast image showing a large hemorrhage (star). **(B)** DNA staining of the cells by DAPI (blue). **(C)** Presence of a few PRV-1 (green) positive cells in the hemorrhage. **(D)** iNOS2 (red) specific transcripts detected in a limited number of cells surrounding a peripheral blood vessel. **(E)** Merged image showing presence of PRV-1 (arrow) but no co-localizing in the M1 macrophage (inset). **(F)** Arg2 (purple) specific transcripts (M2 type macrophages) were undetected. Scale bar = 100μm.

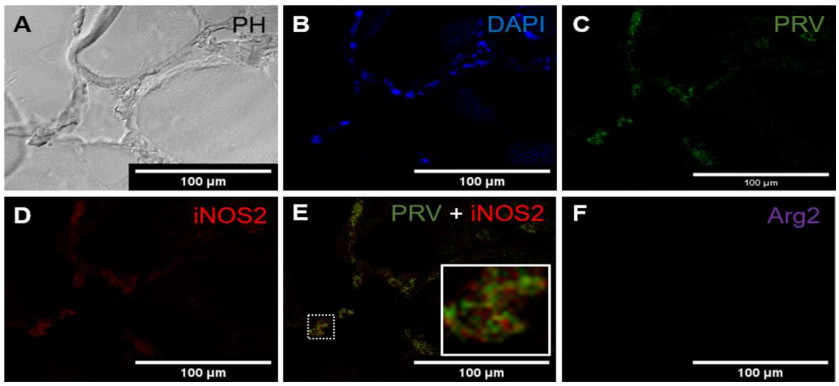

FIGURE 3 | *Fluorescent in situ hybridization of PRV-1, iNOS2 and Arg2 in red focal changes (intermediate phase).* **(A)** Phase contrast image showing infiltrating cells between myocytes. **(B)** Nuclei DNA staining of the cells with DAPI (blue). **(C)** Presence of PRV-1 (green) in infiltrating cells in between myocytes. **(D)** Presence of iNOS2 (red) in infiltrating cells between myocytes. **(E)** Merged image showing co-localization (inset) of PRV-1 and iNOS2 (yellow). **(F)** Arg2 transcripts (purple) were not detected. Scale bar = 100µm.

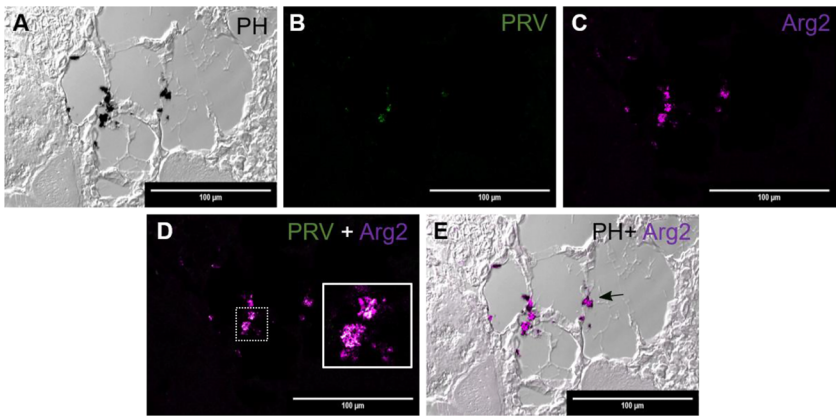

FIGURE 4 | *Fluorescent in situ hybridization of PRV-1 and Arg2 in red focal changes (late phase).* **(A)** Phase contrast image showing structure of the analyzed area and melanin deposit. **(B)** Sporadic presence of PRV-1 (green) in melanized area. **(C)** Arg2 (purple) positive cells **(D)** Merged image showing PRV-1 and Arg2 co-localization (white in the inset). **(E)** Merged image showing Arg2 positive staining of melano-macrophages (arrow). Scale bar = 100µm.

other CD8-positive cells were present around infected cells (**Figures 7A, B**). Granzyme A transcripts were detected in both $CD8^+$ (**Figures 7A–C**) and other cell populations in the infected area (**Figures 7A, B**). Numerous MHC-I positive cells were present at the bleeding site (**Figures 8A–C**), with a limited number also being PRV-1 infected. PRV-1 did not appear to co-localize with MHC-I (**Figures 8B, C**).

b. Black Focal Changes, PRV-1 infected

CD8+ cells were detected in the areas with melanin deposits. Some PRV-1 infected cells were also detected in this area, but the staining did not co-localize (**Figure 9**). Granzyme A specific transcripts were co-localized with CD8+ (**Figures 9C, D**) but also found in other cell subsets (**Figure 9B**). Numerous MHC-I positive cells were detected around a vacuolar area surrounded by melano-macrophages and some PRV-1 infected cells, showing high melanin deposits (**Figures 10A, B**). PRV-1 did co-localize with some MHC-I stained cells (**Figure 10C**).

Gene Expression in Red and Black Spots

a. iNOS2 and Arg2

iNOS2 expression was low in PRV positive (median Ct 30.7), non-spot samples (2 folds)while it was significantly increased (approximately 10 folds, MWU value = 0, n1 = 4, n2 = 5, p-value = 0.0079) in PRV positive (median 27) red focal changes (**Figures 11A**, **S6**). In contrast, iNOS2 was not upregulated in the samples from red focal changes of uninfected fish. In the black focal changes, iNOS2 expression was at the same level as in non-spot samples. Arg2 expression was significantly upregulated in all of the target groups, especially in PRV-1

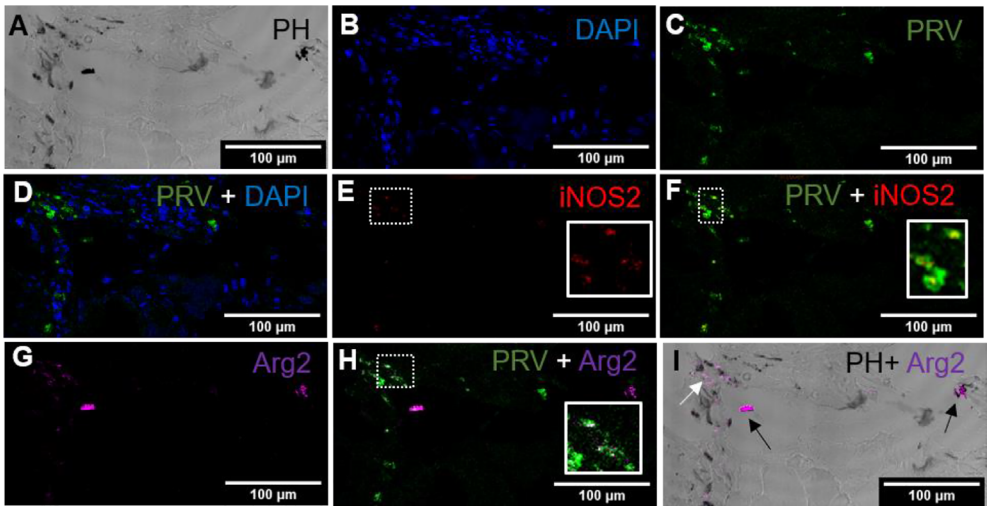

FIGURE 5 | *Fluorescent in situ hybridization of PRV-1, iNOS2 and Arg2 in black focal changes (late phase).* **(A)** Phase contrast image presence of melanin in the infected area. **(B)** Nuclei DNA stained with DAPI (blue). **(C)** PRV-1 (green) detected in severe melanized area **(D)** Merged PRV-1 and DAPI. Number of PRV-1 positive cells compared to total number of cells were low. **(E)** Few iNOS2 (red) positive cells detected at the infected area **(F)** Merged image showing co-localization (yellow in inset) of PRV-1 and iNOS2. **(G)** Presence of Arg2 (purple) positive cells. **(H)** Co-localization of PRV-1 and Arg2 positive cells (white in inset). **(I)** Localization of Arg2 specific transcripts in melanized M2 melano-macrophages (black arrows) and non-melanized M2 macrophages (white arrow). Scale bar = 100µm.

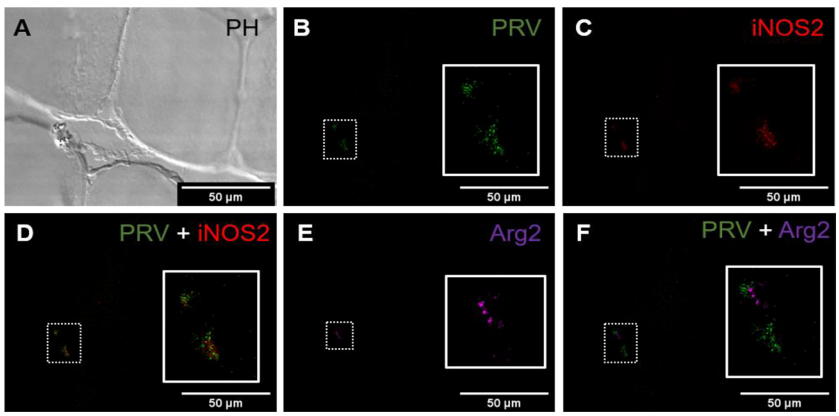

FIGURE 6 | *Fluorescent in situ hybridization of PRV-1, iNOS2 and Arg2 in areas without spots, from PRV-1 infected fish.* **(A)** Phase contrast image showing cells structure. **(B)** PRV-1 (green) specific transcripts detected between muscle cells. **(C)** iNOS2 (red) positive cells in the same area as PRV-1. **(D)** Merged image showing co-localization of PRV-1 and iNOS2 (yellow, insert). **(E)** Arg2 (purple) positive cells were detected partly in same area as PRV-1. **(F)** Merged image of PRV-1 and Arg2 show Arg2 positive cells surrounding PRV-1 infected cells (inset). Scale bar = 50µm.

infected groups. Arg2 was upregulated both in infected, no spot samples (6.5 folds, MWU value = 0, n1 = 4, n2 = 6, p-value = 0.0048) and in red focal changes without PRV infection (4.7 folds, MWU value = 1, n1 = 4, n2 = 6, p-value = 0.0095), compared to the uninfected, no-spot control. Both iNOS2 and Arg2 expression were at the highest level in the PRV infected fish with red focal changes. But in black focal changes only Arg2 expression, in contrast to iNOS2, was significantly upregulated (MWU value = 0, n1 = 4, n2 = 6, p-value = 0.0048) in PRV-1 infected group (median 27.7) (**Figures 11A**, **S6**).

b. CD8α, GzmA and MHC-I

There was a trend towards upregulation of the CD8α gene in the red and black focal changes (**Figure 11B**) but this was not statistically significant. Granzyme A expression level was significantly upregulated in PRV-infected groups with red (16.5 folds, MWU value = 0, n1 = 4, n2 = 5, p-value = 0.0079) and black focal changes (approx. 15 folds, MWU value = 2, n1 = 4, n2 = 5, p-value = 0.0489). Non-infected groups showed no significant induction of CD8α and granzyme A. Increased expression of MHC-1 was spotted in all fish groups infected with PRV-1, compared to non-infected groups, and

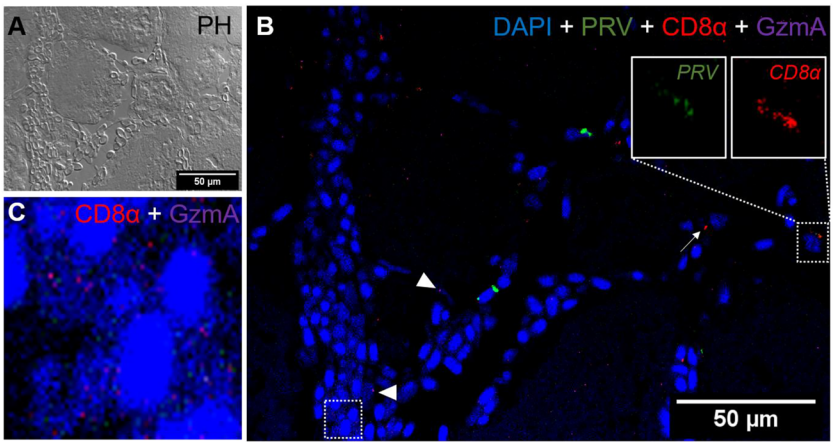

FIGURE 7 | *Fluorescent in situ hybridization of PRV-1, CD8α and GzmA in red focal changes.* **(A)** Phase contrast image showing a bleeding area with a large aggregation of blood cells. **(B)** Merged image of PRV (green), CD8α (red) and GzmA (purple). Localization of PRV-1 in CD8+ cell (dotted rectangle at right top) and co-expression of granzyme A in $CD8^+$ T cells (dotted rectangle in left bottom). Individual T cells detected expressing granzyme A specific transcripts (arrowhead) along with other CD8 cells (arrow). Nuclei DNA stained with DAPI (blue) **(C)** Magnified image of CD8+ and GzmA co-expression from dotted square in image **(B)** Scale Bar = 50 µm.

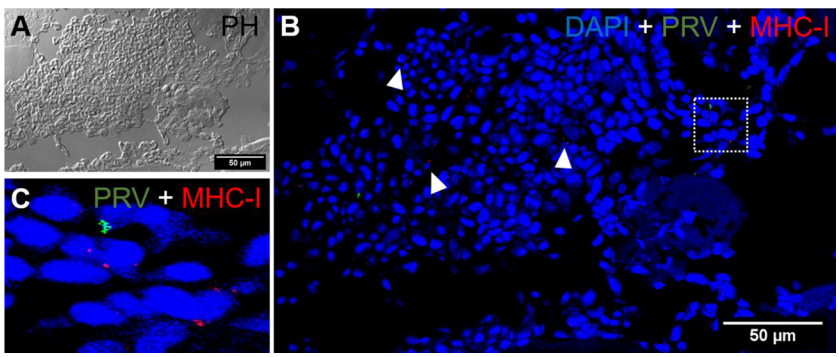

FIGURE 8 | *Fluorescent in situ hybridization of PRV-1, and MHC-I in areas of red focal changes.* **(A)** Phase contrast image showing a large hemorrhage. **(B)** Merged image of PRV-1 and MHC-I showed no co-expression of PRV-1 in MHC-I cells, but a few cells were detected in the bleeding area (arrowhead). **(C)** Magnified image from image B (dotted rectangle) showing PRV-1 infected cells along with MHC-I cells. Scale Bar = 50 µm.

the MHC-I expression level was relatively higher in black focal changes (14 folds, MWU value = 0, n1 = 4, n2 = 6, p-value = 0.0048) than in red focal changes (9 folds, MWU value = 2, n1 = 4, n2 = 5, p-value = 0.0317) (**Figure 11B**).

DISCUSSION

This study aimed to clarify the role of PRV-1 infection and the immune mechanisms involved in the development of melanized foci in white muscle of Atlantic salmon, using immune cell gene markers representing the macrophage polarization pattern, and the cytotoxic immune response.

Macrophages respond to their environment by differentiating into the functional pro-inflammatory phenotypes M1 macrophages, implicated in initiating and sustaining inflammation, or the anti-inflammatory M2 macrophages, implicated in tissue repair (33). In samples from red and black focal changes from non-infected fish there were no obvious detection of macrophage polarization apart from minimal occurrence of M2 macrophages, based on Arg2 transcript detection. Unaffected muscle areas of non-infected fish showed no presence of polarized macrophage markers. These findings were also reflected in the qPCR transcript analysis, which mirrored the *in situ* findings.

On the other hand, our results indicate that in the PRV-1 infected fish, the initial phase of the progress of the red and black spot formation were tightly connected to macrophage polarization and linked to the presence of PRV-1. The development of melanized focal changes is considered to be multifactorial. Viral diseases such as pancreas disease (PD) may affect the white muscle, but

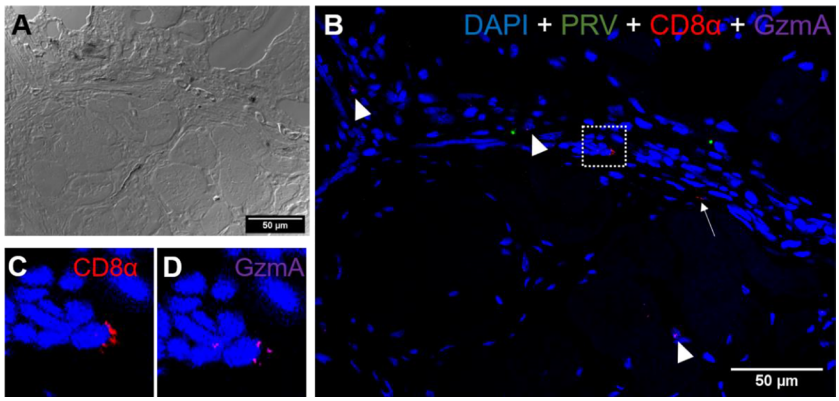

FIGURE 9 | *Fluorescent in situ hybridization of PRV-1, CD8α and GzmA in black focal changes.* **(A)** phase contrast image showing cell structures with melanin accumulation. **(B)** Merged image showing presence of PRV-1 (green) infected cells with $CD8^+$ cells (red) (arrows) and granzyme A (purple) in another cell population (arrowhead). Dotted rectangle showing co-expression of CD8 and GrzmA split in **(C, D)**. Nuclei DNA stained with DAPI (blue) Scale Bar = 50 µm.

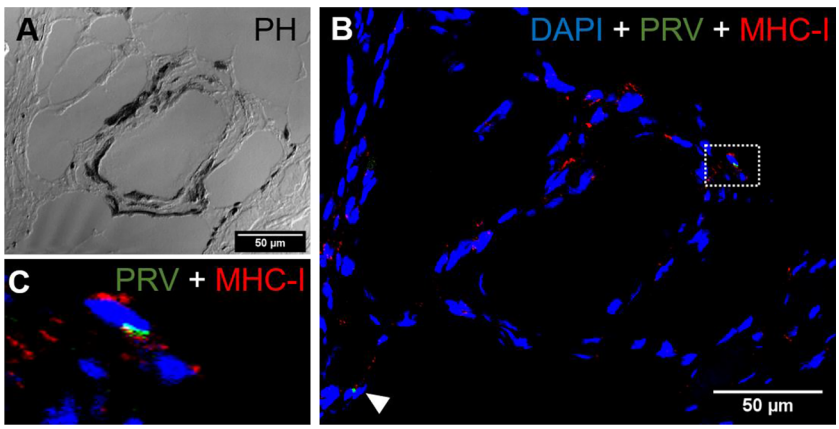

FIGURE 10 | *Fluorescent in situ hybridization of PRV-1 and MHC-I in black focal changes*. **(A)** phase contrast image showing vacuolar area surrounded by melano-macrophages and other immune cells. **(B)** Merged image showing presence of numerous MHC-I positive cells (red) where some are co-staining with PRV-1 (green) (dotted rectangle and arrowhead). **(C)** Magnified area from image B showing co-localization of PRV-1 in some MHC-I cells. Scale Bar = 50 µm.

widespread presence of melanized changes in areas being free from PD historically suggest no etiological role for this disease in the development of melanized focal changes (34). Furthermore, melanized changes have not been found to be influenced by bacterial components (2). We found that local PRV-1 infection was associated with the M1 polarized cell marker iNOS2 in the early developmental phases of melanized foci. PRV-1 was detected in a limited number of erythrocytes in hemorrhages, and only a few M1 macrophages was detected in the initial phase of red spots. Erythrocytes are a primary cell target of PRV-1 both in the acute and persistent phases of infection (7), and infected cells can be detected in any vascularized tissue. We have not found evidence here indicating that the PRV-1 infection initiated these hemorrhages as in previous studies (2, 4). However, for the close PRV relative, Grass carp reovirus (GCRV), it is suggested that iNOS2 activity is implicated in apoptosis of the vascular endothelial cells in hemorrhages characteristic for GCRV infection of Grass carp (*Ctenopharyngodon idella*) (35).

In PRV-1 infected fish, the M1 type macrophages were modestly detected in the early phase of red focal changes. However, in the more developed, intermediate phase of red spots the M1 macrophages were a dominating feature and were almost uniformly positive for PRV-1 specific staining, i.e. PRV-1 infected. The expression analysis by RT-qPCR also demonstrated elevated expression of iNOS2 in this phase. The dominating presence of PRV-1 infected, M1 polarized macrophages in this phase indicates a pro-inflammatory environment, which may be driven by the PRV-1 infection. In an earlier study, a significant downregulation of the anti-inflammatory cytokine IL10 was found associated with red changes (12), which indirectly indicates a pro-inflammatory environment.

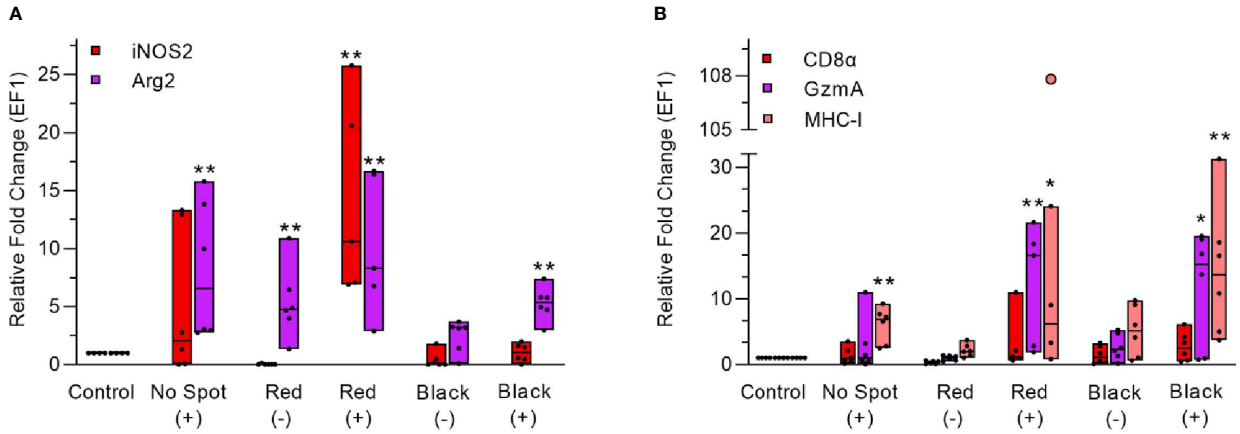

FIGURE 11 | Gene expression analysis during red and black focal changes in PRV infected (+) and uninfected (-) fish groups. **(A)** Relative fold change (median line) for each fish group is shown for iNOS2 and Arg2 (left Y-axis). **(B)** Relative fold change (median line) for each fish group is shown for CD8α, GzmA and MHC-I. Pink dot showing outlier value in the respective group. Each dot within boxes represents individual fish in the group. Gene expression relative to the control group (uninfected and unaffected) fish was normalized against EF1ab. * indicates significantly different from the control group (*$p < 0.05$, **$p < 0.01$).

Red spots with sporadic appearance of melano-macrophages were categorized as late red spot phase. This phase is considered to reflect the transition phase between red and black spots. Upregulation of iNOS2 level during red spots could be an indicator for commencement of melanogenesis. It is noteworthy that iNOS2 contributes to the melanogenesis in mammalian melanocytes (36). Based on the expression of the M2 marker Arg2, we found that the melano-macrophages at the site displayed the properties of anti-inflammatory M2 macrophages. We also found M2 macrophages without melanin. Co-localization pattern revealed PRV-1 abundance in melanized cells. The melano-macrophages of teleost fish are phagocytic cells (37) and they accumulate at long-term antigen retention sites in salmonids (13, 38). Phagocytosis of virus infected cells by macrophage and melano-macrophages have been reported earlier in Atlantic salmon (39). M2 macrophages are cells normally involved in tissue repair, and here they appeared first when melanin started to accumulate in the spots in skeletal muscle tissue.

Our findings indicate that PRV-1 infected macrophages are not innocent bystanders but represent M1 polarized macrophages important in the development of the pro-inflammatory microenvironment of red spots. The melanin accumulation starts in the late phase of red focal changes and will ultimately progress into black focal changes. It therefore seems as if melano-macrophages do not infiltrate the changes as such, but rather as non-pigmented macrophages capable of accumulating melanin over time. Melanogenesis has previously been demonstrated in advanced black spots (3). This putative progression could also be an explanation for the low prevalence of red spots but an increasing prevalence of black spots through the production period in seawater (2).

The black spots demonstrated a more heterogenous macrophage populations, i.e. both M1 and M2 macrophages were present. In advanced melanized areas, few M1 macrophages were positive for PRV-1, whereas PRV-1 co-localization was detected both in melanized (melano-macrophages) and non-melanized M2 type macrophages. In mammals, Arg2 is shown to downregulate the nitric oxide production of the M1 macrophages (40). Our findings indicate that Arg2 specific transcripts are mostly linked to the melanized area and associate with melano-macrophages. Presence of melano-macrophages (M2) was consistent from the late phase of red spots into black spots transformation (**Table 4**).

The correlated upregulation of Arg2 transcripts with the stage of development of the spots in the PRV-1 infected fish indicated a gradual shift from an inflammatory to a healing response

TABLE 4 | Consolidated summary of results.

Type of spot		*Key In situ* findings	Characteristic gene expression level
Red spot	Early	Few M1 macrophages in PRV-1 positive hemorrhages.	Significant upregulation of *iNOS2* expression
	Intermediate	High co-localization of PRV-1 in M1 macrophages.	Significant upregulation of *MHC-I* and *GzmA* expression
	Late	Detection of few M2 melano-macrophages.	
Black spot		Domination of M2 melano-macrophages and co-localization with PRV-1.	Significant upregulation of *Arg2* transcription.

during the transition from red to black macroscopic appearance of the spots. The spots of the non-infected fish with lack of detection of M1 macrophage marker and only a few detected M2 polarized macrophages, strongly indicated that PRV-1 is driving macrophage polarization in the spots of infected fish.

The initial etiological cause(s) of the red spots is unknown. The outcome of the spots in uninfected fish groups is also unknown due to the ubiquitous presence of PRV-1 in farmed Atlantic salmon, and the lack of an experimental model for spot formation (11). However, it could be speculated if the lack of inflammation in spots in non-infected fish argues for a shorter longevity and lower severity of the spots.

To further characterize the inflammatory microenvironment in the spots, the presence of CD8, Granzyme A and MHC-I positive cells was characterized during spot development. There were substantial variations in the presence of these markers among the individual fish, but *in situ* visualization indicated that MHC-I positive, PRV-1 infected cells were targeted by CD8 positive T cells both in red and black spots. The relative low number of CD8 positive cells evenly observed both in red and black focal changes was in line with the RT-qPCR expression analysis. However, a moderate, but not statistically significant up-regulation of CD8α expression in black focal changes compared to red focal changes was observed, and has been reported earlier (12). Mature cytotoxic T cells can use granzyme A for killing of target cells containing intracellular pathogens. Here, granzyme A specific transcripts were observed in cells that were not expressing CD8. By RT-qPCR, expression of Granzyme A was found to be significantly increased in both red and black spots compared to control samples, while CD8 was not. Granzyme A is also be synthesized by natural killer cells (NK-cells) (41) or other immune and non-immune cells in the teleost fish (42).

Mammalian myopathies are often marked by up-regulation of MHC-I (43, 44). By immunolabelling, MHC-I positive cells have earlier been demonstrated to be abundant in red spots (12), and in the present *in situ* study MHC-I cells were common, but perhaps not abundant. In both studies an absence of MHC-I positive myocytes was observed in the affected area, combined with lack of observation of PRV-1. The present study did not indicate that infection of the skeletal muscle cells is an important factor of the spot formation. As for Granzyme A, the MHC-I expression was significantly increased in both PRV-1 infected red and black spots compared to control samples, and co-localization of MHC-I and PRV-1 were seen in some cells especially in the melanized areas. Taken together, the targeted cell mediated immune response by the host tries to resolve and eradicate PRV-1 infection during red and black spots formation.

CONCLUSION

A possible course of events in the pathogenesis of black spots, is that PRV-1 infected erythrocytes in the hemorrhages infect tissue macrophages through phagocytosis. The myocyte degeneration in red muscle caused by PRV-1 (6), could be an additional driver for influx of macrophages, but is probably not the initial cause of red spots, as these are found at similar prevalence prior to PRV infection (2). The iNOS2 expressing M1-polarized non-melanized macrophages are mainly present in the period of the red focal changes, i.e. the time of inflammation, which suggests local production of NO and other oxygen radicals by the M1 macrophages. Melanin is a protector against free oxygen radicals (45), and its accumulation could be a consequence of the pro-inflammatory environment. Melanogenesis has previously been demonstrated in a salmon macrophage-like cell line (46, 47). The increased prevalence and severity of the black spots over time, indicates that the spot forming process is long lasting. The numerous M2-polarized melano-macrophages in black spots indicate that this is a healing phase of the process. Moreover, the presence of cytotoxic T cells and MHC-I positive cells in the focal changes represents the host' ability to target and eliminate PRV-1 infected cells. This suggests a role of PRV-1 infection in driving the development of black spots in white muscle of Atlantic salmon.

DATA AVAILABILITY STATEMENT

The raw data supporting the conclusions of this article will be made available by the authors, without undue reservation.

ETHICS STATEMENT

Ethical review and approval was not required for the animal study because the material was achieved from commercial production.

AUTHOR CONTRIBUTIONS

Conceptualization, MM, HB and ER. Methodology, MM, IN and HB. Software, MM. Validation, MM, ØW and MD. Formal analysis, MM, HB, ØW and ER. Investigation, MM, HB, ØW and ER. Resources, ER and EK. Data curation, MM, IN. Writing—original draft preparation, MM and ER. Writing—review and editing, ØW, MM, MD, HB, EK and ER. Visualization, MM, IN and HB. Supervision, ER, EK, MD and ØW. Project administration, ER. Funding acquisition, ER and EK. All authors contributed to the article and approved the submitted version.

FUNDING

The study was supported by the Norwegian Seafood Research Fund (FHF) grant 901501, and by the Research Council of Norway, grant 280847/E40 (ViVaAct).

SUPPLEMENTARY MATERIAL

The Supplementary Material for this article can be found online at: https://www.frontiersin.org/articles/10.3389/fimmu.2021.664624/full#supplementary-material

REFERENCES

1. Färber F. *Melanin Spots in Atlantic Salmon Fillets: An Investigation of the General Problem, the Frequency and the Economic Implication Based on an Online Survey*. Ås, Norway: Norwegian University of Life Sciences (2017).
2. Bjørgen H, Haldorsen R, Oaland O, Kvellestad A, Kannimuthu D, Rimstad E, et al. Melanized Focal Changes in Skeletal Muscle in Farmed Atlantic Salmon After Natural Infection With Piscine Orthoreovirus (PRV). *J Fish Dis* (2019) 42:935–45. doi: 10.1111/jfd.12995
3. Larsen HA, Austbø L, Mørkøre T, Thorsen J, Hordvik I, Fischer U, et al. Pigment-Producing Granulomatous Myopathy in Atlantic Salmon: A Novel Inflammatory Response. *Fish Shellfish Immunol* (2012) 33:277–85. doi: 10.1016/j.fsi.2012.05.012
4. Bjørgen H, Wessel O, Fjelldal PG, Hansen T, Sveier H, Saebo HR, et al. Piscine Orthoreovirus (PRV) in Red and Melanised Foci in White Muscle of Atlantic Salmon (Salmo Salar). *Vet Res* (2015) 46:89. doi: 10.1186/s13567-015-0244-6
5. Kongtorp R, Taksdal T, Lyngøy A. Pathology of Heart and Skeletal Muscle Inflammation (Hsmi) in Farmed Atlantic Salmon Salmo Salar. *Dis Aquat Org* (2004) 59:217–24. doi: 10.3354/dao059217
6. Wessel Ø, Braaen S, Alarcon M, Haatveit H, Roos N, Markussen T, et al. Infection With Purified Piscine Orthoreovirus Demonstrates a Causal Relationship With Heart and Skeletal Muscle Inflammation in Atlantic Salmon. *PloS One* (2017) 12:e0183781. doi: 10.1371/journal.pone.0183781
7. Finstad ØW, Dahle MK, Lindholm TH, Nyman IB, Løvoll M, Wallace C, et al. Piscine Orthoreovirus (PRV) Infects Atlantic Salmon Erythrocytes. *Vet Res* (2014) 45:35. doi: 10.1186/1297-9716-45-35
8. Wessel Ø, Olsen CM, Rimstad E, Dahle MK. Piscine Orthoreovirus (PRV) Replicates in Atlantic Salmon (Salmo Salar L.) Erythrocytes Ex Vivo. *Vet Res* (2015) 46:26–6. doi: 10.1186/s13567-015-0154-7
9. Wessel Ø, Hansen EF, Dahle MK, Alarcon M, Vatne NA, Nyman IB, et al. Piscine Orthoreovirus-1 Isolates Differ in Their Ability to Induce Heart and Skeletal Muscle Inflammation in Atlantic Salmon (Salmo Salar). *Pathogens (Basel Switzerland)* (2020) 9:1050. doi: 10.3390/pathogens9121050
10. Garver KA, Johnson SC, Polinski MP, Bradshaw JC, Marty GD, Snyman HN, et al. Piscine Orthoreovirus From Western North America is Transmissible to Atlantic Salmon and Sockeye Salmon But Fails to Cause Heart and Skeletal Muscle Inflammation. *PloS One* (2016) 11:e0146229. doi: 10.1371/journal.pone.0146229
11. Malik MS, Bjørgen H, Dhamotharan K, Wessel Ø, Koppang EO, Di Cicco E, et al. Erythroid Progenitor Cells in Atlantic Salmon (Salmo Salar) may be Persistently and Productively Infected With Piscine Orthoreovirus (PRV). *Viruses* (2019) 11:824. doi: 10.3390/v11090824
12. Bjørgen H, Kumar S, Gunnes G, Press CM, Rimstad E, Koppang EO. Immunopathological Characterization of Red Focal Changes in Atlantic Salmon (Salmo Salar) White Muscle. *Vet Immunol Immunopathol* (2020) 222:110035. doi: 10.1016/j.vetimm.2020.110035
13. Agius C, Roberts R. Melano-Macrophage Centres and Their Role in Fish Pathology. *J Fish Dis* (2003) 26:499–509. doi: 10.1046/j.1365-2761.2003.00485.x
14. Gordon S. The Macrophage: Past, Present and Future. *Eur J Immunol* (2007) 37:S9–S17. doi: 10.1002/eji.200737638
15. Gordon S, Taylor PR. Monocyte and Macrophage Heterogeneity. *Nat Rev Immunol* (2005) 5:953–64. doi: 10.1038/nri1733
16. Kanwal Z, Wiegertjes GF, Veneman WJ, Meijer AH, Spaink HP. Comparative Studies of Toll-Like Receptor Signalling Using Zebrafish. *Dev Comp Immunol* (2014) 46:35–52. doi: 10.1016/j.dci.2014.02.003
17. Aoki T, Hikima J-i, Hwang SD, Jung TS. Innate Immunity of Finfish: Primordial Conservation and Function of Viral Rna Sensors in Teleosts. *Fish Shellfish Immunol* (2013) 35:1689–702. doi: 10.1016/j.fsi.2013.02.005
18. Gordon S. Alternative Activation of Macrophages. *Nat Rev Immunol* (2003) 3:23–35. doi: 10.1038/nri978
19. Martinez FO, Helming L, Gordon S. Alternative Activation of Macrophages: An Immunologic Functional Perspective. *Annu Rev Immunol* (2009) 27:451–83. doi: 10.1146/annurev.immunol.021908.132532
20. Mills CD, Ley K. M1 and M2 Macrophages: The Chicken and the Egg of Immunity. *J Innate Immun* (2014) 6:716–26. doi: 10.1159/000364945
21. Martinez FO, Gordon S. The M1 and M2 Paradigm of Macrophage Activation: Time for Reassessment. *F1000prime Rep* (2014) 6. doi: 10.12703/P6-13
22. Wiegertjes GF, Wentzel AS, Spaink HP, Elks PM, Fink IR. Polarization of Immune Responses in Fish: The 'Macrophages First'point of View. *Mol Immunol* (2016) 69:146–56. doi: 10.1016/j.molimm.2015.09.026
23. Wentzel AS, Janssen JJE, de Boer VCJ, van Veen WG, Forlenza M, Wiegertjes GF. Fish Macrophages Show Distinct Metabolic Signatures Upon Polarization. *Front Immunol* (2020) 11:152. doi: 10.3389/fimmu.2020.00152
24. Wentzel AS, Petit J, van Veen WG, Fink IR, Scheer MH, Piazzon MC, et al. Transcriptome Sequencing Supports a Conservation of Macrophage Polarization in Fish. *Sci Rep* (2020) 10:13470. doi: 10.1038/s41598-020-70248-y
25. Nakanishi T, Shibasaki Y, Matsuura YT. Cells in Fish. *Biology* (2015) 4:640–63. doi: 10.3390/biology4040640
26. Trapani JA, Smyth MJ. Functional Significance of the Perforin/Granzyme Cell Death Pathway. *Nat Rev Immunol* (2002) 2:735–47. doi: 10.1038/nri911
27. Mikalsen AB, Haugland O, Rode M, Solbakk IT, Evensen O. Atlantic Salmon Reovirus Infection Causes a Cd8 T Cell Myocarditis in Atlantic Salmon (Salmo Salar L.). *PloS One* (2012) 7:e37269. doi: 10.1371/journal.pone.0037269
28. Løvoll M, Austbø L, Jørgensen JB, Rimstad E, Frost P. Transcription of Reference Genes Used for Quantitative Rt-Pcr in Atlantic Salmon is Affected by Viral Infection. *Vet Res* (2011) 42:8. doi: 10.1186/1297-9716-42-8
29. Pfaffl MW. Relative Quantification. *Real-time PCR* (2006) 63:63–82.
30. Jørgensen SM, Lyng-Syvertsen B, Lukacs M, Grimholt U, Gjøen T. Expression of Mhc Class I Pathway Genes in Response to Infectious Salmon Anaemia Virus in Atlantic Salmon (Salmo Salar L.) Cells. *Fish Shellfish Immunol* (2006) 21:548–60. doi: 10.1016/j.fsi.2006.03.004
31. Munang'andu HM, Fredriksen BN, Mutoloki S, Dalmo RA, Evensen Ø. The Kinetics of Cd4+ and Cd8+ T-Cell Gene Expression Correlate With Protection in Atlantic Salmon (Salmo Salar L) Vaccinated Against Infectious Pancreatic Necrosis. *Vaccine* (2013) 31:1956–63. doi: 10.1016/j.vaccine.2013.02.008
32. Bancroft J, Gamble M. *Theory and Practice of Histological Techniques*. Churchill Livingstone, London, United Kingdom: Elsevier Health Sciences (2008).
33. Mills CD, Kincaid K, Alt JM, Heilman MJ, Hill AM. M-1/m-2 Macrophages and the th1/th2 Paradigm. *J Immunol* (2000) 164:6166–73. doi: 10.4049/jimmunol.164.12.6166
34. Mørkøre T, Taksdal T, Birkeland S. Betydningen Av Pankreas Sykdom (Pd) for Filetkvalitet Av Oppdrettslaks. *Nofima Rapportserie* (2011).
35. Liang B, Su J. Inducible Nitric Oxide Synthase (Inos) Mediates Vascular Endothelial Cell Apoptosis in Grass Carp Reovirus (Gcrv)-Induced Hemorrhage. *Int J Mol Sci* (2019) 20:6335. doi: 10.3390/ijms20246335
36. Lassalle MW, Igarashi S, Sasaki M, Wakamatsu K, Ito S, Horikoshi T. Effects of Melanogenesis-Inducing Nitric Oxide and Histamine on the Production of Eumelanin and Pheomelanin in Cultured Human Melanocytes. *Pigment Cell Res* (2003) 16:81–4. doi: 10.1034/j.1600-0749.2003.00004.x
37. Stosik MP, Tokarz-Deptuła B, Deptuła W. Melanomacrophages and Melanomacrophage Centres in Osteichthyes. *Cent Eur J Immunol* (2019) 44:201. doi: 10.5114/ceji.2019.87072
38. Koppang E, Haugarvoll E, Hordvik I, Aune L, Poppe T. Vaccine-Associated Granulomatous Inflammation and Melanin Accumulation in Atlantic Salmon, Salmo Salar L., White Muscle. *J Fish Dis* (2005) 28:13–22. doi: 10.1111/j.1365-2761.2004.00583.x
39. Falk K, Press CM, Landsverk T, Dannevig BH. Spleen and Kidney of Atlantic Salmon (Salmo Salar L.) Show Histochemical Changes Early in the Course of Experimentally Induced Infectious Salmon Anaemia (Isa). *Vet Immunol Immunopathol* (1995) 49:115–26. doi: 10.1016/0165-2427(95)05427-8
40. Gotoh T, Mori M. Arginase Ii Downregulates Nitric Oxide (No) Production and Prevents No-Mediated Apoptosis in Murine Macrophage-Derived Raw 264.7 Cells. *J Cell Biol* (1999) 144:427–34. doi: 10.1083/jcb.144.3.427
41. Bratke K, Kuepper M, Bade B, Virchow JC Jr, Luttmann W. Differential Expression of Human Granzymes A, B, and K in Natural Killer Cells and During cd8+ T Cell Differentiation in Peripheral Blood. *Eur J Immunol* (2005) 35:2608–16. doi: 10.1002/eji.200526122
42. Chaves-Pozo E, Valero Y, Lozano MT, Rodríguez-Cerezo P, Miao L, Campo V, et al. Fish Granzyme a Shows a Greater Role Than Granzyme B in Fish Innate Cell-Mediated Cytotoxicity. *Front Immunol* (2019) 10:2579. doi: 10.3389/fimmu.2019.02579

43. Pavlath GK. Regulation of Class I Mhc Expression in Skeletal Muscle: Deleterious Effect of Aberrant Expression on Myogenesis. *J Neuroimmunol* (2002) 125:42–50. doi: 10.1016/S0165-5728(02)00026-7
44. Singh P, Kohr D, Kaps M, Blaes F. Skeletal Muscle Cell Mhc I Expression: Implications for Statin-Induced Myopathy. *Muscle Nerve* (2010) 41:179–84. doi: 10.1002/mus.21479
45. Sarna T. Free Radical Scavenging Properties of Melanin. Interaction of Eu and Pheo Melanin Models With Reducing and Oxidizing Agents. *Free Radic Biol Med* (1999) 26:518–25. doi: 10.1016/S0891-5849(98)00234-2
46. Thorsen J, Høyheim B, Koppang EO. Isolation of the Atlantic Salmon Tyrosinase Gene Family Reveals Heterogenous Transcripts in a Leukocyte Cell Line. *Pigment Cell Res* (2006) 19:327–36. doi: 10.1111/j.1600-0749.2006.00319.x
47. Haugarvoll E, Thorsen J, Laane M, Huang Q, Koppang EO. Melanogenesis and Evidence for Melanosome Transport to the Plasma Membrane in a cd83+ Teleost Leukocyte Cell Line. *Pigment Cell Res* (2006) 19:214–25. doi: 10.1111/j.1600-0749.2006.00297.x

Conflict of Interest: The authors declare that the research was conducted in the absence of any commercial or financial relationships that could be construed as a potential conflict of interest.

frontiers in Immunology

ORIGINAL RESEARCH
published: 17 June 2021
doi: 10.3389/fimmu.2021.694965

Multi-Omics Sequencing Provides Insights Into Age-Dependent Susceptibility of Grass Carp (*Ctenopharyngodon idellus*) to Reovirus

Libo He[1,2], *Denghui Zhu*[1,2], *Xinyu Liang*[1,2], *Yongming Li*[1], *Lanjie Liao*[1], *Cheng Yang*[1], *Rong Huang*[1], *Zuoyan Zhu*[1] *and Yaping Wang*[1,3]*

[1] State Key Laboratory of Freshwater Ecology and Biotechnology, Institute of Hydrobiology, Chinese Academy of Sciences, Wuhan, China, [2] College of Advanced Agricultural Sciences, University of Chinese Academy of Sciences, Beijing, China, [3] Innovative Academy of Seed Design, Chinese Academy of Sciences, Beijing, China

OPEN ACCESS

Edited by:
Maria Del Mar Ortega-Villaizan, Miguel Hernández University of Elche, Spain

Reviewed by:
Xiaobo Zhang, Zhejiang University, China
Zhen Xu, Huazhong Agricultural University, China

***Correspondence:**
Yaping Wang
wangyp@ihb.ac.cn

Specialty section:
This article was submitted to Comparative Immunology, a section of the journal Frontiers in Immunology

Received: 14 April 2021
Accepted: 18 May 2021
Published: 17 June 2021

Citation:
He L, Zhu D, Liang X, Li Y, Liao L, Yang C, Huang R, Zhu Z and Wang Y (2021) Multi-Omics Sequencing Provides Insights Into Age-Dependent Susceptibility of Grass Carp (Ctenopharyngodon idellus) to Reovirus. Front. Immunol. 12:694965. doi: 10.3389/fimmu.2021.694965

Grass carp (*Ctenopharyngodon idellus*) is an important aquaculture species in China that is affected by serious diseases, especially hemorrhagic disease caused by grass carp reovirus (GCRV). Grass carp have previously shown age-dependent susceptibility to GCRV, however, the mechanism by which this occurs remains poorly understood. Therefore, we performed transcriptome and metabolome sequencing on five-month-old (FMO) and three-year-old (TYO) grass carp to identify the potential mechanism. Viral challenge experiments showed that FMO fish were susceptible, whereas TYO fish were resistant to GCRV. RNA-seq showed that the genes involved in immune response, antigen presentation, and phagocytosis were significantly upregulated in TYO fish before the GCRV infection and at the early stage of infection. Metabolome sequencing showed that most metabolites were upregulated in TYO fish and downregulated in FMO fish after virus infection. Intragroup analysis showed that arachidonic acid metabolism was the most significantly upregulated pathway in TYO fish, whereas choline metabolism in cancer and glycerophospholipid metabolism were significantly downregulated in FMO fish after virus infection. Intergroup comparison revealed that metabolites from carbohydrate, amino acid, glycerophospholipid, and nucleotide metabolism were upregulated in TYO fish when compared with FMO fish. Moreover, the significantly differentially expressed metabolites showed antiviral effects both *in vivo* and *in vitro*. Based on these results, we concluded that the immune system and host biosynthesis and metabolism, can explain the age-dependent viral susceptibility in grass carp.

Keywords: grass carp, age-dependent viral susceptibility, grass carp reovirus, immune response, biosynthesis, metabolism

INTRODUCTION

Grass carp (*Ctenopharyngodon idellus*) is an important aquaculture species in China, accounting for more than 18% of the total freshwater aquaculture production in the country. Production of grass carp reached 5.53 million tons in 2019, making it the most highly consumed freshwater fish worldwide (1). However, grass carp is susceptible to many pathogens, especially the grass carp reovirus (GCRV), which causes grass carp hemorrhagic disease, a significant threat to the aquaculture of the species (2, 3). Consequently, GCRV has received much attention from fish breeding scientists and fish immunologists who aim to achieve disease-resistant breeding and uncover the mechanism underlying GCRV infection (4–6). Grass carp have shown age-dependent susceptibility to GCRV, with those less than 1 year old being susceptible to GCRV, while those over 3 years of age being resistant to the virus (7). However, the mechanism by which this occurs remains poorly understood.

In mammals, several studies on age-dependent susceptibility to viral infections have been done. Pott et al. (8) showed that neonatal mice were susceptible to rotavirus (8), whereas no clinical signs of infection were observed in adult individuals. This suggests that age-dependent TLR3 expression in the intestinal epithelium contributes to rotavirus susceptibility. In humans, infants and young children are particularly susceptible to viral encephalitis, whereas adults are not. A mouse model-based study revealed that age-dependent susceptibility to reovirus encephalitis was determined by the maturation of type-I interferon response (9). In fish, age is also an important factor that influences susceptibility to viruses. For example, rainbow trout fry showed a decrease in susceptibility to infectious pancreatic necrosis virus (IPNV) with increasing age and ceased to be susceptible at 20 weeks of age (10). Spring viremia of carp virus (SVCV) challenge experiments in multiple North American fish species suggested that host age is a key factor in determining disease outcomes (11). Age-dependent susceptibility to nervous necrosis virus (NNV) was also demonstrated in barramundi (*Lates calcarifer*) whereby infection at 3 and 4 weeks of age caused nervous necrosis disease, while fish at 5, 7, and 9 weeks of age developed subclinical infection (12). However, the mechanism underlying age-dependent susceptibility to viral infections in fish is largely unknown.

For the fish that showed age-dependent susceptibility to virus infection, the younger fish and older fish were considered as sensitive and resistant groups, respectively. Therefore, comparing two groups by specific methods may reveal the key genes or pathways involved in this phenomenon and provide important information for disease-resistant breeding or disease control and prevention. Moreover, the results could also provide useful information on age-dependent viral diseases in humans. In this study, we used five-month-old (FMO) and three-year-old (TYO) grass carp as the sensitive and resistant groups for further study. The age-dependent susceptibility to GCRV in grass carp was confirmed by an artificial viral challenge experiment. Additionally, histopathology, transcriptomics, and metabolomics were employed to uncover the mechanisms underlying this phenomenon. Due to the details of molecular events following GCRV infection have been reported previously (13); therefore, the main aim of the current study was not to identify the genes or pathways associated with GCRV infection again, but to reveal the potential mechanism of age-dependent viral susceptibility in grass carp by comparing susceptible FMO fish with resistant TYO fish. The results will improve our understanding of age-dependent susceptibility to virus infection in grass carp and will benefit disease-resistant breeding programs or GCRV control and prevention.

MATERIALS AND METHODS

Experimental Animals, Virus Exposure, and Sample Collection

Approximately 300 FMO and 300 TYO grass carp were used in the study. FMO fish had an average weight and length of 8 g and 12 cm, respectively, while the average weight and length of TYO fish were 2–3 kg and 50 cm, respectively (**Figure 1A**). All fish were obtained from the Guan Qiao Experimental Station, Institute of Hydrobiology, Chinese Academy of Sciences (CAS), and acclimated in aerated fresh water at 26–28°C for one week before processing. Fish were fed commercial feed twice daily, and water was exchanged daily. If no abnormal symptoms were observed, the fish were selected for further study.

After no abnormal symptoms were observed in the two groups, a viral challenge experiment was performed. Fish were infected with GCRV (GCRV subtype II, 2.97×10^3 RNA copies/μL) at a dose of 20 μL per gram of body weight by intraperitoneal injection. At the time before injection (0 days) and 1-5 days after injection, 15 fish from each group were anesthetized and euthanized with MS-222 (100 mg/L), and the spleens were removed for analysis. The collected samples were used for RT-qPCR analysis, histological section preparation, and transcriptome and metabolome sequencing. The remaining fish were carefully monitored, and the number of daily deaths was recorded. The experiment was concluded when no mortality was recorded for seven consecutive days, and the overall mortality rate could be calculated.

Histopathology

Histological sections were prepared as described previously (14). Briefly, spleen samples from three individuals of each group that were collected at 0, 1, 3, 5, and 7 days post-infection (dpi) were fixed in 4% paraformaldehyde overnight at 4°C. Following dehydration, the samples were embedded in HistoResin (Leica). Serial sections of 4 μm thickness were cut using a microtome (Leica), dried on slides at 42°C overnight, stained with hematoxylin and eosin (H&E), mounted in Permount (Fisher), and imaged with phase contrast with a 100× oil immersion objective lens.

Transcriptome Sequencing

RNA was isolated from the spleens using TRIzol reagent (Invitrogen, USA) according to the manufacturer's protocol.

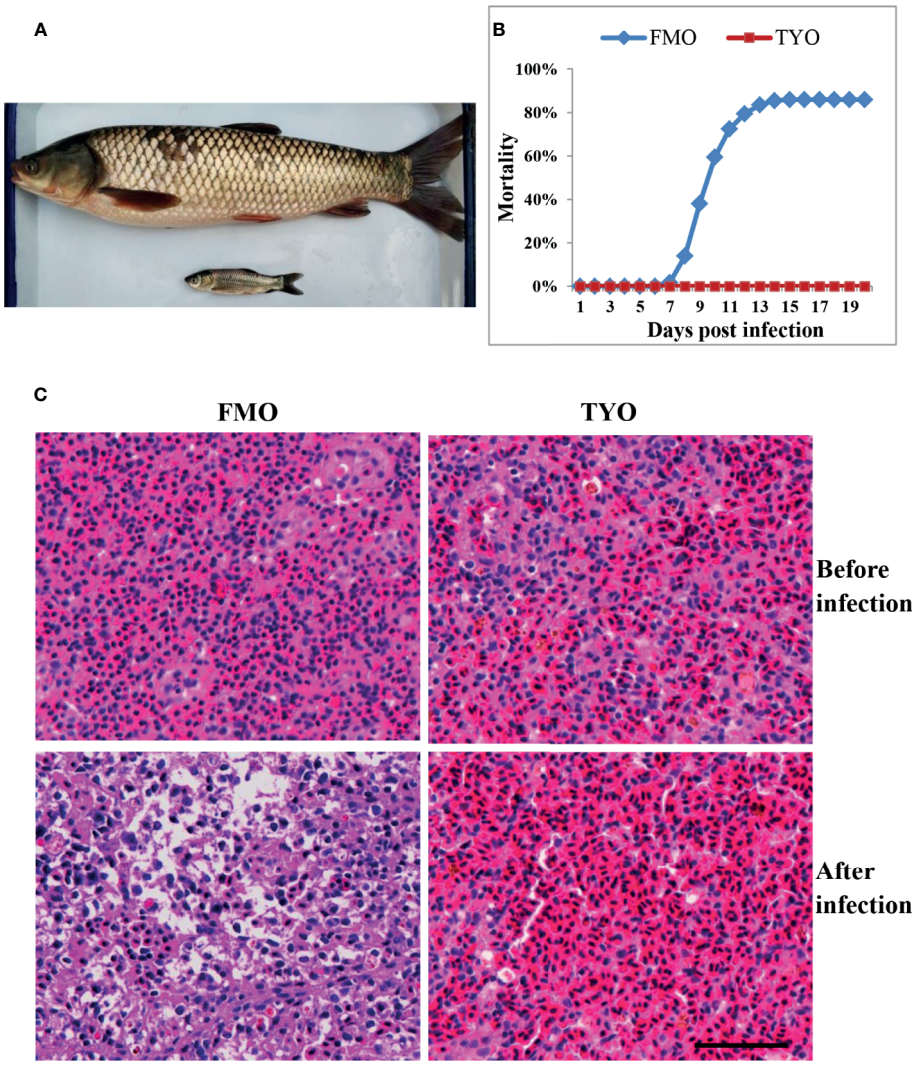

FIGURE 1 | The age-dependent susceptibility to GCRV in grass carp. **(A)** The representative picture of FMO grass carp and TYO grass carp. **(B)** The cumulative mortality of two groups of grass carp after GCRV infection. The total mortality of FMO fish group was reached to 86% while no dead fish was observed in the TYO fish group. **(C)** Histological section observation of two fish groups before and after GCRV infection. The spleen samples from two groups that that collected before and after (7 days post infection) GCRV infection were subjected histological section preparation and observed under microscope. Scale bars = 100 um.

Sequencing libraries were generated using the NEBNext Ultra RNA Library Prep Kit for Illumina (New England Biolabs, USA) following the manufacturer's protocol. Libraries were sequenced on an Illumina Novaseq platform, and 150 bp pair-end reads were generated. The output raw data reads were processed as described previously to obtain clean data (13). The clean reads were mapped to the reference genome of grass carp using Hisat2 software (15), and gene expression levels were calculated by FPKM (expected number of fragments per kilobase of transcript sequence per million base pairs sequenced) methods (16).

Differential expression analysis of the two groups/conditions was performed using the DESeq package (17). The resulting P-values were adjusted using the Benjamini and Hochberg approach to control the false discovery rate. Genes with an adjusted P-value < 0.05 (q value < 0.05) in DESeq analysis were assigned as differentially expressed genes (DEGs). All the DEGs identified in this study were used as references for the Gene Ontology (GO) and Kyoto Encyclopedia of Genes and Genomes (KEGG) enrichment analysis using the GOseq R package and KOBAS software (18, 19).

Examining the Expression Patterns of Immune Related Genes by RT-qPCR

Eight genes involved in the immune response were selected for RT-qPCR analysis to confirm the reliability of the RNA-seq data. Spleen samples from the two groups before and after GCRV infection were obtained, and RNA samples were prepared. First-strand cDNA was obtained using a random hexamer primer and ReverTra Ace kit (Toyobo, Japan). RT-qPCR was performed using a fluorescence quantitative PCR instrument (Bio-Rad, USA). Each RT-qPCR

mixture contained 0.8 μL forward and reverse primers (for each primer), 1 μL template, 10 μL 2× SYBRgreen master mix (TOYOBO, Japan), and 7.4 μL ddH2O. Three replicates were included for each sample, and the β-actin gene was used as an internal control for normalization of gene expression. The relative expression levels of genes in the TYO group were calculated as the ratio of gene expression levels relative to those in the FMO group at the corresponding time point. The primers are listed in **Table S1**. The RT-qPCR program was as follows: 95°C for 10 s, 40 cycles of 95°C for 15 s, 55°C for 15 s, and 72°C for 30 s, followed by melt curve construction. Relative expression levels were calculated using the $2^{-\triangle\triangle Ct}$ method (20). Data represent the mean ± standard deviation of three replicates.

Extraction of Metabolites

The spleen samples collected were frozen immediately in liquid nitrogen and then preserved at – 80°C. For metabolite extraction, the samples were thawed slowly on ice. Samples (50 mg) were homogenized with 1000 μL of ice-cold methanol/water (70%, v/v) using an Ultra-Turrax homogenizer. Cold steel balls were added to the mixture and homogenized at 30 Hz for 3 min. The mixtures were stirred for 1 min, centrifuged at 12,000 rpm at 4°C for 10 min, and the collected supernatant was used for further analysis.

UPLC -MS/MS Analysis

Metabolites were determined *via* ultra-performance liquid chromatography-tandem mass spectrometry (UPLC-MS/MS), as described previously (21, 22). Briefly, the UPLC system (Shim-pack UPLC SHIMADZU CBM30A) combined with MS/MS (QTRAP 6500+) was set at 30,000 resolution to obtain UPLC-MS/MS statistics. Sample analysis was performed in positive ion modes, a spray voltage of 5.5 kV, negative ion modes, spray voltage of -4.5 kV, and capillary temperature of 500°C. The mass scanning scope was set from 50 to 1,500 m/z. The nitrogen sheath and nitrogen auxiliary gas were set at 30 L/min and 10 L/min, respectively. Solvent A was 0.04% acetic acid (Fisher Scientific)/water (Millipore) (v/v), and solvent B was 0.04% acetic acid/acetonitrile (Fisher Scientific) (v/v). The gradient flow rate was 0.4 mL/min and the column temperature was 40°C, and the process was as follows: 5% B at 0 min, 95% B at 11.0 min, 95% B at 12.0 min, 5% B at 12.1 min, and 5% B at 14 min. The QC samples were injected four times at the start to ensure system consistency. A Waters ACQUITY UPLC HSS T3 C18 column (100 × 2.1 mm, 1.8 μm) was used for all analyses.

Metabolite Identification and Data Processing

Metabolite identification was based on the primary and secondary spectral data annotated against the self-compiled database MWDB (WuhanMetware Biotechnology Co., Ltd.) and publicly available metabolite databases, including MassBank (http://www.massbank.jp/), KNApSAcK (http://kanaya.naist.jp/KNApSAcK/), HMDB (http://www.hmdb.ca/), MoToDB (http://www.ab.wur.nl/moto/), and METLIN (http://metlin.scripps.edu/index.php). Metabolite quantification was performed using the multiple reaction monitoring (MRM) mode (23). Orthogonal partial least squares discrimination analysis (OPLS-DA) was used to study the identified metabolites. Those with significant differences in content were set with thresholds of variable importance in projection (VIP) ≥ 1 and | Log2fold change | ≥ 1.

CCK-8 Assay

A CCK-8 detection kit (Beyotime, Shanghai, China) was used to investigate the effects of the metabolites on cell viability according to the manufacturer's instructions. Briefly, approximately 5×10^3 *Ctenopharyngodon idellus* kidney (CIK) cells were seeded in 96 well plates and cultured in M199 medium supplemented with 10% fetal bovine serum (FBS) at 28°C for 24 h. Cells were treated with metabolites at different concentrations for 24 h. Then, 10 μL of CCK-8 solution was added to each well and incubated at 28°C for 4 h, and the absorbance at 450 nm was measured using a microplate reader (BIO-RAD, Hercules, CA, USA). The untreated cells were considered as the positive control, while the wells containing no cells but only culture medium were used as blank controls. The data are represented as the mean ± standard deviation (SD) values of three replicates.

Investigating the Anti-Viral Effects of Significantly Dems *In Vitro* and *In Vivo*

CIK cells were seeded in 6-well plates and grown until they formed a monolayer with 90% confluency. Before GCRV infection, the medium was replaced with a metabolite-supplemented medium at different concentrations and incubated for 4 h. Cells were then infected with GCRV at a multiplicity of infection (MOI) of 0.1 and harvested at 24 h post infection. The copy numbers of non-structural protein NS80 and structural protein VP7 were determined by RT-qPCR as described above. Additionally, plaque assays were performed to investigate the antiviral effects of the metabolites. Briefly, the infected cells in 12-well plates were overlaid with a medium containing 0.7% melted soft agar. After 24–48 h post-infection, the plaques formed and the medium was removed. The cells were then fixed with 20% formaldehyde and stained with 1% crystal violet. Three biological duplications were performed for the plaque assays and therefore the statistic data of the plaques in different groups were calculated and compared.

Approximately 400 FMO grass carp were randomly divided into four groups, one hundred each. The fish were then intraperitoneally injected with different metabolites (arachidonic acid: 100 μM; L-tryptophan: 5 mM; adenosine: 500 μM) at a volume of 200 μL or the same volume of PBS (control group), once daily for 3 days. After that, a viral challenge experiment was carried out for these fish by intraperitoneal injection as described above. The experiment was concluded when no mortality was recorded for seven consecutive days, and the total mortality in each group was calculated.

Statistical Analysis

The statistical significance between different groups was determined by one-way analysis of variance (ANOVA) and

Fisher's least significant difference (LSD) posttest. Differences were considered significant at $P < 0.05$. $P < 0.05$ was denoted by *.

RESULTS

Age-Dependent Susceptibility to GCRV in Grass Carp

Representative images of FMO and TYO grass carp are shown in **Figure 1A**. A viral challenge was performed for FMO and TYO grass carp. **Figure 1B** shows that a mortality rate of 86% in the FMO fish group was reached at 15 days after infection with GCRV, with the first death recorded 8 days post-infection (dpi). In contrast, no dead fish were observed in the TYO fish group. Histological sections from both groups showed no visible difference between spleen samples before GCRV infection; cells in both groups had an orderly arrangement, and the nuclei were intact (**Figure 1C**). However, the post-infection spleen samples from FMO fish showed severe necrotic lesions, vacuolization, and hypertrophied nuclei with karyorrhexis, while no obvious change was observed in the spleen samples from TYO fish. Therefore, these results further confirm age-dependent susceptibility to GCRV in grass carp.

Transcriptome Analysis of Grass Carp With Different Ages Before and After Viral Challenge

To further elucidate the mechanism of age-dependent susceptibility to GCRV in grass carp, we performed RNA-seq analysis on samples collected from the two age groups before (0 d) and after (1, 3, and 5 d) infection. The samples in the FMO group were named S1-0, S1-1, S1-3, and S1-5, while samples in the TYO group were named as S3-0, S3-1, S3-3, and S3-5. Three duplicates of each sample were processed, yielding a total of 24 libraries, which were sequenced on an Illumina Novaseq platform to generate 150 bp pair-end reads. In total, each library yielded clean bases ≥ 6 GB, Q20 ≥ 95%, Q30 ≥ 87%, and uniquely mapped percentage ≥ 85% (**Table S2**), confirming the high quality of the sequence data and its suitability for further analysis. The sequence data from this study were deposited in the Sequence Read Archive (SRA) at the National Center for Biotechnology Information (NCBI) (accession number: PRJNA600033). These data were subjected to a series of intergroup comparisons to identify the DEGs. Briefly, data from the TYO fish group (S3-0, S3-1, S3-3, and S3-5) were compared with data from the FMO fish group (S1-0, S1-1, S1-3, and S1-5) at the same time points. In detail, 300, 898, 393, and 428 DEGs were upregulated, whereas 569, 1040, 555, and 724 DEGs were downregulated at 0, 1, 3, and 5 dpi, respectively (**Table S3**). Detailed information on these DEGs is presented in **Table S4**.

Enrichment Analysis of the DEGs

GO and KEGG enrichment analyses were used to identify the specific roles of the DEGs. To discriminate the virus infection process in fish between the different groups, the upregulated and downregulated DEGs from each time point were separately subjected to enrichment analysis. As shown in **Table 1**, before GCRV infection (0 d), GO enrichment analysis showed that the upregulated DEGs were significantly enriched with terms involved in proteasome and metal ion homeostasis, while the downregulated DEGs were mainly enriched with terms related to enzyme activity. At 1 and 3 dpi, GO terms involved in immune response, antigen presentation, and chemokine and cytokine activity were significantly enriched for upregulated DEGs, whereas terms responsible for enzyme activity and the oxidation-reduction process were enriched for downregulated DEGs. Finally, binding-related GO terms were enriched for the upregulated DEGs from 5 dpi, whereas chemokine and cytokine activity-related terms were enriched for the downregulated DEGs. The results support that the immune response of TYO fish started immediately, while in FMO fish it was activated slowly. The top five enriched GO terms (up and downregulated) at each time point are listed in **Table 1** and full details of the GO terms are given in **Table S5**.

KEGG enrichment analysis of the DEGs showed similar results (**Figure 2**). The pathways involved in proteasome, lysosome, glutathione metabolism, and drug metabolism were significantly enriched for the upregulated DEGs before GCRV infection, while downregulated DEGs were enriched in metabolism-related pathways (galactose, starch, and sucrose metabolism) (**Figure 2A**). At 1 and 3 dpi, pathways participating in immune response and phagocytosis, such as NOD-like receptor signaling pathways, phagosomes, lysosomes, and proteasomes, were significantly enriched for the upregulated DEGs. The biosynthesis-and metabolism-related pathways were enriched for the downregulated DEGs (**Figures 2B, C**). Finally, metabolism-related pathways, such as glutathione metabolism and drug metabolism-cytochrome P450, were enriched for upregulated DEGs, while immune-related signaling pathways were enriched for the downregulated DEGs (**Figure 2D**). The results of KEGG enrichment further supported that TYO fish could respond rapidly to virus infection by initiating the immune response at the early stage of infection, whereas FMO fish had blunted immune responses that were only activated at the late stage of infection. The top five enriched KEGG terms (up and downregulated) at each time point are shown in **Figure 2**, and full details of the KEGG terms given in **Table S6**.

Expression Patterns of DEGs in the Immune Related GO or KEGG Terms

The gene expression patterns of DEGs in the immune-related GO or KEGG terms (immune response, chemokine/cytokine, antigen processing and presentation, proteasome, phagosome, and lysosome) were selected for further analysis. As shown in **Figure 3**, in terms of immune response and chemokine/cytokine, most of the genes showed no significant difference before GCRV infection between the two age groups. However, more than half of the genes were upregulated at 1 and 3 dpi in the TYO fish group, whereas this trend ceased at 5 dpi. The genes involved in antigen presentation were almost upregulated throughout the

TABLE 1 | The top 5 significant enriched GO terms for the DEGs.

Comparisons	UP/down	GO terms	Corrected P-value
S3-0/S1-0	UP	proteasome complex	1.31E-08
		proteasome core complex	3.27E-08
		cellular iron ion homeostasis	1.59E-05
		cellular transition metal ion homeostasis	1.59E-05
		iron ion homeostasis	1.59E-05
	Down	serine-type endopeptidase activity	3.61E-06
		proteolysis	3.56E-05
		serine-type peptidase activity	5.84E-05
		serine hydrolase activity	5.84E-05
		peptidase activity, acting on L-amino acid peptides	0.00012568
S3-1/S1-1	UP	immune response	0.000653
		immune system process	0.000653
		antigen processing and presentation	0.005695
		MHC protein complex	0.0239
		MHC class II protein complex	0.0239
	Down	oxidoreductase activity	4.60E-25
		oxidation-reduction process	2.37E-20
		catalytic activity	4.52E-20
		single-organism metabolic process	4.56E-15
		serine-type endopeptidase activity	3.32E-14
S3-3/S1-3	UP	G-protein coupled receptor binding	3.53E-06
		chemokine activity	3.53E-06
		chemokine receptor binding	3.53E-06
		cytokine activity	1.73E-05
		cytokine receptor binding	9.19E-05
	Down	serine-type endopeptidase activity	2.81E-16
		endopeptidase inhibitor activity	6.99E-15
		endopeptidase regulator activity	6.99E-15
		serine-type peptidase activity	6.99E-15
		serine hydrolase activity	6.99E-15
S3-5/S1-5	UP	oxygen binding	9.28E-07
		heme binding	0.016744
		tetrapyrrole binding	0.021006
	Down	NAD+ ADP-ribosyltransferase activity	2.14E-05
		transferase activity, transferring pentosyl groups	0.001779
		chemokine activity	0.003354
		chemokine receptor binding	0.003354
		cytokine activity	0.003485

entire infection process. For the terms proteasome, lysosome, and phagosome, over half of the genes showed upregulated expression patterns at 0, 1, and 3 dpi, but no difference was observed at 5 dpi. Moreover, we performed RT-qPCR for eight genes participating in immune-related biological processes in order to confirm the reliability of the RNA-seq data. As shown in **Supplementary Figure 1**, most genes showed expression patterns similar to those obtained by RNA-seq, although the relative expression levels were not completely consistent (**Supplementary Figure 1**). Collectively, these results show that most genes in the immune-related terms or pathways were upregulated in the TYO fish group before (0 d), or at the early stage (1 and 3 d) of GCRV infection, indicating their contribution to the age-dependent viral susceptibility in grass carp.

Metabolome Analysis of Grass Carp Age Groups Before and After Viral Challenge

To further elucidate the mechanism of age-dependent susceptibility to GCRV in grass carp, a widely targeted metabolome analysis was performed on samples collected from the two groups before (0 d) and after GCRV infection (1, 3, and 5 d). The sample names were consistent with those in RNA-seq, and three duplicates were also performed for each sample. A total of 516 metabolites, including carbohydrates, amino acids, amino acid derivatives, fatty acids, carnitines, nucleotide derivatives (purine and pyrimidine derivatives), phospholipids (lysophosphatidylcholine [lysoPC] class, lysophosphatidylethanolamine [lysoPE] class), organic acid derivatives, oxidized lipids, benzene and substituted derivatives, and vitamins, were identified in all samples (**Table S7**). The two score plots of the principal component analysis (PCA) model show a clear separation of samples from the two age groups, indicating the difference between two groups (**Supplementary Figure 2**). Moreover, samples before GCRV infection also separated significantly from GCRV-infected samples in both groups (**Supplementary Figure 2**), implying the efficiency of GCRV infection. OPLS-DA was employed to identify differentially expressed metabolites (DEMs). Data from the TYO fish group (S3-0, S3-1, S3-3, and S3-5) were compared with data from the FMO fish group (S1-0, S1-1, S1-3, and S1-5) at the same time

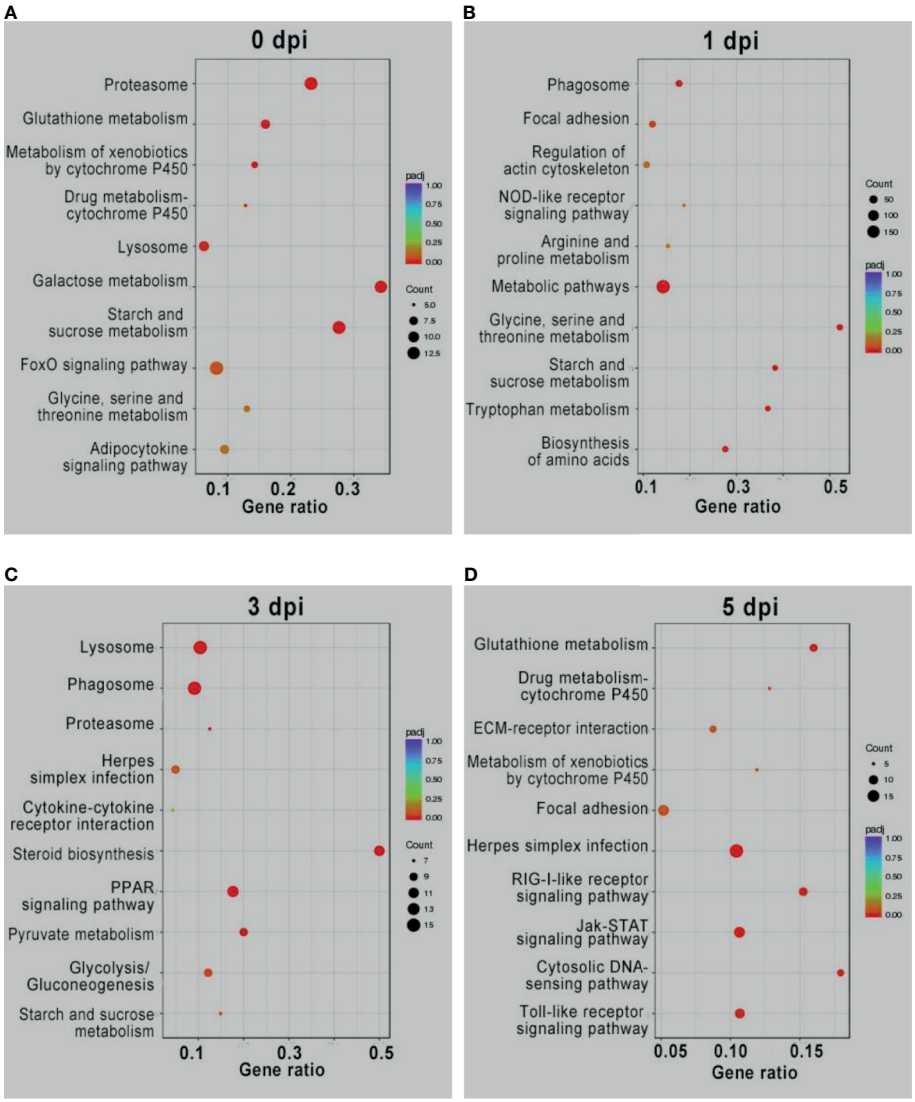

FIGURE 2 | KEGG enrichment analysis of DEGs from intergroup comparisons before **(A)** and at 1 **(B)**, 3 **(C)**, and 5 **(D)** days after GCRV infection. In each time points, the upper five terms indicated the terms enriched in upregulated genes, while the bottom five terms represented the terms enriched in downregulated genes.

points. Intergroup comparisons showed that 55, 158, 190, and 190 DEMs were upregulated, whereas 67, 15, 26, and 11 DEMs were downregulated at 0, 1, 3, and 5 dpi, respectively (**Supplementary Figure 3A**). Moreover, intragroup comparisons between samples before and after GCRV infection were also done. The results showed that 146, 151, and 175 DEMs were identified in the FMO fish group (**Supplementary Figure 3B**), while 88, 107, and 110 DEMs were identified in the TYO fish group (**Supplementary Figure 3C**) at 1, 3, and 5 dpi, respectively. Detailed information on these DEMs is shown in **Table S8**. Interestingly, both inter and intragroup comparisons showed that most DEMs were upregulated in the TYO fish group and downregulated in the FMO fish group after virus infection. These results suggest that the TYO fish responded positively to virus infection, resulting in the upregulation of most metabolites, while the FMO fish were severely affected by virus infection, inducing the downregulation of most metabolites.

Enrichment Analysis of DEMs From Intergroup and Intragroup Comparisons

To understand the functions of DEMs and the biological processes related to GCRV infection, all DEMs from intergroup comparisons were mapped to terms in the KEGG database. As shown in **Figure 4**, before GCRV infection, KEGG terms arachidonic acid metabolism, pyrimidine metabolism, and platelet activation were enriched (**Figure 4A**). Three metabolism-related terms (purine metabolism, pentose phosphate pathway, and pyrimidine metabolism) were enriched at 1 dpi (**Figure 4B**). At 3 dpi, four metabolism-related terms (purine metabolism, choline

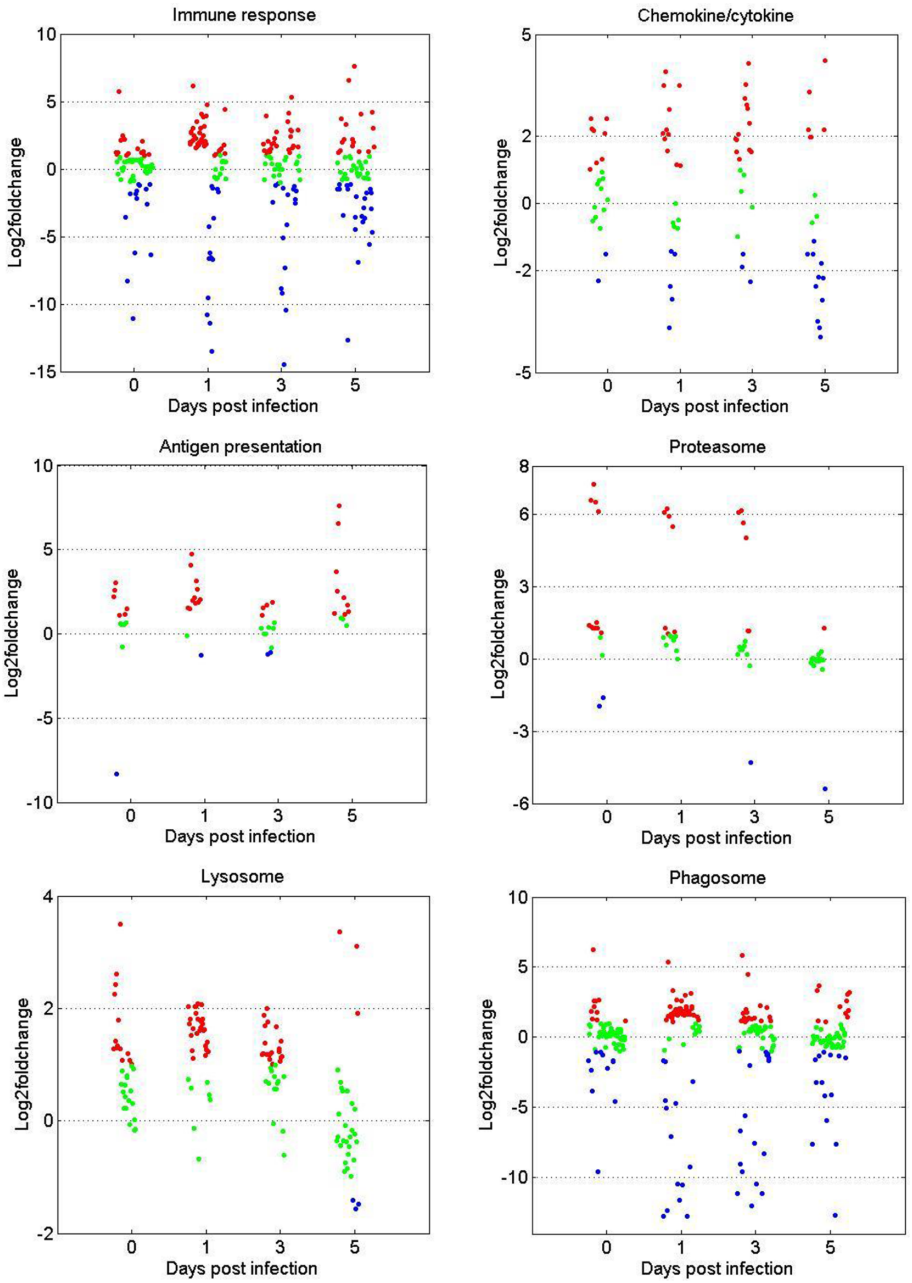

FIGURE 3 | Scatterplots of gene expression pattern of DEGs in the immune related GO or KEGG terms. Scatterplots showing the log2fold change values of DEGs from intergroup comparisons in GO or KEGG terms that involved in immune response, chemokine/cytokine, antigen presentation, proteasome, phagosome, and lysosome. The red dots indicated DEGs with log2foldchange ≥ 1, the green dots represented DEGs with |log2foldchange| ≤ 1, and the blue dots stand for DEGs with log2foldchange ≤ -1.

metabolism in cancer, tryptophan metabolism, and glycerophospholipid metabolism) were also enriched (**Figure 4C**). Finally, KEGG terms purine metabolism, tryptophan metabolism, and axon regeneration were enriched for the DEMs from 5 dpi (**Figure 4D**). Many of the enriched terms were involved in carbohydrate, nucleotide, and amino acid metabolism, indicating the different metabolism patterns between fish of different ages after virus infection. The enriched KEGG terms for the DEMs are shown in **Table S9**.

DEMs from intragroup comparisons were subjected to KEGG enrichment analysis. For the FMO fish groups, the KEGG terms choline metabolism in cancer and glycerophospholipid metabolism were significantly enriched at all time-points after GCRV infection (**Table 2**). Because most of the DEMs were

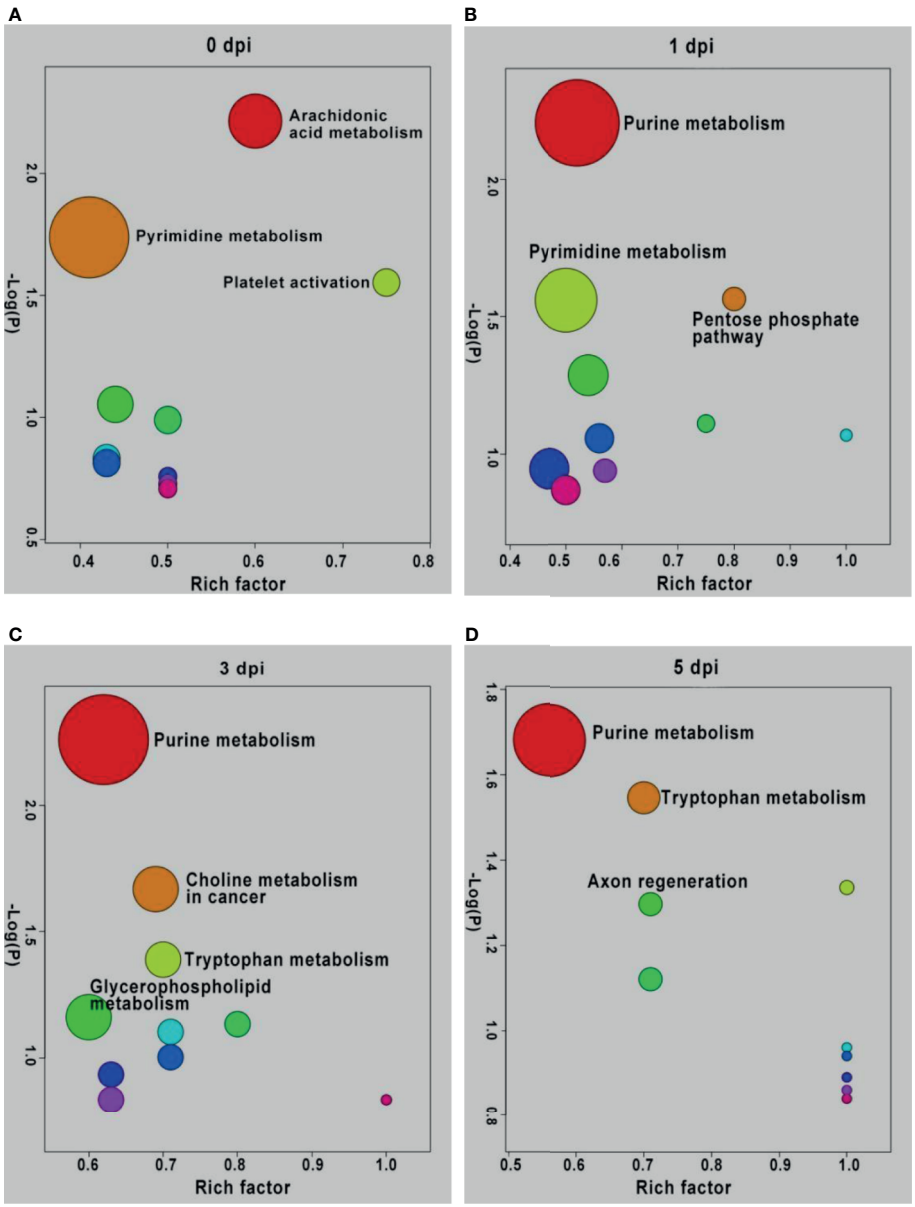

FIGURE 4 | KEGG enrichment analyses of DEMs and the top ten significant DEMs from from intergroup comparisons before **(A)** and at 1 **(B)**, 3 **(C)**, and 5 **(D)** days after GCRV infection. In each time points, the top ten enriched terms were shown as dots. The size of dots indicated the enriched metabolite number and the labeled dots represented the significant enriched KEGG terms ($p < 0.05$).

downregulated in FMO fish, we propose that the two pathways were inhibited in FMO fish after GCRV infection. For the TYO fish, arachidonic acid metabolism was the most significantly enriched KEGG term after GCRV infection, followed by serotonergic synapse, inflammatory mediator regulation of TRP channels, and purine metabolism at different time points (**Table 2**). These pathways may have been activated because most DEMs in this group were upregulated after GCRV infection. These results further support different metabolic patterns between fish of different ages.

Identification of Significant DEMs Between Two Groups

It is generally recognized that more significant DEMs may play an important role in response to stimulation; therefore, the top 10 significant DEMs (upregulated and downregulated) from intergroup comparisons at each time point were identified. Before GCRV infection, the top 10 upregulated DEMs were mainly classified into three classes: organic acid and its derivatives (citraconic acid and kinic acid), amino acid metabolomics (tryptophan betaine, citric acid, and hippuric acid), and

TABLE 2 | KEGG enrichment analysis of DEMs from intragroup comparisons.

Groups	Dpi (dpi)	KEGG terms	P value
Five months group	1 dpi	Choline metabolism in cancer	0.001423
		Glycerophospholipid metabolism	0.006047
	3 dpi	Choline metabolism in cancer	0.00058
		Glycerophospholipid metabolism	0.002626
	5 dpi	Choline metabolism in cancer	0.0004
		Glycerophospholipid metabolism	0.002411
		Pyrimidine metabolism	0.028428
Three years group	1 dpi	Arachidonic acid metabolism	0.00017
		Serotonergic synapse	0.015474
		Inflammatory mediator regulation of TRP channels	0.015474
		Purine metabolism	0.029674
	3 dpi	Arachidonic acid metabolism	0.004301
		Purine metabolism	0.076058
	5 dpi	Arachidonic acid metabolism	0.000963
		Propanoate metabolism	0.001838
		Antifolate resistance	0.0195
		Purine metabolism	0.021864
		Pyruvate metabolism	0.030814
		Serotonergic synapse	0.038322
		Inflammatory mediator regulation of TRP channels	0.038322
		Lysosome	0.044187
		Phototransduction	0.044187
		C-type lectin receptor signaling pathway	0.044187

glycerophospholipids (lysoPE 22:4 [2n isomer1], lysoPC 18:3 [2n isomer2], lysoPC 18:3 [2n isomer1], and lysoPE 20:3). The top 10 downregulated DEMs were divided into two classes: carnitines (carnitine [CAR] C12:1-OH, and CAR C8:1), oxidized lipid or other lipid (5S,15S-dihydroxy-6E,8Z,10Z,13E-eicosatetraenoic acid [5(S),15(S)- DiHETE], lipoxin A4, 14S-hydroxy-4Z,7Z,10Z, 12E,16Z,19Z-docosahexaenoic acid [14(S)-HDHA], 24,25-Dihydrolanosterol, and (±)-5-hydroxy-6E, 8Z,11Z,14Z,17Z -eicosapentaenoic acid [(±)5-HEPE]) (**Figure 5A**). At 1 dpi, for the top 10 upregulated DEMs, most of them were glycerophospholipids (lysoPC 20:1 [2n isomer], lysoPC 20:1, lysoPE 20:2, lysoPC 18:3 [2n isomer1], lysoPC 18:3 [2n isomer2], and lysoPC 20:2), while the others were tryptophan betaine, Indole-3-acetamide, CAR C15:DC*, and xanthosine. The top 10 downregulated DEMs were divided into three classes: oxidized lipid or other lipids (24,25-Dihydrolanosterol, 5(S),15(S)-DiHETE, lipoxin A4, (±)5-HEPE, and 14(S)-HDHA), amino acid metabolomics (4-Hydroxy-L-Glutamic acid, N2-Acetyl-L-ornithine, and L-arginine), and others (CAR C8:1 and ADP-ribose) (**Figure 5B**). Most of the top 10 upregulated DEMs at 3 dpi were also glycerophospholipids, followed by Indole-3-acetamide, tryptophan betaine, and CAR ph-C1. The top 10 downregulated DEMs were CAR C8:1, 5(S),15(S)-DiHETE, ADP-ribose, 24,25-Dihydrolanosterol, d-glucosamine 6-Phosphate, guanosine 3',5'-cyclic monophosphate, glycylphenylalanine, Sn-Glycero-3-Phosphocholine, CAR C21:2, and LipoxinA4 (**Figure 5C**). For the last period (5 dpi), half of the top 10 upregulated DEMs were also glycerophospholipids (lysoPC and lysoPE), while the others were carnitines (CAR C15:DC* and CAR ph-C1), tryptophan betaine, Indole-3-acetamide, and biliverdin. The top 10 downregulated DEMs contained organic acid derivatives (2-Methylsuccinic acid, glutaric acid, ethylmalonate, and ethylene glycol sulfate) and others (CAR C8:1, ADP-ribose, 24, 25-Dihydrolanosterol, d-glucosamine 6-Phosphate, glycylphenylalanine, and biotin) (**Figure 5D**). Apparently, glycerophospholipids (lysoPC and lysoPE) were significantly upregulated in TYO fish at all time-points, indicating it is an important role in defense against virus infection.

DEMs Related to the Metabolism of Carbohydrates, Amino Acids, Glycerophospholipids, and Nucleotides

The expression patterns of metabolites involved in the metabolism of carbohydrates, amino acids, glycerophospholipids, and nucleotides were compared between the two age groups. **Figure 6** shows that for the four metabolite categories, most of them showed no significant difference between the two groups before GCRV infection (**Figure 6**). However, more than half of them were upregulated at 1, 3, and 5 dpi in the TYO fish, with only a few being downregulated. The upregulation of metabolites in TYO fish indicated their ongoing transcription, translation, and biosynthesis to defend against viral infection, whereas in FMO fish, the downregulation of metabolites indicated that the host translation machinery was hijacked by the virus, resulting in death.

The Anti-Viral Effects of DEMs

The above results showed that many metabolites were differentially expressed between the two age groups, whereas their role during virus infection was unclear. Three DEMs, arachidonic acid, L-tryptophan, and adenosine, were selected for further analysis. The CCK-8 assay indicated that the three metabolites showed no cytotoxicity at concentrations of 100 μM, 5 mM, and 500 μM, respectively (**Supplementary Figure 4**). Therefore, cells were treated with three metabolites at these

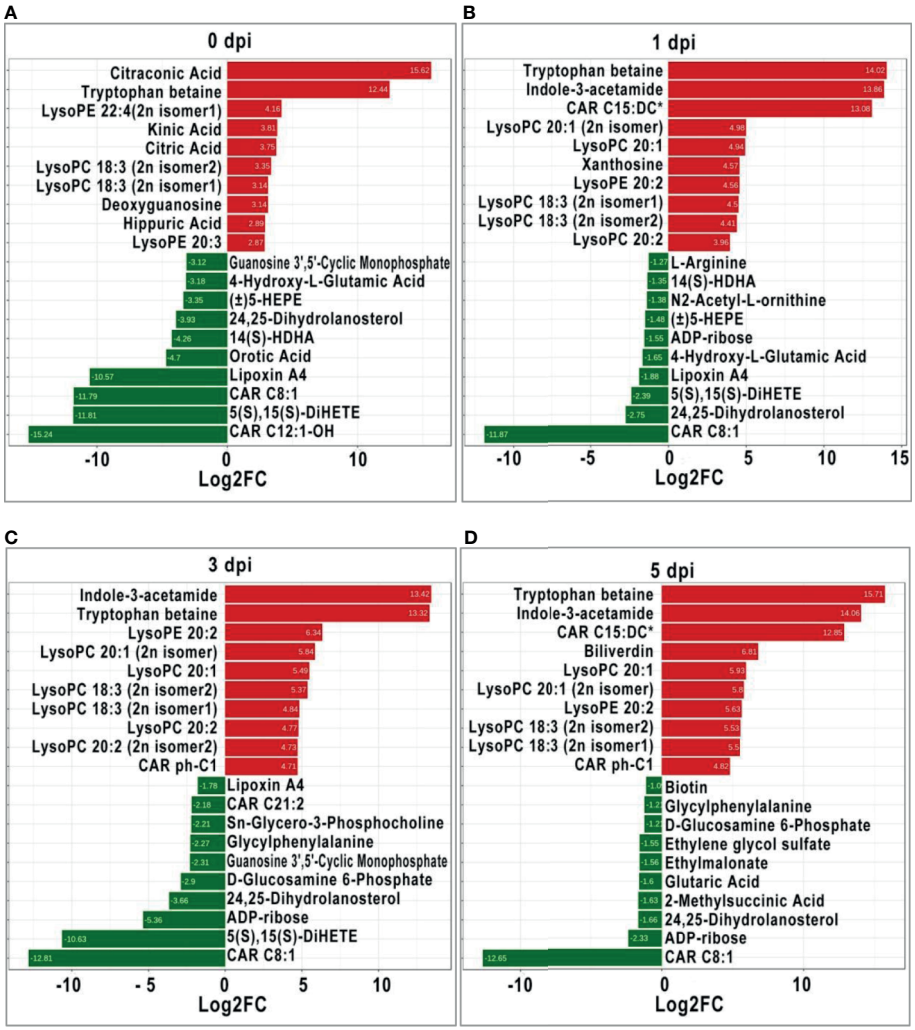

FIGURE 5 | The top ten significant DEMs (up-regulated and down-regulated) from from intergroup comparisons before **(A)** and at 1 (B), 3 **(C)**, and 5 **(D)** days after GCRV infection. The red bars represented the up-regulated metabolites while the green bars indicated the down-regulated between intergroup comparisons.

concentrations to investigate their role during viral infection. As shown in **Figure 7**, all three metabolites inhibited GCRV replication in a dose-dependent manner, especially adenosine. RT-qPCR revealed that the copy number of NS80 and VP7 in metabolite-treated cells was significantly lower than that in untreated cells (**Figure 7A** and **Supplementary Figure 4**). The plaque assay also showed that the number of plaques in the metabolite-treated cells was significantly less than that in the untreated cells (**Figures 7B, C**). Moreover, to further investigate the role of metabolites during virus infection *in vivo*, FMO grass carp were injected with different doses of metabolites or the same volume of PBS (control group) and then subjected to viral challenge experiments. **Figure 7D** shows that all three metabolites reduced the mortality of grass carp after GCRV infection, whereas PBS did not. Specifically, the mortality rates in the arachidonic acid, L-tryptophan, and adenosine injected groups were 58.0%, 60.1%, and 48.5%, respectively, while mortality in control group was up to 83.0%. Collectively, these results indicate the antiviral effects of differentially expressed metabolites.

DISCUSSION

The grass carp is an important farmed fish in China, accounting for approximately 16% of global freshwater aquaculture. Their significant economic value is threatened by their susceptibility to viral infections, has raised concerns among scientists (14, 24–26). Before this study, it was known that grass carp showed age-dependent susceptibility to GCRV, with those less than one year old considered susceptible, and those older than three years of age resistant. However, the mechanisms causing this discrepancy

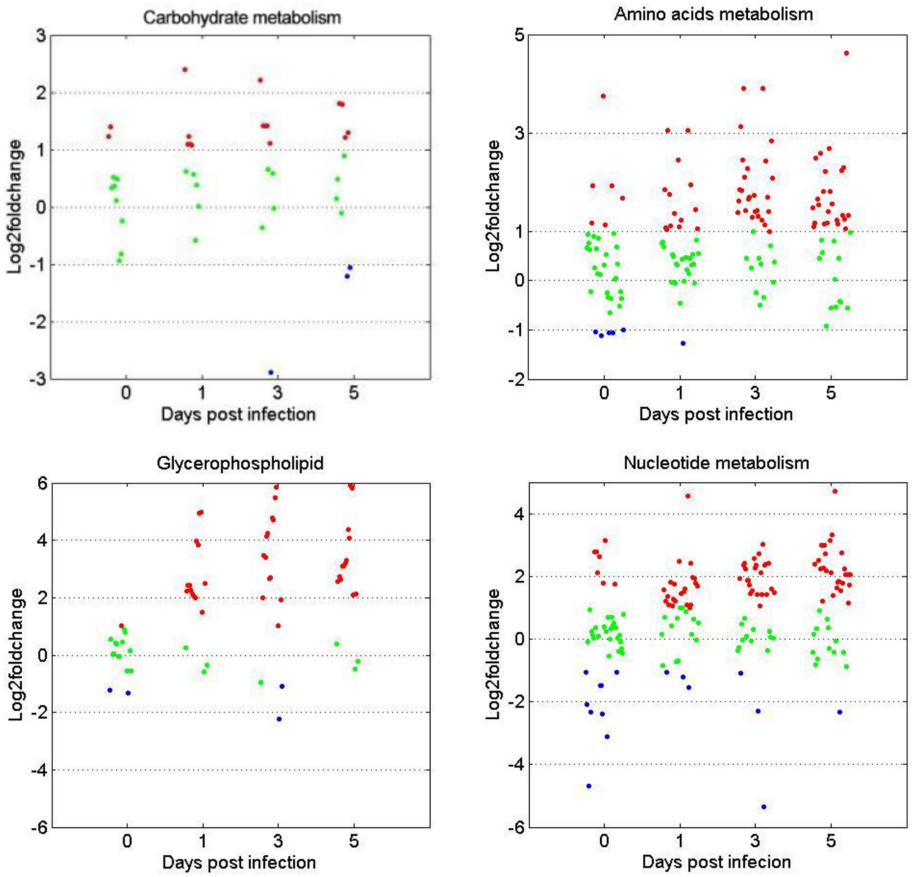

FIGURE 6 | Scatterplots of gene expression pattern of DEMs in the reprehensive metabolism pathways. Scatterplots showing the log2fold change values of DEMs from intergroup comparisons in in the reprehensive metabolism pathways (carbohydrate metabolism, amino acids metabolism, glycerophospholipids, and nucleotides metabolism). The red dots indicated DEMs with log2fold change ≥ 1, the green dots represented DEGs with |log2foldchange| ≤ 1, and the blue dots stand for DEGs with log2foldchange < -1.

remained poorly understood. In this study, we compared susceptible FMO fish with resistant TYO fish using different methods to elucidate the mechanisms underlying this phenomenon.

Immune Response

It is well known that the immune response plays an important role in host defense against pathogen invasion. Properly regulated immune responses can eliminate invading pathogens, while a disordered or immoderate immune response can lead to organism damage (14, 27, 28). The transcriptome sequencing results from this study are particularly interesting. At 0, 1, and 3 dpi, the immune-related terms, including proteasome, lysosome, phagosome, antigen processing and presentation, and chemokine/cytokine activity were enriched in upregulated genes of TYO fish. Moreover, other terms, such as glutathione metabolism, iron ion homeostasis, and drug metabolism-cytochrome P450, were also enriched in upregulated genes at the same time points. It is known that glutathione plays important roles in antioxidant defense, cell proliferation and apoptosis, signal transduction, cytokine production, and immune responses and iron ion homeostasis is important for host defense against pathogen infection (29–32). The expansion of the cytochrome P450 gene family was accounted for the koala's ability to detoxify eucalyptus foliage (33). The upregulation of these terms, combined with the immune-related terms in the TYO fish group, suggests that the fish could recognize the virus rapidly and then initiate the immune response to eliminate the invading virus. Nevertheless, the immune-related pathways were not activated until 5 dpi in the younger fish group, implying that the immune response was repressed to benefit virus replication. Therefore, these results may be one of the reasons for age-dependent susceptibility to GCRV.

Carbohydrate and Amino Acid Metabolism

Carbohydrates are the main energy source for cells and other life processes. Amino acids play several roles, including functioning as building blocks of proteins and taking part in the synthesis of ATP and metabolites with various biological functions (34, 35). Many of the metabolites related to carbohydrate and amino acid metabolism showed no significant difference in expression levels between the two fish groups before GCRV infection.

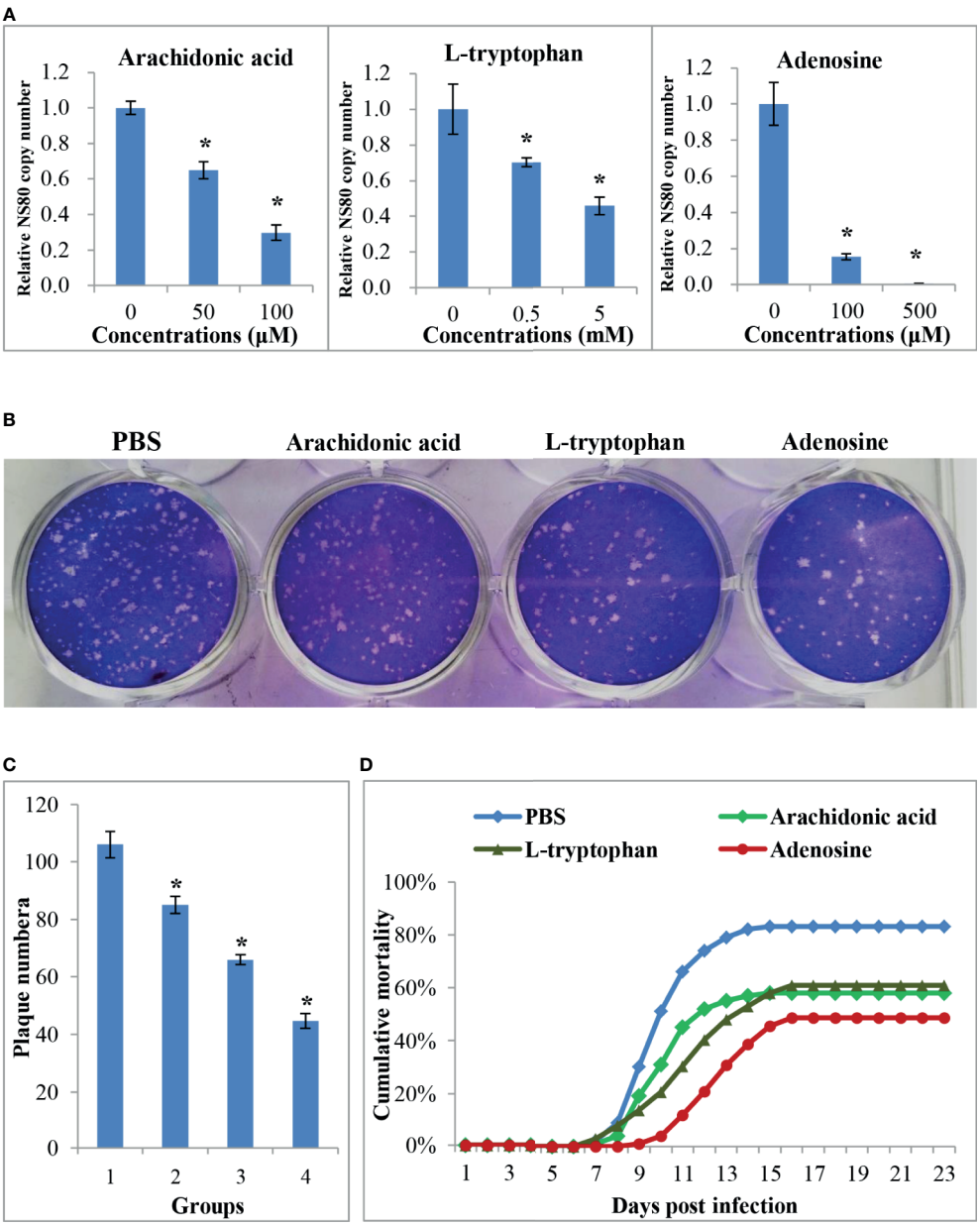

FIGURE 7 | The anti-viral effects of differential expressed metabolites. **(A)** The relative copy number of GCRV nonstructural protein gene NS80 in different metabolites treated cells or in untreated cells. **(B)** Plaque assay of different metabolites treated cells or in untreated cells. **(C)** The plaque numbers of different groups that calculated from three biological duplications. 1: PBS treated group; 2: arachidonic acid treated group; 3: L-tryptophan treated group; 4: adenosine treated group. **(D)** Survival curve of different metabolites treated or PBS treated fish after GCRV infection. Significant difference ($P < 0.05$) between the control and treated groups was indicated with asterisks (*).

Additionally, most DEMs, especially the metabolites involved in amino acid metabolism, were upregulated in the TYO fish group. Of relevance is a study on virus-infected olive flounder fish, whereby it was found that amino acid metabolism was suppressed in viral hemorrhagic septicemia for the biosynthesis of viral proteins (36). Another study found that glucose was the most crucial biomarker between survival and death in tilapia, and that glucose enhances their defense against *Edwardsiella tarda* infection through metabolome reprogramming (37, 38). Considering that the TYO fish were resistant while FMO fish were susceptible to GCRV, we proposed that TYO fish respond to virus infection effectively, resulting in the upregulation of carbohydrates and amino acids to provide materials and energy for improved defense against the virus. Nevertheless, the FMO fish failed to defend against virus infection and the cell components may be utilized by viruses for viral protein

synthesis, leading to the downregulation of metabolites involved in carbohydrate and amino acid metabolism.

Glycerophospholipid Metabolism

Metabolomics showed that the glycerophospholipid metabolism pathway was activated in TYO fish and repressed in FMO fish. The expression patterns of DEMs related to glycerophospholipid metabolism were upregulated in TYO fish. Glycerophospholipids are ubiquitous in nature and play a crucial role as components of cellular membranes or subcellular organelle membranes (39). Moreover, glycerophospholipids act as binding sites for intracellular and intercellular proteins and are involved in metabolism and signaling (40). Coincidently, we also observed cell necrosis in the spleen of FMO fish, indicating that the cell

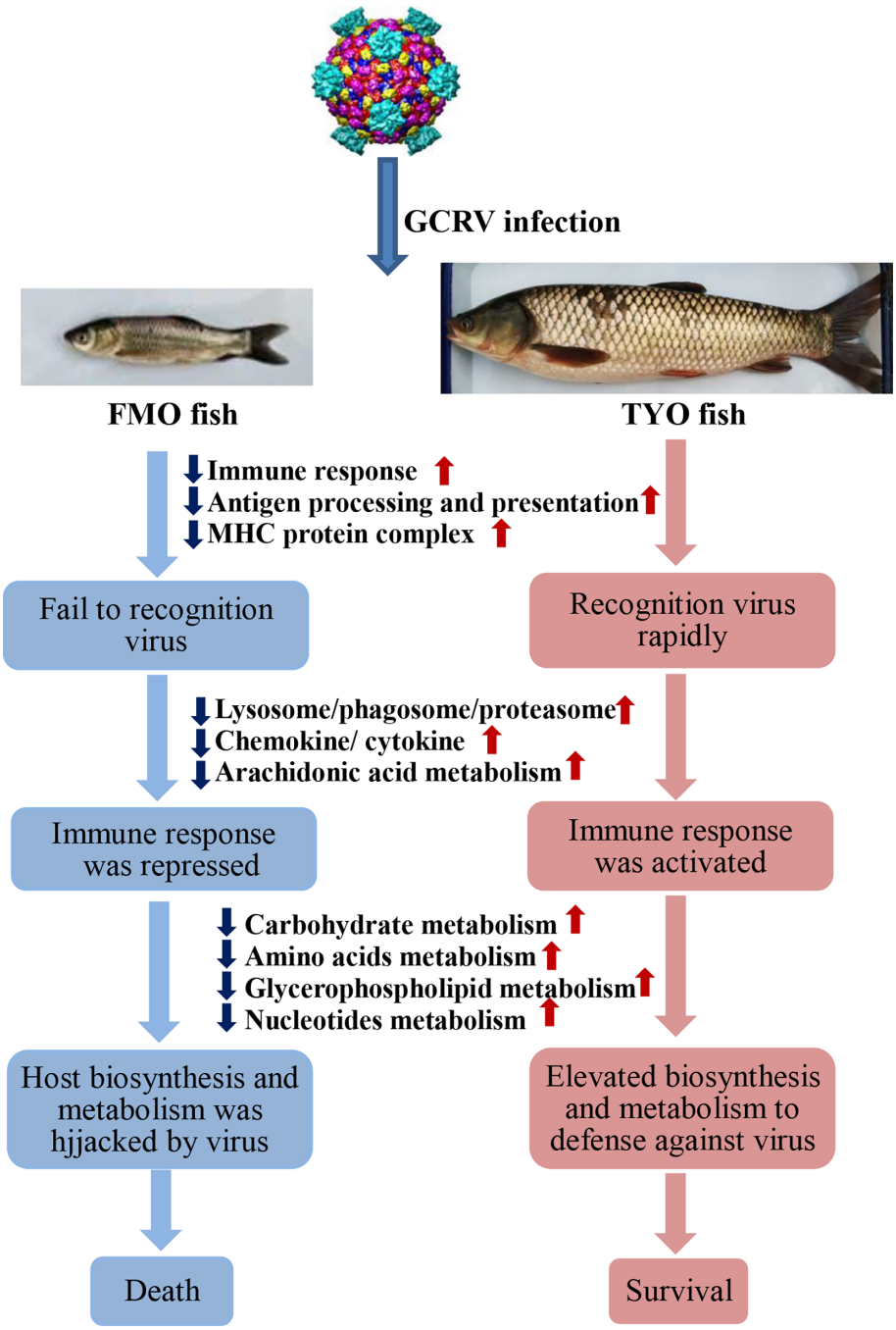

FIGURE 8 | The schematic diagram of the reasons for the age-dependent viral susceptibility in grass carp. The downward dark blue arrows indicated these representative pathways were down-regulated in FMO fish groups, while the upward red arrows represented these pathways were up-regulated in TYO fish.

membranes were broken in FMO fish after virus infection, resulting in the downregulation of the glycerophospholipid metabolism pathway. Nevertheless, the activation of pathways related to membrane-structure organelles (proteasome, lysosome, and phagosome) in TYO fish indicated the formation of membrane-structured organelles to eliminate the virus. Therefore, these results highlight the important role of glycerophospholipids in host defense against viral infections.

Nucleotide Metabolism

The nucleotide metabolism-related pathways (pyrimidine metabolism and purine metabolism) were activated in TYO fish after virus infection, and DEMs related to these pathways were mainly upregulated in this group. Nucleotides are central to biological signaling and the transfer of genetic information, which are essential for DNA and RNA synthesis, and therefore, for protein synthesis (41, 42). The upregulation of these pathways in TYO fish may be due to them responding positively to virus infection and the initiation of DNA replication, RNA transcription and translation, as well as protein synthesis, in order to eliminate the virus. The downregulation of these pathways in FMO fish implies that the host translation machinery is hjjacked or shut down by GCRV to facilitate the replication and spread of the virus. Similarly, the nucleotide metabolism-related pathways were downregulated in classical swine fever virus-infected piglets (43), and purine metabolism was downregulated in bisphenol A-treated zebrafish (44, 45). Collectively, these results show the vital role of nucleotide metabolism in response to virus infection or toxicity stimulation.

Arachidonic Acid Metabolism

We found that the arachidonic acid metabolism pathway was also significantly upregulated in TYO fish after virus infection. Arachidonic acid is a polyunsaturated omega-6 fatty acid and a precursor in the biosynthesis of prostaglandins, thromboxanes, and leukotrienes. Additionally, arachidonic acid has been reported to act as a key inflammatory intermediate and play an important role in the immune response (46). As found for carbohydrate and amino acid metabolism, virus-infected olive flounder fish had increased levels of arachidonic acid with viral hemorrhagic septicemia, suggesting an inflammatory response occurred (36). Arachidonic acid also showed an elevated trend in the serum of adult human patients with primary dengue infection (47), and in hepatitis C-infected tree shrews, metabolomic analysis revealed that arachidonic acid is one of the most significant differential metabolites (48). Therefore, the upregulation of the arachidonic acid metabolism pathway in TYO fish after virus infection may be responsible for the elevated immune response and inflammatory response in this group at the early stage of infection, which is beneficial for host defense against virus invasion.

In summary, based on the results obtained in this study, we concluded that not only the immune system, but also host biosynthesis and metabolism, account for the age-dependent susceptibility to GCRV in grass carp. As shown in **Figure 8**, The FMO fish failed to recognize the invaded virus, failed to initiate the immune response immediately, and the host translation machinery was hijacked by the virus for viral protein synthesis, resulting in death. However, the older, TYO fish recognized the virus immediately, rapidly activated the immune response, and elevated host translation machinery involved in DNA replication, RNA transcription and translation, as well as biosynthesis and metabolism to defend against viruses (**Figure 8**).

DATA AVAILABILITY STATEMENT

The datasets presented in this study can be found in online repositories. The names of the repository/repositories and accession number(s) can be found in the article/**Supplementary Material**.

ETHICS STATEMENT

The animal study was reviewed and approved by the committee of the Institute of Hydrobiology, Chinese Academy of Sciences.

AUTHOR CONTRIBUTIONS

LH, YW, and ZZ designed research. LH, DZ, XL, and YL performed research. RH, CY, and LL contributed new reagents or analytic tools. LH, DZ, and XL analyzed data. LH and YW wrote the paper. All authors contributed to the article and approved the submitted version.

FUNDING

This work was supported by the National Natural Science Foundation of China (NO. 32073017 and 31702322 to LH), the Strategic Pilot Science and Technology Projects (A) Category of CAS (No. XDA24030203 to YW), the Youth Innovation Promotion Association CAS (No. 2021338 to LH), and State Key Laboratory of Freshwater Ecology and Biotechnology (NO. 2019FBZ05 to YW).

ACKNOWLEDGMENTS

Metabolic extraction and detection were performed by Wuhan Metware Biotechnology Co., Ltd. The authors thank the director, Jianghua Wei, for help with sample collection, metabolic extraction, and detection.

SUPPLEMENTARY MATERIAL

The Supplementary Material for this article can be found online at: https://www.frontiersin.org/articles/10.3389/fimmu.2021.694965/full#supplementary-material

REFERENCES

1. Fisheries Bureau of Ministry of Agriculture in China. In: *China Fishery Statistical Yearbook of 2019*. Beijing: China Agriculture Press. p. 24p–5p.
2. Attoui H, Mertens PPC, Becnel J, Belaganahalli S, Bergoin M, Brussaard CP, et al. Family ReoviridaeVirus Taxonomy. In: AMQ King, MJ Adams, EB Carstens, EJ Lefkowitz, editors. *Ninth Report of the International Committee on Taxonomy of Viruses*. San Diego: Elsevier (2012). pp. 475–637.
3. Rao Y, Su J. Insights Into the Antiviral Immunity Against Grass Carp (*Ctenopharyngodon Idella*) Reovirus (GCRV) in Grass Carp. *J Immunol Res* (2015) 2015):670437. doi: 10.1155/2015/670437
4. Ji J, Rao Y, Wan Q, Liao Z, Su J. Teleost-Specific TLR19 Localizes to Endosome, Recognizes Dsrnaand NF-κb Pathways, and Protects Cells From Grass Carp Reovirus Infection. *J Immunol* (2018) 200(2):573–85. doi: 10.4049/jimmunol.1701149
5. Xue Y, Jiang X, Gao J, Li X, Xu J, Wang J, et al. Functional Characterisation of Interleukin 34 in Grass Carp. *Ctenopharyngodon idella*. *Fish Shellfish Immunol* (2019) 92:91–100. doi: 10.1016/j.fsi.2019.05.059
6. Shen Y, Wang L, Fu J, Xu X, Yue GH, Li J. Population Structure, Demographic History and Local Adaptation of The Grass Carp. *BMC Genomics* (2019) 20 (1):467. doi: 10.1186/s12864-019-5872-1
7. Chen G, Xiong L, Wang Y, He L, Huang R, Liao L, et al. Different Responses in One-Year-Old and Three-Year-Old Grass Carp Reveal the Mechanism of Age Restriction of GCRV Infection. *Fish Shellfish Immunol* (2019) 86:702–12. doi: 10.1016/j.fsi.2018.11.074
8. Pott J, Stockinger S, Torow N, Smoczek A, Lindner C, McInerney G, et al. Age-Dependent TLR3 Expression of the Intestinal Epithelium Contributes to Rotavirus Susceptibility. *PloS Pathog* (2012) 8(5):e1002670. doi: 10.1371/journal.ppat.1002670
9. Wu AG, Pruijssers AJ, Brown JJ, Stencel-Baerenwald JE, Sutherland DM, Iskarpatyoti JA, et al. Age-Dependent Susceptibility to Reovirus Encephalitis in Mice is Influenced by Maturation of the Type-I Interferon Response. *Pediatr Res* (2018) 83(5):1057–66. doi: 10.1038/pr.2018.13
10. Dorson M, Touchy C. The Influence of fish Age and Water Temperature on Mortalities of Rainbow Trout, *Salmo Gairdneri Richardson*, Caused by a European Strain of Infectious Pancreatic Necrosis Virus. *J Fish Dis* (1981) 4 (3):213–21. doi: 10.1111/j.1365-2761.1981.tb01128.x
11. Emmenegger EJ, Sanders GE, Conway CM, Binkowski FP, Winton JR, Kurath G. Experimental Infection of Six North American Fish Species With the North Carolina Strain of Spring Viremia of Carp Virus. *Aquaculture* (2016) 450:273–82. doi: 10.1016/j.aquaculture.2015.07.007
12. Jaramillo D, Hick P, Whittington RJ. Age Dependency of Nervous Necrosis Virus Infection in Barramundi *Lates Calcarifer* (Bloch). *J Fish Dis* (2017) 40 (8):1089–101. doi: 10.1111/jfd.12584
13. He L, Zhang A, Pei Y, Chu P, Li Y, Huang R, et al. Differences in Responses of Grass Carp to Different Types of Grass Carp Reovirus (GCRV) and the Mechanism of Hemorrhage Revealed by Transcriptome Sequencing. *BMC Genomics* (2017) 18(1):452. doi: 10.1186/s12864-017-3824-1
14. Tzung KW, Goto R, Saju JM, Sreenivasan R, Saito T, Arai K, et al. Early Depletion of Primordial Germ Cells in Zebrafish Promotes Testis Formation. *Stem Cell Rep* (2015) 5(1):156. doi: 10.1016/j.stemcr.2015.07.001
15. Kim D, Langmead B, Salzberg SL. Hisat: A Fast Spliced Aligner With Low Memory Requirements. *Nat Methods* (2015) 12(4):357–60. doi: 10.1038/nmeth.3317
16. Trapnell C, Williams BA, Pertea G, Mortazavi A, Kwan G, van Baren MJ, et al. Transcript Assembly and Quantification by RNA-Seq Reveals Unannotated Transcripts and Isoform Switching During Cell Differentiation. *Nat Biotechnol* (2010) 28(5):511–5. doi: 10.1038/nbt.1621
17. Anders S, Huber W. Differential Expression Analysis for Sequence Count Data. *Genome Bio* (2010) 11(10):R106. doi: 10.1186/gb-2010-11-10-r106
18. Young MD, Wakefield MJ, Smyth GK, Oshlack A. Gene Ontology Analysis for RNA-seq: Accounting for Selection Bias. *Genome Biol* (2010) 11(2):R14. doi: 10.1186/gb-2010-11-2-r14
19. Xie C, Mao X, Huang J, Ding Y, Wu J, Dong S, et al. Kobas 2.0: Web Server for Annotation and Identification of Enriched Pathways and Diseases. *Nucleic Acids Res* (2011) 39:W316–322. doi: 10.1093/nar/gkr483
20. Livak KJ, Schmittgen TD. Analysis of Relative Gene Expression Data Using Real-Time Quantitative PCR and the 2(-Delta(T)) Method. *Methods* (2001) 25 (4):402–8. doi: 10.1006/meth.2001.1262
21. Liu R, Hong J, Xu X, Feng Q, Zhang D, Gu Y, et al. Gut Microbiome and Serum Metabolome Alterations in Obesity and After Weight-Loss Intervention. *Nat Med* (2017) 23(7):859–68. doi: 10.1038/nm.4358
22. Zeng X, Yuan H, Dong X, Peng M, Jing X, Xu Q, et al. Genome-Wide Dissection of Co-selected Uv-B Responsive Pathways in the UV-B Adaptation of Qingke. *Mol Plant* (2020) 13(1):112–27. doi: 10.1016/j.molp.2019.10.009
23. Fraga CG, Clowers BH, Moore RJ, Zink EM. Signature-Discovery Approach for Sample Matching of Nerve-Agent Precursorusing Liquid Chromatography-Mass Spectrometry, XCMS, and Chemometrics. *Anal Chem* (2010) 82(10):4165–73. doi: 10.1021/ac1003568
24. Wang Y, Lu Y, Zhang Y, Ning Z, Li Y, Zhao Q, et al. The Draft Genome of the Grass Carp (*Ctenopharyngodon Idellus*) Provides Insights Into its Evolution and Vegetarian Adaptation. *Nat Genet* (2015) 47(6):625–31. doi: 10.1038/ng.3280
25. Zhao H, Chong J, Tang R, Li L, Xia J, Li D. Metabolomics Investigation of Dietary Effects on Flesh Quality in Grass Carp (*Ctenopharyngodon Idellus*). *Gigascience* (2018) 7(10):1–18. doi: 10.1093/gigascience/giy111
26. Tang M, Lu Y, Xiong Z, Chen M, Qin Y. The Grass Carp Genomic Visualization Database (Gcgvd): An Informational Platform For Genome Biology Of Grass Carp. *Int J Biol Sci* (2019) 15(10):2119–27. doi: 10.7150/ijbs.32860
27. Shibutani ST, Saitoh T, Nowag H, Münz C, Yoshimori T. Autophagy and Autophagy-Related Proteins in the Immune System. *Nat Immunol* (2015) 16 (10):1014–24. doi: 10.1038/ni.3273
28. Martin-Mateos R, Alvarez-Mon M, Albillos A. Dysfunctional Immune Response in Acute-on-Chronic Liver Failure: It Takes Two to Tango. *Front Immunol* (2019) 10:973. doi: 10.3389/fimmu.2019.00973
29. Wu G, Fang YZ, Yang S, Lupton JR, Turner ND. Glutathione Metabolism and its Implications for Health. *J Nutr* (2004) 134(3):489–92. doi: 10.1093/jn/134.3.489
30. Doherty CP. Host-Pathogen Interactions: The Role Of Iron. *J Nutr* (2007) 137 (5):1341–4. doi: 10.1093/jn/137.5.1341
31. Cherayil BJ. The Role Of Iron in the Immune Response to Bacterial Infection. *Immunol Res* (2011) 50(1):1–9. doi: 10.1007/s12026-010-8199-1
32. Sikorska K. The Iron Homeostasis Network and Hepatitis C Virus - a New Challenge in the Era of Directly Acting Antivirals. *Virulence* (2016) 7(6):620–2. doi: 10.1080/21505594.2016.1191739
33. Johnson RN, O'Meally D, Chen Z, Etherington GJ, Ho SYW, Nash WJ, et al. Adaptation and Conservation Insights From The Koala Genome. *Nat Genet* (2018) 50(8):1102–11. doi: 10.1038/s41588-018-0153-5
34. Wu G. Amino Acids: Metabolism, Functions, and Nutrition. *Amino Acids* (2009) 37(1):1–17. doi: 10.1007/s00726-009-0269-0
35. Mulukutla BC, Khan S, Lange A, Hu WS. Glucose Metabolism in Mammalian Cell Culture: New Insights for Tweaking Vintage Pathways. *Trends Biotechnol* (2010) 28(9):476–84. doi: 10.1016/j.tibtech.2010.06.005
36. Cho SY, Kwon YK, Nam M, Vaidya B, Kim SR, Lee S, et al. Integrated Profiling of Global Metabolomic and Transcriptomic Responses to Viral Hemorrhagic Septicemia Virus Infection in Olive Flounder. *Fish Shellfish Immunol* (2017) 71:220–9. doi: 10.1016/j.fsi.2017.10.007
37. Peng B, Ma YM, Zhang JY, Li H. Metabolome Strategy Against Edwardsiella Tarda Infection Through Glucose-Enhanced Metabolic Modulation in Tilapias. *Fish Shellfish Immunol* (2015) 45(2):869–76. doi: 10.1016/j.fsi.2015.06.004
38. Zeng ZH, Du CC, Liu SR, Li H, Peng XX, Peng B. Glucose Enhances Tilapia Against *Edwardsiella Tarda* Infection Through Metabolome Reprogramming. *Fish Shellfish Immunol* (2017) 61:34–43. doi: 10.1016/j.fsi.2016.12.010
39. Yang Y, Lee M, Fairn GD. Phospholipid Subcellular Localization and Dynamics. *J Biol Chem* (2018) 293(17):6230–40. doi: 10.1074/jbc.R117.000582
40. Hermansson M, Hokynar K, Somerharju P. Mechanisms of Glycerophospholipid Homeostasis in Mammalian Cells. *Prog Lipid Res* (2011) 50(3):240–57. doi: 10.1016/j.plipres.2011.02.004
41. Nyhan WL. Disorders of Purine and Pyrimidine Metabolism. *Mol Genet Metab* (2005) 86(1-2):25–33. doi: 10.1016/j.ymgme.2005.07.027
42. Chitrakar I, Kim-Holzapfel DM, Zhou W, French JB. Higher Order Structures In Purine And Pyrimidine Metabolism. *J Struct Biol* (2017) 197(3):354–64. doi: 10.1016/j.jsb.2017.01.003
43. Gong W, Jia J, Zhang B, Mi S, Zhang L, Xie X, et al. Serum Metabolomic Profiling of Piglets Infected With Virulent Classical Swine Fever Virus. *Front Microbiol* (2017) 8:731. doi: 10.3389/fmicb.2017.00731
44. Yoon C, Yoon D, Cho J, Kim S, Lee H, Choi H, et al. ^{1}h-NMR-Based Metabolomic Studies of Bisphenol A in Zebrafish (*Danio Rerio*). *J Environ Sci Health B* (2017) 52(4):282–9. doi: 10.1080/03601234.2016.1273009

45. Ortiz-Villanueva E, Navarro-Martín L, Jaumot J, Benavente F, Sanz-Nebot V, Piña B, et al. Metabolic Disruption of Zebrafish (Danio Rerio) Embryos by Bisphenol a. An Integrated Metabolomic and Transcriptomic Approach. *Environ Pollut* (2017) 231(Pt 1):22–36. doi: 10.1016/j.envpol.2017.07.095
46. Harizi H, Corcuff JB, Gualde N. Arachidonic-Acid-Derived Eicosanoids: Roles in Biology and Immunopathology. *Trends Mol Med* (2008) 14(10):461–9. doi: 10.1016/j.molmed.2008.08.005
47. Cui L, Lee YH, Kumar Y, Xu F, Lu K, Ooi EE, et al. Serum Metabolome and Lipidome Changes in Adult Patients With Primary Dengue Infection. *PloS Negl Trop Dis* (2013) 7(8):e2373. doi: 10.1371/journal.pntd.0002373
48. Sun H, Zhang A, Yan G, Piao C, Li W, Sun C, et al. Metabolomic Analysis of Key Regulatory Metabolites in Hepatitis C Virus-Infected Tree Shrews. *Mol Cell Proteomics* (2013) 12(3):710–9. doi: 10.1074/mcp.M112.019141

Conflict of Interest: The authors declare that the research was conducted in the absence of any commercial or financial relationships that could be construed as a potential conflict of interest.

frontiers in Immunology

ORIGINAL RESEARCH
published: 05 July 2021
doi: 10.3389/fimmu.2021.687151

Integrative Transcriptomic Analysis Reveals the Immune Mechanism for a CyHV-3-Resistant Common Carp Strain

Zhiying Jia[1,2,3†], Nan Wu[4,5†], Xiaona Jiang[1,2], Heng Li[4,5], Jiaxin Sun[1,2], Mijuan Shi[4], Chitao Li[1,2], Yanlong Ge[1,2], Xuesong Hu[1,2], Weidong Ye[4,5], Ying Tang[4], Junwei Shan[4,6], Yingyin Cheng[4], Xiao-Qin Xia[4,5,7] and Lianyu Shi[1,2*]*

[1] Heilongjiang River Fisheries Research Institute, Chinese Academy of Fishery Sciences, Harbin, China, [2] National and Local Joint Engineering Laboratory for Freshwater Fish Breeding, Harbin, China, [3] Key Laboratory of Aquatic Genomics, Ministry of Agriculture, Chinese Academy of Fishery Sciences, Beijing, China, [4] Institute of Hydrobiology, Chinese Academy of Sciences, Wuhan, China, [5] College of Advanced Agricultural Sciences, University of Chinese Academy of Sciences, Beijing, China, [6] College of Fisheries and Life Science, Dalian Ocean University, Dalian, China, [7] The Innovative Academy of Seed Design, Chinese Academy of Sciences, Beijing, China

OPEN ACCESS

Edited by:
Maria Del Mar Ortega-Villaizan, Miguel Hernández University of Elche, Spain

Reviewed by:
Paulina Schmitt, Pontificia Universidad Católica de Valparaíso, Chile
Jing Xing, Ocean University of China, China

***Correspondence:**
Lianyu Shi
sly2552@aliyun.com
Xiao-Qin Xia
xqxia@ihb.ac.cn

†These authors share first authorship

Specialty section:
This article was submitted to Comparative Immunology, a section of the journal Frontiers in Immunology

Received: *29 March 2021*
Accepted: *14 June 2021*
Published: *05 July 2021*

Citation:
Jia Z, Wu N, Jiang X, Li H, Sun J, Shi M, Li C, Ge Y, Hu X, Ye W, Tang Y, Shan J, Cheng Y, Xia X-Q and Shi L (2021) Integrative Transcriptomic Analysis Reveals the Immune Mechanism for a CyHV-3-Resistant Common Carp Strain. Front. Immunol. 12:687151. doi: 10.3389/fimmu.2021.687151

Anti-disease breeding is becoming the most promising solution to cyprinid herpesvirus-3 (CyHV-3) infection, the major threat to common carp aquaculture. Virus challenging studies suggested that a breeding strain of common carp developed resistance to CyHV-3 infection. This study illustrates the immune mechanisms involved in both sensitivity and anti-virus ability for CyHV3 infection in fish. An integrative analysis of the protein-coding genes and long non-coding RNAs (lncRNAs) using transcriptomic data was performed. Tissues from the head kidney of common carp were extracted at days 0 (the healthy control) and 7 after CyHV-3 infection (the survivors) and used to analyze the transcriptome through both Illumina and PacBio sequencing. Following analysis of the GO terms and KEGG pathways involved, the immune-related terms and pathways were merged. To dig out details on the immune aspect, the DEGs were filtered using the current common carp immune gene library. Immune gene categories and their corresponding genes in different comparison groups were revealed. Also, the immunological Gene Ontology terms for lncRNA modulation were retained. The weighted gene co-expression network analysis was used to reveal the regulation of immune genes by lncRNA. The results demonstrated that the breeding carp strain develops a marked resistance to CyHV-3 infection through a specific innate immune mechanism. The featured biological processes were autophagy, phagocytosis, cytotoxicity, and virus blockage by lectins and MUC3. Moreover, the immune-suppressive signals, such as suppression of IL21R on STAT3, PI3K mediated inhibition of inflammation by dopamine upon infection, as well as the inhibition of NLRC3 on STING during a steady state. Possible susceptible factors for CyHV-3, such as ITGB1, TLR18, and CCL4, were also revealed from the non-breeding strain. The results of this study also suggested that Nramp and PAI regulated by LncRNA could facilitate virus infection and proliferation for infected cells respectively, while T cell leukemia homeobox 3

(TLX3), as well as galectin 3 function by lncRNA, may play a role in the resistance mechanism. Therefore, immune factors that are immunogenetically insensitive or susceptible to CyHV-3 infection have been revealed.

Keywords: transcriptome, lncRNA, CyHV-3, resistant immune mechanism, common carp

INTRODUCTION

Cyprinid herpesvirus-3 (CyHV-3) infection is a major threat to common carp aquaculture (1), leading to widespread mortality and substantial economic loss. CyHV-3 is thought to cause death by weakening the host's immune system, resulting in susceptibility to pathogenic microbes (1). In common carp, clinical signs of the disease develop rapidly and may induce morbidity and mortality within a period of 6 to 10 days following infection (2).

Carp that survive a primary infection with CyHV-3 can be resistant to future infection with this virus. Since latency and persistent carrying of CyHV-3 exist in carp (2–4), genetic backgrounds are crucial in developing an understanding of resistance against the virus. Experimental infections of carp from pure lines or crosses have indicated the existence of a genetic background of resistance by divergent survival rates (2). For example, a markedly higher expression of immune-related genes involved in pathogen recognition, complement activation, major histocompatibility complex class I (MHC I)-restricted antigen presentation, and the development of adaptive mucosal immunity was noted in the more resistant R3 line. Higher activation of $CD8^+$ T cells was also observed (5). The diallelic cross of four European carp lines, including Polish 'K' and 'R6', Hungarian 'R7' and French 'F' also has been done to select the resistant fish, and then found that MH class II B genes of carp can affect immunity against CyHV-3 infection (6). Additionally, carp strains of Asian origin, particularly Amur wild carp, were shown to be more resistant to CyHV-3 than strains originating from Europe, such as the Prerov scale carp or koi carp from a breed in the Czech Republic (7).

The immune response of carp to CyHV-3 involves both innate and adaptive aspects with the outcome of the disease largely depending on whether the balance is tipped in favor of the host's immune response or virus's evasion strategy (2). In general, transcriptomic analysis has revealed that three immune-related pathways, namely the mitogen-activated protein kinase (MAPK) signaling pathway, the innate immune response, and the cytokine-mediated signaling pathway, were highly involved in the infection with CyHV-3 (8). In red common carp × koi, the expression of interleukin 12 (IL12) p35, interferon (IFN) αβ, and toll-like receptor 9 (TLR9) may provide potential genes related to resistance against KHV (another term for CyHV-3) (9). However, the magnitude of type I IFN response did not correlate with a higher resistance in CyHV-3-infected carp, during the challenge test among different strains, although CyHV-3 infection can induce type I IFNs (7, 10). Regarding the innate resistance in carp, the mapped CyHV-3 survival quantitative trait loci have been reported mainly in *IL10* and *MHC II* (11). Recently, by quantitative trait locus mapping and genome-wide association study, *tumor necrosis factor-alpha* (*tnfa*), *hypoxia inducible factor 1 subunit alpha* (*hif1a*), *galectin-8* (*LGALS8*), *rootletin*, and *paladin*, have also been related to resistance against CyHV-3 (12). Adaptive immunity through both cytotoxicity and immunoglobulin (Ig) secretion may be involved in resistance. Matthew et al. revealed that, in the anterior kidney, Ig secretion plays an important role in the resistance during the persistent infection or reactivation phases of CyHV-3 (1). In addition, CyHV-3 profoundly influences the expression of host miRNA, although the regulation of immune processes by miRNA in the clinical and latent phases differs (4). This suggests an important role of non-coding RNAs in anti-CyHV-3 immunity.

Transcriptomic studies have been a widely used tool to reveal molecular pathology (13, 14) and even pathogen discovery (15) during fish viral infection. This could facilitate understanding the pathogenic mechanisms of diseases and the immune system of fish (16). For CyHV-3 infection, the first transcriptional analysis of carp anterior kidney mainly pointed out the important role of humoral immune responses, especially those related to immunoglobulin (1). Spleen transcriptomic analyses comparing the susceptible and resistant common carp revealed that the susceptible fish elicited a typical anti-viral interferon response, while the upregulated IL-8 attracted innate immune cells and related response may play an essential role in resistant fish (17). Recent studies have demonstrated that lncRNAs are widely modulated during fish viral or bacterial infections (18–21). As for virus infection, lncRNAs could be involved in regulating the host response during ISAV infection in salmon (18). In zebrafish, SVCV could induce both immune and antiviral processes related to LncRNA (21). The widespread differential expression of lncRNAs in response to infections with different types of pathogens suggested that lncRNAs are pivotal players during immune responses in fish. However, the specific LncRNA modulation of the immune response during CyHV-3 infection has not been accessed in carp.

German mirror carp selection G_4 is a strain of common carp cultivated widely in China, yet with high mortality caused by the CyHV-3 virus. Based on our previous study, a strain of common carp from German mirror carp selection G_4 has already shown a higher survival rate after breeding for three generations. Among fish from the G_3 generation, 1,000 individuals were genotyped by four SNP loci, including carp065309, carp070076, carp183811 and carp160380, and then four main groups, with genotypes of GG/GT/GG/AA, GG/TT/TT/AA, AG/TT/AG/AT and GG/GG/GG/AA, whose survival rates were 89.9, 94.7, 88.0 and 92.7% respectively, were propagated (22). While the unselected mirror carp was 62.6%. Since decreased viral load in tissues directly indicates resistance to CyHV-3 (23), the fact that it has displayed a better immunological index as well as a reduced virus load in

immune organs, such as the kidneys and spleen (24, 25), strongly suggests resistance to CyHV-3 in current breeding strain. In detail, acid phosphatase in the spleen, glutathione and total antioxidation capacity in the kidney, lysozyme and immunoglobulin M in the serum, and alkaline phosphatase in the spleen and kidney also showed significant differences between G_1 and G_3 or G_1 and G_2/G_3. Meanwhile, the survival rate after the CyHV-3 challenge increased generation by generation. The strong resistance to CyHV-3 has been stable for G_3 (24). Recently, Sun has revealed that virus genes *TK* and *ORF72* in the G_4 were expressed at levels significantly lower than those in the non-breeding strain (25). Thus, the resistance to CyHV-3 in G_4 was strongly deduced.

However, there is a lack of systemic studies focusing on a detailed network of the immune system for the anti-CyHV-3 immune mechanism in this resistant strain. The third-generation sequencing method, such as PacBio, can decode the genetic sequences that are markedly longer compared with the second-generation method, such as Illumina (26). Therefore, a higher quality assembly of transcripts, including both mRNA and non-coding RNAs, may provide a more detailed understanding of the mechanism of genetic resistance.

In this study, to reveal the immune mechanisms involved in anti-CyHV3 breeding for common carp, integrative transcriptomic analysis was performed for both mRNA and long non-coding RNA (lncRNA) during the CyHV-3 challenge, using the strategy shown in **Figure 1**. Immune-related transcripts, from both survivors and healthy controls of either breeding or non-breeding strains, were analyzed. By comparing data from different groups for different strains obtained through both Illumina (New England Biolabs, Ipswich, MA, USA) and Pacific Biosciences (PacBio) sequencing, both immune-related differentially expressed genes (DEG) and lncRNA have been revealed for the Kyoto Encyclopedia of Genes and Genomes (KEGG) pathways and/or Gene Ontology (GO) terms involved. The immune gene-related lncRNA was also explored. This study may shed some light on molecular breeding for virus-resistant fish strains.

MATERIALS AND METHODS

Ethics Statement

All procedures involving animals in this study were conducted according to the guidelines for the care and use of laboratory animals of Heilongjiang River Fisheries Research Institute, Chinese Academy of Fishery Sciences (Harbin, China). The studies involving animals were reviewed and approved by the Committee for the Welfare and Ethics of Laboratory Animals of Heilongjiang River Fisheries Research Institute, Chinese Academy of Fishery Sciences.

Animals and Virus Challenge

German mirror carp selection G_4 used in this study were obtained from Kuandian Research Base of Heilongjiang River Fisheries Research Institute (Liaoning, China). The breeding strain was the fourth generation after the selection of resistance to CyHV-3 (25). Two G_4 groups with survival rates of 94.7 and 92.7% were mixed with the ratio 1:1 and used as the experimental

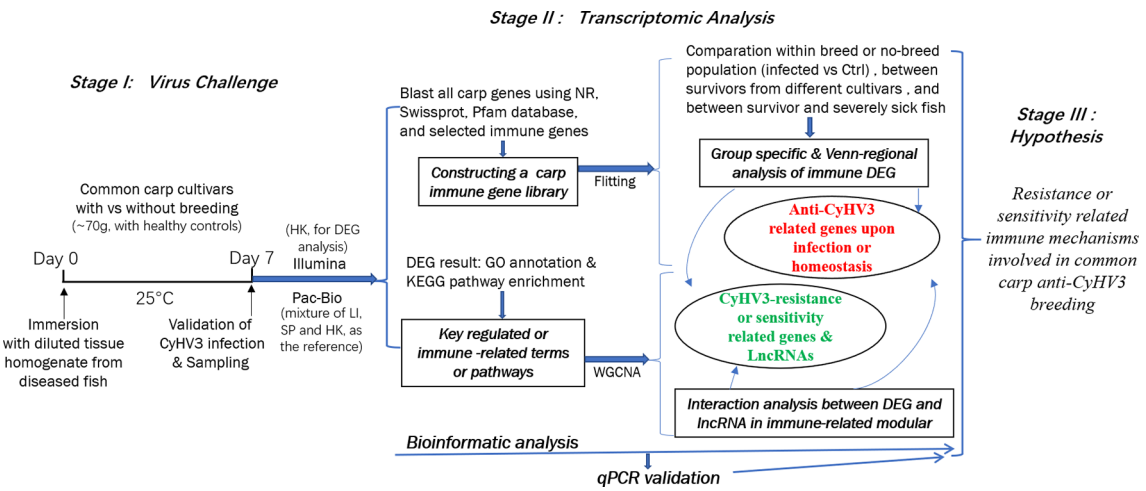

FIGURE 1 | The strategy of integrative transcriptomic analysis for revealing immune mechanisms involved for resistance or sensitivity for current anti-CyHV3 breeding in common carp. During stage I, the disease modelling for CyHV3 infection was established using immersion of virus-containing tissue homogenate and then validated by checking the expression of virus genes. The transcriptomic sampling was done on day 7 post-infection for sequencing using both Illumina and Pac-Bio platforms. In stage II, the bioinformatic analysis was carried out for the transcriptomic data. DEG was generated from five comparison groups, including SvC-B, SvC-N, SvS-BvN-D7, CvC-BvN-D0, and SvI-B&N. The fish with severe illness swam very slowly or even floated on the water. The revealed DEGs were annotated by GO terms and KEGG pathways. Further, a common carp immune gene library was constructed for further immune-related analysis. Additionally, to reveal the LncRNA regulation, WGCNA was used to reveal the interaction between differential expressed transcripts and LncRNA in immune-related module. Thereafter, the resistance or sensitivity related immune mechanisms involved in common carp anti-CyHV3 breeding could be enlightened accordingly.

populations in this study. Both the breeding strain G_4 and non-breeding strain were used for the virus challenge. Since CyHV-3 has a mucosal route of infection mainly *via* the skin rather than the gut (2), this study induced infection with CyHV-3 by adding the homogenate solution of internal organs from sick fish into the water of the tanks following the previously published methods (24, 25, 27). The homogenate solution was prepared using organs from 10 severely sick fish, which swam very slowly or floated on the water. Before using the homogenate to infect fish, the head kidney tissues from those sick fish were checked for the CyHV-3 infection by PCR of virus genes *TK* and *Sph* following the method described in the industry-standard SC/T 7212.1-2011 (28). The CyHV-3 that contained internal organs from sick fish was homogenized to generate 100 ml homogenate, which contained 1.5×10^7 copy CyHV-3 per mg homogenate by PCR-checking virus gene *Sph*. Then the homogenate was used to infect the experimental fish, 17 ml homogenate was used for each tank. For either the breeding or non-breeding strains, the virus challenging group (using diseased fish tissue's homogenate) was paralleled with the control group (using saline instead). For each treatment groups, three replicates have been done. In each tank (1.6 m × 1.2 m × 0.6 m), which contained around 1 m^3 water, healthy juvenile common carp (~70 g; N = 100 fish) were used. The water temperature during the experiment was maintained at 25 ± 1°C.

Sampling and Pathological Analysis

A selection of common carp, from either the breeding or non-breeding strains, were sacrificed. Head kidney samples were obtained at days 0 and 7 after challenge, representing the control and survivor carp. For each tissue sample, three fish were used. For transcriptomic analysis, the samples (N = 3) were collected immediately and soaked in 10 volumes of RNAlater (Qiagen, Hilden, Germany), for sequencing using Illumina (New England Biolabs). Further, to better sequence and generate the lncRNAs, PacBio sequencing was applied to analyze the mixture of liver, spleen, and kidney, with two sample replicates. Additionally, for the validation of transcriptomic data, the qPCR samples (N = 3) were also collected using RNAlater. The number of dead fish during the experiment was counted daily to calculate the mortality rate. Meanwhile, to analyze the degree of swelling of inner organs, the proportion of trunk kidney to the whole trunk area was calculated by ImageJ (https://imagej.en.softonic.com/). In detail, the area of both trunk kidney and trunk regions were selected and measured, and the percentages between them were calculated based on eight survivors of breeding or non-breeding strain. T-tests were applied to test the significance of the difference.

RNA Extraction

RNA was isolated using the AllPrep DNA/RNA FFPE Kit (Qiagen, Hilden, Germany), according to the instructions provided by the manufacturer. RNA degradation and contamination were monitored on 1% agarose gels. RNA purity was checked using the NanoPhotometer spectrophotometer (Implen Inc., Westlake Village, CA, USA). RNA concentration was measured using the Qubit RNA Assay Kit in a Qubit 2.0 Flurometer (Life Technologies, Carlsbad, CA, USA). RNA integrity was assessed using the RNA Nano 6000 Assay Kit of the Agilent Bioanalyzer 2100 system (Agilent Technologies, Santa Clara, CA, USA).

Library Preparation and Sequencing for Transcriptomic Analysis

Optimized RNA-Seq strategies, including both PacBio and Illumina (New England Biolabs) sequencing (29), were used to more precisely resolve the sequence of transcripts. Firstly, the total RNA isolated from the head kidney was used to construct the cDNA library. Subsequently, the library was sequenced on a PacBio RS II platform (Biomarker Technologies, Beijing, China). For the PacBio Long Read Processing, raw reads were processed into error-corrected reads of insert using Iso-seq pipeline with minFullPass = 0 and minPredictedAccuracy = 0.90. Next, full-length, non-chemiric transcripts were determined by searching for the polyA tail signal and the 5' and 3' cDNA primers in reads of the insert. Iterative Clustering for Error Correction (ICE) was used to obtain consensus isoforms, and full-length consensus sequences from ICE were polished using Quiver. High-quality transcripts with post-correction accuracy of >99% were retained for further analysis.

The illustration of transcripts obtained from the results of PacBio could provide reference transcriptional sequences for the assembly of Illumine sequencing data, to improve sequencing quality. Therefore, Illumina (New England Biolabs) sequencing was performed on all head kidney samples. The procedure used for the preparation of the gene library and sequencing of the transcriptome followed previously published methods (30). Briefly, sequencing libraries were generated using the NEBNext UltraTM RNA Library Prep Kit for Illumina (New England Biolabs), and the library quality was assessed on the Agilent Bioanalyzer 2100 system. The library preparations were sequenced on an Illumina platform, and 150 bp paired-end reads were generated.

Annotation and Functional Analysis of Transcripts by Public Databases

All reads in the transcriptome data were mapped on the common carp genome (https://asia.ensembl.org/Cyprinus_carpio_german_mirror/Info/Index) (31) for annotation. In detail, GMAP (Genomic Mapping and Alignment Program) and BLAST (version 2.2.26) were applied for mapping the transcriptome data to carp genome and obtaining annotation respectively. The data from the Illumina platform were also used to check and replace errors by proovread (version 2.14.1) in the data from the PacBio platform. Both the annotation of genes and lncRNAs were subsequently generated. The protein-coding transcripts were annotated by NR, swissprot and Pfam database. DEGs were detected from five comparison groups, including intra-strain comparison groups SvC-B (survivors *vs.* controls in the breeding strain) and SvC-N (survivors *vs.* controls in the non-breeding strain), inter-strain comparison groups SvS-BvN-D7 (the comparison between survivors at day 7 for the two strains to compare survivors from the breeding to non-breeding

strain) and CvC-BvN-D0 (the comparison between control fish at day 0 for the two strains to compare controls from the breeding to non-breeding strain), and group SvI-B&N. The vital genes for survival were investigated through group SvI-B&N, in which the DEGs with no significant differences (p >0.05) were compared between the survivors from the two strains with the transcripts from fish with severe illness. The revealed DEGs were annotated by GO terms and KEGG pathways, following a previously published protocol (30, 32). In brief, functional annotation and the classification of genes were determined by both employing local genes blasts against GO Consortium (http://geneontology.org/) and KEGG (https://www.kegg.jp/kegg/pathway.html). Enrichment of the KEGG pathways was carried out for both upregulated and downregulated genes for all comparison groups. Then to demonstrate the immune DEGs involved pathways more clearly, the gene list of the current construct common carp immune gene library was used as follows. In addition, the LncRNAs were also annotated by GO terms.

Construction of the Common Carp Immune Gene Library

The common carp immune library was constructed by following our previously published method, which was applied to grass carp (30) and tilapia (32), with some adjustment for viral infection-related immune genes. The modifications were based on gene information obtained by blasting each sequence to databases, including NCBI NR database, as well as Swiss-Prot and Pfam databases. The common carp immune gene library contained information for immune genes at two levels. For the first level, nine categories of immune processes, namely "acute phase reactions", "pattern recognition", "antigen processing and regulators", "complement system", "inflammatory cytokines and receptors", "adapters, effectors and signal transducers", "innate immune cells related", "T/B cell antigen activation", and "other genes related to immune response", were proposed. Subsequently, many categories of immune genes for each immune process (detailed in **Table S1**) were applied for the second level. The library was used to filter transcriptome data and obtain details of the immune processes and particular immune genes for each comparison group, during the GO term and KEGG pathway enrichment.

Statistical Analysis

The DEG was generated by comparing the RPKM (Reads Per Kilobase of transcript, per Million mapped reads) using the DESeq2 R package (1.16.1). The resulting p values were adjusted using the Benjamini and Hochberg approach for controlling the false discovery rate. Genes with an adjusted p <0.05 found by DESeq2 were assigned as being differentially expressed. The following bioinformatics analysis was performed to select immune-related transcripts from the common carp immune gene library and construct the bar plots for the major immune processes and immune categories. The t-test was used to assess differences, with a false discovery rate adjusted p <0.05. Qualitative comparisons were performed between samples by counting the number of DEG. The data were rearranged in Microsoft EXCEL, and applied to plot charts by ggplot2 (2.2.1) using R language.

Correlation Analysis Between LncRNA and Genes Involved in Immune-Related GO Terms

The weighted gene co-expression network analysis (WGCNA) was performed using the R package "WGCNA" (33). Specifically, all genes with an expression variance ranked in the top 75 percentile of the data set were retained (34). The R package WGCNA was used to construct the weighted gene co-expression network (35). A matrix of signed Pearson correlations between all gene pairs was computed, and the transformed matrix was used as input for linkage hierarchical clustering. All transcripts in current transcriptome data with similar expression patterns were clustered together as one module. Subsequently, using the R package clusterProfiler (36), enriched GO terms for lncRNA-related protein-coding genes were generated for the DET list of every module. The p values of enriched GO terms were produced from the Kolmogorov–Smirnov test. To elucidate the detailed lncRNA-mRNA network, the immune-related GO term containing module was selected, and the relationship of involved top 100 transcripts and related lncRNAs were shown by the cystoscope software. In addition, the immune DETs (differentially expressed transcripts) involved in the immune-related module were classified into comparison groups SvC-B, SvC-N and SvS-BvN-D7, to reveal the LncRNA modulation of immunity at the aspect of surviving from CyHV-3 infection.

Quantitative Reverse Transcription Polymerase Chain Reaction (qPCR)

The mRNA samples used for transcriptome sequencing were also subjected to qPCR validation (n = 3), using SYBR Green PCR master mix (Bio-Rad) and CFX real-time PCR detection system (Bio-Rad), following a previously published protocol (37, 38). After RNA isolation, reverse transcription and qPCR experiments were carried out for 11 genes. Gene-specific primers (**Table S4**) were designed with the Primer Premier 5.0 software. Housekeeping gene 18s RNA was used to normalize data, and 2-DDCt formula was used to calculate the relative expression.

RESULTS

Virus Identification, Mortality Rate and Pathological Appearance

The successful infection of CyHV-3 has been validated using PCR, to check the expression of virus genes (*TK* and *Sph*), in randomly sampled severely sick fish (N = 10) at day 7 after challenge (**Figure 2A**). Further, to reveal the mortality, the number of dead fish was recorded from days 1 to 15 after challenge (**Table S1**), the mortality rate was then calculated for all groups (**Table S2**). For the challenged non-breeding strain (**Figure 1B**), the mortality rate increased daily, except for a decrease observed on day 5. Mortality peaked at day 7 (69%) and

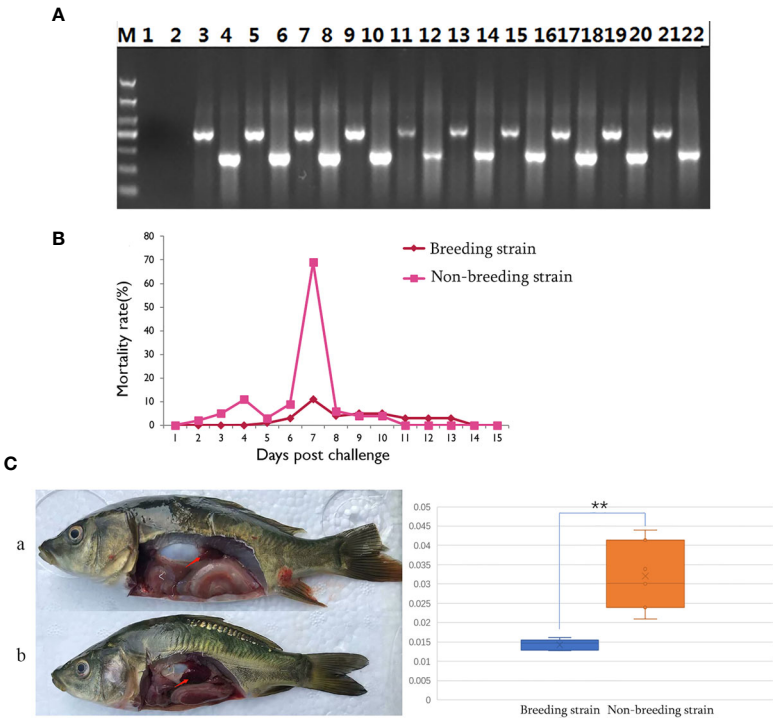

FIGURE 2 | Differential appearance of general mortality and pathology between fish from the breeding and non-breeding strains. **(A)** The PCR validation of the CyHV-3 virus genes TK and Sph. Lane 1-2 represents the negative control, and afterwards, lane 3-22 represents the result for tested 10 virus infected fish. The lanes of odd and even numbers showed the PCR result of TK and Sph genes, respectively. M is the abbreviation of "marker". **(B)** Comparison of daily mortality between the breeding and non-breeding strains. The mortality was monitored within 15 days post challenge. N=300 per group. **(C)** The degree of swelling trunk kidney was limited in the survivors from the breeding strain (a) compared with the markedly enlarged trunk kidney observed in fish from the non-breeding strain (b). The arrow indicates the trunk kidney region. "**" means the very significant difference ($p < 0.01$) between current compared two groups.

decreased to a markedly low level thereafter. For the challenged breeding strain (**Figure 2B**), the mortality rate remained at a markable low level, with the highest value (11%) recorded at day 7. The mortality rates of the two challenged groups were very significantly different (p <0.01). The number of dead fish for each day is listed in **Table 1** for the breeding or non-breeding strain, while in the two unchallenged controls, there were no dead fish (data not shown). Compared with the organs in survivors of the breeding strain, pathological swelling and hyperemia of the internal organs (particularly the kidney) were obvious in survivors from the non-breeding strain on day 7 (**Figure 2C**). In detail, the proportion of kidney area to the whole trunk area in the breeding strain was significantly different from that of the non-breeding strain (p <0.01) (**Figure 2D**). The reduced immune organ swelling was reflected by the ratio of 0.44 comparing the proportions between the breeding and non-breeding strains (**Table S2**).

Quality and Validation of Transcriptomic Data

Sequencing was performed with both the PacBio RS II and Illumina platforms to analyze the gene information of the common carp. Through PacBio sequencing, 19.49 G data were obtained. Of the 258,346 ccs, 79.79% were full-length sequences, and 17,769 polished high-quality isoforms were also revealed (**Table S3**, sheet 1). Meanwhile, the Illumina data were also characterized by high quality, and the information for each sample is provided in **Table S3** (sheet 2). To validate the transcriptomic data, qPCR was conducted. A total of 24 reactions were performed to validate the transcripts of 11 genes, most of which were immune genes. The correlation analysis showed that fold changes between transcriptome and qPCR results correlated well (R^2 = 0.929718564). The gene ID, annotation, primers, and fold-change information are listed in **Table S4**.

TABLE 1 | The number of dead fish for each day during the CyHV-3 challenging for breeding or non-breeding stain.

Stain	D1	D2	D3	D4	D5	D6	D7	D8	D9	D10	D11	D12	D13	D14	D15
Breeding	0	0	0	0	1	3	11	4	5	5	3	3	3	0	0
Non-breeding	0	2	5	11	3	9	69	6	4	4	0	0	0	0	0

GO Analysis of Immune-Related DEGs Among Tested Fish

According to the enriched general GO terms (**Figure 3**) of immune-related DEGs, there are "immune system process" and "antioxidant activity" for all comparison groups, "chemoattractant activity" only in comparison group SvC-B, "rhythmic process" only in comparison group SvC-N, "cell killing" in both comparison groups SvC-B and SvS-BvN-D7, and "virion" in both comparison groups SvC-N and SvS-BvN-D7. The detailed significant enriched GO terms involved in biological processes (BP), cellular components (CC), and molecular functions (MF) were detailed in **Tables S5–S9** for all comparison groups. The immune-related significant regulated BP terms (p <0.01) were in the largest number (**Table 2**), for example, "positive regulation of cell migration" in group SvC-B; "activation of MAPK activity", "regulation of protein ubiquitination involved in ubiquitin-dependent protein catabolic process", "oxication-reduction process" and "positive regulation of cell migration" in group SvC-N; "activation of MAPK activity" and "dopaminergic neuron differentiation" in group SvS-BvN-D7. Besides, the CC terms (p <0.01) includes "Pre-autophagosomal structure membrane" in group SvC-B, SvC-N, CvC-BvN-D0 and SvI-B&N, and the MF terms (p <0.01) includes "NF-KappaB binding" and "lysozyme activity" in group SvC-N; "cytokine activity" in group SvS-BvN-D7; "Lysozyme activity", "MAP kinase activity" and "ubiquitin-like protein binding" in group CvC-BvN-D0.

KEGG Analysis of DEGs Among Tested Fish

Compared with group SvC-B, there were markedly more genes involved in immune and related pathways in group SvC-N. Current revealed immune pathways in group SvC-B were "phagosome", "regulation of autophagy", "ubiquitin mediated proteolysis", and "plant-pathogen interaction" (**Figure 4Aa**). Meanwhile, there are four immune pathways, including "endocytosis", "phagosome", "FoxO signaling pathway", "ubiquitin mediated proteolysis", "DNA replication", "fructose and mannose metabolism", "oxidative phosphorylation", and "plant–pathogen interaction" in group SvC-N (**Figure 4Ab**). To get a better understanding of the different survival mechanism, the pathways revealed in group SvS-BvN-D7 includes "endocytosis", "phagosome", "ubiquitin mediated proteolysis", "DNA replication", "fructose and mannose metabolism", and "oxidative phosphorylation" (**Figure 4Ac**, left).

To better illustrate the immune and related pathways more clearly, filtering of DEG was conducted using the gene list of the common carp immune gene library (**Table S1**), and then a bubble chart was used to clarify both the enrichment factors and gene numbers for revealed immune pathways. For group SvS-BvN-D7, which reflected differential surviving mechanism [**Figure 4A** (c, right)], the revealed immune pathways include "TNF signaling pathway", "T cell receptor signaling pathway", "inflammatory mediator regulation of TRP channels", "Epstein–Barr virus infection", "Toll-like receptor signaling pathway", "NOD-like receptor signaling pathway" and "cytokine-cytokine receptor interaction". In addition, "dopaminergic synapse" was also found. While, groups CvC-BvN-D0 and SvI-B&N, revealed the difference and similarity for maintaining basic homeostasis, respectively. The most enriched immune pathways were the "p53 signaling pathway", "NOD-like receptor signaling pathway", "lysosome", "oxidative phosphorylation", and "proteasome" in group CvC-BvN-D0 (**Figure 4Ba**), yet only "phagosome" in group SvI-B&N (**Figure 4Bb**).

Classification of DEG From Different Comparison Groups Into Immune Process and Immune Gene Category

The current construction of the common carp immune gene library (**Table S4**) was used to classify the revealed immune transcripts and refine the involved immune processes and immune gene categories. The details of DEG involved in all comparison groups were provided in **Tables S5–S9**. At the level of immune processing, in group SvC-B (**Figure 5A**, **Tables 3A** and **S5**), most immune mRNAs were upregulated in the immune processes of "pattern recognition", "inflammatory cytokines and receptors", and "T/B cell antigen activation", while downregulated in the immune process of "inflammatory cytokines and receptors", "complement system", "adapters, effectors and signal transducers", and "pattern recognition". Interestingly, there were no genes in "antigen processing and regulators" for group SvC-B. In addition, there were only downregulated genes in "acute phase reactions", as well as only upregulated genes in "innate immune cells related" in group SvC-B. In group SvC-N (**Figure 5A**, **Tables 3A** and **S6**), immune genes were upregulated in the immune processes, such as "other genes related to immune response", "inflammatory cytokines and receptors", and "adapters, effectors and signal transducers". Meanwhile, the downregulated genes were involved in the immune processes, such as "pattern recognition", "inflammatory cytokines and receptors" and "other genes related immune response". The largest number of immune mRNAs was observed in group SvS-BvN-D7 (**Figure 5A**, **Tables 3A**, and **S7**). The upregulated immune DEGs (BS-advantage) were mainly involved in "inflammatory cytokines and receptors", "other genes related to immune response", "T/B cell antigen activation", "pattern recognition", and "adapters, effectors and signal transducers", whereas the downregulated immune DEGs (NBS-advantage) were mainly involved in "other genes related to immune response", "adapters, effectors and signal transducers", "inflammatory cytokines and receptors", "T/B cell antigen activation", "pattern recognition", and "antigen processing and regulators". Meanwhile, in group CvC-BvN-D0 (**Figure 5A**, **Tables 3B** and **S8**), the upregulated immune DEGs (BS-advantage), were found mostly in "adapters, effectors and signal transducers", and noted in "antigen processing and regulators" and "T/B cell antigen activation", while downregulated immune DEGs (NBS-advantage), were mostly involved in "inflammatory cytokines and receptors", and also noted in "pattern recognition" and "complement system". In group SvI-B&N (**Figure 5B**, **Tables 3B** and **S9**), among the revealed six processes, "T/B cell antigen activation" and "other genes related to immune response" exhibited the

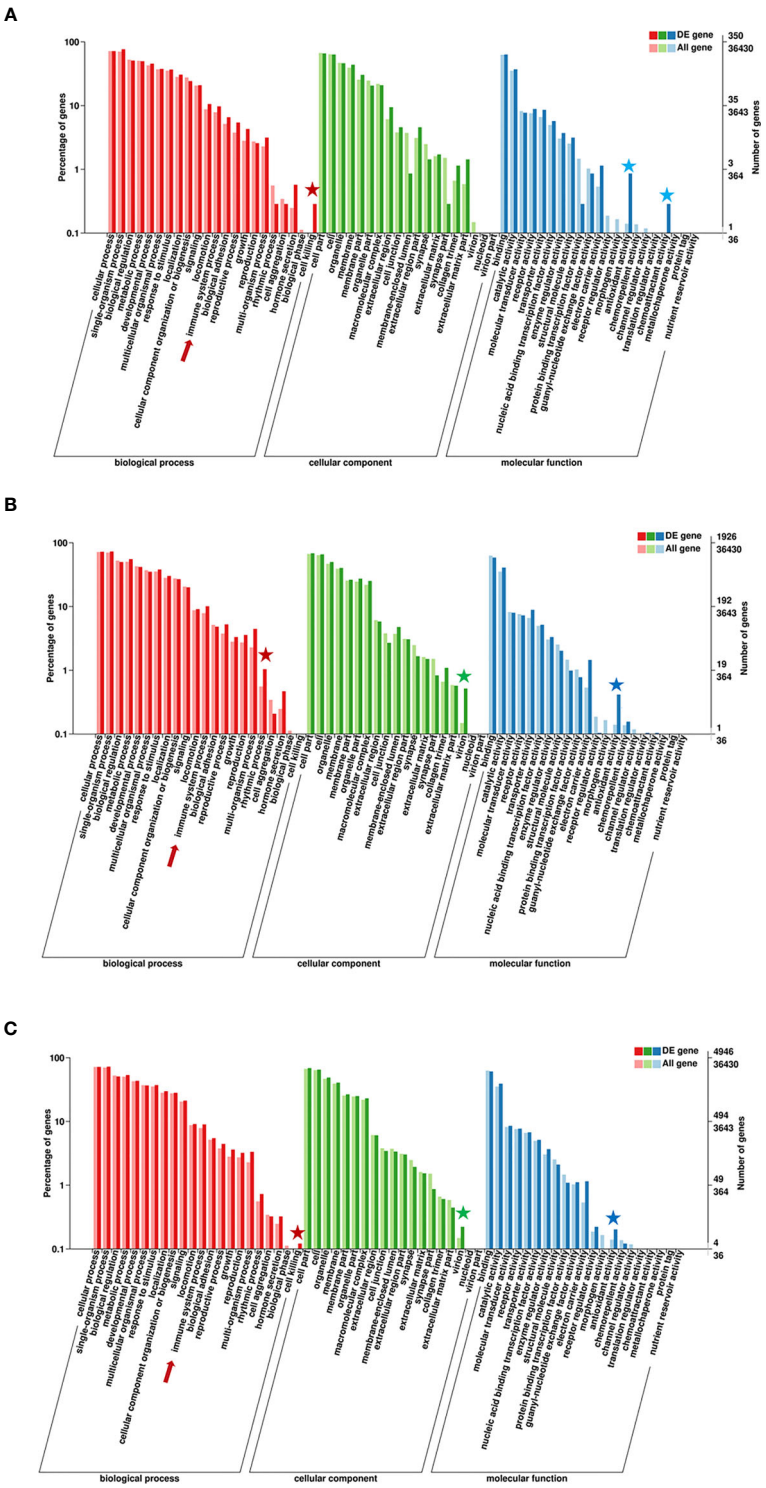

FIGURE 3 | GO (Gene Ontology) terms of comparison groups SvC-B, SvC-N, and SvS-BvN-D7. The different colors of the bar indicate the comparison of the GO terms between all genes and immune-related genes. In detail, red and pink bars represent all genes and immune-related genes respectively for the biological process (BP, in part **A**), green and light green bars represent those for the cellular component (CC, in part **B**), blue and light blue bars represent those for the molecular function (MF, in part **C**). The immune-related terms are labeled with stars.

TABLE 2 | Featured immune-related GO biological process terms for all comparison groups.

Compared group	GO terms ($P < 0.01$).
Group SvC-B	Phagocytosis, positive regulation of immune system process, positive regulation of I-kappa B kunase/NF-kappaB signaling, integrin-mediated signaling pathway, regulation of B cell activation, macrophage activation, lymphocyte-mediated immunity
Group SvC-N	Response to lipopolysaccharide, regulation of granulocyte differentiation, toll-like receptor signaling pathway, positive regulation of immune system process, macrophage differentiation, phagocytosis, engulfment, lymphocyte activation, integrin-mediated signaling pathway, leukocyte activation
Group SvS-BvN-D7	Response to lipopolysaccharide, negative regulation of B cell apoptotic process, positive regulation of TOR signaling, macrophage differentiation, endosome to lysosome transport, regulation of granulocyte differentiation, toll-like receptor signaling pathway, defense response to fungus, phagocytosis, engulfment, T cell proliferation, mast cell activation, myeloid cell activation involved in immune response, regulation of T cell differentiation in thymus, phagosome maturation, positive regulation of T cell activation
Group CvC-BvN-D0	Phagocytosis, positive regulation of immune system process, positive regulation of I-kappaB kinase/NF-kappaB signaling, integrin mediated signaling pathway, regulation of B cell activation, lymphocyte mediated immunity, macrophage activation, response to lipopolysaccharide
Group SvI-B&N	Phagocytosis, positive regulation of cell migration, positive regulation of I-kappaB kinase/NF-kappaB signaling, positive regulation of myeloid leukocyte differentiation, integrin-mediated signaling pathway, regulation of B cell activation, leukocyte activation, regulation of immune response, and macrophage activation

The details of the GO terms involved in biological process were listed in ***Tables S5–S9****.*

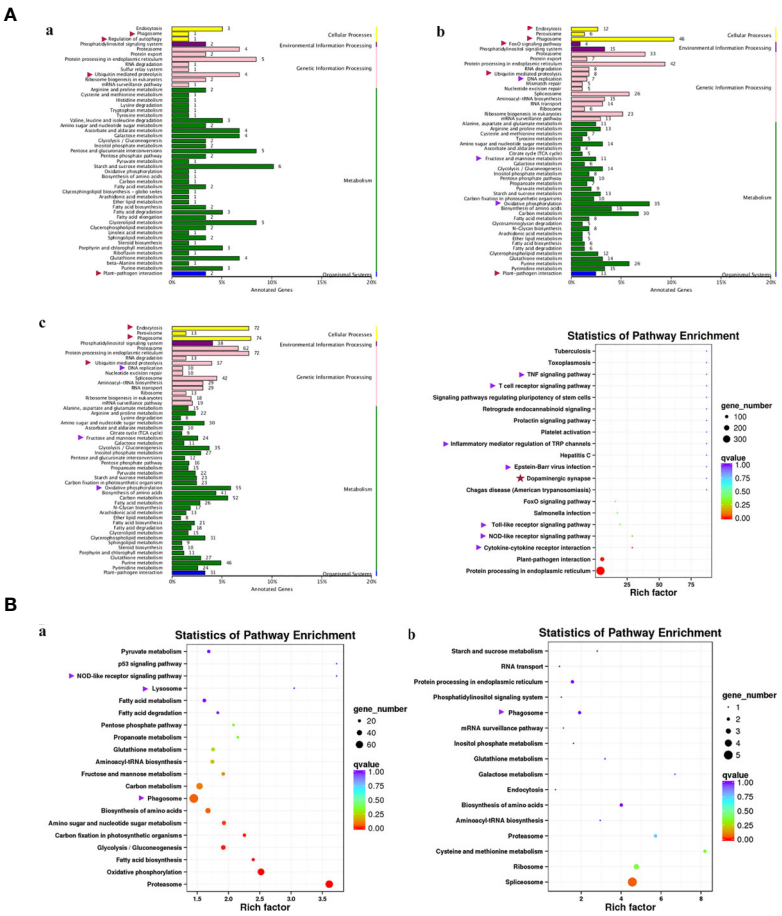

FIGURE 4 | KEGG (Kyoto Encyclopedia of Genes and Genomes) pathways revealed for all comparison groups. In part **(A)**, the enriched pathways for comparison group SvC-B (a), SvC-N (b) and SvS-BvN-D7 (c) were shown mainly in bar plots. In addition, for the comparison group SvS-BvN-D7, the babble plot of pathways for immune-related DEG was also given in the right to illustrate the rich factor. In part **(B)**, the pathways of immune-related DEG for both comparison group CvC-BvN-D0 (a), which compared controls of both stains, and group SvI-B&N (b), which has compared similar genes of survivors from both strains with protein-coding transcripts of severely sick fish, were demonstrated in babble plots. The immune-related terms are labeled with arrows. Red and purple arrows indicate the immune and related pathways representatively.

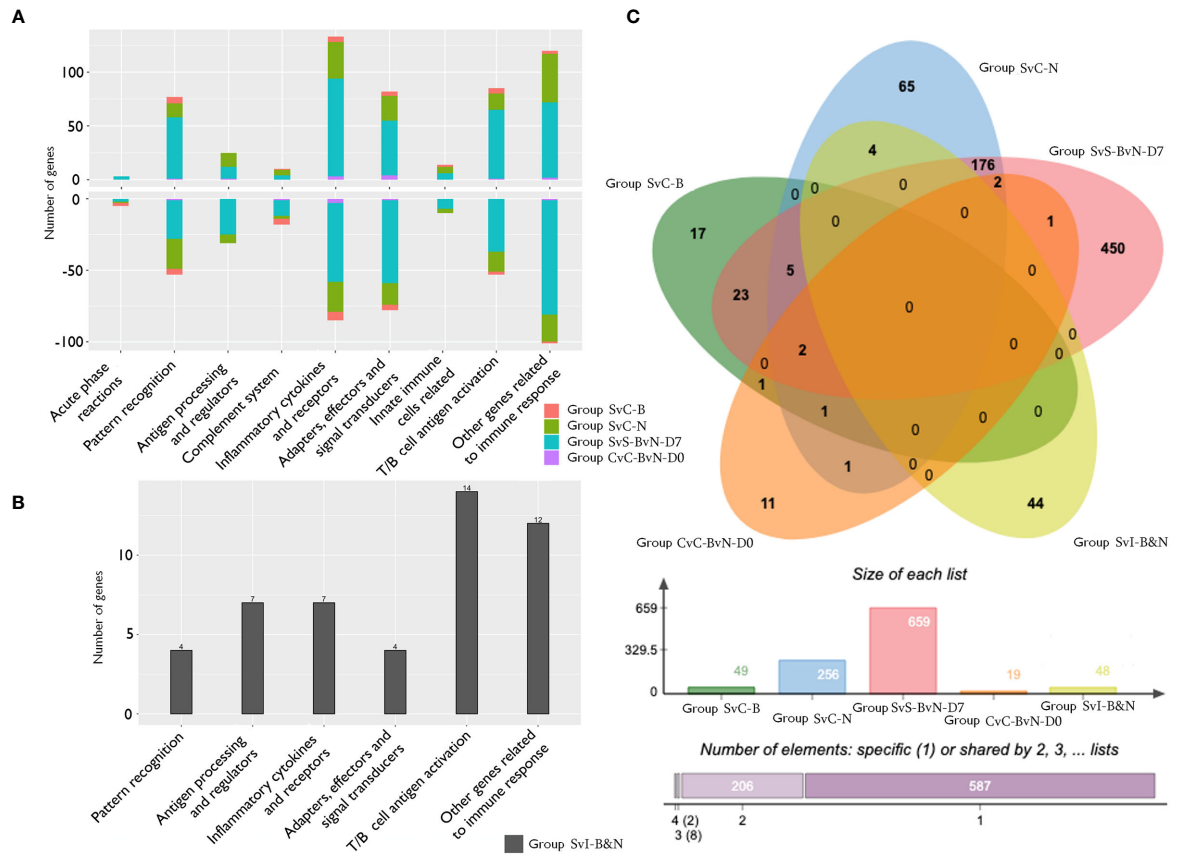

FIGURE 5 | The analysis of immune processes of DEG among different comparison groups. **(A)** The bar plots of gene number for the involved immune processes of up or down-regulated DEGs in groups SvC-B, SvC-N, SvS-BvN-D7, and CvC-BvN-D0; **(B)** The barplot of gene number for the involved immune processes in group SvI-B&N; **(C)** The Venn diagram of gene number for all comparison groups. DEG, differentially expressed gene.

greatest DEG number. To illustrate the immune process, the involved immune gene categories of the immune-related DEG in all comparisons were listed in **Table 3**.

Venn-Regional Analysis of Immune-Related DEG From Different Comparison Groups

A Venn diagram was created to demonstrate the relationship between the immune-related DEG among all comparison groups (**Figure 5C**). The details for all regions were in **Table S10**. Though the region-specific DEGs accounted for a large proportion of each comparison group, with immune gene categories for region-specific DEG underlined in **Table 3**, the overlapping DEGs (**Table 4**), which contained important genes, were listed with the corresponding immune process and immune gene category.

Immune-Related GO Terms as Well as Network Correlation Between LncRNAs and Genes in Immune-Related Module

The results of "WGCNA" were selected to determine the biological processes involved in CyHV-3-induced modulation of genes by lncRNAs, from an immune perspective. Among the currently divided 35 gene modules (**Figure 6A**), 12 modules were found with immune-related GO terms (**Figure S1**). Generally, "double-stranded DNA binding", "receptor-mediated endocytosis", "response to bacterium", "lysosome", "defense response to fungus", "killing of cells of other organism", "oxygen carrier activity", "oxygen binding", "defense response to bacterium", "killing of cells of other organism", "NuA4 histone acetyltransferase complex", "defense response to gram-negative bacterium", "defense response to gram-positive bacterium", "immune response", "regulation of cytokine secretion", "cytolysis", "execution phase of apoptosis", "cellular response to gamma radiation", "nucleic acid metabolic process", "TOR signaling", "DNA replication", "ubiquitin-dependent protein catabolic process", "granulocyte differentiation", and "macrophage differentiation" were revealed after the "WGCNA" analysis. The top five immune-related modules containing most immune-related GO terms (**Figure 6B**) were analyzed for the relationship between LncRNA and transcripts by PPI networks in cystoscope (**Figure 6C**, with details in **Table S11**). The LncRNA regulated genes, which upregulated in group SvS-BvN-D7, such as Semaphorin-4E in the blue module, can be

TABLE 3A | Immune gene categories involved in differentially expressed mRNA for comparison groups SvC-B, SvC-N, and SvS-BvN-D7.

Compared group	Immune gene category	
	1<FC<2	2<FC
Up-regulated in group SvC-B (26)	LRR-containing proteins, MRC, NFIL3, perforin, UBE, PIGR, TRIM, TLX.	CSF, UBE, C3, GVIN, IL21R, IL23R, integrin alpha, MMR, NCAM, cathepsin, ubiquitin ligase ladderlectin, LRR-containing proteins, Ig heavy chain, Ig light chain, PIGR, SEMA.
Down-regulated in group SvC-B (23)	CXCL, integrin alpha, myeloid cell related, galectin.	Fibrinogen, NALP12, NLRC3, C3, GVIN, IFI, IL1R, C-type lectin, galectin, TLR18, Ig light chain, TIP.
Up-regulated in group SvC-N (155)	FBXL, fucolectin, MPR, nattectin, TLR1, TLR5, CDK, CDK related, CDKIs, HA, MHC I, MHC II, TGFB, TNF, TNFAIP3-interacting protein, C3aR, C7, CCL, CCR, CFLAR, CXCL, CXCR, cytokine receptor, IFI, IFIT, IL1R related, IRF8, NFIL3, MAPK, MAPKKK, NALP12, NLRC3, programmed cell death protein, SOCS1, SOCS3, SOCS7, TRAF, TTRAP, UBE, MIF, NCF, NCK and related, BCL, BLNK, FCR, HDAC, HMG, Ig light chain, PBX, TAGAP, AP-3, CARD, cathepsin, CEBP, hepcidin, HSP, lymphocyte antigen, myeloid cell related, PIN1, platelet related, TMED, ubiquitin ligase, ubiquitin related, TRIM, UBL.	MAPK, MAPKKK, NLRC3, MHC II, C3, CCL, CXCL, CXCR, IL-1, IL1R, IL-6, IL6R, IL-8, IRF8, MX, NRAMP, AP-3, cathepsin, HSP5, HSP70, mucin, myeloid cell related, platelet related, ubiquitin ligase, NITR, TLR18, TLR22, TLR25, CD22, HMG, TCIRG1,
Down-regulated in group SvC-N (102)	Plasminogen, C-type lectin, Hepatic lectin, LRR-containing proteins, RBL, SITR, TLR13, CD22, Ig heavy chain, Ig light chain, SEMA, TCR, CDK, VEGF, VEGFR, C3aR, ACRs, CCR, EGFR, FGFR, GVIN, IL17R, IL21R, IL2R, integrin alpha, integrin beta, ACTININ, MALT1, paladin, RTK, TRIM, ubiquitin ligase, UBL, granzyme, MAPKKK, NALP12, NALP3, perforin, UBE, CDK, TRIM.	perforin, CD59, CCL, IL6R, IL-8, IRF related, TITIN, NCAM, CD33, HSP90, Kruppel-like factor, ubiquitin ligase, UBL, collectin, galectin, LRR-containing proteins, B-cell CLL/lymphoma, JAG, NFAT, SEMA
BS-advantage immune DEGs in group SvS-BvN-D7 (357)	Fibrinogen, MBL, collectin, C-type lectin, FBXL, fucolectin, galectin, intelectin, LRR-containing proteins, RBL, TLR8, TLR13, TLR3, TLR9, CDKIs, CIITA, LRMP, TGBR, VEGF, C3, C5, ACRs, CCL, CCR, CXCR, EGF, FGFR, GVIN, IFI, IL10R, IL13R, IL17R, IL1R related, IL21R, IL23R, IL2R, IL6R, IL-8, integrin alpha, integrin beta, IRF4, IRF5, IRF7, MX, XCR, CBX4, CSFR, granzyme, MAPK, MAPKKK, NALP12, NALP3, NDRG1, perforin, Programmed cell death protein, TRAF, TRAIL, UBE, MMR, NCAM, B-cell CLL/lymphoma, CD2, CD22, CD276, CD6, FCR, GATA and related, Ig heavy chain, Ig light chain, immunoglobulin superfamily, JAG, LAG, MAL, NFAT, PIGR, PKC, SEMA, T-bet, VTCN, ZAP, ACTININ, cathepsin, CD302, lymphocyte antigen, lymphocyte related, myeloid cell related, nectin, palladin, PI3K, TIAM, ubiquitin ligase, ubiquitin related, TRIM.	Fibrinogen, CSF, granzyme, MAPKKK, NALP12, NALP3, NLRC3, EGF, perforin, TRAF, UBE, CDK, LRMP, MHC I, MHC II, C3aR, C8, CCL, CCR, FGFR, GVIN, IFI, IFIT, IL17R, IL1R related, IL21R, IL23R, IL2R, IL6R, IL-8, integrin alpha, integrin beta, NFIL3, TITIN, MCP, NCAM, cathepsin, HSPb1, lymphocyte antigen, mucin, PI3K, rootletin, RTK, TRIM, ubiquitin ligase, ubiquitin related, UBL, collectin, c-type lectin, fucolectin, Lgals3bpa, galectin, Hepatic lectin, ladderlectin, LRR-containing proteins, MRC, NITR, scavenger receptor, SIGLEC, CD22, CD4, FCR, HDAC, Ig heavy chain, Ig light chain, immunoglobulin superfamily, JAG, NFAT, PIGR, PKC, SEMA, VSIG.
NBS-advantage immune DEGs in group SvS-BvN-D7 (303)	c-type lectin, FBXL, LPS-anchor protein, LRR-containing proteins, MPR, TLR1, TLR22, CDK, CDK related, CDKIs, HA, MHC II, TGFB, TNFAIP3-interacting protein, C3, C3aR, C4, C7, ACRs, CD11, CFLAR, CXCR, cytokine receptor, FAM, GVIN, HB-EGF, IL12R, IL1R related, IL-6, IL6R, integrin alpha, integrin beta, IRF1, IRF8, NFIL3, CSFR, JAK1, MAPK, MAPKKK, NALP12, NALP3, NLRC3, Programmed cell death protein, SOCS1, SOCS3, SOCS7, STAT3, UBE, MIF, NCF, NCK and related, BAFF, B-cell CLL/lymphoma, BCL, BLNK, CD22, CD276, FCR, HDAC, HMG, Ig light chain, PBX, PIGR, SEMA, TAL, VSIG, WWP, AP-3, CARD, cathepsin, CEBP, HSP, HSP4, HSP5, HSP70, HSP90, Kruppel-like factor, lymphocyte antigen, MALT1, mucin, myeloid cell related, PAXILLIN, PIN1, platelet related, TMED, ubiquitin ligase, ubiquitin related, TRIM, UBL.	Macroglobulin, CSF, MAPK, MAPKKK, NALP12, NALP3, NLRC3, SOCS3, UBE, CDK, CDKIs, MHC II, TNF, FGF, TNFAIP3-interacting protein, C3, C3aR, C7, CD59, CCL, CCR, CXCL, CXCR, GVIN, IL-1, IL-12, IL1R, IL1R related, IL2R, IL-6, IL-8, integrin alpha, IRF8, NFIL3, NRAMP, ACTININ, AP-3, caspase, cathepsin, CEBP, hepcidin, HSP70, lymphocyte antigen, ubiquitin ligase, UBL, CD209, C-type lectin, galectin, intelectin, LRR-containing proteins, TLR18, TLR25, TLR4, TLR5, BCL, CD22, CD276, HDAC, Ig light chain, PIGR, SEMA, TAGAP, TCIRG1, TCIRG2, TCIRG3.

For group SvS-BvN-D7, "BS-advantage" represented the upregulated genes related to the breeding strain, while "NBS-advantage" represented the downregulated genes related to non-breeding strain, after the comparison between survivors from breeding strain and survivors from the non-breeding strain.

the factor associated with the resistance in the breeding strain. The LncRNA regulated genes, which downregulated in group SvS-BvN-D7, such as Lgals3l in the grey60 module, can be the factor associated with less accessibility to CyHV-3 in the breeding strain. The LncRNA regulated genes, which was upregulated in group SvC-N and downregulated in group SvS-BvN-D7, such as natural resistance-associated macrophage protein (Nramp), plasminogen activator inhibitor (PAI) in the brown module, could be the key clues for susceptibility of CyHV-3 in the non-breeding strain. Specifically, for detailed correlations of lncRNAs and DEG in groups SvC-B, SvC-N, and SvS-BvN-D7 (**Table S12**), T cell leukemia homeobox 3 (TLX3) and LGALS3 were revealed, respectively, in the survivors of the breeding strain.

DISCUSSION

This study demonstrated that the anti-CyHV-3 immune mechanisms of a breeding strain of common carp. This demonstrated dramatically decreased levels of mortality and less inner tissues swelling together with the previously revealed reduced virus load of tissues (24, 25), proving resistance to CyHV-3. The current studies of biological processes and

TABLE 3B | Immune gene categories involved in differentially expressed mRNA each comparison group CvC-BvN-D0 and SvI-B&N.

Compared group	Immune gene category
BS-advantage immune DEGs in group CvC-BvN-D0 (12)	1<FC<2: MHC I, GVIN, IL21R, NLRC3; 2<FC: NALP3, perforin, STAT3, integrin alpha, platelet related, ubiquitin related, MRC, HDAC.
NBS-advantage immune DEGs in group CvC-BvN-D0 (7)	1<FC<2: TLR18, C3, CCL, integrin beta. 2<FC: perforin, IFI, myeloid cell related
All in group SvI-B&N (48)	LRR-containing proteins, VEGFR, VEGF, CDKIs, CDK, NFIL3, LIFR, integrin beta, FAM, CCR, CD166, MAPK, CD97, SEMA, PIGR, NFAT, Ig light chain, HMG, HDAC, BTG, BCL, ubiquitin ligase, platelet related, HIF1a, CEBP.

*The number (>1) of DEG is shown in the brackets. The full names of all gene abbreviations could be found in **Tables S5–S9**. The underlined up or down-regulated immune gene categories are the regional specific in the Venn diagram for every group (detailed in **Table S10**). For group CvC-BvN-D0, "BS-advantage" represented the upregulated genes related to the breeding strain, while "NBS-advantage" represented the downregulated genes related to non-breeding strain, after the comparison between controls from breeding strain and controls from the non-breeding strain.*

TABLE 4 | The immune process and immune gene category for overlapping genes in the Venn regional analysis.

Overlapping regions	Immune process	Immune gene category
Groups SvC-B & SvS-BvN-D7 (23)	pattern recognition (7), complement system (4), inflammatory cytokines and receptors (3), adapters, effectors and signal transducers (4), innate immune cells related, T/B cell antigen activation (2), other genes related to immune response (2)	CSF, NALP12, UBE, C3, GVIN, IL23R, integrin alpha, NCAM, ubiquitin ligase, C-type lectin, galectin, ladderlectin, LRR-containing proteins, MRC, PIGR
Groups SvC-B & CvC-BvN-D0 (1)	inflammatory cytokines and receptors	IFI
Group SvC-N & SvS-BvN-D7 (176)	pattern recognition (18), antigen processing and regulators (14), complement system (4), inflammatory cytokines and receptors (38), adapters, effectors and signal transducers (23), innate immune cells related (8), T/B cell antigen activation (24), other genes related to immune response (47)	Granzyme, MAPK, MAPKKK, NALP12, NALP3, NLRC3, perforin, Programmed cell death protein, SOCS1, SOCS3, SOCS7, UBE, CDK, CDK related, CDKIs, HA, MHC II, TGFB, TNF, TNFAIP3-interacting protein, VEGF, C3aR, C7, ACRs, CCL, CCR, CFLAR, CXCL, CXCR, cytokine receptor, FGFR, GVIN, IL1, IL17R, IL1R related, IL2R, IL6, IL6R, IL8, integrin alpha, IRF8, NFIL3, TITIN, MIF, NCAM, NCF, NCK and related, NRAMP, ACTININ, AP-3, CARD, cathepsin, CEBP, hepcidin, HSP, HSP5, HSP70,lymphocyte antigen, paladin, PIN1, platelet related, RTK, TMED, TRIM, ubiquitin ligase, ubiquitin related, UBL, collectin, C-type lectin, FBXL, galectin, LRR-containing proteins, MPR, RBL, TLR1, TLR13, TLR22, TLR25, TLR5, BCL, BLNK, CD22, FCR, HDAC, HMG, Ig heavy chain, Ig light chain, JAG, NFAT, PBX, SEMA, TAGAP, TCIRG1
Groups SvC-N & SvI-B&N (4)	antigen processing and regulators (3), other genes related to immune response	CEBP, VEGFR
Groups SvC-N & CvC-BvN-D0 (1)	inflammatory cytokines and receptors	integrin alpha
Groups SvS-BvN-D7 & CvC-BvN-D0 (1)	inflammatory cytokines and receptors	CCL
Groups SvC-B & SvC-N & SvS-BvN-D7 (5)	pattern recognition, inflammatory cytokines and receptors (3), adapters, effectors and signal transducers	LRR-containing proteins, CXCL, IL1R, perforin
Groups SvC-B & SvC-N & SvI-B&N (1)	complement system	C3
Groups SvC-N & SvS-BvN-D7 & CvC-BvN-D0 (2)	adapters, effectors and signal transducers (2)	perforin
Groups SvC-B & SvC-N & SvS-BvN-D7 & CvC-BvN-D0 (2)	pattern recognition, inflammatory cytokines and receptors,	TLR18, IL21R

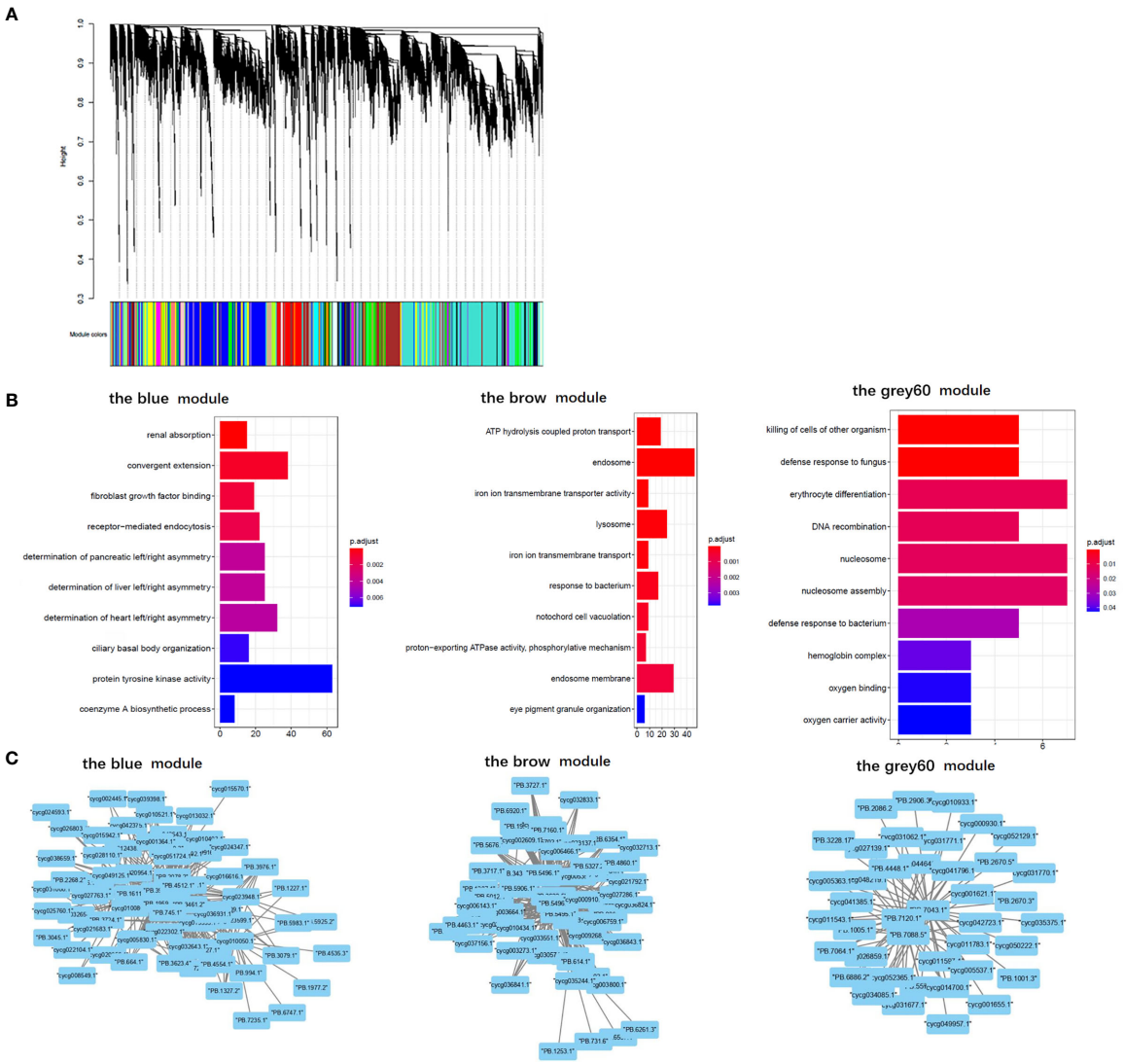

FIGURE 6 | Gene ontology analysis and cystoscopes of key matched lncRNA and transcripts in the immune-related module. **(A)** the cluster dendrogram of all gene module. **(B)** The GO terms involved in the immune-related module, including the blue, brow, and the grey60 module, which contain the matched lncRNA and transcripts involved in current analyzed comparison groups. The star, triangle, and arrow represent the revealed GO term for comparison groups SvC-B, SvC-N, and SvS-BvN-D7, respectively. **(C)** Cystoscopes of key matched lncRNA and transcripts in the immune-related module, as shown for blue, brow and grey60 module, respectively. The PPI network here just showed the pattern of closely related genes and LncRNAs, and to access the detailed information of genes and LncRNAs, please refer to **Table S11**.

pathways discovered through transcriptomic analysis have been merged to improve clarity. Afterwards, by comparing the survivors and healthy fish in either breeding or non-breeding strains, key genes and related lncRNAs involved in immune processes were also revealed. Accordingly, the immunogenetically insensitive or susceptible factors to CyHV-3 infection were determined.

From the aspect of cell surface receptors, which could participate in virus-host interaction, current comparison results suggested potential components involved in virus entry and downstream proinflammatory signaling. Firstly, integrin acts as a herpesvirus receptor (39), and the integrin-dependent signalosome in herpesvirus-infected cells mediated or coactivated numerous inflammatory responses and signaling transductions (39). Therefore, the finding that there was more expression of integrin beta 1 (ITGB1) in the survivors from non-breeding strain compared with those from the breeding strain, even during the steady status, may indicate that ITGB1 facilitates the binding of herpes virus glycoprotein for entry (40). This coincides with the finding that integrin signaling promotes the release of intracellular calcium stores and contributes to viral entry and cell-to-cell

spreading *via* glycoprotein H, during herpes simplex virus infection in humans (41). Recent reports have also demonstrated that some integrins on lymphocytes, such as B cells, could facilitate mucosa-specific homing (42). Secondly, higher TLR expression in survivors of the non-breeding strain compared with that of the breeding strain also indicated its role in facilitating the virus infection. Of note, TLR4 signaling leads to the production of proinflammatory cytokines in human lymphatic endothelial cells (39). In addition, fish-specific and virus-responding TLR18 (43, 44) (the most overlapping gene among groups) was downregulated in the comparison group SvC-B, whereas it was upregulated in group SvC-N. Also, TLR18 was higher in steady-state in the nonbreeding strain. This suggested its possibility to enhance the severity of CyHV-3 infection. MAPK signaling, as the downstream process of pattern recognition receptors, could facilitate the tnf-alpha-induced suppressor of cytokine signaling 3 (SOCS3) expression. This can lead to both pro-inflammatory immune response and failure in growth (45), according to the upregulated DEGs upon infection observed in the group SvC-N.

To reveal the breeding driven improvement for the resistance from CyHV-3 infection, by comparing the survivors from different strains, DEGs of the inflammatory status also provide clues for how to block the virus. Non-specific binding of the virus by lectins played a protective role in preventing virus entry. Both upregulated ladderlectins and higher galectin expression were detected in survivors of breeding strains compared with non-breeding strains. This is suggestive of their blocking ability for viral proteins (46, 47), such as glycoprotein (48). Moreover, as the head kidney is one of the major reticuloendothelial systems in fish (49), mucin was also found to be upregulated as the anti-virus barrier. This was shown in the comparison group SvC-N as the gel-forming mucin 5B (MUC5B) (50) was upregulated in the survivors of the non-breeding strain. However, higher expression levels of membrane-bound MUC3 (51) were found in survivors of the breeding strain versus the non-breeding strain. Additionally, as shown in the comparison group SvS-BvN-D7, the complement system functioned differently. BS-advantage complement components C8 indicate the formation of terminal complement complex (52), while NBS-advantage CD59, which is the inhibitor of complement membrane attack complex (MAC) (52), suggesting the inhibition of f complement-dependent cytotoxicity (CDC). Thus, the effective CDC may be more helpful for surviving. These findings suggested that more mucus was secreted, thereby causing tissue swelling upon CyHV-3 infection in the non-breeding strain. For the survivors of the breeding strain, the membrane-bound mucin could effectively bind the virus with no gel.

For the anti-viral biological process for the breeding strain, the lectin complement pathway has been involved in the clearance of apoptotic cells, reflected by the GO term "cell killing" in both comparison groups SvC-B and SvS-BvN-D7, as well as more types of lectins in survivors from breeding strains. Hence, in survivors of the breeding strain, the complement components reported in the acute phase in common carp during CyHV-3 infection (53), could facilitate the phagocytic process *via* binding of MRC (Mannose-Receptor C) in fish (54). The interleukin 21 receptor (IL21R), which was found regulated in the survivors of the breeding strain for group SvC-B and the healthy control of the non-breeding strain for group SvC-N, indicated the control of inflammation by suppressing STAT3 signaling (55). The upregulated IL23R in the survivors of the breeding strain for group SvC-B can promote cytotoxic ability (56), which may immediately kill infected cells. The lack of antigen presentation in comparison group SvC-B suggested that the infection was overcome before the amplification of CyHV-3 in the breeding strain. As to the BS-advantage interferon related genes in group SvS-BvN-D7, the activator of IRF7 (57) as well as MX, the inhibitor of virus replication, may elicit the interferon antiviral response. Meanwhile, for proinflammatory cytokine, echoed with upregulated IL-1, IL-6, and IL-8 in group SvC-N, the NBS-advantage proinflammatory signaling dominated in the survivors from non-breeding strain, and also numerous upregulated genes were involved in antigen presentation in the non-breeding strain in group SvC-N. Therefore, the survivors from breeding strains overcame the infection mainly through phagocytosis and cytotoxicity at the cellular level and may elicit IFN response, without activating the typical process of proinflammation as in survivors from the non-breeding strain.

Thus, there are different signatures between the two strains, regarding the survival strategy. For the survivors in the breeding strain, self-repairing related autophagy was detected as both the KEGG pathways "regulation of autophagy" and autophagy-related fish antiviral tripartite motif (TRIM) protein (58) were found in group SvC-B. These findings were in line with TRIMs, which were found regulated in the survivors of breeding strain for group SvC-B and in the healthy control of non-breeding strain for group SvC-N. The above finding of TRIM is coincident with one of the recently revealed CyHV-3 resistant related DEGs with identified QTLs (17). In the survivors from the breeding strain, the higher PI3K also suggests higher autophagy, since the PI3K/AKT/mTOR pathway enhances this process (59). In the breeding strain, the suppressed IFN activation was also suggested, for that fish TRIM may inhibit the activation of IFN and attenuate IFN regulatory factor (IRF) (60, 61). The factor that there was more expression of TRAF6 in survivors of breeding strain compared with those of non-breeding strain, is in line with the resistant related SNP on TRAF6 (62) and suggests the possible repression on the production of type I IFN (63). In addition, nuclear factor, interleukin 3 regulated (NFIL3) can control Treg cell function *via* directly binding to and negatively regulates the expression of Foxp3 (64), and has been revealed stimulating both proinflammatory (e.g., NF-kappa B [NF-κB]) and anti-inflammatory factors (e.g., IL10) in carp (65). Thus, the upregulated NFIL3 in the survivors of the breeding strain for group SvC-B may suggest the extensive activation of immune cells, with diminished immune regulation. The directed lymphocytes response could be

present as there was upregulation of IL23R, which significantly enhances the expression of cytotoxic mediators (56), as well as cathepsin L (a component of lysosomes) (66). This indicated an enhanced activation of the cytotoxic ability of T cells in survivors from the breeding strain. For B cells, the secretion of Ig-related genes (e.g., polymeric immunoglobulin receptor [PIGR], Ig heavy chain and light chain) was also upregulated in the survivors of breeding strain for group SvC-B. To fight the virus, the survivors from the non-breeding strain developed typical inflammatory cascades, including pro-inflammatory cytokines (e.g., IL-1, IL-6, and IL-8), as well as MAPK signaling, which is profoundly involved in cell survival functions during viral infection (67). For the control of inflammation, the survivors from the common strain exhibited suppression of the IFN response, which was also reflected by the upregulated IRF1 and IRF8, the inhibitor of the MYD88-mediated NF-κB signaling pathway (68, 69). Downstream hypoxia was also found, as indicated by the "p53 signaling pathway" and "oxidative phosphorylation". The hypoxic status could also protect survivors of the non-breeding strain from death since p53 suppresses cell apoptosis (70), and HIF1A regulates virus-induced glycolytic genes (71).

Furthermore, the DEGs generated by comparing the survivors from the two strains in comparison group SvS-BvN-D7, which can provide clues for how to develop the resistance to CyHV-3 infection. The BS-advantage semaphorin, which was also regulated by LncRNA, is related to immunoregulation (72, 73). This indicated a possible tolerance of viral replication or latency after primary infection in the survivors (2), while had no negative effects on the proliferation of host cells (74). There was less cyclin-dependent kinase inhibitor 1D (CDKN1D) in survivors from the breeding strain compared with the non-breeding strain. This indicated that there was an interrupted circadian cell-cycle timing in the survivors from non-breeding strains (75). The higher levels of STAT3 and possible its upregulated integrins (76) in survivors from the non-breeding strain may facilitate the effect of enhanced IL6 signaling. Apart from the typical immune signals in comparison group SvS-BvN-D7, there was relatively higher PI3K activity, which was involved in the KEGG pathway "dopaminergic synapse". This indicated that dopamine inhibited inflammation (77) in survivors from the breeding strain. This is because PI3K is dependent on the accumulation of DOPA decarboxylase, the enzyme involved in the production of dopamine, which is reduced by a viral infection (78). Additionally, genes responsive to the secretion of immunoglobulin (e.g., PIGR and Ig light chain), which is important for anti-virus immunity, were common (in comparison group SvI-B&N) between the two strains.

Additionally, the comparison of two strains with health status in group CvC-BvN-D0 suggested the differential basal properties for immune homeostasis. Among BS-advantage immune DEGs, which was related to the healthy control of breeding strain, the expression of NACHT, LRR, and PYD domains-containing protein 3 (NALP3) indicated a stronger ability to form the inflammasome in the breeding strain. The higher levels of NLR family CARD domain containing 3 (NLRC3), which is a negative regulator of the DNA sensor STING, suggest less sensitivity to the DNA virus in the breeding strain. The higher levels of MHC I indicate greater potential to activate response by cytotoxic $CD8^+$ T cells upon herpes virus infection, as previously revealed in the resistant strain R3 (79). For the potential T helper cell differentiation-related JAK/STAT pathway, the upregulation of both STAT3 and histone deacetylase (HDAC) indicated an easier differentiation of both T helper 17 and regulatory T directions (80), respectively, in the breeding strain even in the steady state (81, 82). Upregulation of HDAC in the healthy control of breeding strain for group CvC-BvN-D0, which could inhibit the function of macrophages in fish (83), also suggests a more delicate immune regulation during the steady state in the breeding strain. The macrophage related MRC (Mannose-Receptor C) in fish could potentially induce the phagocytic process if necessary (54). However, among NBS-advantage immune DEGs, which indicated higher expression in the non-breeding stain at a steady state, myeloid-associated differentiation marker-like protein 2 (myadml2) suggested the basic more differentiation of monocyte cell types (84) As the surface receptor, TLR18 and ITGB1 suggested susceptibility to virus binding. Moreover, C-C motif chemokine ligand 4 (CCL4), which can protect infected cells with the viral burden (85), may be a risk factor for the non-breeding strain. In addition, the downregulated DEGs in group SvC-B and SvC-N also provided clues for how to maintain immune homeostasis, which can prevent the virus challenge. Among the downregulated DEGs in group SvC-B, both the existence of C3 and IFI suggested a restricting effector on the virus, since that C3b can bind directly to purified glycoprotein C of herpesvirus (86), and interferon-induced protein 44 (IFI44) may restrict virus replication (87). These factors were also revealed in NBS-advantage immune DEGs in group CvC-BvN-D0. Therefore, upon steady state, C3b and IFI44 also served as the basic defense function even in the virus carrier state, which could be especially important for the non-breeding strain.

The revealed regulation of resistance to CyHV-3 by lncRNA involved numerous biological processes. Among the revealed GO terms in comparison group SvC-N, "DNA replication" could indicate virus proliferation in the non-breeding strain. In survivors from the non-breeding strain, the lncRNA-regulated genes were mainly involved in innate immune cell function (e.g., macrophage protein and cathepsin, as components of lysosomes) and cell apoptosis. Nramp and PAI were found regulated by LncRNA in comparison groups SvC-N (up) and SvS-BvN-D7 (down). This finding indicates the more expression of Nramp and PAI in the survivors of non-breeding strain, could facilitate virus infection and proliferation for infected cell respectively, since that Nramp may serve as a virus receptor (88), meanwhile, PAI can inhibit apoptosis in cell lines infected with viruses (89). While, in survivors from the breeding strain, the only lncRNA-modulated gene, TLX3, is strongly methylated. This indicates

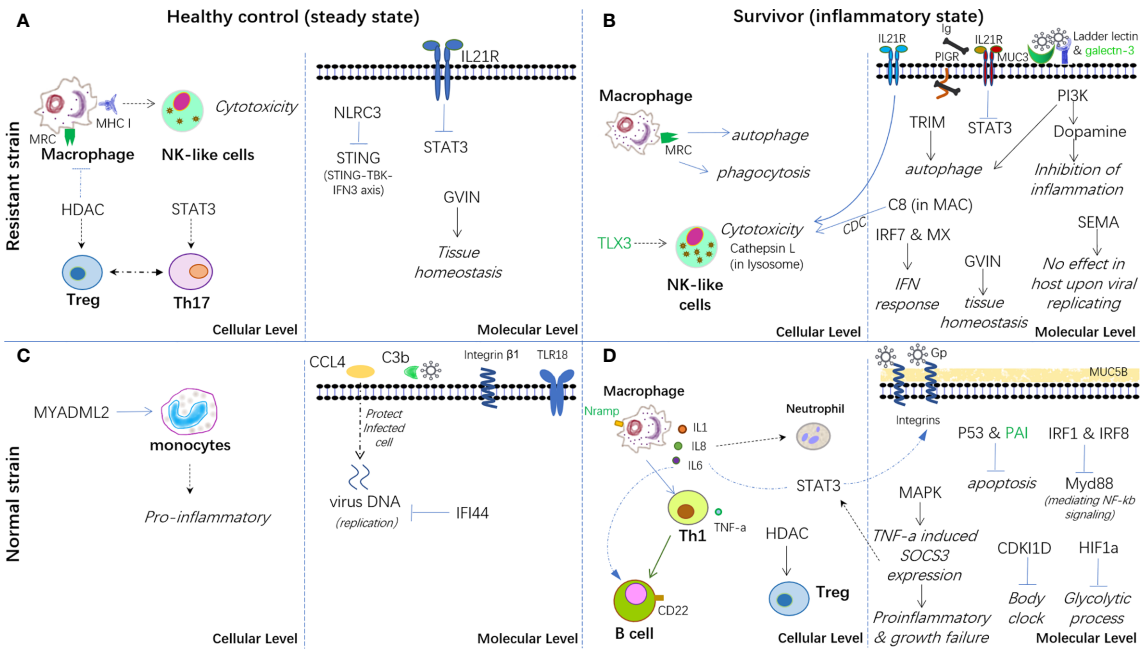

FIGURE 7 | Hypothesis of the carp immune mechanism in both breeding (resistant) and non-breeding (normal) strains, either at the steady-state or upon surviving for CyHV-3 infection. **(A)** Healthy control in the steady state in the breeding strain. **(B)** Survivors in an inflammatory state in the breeding strain. **(C)** Healthy control in the steady state in non-breeding strain. **(D)** Survivors in an inflammatory state in the non-breeding strain. The words in italics, bold, and green represent the biological process, cell type, and lncRNA-modulated immune genes, respectively. The arrow denotes facilitation or promotion, and — denotes inhibition. The dashed line indicates a possible correlation.

that TLX3 expression was suppressed during hepatitis B virus-related cancer (90). This suggests that TLX3 in survivors from the breeding strain may play a protective role, and participate in lymphocyte proliferation in the head kidney. Meanwhile, echoing with the recent finding of the participation of zebrafish galectin proteins in immunity against viral infection (48, 91), in comparison group SvS-BvN-D7 the LncRNA regulated transcripts Lgals3l (down) and Lgals3bpa (up), as well as BS-advantage Lgals3bpa and galectin 3 suggested the regulation of galectin-3 related biological activities could be related to reduce the viral attachment for survivors of the breeding strain.

Therefore, based on the present findings, a hypothesis has been proposed for the immune mechanisms involved in both healthy controls and survivors from infection in both strains (**Figure 7**). In conclusion, the breeding strain of common carp showed a better ability to maintain immune homeostasis in both steady and inflammatory states and displayed enhanced blockage of CyHV-3 infection compared with the non-breeding strain. Thus, this strain could be termed as a resistant strain accordingly. Since the modulation of mRNA and lncRNA expression dynamics currently remains a hypothesis, further molecular evidence is needed to elucidate the mechanism of both resistance and susceptibility. In addition, the finding that both the inhibition of inflammation by dopamine in the breeding strain and the disrupted bio-clock in the non-breeding strain upon CyHV-3 infection suggested better growth performance for the breeding strain. Therefore, the possible advantage of this resistant strain for growth performance warrants further study.

DATA AVAILABILITY STATEMENT

The datasets presented in this study can be found in online repositories. The names of the repository/repositories and accession number(s) can be found in the article/**Supplementary Material**.

ETHICS STATEMENT

The animal study was reviewed and approved by The Committee for the Welfare and Ethics of Laboratory Animals, Heilongjiang River Fisheries Research Institute, Chinese Academy of Fishery Sciences.

AUTHOR CONTRIBUTIONS

LS and ZJ conceived the project and designed the experiments. NW and ZJ wrote the manuscript. ZJ performed the experiments. ZJ and JXS conducted the CyHV-3 infection experiment and collected samples. CL, XH, and YG performed fish propagation and culture. XJ conducted the RT-PCR experiment. NW and X-QX coordinated the data analysis tasks. NW, HL, MS, WY, YT, JWS, and YC

analyzed the data. The manuscript was revised and approved by X-QX and LS. All authors contributed to the article and approved the submitted version.

FUNDING

This work was funded by grants from the National Key R&D Program of China (2018YFD0900302-6), The Natural Science Foundation of Heilongjiang Province (TD2019C004), China Aquaculture Research System (CARS-45-06), and Central Public-interest Scientific Institutional Basal Research Fund (2020TD31).

ACKNOWLEDGMENTS

We thank Mr. Bruno Unger from the University of Canterbury in New Zealand for language editing.

SUPPLEMENTARY MATERIAL

The Supplementary Material for this article can be found online at: https://www.frontiersin.org/articles/10.3389/fimmu.2021.687151/full#supplementary-material

REFERENCES

1. Neave MJ, Sunarto A, McColl KA. Transcriptomic Analysis of Common Carp Anterior Kidney During Cyprinid Herpesvirus 3 Infection: Immunoglobulin Repertoire and Homologue Functional Divergence. *Sci Rep* (2017) 7:41531. doi: 10.1038/srep41531
2. Adamek M, Steinhagen D, Irnazarow I, Hikima J, Jung TS, Aoki T. Biology and Host Response to Cyprinid Herpesvirus 3 Infection in Common Carp. *Dev Comp Immunol* (2014) 43:151–9. doi: 10.1016/j.dci.2013.08.015
3. Sunarto A, McColl KA. Expression of Immune-Related Genes of Common Carp During Cyprinid Herpesvirus 3 Infection. *Dis Aquat Organ* (2015) 113:127–35. doi: 10.3354/dao02824
4. Reichert M, Lukasik A, Zielenkiewicz P, Matras M, Maj-Paluch J, Stachnik M, et al. Host microRNA Analysis in Cyprinid Herpesvirus-3 (CyHV-3) Infected Common Carp. *BMC Genomics* (2019) 20:46. doi: 10.1186/s12864-018-5266-9
5. Rakus KL, Irnazarow I, Adamek M, Palmeira L, Kawana Y, Hirono I, et al. Gene Expression Analysis of Common Carp (Cyprinus Carpio L.) Lines During Cyprinid Herpesvirus 3 Infection Yields Insights Into Differential Immune Responses. *Dev Comp Immunol* (2012) 37:65–76. doi: 10.1016/j.dci.2011.12.006
6. Rakus KL, Wiegertjes GF, Adamek M, Siwicki AK, Lepa A, Irnazarow I. Resistance of Common Carp (*Cyprinus Carpio L.*) to Cyprinid Herpesvirus-3 is Influenced by Major Histocompatibility (MH) Class II B Gene Polymorphism. *Fish Shellfish Immun* (2009) 26:737–43. doi: 10.1016/j.fsi.2009.03.001
7. Adamek M, Matras M, Dawson A, Piackova V, Gela D, Kocour M, et al. Type I Interferon Responses of Common Carp Strains With Different Levels of Resistance to Koi Herpesvirus Disease During Infection With CyHV-3 or SVCV. *Fish Shellfish Immunol* (2019) 87:809–19. doi: 10.1016/j.fsi.2019.02.022
8. Lee X, Yi Y, Weng S, Zeng J, Zhang H, He J, et al. Transcriptomic Analysis of Koi (*Cyprinus Carpio*) Spleen Tissue Upon Cyprinid Herpesvirus 3 (CyHV3) Infection Using Next Generation Sequencing. *Fish Shellfish Immunol* (2016) 49:213–24. doi: 10.1016/j.fsi.2015.12.007
9. Hwang JA, Kim JE, Kim HS, Lee JH. Immune Response to Koi Herpesvirus (KHV) of Koi and Koi X Red Common Carp (*Cyprinus Carpio*). *Dev Reprod* (2017) 21:361–70. doi: 10.12717/DR.2017.21.4.361
10. Adamek M, Rakus KL, Brogden G, Matras M, Chyb J, Hirono I, et al. Interaction Between Type I Interferon and Cyprinid Herpesvirus 3 in Two Genetic Lines of Common Carp (*Cyprinus Carpio*). *Dis Aquat Organ* (2014) 111:107–18. doi: 10.3354/dao02773
11. Tadmor-Levi R, Hulata G, David L. Multiple Interacting QTLs Affect Disease Challenge Survival in Common Carp (*Cyprinus Carpio*). *Heredit (Edinb)* (2019) 123:565–78. doi: 10.1038/s41437-019-0224-0
12. Jia ZY, Chen L, Ge YL, Li SW, Peng WZ, Li CT, et al. Genetic Mapping of Koi Herpesvirus Resistance (KHVR) in Mirror Carp (*Cyprinus Carpio*) Revealed Genes and Molecular Mechanisms of Disease Resistance. *Aquaculture* (2020) 519:1–10. doi: 10.1016/j.aquaculture.2019.734850
13. Ren X, Liu P, Li J. Comparative Transcriptomic Analysis of *Marsupenaeus Japonicus* Hepatopancreas in Response to *Vibrio Parahaemolyticus* and White Spot Syndrome Virus. *Fish Shellfish Immunol* (2019) 87:755–64. doi: 10.1016/j.fsi.2019.02.030
14. Liu X, Qin Z, Babu VS, Zhao L, Li J, Zhang X, et al. Transcriptomic Profiles of Striped Snakehead Cells (SSN-1) Infected With Snakehead Vesiculovirus (SHVV) Identifying IFI35 as a Positive Factor for SHVV Replication. *Fish Shellfish Immunol* (2019) 86:46–52. doi: 10.1016/j.fsi.2018.11.031
15. Tengs T, Rimstad E. Emerging Pathogens in the Fish Farming Industry and Sequencing-Based Pathogen Discovery. *Dev Comp Immunol* (2017) 75:109–19. doi: 10.1016/j.dci.2017.01.025
16. Sudhagar A, Kumar G, El-Matbouli M. Transcriptome Analysis Based on RNA-Seq in Understanding Pathogenic Mechanisms of Diseases and the Immune System of Fish: A Comprehensive Review. *Int J Mol Sci* (2018) 19 (1):245. doi: 10.3390/ijms19010245
17. Tadmor-Levi R, Doron-Faigenboim A, Marcos-Hadad E, Petit J, Hulata G, Forlenza M, et al. Different Transcriptional Response Between Susceptible and Resistant Common Carp (*Cyprinus Carpio*) Fish Hints on the Mechanism of CyHV-3 Disease Resistance. *BMC Genomics* (2019) 20(1):1019. doi: 10.1186/s12864-019-6391-9
18. Boltana S, Valenzuela-Miranda D, Aguilar A, Mackenzie S, Gallardo-Escarate C. Long Noncoding RNAs (lncRNAs) Dynamics Evidence Immunomodulation During ISAV-Infected Atlantic Salmon (*Salmo Salar*). *Sci Rep* (2016) 6:22698. doi: 10.1038/srep22698
19. Tarifeno-Saldivia E, Valenzuela-Miranda D, Gallardo-Escarate C. In the Shadow: The Emerging Role of Long Non-Coding RNAs in the Immune Response of Atlantic Salmon. *Dev Comp Immunol* (2017) 73:193–205. doi: 10.1016/j.dci.2017.03.024
20. Sun W, Feng J. Differential lncRNA Expression Profiles Reveal the Potential Roles of lncRNAs in Antiviral Immune Response of *Crassostrea Gigas*. *Fish Shellfish Immunol* (2018) 81:233–41. doi: 10.1016/j.fsi.2018.07.032
21. Valenzuela-Munoz V, Pereiro P, Alvarez-Rodriguez M, Gallardo-Escarate C, Figueras A, Novoa B. Comparative Modulation of lncRNAs in Wild-Type and Rag1-Heterozygous Mutant Zebrafish Exposed to Immune Challenge With Spring Viraemia of Carp Virus (SVCV). *Sci Rep* (2019) 9:14174. doi: 10.1038/s41598-019-50766-0
22. Jia Z, Shi L, Shi J, Li C, Hu X, Ge Y, et al. *Identification Methods of Carp Germplasm Resources*. ZL201610945256.9, the National Invention Patent in China.
23. Tadmor-Levi R, Asoulin E, Hulata G, David L. Studying the Genetics of Resistance to CyHV-3 Disease Using Introgression From Feral to Cultured Common Carp Strains. *Front Genet* (2017) 8:24. doi: 10.3389/fgene.2017.00024
24. Jia ZY, Wang SH, Bai SS, Ge YL, Li CT, Hu XS, et al. Survival Rate and Immunological Responses of Mirror Carp Selective Breeding Generations to CyHV-3. *J World Aquacult Soc* (2018) 49:388–95. doi: 10.1111/jwas.12511
25. Sun JX, Shi LY, Jiang XN, Li CT, Ge YL, Hu XS, et al. Research on Expression of Virus in Cyprinid Herpesvirus 3 (CyHV-3) F4 Disease Resistant Strains. *J Shanghai Ocean Univ* (2020) 30(02):258–65. doi: CN 31-2024/S
26. Conte MA, Gammerdinger WJ, Bartie KL, Penman DJ, Kocher TD. A High Quality Assembly of the Nile Tilapia (*Oreochromis Niloticus*) Genome Reveals the Structure of Two Sex Determination Regions. *BMC Genomics* (2017) 18:341. doi: 10.1186/s12864-017-3723-5
27. Adamek M, Syakuri H, Harris S, Rakus KL, Brogden G, Matras M, et al. Cyprinid Herpesvirus 3 Infection Disrupts the Skin Barrier of Common Carp (Cyprinus Carpio L.). *Vet Microbiol* (2013) 162:456–70. doi: 10.1016/j.vetmic.2012.10.033

28. Tan A, Ye X, Jiang L, Zhao F, Zou W, Lin Z, et al. *Detection Methods of Cyprinid Herpesvirus (CyHv)*. Beijing: China MoAaRAotPsRo (2011).
29. Zhang X, Li G, Jiang H, Li L, Ma J, Li H, et al. Full-Length Transcriptome Analysis of *Litopenaeus Vannamei* Reveals Transcript Variants Involved in the Innate Immune System. *Fish Shellfish Immunol* (2019) 87:346–59. doi: 10.1016/j.fsi.2019.01.023
30. Wu N, Wang B, Cui ZW, Zhang XY, Cheng YY, Xu X, et al. Integrative Transcriptomic and Micrornaomic Profiling Reveals Immune Mechanism for the Resilience to Soybean Meal Stress in Fish Gut and Liver. *Front Physiol* (2018) 9:1154. doi: 10.3389/fphys.2018.01154
31. Xu P, Zhang X, Wang X, Li J, Liu G, Kuang Y, et al. Genome Sequence and Genetic Diversity of the Common Carp. *Cyprinus Carpio Nat Genet* (2014) 46:1212–9. doi: 10.1038/ng.3098
32. Wu N, Song YL, Wang B, Zhang XY, Zhang XJ, Wang YL, et al. Fish Gut-Liver Immunity During Homeostasis or Inflammation Revealed by Integrative Transcriptome and Proteome Studies. *Sci Rep* (2016) 6:36048. doi: 10.1038/srep36048
33. Wang J, Fu L, Koganti PP, Wang L, Hand JM, Ma H, et al. Identification and Functional Prediction of Large Intergenic Noncoding RNAs (lincRNAs) in Rainbow Trout (*Oncorhynchus Mykiss*). *Mar Biotechnol (NY)* (2016) 18:271–82. doi: 10.1007/s10126-016-9689-5
34. Liao Q, Liu C, Yuan X, Kang S, Miao R, Xiao H, et al. Large-Scale Prediction of Long Non-Coding RNA Functions in a Coding-Non-Coding Gene Co-Expression Network. *Nucleic Acids Res* (2011) 39:3864–78. doi: 10.1093/nar/gkq1348
35. Langfelder P, Horvath S. WGCNA: An R Package for Weighted Correlation Network Analysis. *BMC Bioinf* (2008) 9:559. doi: 10.1186/1471-2105-9-559
36. Yu GC, Wang LG, Han YY, He QY. Clusterprofiler: An R Package for Comparing Biological Themes Among Gene Clusters. *Omics* (2012) 16:284–7. doi: 10.1089/omi.2011.0118
37. Zhang XJ, Zhang XY, Zhang N, Guo X, Peng KS, Wu H, et al. Distinctive Structural Hallmarks and Biological Activities of the Multiple Cathelicidin Antimicrobial Peptides in a Primitive Teleost Fish. *J Immunol* (2015) 194:4974–87. doi: 10.4049/jimmunol.1500182
38. Wu N, Zhang XY, Huang B, Zhang N, Zhang XJ, Guo X, et al. Investigating the Potential Immune Role of Fish NCAMs: Molecular Cloning and Expression Analysis in Mandarin Fish. *Fish Shellfish Immun* (2015) 46:765–77. doi: 10.1016/j.fsi.2015.08.006
39. Campadelli-Fiume G, Collins-McMillen D, Gianni T, Yurochko AD. Integrins as Herpesvirus Receptors and Mediators of the Host Signalosome. *Annu Rev Virol* (2016) 3:215–36. doi: 10.1146/annurev-virology-110615-035618
40. Azab W, Gramatica A, Herrmann A, Osterrieder N. Binding of Alphaherpesvirus Glycoprotein H to Surface Alpha4beta1-Integrins Activates Calcium-Signaling Pathways and Induces Phosphatidylserine Exposure on the Plasma Membrane. *mBio* (2015) 6:e01552–01515. doi: 10.1128/mBio.01552-15
41. Cheshenko N, Trepanier JB, Gonzalez PA, Eugenin EA, Jacobs WRJr., Herold BC. Herpes Simplex Virus Type 2 Glycoprotein H Interacts With Integrin Alphavbeta3 to Facilitate Viral Entry and Calcium Signaling in Human Genital Tract Epithelial Cells. *J Virol* (2014) 88:10026–38. doi: 10.1128/JVI.00725-14
42. Delecluse S, Tsai MH, Shumilov A, Bencun M, Arrow S, Beshirova A, et al. Epstein-Barr Virus Induces Expression of the LPAM-1 Integrin in B Cells. *Vitro Vivo J Virol* (2019) 93(5):e01618–18. doi: 10.1128/JVI.01618-18
43. Huang WJ, Shen Y, Xu XY, Hu MY, Li JL. Identification and Characterization of the TLR18 Gene in Grass Carp (*Ctenopharyngodon Idella*). *Fish Shellfish Immunol* (2015) 47:681–8. doi: 10.1016/j.fsi.2015.09.052
44. Lee PT, Zou J, Holland JW, Martin SA, Collet B, Kanellos T, et al. Identification and Characterisation of TLR18-21 Genes in Atlantic Salmon (*Salmo Salar*). *Fish Shellfish Immunol* (2014) 41:549–59. doi: 10.1016/j.fsi.2014.10.006
45. Jiang X, He M, Bai J, Chan CB, Wong AOL. Signal Transduction for TNFalpha-Induced Type II SOCS Expression and Its Functional Implication in Growth Hormone Resistance in Carp Hepatocytes. *Front Endocrinol (Lausanne)* (2020) 11:20. doi: 10.3389/fendo.2020.00020
46. Wang W, Cole AM, Hong T, Waring AJ, Lehrer RI. Retrocyclin, an Antiretroviral Theta-Defensin, Is a Lectin. *J Immunol* (2003) 170:4708–16. doi: 10.4049/jimmunol.170.9.4708
47. Zhu D, Fu P, Huang R, Xiong L, Wang Y, He L, et al. Molecular Characterization, Tissue Distribution and Functional Analysis of Galectin 1-Like 2 in Grass Carp (*Ctenopharyngodon Idella*). *Fish Shellfish Immunol* (2019) 94:455–63. doi: 10.1016/j.fsi.2019.09.041
48. Ghosh A, Banerjee A, Amzel LM, Vasta GR, Bianchet MA. Structure of the Zebrafish Galectin-1-L2 and Model of its Interaction With the Infectious Hematopoietic Necrosis Virus (IHNV) Envelope Glycoprotein. *Glycobiology* (2019) 29:419–30. doi: 10.1093/glycob/cwz015
49. Wu C, Zhao X, Babu VS, Yuan G, Wang W, Su J, et al. Distribution of Mannose Receptor in Blunt Snout Bream (*Megalobrama Amblycephala*) During the Embryonic Development and its Immune Response to the Challenge of Aeromonas Hydrophila. *Fish Shellfish Immunol* (2018) 78:52–9. doi: 10.1016/j.fsi.2018.03.049
50. Schneider JR, Shen X, Orlandi C, Nyanhete T, Sawant S, Carias AM, et al. A MUC16 IgG Binding Activity Selects for a Restricted Subset of IgG Enriched for Certain Simian Immunodeficiency Virus Epitope Specificities. *J Virol* (2020) 94(5):e01246–19.94. doi: 10.1128/JVI.01246-19
51. Tang MLK. The Physiological Induction of Tolerance to Allergens, Allergy. In: *Allergy, Immunity and Tolerance in Early Childhood*. Academic Press, Elsevier Inc (2016).
52. Li L, Yang W, Shen Y, Xu X, Li J. Fish Complement C8 Evolution, Functional Network Analyses, and the Theoretical Interaction Between C8 Alpha Chain and CD59. *Mol Immunol* (2020) 128:235–48. doi: 10.1016/j.molimm.2020.10.013
53. Pionnier N, Adamek M, Miest JJ, Harris SJ, Matras M, Rakus KL, et al. C-Reactive Protein and Complement as Acute Phase Reactants in Common Carp (*Cyprinus Carpio*) During CyHV-3 Infection. *Dis Aquat Organ* (2014) 109:187–99. doi: 10.3354/dao02727
54. Magnadottir B, Gudmundsdottir S, Lange S. A Novel Ladder-Like Lectin Relates to Sites of Mucosal Immunity in Atlantic Halibut (*Hippoglossus Hippoglossus L.*). *Fish Shellfish Immunol* (2019) 87:9–12. doi: 10.1016/j.fsi.2018.12.034
55. Ryu JG, Lee J, Kim EK, Seo HB, Park JS, Lee SY, et al. Treatment of IL-21r-Fc Control Autoimmune Arthritis *via* Suppression of STAT3 Signal Pathway Mediated Regulation of the Th17/Treg Balance and Plasma B Cells. *Immunol Lett* (2015) 163:143–50. doi: 10.1016/j.imlet.2014.09.007
56. Moens E, Brouwer M, Dimova T, Goldman M, Willems F, Vermijlen D. IL-23R and TCR Signaling Drives the Generation of Neonatal Vgamma9Vdelta2 T Cells Expressing High Levels of Cytotoxic Mediators and Producing IFN-Gamma and IL-17. *J Leukoc Biol* (2011) 89:743–52. doi: 10.1189/jlb.0910501
57. Zhang YB, Gui JF. Molecular Regulation of Interferon Antiviral Response in Fish. *Dev Comp Immunol* (2012) 38:193–202. doi: 10.1016/j.dci.2012.06.003
58. Langevin C, Levraud JP, Boudinot P. Fish Antiviral Tripartite Motif (TRIM) Proteins. *Fish Shellfish Immunol* (2019) 86:724–33. doi: 10.1016/j.fsi.2018.12.008
59. Shanware NP, Bray K, Abraham RT. The PI3K, Metabolic, and Autophagy Networks: Interactive Partners in Cellular Health and Disease. *Annu Rev Pharmacol* (2013) 53:89–106. doi: 10.1146/annurev-pharmtox-010611-134717
60. Wu M, Dan C, Gui JF, Zhang YB. Fish Species-Specific TRIM Gene FTRCA1 Negatively Regulates Interferon Response Through Attenuating IRF7 Transcription. *Fish Shellfish Immunol* (2019) 90:180–7. doi: 10.1016/j.fsi.2019.04.297
61. Wu M, Zhao X, Gong XY, Wang Y, Gui JF, Zhang YB. FTRCA1, a Species-Specific Member of finTRIM Family, Negatively Regulates Fish IFN Response Through Autophage-Lysosomal Degradation of TBK1. *J Immunol* (2019) 202:2407–20. doi: 10.4049/jimmunol.1801645
62. Kongchum P, Palti Y, Hallerman EM, Hulata G, David L. SNP Discovery and Development of Genetic Markers for Mapping Innate Immune Response Genes in Common Carp (*Cyprinus Carpio*). *Fish Shellfish Immunol* (2010) 29:356–61. doi: 10.1016/j.fsi.2010.04.013
63. Wei JG, Zang SQ, Xu M, Zheng QJ, Chen XL, Qin QW. TRAF6 is a Critical Factor in Fish Immune Response to Virus Infection. *Fish Shellfish Immun* (2017) 60:6–12. doi: 10.1016/j.fsi.2016.11.008
64. Kim HS, Sohn H, Jang SW, Lee GR. The Transcription Factor NFIL3 Controls Regulatory T-Cell Function and Stability. *Exp Mol Med* (2019) 51:80. doi: 10.1038/s12276-019-0280-9
65. Yu H, Shen Y, Sun J, Xu X, Wang R, Xuan Y, et al. Molecular Cloning and Functional Characterization of the NFIL3/E4BP4 Transcription Factor of

Grass Carp, Ctenopharyngodon Idella. *Dev Comp Immunol* (2014) 47:215–22. doi: 10.1016/j.dci.2014.07.019
66. Szymczak M. Distribution of Cathepsin D Activity Between Lysosomes and a Soluble Fraction of Marinating Brine. *J Food Sci* (2016) 81:E1966–70. doi: 10.1111/1750-3841.13375
67. Kumar R, Khandelwal N, Thachamvally R, Tripathi BN, Barua S, Kashyap SK, et al. Role of MAPK/MNK1 Signaling in Virus Replication. *Virus Res* (2018) 253:48–61. doi: 10.1016/j.virusres.2018.05.028
68. Xuan MH, Yan XL, Liu XZ, Xu TJ. IRF1 Negatively Regulates NF-Kappa B Signaling by Targeting MyD88 for Degradation in Teleost Fish. *Dev Comp Immunol* (2020) 110:103709. doi: 10.1016/j.dci.2020.103709
69. Yan X, Zhao X, Huo R, Xu T. IRF3 and IRF8 Regulate NF-kappaB Signaling by Targeting MyD88 in Teleost Fish. *Front Immunol* (2020) 11:606. doi: 10.3389/fimmu.2020.00606
70. Feng X, Liu X, Zhang W, Xiao W. P53 Directly Suppresses BNIP3 Expression to Protect Against Hypoxia-Induced Cell Death. *EMBO J* (2011) 30:3397–415. doi: 10.1038/emboj.2011.248
71. Godoy-Lugo JA, Miranda-Cruz MM, Rosas-Rodriguez JA, Adan-Bante NP, Icedo-Garcia R, Sonanez-Organis JG. Hypoxia Inducible Factor -1 Regulates WSSV-Induced Glycolytic Genes in the White Shrimp Litopenaeus Vannamei. *Fish Shellfish Immunol* (2019) 92:165–71. doi: 10.1016/j.fsi.2019.05.040
72. Lepelletier Y, Moura IC, Hadj-Slimane R, Renand A, Fiorentino S, Baude C, et al. Immunosuppressive Role of Semaphorin-3A on T Cell Proliferation is Mediated by Inhibition of Actin Cytoskeleton Reorganization. *Eur J Immunol* (2006) 36:1782–93. doi: 10.1002/eji.200535601
73. Alamri A, Soussi Gounni A, Kung SKP. View Point: Semaphorin-3E: An Emerging Modulator of Natural Killer Cell Functions? *Int J Mol Sci* (2017) 18:2337. doi: 10.3390/ijms18112337
74. Yan Y, Cui H, Guo C, Wei J, Huang Y, Li L, et al. Singapore Grouper Iridovirus-Encoded Semaphorin Homologue (SGIV-Sema) Contributes to Viral Replication, Cytoskeleton Reorganization and Inhibition of Cellular Immune Responses. *J Gen Virol* (2014) 95:1144–55. doi: 10.1099/vir.0.060608-0
75. Laranjeiro R, Tamai TK, Peyric E, Krusche P, Ott S, Whitmore D. Cyclin-Dependent Kinase Inhibitor P20 Controls Circadian Cell-Cycle Timing. *Proc Natl Acad Sci USA* (2013) 110:6835–40. doi: 10.1073/pnas.1217912110
76. Rivera-Soto R, Dissinger NJ, Damania B. Kaposi's Sarcoma-Associated Herpesvirus Viral Interleukin-6 Signaling Upregulates Integrin Beta3 Levels and Is Dependent on STAT3. *J Virol* (2020) 94(5):e01384–19. doi: 10.1128/JVI.01384-19
77. Kalkman HO, Feuerbach D. Antidepressant Therapies Inhibit Inflammation and Microglial M1-Polarization. *Pharmacol Ther* (2016) 163:82–93. doi: 10.1016/j.pharmthera.2016.04.001
78. Frakolaki E, Kalliampakou KI, Kaimou P, Moraiti M, Kolaitis N, Boleti H, et al. Emerging Role of L-Dopa Decarboxylase in Flaviviridae Virus Infections. *Cells* (2019) 8(8):837. doi: 10.3390/cells8080837
79. Rakus KL, Irnazarow I, Adamek M, Palmeira L, Kawana Y, Hirono I, et al. Gene Expression Analysis of Common Carp (Cyprinus Carpio L.) Lines During Cyprinid Herpesvirus 3 Infection Yields Insights Into Differential Immune Responses. *Dev Comp Immunol* (2012) 37:65–76. doi: 10.1016/j.dci.2011.12.006
80. Zhang H, Xiao Y, Zhu Z, Li B, Greene MI. Immune Regulation by Histone Deacetylases: A Focus on the Alteration of FOXP3 Activity. *Immunol Cell Biol* (2012) 90:95–100. doi: 10.1038/icb.2011.101
81. Jin H, Guo X. Valproic Acid Ameliorates Coxsackievirus-B3-Induced Viral Myocarditis by Modulating Th17/Treg Imbalance. *Virol J* (2016) 13:168. doi: 10.1186/s12985-016-0626-z
82. Sugimoto K, Itoh T, Takita M, Shimoda M, Chujo D, SoRelle JA, et al. Improving Allogeneic Islet Transplantation by Suppressing Th17 and Enhancing Treg With Histone Deacetylase Inhibitors. *Transpl Int* (2014) 27:408–15. doi: 10.1111/tri.12265
83. Moreira JD, Koch BEV, van Veen S, Walburg KV, Vrieling F, Guimaraes TMPD, et al. Functional Inhibition of Host Histone Deacetylases (HDACs) Enhances *In Vitro* and *In Vivo* Anti-Mycobacterial Activity in Human Macrophages and in Zebrafish. *Front Immunol* (2020) 11:36. doi: 10.3389/fimmu.2020.00036
84. Wang QQ, Li N, Wang XJ, Shen JG, Hong XJ, Yu H, et al. Membrane Protein hMYADM Preferentially Expressed in Myeloid Cells Is Up-Regulated During Differentiation of Stem Cells and Myeloid Leukemia Cells. *Life Sci* (2007) 80:420–9. doi: 10.1016/j.lfs.2006.09.043
85. Parekh NJ, Krouse TE, Reider IE, Hobbs RP, Ward BM, Norbury CC. Type I Interferon-Dependent CCL4 Is Induced by a cGAS/STING Pathway That Bypasses Viral Inhibition and Protects Infected Tissue, Independent of Viral Burden. *PloS Pathog* (2019) 15(10):e1007778. doi: 10.1371/journal.ppat.1007778
86. Eisenberg RJ, Ponce de Leon M, Friedman HM, Fries LF, Frank MM, Hastings JC, et al. Complement Component C3b Binds Directly to Purified Glycoprotein C of Herpes Simplex Virus Types 1 and 2. *Microb Pathog* (1987) 3:423–35. doi: 10.1016/0882-4010(87)90012-x
87. Busse DC, Habgood-Coote D, Clare S, Brandt C, Bassano I, Kaforou M, et al. Interferon-Induced Protein 44 and Interferon-Induced Protein 44-Like Restrict Replication of Respiratory Syncytial Virus. *J Virol* (2020) 94(18):e00297–20. doi: 10.1128/JVI.00297-20
88. Rose PP, Hanna SL, Spiridigliozzi A, Wannissorn N, Beiting DP, Ross SR, et al. Natural Resistance-Associated Macrophage Protein Is a Cellular Receptor for Sindbis Virus in Both Insect and Mammalian Hosts. *Cell Host Microbe* (2011) 10:97–104. doi: 10.1016/j.chom.2011.06.009
89. Jensen P. Structure and Function of Plasminogen Activator Inhibitor-2. *Int J Oncol* (1997) 11:557–70. doi: 10.3892/ijo.11.3.557
90. Tao R, Li J, Xin J, Wu J, Guo J, Zhang L, et al. Methylation Profile of Single Hepatocytes Derived From Hepatitis B Virus-Related Hepatocellular Carcinoma. *PloS One* (2011) 6:e19862. doi: 10.1371/journal.pone.0019862
91. Nita-Lazar M, Mancini J, Feng C, Gonzalez-Montalban N, Ravindran C, Jackson S, et al. The Zebrafish Galectins Drgal1-L2 and Drgal3-L1 Bind *In Vitro* to the Infectious Hematopoietic Necrosis Virus (IHNV) Glycoprotein and Reduce Viral Adhesion to Fish Epithelial Cells. *Dev Comp Immunol* (2016) 55:241–52. doi: 10.1016/j.dci.2015.09.007

Conflict of Interest: The authors declare that the research was conducted in the absence of any commercial or financial relationships that could be construed as a potential conflict of interest.

frontiers in Immunology

ORIGINAL RESEARCH
published: 24 August 2021
doi: 10.3389/fimmu.2021.725150

Cyprinus carpio TRIF Participates in the Innate Immune Response by Inducing NF-κB and IFN Activation and Promoting Apoptosis

Rongrong Liu†, Xiaoye Liu†, Meijiao Song, Yue Qi, Hua Li, Guiwen Yang and Shijuan Shan**

Shandong Provincial Key Laboratory of Animal Resistance Biology, College of Life Sciences, Shandong Normal University, Jinan, China

TRIF, an important adaptor downstream of Toll-like receptor signaling, plays a critical role in the innate immune response. In this study, the full-length coding sequence of TRIF from common carp (*Cyprinus carpio* L.) was cloned and characterized. Bioinformatics analysis showed that common carp TRIF exhibited a conserved TIR domain and had the closest relationship with grass carp TRIF. Expression analysis revealed that TRIF was constitutively expressed in the examined tissues of common carp, with the highest expression in the spleen and the lowest expression in the head kidney, and could be upregulated under *Aeromonas hydrophila* and poly(I:C) stimulation *in vivo* and under poly (I:C), LPS, PGN, flagellin, and Pam3CSK4 stimulation *in vitro*. Laser confocal microscopy showed that common carp TRIF colocalized with the Golgi apparatus. A luciferase reporter assay showed that carp TRIF elicited the activity of ifn-1 and nf-κb through the C-terminal domain. Additionally, crystal violet staining and qPCR assays revealed that carp TRIF inhibited the replication of SVCV in epithelioma papulosum cyprini (EPC) cells. Then, the signaling downstream of carp TRIF was investigated. Coimmunoprecipitation and Western blotting analysis demonstrated that carp TRIF interacted with TBK1 and augmented the expression of TRAF6 and phosphorylation of TBK1. Overexpression of carp TRIF significantly enhanced the expression of interferon-stimulated genes and inflammatory cytokines. Furthermore, flow cytometric (FCM) analysis suggested that carp TRIF induced apoptosis through the activation of caspase-8. In summary, our study indicated that TRIF plays an essential role in the innate immune responses of common carp against bacterial and viral infection.

Keywords: ***Cyprinus carpio*** **L., TRIF, cellular localization, signaling pathway, apoptosis**

OPEN ACCESS

Edited by:
Maria Del Mar Ortega-Villaizan, Miguel Hernández University of Elche, Spain

Reviewed by:
Patricia Pereiro, Consejo Superior de Investigaciones Científicas (CSIC), Spain
Magdalena Chadzińska, Jagiellonian University, Poland

****Correspondence:***
Guiwen Yang
yanggw@sdnu.edu.cn
Shijuan Shan
shansj@sdnu.edu.cn

†These authors have contributed equally to this work and share first authorship

Specialty section:
This article was submitted to Comparative Immunology, a section of the journal Frontiers in Immunology

Received: *15 June 2021*
Accepted: *02 August 2021*
Published: *24 August 2021*

Citation:
Liu R, Liu X, Song M, Qi Y, Li H, Yang G and Shan S (2021) Cyprinus carpio TRIF Participates in the Innate Immune Response by Inducing NF-κB and IFN Activation and Promoting Apoptosis. Front. Immunol. 12:725150. doi: 10.3389/fimmu.2021.725150

INTRODUCTION

Innate immunity plays a crucial role as the first line of defense protecting both lower and higher eukaryotes against pathogenic invasion (1). The mechanism of innate immunity relies on a family of proteins characterized by a highly specialized structure often termed pattern recognition receptors (PRRs) that recognize conserved pathogen-associated molecular patterns (PAMPs) or damage-associated molecular patterns (DAMPs) (2). Toll-like receptors (TLRs), an evolutionary ancient family of PRRs, have been extensively studied over the recent decades (3). Upon the recognition of microbes, TLRs immediately recruit and bind distinct Toll/IL-1 recruitment (TIR) domain-containing adaptor molecules in the cytoplasm (4). To date, six adaptors of TLRs have been identified, although the Toll receptor–associated molecule (TRAM) is absent in teleost genomes (5).

Toll-interleukin 1 receptor domain-containing adaptor molecule (TICAM-1, also named TRIF) is the third TIR domain-containing adaptor protein to be described (6). It has been well documented that TRIF is essential for the TLR3- and TLR4-mediated production of type-I IFN and other proinflammatory mediators in mammals (6, 7). Mammalian TRIF consists of an N-terminal proline-rich region (PRR), a highly conserved TIR domain, and a C-terminal domain that harbors a receptor-interacting protein 1 (RIP1) interaction motif (RHIM) (8). TNF receptor-associated factor (TRAF) 6 and TANK-binding kinase (TBK)-1 interact with TRIF through the N-terminal portion of TRIF, which is crucial for IRF3 and NF-κB activation (7, 9). The TIR domain of TRIF interacts with the TIR domain of TLR3 as well as the TLR4-bridging adaptor TRAM (6, 10). The C-terminal RIP homotypic interaction motif (RHIM) is crucial for NF-κB activation and apoptosis (11–13).

The first sequence of nonmammalian TRIF was found in the catfish genome (14). To date, the complete coding sequence of TRIF has been reported only in the channel catfish (*Ictalurus punctatus*) (15), zebrafish (*Danio rerio*) (16), grass carp (*Ctenopharyngodon idella*) (17), orange-spotted grouper (*Epinephelus coioides*) (18), large yellow croaker (*Larimichthys crocea*) (19), fugu (*Takifugu rubripes*) (20), and black carp (*Mylopharyngodon piceus*) (21). An increasing number of studies have recognized that fish TRIF gene expression can be modulated by bacterial PAMPs, including channel catfish, orange-spotted grouper, and large yellow croaker (15, 18, 19). In other teleost fish, such as zebrafish and grass carp, TRIF can respond to poly(I:C) and grass carp reovirus (GCRV) stimulation (16, 22). In addition, as an adaptor, fish TRIF can execute signal transduction by associating with TBK1 and then phosphorylating IRF3/7, inducing the transcription of IFN-β and other IFN-regulated genes (8). Furthermore, fish TRIF was reported to inhibit virus replication (17, 18). However, the mechanism remains unclear.

Common carp (*Cyprinus carpio* L.) is one of the most important freshwater aquaculture species and an important economic asset for angling and fisheries (23). However, various viruses and bacteria cause serious diseases in common carp, resulting in a high mortality rate and enormous economic losses to the aquaculture industry (24). Therefore, it is imperative to study the immune-related genes of common carp to develop useful treatment strategies for disease prevention and control in common carp (25). In this study, the TRIF gene from common carp was cloned. Its gene expression pattern and immune modulation function were analyzed. In addition, the role of common carp TRIF in the host innate immune responses was studied. These results can lay a foundation for research on the mechanisms of resistance to pathogens and help us to better understand the biological characteristics of TRIF in teleosts.

MATERIALS AND METHODS

Animals and Immune Challenge

Healthy common carp (average weight: 180 g) were purchased from a local fish farm and cultured at 22–25°C in recirculating tap water with commercial fish feed for more than one week prior to experimental use. The immune challenges method and concentration were performed according to the previously described protocols (26). Briefly, fish were injected intraperitoneally with formalin (overnight at 4°C in 0.5% formalin), inactivated *Aeromonas hydrophila* (2×10^7 CFU per fish) and poly(I:C) (1.6 mg/ml) in a volume of 500 μl. Fish in the control group were injected with the same amount of PBS. The samples were collected from three infected fish at different time points after stimulation (0, 3, 6, 12, 24, 72, and 168 h). Tissue samples were stored in liquid nitrogen until subsequent analyses.

Ribonucleic Acid (RNA) Extraction, Complementary DNA (cDNA) Synthesis, and Real-Time Polymerase Chain Reaction (PCR)

The total RNA of cells and various tissues were extracted using the RNA simple Total RNA Kit (Tiangen, China) according to the instructions of the manufacturer. The total RNA concentration and quality were measured by ultraviolet spectrophotometry (Thermo Fisher Scientific, USA). First-strand cDNA was then synthesized using the FastQuant RT Kit (with gDNase) (Tiangen) following the protocol of the manufacturer. The mRNA expression of target genes was quantified using the SYBR Premix Ex Taq II reagent (Takara, China) and a LightCycler 96 real-time PCR system (Roche, Switzerland). The amplification scheme was as follows: incubation for 30 s at 94°C followed by 40 cycles of 5 s at 94°C, 30 s at 60°C, and 50 s at 70°C. The mRNA expression levels of tissues and cells were normalized to the expression levels of s11 and EF-1α, respectively. The data were analyzed using the $2^{-\Delta\Delta CT}$ method as described previously (27). Primers are listed in **Supplementary Table 1**.

Gene Cloning and Plasmid Construction

To obtain the full-length cDNA of the sequence of common carp TRIF, the partial sequence of TRIF was cloned from common carp using a pair of primers specific to the conserved region of the reported TRIF sequence. Then, 5′ and 3′ RACE-PCR were performed using a 3′-full RACE core set (Takara, China) and

SMARTer® RACE 5′ Kit (Clontech, USA) according to the instructions of the manufacturer.

To construct the expression of plasmid for GFP-tagged, carp TRIF, or truncated forms including △N (deletion of amino acids 9–158), △TIR domain (deletion of amino acids 324–451), and △C (deletion of amino acids 452–578) were amplified by PCR and inserted into the pEGFP-N1 vector through the appropriate enzyme digestion site to obtain the TRIF-FL-EGFP, TRIF-△N-EGFP, TRIF-△TIR-EGFP, and TRIF-△C-EGFP vectors, respectively. The open reading frames (ORFs) of carp TBK1 was subcloned into the pCMV-HA vector and obtained HA-tagged TBK1 plasmid. For dual-luciferase reporter assays, the 5′ flanking region upstream of the start codon ATG in the *ifn-1* gene was cloned into the PGL4.10 basic plasmid. The generated recombined plasmid was named Luci-*ifn-1*. All constructs were verified by DNA sequencing. The primers used in this study are listed in **Supplementary Table 1**. The luciferase reporter plasmid of *nf-κb* was kindly provided by GuangXun Meng (Institute Pasteur of Shanghai, Chinese Academy of Sciences, China).

Sequence Analysis

The protein structures of the target genes were predicted by NCBI and SWISS-MODEL. Multiple alignment analysis was performed using Clustal W, and the results were viewed and edited with the BioEdit software. A phylogenetic tree was constructed using the neighbor-joining method and MEGA 6.0 software. To derive the confidence value for the phylogenetic analysis, boot-strap trials were replicated 1,000 times. The GenBank accession numbers for these sequences are shown in **Supplementary Table 2**.

Isolation and Stimulation of Common Carp Peripheral Blood Leukocytes (PBLs)

Common carp PBLs were prepared by density gradient centrifugation with Percoll (Sigma-Aldrich, Germany) according to a previous protocol (27). Briefly, for the isolation of PBLs, diluted blood was layered on top of 65% Percoll and centrifuged. After 25 min of centrifugation at 800 × g, the cells present on the interface of the gradient were collected and washed three times with PBS. The cells were resuspended in complete L-15 (Gibco, USA) supplemented with 10% fetal bovine serum (Gibco) and 1% penicillin-streptomycin (Gibco). Approximately 10^7 cells/well were seeded in 24-well plates with 500 μl of complete medium. After recovering overnight at 25°C, drug treatment was performed using poly(I:C) (a synthetic analogue of double-stranded RNA) (5 μg/ml, Sigma-Aldrich), LPS (a component of the outer membranes of gram-negative bacteria) (10 μg/ml, Sigma-Aldrich), peptidoglycan (PGN) (the main PAMP of gram-positive bacteria) (10 μg/ml, Sigma-Aldrich), flagellin (a principal component of bacterial flagella) (10 ng/ml, Sigma-Aldrich), and Pam3CSK4 (a synthetic triacylated lipopeptide that can be recognized by TLR1/2) (10 ng/ml, Invitrogen, USA) at different time points (3, 6, 12, and 24 h) according to the previously described protocols (28). The cells in the control group were stimulated with the same amounts of PBS (denoted by 0 h).

Cell Culture, Transfections, and Virus

The 293T and HeLa cells maintained in our laboratory were cultured in DMEM (Gibco) supplemented with 10% fetal bovine serum (Gibco) and 1% penicillin-streptomycin (Gibco) in an incubator at 37°C and 5% CO_2. Epithelioma papulosum cyprini (EPC) cells were cultured at 25°C in M199 medium (Gibco) supplemented with 10% fetal bovine serum (Gibco) and 1% penicillin-streptomycin (Gibco). Lipofectamine 2000 (Invitrogen), Fugene HD (Promega, USA), and jetPRIME reagent (Polyplus, France) were used for 293T, HeLa, and EPC cell transfection, respectively.

Spring viremia of carp virus (SVCV) were kept in the lab and propagated in EPC cells. Viral titers were measured according to the method of Reed and Muench (29). Cytopathic effect (CPE) was observed by crystal violet staining. Briefly, EPC cells were seeded in 24-well plates and transfected with the indicated plasmids. After 24 h, the cells were infected with SVCV for 24 h. The infected EPC cells were washed with PBS and fixed with 4% formaldehyde for 30 min at room temperature, stained with 1% (w/v) crystal violet for 10 min, and then washed with PBS and observed for CPE by a microscope.

Luciferase Activity Assays

To determine the effects of carp TRIF on the regulation of *nf-κb* and *ifn-1* activity, luciferase assays were performed. 293T cells were seeded in 96-well plates 12 h before transfection. Cells were transfected with Luci-*ifn-1* or Luci-*nf-κb* and pRL-TK (internal control) along with different carp TRIF-overexpressing plasmids. After 24 h of transfection, cells were lysed and analyzed for luciferase activity by Dual-Glo® Reagent (Promega). The relative luciferase activity was calculated by normalizing *Firefly* to *Renilla* luciferase activity. All experiments were performed in triplicate and repeated at least three times.

Confocal Fluorescence Microscopy

HeLa cells were seeded onto coverslips in 24-well plates. After reaching 70–90% confluence, cells were transfected with TRIF-FL-EGFP, TRIF-△N-EGFP, TRIF-△TIR-EGFP, and TRIF-△C-EGFP for 24 h, respectively. Then, cells on coverslips were washed once with PBS, fixed with 4% paraformaldehyde for 30 min, and stained with WGA (cytomembrane-Tracker) (InvivoGen, France) for 10 min and DAPI (Sigma-Aldrich) for 15 min. For Golgi staining, the cells were washed once with HBSS and stained with Golgi-Tracker (Beyotime, China) at 4°C for 30 min. Finally, the coverslips were washed with PBS and observed by the Leica laser scanning confocal microscope. The results were indicated from three independent replicates.

Coimmunoprecipitation (Co-IP) and Western Blotting Analysis

For immunoprecipitation (IP) experiments, 3 μg of the indicated plasmids were transfected into 293T cells, which were cultured in 6-well plates overnight. After 48 h of transfection, the medium was removed carefully and washed twice with PBS. Then, the cells were lysed with 600 μl of lysis buffer (1% NP-40, 50 mM Tris-HCl, 150

mM NaCl, 15 mM EDTA, 1 mM NaF, 1 mM Na3VO4, pH 8.0) containing a protease inhibitor cocktail at 4°C for 30 min. The cellular fragments were separated by centrifugation at 12,000 × g for 10 min at 4°C. After centrifugation, the supernatants were transferred into a new centrifuge tube (50 μl of cell lysate was designated as the input). The remaining cell lysates were incubated with protein A/G agarose (Santa Cruz, USA) and monoclonal anti-GFP (Solarbio, China, K106580P, 1:10 diluted with lysis buffer) overnight at 4°C with soft agitation. The agarose-protein complex was harvested and washed three times with a lysis buffer and resuspended in 15 μl of 2 × SDS-PAGE loading buffer (designated as IP). Equal loadings of samples (IP and input) were analyzed by Western blot (WB) with anti-GFP and anti-HA (Abcam, England, ab9110) Abs, respectively.

The generated cell lysates were boiled for 10 min, subjected to 10% SDS-PAGE, and transferred onto PVDF membranes (Sigma-Aldrich). The membranes were blocked with 5% nonfat milk (diluted in TBST buffer; 150 mM NaCl, 3 mM EDTA, 0.1% Tween-20, 50 mM Tris-HCl, pH 8.0) for 1 h at room temperature and incubated with primary antibodies: anti-GFP, anti-TRAF6 (Abcam, ab245319), anti-pTBK1 (CST, USA, D52C2), anti-HA, anti-caspase-8 (CST, 8592S), and anti-β-actin (Solarbio, K200058M) (1:1,000 dilution in blocking milk solution) at 4°C overnight. The membrane was washed three times with TBST and probed with the relevant horseradish peroxidase (HRP)-conjugated secondary antibodies (Proteintech, USA) (1:10,000 dilution in 1% BSA dissolved in TBST) for 1 h at room temperature. Finally, the membrane was washed three times with TBST and processed for ECL Western blotting Detection Reagents (Meilunbio, China). The experiments were performed at least three times.

Flow Cytometric (FCM) Detection of Apoptotic Cells

Apoptotic cells were evaluated using the Annexin V-mCherry apoptosis detection kit (Beyotime, C1070S). The staining procedure was carried out according to the instructions of the manufacturer. In brief, the EPC cells were seeded in 24-well plates overnight and transfected with pEGFP-N1 or carp TRIF-EGFP. At 24 h post-transfection, cells were harvested, then washed with PBS, and resuspended in Annexin V-mCherry Binding Buffer. Stained cells were incubated with 5 μl of Annexin V-mCherry for 10 min at room temperature in the dark. Then, the stained cells were checked with the FACS Calibur system (BD Biosciences, USA) and evaluated with the FlowJo software (TreeStar, Ashland, OR, USA). The results were calculated from three independent replicates.

Statistical Analysis

Values are presented as the mean ± SD of three independent experiments with technical replicates for each experiment. Data are processed using one- or two-way ANOVA or Tukey's test. A value of $P < 0.05$ was considered statistically significant ($^{*}P < 0.05$, $^{**}P < 0.01$, $^{***}P < 0.001$, $^{****}P < 0.0001$).

RESULTS

Identification of the TIR-Domain-Containing Adapter-Inducing Interferon-β (TRIF) Gene in Common Carp

In this study, we cloned and identified a novel TRIF cDNA sequence from common carp (*C. carpio* L.). The complete sequence of the carp TRIF cDNA (GenBank accession No. MZ169546) was 2,667 bp, containing a 5′ untranslated terminal region (UTR) of 343 bp, a 3′ UTR of 590 bp, and an open reading frame (ORF) of 1,734 bp encoding a polypeptide of 578 amino acids (aa) (**Supplementary Figure 1**). The protein structure predicted by SWISS-MODEL showed that carp TRIF exhibited the typical characteristics of an N-terminal domain, a TIR domain close to its C-terminus, and a C-terminal domain (**Figures 1A, B**). Multiple sequence alignment showed that the TIR domain of TRIF was conserved between common carp and other species, containing three highly conserved regions: Box 1, Box 2, and Box 3. In addition, carp TRIF lacks the N-terminal and C-terminal proline-rich domains (**Figure 1C** and **Supplementary Figure 2**).

To examine the evolutionary relationships of TRIF in common carp and other species, a phylogenetic tree was constructed using the neighbor-joining method based on the MEGA 6.0 program. Phylogenetic analysis showed that fish TRIF members formed an independent cluster and carp TRIF had the closest relationship with TRIF in *Ctenopharyngodon idella* and *Danio rerio* (**Figure 1D**). In addition, the identities of TRIF between common carp and other teleosts were 22.3–73.1%. Carp TRIF was highly similar to *C. idella* TRIF (73.1%) and had the lowest identity with *Takifugu rubripes* TRIF (30.5%) (**Supplementary Table 3**).

Tissue Expression Profile and Cellular Localization of TIR-Domain-Containing Adapter-Inducing Interferon-β (TRIF)

The expression patterns of TRIF were detected by qRT-PCR in 11 tissues of healthy common carp, including the liver, spleen, head kidney, foregut, hindgut, gills, gonad, skin, muscle, buccal epithelium, and brain. The results showed that carp TRIF mRNA was detected in all examined tissues, with the highest expression in the spleen, the lowest expression in the head kidney, and moderate expression in the other nine tissues (**Figure 2**).

To gain a better understanding of the functions of carp TRIF, its subcellular localization was investigated. HeLa cells were transfected with the TRIF-FL-EGFP, TRIF-△N-EGFP, TRIF-△TIR-EGFP, and TRIF-△C-EGFP recombinant vectors and then visualized by confocal microscopy. As illustrated in **Figure 3A**, carp TRIF was localized near the nuclear membrane with the formation of speckle-like structures. The site and structure were likely to be the Golgi apparatus. However, truncated carp TRIF segments had different localizations. The mutant in which the N-terminal domain was deleted showed the same localization as TRIF-FL-EGFP. The two mutants with truncated C-termini or TIR domains were ubiquitously

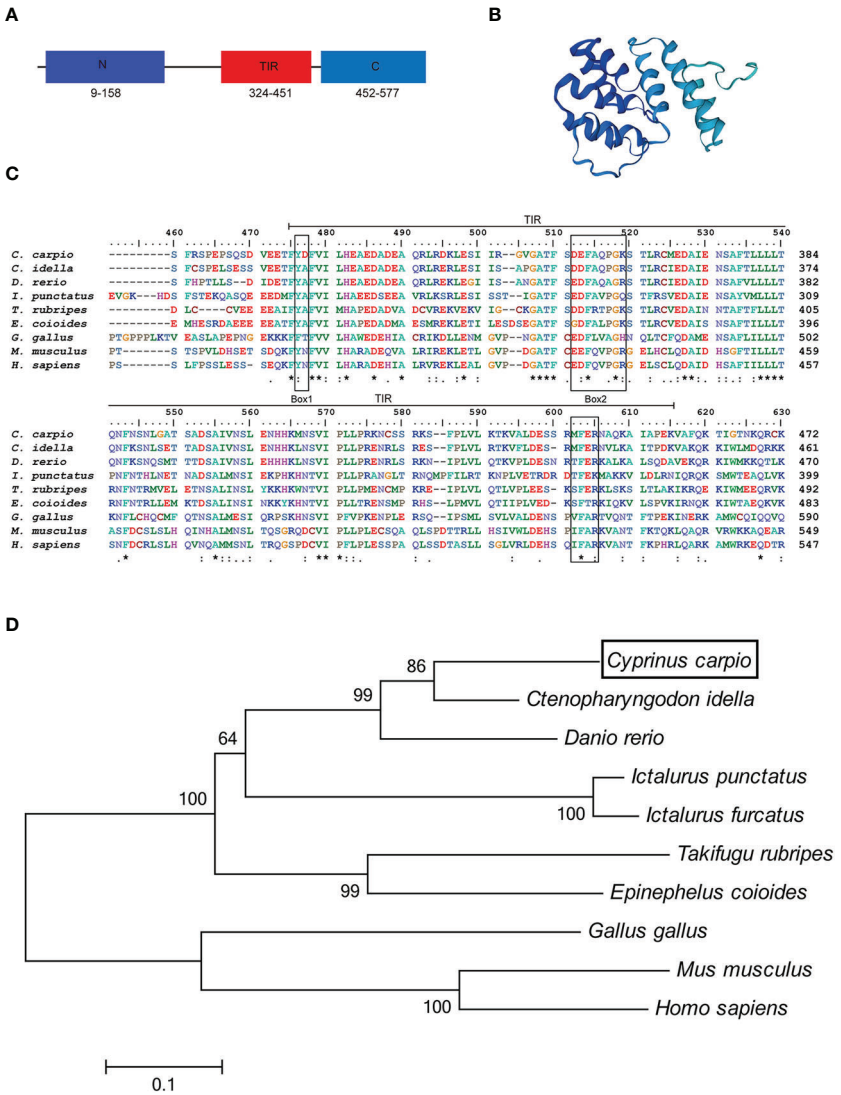

FIGURE 1 | Alignment of TRIF TIR domain sequences and phylogenetic tree. **(A)** A schematic diagram showing the domain architecture of common carp TRIF. **(B)** Modeled three-dimensional structure of common carp TRIF shown as a cartoon. **(C)** The sequences were aligned using the Clustal W method. The identical, conserved, and highly conserved substituted amino acid residues were indicated in (*), (.), and (:) respectively. The three boxes of the TIR domain were outlined in black. **(D)** Phylogenetic analysis of TRIF amino acid sequences. The phylogenetic tree was constructed using amino acid multiple alignments generated by the neighbor-joining method within the MEGA 6.0. program. Black box denoted carp TRIF. The GenBank accession numbers of these sequences are listed in **Supplementary Table 2**. A "*" represents amino acid residues identical among all the nine species in the designated site. One "*" represents amino acid residues identical among all the nine species in the column. "**" or "*****" indicates that the amino acid residues of the two or four consecutive sites are identical.

distributed in the cytoplasm. To further investigate whether carp TRIF was accurately localized to the Golgi apparatus, transfection and laser confocal imaging were conducted. The results demonstrated that TRIF-FL and the segment deleting the N-terminal domain were colocalized with the Golgi apparatus, while the two segments with truncated C termini or TIR domains were not similar (**Figure 3B**). These results reveal that carp TRIF is a Golgi-localized protein, and the sequence spanning the TIR domain and C-terminus contributes to its unique subcellular localization.

Expression Profiles of Carp TIR-Domain-Containing Adapter-Inducing Interferon-β (TRIF) After *A. hydrophila* and Poly(I:C) Injection

A. hydrophila, a well-known fish-pathogenic bacterium, is primarily found in temperate and freshwater environments and causes infections in various organisms (27). The expression profile of carp TRIF was examined in immune-related tissues after bacterial challenge. As illustrated in **Figure 4**, a significant upregulation of TRIF was observed in

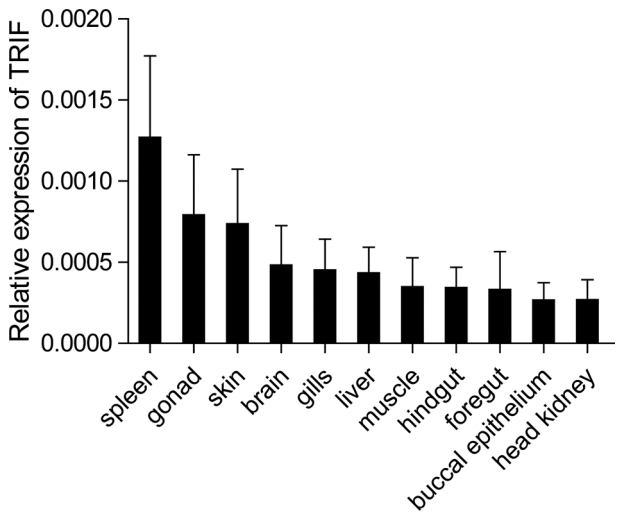

FIGURE 2 | Tissue expression of TRIF in normal common carp. The mRNA expression of carp TRIF in the liver, spleen, head kidney, foregut, hindgut, skin, gills, gonad, muscle, buccal epithelium, and brain was detected by real-time PCR. The 40S ribosomal protein s11 was amplified in each tissue sample as an internal control, n = 3.

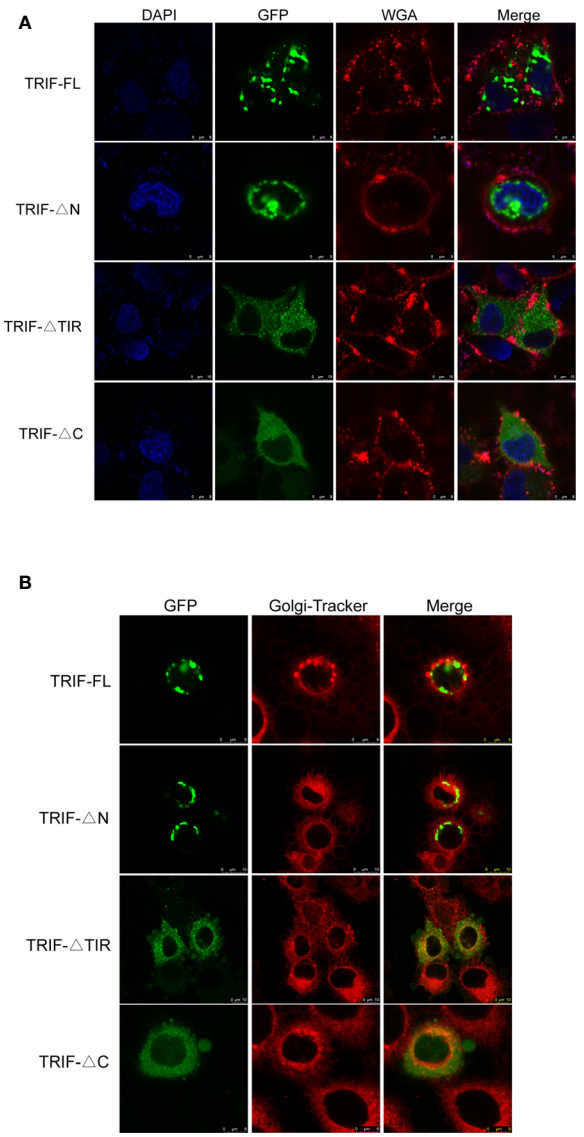

FIGURE 3 | Localization of full-length and truncated forms of carp TRIF. **(A)** Different mutants of carp TRIF, including TRIF-EGFP, TRIF-△N-EGFP, TRIF-△TIR-EGFP, or TRIF-△C-EGFP, were transfected into HeLa cells. At 24 h post-transfection, the cells were stained with WGA (cell membrane marker) and DAPI, then visualized by confocal laser microscopy. Red, green, and blue represented the cell membrane, carp TRIF, and nucleus, respectively. **(B)** HeLa cells were transfected with different mutants of carp TRIF, including TRIF-EGFP, TRIF-△N-EGFP, TRIF-△TIR-EGFP, or TRIF-△C-EGFP. At 24 h post-transfection, the cells were stained with Golgi-Tracker Red and imaged using a laser scanning confocal microscope. Green indicated the TRIF protein. The Golgi complex was stained in red.

the spleen, foregut, hindgut, and skin, whereas a downregulation was observed in the liver and head kidney. In the spleen and skin, TRIF expression was initially reduced, then increased and reached a peak at 168 h (1.8-fold) and 72 h (2.7-fold), respectively (**Figures 4B, F**). The expression of TRIF in the foregut and hindgut was significantly elevated and reached maximum levels at 3 h (2.0-fold and 7.5-fold, respectively) (**Figures 4D, E**). However, in the liver and head kidney, the expression of TRIF was downregulated (**Figures 4A, C**). These data suggest that TRIF, as an important adaptor of the TLR signaling pathway, has an important role in antibacterial immune responses.

Poly (I:C) is a synthetic analogue of double-stranded RNA (dsRNA) that is usually used as a viral infection mimic to induce the immune response (28). The role of carp TRIF in antiviral immunity was investigated. Common carp were injected intraperitoneally with poly(I:C), and the mRNA expression level of carp TRIF was detected at 3, 6, 12, 24, 48, 72, and 168 h post injection. After injection with poly(I:C), a significant upregulation of carp TRIF was observed in the liver, spleen, head kidney, foregut, and skin and reached the highest expression level at different time points (1.9-fold in liver, 5.4-fold in spleen, 3.1-fold in head kidney, 1.8-fold in foregut, and 1.8-fold in skin). No significant differences in carp TRIF expression was observed in the hindgut (**Figure 5**).

Carp TIR-Domain-Containing Adapter-Inducing Interferon-β (TRIF) mRNA Expression in Response to Different Stimuli *In Vitro*

As a TLR adapter, it was examined whether carp TRIF gene can respond to TLR ligands. Then, carp TRIF expression was determined after treatment with different immunostimulants in isolated PBLs. As shown in **Figure 6**, the expression of carp TRIF was significantly upregulated at 3 h and peaked at 6 and 12 h (53.54-fold, 3.12-fold) after stimulation with poly(I:C) and PGN, respectively (**Figures 6A, C**). After a challenge with LPS and Pam3CSK4, the expression of carp TRIF increased and reached the highest level at 12 h (4.79-fold and 5.77-fold, respectively)

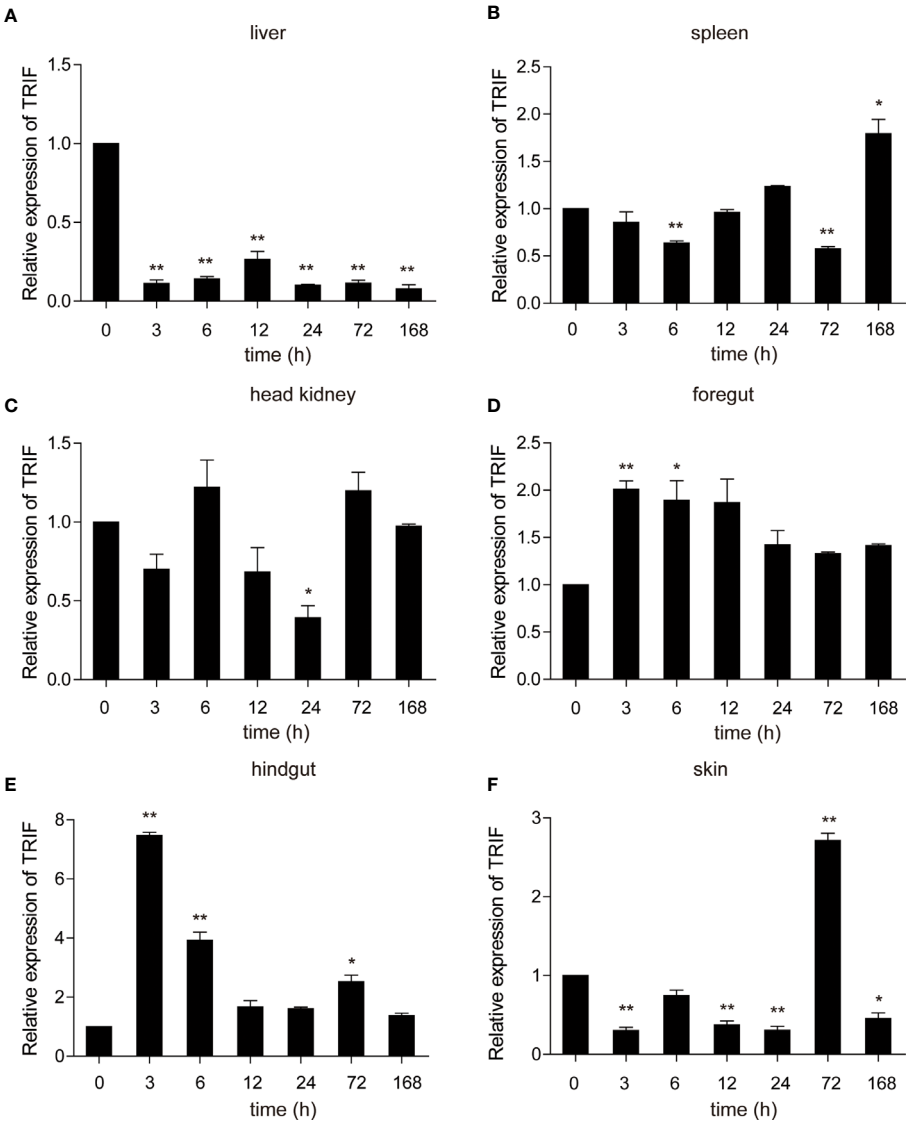

FIGURE 4 | The relative expression of carp TRIF in various tissues of common carp after intraperitoneal injection with *A. hydrophila*. The expression of carp TRIF in the liver **(A)**, spleen **(B)**, head kidney **(C)**, foregut **(D)**, hindgut **(E)**, and skin **(F)** at different time points are shown. The results were calculated relative to the expression of the 40S ribosomal protein s11. Data were presented as a fold increase compared to the unstimulated control group (denoted by 0 h). Means ± SD (n = 3), $^{*}P < 0.05$, $^{**}P < 0.01$.

(**Figures 6B, E**). In addition, carp TRIF expression was induced at 3 h and reached a peak value at 24 h (8.43-fold) after flagellin stimulation (**Figure 6D**).

These results indicate that carp TRIF plays a critical role in the immune responses triggered by bacteria and viruses.

Carp TIR-Domain-Containing Adapter-Inducing Interferon-β (TRIF) Activates IFN and NF-κB Through the C-Terminal Domain

To further elucidate the mechanisms by which carp TRIF induces an inflammatory response, a luciferase reporter assay was used to test the promoter activities of *ifn-1* and *nf-κb*. As illustrated in **Figure 7A**, carp TRIF-expressing plasmids significantly induced the luciferase activity of *ifn-1* and *nf-κb*, and this induction occurred in a dose-dependent manner in the *ifn-1* promoter activity assay. Moreover, we tested the effects of different carp TRIF mutants on *ifn-1* and *nf-κb* promoter luciferase activities. The results showed that carp TRIF-FL, TRIF-△N, and TRIF-△TIR had significantly increased the relative activity of *ifn-1* and *nf-κb*; however, TRIF-△C showed no influence compared with that of the control group (**Figure 7B**). As shown in **Figure 7C**, TRIF-FL, TRIF-△N, TRIF-△TIR, and TRIF-△C proteins were strongly expressed

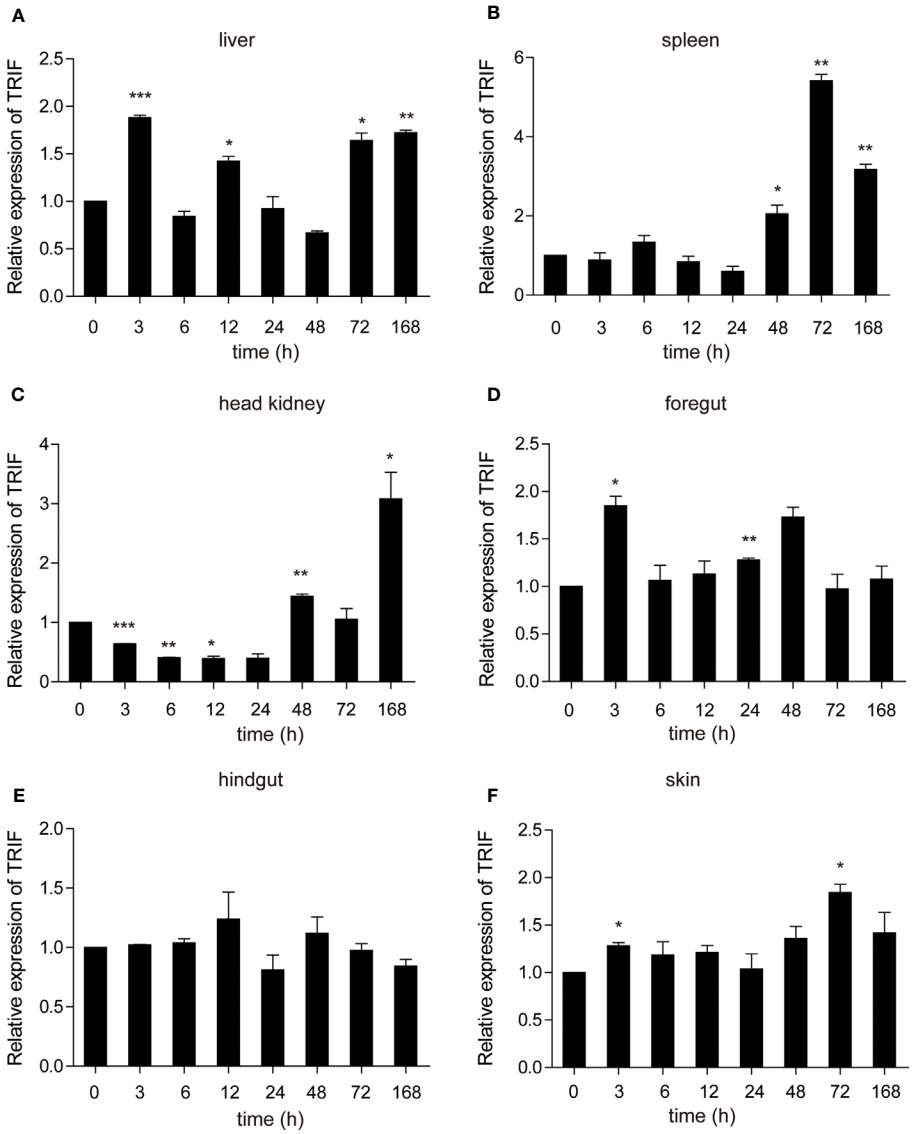

FIGURE 5 | The relative expression of carp TRIF in various tissues of common carp after intraperitoneal injection with poly(I:C). The mRNA expression levels of carp TRIF in the liver **(A)**, spleen **(B)**, head kidney **(C)**, foregut **(D)**, hindgut **(E)**, and skin **(F)** at different time points are shown. Gene expression results were calculated relative to the expression of 40S ribosomal protein s11. Data were presented as the fold changes based on the unstimulated control group (denoted by 0 h). Means ± SD (n = 3), $^{*}P < 0.05$, $^{**}P < 0.01$, $^{***}P < 0.001$.

in 293T cells at 48 h post-transfection. These results imply that carp TRIF relies on the C-terminal domain to activate the transcription factors.

Carp TIR-Domain-Containing Adapter-Inducing Interferon-β (TRIF) Involved in the Antiviral Response *via* the TRAF6-TBK1 Axis

To further investigate the impact of carp TRIF on the antiviral activity, EPC cells were transfected with plasmid expressing carp TRIF and subjected to SVCV infection for 24 h. Crystal violet staining showed apparent CPE in the control cells, whereas the CPE was markedly reduced in TRIF-overexpressing cells after SVCV infection **(Figure 8A).** As shown in **Figure 8B**, the transcriptional levels of two SVCV genes (SVCV-G and SVCV-N) were significantly attenuated in carp TRIF-overexpressing cells at 3 and 6 h after SVCV infection, which suggest that carp TRIF can inhibit SVCV replication. To further explore the antiviral mechanism of carp TRIF, the expression of TRAF6 and TBK1, the downstream signaling of TRIF, was measured by WB analysis at 48 h post-transfection. As shown in **Figure 8C**, an enhanced Western blotting band was detected

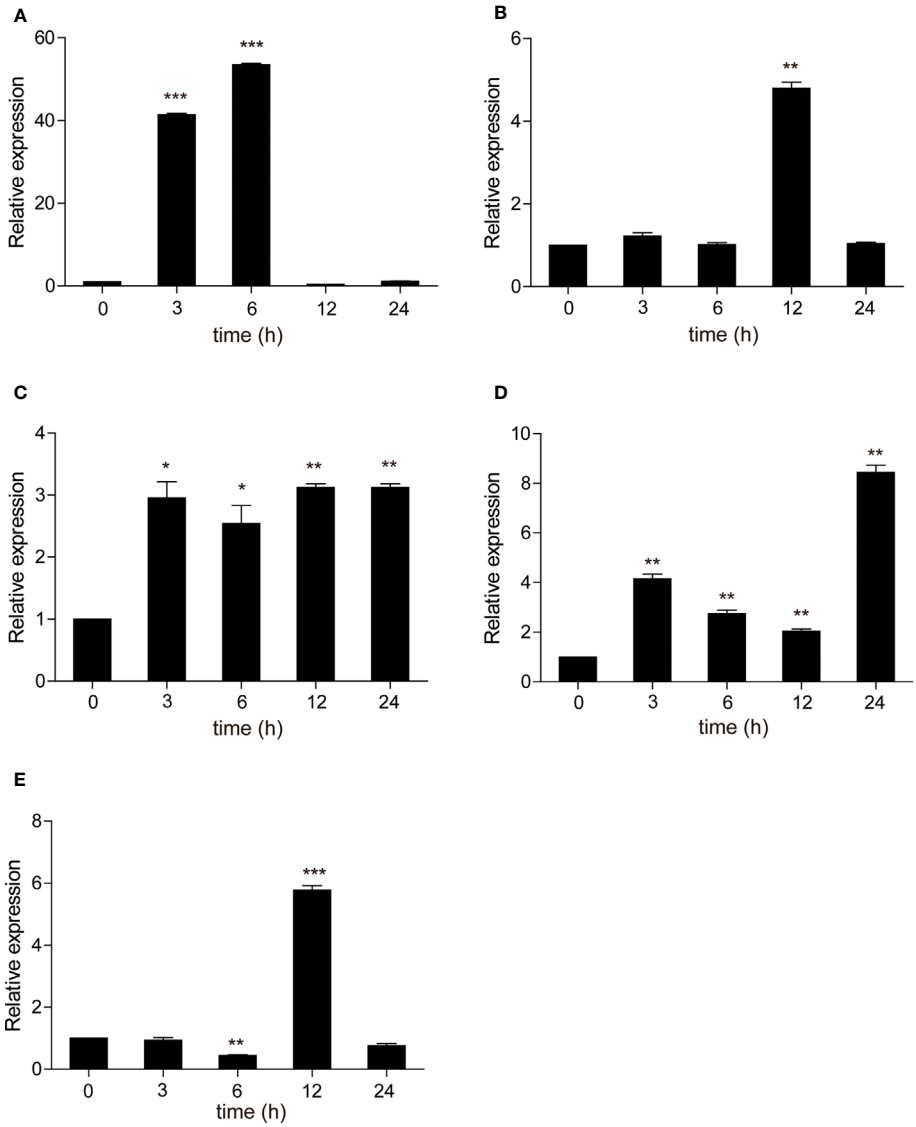

FIGURE 6 | The relative expression of carp TRIF in the PBLs after treatment with poly(I:C) **(A)**, LPS **(B)**, PGN **(C)**, flagellin **(D)**, and Pam3CSK4 **(E)** at different time points. The results were calculated relative to the expression of 40S ribosomal protein s11. Data were presented as the fold change based on the control group (denoted by 0 h). Means ± SD (n = 3), $^{*}P < 0.05$, $^{**}P < 0.01$, $^{***}P < 0.001$.

for TRAF6 and the phosphorylated form of TBK1 in carp TRIF-overexpressing cells. To further investigate the role of carp TRIF in the downstream signaling, EPC cells were stimulated with poly (I:C), in which poly(I:C) induced the expression of TRAF6 and phosphorylation of TBK1. The densitometric analysis of protein bands using the ImageJ software confirmed the results. Previous studies demonstrated that human TRIF forms a complex with TBK1 and TRAF6 (9). However, fish TRIF lacks the TRAF6 binding motif. Then, the interaction between carp TRIF and TBK1 was examined. Coimmunoprecipitation experiments indicated that carp TRIF was directly bound to TBK1 (**Figure 8D**). Next, the expression of IFN-stimulated genes and proinflammatory cytokines was detected in the carp TRIF-mediated immune response. After SVCV stimulation, the expression of *ifn*, *viperin*, *isg15*, *mx*, and proinflammatory cytokines such as *il-1β* and *tnf-α* were significantly upregulated in the carp TRIF-overexpressing group compared with the control (**Figure 8E**). These results indicate that carp TRIF is involved in the antiviral response *via* the TRAF6-TBK1 axis.

Carp TIR-Domain-Containing Adapter-Inducing Interferon-β (TRIF) Induces Apoptosis Through the Caspase-8 Axis

Apoptosis is a host defense against pathogen invasion. To investigate whether carp TRIF can mediate apoptosis, EPC cells were transfected with carp TRIF and the early apoptosis was

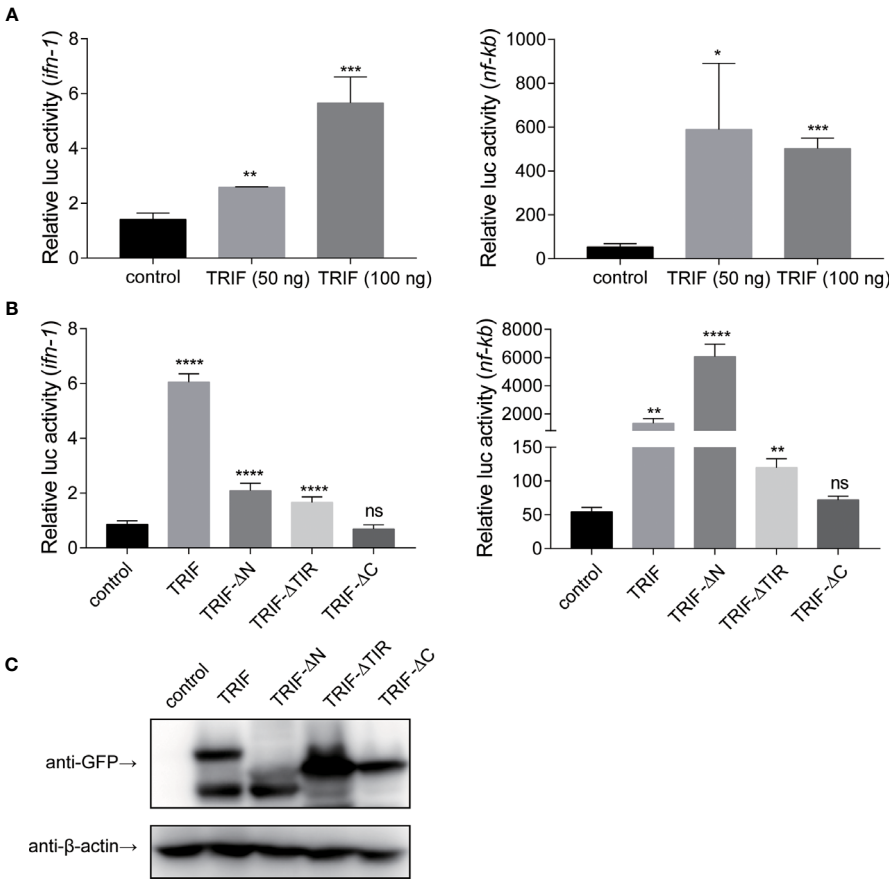

FIGURE 7 | Carp TRIF enhances the promoter activities of *ifn* and *nf-κb* through the C-domain. **(A)** 293T cells were transfected with pEGFP-N1 (control) or different amounts (50 and 100 ng) of carp TRIF-EGFP together with *ifn-1* or *nf-κb* promoter luciferase reporter vector and pRL-TK. After transfection for 48 h, *Firefly* and *Renilla* luciferase activities were measured. **(B)** 293T cells were transfected with the indicated plasmid. After transfection for 48 h, *Firefly* and *Renilla* luciferase activities were measured. **(C)** 293T cells were seeded in 6-well plates and transfected with the pEGFP-N1 (control) and different mutants of carp TRIF (TRIF-△N-EGFP, TRIF-△TIR-EGFP, or TRIF-△C-EGFP) for 48 h. The cell lysates were subjected to Western blot analysis with anti-GFP and anti-β-actin Abs. All data represented the means ± SD (n = 3) from three independent triplicate experiments, $^{*}P < 0.05$, $^{**}P < 0.01$, $^{***}P < 0.001$, $^{****}P < 0.0001$ and ns, no significant.

examined. The results demonstrated that the number of early apoptotic cells significantly increased in carp TRIF-overexpressing cells (97.8%) compared with the control group (62.2%) **(Figure 9A)**. To better define the mechanism by which carp TRIF initiates apoptosis, we examined the expression of caspase-8. As shown in **Figure 9B**, carp TRIF promoted caspase-8 activation. Hence, carp TRIF induces apoptosis through the caspase-8 axis.

DISCUSSION

TRIF is an essential adaptor protein required for innate immune responses mediated by TLRs (30). In teleost fish, several fish-specific TLRs, such as Tlr22 and Tlr19, can recruit TRIF and subsequently activate the TRIF-dependent pathway (20, 31), collectively implying that fish TRIF has an important role in the defensive immune responses. In the current study, the TRIF gene of common carp was cloned and characterized. Carp TRIF lacks the N-terminal and C-terminal proline-rich domains, which was reported in zebrafish, large yellow croaker, black carp, and orange spotted grouper (16, 18, 19, 21). Furthermore, multiple sequence alignment of the TIR domain among different species showed that carp TRIF displayed a typical TIR domain and had three highly conserved regions, Box 1, Box 2, and Box 3, which are conserved in mammalian TRIF and essential for TRIF- and MyD88-mediated signal transduction (6). In addition, phylogenetic analysis revealed that carp TRIF clustered with other fish TRIF and was highly similar to grass carp.

Tissue expression analysis showed that carp TRIF was constitutively expressed in several studied tissues of healthy common carp, with the highest expression levels detected in the spleen, indicating a possible role of TRIF in the immune defense system of common carp. However, the expression pattern was different in various species. Grass carp TRIF is highly expressed in the foregut and skin (17). Channel catfish TRIF has the highest expression in the ovary and spleen (15). In the amphioxus,

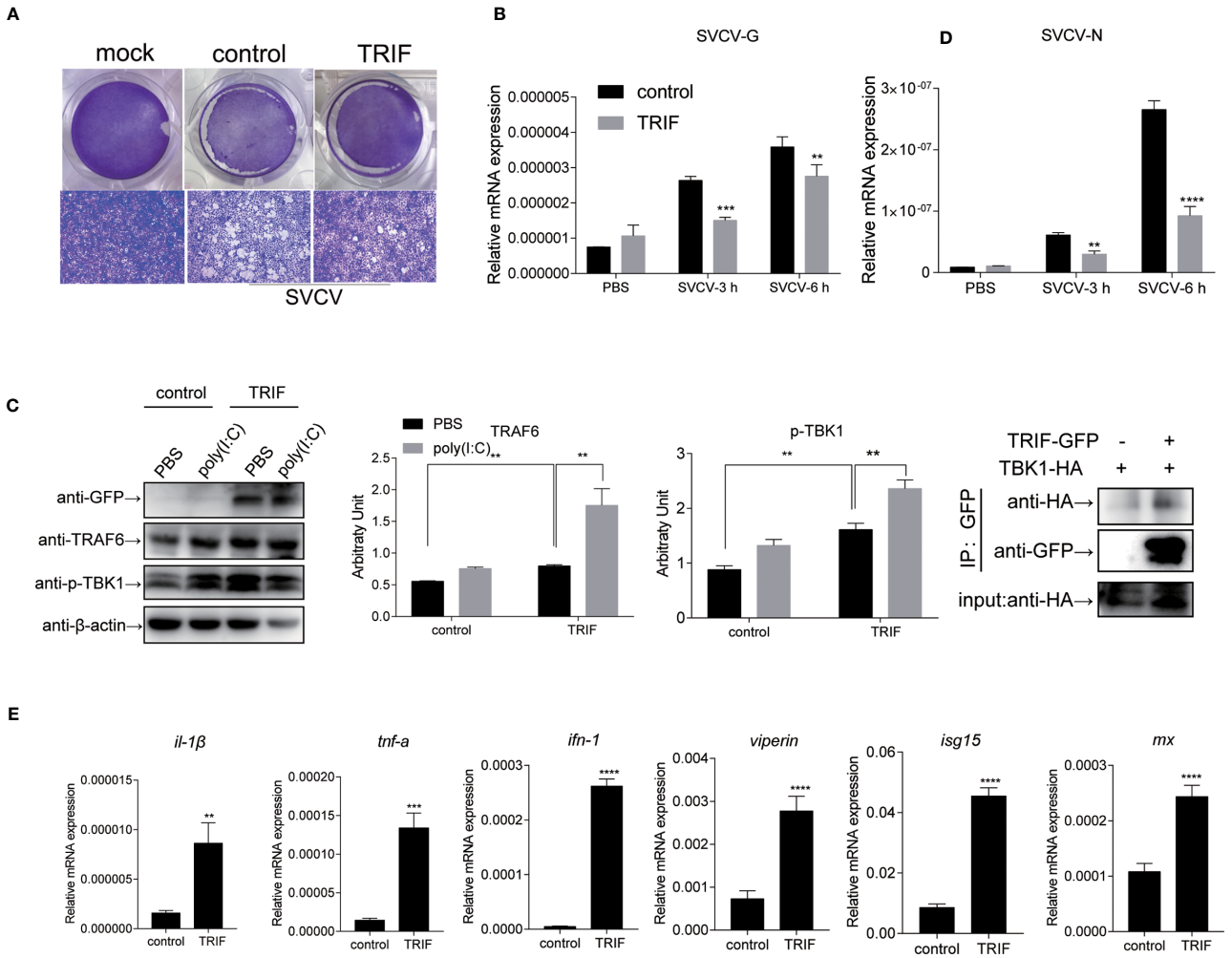

FIGURE 8 | Carp TRIF involved in the antiviral response *via* the TRAF6-TBK1 axis. **(A)** EPC cells were seeded in 24-well plated overnight and transfected with pEGFP-N1 (control) or carp TRIF-EGFP. At 24 h post-transfection, the cells were infected with SVCV (MOI = 0.01) per well and incubated at 25°C for 24 h. This experiment was divided into two groups. **(A)** One group of cells stained with crystal violet for CPE. The cell monolayers were stained with crystal violet, and CPE was observed. **(B)** The second group of cells was used to extract the total RNA. The expression levels of SVCV-G and SVCV-N transcripts of SVCV by qRT-PCR analysis. **(C)** Cells were transiently transfected with above-mentioned plasmids in six-well plates. After 24 h of transfection, poly(I:C) stimulation was administered for 24 h, and then immunoblotted was conducted with the indicated antibodies. β-actin was used as a loading control. TRAF6/β-actin and p-TBK1/β-actin levels were quantified by the Image J software. **(D)** 293T cells were transfected with the indicated plasmids. At 48 h post-transfection, cell lysates were immunoprecipitated with anti-GFP, and immunoblotted analyzed with the indicated Abs. **(E)** EPC cells were transiently transfected with the indicated plasmids and harvested to quantify the relative expression levels of IFN-stimulated genes and proinflammatory genes at 6 h post SVCV infection. The results were calculated relative to the expression of EF-1α. All experiments were repeated at least three times with similar results. $^{**}P < 0.01$, $^{***}P < 0.001$, $^{****}P < 0.0001$.

transcripts of TRIF are strongly detected in the epithelial cells of the gut, skin, and gill (32). In zebrafish, a high TRIF transcript level is found in the liver (33). The differences in tissue distribution imply that TRIF performs divergent roles in various organs in different species. TLRs and their adaptors have a specific localization in the cells for their functions (34). In the current study, carp TRIF localized to a unique site near the nuclear membrane and was a Golgi apparatus-localized protein, which was consistent with demonstrations in other species, such as zebrafish (16) and orange-spotted grouper (18).

Bacteria are pathogenic agents of fish disease, and fish TRIF is reported to play important roles in the innate immune responses against bacterial pathogens. Channel catfish TRIF mRNA shows an enhanced expression in the head kidney and spleen after *Edwardsiella ictalurid* infection (15). The mRNA expressions of *TRIF* from orange-spotted grouper and mandarin fish are upregulated after LPS stimulation (18, 35). The transcription of amphioxus TRIF is upregulated after a challenge with gram-negative and gram-positive bacteria (32). Similarly, in the current study, the transcription of carp TRIF was upregulated in immune-related tissues after it was challenged with killed *A. hydrophila*, except in the liver. Additionally, fish TRIF is found to take part in the antiviral immune response. For example, the miiuy croaker TRIF contributes to IFN antiviral immunity

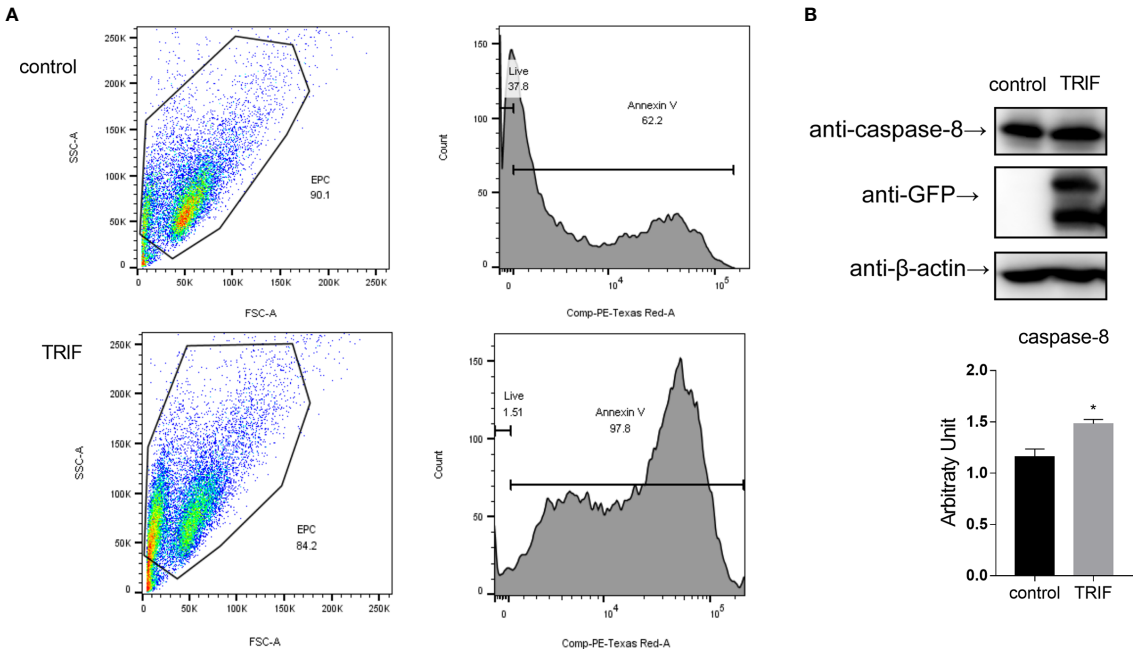

FIGURE 9 | Carp TRIF induces apoptosis. **(A)** EPC cells in 24-well plates were transfected with pEGFP-N1 (control) or carp TRIF-EGFP. The early apoptosis cells were stained with Annexin V-mCherry. Flow cytometric analysis was undertaken to detect Annexin V in cells. The percent of apoptotic cells were determined using the FlowJo software. **(B)** 293T cells were transfected with pEGFP-N1 (control) or carp TRIF-EGFP. After transfection for 24 h, the cell lysates were collected. Western blot was performed with anti-caspase-8 Abs. The level of caspase-8 was quantified by densitometry analysis of the band intensity using the Image J software, and normalized to the β-actin. Data were shown as the mean ± SD of the relative ratios of the intensity (caspase-8/β-actin). All experiments were repeated at least three times. $^*P < 0.05$.

following infection with Siniperca chuatsi rhabdovirus (SCRV) (36). In addition, TRIF expression was significantly upregulated in immune-related tissues in grass carp (17), large yellow croaker (34), zebrafish (16), and orange-spotted grouper (18) after poly(I:C) stimulation. Similarly, carp TRIF was upregulated after poly(I:C) stimulation *in vivo* and *in vitro*. These results indicate that fish TRIF exhibits extraordinarily broad roles in host antibacterial and antiviral innate immunity, which may be related to TLR recognition (20, 31).

To characterize the antiviral effects of carp TRIF, antiviral activity was investigated in carp TRIF-overexpressing cells. The results demonstrated that carp TRIF can inhibit the replication of SVCV *in vitro*. Similarly, in grass carp TRIF-overexpressing cells, the viral load and titer are significantly lower than those in the controls after GCRV challenge, and viral replication is obviously inhibited (17). Overexpression of grouper TRIF in grouper brain cells restrains the replication of red-spotted grouper nervous necrosis virus (RGNNV) (18). The possible mechanism of host defense against pathogens is inducing the expression of proinflammatory cytokines or interferon-stimulated genes. It is reported that mammalian TRIF can induce NF-κB and IFN-β (11). The activation of NF-κB in the TRIF-dependent pathway is verified to occur through the recruitment of TRAF6 and RIP1 by the TRAF6 binding motif and C-terminal RHIM domain, respectively (37–39). However, fish TRIF lacks the TRAF6 binding motif and C-terminal RHIM domain. Interestingly, carp TRIF significantly activated NF-κB, which was consistent with the findings in zebrafish, orange-spotted grouper, and large yellow croaker (16, 18, 34), implying the conserved function of fish TRIF in the NF-κB-mediating signaling cascade. Additionally, zebrafish TRIF is documented to associate with RIP1 but not TRAF6, and mutation of the TRIF RHIM domain disrupts NF-κB activation (16). Similarly, the absence of the C-terminus in carp TRIF suppressed the activation of NF-κB, indicating a fish TRIF-dependent NF-κB signaling *via* interaction with RIP1.

Mammalian TRIF is demonstrated to induce the production of IFN-β *via* the association of TRIF-TBK1 through the TBK1 binding motif (9). However, the TBK1 binding motif mentioned above is not conserved in fish TRIF. Intriguingly, carp TRIF could interact with TBK1, as found in zebrafish, indicating the conserved TRIF-TBK1 signaling cascade in teleost fish. Moreover, carp TRIF was capable of activating type I IFN, and a similar phenomenon was also observed in large yellow croaker (19), suggesting that type I IFN signaling pathways are involved in the TRIF-mediated immune response. Notably, it has been revealed that mutation of the C-terminal RHIM domain in common carp diminishes the activation of IFN, as shown in zebrafish (16), indicating that not only does the TBK1-mediated signaling cascade participate in TRIF-induced type I IFN production, but other molecules, such as RIP1, may also be involved in IFN activation. These results collectively suggest that fish TRIF may have different ways to induce IFN responses.

Apoptosis is a host defense against pathogen invasion that can be triggered by TLR ligands (40). Apoptosis occurs through the activation of members of the caspase family of cysteine proteases (41). Studies in mammals have demonstrated that protein-protein interactions resulting from the death domain (DD) are often involved in caspase activation (42). However, TRIF, which lacks DD, efficiently induces apoptosis (11). In this study, we found that carp TRIF overexpression induced apoptosis in EPC cells. Additionally, mammalian TRIF-induced apoptosis occurred through the activation of the FADD-caspase-8 axis (11). Similarly, carp TRIF overexpression enhanced the expression of caspase-8, suggesting that carp TRIF can induce apoptosis *via* the caspase-8 axis.

In summary, this study reported the identification and characterization of the TRIF gene from common carp. Carp TRIF participated in antibacterial and antiviral immune responses. In addition, overexpression of carp TRIF activated interferons and proinflammatory cytokines *via* the *ifn* and *nf-κb* pathways and inhibited SVCV replication in EPC cells. Furthermore, carp TRIF induced apoptosis through the activation of caspase-8. These results contribute to developing strategies for defense against virus infections in teleosts.

DATA AVAILABILITY STATEMENT

The datasets presented in this study can be found in online repositories. The names of the repository/repositories and accession number(s) can be found in the article/**Supplementary Material**.

ETHICS STATEMENT

The animal study was reviewed and approved by the Animal Experimental Ethics Committee of Shandong Normal University.

AUTHOR CONTRIBUTIONS

SS conceived and designed the experiments. RL, XL, and MS performed the experiments and analyzed the data. YQ, HL, and GY participated in the discussion of the results. SS, RL, and GY designed the study and wrote the paper. All authors contributed to the article and approved the submitted version.

FUNDING

This work was supported by the National Natural Science Foundation of China (32002419, 31972828) and the National Key R&D Program of China (2018YFD0900302-8).

ACKNOWLEDGMENTS

We thank all the staff members who provided laboratory assistance.

SUPPLEMENTARY MATERIAL

The Supplementary Material for this article can be found online at: https://www.frontiersin.org/articles/10.3389/fimmu.2021.725150/full#supplementary-material

Supplementary Figure 1 | Nucleotide and deduced amino acid sequence of carp TRIF. The cDNA sequence and amino acid sequence of TRIF in Carp. Uppercase letters denote the coding region and lowercase letters show the UTR. The deduced amino acid sequence is shown below the coding regions and the polyadenylation signal attaaa is in bold font. The red box represents the TIR domain.

Supplementary Figure 2 | The multiple alignment of TRIF across species. The sequences were aligned using the Clustal W method. The identical, conservative and similar substituted amino acid residues are indicated in (*), (: or .), respectively.

REFERENCES

1. Akira S, Uematsu S, Takeuchi O. Pathogen Recognition and Innate Immunity. *Cell* (2006) 124(4):783–801. doi: 10.1016/j.cell.2006.02.015
2. Meylan E, Tschopp J, Karin M. Intracellular Pattern Recognition Receptors in the Host Response. *Nature* (2006) 442(7098):39–44. doi: 10.1038/nature04946
3. Akira S, Takeda K, Kaisho T. Toll-Like Receptors: Critical Proteins Linking Innate and Acquired Immunity. *Nat Immunol* (2001) 2(8):675–80. doi: 10.1038/90609
4. O'Neill LA, Bowie AG. The Family of Five: TIR-Domain-Containing Adaptors in Toll-Like Receptor Signalling. *Nat Rev Immunol* (2007) 7 (5):353–64. doi: 10.1038/nri2079
5. Kanwal Z, Wiegertjes GF, Veneman WJ, Meijer AH, Spaink HP. Comparative Studies of Toll-Like Receptor Signalling Using Zebrafish. *Dev Comp Immunol* (2014) 46(1):35–52. doi: 10.1016/j.dci.2014.02.003
6. Oshiumi H, Matsumoto M, Funami K, Akazawa T, Seya T. TICAM-1, an Adaptor Molecule That Participates in Toll-Like Receptor 3-Mediated Interferon-Beta Induction. *Nat Immunol* (2003) 4(2):161–7. doi: 10.1038/ni886
7. Fitzgerald KA, Rowe DC, Barnes BJ, Caffrey DR, Visintin A, Latz E, et al. LPS-TLR4 Signaling to IRF-3/7 and NF-KappaB Involves the Toll Adapters TRAM and TRIF. *J Exp Med* (2003) 198(7):1043–55. doi: 10.1084/jem.20031023
8. Yamamoto M, Sato S, Hemmi H, Hoshino K, Kaisho T, Sanjo H, et al. Role of Adaptor TRIF in the Myd88-Independent Toll-Like Receptor Signaling Pathway. *Science* (2003) 301(5633):640–3. doi: 10.1126/science.1087262
9. Sato S, Sugiyama M, Yamamoto M, Watanabe Y, Kawai T, Takeda K, et al. Toll/IL-1 Receptor Domain-Containing Adaptor Inducing IFN-Beta (TRIF) Associates With TNF Receptor-Associated Factor 6 and TANK-Binding Kinase 1, and Activates Two Distinct Transcription Factors, NF-Kappa B and IFN-Regulatory Factor-3, in the Toll-Like Receptor Signaling. *J Immunol* (2003) 171(8):4304–10. doi: 10.4049/jimmunol.171.8.4304
10. Funami K, Matsumoto M, Oshiumi H, Inagaki F, Seya T. Functional Interfaces Between TICAM-2/TRAM and TICAM-1/TRIF in TLR4 Signaling. *Biochem Soc Trans* (2017) 45(4):929–35. doi: 10.1042/BST20160259
11. Kaiser WJ, Offermann MK. Apoptosis Induced by the Toll-Like Receptor Adaptor TRIF is Dependent on its Receptor Interacting Protein Homotypic Interaction Motif. *J Immunol* (2005) 174(8):4942–52. doi: 10.4049/jimmunol.174.8.4942
12. Meylan E, Burns K, Hofmann K, Blancheteau V, Martinon F, Kelliher M, et al. RIP1 is an Essential Mediator of Toll-Like Receptor 3-Induced NF-Kappa B Activation. *Nat Immunol* (2004) 5(5):503–7. doi: 10.1038/ni1061
13. Yamamoto M, Sato S, Mori K, Hoshino K, Takeuchi O, Takeda K, et al. Cutting Edge: A Novel Toll/IL-1 Receptor Domain-Containing Adapter That Preferentially Activates the IFN-Beta Promoter in the Toll-Like Receptor Signaling. *J Immunol* (2002) 169(12):6668–72. doi: 10.4049/jimmunol.169.12.6668
14. Rebl A, Goldammer T, Seyfert HM. Toll-Like Receptor Signaling in Bony Fish. *Veterinary Immunol Immunopathol* (2010) 134(3-4):139–50. doi: 10.1016/j.vetimm.2009.09.021

15. Baoprasertkul P, Peatman E, Somridhivej B, Liu Z. Toll-Like Receptor 3 and TICAM Genes in Catfish: Species-Specific Expression Profiles Following Infection With Edwardsiella Ictaluri. *Immunogenetics* (2006) 58(10):817–30. doi: 10.1007/s00251-006-0144-z
16. Fan S, Chen S, Liu Y, Lin Y, Liu H, Guo L, et al. Zebrafish TRIF, a Golgi-Localized Protein, Participates in IFN Induction and NF-Kappab Activation. *J Immunol* (2008) 180(8):5373–83. doi: 10.4049/jimmunol.180.8.5373
17. Yang C, Li Q, Su J, Chen X, Wang Y, Peng L. Identification and Functional Characterizations of a Novel TRIF Gene From Grass Carp (Ctenopharyngodon Idella). *Dev Comp Immunol* (2013) 41(2):222–9. doi: 10.1016/j.dci.2013.05.018
18. Wei J, Zhang X, Zang S, Qin Q. Expression and Functional Characterization of TRIF in Orange-Spotted Grouper (Epinephelus Coioides). *Fish Shellfish Immunol* (2017) 71:295–304. doi: 10.1016/j.fsi.2017.09.063
19. Zou PF, Shen JJ, Li Y, Yan Q, Zou ZH, Zhang ZP, et al. Molecular Cloning and Functional Characterization of TRIF in Large Yellow Croaker Larimichthys Crocea. *Fish Shellfish Immunol* (2019) 91:108–21. doi: 10.1016/j.fsi.2019.05.011
20. Matsuo A, Oshiumi H, Tsujita T, Mitani H, Kasai H, Yoshimizu M, et al. Teleost TLR22 Recognizes RNA Duplex to Induce IFN and Protect Cells From Birnaviruses. *J Immunol* (2008) 181(5):3474–85. doi: 10.4049/jimmunol.181.5.3474
21. Peng F, Jin S, Chen Z, Chang H, Xiao J, Li J, et al. TRIF-Mediated Antiviral Signaling is Differentially Regulated by TRAF2 and TRAF6 in Black Carp. *Dev Comp Immunol* (2021) 121:104073. doi: 10.1016/j.dci.2021.104073
22. Huang WJ, Shen Y, Xu XY, Hu MY, Li JL. Identification and Characterization of the TLR18 Gene in Grass Carp (Ctenopharyngodon Idella). *Fish Shellfish Immunol* (2015) 47(2):681–8. doi: 10.1016/j.fsi.2015.09.052
23. Bostock J, McAndrew B, Richards R, Jauncey K, Telfer T, Lorenzen K, et al. Aquaculture: Global Status and Trends. *Philosophical Transactions of the Royal Society of London. Ser B Biol Sci* (2010) 365(1554):2897–912. doi: 10.1098/rstb.2010.0170
24. Zrncic S, Oraic D, Zupicic IG, Pavlinec Z, Brnic D, Rogic ZA, et al. Koi Herpesvirus and Carp Edema Virus Threaten Common Carp Aquaculture in Croatia. *J Fish Dis* (2020) 43(6):673–85. doi: 10.1111/jfd.13163
25. Zhang F, Shan S, Xu X, Wang Y, Zhang Y, Yin M, et al. Molecular Characterization and Expression Analysis of Two Peptidoglycan Recognition Proteins (Ccpgrp5, Ccpgrp6) in Larvae Ontogeny of Common Carp Cyprinus Carpio L. And Upon Immune Stimulation by Bacteria. *BMC Veterinary Res* (2019) 15(1):10. doi: 10.1186/s12917-018-1744-1
26. Shan S, Liu D, Liu R, Zhu Y, Li T, Zhang F, et al. Non-Mammalian Toll-Like Receptor 18 (Tlr18) Recognizes Bacterial Pathogens in Common Carp (Cyprinus Carpio L.): Indications for a Role of Participation in the NF-KappaB Signaling Pathway. *Fish Shellfish Immunol* (2018) 72:187–98. doi: 10.1016/j.fsi.2017.09.081
27. Shan S, Liu R, Jiang L, Zhu Y, Li H, Xing W, et al. Carp Toll-Like Receptor 8 (Tlr8): An Intracellular Tlr That Recruits TIRAP as Adaptor and Activates AP-1 Pathway in Immune Response. *Fish Shellfish Immunol* (2018) 82:41–9. doi: 10.1016/j.fsi.2018.08.001
28. Shan S, Liu R, Feng H, Zhang Y, Zhang F, Lv C, et al. Identification and Functional Characterization of the Transcription Factor NF-Kappab Subunit P65 in Common Carp (Cyprinus Carpio L.). *Fish Shellfish Immunol* (2019) 95:25–34. doi: 10.1016/j.fsi.2019.10.014
29. Han N, Chen Z, Wan H, Huang G, Li J, Jin BR. A Rapid Method for Titration of Ascovirus Infectivity. *J Virological Methods* (2018) 255:101–6. doi: 10.1016/j.jviromet.2018.02.011
30. Wu X, Lei C, Xia T, Zhong X, Yang Q, Shu HB. Regulation of TRIF-Mediated Innate Immune Response by K27-Linked Polyubiquitination and Deubiquitination. *Nat Commun* (2019) 10(1):4115. doi: 10.1038/s41467-019-12145-1
31. Ji J, Rao Y, Wan Q, Liao Z, Su J. Teleost-Specific TLR19 Localizes to Endosome, Recognizes Dsrna, Recruits TRIF, Triggers Both IFN and NF-KappaB Pathways, and Protects Cells From Grass Carp Reovirus Infection. *J Immunol* (2018) 200(2):573–85. doi: 10.4049/jimmunol.1701149
32. Yang M, Yuan S, Huang S, Li J, Xu L, Huang H, et al. Characterization of Bbtticam From Amphioxus Suggests the Emergence of a Myd88-Independent Pathway in Basal Chordates. *Cell Res* (2011) 21(10):1410–23. doi: 10.1038/cr.2011.156
33. Luo K, Li Y, Xia L, Hu W, Gao W, Guo L, et al. Analysis of the Expression Patterns of the Novel Large Multigene TRIM Gene Family (Fintrim) in Zebrafish. *Fish Shellfish Immunol* (2017) 66:224–30. doi: 10.1016/j.fsi.2017.04.024
34. Zhu S, Xiang X, Xu X, Gao S, Mai K, Ai Q. TIR Domain-Containing Adaptor-Inducing Interferon-Beta (TRIF) Participates in Antiviral Immune Responses and Hepatic Lipogenesis of Large Yellow Croaker (Larimichthys Crocea). *Front Immunol* (2019) 10:2506. doi: 10.3389/fimmu.2019.02506
35. Wang KL, Chen SN, Li L, Huo HJ, Nie P. Functional Characterization of Four TIR Domain-Containing Adaptors, Myd88, TRIF, MAL, and SARM in Mandarin Fish Siniperca Chuatsi. *Dev Comp Immunol* (2021) 122:104110. doi: 10.1016/j.dci.2021.104110
36. Zheng W, Chu Q, Yang L, Sun L, Xu T. Circular RNA Circdtx1 Regulates IRF3-Mediated Antiviral Immune Responses Through Suppression of MiR-15a-5p-Dependent TRIF Downregulation in Teleost Fish. *PloS Pathog* (2021) 17(3):e1009438. doi: 10.1371/journal.ppat.1009438
37. Seya T, Oshiumi H, Sasai M, Akazawa T, Matsumoto M. TICAM-1 and TICAM-2: Toll-Like Receptor Adapters That Participate in Induction of Type 1 Interferons. *Int J Biochem Cell Biol* (2005) 37(3):524–9. doi: 10.1016/j.biocel.2004.07.018
38. Hyun J, Kanagavelu S, Fukata M. A Unique Host Defense Pathway: TRIF Mediates Both Antiviral and Antibacterial Immune Responses. *Microbes Infect* (2013) 15(1):1–10. doi: 10.1016/j.micinf.2012.10.011
39. Fitzgerald KA. LPS-TLR4 Signaling to IRF-3/7 and NF-Kappa B Involves the Toll Adapters TRAM and TRIF. *J Exp Med* (2003) 198(9):1043. doi: 10.1084/jem.20031023
40. Barber GN. Host Defense, Viruses and Apoptosis. *Cell Death Differentiation* (2001) 8(2):113–26. doi: 10.1038/sj.cdd.4400823
41. Creagh EM, Conroy H, Martin SJ. Caspase-Activation Pathways in Apoptosis and Immunity. *Immunological Rev* (2003) 193:10–21. doi: 10.1034/j.1600-065x.2003.00048.x
42. Thorburn A. Death Receptor-Induced Cell Killing. *Cell Signalling* (2004) 16 (2):139–44. doi: 10.1016/j.cellsig.2003.08.007

Conflict of Interest: The authors declare that the research was conducted in the absence of any commercial or financial relationships that could be construed as a potential conflict of interest.

frontiers in Immunology

ORIGINAL RESEARCH
published: 31 August 2021
doi: 10.3389/fimmu.2021.702971

Divergent Antiviral Mechanisms of Two *Viperin* Homeologs in a Recurrent Polyploid Fish

Cheng-Yan Mou[1,2], *Shun Li*[1,2], *Long-Feng Lu*[1,2], *Yang Wang*[1,2], *Peng Yu*[1,2], *Zhi Li*[1], *Jin-Feng Tong*[1,2], *Qi-Ya Zhang*[1,2], *Zhong-Wei Wang*[1,2], *Xiao-Juan Zhang*[1], *Guang-Xin Wang*[1], *Li Zhou*[1,2,3*] *and Jian-Fang Gui*[1,2,3*]

[1] State Key Laboratory of Freshwater Ecology and Biotechnology, Institute of Hydrobiology, The Innovative Academy of Seed Design, Chinese Academy of Sciences, Wuhan, China, [2] College of Life Sciences, University of Chinese Academy of Sciences, Beijing, China, [3] Hubei Hongshan Laboratory, Chinese Academy of Sciences, Wuhan, China

OPEN ACCESS

Edited by:
Verónica Chico Gras, Universidad Miguel Hernández de Elche, Spain

Reviewed by:
Sarah J. Poynter, Wilfrid Laurier University, Canada
Khalil Eslamloo, Memorial University of Newfoundland, Canada

***Correspondence:**
Li Zhou
zhouli@ihb.ac.cn
Jian-Fang Gui
jfgui@ihb.ac.cn

Specialty section:
This article was submitted to Comparative Immunology, a section of the journal Frontiers in Immunology

Received: 30 April 2021
Accepted: 09 August 2021
Published: 31 August 2021

Citation:
Mou C-Y, Li S, Lu L-F, Wang Y, Yu P, Li Z, Tong J-F, Zhang Q-Y, Wang Z-W, Zhang X-J, Wang G-X, Zhou L and Gui J-F (2021) Divergent Antiviral Mechanisms of Two Viperin Homeologs in a Recurrent Polyploid Fish. Front. Immunol. 12:702971. doi: 10.3389/fimmu.2021.702971

Polyploidy and subsequent diploidization provide genomic opportunities for evolutionary innovations and adaptation. The researches on duplicated gene evolutionary fates in recurrent polyploids have seriously lagged behind that in paleopolyploids with diploidized genomes. Moreover, the antiviral mechanisms of Viperin remain largely unclear in fish. Here, we elaborate the distinct antiviral mechanisms of two *viperin* homeologs (*Cgviperin-A* and *Cgviperin-B*) in auto-allo-hexaploid gibel carp (*Carassius gibelio*). First, *Cgviperin-A* and *Cgviperin-B* showed differential and biased expression patterns in gibel carp adult tissues. Subsequently, using co-immunoprecipitation (Co-IP) screening analysis, both *Cg*Viperin-A and *Cg*Viperin-B were found to interact with crucian carp (*C. auratus*) herpesvirus (*Ca*HV) open reading frame 46 right (ORF46R) protein, a negative herpesvirus regulator of host interferon (IFN) production, and to promote the proteasomal degradation of ORF46R *via* decreasing K63-linked ubiquitination. Additionally, *Cg*Viperin-B also mediated ORF46R degradation through autophagosome pathway, which was absent in *Cg*Viperin-A. Moreover, we found that the N-terminal α-helix domain was necessary for the localization of *Cg*Viperin-A and *Cg*Viperin-B at the endoplasmic reticulum (ER), and the C-terminal domain of *Cg*Viperin-A and *Cg*Viperin-B was indispensable for the interaction with degradation of ORF46R. Therefore, the current findings clarify the divergent antiviral mechanisms of the duplicated *viperin* homeologs in a recurrent polyploid fish, which will shed light on the evolution of teleost duplicated genes.

Keywords: *viperin*, polyploid, homeolog, herpesvirus, proteasomal degradation, autophagosome

INTRODUCTION

Genome sequencing explosion has highlighted a profound impact of polyploidy and subsequent post-polyploid diploidization (PPD) on evolutionary innovations and adaptation. As the impact might lead to genomic diversity, variability, and complexity, polyploidy is generally considered to have far-reaching consequences in shaping species speciation, diversification, and ecological adaption (1–10). The evolutionary fates of duplicated genes are dynamic and complex and

include pseudogenization or gene deletion, subfunctionalization, or neofunctionalization under relaxed purifying selection (3). In animals, the evolution of duplicated genes has been documented in more easily discernible paleopolyploids, which are characterized by highly diploidized genomes after several rounds of whole-genome duplications (WGD) at the root of the vertebrate (11, 12). However, research on recurrent polyploids, which are much more difficult to disentangle bioinformatically and experimentally, has seriously lagged behind that on animal paleopolyploids (13).

Viperin (also known as Vig1 in rainbow trout) was first identified as an antiviral protein induced by human cytomegalovirus in 2001 (14, 15). It belongs to the radical S-adenosylmethionine (SAM) enzyme family (14, 16, 17) and is composed of three distinct domains (18). Its N-terminal domain contains an amphipathic α-helix, which localizes Viperin to the ER, lipid droplets, or mitochondria (19–21). The central SAM domain has a characteristic CxxxCxxC motif responsible for binding proteins containing an iron-sulfur cluster (22, 23). The C-terminal domain is highly conserved, but its role remains poorly defined (24). This domain has been proposed to be involved in protein–protein interactions (19).

Viperin is known as an interferon (IFN)-stimulated gene (ISG) with broad-spectrum antiviral activities. Its expression can be induced by lipopolysaccharide (LPS), polyinosinic: polycytidylic acid [poly (I:C)], or various viruses (19, 25). Studies on mammalian Viperin have shown that its antiviral mechanisms appear to be virus-specific, owing to the distinct infection routes and replication strategies of different viruses (26). Recently, Ghosh and Marsh (2020) listed the different viruses reported to be restricted by viperin and the known mechanisms of restriction, and summarized two major ways of the antiviral activities of viperin (27). Viperin has been found to interact with a wide variety of host and viral proteins, and the complex network of interactions inhibits viral RNA transcription and replication (28–30), interrupts viral particle assembly and maturation (14), or impairs viral budding and release (20, 31, 32). Another way relies on the catalytic activity of Viperin to generate 3′-deoxy-3′,4′-didehydro-CTP (ddhCTP), which can directly interfere with RNA synthesis and the replication of flaviviruses (33). Similar to mammal, fish *viperin* is considered an important antiviral gene because its expression is also induced by LPS, poly(I:C), or viruses (15, 34–40). However, little is known about the molecular mechanism underlying the antiviral effect of fish Viperin.

Gibel carp (*Carassius gibelio*), widely distributed across the Eurasian continent, can reproduce by unisexual gynogenesis or sexual reproduction (41–43). Along with a large-scale culture of several improved varieties, such as allogynogenetic gibel carp "CAS III" (clone A^+) and "CAS III" (clone F) (44, 45), gibel carp has become one of the most important aquaculture species in China with about 3 million tons of annual production capacity (46). However, a serious outbreak of an epizootic disease caused by *Ca*HV has resulted in enormous economic losses since 2012 (47). In previous studies, we identified distinct immune responses and the differential expression of innate and adaptive immune genes among three clones (A^+, F, and H) after *Ca*HV challenge (48–51). Eight IFN system genes, including *viperin*, were identified as candidate resistant-related genes for disease-resistance breeding of gibel carp. *Viperin* was sharply upregulated among three clones at post infection (52). Additionally, gibel carp has over 150 chromosomes and is considered an auto-allo-hexaploid in comparison with goldfish (*Carassius auratus*) with 100 chromosomes (53, 54). It had been speculated that two rounds (2R) of polyploidy events, an allotetraploidy and an autotriploidy, occurred during its evolution (55). *Viperin* unigenes in transcriptomic data have been classified into two divergent homeologs with biased expression after *Ca*HV infection (52). It is necessary to further analyze expression and function divergence of the two *viperin* homeologs. Therefore, in this study, we first characterized two gibel carp *viperin* homeologs (*Cgviperin-A* and *Cgviperin-B*), and then investigated their divergent antiviral mechanisms through subcellular localization, overexpression, Co-IP, and *in vitro* ubiquitination assay.

MATERIALS AND METHODS

Cells, Gibel Carp, and Virus

Fish cell line *Carassius auratus* L. blastulae embryonic (CAB) cell was cultured at 28°C in 5% CO2 in medium 199 (Invitrogen) supplemented with 10% fetal bovine serum (FBS) (Invitrogen) as described previously (56–58). Female gibel carp clone F (about 67.68 ± 2.16 g) were obtained from the National Aquatic Biological Resource Center (NABRC), Institute of Hydrobiology (IHB), Chinese Academy of Sciences (CAS). *Ca*HV was provided by Prof. Q. Y. Zhang (Institute of Hydrobiology, Chinese Academy of Sciences) and propagated by intraperitoneal injection into healthy gibel carp. The isolation method of *Ca*HV was used as previously described (48, 59). Before sampling, fish were deeply euthanized by overdosed anesthesia styrylpyridine (30–50 mg/L; Aladdin, Shanghai, China) and immediately cut off spinal cord adjacent to the head. All procedures were approved by the Institutional Animal Care and Use Committee of IHB, CAS (protocol number 2016-018).

Gene Identification and Sequence Analysis

According to the genome sequences of gibel carp clone F (CI01000363_00413629_00414546 and ENSONIP00000026093-D2), specific primers (**Supplementary Table S1**) were designed to amplify *viperin* from gibel carp clone F head kidney cDNA library by 3' and 5' rapid amplification of cDNA ends (RACE) (SMARTer® RACE 5'/3' Kit, Clontech).

The cDNA sequences of six *viperin* transcripts were deposited in GenBank (accession numbers from MZ055409 to MZ055414). The specificity of RACE primer was confirmed by sequence analysis. The sequence assembly was performed by DNAstar software, and the assembly validation was confirmed by full-length sequence amplification and sequence analysis. The validation of open reading frame (ORF), multiple sequence

alignments, and neighbor-joining (NJ) phylogeny construction were analyzed by using ORF finder (https://www.ncbi.nlm.nih.gov/orffinder/), ClustalW program, and MEGA 7.0 software, respectively.

Chromosome Preparation and Fluorescence *In Situ* Hybridization

The bacterial artificial chromosome (BAC) clones containing *Cgviperin-A* and *Cgviperin-B* were screened by Polymerase Chain Reaction (PCR). Then, *Cgviperin-A*-BAC-DNA and *Cgviperin-B*-BAC-DNA were labeled by Biotin-Nick Translation Mix (Roche) and DIG-Nick Translation Mix, respectively. Chromosome preparation and FISH analyses were performed as described previously (55, 60). All metaphase chromosomes were counterstained with 4', 6-diamidino-2-phenylindole (DAPI).

RNA Extraction and Quantitative Real-Time PCR

RNA extraction and qPCR were performed as described previously (51, 52). Total RNAs from 10 adult tissues (including intestine, gill, muscle, head-kidney, trunk kidney, liver, spleen, thymus, gonad, and brain) were isolated using SV Total RNA isolation System (Promega) according to the manufacturer's protocols. Subsequently, the primeScript™ RT reagent Kit with gDNA Eraser (TaKaRa) was used to solve the DNA contamination of total RNA. The quantity of total RNA was detected by Nanodrop 2000 (Thermo Scientific), and the quality was assessed by agarose gel electrophoresis. One μg of total RNAs was used to synthesize first-strand cDNAs in a 20 μl reaction volume following the protocol of GoldScript cDNA synthesis Kit (Invitrogen).

qPCR was performed by using iTaq™ Universal SYBR® Green Supermix (Bio-Rad) according to the manufacturer's protocol. The reference gene, *eukaryotic translation elongation factor 1 alpha 1, like 1* (*eef1a1l1*) (M value=0.74 < 1.5) was selected as the normalizer for qPCR as described previously (52). The primers (**Supplementary Table S1**) used for qPCR analysis were designed with http://biotools.nubic.northwestern.edu/OligoCalc.html. The specificity of each pair of primers was analyzed by sequencing, and the primer efficiency and R^2 were assessed by constructing standard curve using the dilutions of cDNA as the template. All samples (n = 3) were analyzed in triplicate. The relative gene expression levels were calculated using the $2^{-\Delta\Delta CT}$ method. IBM® SPSS® statistics 20 software was used for statistical analysis. A probability (p) of <0.05 was considered statistically significant.

Plasmid Constructs

According to the genome sequences of gibel carp clone F (Wang et al., unpublished data), 5' flanking sequences and partial sequences of exon 1 of *Cgviperin*-A and *Cgviperin*-B (accession numbers from MZ055415-MZ055420) were also amplified from gibel carp clone F. For luciferase activity assays, these sequences were cloned into Kpn I/Xho I sites of pGL3-Basic luciferase reporter vector (Promega) to construct promoter-driven luciferase vector, respectively. For overexpression, the wild type (WT) *Cgviperin-A* ORF, *Cgviperin-B* ORF, and their corresponding sequences of mutants with a C-terminal hemagglutinin (HA)-tag or a C-terminal Flag-tag were cloned into pcDNA3.1(+) vector, respectively. The *Cgviperin-A* ORF and *Cgviperin-B* ORF were also inserted into pEGFP (enhanced green fluorescent protein)-N3 and pDsRed-N1 vector, respectively. The ORF of *Ca*HV gene ORF46R with a C-terminal HA-tag, Flag-tag, or Myc-tag were cloned into pcDNA3.1(+) vector, respectively. *Ca*IFN-Luc, IFN-stimulated response elements (ISRE)-Luc, and ER-DsRed were constructed previously (61). All constructs were confirmed by sequence analysis.

Transfection and Luciferase Activity Assays

Luciferase activity assays were performed as described previously (49, 50). CAB cells were seeded in 24-well plates overnight and co-transfected with various plasmid constructs at a ratio of 10:10:1 (promoter-driven luciferase plasmid/expression plasmid/Renilla luciferase plasmid pRL-TK) using FuGENE HD Transfection Reagent (Promega). Empty vector pGL3-Basic luciferase reporter vector (Promega) was used as control. If necessary, the cells were transfected again with poly (deoxyadenylic-deoxythymidylic) acid sodium salt [poly (dA:dT)] (Invivogen) or poly (I:C) (Sigma-Aldrich) (1μg/ml) at 24 h post-transfection. Then, the cells were harvested at 24 h post-transfection and lysed according to the Dual-Luciferase Reporter Assay System (Promega). Luciferase activities were measured by a Junior LB9509 luminometer (Berthold, Pforzheim, Germany) and normalized to the amounts of Renilla luciferase activities. The results were representative of more than three independent experiments, and each was performed in triplicate. The significant differences were calculated by IBM® SPSS® statistics 20 software.

Co-IP Assay and Western Blotting

Co-IP and western blotting were performed as described previously (62). Briefly, the CAB or 293T cells were seeded into 10 cm^2 dishes overnight, and transfected with different plasmids (a total of 10 μg) indicated on the Figure using FuGENE HD Transfection Reagent (Promega). At 24 h post-transfection, the cells were lysed by radioimmunoprecipitation (RIPA) lysis buffer with protease inhibitor cocktail (Sigma-Aldrich). After removing cellular debris, the supernatants were incubated with 15 μl anti-Flag or anti-Myc affinity gel (Sigma-Aldrich) overnight at 4°C. Immunoprecipitated proteins were resuspended in 100 μl SDS-PAGE protein loading buffer (Beyotime) after collecting by centrifugation and washing three times with lysis buffer. The whole cell lysates (WCL) or immunoprecipitated proteins were separated by 10–15% SDS-PAGE and then transferred to polyvinylidene fluoride membranes (Bio-Rad). The membranes were incubated with anti-β-actin (Cell Signaling Technology) at 1:3,000, anti-Flag/HA (Sigma-Aldrich) at 1:3,000, or anti-Myc (Santa Cruz Biotechnology) at 1:3,000, and then hybridized with the secondary HRP-conjugated anti-mouse IgG or anti-rabbit IgG

(Thermo Scientific) at 1:5,000. Results are captured by using an ImageQuant LAS 4000 system (GE Healthcare) and are representative of three independent experiments.

In Vitro Ubiquitination Assay

Ubiquitination assay was performed as described previously (62, 63). Briefly, CAB cells were transiently co-transfected with different overexpression plasmids (a total of 10 μg) indicated on the Figure and 1 μg HA-Ub or HA-Ub-K63O expression plasmids. At 18 h post-transfection, the cells were treated with 20 mM MG132 (Sigma-Aldrich) for 6 h and then were lysed using a RIPA lysis buffer containing 1% SDS and denatured by heating for 10 min. After denaturing and diluting, the supernatants were immunoprecipitated overnight at 4°C with 30 μl anti-Flag or anti-Myc agarose conjugate (Sigma-Aldrich). The whole cell lysates or immunoprecipitated proteins were analyzed by western blot as above described.

RESULTS

Molecular Characterization and Biased Expression Patterns of *Cgviperin* Homeologs

Six *Cgviperin* transcripts were cloned from the head-kidney of gibel carp clone F using RACE-PCR (**Supplementary Figure S1**). Analysis of multiple nucleotide alignments and their locations in the assembled genome (Wang et al., unpublished data) showed that they were clustered into two homeologs, each possessing three alleles (**Supplementary Figure S1**). The average identities among the three *Cgviperin-A* and *Cgviperin-B* alleles are 99.5 ± 0.3 and 99.4 ± 0.1%, respectively, while the average identity between the *Cgviperin-A* and *Cgviperin-B* homeologs is 91.3 ± 0.1%. The cDNAs of *Cgviperin-A* and *Cgviperin-B* were predicted to encode one *Cg*Viperin-A protein (359aa, *Cg*Viperin-A1/A2/A3) and three *Cg*Viperin-B proteins (371aa, *Cg*Viperin-B1, *Cg*Viperin-B1 and *Cg*Viperin-B3), respectively. Only two amino acid differences were observed among the three *Cg*Viperin-B proteins. *Cg*Viperin-A and *Cg*Viperin-B have about 90.1 ± 0.3% amino acid identity (**Supplementary Figure S2**). Phylogenetic analysis (**Figure 1B**) confirmed that *Cgviperin-A* and *Cgviperin-B* might be a pair of homeologs derived from early allotetraploidy (4R), and they both have three alleles because of late autotriploidy (5R).

Subsequently, the genomic structure and syntenic alignment were analyzed. *Cgviperin-A*s and *Cgviperin-B*s all contain six exons and five introns, and major differences between *Cgviperin-A* and *Cgviperin-B* homeologs exist in the introns (**Figure 1A**). The lengths of five introns vary between the two homeologs, especially the length of first and second introns. The average identity of the corresponding introns among three alleles is 99.3 ± 0.3%, but the average identity between two homeologs is 75.1 ± 0.1%, which is remarkably lower than that of the cDNAs (91.3 ± 0.1%). *Cgviperin-A*s and *Cgviperin-B*s are located on chromosome *Cg*A17 and *Cg*B17 of the gibel carp assembled genome, respectively, and the three alleles of each homeolog in

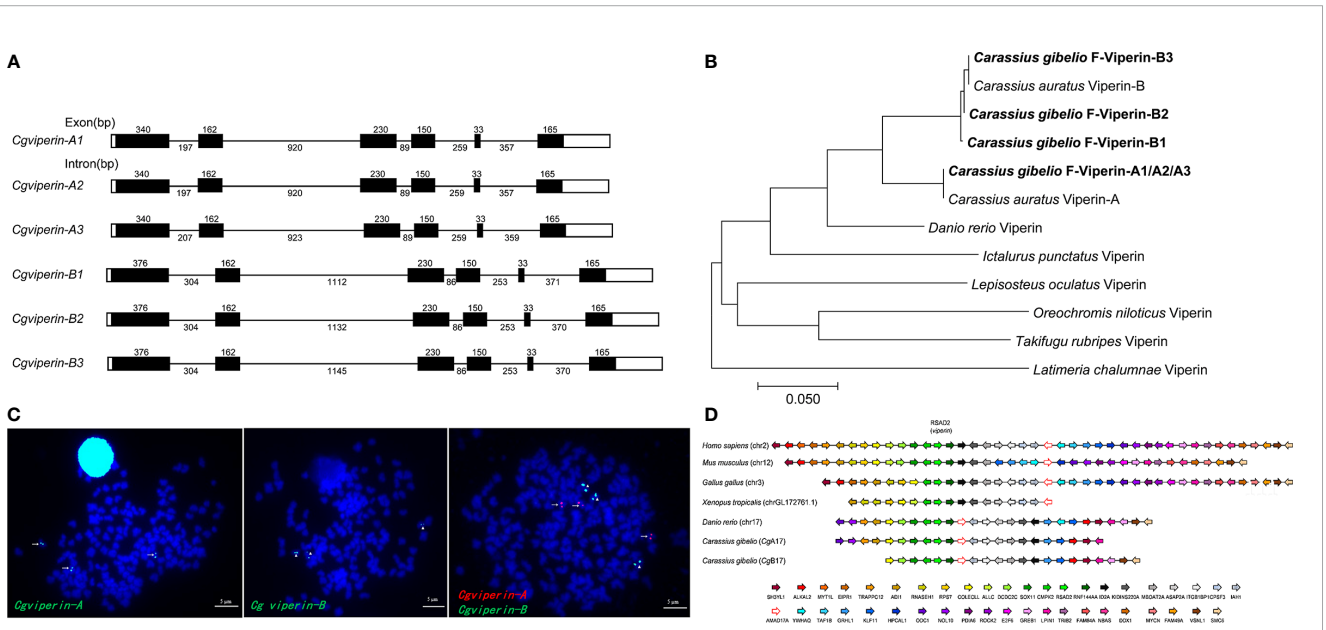

FIGURE 1 | Molecular characterization of *Cgviperin*-A and *Cgviperin*-B in gibel carp. **(A)** Genomic structure of six *Cgviperin* genes. Exons and introns are depicted by rectangle boxes and thick lines, respectively, and ORFs are highlighted by black boxes. Sizes (bp) are indicated upon or below themselves. **(B)** Phylogenetic tree of vertebrate Viperin. **(C)** Localization of *Cgviperin*-A and *Cgviperin*-B on gibel carp metaphase chromosomes. *Cgviperin*-A-BAC-DNA probe was labeled with DIG (green signals) or Biotin (red signals) (indicated by arrows), and *Cgviperin*-B-BAC-DNA probe was labeled with DIG (indicated by arrowheads). All metaphase chromosomes (blue) were counterstained with DAPI. **(D)** Gene synteny of vertebrate *viperin*. Conserved gene blocks are represented in matching colors. Transcription orientations are indicated by arrows.

three homologous chromosomes were confirmed by FISH. Three red *Cgviperin-A*s signals and three green *Cgviperin-B*s signals were observed on three different homologous chromosomes when *Cgviperin-A*-BAC-DNA and *Cgviperin-B*-BAC-DNA were simultaneously used as probes (**Figure 1C**). The *Cgviperin* homologous genes were found in zebrafish chromosome (*Danio rerio*) 17 (chr17), human (*Homo sapiens*) chr2, mouse (*Mus musculus*) chr12, chicken (*Gallus gallus*) chr3, and tropical clawed frog (*Xenopus tropicalis*) chrLG172761.1 with a conserved gene cluster (CMPK2-RSAD2/viperin-RNF144AA) (**Figure 1D**). Compared to zebrafish chr17, gibel carp *Cg*A17 and *Cg*B17 both retain most of the zebrafish homologous genes except *ywhaq*.

To confirm the potential antivirus activities of *Cgviperin-A* and *Cgviperin-B*, we compared their expression differences in the adult tissues of healthy individuals (**Figure 2**). *Cgviperin-A* and *Cgviperin-B* were constitutively expressed in the 10 tissues examined. However, obvious expression differences between *Cgviperin-A* and *Cgviperin-B* were observed. Both *Cgviperin-A* and *Cgviperin-B* showed high expression in immune tissue spleen. Additionally, *Cgviperin-A* and *Cgviperin-B* had differentially biased expression among different tissues. *Cgviperin-A* was abundantly expressed and showed higher expression than *Cgviperin-B* in the spleen and liver, while *Cgviperin-B* was highly expressed in the gill.

*Cg*Viperin-A and *Cg*Viperin-B Both Interact and Colocalize With ORF46R at ER

To further uncover their antiviral mechanisms, we analyzed the roles of different *Cg*Viperin domains and tried to determine their viral interactome. Firstly, we analyzed subcellular the localization of *Cg*Viperin-A and *Cg*Viperin-B in CAB cells (**Figure 3**). After co-transfection of *Cg*Viperin-A- EGFP or *Cg*Viperin-B-EGFP with ER-DsRed, confocal microscopy revealed that both *Cg*Viperin-A and *Cg*Viperin-B (green) mainly overlapped the red ER signals (**Figure 3A**). Then, we performed domain mapping to determine which domain was necessary for *Cg*Viperin-A and *Cg*Viperin-B ER localization. Three mutants of *Cg*Viperin-A and *Cg*Viperin-B were constructed, i.e., Vip-A-ΔN (lacking aa 1-74 in the N-terminal α-helix domain), Vip-A-ΔM (lacking CxxxCxxC motif in the middle SAM domain), and Vip-A-ΔC (339–359) (lacking aa 339-359 in the C terminus) (**Figure 3B**). Similar to WT *Cg*Viperin-A, Vip-A-ΔM and Vip-A-ΔC could localize at the ER, but Vip-A-ΔN was diffusely distributed in the cytoplasm and nucleus (**Figure 3C**). Similar subcellular localization was observed in the mutants of *Cg*Viperin-B (**Figure 3D**). The results indicate that the N-terminal α-helix domain is necessary for the localization of *Cg*Viperin-A and *Cg*Viperin-B at the ER.

Subsequently, to clarify the relevance of *Cg*Viperins and *Ca*HV, the Co-IP experiments were performed, which demonstrated that both *Cg*Viperin-A and *Cg*Viperin-B were efficiently associated with *Ca*HV ORF46R (**Figure 4A**). Next, the subcellular locations of *Cg*Viperins and ORF46R were monitored in CAB cells. Confocal microscopy revealed that the signals of ORF46R were mainly overlapped with those of *Cg*Viperin-A and *Cg*Viperin-B (**Figure 4B**), indicating that both *Cg*Viperin-A and *Cg*Viperin-B partly colocalize with ORF46R at the ER. Finally, we analyzed which domain was essential for the colocalization of *Cg*Viperins with ORF46R. Interestingly, the signals of ORF46R almost overlapped with those of Vip-A-ΔN and partly colocalized with Vip-A-ΔM, but was not with Vip-A-ΔC (**Figure 4C**), and similar subcellular localization was observed among three mutants of *Cg*Viperin-B (**Figure 4D**). These data imply that the C-terminal domain of *Cg*Viperin-A and *Cg*Viperin-B is indispensable for the colocalization with ORF46R.

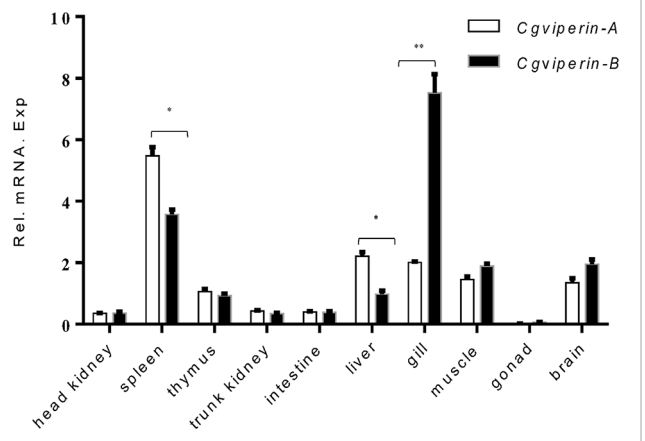

FIGURE 2 | qPCR analysis of *Cgviperin-A* and *Cgviperin-B* expression in adult tissue from healthy gibel carp clone F. *Eukaryotic translation elongation factor 1 alpha 1, like 1(eef1a1l1)* was used as control. Each bar represents mean ± standard deviation (SD) (n = 3). *$P < 0.05$, **$P < 0.01$.

*Ca*HV ORF46R Blocks IFN Induction

To obtain a clear picture of the functions of *Cg*Viperin-A and *Cg*Viperin-B in the cellular antiviral immunity, the role of ORF46R for immune response was investigated. As shown in **Figure 5A**, poly(dA:dT) and poly(I:C) could induce the activation of the crucian carp *Ca*IFN promoter (64). However, such induction was significantly impeded by ORF46R in a dose-dependent manner. ISRE, a transcription factor binding motif in the IFN promoter region, facilitates gene transcription (64). Consistently, the same results were also observed in ISRE (**Figure 5B**). For viperin, which was focused in this study, had been identified as an antiviral factor, their promoter activities were checked under ORF46R overexpression as well. The six *Cgviperin* promoters stimulated by poly(dA:dT) or poly(I:C) were blunted ORF46R as expected (**Figures 5C, D**). These results suggest that *Ca*HV ORF46R serves as a negative regulator to block host IFN production or this suppression happened following an induction.

*Cg*Viperin-A and *Cg*Viperin-B Promote *Ca*HV ORF46R Proteasomal Degradation *via* Decreasing Lysine 63 (K63)-Linked Ubiquitination

To determine the effect of *Cg*Viperin-A and *Cg*Viperin-B on the ORF46R of *Ca*HV, Vip-A-Flag or Vip-B-Flag was co-transfected

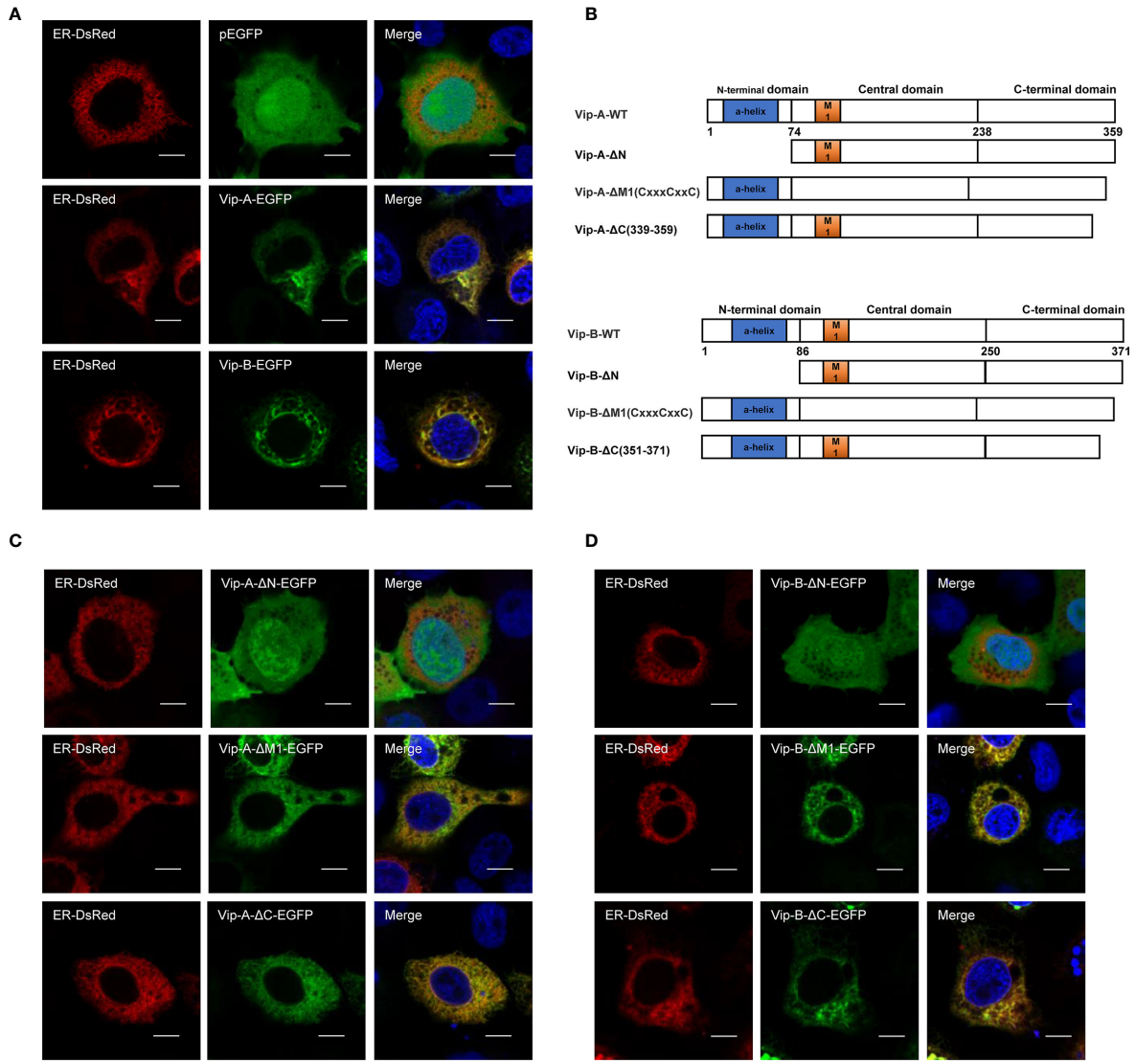

FIGURE 3 | *Cg*Viperin-A and *Cg*Viperin-B colocalize at ER through N-terminus domain. **(A)** Subcellular localization of WT *Cg*Viperin-A, *Cg*Viperin-B, and ER-DsRed. CAB cells were plated onto coverslips in six-well plates and co-transfected *Cg*Viperin-A-EGFP or *Cg*Viperin-B-EGFP with ER-DsRed. After 24 h, the cells were fixed and observed under confocal microscopy. Nuclear was stained with DAPI. Scale bars = 5 μm. **(B)** Diagrammatic representation of WT and three mutants of *Cg*Viperin-A or *Cg*Viperin-B. **(C, D)** Subcellular localization of three mutants of *Cg*Viperin-A **(C)** or *Cg*Viperin-B **(D)** with ER-DsRed.

with ORF46R-HA. The overexpression of *Cg*Viperin-A and *Cg*Viperin-B caused a significant reduction of ORF46 protein in a dose-dependent manner, respectively (**Figures 6A, B**). We also used the mutants to determine which domain was indispensable for the capacity of *Cg*Viperin-A or *Cg*Viperin-B to influence the stability of ORF46R. Consistent with WT *Cg*Viperin-A, Vip-A-ΔN and Vip-A-ΔM still could reduce the expression of ORF46R, whereas such an effect was abrogated in the Vip-A-ΔC group (**Figure 6C**). Similar results were obtained in the three mutants of *Cg*Viperin-B (**Figure 6D**), implying that the C-terminus of *Cg*Viperin is necessary for the regulation on ORF46R stability.

To determine how *Cg*Viperin-A and *Cg*Viperin-B regulate ORF46R at the protein level, a proteasome inhibitor (MG132), two lysosomal inhibitors [NH_4Cl and CQ (Chloroquine)], and an autophagosome inhibitor 3-methyladenine (3-MA) were used to examine the manner of *Cg*Viperin-A and *Cg*Viperin-B-mediated ORF46R degradation. In comparison with the control group (DMSO treatment), MG132 could effectively inhibit the degradation of ORF46R induced by *Cg*Viperin-A (**Figure 7A**). Significantly, the reduction of ORF46R was rescued by MG132 dose-dependently (**Figure 7B**). Similar results were also observed in *Cg*Viperin-B group (**Figures 7C, D**). These observations suggest that both *Cg*Viperin-A and *Cg*Viperin-B

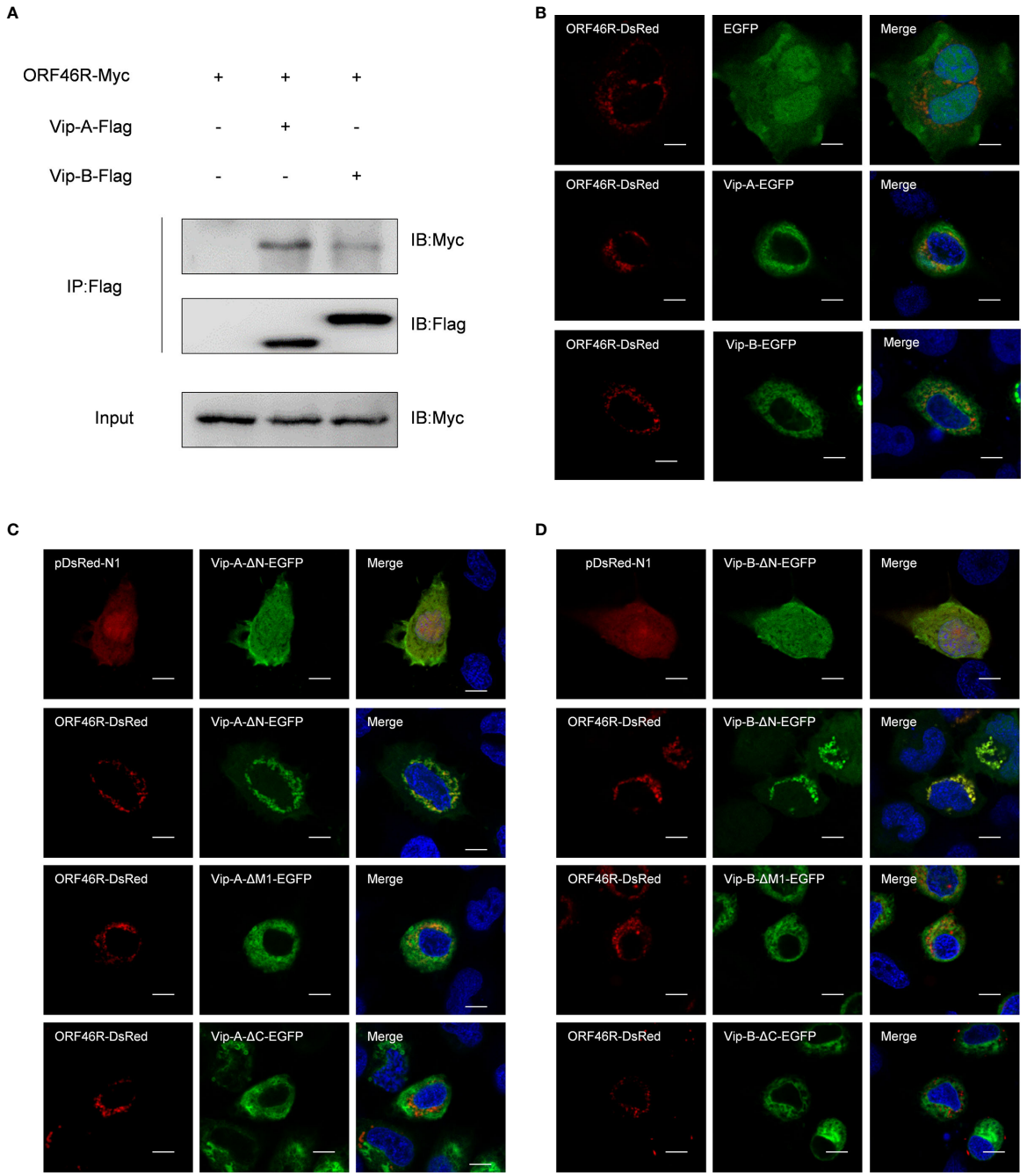

FIGURE 4 | Both *Cg*Viperin-A and *Cg*Viperin-B interact with ORF46R of *Ca*HV. **(A)** Co-IP of Vip-A-Flag or Vip-B-Flag with Myc-ORF46R in CAB cells transfected with the indicated plasmids. Anti-Flag Ab was used for Co-IP. **(B)** Subcellular localization of WT *Cg*Viperin-A, *Cg*Viperin-B, and ORF46R. CAB cells were plated onto coverslips in six-well plates and co-transfected *Cg*Viperin-A-EGFP or *Cg*Viperin-B-EGFP with ORF46R-DsRed. After 24 h, the cells were fixed and observed under confocal microscopy. Nuclear was stained with DAPI. Scale bars = 5 μm. **(C, D)** Subcellular localization of three mutants of *Cg*Viperin-A or *Cg*Viperin-B with ORF46R-DsRed. Scale bars = 5 μm.

could promote the proteasomal degradation of ORF46R. Protein ubiquitination is critical for the proteasomal degradation pathway (65). Whether *Cg*Viperin-A and *Cg*Viperin-B induce the polyubiquitination of ORF46R was further investigated. As shown in **Figure 7E**, both *Cg*Viperin-A and *Cg*Viperin-B suppressed the polyubiquitination of ORF46R. Previous studies suggested that target proteins were stabilized by K63-linked polyubiquitin chains (66, 67). Therefore, we tested a ubiquitin mutant, K63-only (K63O) (in which lysine at position 63 was ubiquitinated and linked with polyubiquitin chains, while all

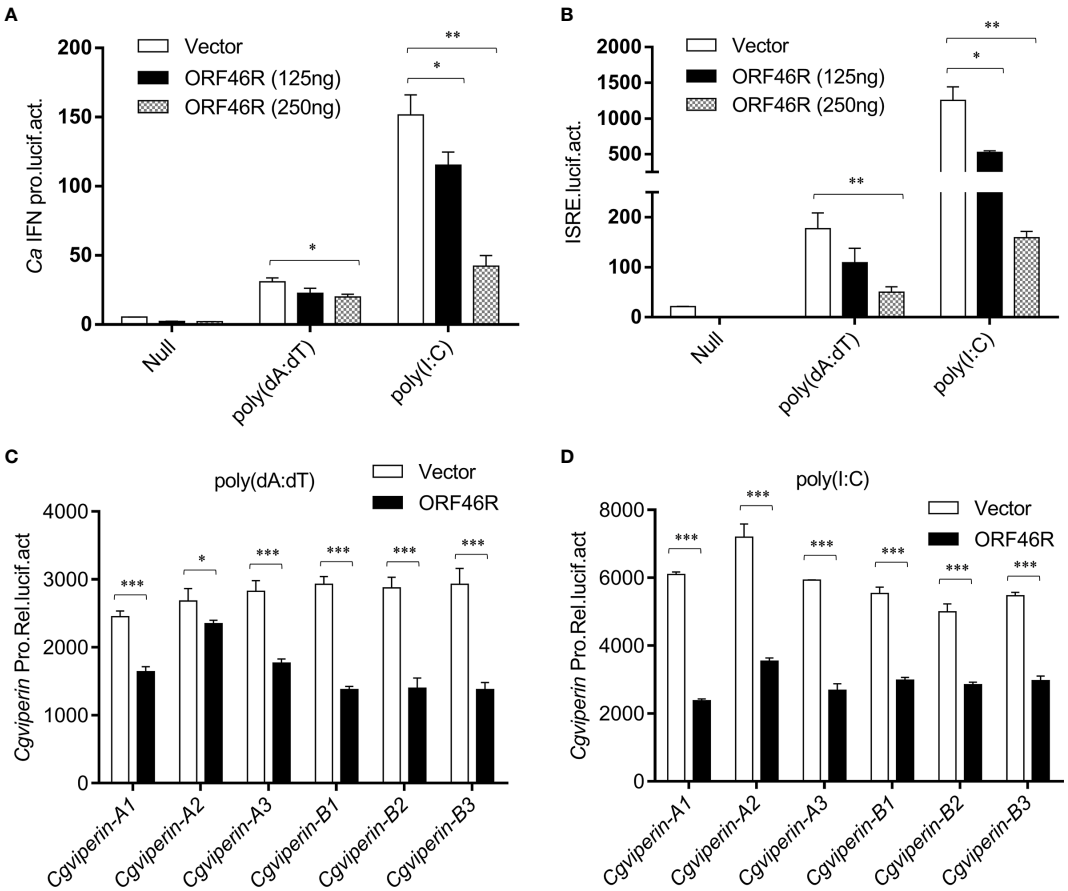

FIGURE 5 | *Ca*HV ORF46R blocks poly (dA:dT) or poly (I:C)-triggered activation of *CaIFN* promoter **(A)**, ISRE luciferase reporter **(B),** and six *Cgviperin* promoters **(C, D)**. CAB cells seeded overnight were co-transfected the empty vector or ORF46R (250 ng) and 25 ng pRL-TK plus 250 ng *Ca*IFNpro-luc or ISRE-luc. At 24 h post-transfection, cells were untreated (null) or transfected with 1 μg poly (dA:dT) or poly (I:C). The luciferase activities were monitored 24 h after stimulation. Each bar represents mean ± standard deviation (SD) (n = 3). $^{*}P < 0.05$, $^{**}P < 0.01$, $^{***}P < 0.001$.

other lysine residues were mutated to arginine residues), to determine whether the attenuation of ORF46R was mediated by the decrease of K63-ubiquitination. Consistent with prediction, the K63-linked ubiquitination of ORF46R was significantly impaired under *Cg*Viperin-A regulation (**Figure 7F**). Similar results were also obtained in *Cg*Viperin-B group (**Figure 7G**). The above results suggest that both *Cg*Viperin-A and *Cg*Viperin-B promote ORF46R proteasomal degradation *via* decreasing K63-linked ubiquitination.

*Cg*Viperin-B Mediates Autophagic Degradation of *Ca*HV ORF46R

In **Figure 7C**, we noticed that 3-MA could efficiently block ORF46R degradation induced by *Cg*Viperin-B, implying that *Cg*Viperin-B might promote ORF46R degradation through autophagosome pathway, which was distinguished with *Cg*Viperin-A, meaning that the *Cg*Viperin-A and *Cg*Viperin-B functional divergence occurs during the progression of ORF46R degradation. To identify our hypothesis, 3-MA treatment was employed for ORF46R degradation experiments subsequently. Consistent with the results above, increasing doses of 3-MA could not block the ORF46R degradation induced by *Cg*Viperin-A (**Figure 8A**), but *Cg*Viperin-B-mediated ORF46R degradation was obviously rescued by 3-MA in a dose-dependent manner (**Figure 8B**). These results suggest that *Cg*Viperin-B degrade ORF46R *via* an autophagic pathway that is absent in *Cg*Viperin-A. To further illustrate the exact mechanism in this process, we identified that the conversion of Microtubule-associated Protein 1A/1B-Light Chain 3 (LC3)-I to LC3-II was promoted by *Cg*Viperin-B, which means that autophagy is enhanced by the overexpression of *Cg*Viperin-B (**Figure 8C**). Co-IP assays showed that *Cg*Viperin-B interacted with many autophagic components, such as LC3, Beclin1, and autophagy-related gene 5 (ATG5) (**Figure 8D**). Meanwhile, interactions between ORF46R and these autophagic components were also confirmed (**Figure 8E**). Confocal immunofluorescence analysis showed that *Cg*Viperin-B overexpression caused the aggregation of LC3-GFP, demonstrating that cellular autophagy is enhanced (**Figure 8F**). These results suggest that *Cg*Viperin-B mediates the autophagic degradation of ORF46R, which is not possessed by *Cg*Viperin-A.

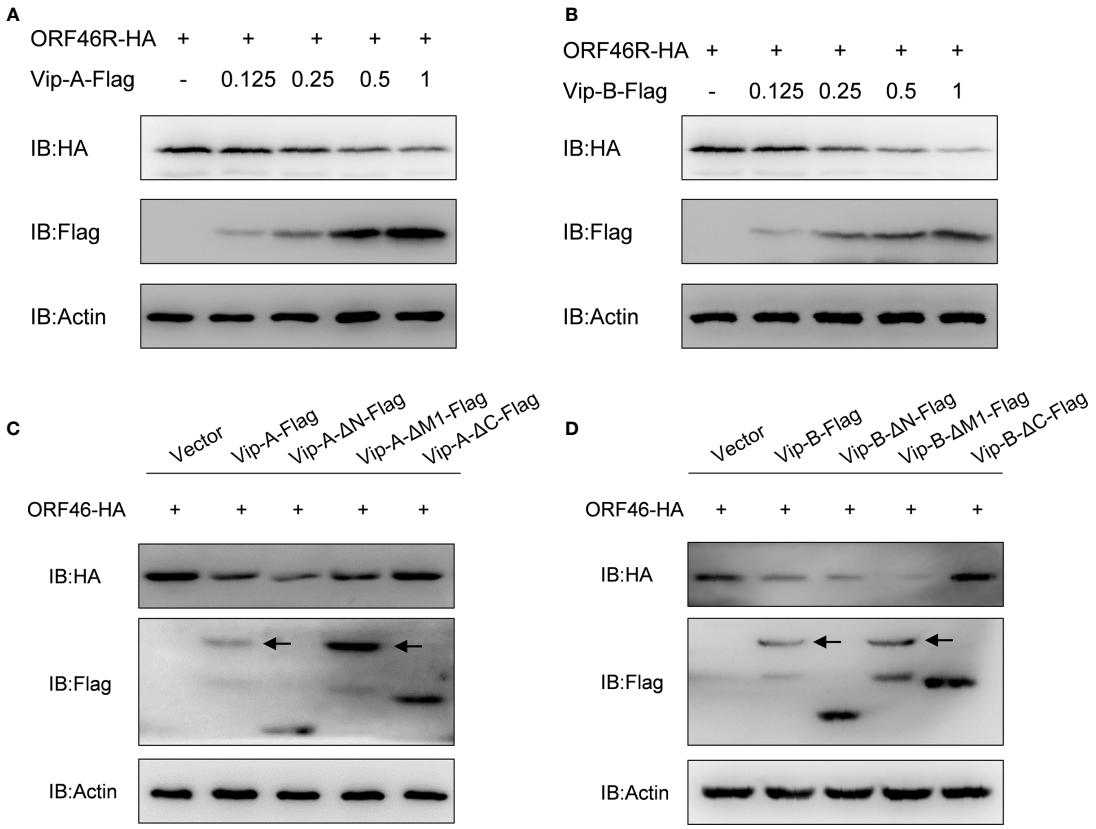

FIGURE 6 | Overexpression of *Cg*Viperin-A and *Cg*Viperin-B induce the reduction of *Ca*HV ORF46R protein *via* its C-terminus. **(A, B)** Overexpression of *Cg*Viperin-A **(A)** or *Cg*Viperin-B **(B)** induced the reduction of ORF46 protein in a dose-dependent manner in CAB cells. CAB cells were transfected with the indicated expression vectors and harvested for western blot analysis after 18–24 h **(C, D)** Domain mapping for *Cg*Viperin-A **(C)** or *Cg*Viperin-B **(D)** domains acting on ORF46R. CAB cells were transfected with the indicated expression vectors (2 μg/well) and harvested for western blot analysis after 18–24 h Diagrammatic representation of three mutants of *Cg*Viperin-A or *Cg*Viperin-B is shown in **Figure 3B**. Data are presented based on three independent experiments.

DISCUSSION

After WGD, duplicated genes step into complex and dynamic evolutionary routes under relaxed purifying selection. One of the two duplicates may be fractionated (deleted), or both may be retained, or diverge and evolve (sub- or neofunctionalization) (3). Recently, we revealed the biased expression and sub-/neofunctionalization of multiple duplicated *foxl2* homeologs and alleles in gibel carp (60). Innate immunity plays a vital role in the first barrier protecting the host from invading viruses (68). In this study, we focused on *viperin*, which is increasingly considered as a central player in the mammal antiviral response (27), and elucidated the divergent antiviral mechanisms of two homeologs in a polyploid fish.

In addition to the "fish-specific" (3R) WGD event about 320–350 million years ago (Mya), gibel carp was supposed to be experienced two extra rounds of polyploidy [an early allo-polyploidy (4R) and a late auto-polyploidy (5R)] at approximately 18.49 and 0.51 Mya, respectively (55, 60, 69, 70). In this study, we identified two homeologs of *Cgviperin*s with about 91% identity, and each homeolog has three alleles with high identities (≥99.0%) and located on three homologous chromosomes separately (**Supplementary Figure S1** and **Figure 1C**). Compared to zebrafish, our results (**Figures 1B, D**) indicated that the duplication of *Cgviperin*, same as gibel carp other genes (i.e., *dmrt1*, *foxl2*, *nanos2* and *bmp15*) (55, 60, 69, 70), may derive from the early allotetraploidy (4R) and a late autotriploidy (5R) event. In addition, *Cgviperin-A* and *Cgviperin-B* showed a different tissue-dependent constitutive expressions, suggesting A or B homologs might occur dominant or biased expression of homeologs during gibel carp evolution. In our previous study, we also found that *Cgviperin-A* and *Cgviperin-B* exhibited a biased expression pattern after *Ca*HV infection. Significantly, the upregulation folds of them in clone A^+, F, and H were related to their resistance ability to *Ca*HV, progressively increasing from susceptible clone to resistant clone at 1 dpi (52), which implies that *Cgviperin-A* and *Cgviperin-B* might play an important role in the battle between gibel carp and *Ca*HV.

Consistent with other vertebrate Viperin, both *Cg*Viperin-A and *Cg*Viperin-B contain three domains. The N-terminal domain shows considerable variability between species and

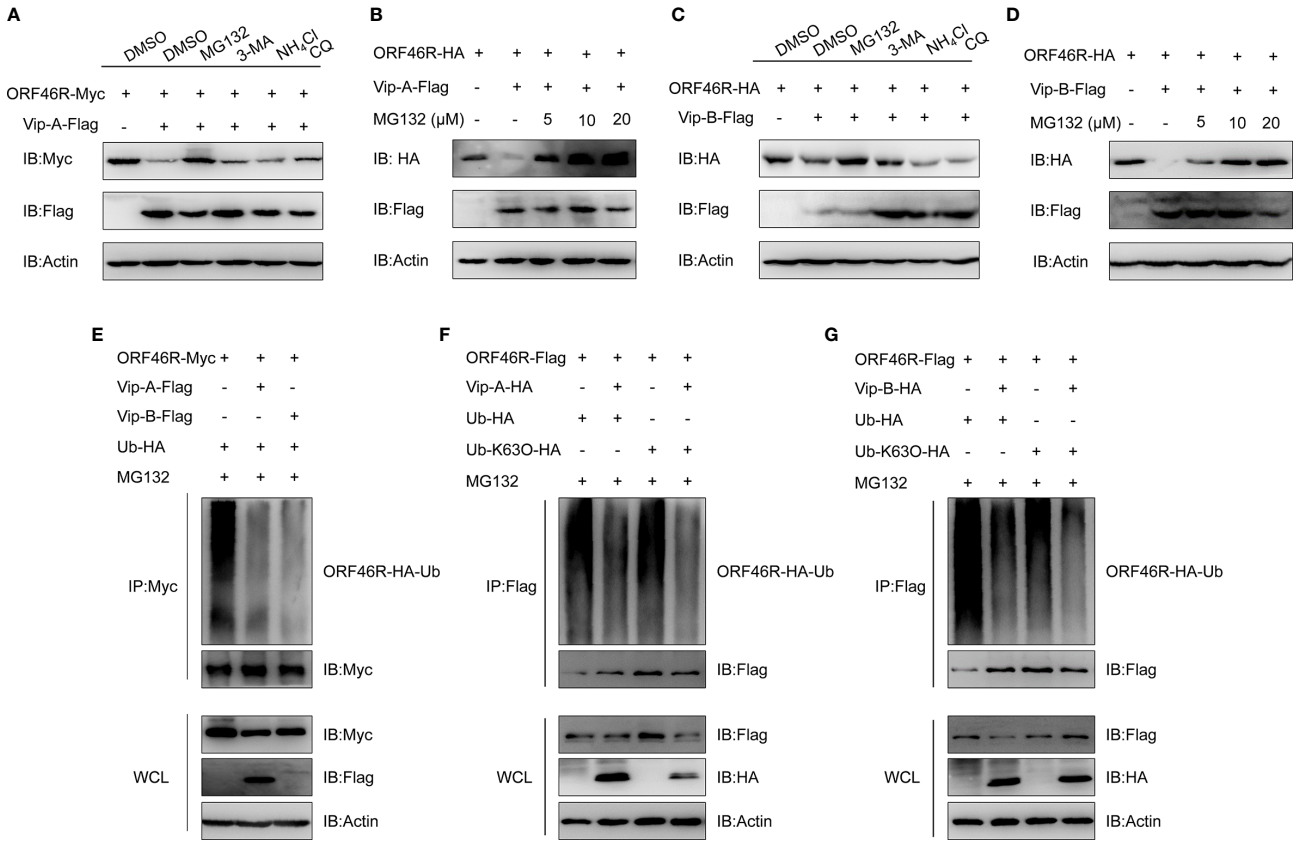

FIGURE 7 | *Cg*Viperin-A and *Cg*Viperin-B promote *Ca*HV ORF46R proteasomal degradation *via* decreasing K63-linked ubiquitination. **(A, C)** Effects of inhibitors on *Cg*Viperin-A **(A)** or *Cg*Viperin-B-mediated **(C)** destabilization of ORF46R. CAB cells were seeded in six-well overnight and transfected with the indicated expression vectors (2 μg/well). The cells were treated with the indicated inhibitors at 18 h post-transfection and harvested for western blot analysis with the anti-Flag and anti-β-actin Abs. **(B, D)** ORF46R degradation induced by *Cg*Viperin-A **(B)** or *Cg*Viperin-B **(D)** was rescued by MG132 in a dose-dependent manner. CAB cells were transfected with the indicated expression vectors (2 μg/well) and treated with DMSO or MG132 (5, 10, or 20 μM) for 6 h at 18 h post-transfection. Then, the WCL were subjected to western blot analysis with the indicated Abs. **(E)** *Cg*Viperin-A and *Cg*Viperin-B decreased the ubiquitination of ORF46R. CAB cells were seeded in 10 cm^2 dishes and transfected with 5 μg ORF46R-Myc, 4 μg *Cg*Viperin-A-Flag or *Cg*Viperin-B-Flag, and 1 μg HA-Ub and were treated with DMSO or MG132 for 6 h at 18 h post-transfection. After IP with anti-Myc-affinity gels, the immunoprecipitates and WCL were analyzed by western blot analysis with the indicated Abs. **(F, G)** *Cg*Viperin-A **(F)** and *Cg*Viperin-B **(G)** decreased the K63-linked ubiquitination of ORF46R. CAB cells were seeded in 10 cm^2 dishes were co-transfected with the indicated expression vectors (5 μg ORF46R-Flag, 4 μg *Cg*Viperin-A-HA, or *Cg*Viperin-B-HA) and 1 μg HA-Ub or Ub-K63O-HA, and were treated with MG132 for 6 h at 18 h post-transfection. After IP with anti-Flag-affinity gels, the immunoprecipitates and WCL were analyzed by western blot analysis with the indicated Abs. Data are presented based on three independent experiments.

aims at the localization of Viperin to the ER, lipid droplets, or mitochondria (19–21). Major sequence differences between *Cg*Viperin-A and *Cg*Viperin-B also exist in their N-terminal region (**Supplementary Figure S2**), and the two N-terminal truncated mutants (Vip-A-ΔN and Vip-B-ΔN) both result in the delocalization of Viperin from the ER membrane (**Figure 3**). The other two domains, the middle SAM and C-terminal domains, are highly conserved across species. The role of the C-terminal domain remains poorly defined (24). Mutating the C-terminal tryptophan residue of human VIPERIN could prevent its binding to iron-sulfur cluster–installing protein CIAO1 (71, 72). In this study, the C-terminal truncated mutants (Vip-A-ΔC and Vip-B-ΔC) failed to colocalize with and degrade *Ca*HV ORF46R (**Figures 4C, D**, **6C, D**), implying that the C-terminus is necessary for *Cg*Viperin-ORF46R interactions.

Mammalian Viperin has been found to interact with three groups of proteins: host proteins involved in innate immune signaling [i.e., Interleukin 1 Receptor Associated Kinase 1 (IRAK1), TNF Receptor Associated Factor 6 (TRAF6), Stimulator of Interferon Genes (STING), and TBK1], host metabolic enzymes [i.e., Farnesyl Pyrophosphate (FPPS) and Microsomal Triglyceride Transfer Protein (MTP)], and viral structural and non-structural proteins [i.e., Non-structural Protein 3 (NS3) and NS5A of flaviviruses] (27). The interactions between mammalian Viperin and viral proteins appear idiosyncratic. Viperin can inhibit viral RNA replication by interfering with the interactions between host proteins and viral non-structural proteins (28–30), inducing the degradation of viral proteins (27, 73), or acting through Fe-S cluster-dependent enzymatic activity (72). In this study, we found that

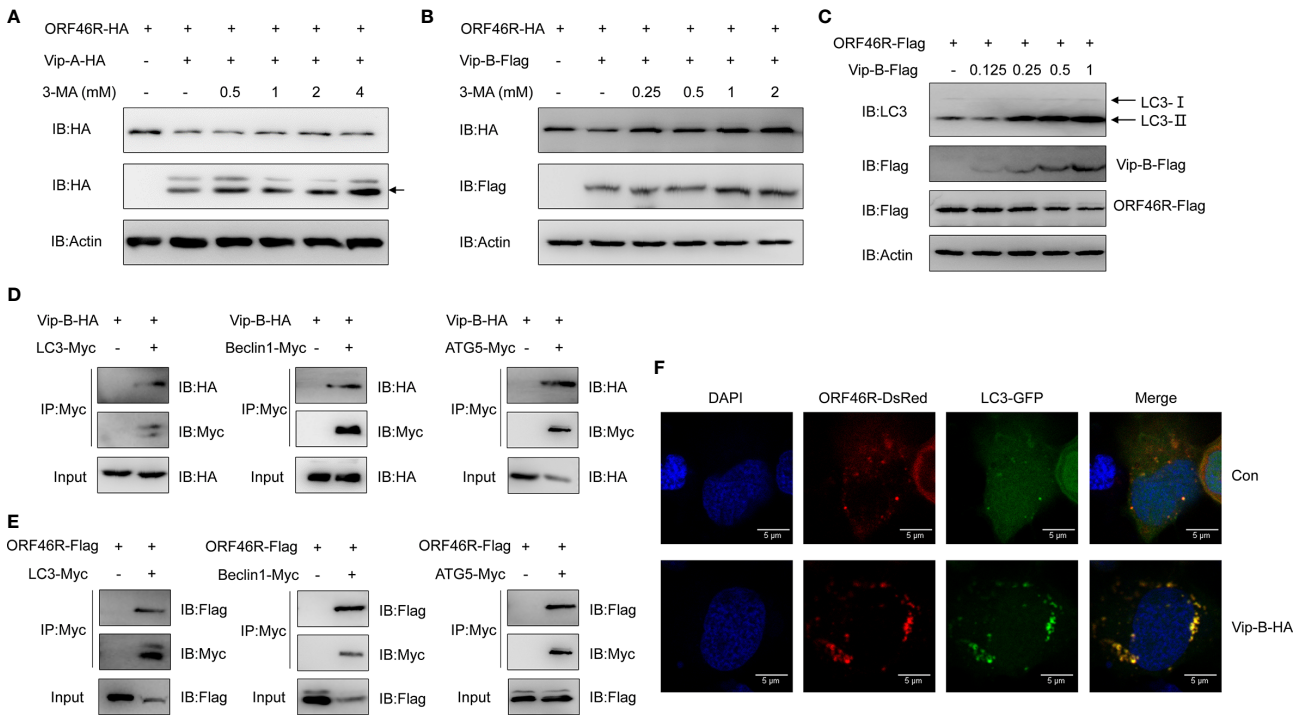

FIGURE 8 | *Cg*Viperin-B mediates degradation of *Ca*HV ORF46R *via* an autophagic pathway. **(A, B)** Effects of 3-MA on *Cg*Viperin-A- **(A)** or *Cg*Viperin-B-mediated **(B)** destabilization of ORF46R. CAB cells were transfected with the indicated expression vectors (2 μg/well) and treated with DMSO or 3-MA (0.5, 1, 2, or 4 mM in A and 0.25, 0.5, 1, or 2 mM in B) for 6 h at 18 h post-transfection. Then, the WCL were subjected to western blot analysis with the indicated Abs. **(C)** Effects of *Cg*Viperin-B on the conversion of LC3B-I to LC3B-II. CAB cells were transfected with increasing amounts of *Cg*Viperin-B-Flag (0.125, 0.25, 0.5, and 1 μg), analyzed by western blot analysis with the indicated Abs. **(D, E)** Co-IP of Vip-B-HA **(D)** or ORF46R-Flag **(E)** with LC3-Myc, Beclin1-Myc, and ATG5-Myc in HEK 293T cells transfected with the indicated plasmids. Anti-Myc Ab was used for Co-IP. **(F)** Subcellular colocalization of ORF46R and *Cg*Viperin-B with LC3-DsRed. CAB cells were plated onto coverslips in six-well plates and co-transfected with the indicated plasmids. After 24 h, the cells were fixed and observed under confocal microscopy. Nuclear was stained with DAPI. Scale bars = 5 μm.

both *Cg*Viperin-A and *Cg*Viperin-B could interact and promote *Ca*HV ORF46R protein degradation (**Figures 4A** and **6**). Our preliminary study showed that *Ca*HV ORF46R is a negative regulator of host IFN production because the overexpression of ORF46R could inhibit activation of the *Ca*IFN promoter and ISRE luciferase reporter activity stimulated by poly (dA:dT) (**Figure 5**). Up to now, the domain and exact function of ORF46R are unknown. By bioinformatics analysis, we did not find any known domain in ORF46R and any viral protein similar to ORF46R that had been studied. Further research will be required to determine which region can interact with *Cg*Viperins and to reveal the exact function of ORF46R in *Ca*HV invasion, replication, assembly, or release, especially in *Ca*HV evasion from the host IFN response.

Among the diverse antiviral mechanisms, one emerging theme is that Viperin seems to promote the ubiquitin-dependent proteasomal degradation of some target proteins (27). For example, human VIPERIN can promote the degradation of viral NS5A through the proteasomal degradation pathway (27). It was also found to be capable of stimulating K63-linked polyubiquitination of IRAK1, which phosphorylated interferon regulatory factor (IRF) 7 and ultimately led to IFN production (74). In this study, we found that both *Cg*Viperin-A and *Cg*Viperin-B could promote *Ca*HV ORF46R proteasomal degradation, most likely by decreasing the K63-linked ubiquitination of ORF46R (**Figure 7**). Our findings suggest that *Cg*Viperin-A and *Cg*Viperin-B, like their human homologous genes, may have a general role in engaging with E3 ubiquitin ligases, which are responsible for tagging proteins with polyubiquitin chains. The ubiquitin molecule contains seven lysine residues (K6, K11, K27, K29, K33, K48, and K63) and an amino terminus (M1), which can conjugate with other ubiquitin molecules to form polymeric chains (66, 67). Among them, the K63-based polymeric chain is one of the best described codes and mainly involves in signal transduction, protein sorting and trafficking, and enzymatic activity (67). A growing number of studies suggest that ubiquitin chains play an important role in the modulation of innate immunity (75). Altogether, our results suggest that the overexpression of *Cg*Viperin-A or *Cg*Viperin-B can decrease the K63-linked ubiquitination of endogenous ORF46R protein, which reduces the stability of ORF46R protein and ultimately results in its degradation by the proteasome. There is still much to study on this topic, including which of the ubiquitin ligases *Cg*Viperin and

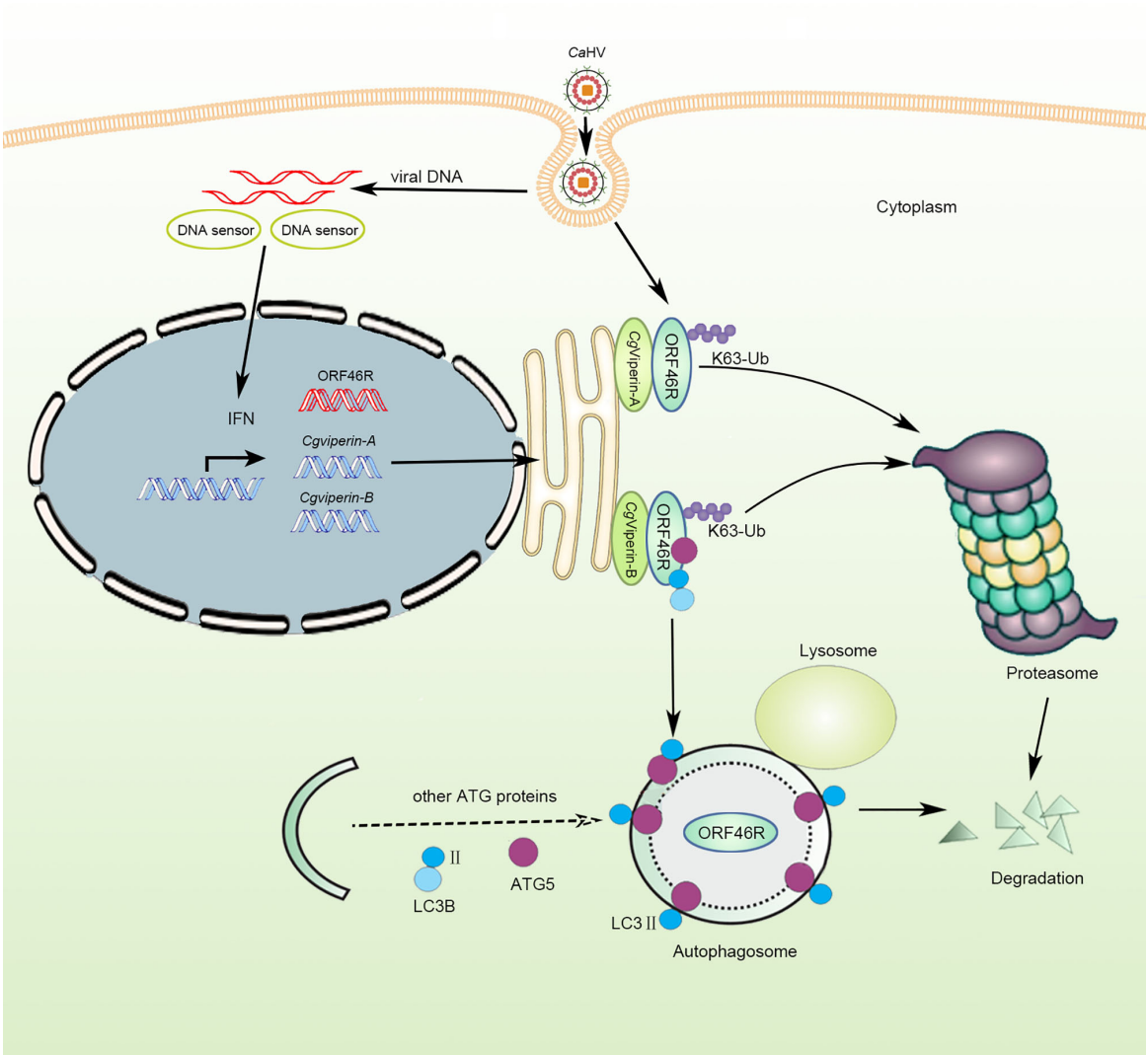

FIGURE 9 | Schematic diagram of divergent antiviral mechanisms of *Cg*Viperin-A and *Cg*Viperin-B in gibel carp resistance against herpesvirus *Ca*HV. Both *Cg*Viperin-A and *Cg*Viperin-B directly interact and promote proteasomal degradation of *Ca*HV ORF46R *via* decreasing K63-linked ubiquitination. In addition, *Cg*Viperin-B induces ORF46R degradation through autophagosome pathway.

*Cg*Viperin-B interact with and how they cooperate to degrade viral ORF46R.

Eukaryote organisms possess two major cellular degradation machineries: the ubiquitin–proteasome system (UBS) and autophagy-lysosome pathway (ALP) (76, 77). As described above, *Cg*Viperin-A and *Cg*Viperin-B could both promote *Ca*HV ORF46R proteasomal degradation in CAB cells (**Figure 7**). In this study, *Cg*Viperin-B-mediated ORF46R degradation is blocked by autophagy inhibitor 3-MA, and both of them are interacted with the same autophagic components; meanwhile the transformation of LC3 from type I to type II is increased, demonstrating autophagy is one mechanism of *Cg*Viperin-B to degrade viral protein. On the other hand, our data also suggest that ORF46R can also be eliminated by *Cg*Viperin-B during the ubiquitination. Whether there is association between these two mechanisms is still unclear. Which one exerts the major antiviral function is also unknown. Both of that need to be clarified in further study. For unknown reasons, the CAB cells and other cell lines used in our laboratory failed to proliferate *Ca*HV. Therefore, we could not perform the antiviral studies *in vitro* where the proteins are overexpressed or knocked out, followed by a virus infection. In the further study, we will mutate *Cgviperin-A* and *Cgviperin-B*, respectively, in gibel carp by using CRISPR/Cas9 and compare the antiviral differences between them, which would help to complete the story and highlight their antiviral activity.

Based on the above results of functional analysis *in vitro*, we propose a schematic diagram for divergent antiviral mechanisms of *Cg*Viperin-A and *Cg*Viperin-B in the gibel carp resistance against herpesvirus *Ca*HV (**Figure 9**). After *Ca*HV invasion, both *Cg*Viperin-A and *Cg*Viperin-B could promote the proteasomal degradation of *Ca*HV ORF46R *via* decreasing K63-linked ubiquitination. Additionally, *Cg*Viperin-B also mediated ORF46R degradation through autophagosome pathway. In conclusion, the current findings shed light on the antiviral activities of teleost Viperin as well as the divergent functions and regulative mechanisms of two duplicated *viperin* homeologs. Meanwhile, the above data also imply that the two *viperin* homeologs have subfunctionalized and cooperate to regulate antiviral response.

DATA AVAILABILITY STATEMENT

The datasets presented in this study can be found in online repositories. The names of the repository/repositories and accession number(s) can be found below: MZ055409 (https://www.ncbi.nlm.nih.gov/nuccore/MZ055409); MZ055410 (https://www.ncbi.nlm.nih.gov/nuccore/MZ055410); MZ055411 (https://www.ncbi.nlm.nih.gov/nuccore/MZ055411); MZ055412 (https://www.ncbi.nlm.nih.gov/nuccore/MZ055412); MZ055413 (https://www.ncbi.nlm.nih.gov/nuccore/MZ055413); MZ055414 (https://www.ncbi.nlm.nih.gov/nuccore/MZ055414); MZ055415 (https://www.ncbi.nlm.nih.gov/nuccore/MZ055415); MZ055416 (https://www.ncbi.nlm.nih.gov/nuccore/MZ055416); MZ055417 (https://www.ncbi.nlm.nih.gov/nuccore/MZ055417); MZ055418 (https://www.ncbi.nlm.nih.gov/nuccore/MZ055418); MZ055419 (https://www.ncbi.nlm.nih.gov/nuccore/MZ055419); MZ055420 (https://www.ncbi.nlm.nih.gov/nuccore/MZ055420).

ETHICS STATEMENT

The animal study was reviewed and approved by the Institutional Animal Care and Use Committee of IHB, CAS (protocol number 2016-018).

AUTHOR CONTRIBUTIONS

J-FG, LZ, and C-YM designed the study. C-YM, SL, L-FL, PY, ZL, J-FT, Q-YZ, Z-WW, X-JZ, and G-XW prepared the samples and carried out the experiments. C-YM, LZ, J-FG, SL, and YW analyzed and discussed the results. LZ, J-FG, SL, YW, and C-YM wrote the paper. All authors contributed to the article and approved the submitted version.

FUNDING

This work was supported by the Strategic Priority Research Program of the Chinese Academy of Sciences (XDA24030203 and XDA24030104), the National Natural Science Foundation (31772838), and China Agriculture Research System of MOF and MARA (CARS-45-07). The funding bodies had no role in the design of the study and collection, analysis, and interpretation of data and in writing the manuscript.

ACKNOWLEDGMENTS

We thank the reviewers for helpful discussion in editing this manuscript. The research was supported by the Analytical & Testing Center, IHB, CAS and Wuhan Branch, Supercomputing Centre, CAS, China.

SUPPLEMENTARY MATERIAL

The Supplementary Material for this article can be found online at: https://www.frontiersin.org/articles/10.3389/fimmu.2021.702971/full#supplementary-material

Supplementary Figure S1 | Multiple nucleotide sequence alignment of six *Cgviperin* transcripts from gibel carp clone F. ORF is highlighted by red box.

Supplementary Figure S2 | Multiple amino acid sequence alignment of *Cg*Viperin proteins from gibel carp clone F.

Supplementary Table S1 | Primers used in this study.

REFERENCES

1. Soltis DE, Visger CJ, Soltis PS. The Polyploidy Revolution Then … and Now: Stebbins Revisited. *Am J Bot* (2014) 101(7):1057–78. doi: 10.3732/ajb.1400178
2. Soltis PS, Soltis DE. Ancient WGD Events as Drivers of Key Innovations in Angiosperms. *Curr Opin Plant Biol* (2016) 30:159–65. doi: 10.1016/j.pbi.2016.03.015
3. Cheng F, Wu J, Cai X, Liang JL, Freeling M, Wang XW. Gene Retention, Fractionation and Subgenome Differences in Polyploid Plants. *Nat Plants* (2018) 4(5):258–68. doi: 10.1038/s41477-018-0136-7
4. Clark JW, Donoghue PCJ. Whole-Genome Duplication and Plant Macroevolution. *Trends Plant Sci* (2018) 23(10):933–45. doi: 10.1016/j.tplants.2018.07.006
5. Mandakova T, Lysak MA. Post-Polyploid Diploidization and Diversification Through Dysploid Changes. *Curr Opin Plant Biol* (2018) 42:55–65. doi: 10.1016/j.pbi.2018.03.001
6. Van de Peer Y, Maere S, Meyer A. The Evolutionary Significance of Ancient Genome Duplications. *Nat Rev Genet* (2009) 10(10):725–32. doi: 10.1038/nrg2600
7. Van De Peer Y, Mizrachi E, Marchal K. The Evolutionary Significance of Polyploidy. *Nat Rev Genet* (2017) 18(7):411–24. doi: 10.1038/nrg.2017.26
8. Fox DT, Soltis DE, Soltis PS, Ashman TL, Van de Peer Y. Polyploidy: A Biological Force From Cells to Ecosystems. *Trends Cell Biol* (2020) 30(9):688–94. doi: 10.1016/j.tcb.2020.06.006
9. Carretero-Paulet L, Van de Peer Y. The Evolutionary Conundrum of Whole-Genome Duplication. *Am J Bot* (2020) 107(8):1101–5. doi: 10.1002/ajb2.1520
10. Zhou L, Gui JF. Natural and Artificial Polyploids in Aquaculture. *Aquac Fish* (2017) 3(2):103–11. doi: 10.1016/j.aaf.2017.04.003
11. Amores A, Force A, Yan YL, Joly L, Amemiya C, Fritz A, et al. Zebrafish Hox Clusters and Vertebrate Genome Evolution. *Science.* (1998) 282(5394):1711–4. doi: 10.1126/science.282.5394.1711
12. Jaillon O, Aury JM, Wincker P. "Changing by Doubling", the Impact of Whole Genome Duplications in the Evolution of Eukaryotes. *Cr Biol* (2009) 332(2-3):241–53. doi: 10.1016/j.crvi.2008.07.007
13. Rodriguez F, Arkhipova IR. Transposable Elements and Polyploid Evolution in Animals. *Curr Opin Genet Dev* (2018) 49:115–23. doi: 10.1016/j.gde.2018.04.003

14. Chin KC, Cresswell P. Viperin (Cig5), an IFN-Inducible Antiviral Protein Directly Induced by Human Cytomegalovirus. *Proc Natl Acad Sci U S A* (2001) 98(26):15125–30. doi: 10.1073/pnas.011593298
15. Boudinot P, Massin P, Blanco M, Riffault S, Benmansour A. *Vig-1*, a New Fish Gene Induced by the Rhabdovirus Glycoprotein, has a Virus-Induced Homologue in Humans and Shares Conserved Motifs With the MoaA Family. *J Virol* (1999) 73(3):1846–52. doi: 10.1128/JVI.73.3.1846-1852.1999
16. Fenwick MK, Li Y, Cresswell P, Modis Y, Ealick SE. Structural Studies of Viperin, an Antiviral Radical SAM Enzyme. *Proc Natl Acad Sci U S A* (2017) 114(26):6806–11. doi: 10.1073/pnas.1705402114
17. Zhu H, Cong JP, Shenk T. Use of Differential Display Analysis to Assess the Effect of Human Cytomegalovirus Infection on the Accumulation of Cellular RNAs: Induction of Interferon-Responsive RNAs. *Proc Natl Acad Sci U S A* (1997) 94(25):13985–90. doi: 10.1073/pnas.94.25.13985
18. Mattijssen S, Pruijn GJ. Viperin, a Key Player in the Antiviral Response. *Microbes Infect* (2012) 14(5):419–26. doi: 10.1016/j.micinf.2011.11.015
19. Seo JY, Yaneva R, Cresswell P. Viperin: A Multifunctional, Interferon-Inducible Protein That Regulates Virus Replication. *Cell Host Microbe* (2011) 10(6):534–9. doi: 10.1016/j.chom.2011.11.004
20. Hinson ER, Cresswell P. The N-Terminal Amphipathic Alpha-Helix of Viperin Mediates Localization to the Cytosolic Face of the Endoplasmic Reticulum and Inhibits Protein Secretion. *J Biol Chem* (2009) 284(7):4705–12. doi: 10.1074/jbc.M807261200
21. Hinson ER, Cresswell P. The Antiviral Protein, Viperin, Localizes to Lipid Droplets *via* its N-Terminal Amphipathic Alpha-Helix. *Proc Natl Acad Sci U S A* (2009) 106(48):20452–7. doi: 10.1073/pnas.0911679106
22. Duschene KS, Broderick JB. The Antiviral Protein Viperin is a Radical SAM Enzyme. *FEBS Lett* (2010) 584(6):1263–7. doi: 10.1016/j.febslet.2010.02.041
23. Shaveta G, Shi JH, Chow VTK, Song JX. Structural Characterization Reveals That Viperin is a Radical S-Adenosyl-L-Methionine (SAM) Enzyme. *Biochem Biophys Res Commun* (2010) 391(3):1390–5. doi: 10.1016/j.bbrc.2009.12.070
24. Ng LFP, Hiscox JA. Viperin Poisons Viral Replication. *Cell Host Microbe* (2018) 24(2):181–3. doi: 10.1016/j.chom.2018.07.014
25. Helbig KJ, Beard MR. The Role of Viperin in the Innate Antiviral Response. *J Mol Biol* (2014) 426(6):1210–9. doi: 10.1016/j.jmb.2013.10.019
26. Lindqvist R, Overby AK. The Role of Viperin in Antiflavivirus Responses. *DNA Cell Biol* (2018) 37(9):725–30. doi: 10.1089/dna.2018.4328
27. Ghosh S, Marsh ENG. Viperin: An Ancient Radical SAM Enzyme Finds its Place in Modern Cellular Metabolism and Innate Immunity. *J Biol Chem* (2020) 295(33):11513–28. doi: 10.1074/jbc.REV120.012784
28. Jiang D, Guo H, Xu C, Chang J, Gu B, Wang L, et al. Identification of Three Interferon-Inducible Cellular Enzymes That Inhibit the Replication of Hepatitis C Virus. *J Virol* (2008) 82(4):1665–78. doi: 10.1128/JVI.02113-07
29. Helbig KJ, Eyre NS, Yip E, Narayana S, Li K, Fiches G, et al. The Antiviral Protein Viperin Inhibits Hepatitis C Virus Replication *via* Interaction With Nonstructural Protein 5a. *Hepatology* (2011) 54(5):1506–17. doi: 10.1002/hep.24542
30. Helbig KJ, Carr JM, Calvert JK, Wati S, Clarke JN, Eyre NS, et al. Viperin Is Induced Following Dengue Virus Type-2 (DENV-2) Infection and Has Anti-Viral Actions Requiring the C-Terminal End of Viperin. *PloS Negl Trop D* (2013) 7(4):e2178. doi: 10.1371/journal.pntd.0002178
31. Wang XY, Hinson ER, Cresswell P. The Interferon-Inducible Protein Viperin Inhibits Influenza Virus Release by Perturbing Lipid Rafts. *Cell Host Microbe* (2007) 2(2):96–105. doi: 10.1016/j.chom.2007.06.009
32. Nasr N, Maddocks S, Turville SG, Harman AN, Woolger N, Helbig KJ, et al. HIV-1 Infection of Human Macrophages Directly Induces Viperin Which Inhibits Viral Production. *Blood* (2012) 120(4):778–88. doi: 10.1182/blood-2012-01-407395
33. Gizzi AS, Grove TL, Arnold JJ, Jose J, Jangra RK, Garforth SJ, et al. Publisher Correction: A Naturally Occurring Antiviral Ribonucleotide Encoded by the Human Genome. *Nature* (2018) 562(7725):610–4. doi: 10.1038/s41586-018-0355-0
34. Sun BJ, Nie P. Molecular Cloning of the Viperin Gene and its Promoter Region From the Mandarin Fish Siniperca Chuatsi. *Vet Immunol Immunopathol* (2004) 101(3-4):161–70. doi: 10.1016/j.vetimm.2004.04.013
35. Chen ZY, Lei XY, Zhang QY. The Antiviral Defense Mechanisms in Mandarin Fish Induced by DNA Vaccination Against a Rhabdovirus. *Vet Microbiol* (2012) 157(3-4):264–75. doi: 10.1016/j.vetmic.2011.12.025
36. Lee SH, Peng KC, Lee LH, Pan CY, Hour AL, Her GM, et al. Characterization of Tilapia (*Oreochromis Niloticus*) Viperin Expression, and Inhibition of Bacterial Growth and Modulation of Immune-Related Gene Expression by Electrotransfer of Viperin DNA Into Zebrafish Muscle. *Vet Immunol Immunopathol* (2013) 151(3-4):217–28. doi: 10.1016/j.vetimm.2012.11.010
37. Wang B, Zhang YB, Liu TK, Shi J, Sun F, Gui JF. Fish Viperin Exerts a Conserved Antiviral Function Through RLR-Triggered IFN Signaling Pathway. *Dev Comp Immunol* (2014) 47(1):140–9. doi: 10.1016/j.dci.2014.07.006
38. Eslamloo K, Ghorbani A, Xue X, Inkpen SM, Larijani M, Rise ML. Characterization and Transcript Expression Analyses of Atlantic Cod Viperin. *Front Immunol* (2019) 10:311. doi: 10.3389/fimmu.2019.00311
39. Wang F, Jiao HQ, Liu WM, Chen B, Wang YD, Chen BX, et al. The Antiviral Mechanism of Viperin and its Splice Variant in Spring Viremia of Carp Virus Infected Fathead Minnow Cells. *Fish Shellfish Immunol* (2019) 86:805–13. doi: 10.1016/j.fsi.2018.12.012
40. Zhang SH, Lv XY, Deng D, Zeng L, Huang W, Tang DD, et al. Gene Characterization and Expression Pattern of Mx and Viperin Genes in Dabry's Sturgeon Acipenser Dabryanus. *J Appl Ichthyol* (2019) 35(2):408–19. doi: 10.1111/jai.13876
41. Gui JF, Zhou L. Genetic Basis and Breeding Application of Clonal Diversity and Dual Reproduction Modes in Polyploid *Carassius Auratus Gibelio*. *Sci China Life Sci* (2010) 53(4):409–15. doi: 10.1007/s11427-010-0092-6
42. Li XY, Gui JF. Diverse and Variable Sex Determination Mechanisms in Vertebrates. *Sci China Life Sci* (2018) 61(12):1503–14. doi: 10.1007/s11427-018-9415-7
43. Li XY, Liu XL, Zhu YJ, Zhang J, Ding M, Wang MT, et al. Origin and Transition of Sex Determination Mechanisms in a Gynogenetic Hexaploid Fish. *Heredity (Edinb)* (2018) 121(1):64–74. doi: 10.1038/s41437-017-0049-7
44. Wang ZW, Zhu HP, Wang D, Jiang FF, Guo W, Zhou L, et al. A Novel Nucleo-Cytoplasmic Hybrid Clone Formed *via* Androgenesis in Polyploid Gibel Carp. *BMC Res Notes* (2011) 4:82. doi: 10.1186/1756-0500-4-82
45. Chen F, Li XY, Zhou L, Yu P, Wang ZW, Li Z, et al. Stable Genome Incorporation of Sperm-Derived DNA Fragments in Gynogenetic Clone of Gibel Carp. *Mar Biotechnol* (2020) 22(1):54–66. doi: 10.1007/s10126-019-09930-w
46. Zhou L, Wang ZW, Wang Y, Gui JF. Crucian Carp and Gibel Carp Culture. In: . *Aquaculture in China: Success Stories and Modern Trends*. Oxford: John Wiley & Sons Ltd (2018). p. 149–57.
47. Zeng XT, Chen ZY, Deng YS, Gui JF, Zhang QY. Complete Genome Sequence and Architecture of Crucian Carp *Carassius Auratus* Herpesvirus (*Ca*HV). *Arch Virol* (2016) 161(12):3577–81. doi: 10.1007/s00705-016-3037-y
48. Gao FX, Wang Y, Zhang QY, Mou CY, Li Z, Deng YS, et al. Distinct Herpesvirus Resistances and Immune Responses of Three Gynogenetic Clones of Gibel Carp Revealed by Comprehensive Transcriptomes. *BMC Genomics* (2017) 18(1):561. doi: 10.1186/s12864-017-3945-6
49. Gao FX, Lu WJ, Wang Y, Zhang QY, Zhang YB, Mou CY, et al. Differential Expression and Functional Diversification of Diverse Immunoglobulin Domain-Containing Protein (DICP) Family in Three Gynogenetic Clones of Gibel Carp. *Dev Comp Immunol* (2018) 84:396–407. doi: 10.1016/j.dci.2018.03.013
50. Lu WJ, Zhou L, Gao FX, Zhou YL, Li Z, Zhang XJ, et al. Dynamic and Differential Expression of Duplicated *Cxcr4/Cxcl12* Genes Facilitates Antiviral Response in Hexaploid Gibel Carp. *Front Immunol* (2020) 11:2176. doi: 10.3389/fimmu.2020.02176
51. Lu WJ, Gao FX, Wang Y, Zhang QY, Li Z, Zhang XJ, et al. Differential Expression of Innate and Adaptive Immune Genes in the Survivors of Three Gibel Carp Gynogenetic Clones After Herpesvirus Challenge. *BMC Genomics* (2019) 20:432. doi: 10.1186/s12864-019-5777-z
52. Mou CY, Wang Y, Zhang QY, Gao FX, Li Z, Tong JF, et al. Differential Interferon System Gene Expression Profiles in Susceptible and Resistant Gynogenetic Clones of Gibel Carp Challenged With Herpesvirus *Ca*HV. *Dev Comp Immunol* (2018) 86:52–64. doi: 10.1016/j.dci.2018.04.024
53. Lu M, Li XY, Li Z, Du WX, Zhou L, Wang Y, et al. Regain of Sex Determination System and Sexual Reproduction Ability in a Synthetic Octoploid Male Fish. *Sci China Life Sci* (2021) 64(1):77–87. doi: 10.1007/s11427-020-1694-7
54. Yu P, Wang Y, Yang WT, Li Z, Zhang XJ, Zhou L, et al. Upregulation of the PPAR Signaling Pathway and Accumulation of Lipids are Related to the

Morphological and Structural Transformation of the Dragon-Eye Goldfish Eye. *Sci China Life Sci* (2021) 64(7):1031–49. doi: 10.1007/s11427-020-1814-1
55. Li XY, Zhang XJ, Li Z, Hong W, Liu W, Zhang J, et al. Evolutionary History of Two Divergent *Dmrt1* Genes Reveals Two Rounds of Polyploidy Origins in Gibel Carp. *Mol Phylogenet Evol* (2014) 78:96–104. doi: 10.1016/j.ympev.2014.05.005
56. Zhang YB, Zhang QY, Xu DQ, Hu CY, Gui JF. Identification of Antiviral-Relevant Genes in the Cultured Fish Cells Induced by UV-Inactivated Virus. *Chin Sci Bull* (2003) 48(6):581–8. doi: 10.1360/03tb9124
57. Liu TK, Zhang YB, Liu Y, Sun F, Gui JF. Cooperative Roles of Fish Protein Kinase Containing Z-DNA Binding Domains and Double-Stranded RNA-Dependent Protein Kinase in Interferon-Mediated Antiviral Response. *J Virol* (2011) 85(23):12769–80. doi: 10.1128/JVI.05849-11
58. Liu Y, Zhang YB, Liu TK, Gui JF. Lineage-Specific Expansion of IFIT Gene Family: An Insight Into Coevolution With IFN Gene Family. *PloS One* (2013) 8(6):e66859. doi: 10.1371/journal.pone.0066859
59. Xu L, Podok P, Xie J, Lu L. Comparative Analysis of Differential Gene Expression in Kidney Tissues of Moribund and Surviving Crucian Carp (*Carassius Auratus Gibelio*) in Response to Cyprinid Herpesvirus 2 Infection. *Arch Virol* (2014) 159(8):1961–74. doi: 10.1007/s00705-014-2011-9
60. Gan RH, Wang Y, Li Z, Yu ZX, Li XY, Tong JF, et al. Functional Divergence of Multiple Duplicated *Foxl2* Homeologs and Alleles in a Recurrent Polyploid Fish. *Mol Biol Evol* (2021) 38(5):1995–2013. doi: 10.1093/molbev/msab002
61. Lu LF, Li S, Wang ZX, Du SQ, Chen DD, Nie P, et al. Grass Carp Reovirus VP41 Targets Fish MITA To Abrogate the Interferon Response. *J Virol* (2017) 91(14):e00390–17. doi: 10.1128/JVI.00390-17
62. Li S, Lu LF, Liu SB, Zhang C, Li ZC, Zhou XY, et al. Spring Viraemia of Carp Virus Modulates P53 Expression Using Two Distinct Mechanisms. *PloS Pathog* (2019) 15(3):e1007695. doi: 10.1371/journal.ppat.1007695
63. Lu LF, Li S, Lu XB, LaPatra SE, Zhang N, Zhang XJ, et al. Spring Viremia of Carp Virus N Protein Suppresses Fish IFN Phi 1 Production by Targeting the Mitochondrial Antiviral Signaling Protein. *J Immunol* (2016) 196(9):3744–53. doi: 10.4049/jimmunol.1502038
64. Sun F, Zhang YB, Liu TK, Shi J, Wang B, Gui JF. Fish MITA Serves as a Mediator for Distinct Fish IFN Gene Activation Dependent on IRF3 or IRF7. *J Immunol* (2011) 187(5):2531–9. doi: 10.4049/jimmunol.1100642
65. Deribe YL, Pawson T, Dikic I. Post-Translational Modifications in Signal Integration. *Nat Struct Mol Biol* (2010) 17(6):666–72. doi: 10.1038/nsmb.1842
66. Ikeda F, Dikic I. Atypical Ubiquitin Chains: New Molecular Signals - 'Protein Modifications: Beyond the Usual Suspects' Review Series. *EMBO Rep* (2008) 9 (6):536–42. doi: 10.1038/embor.2008.93
67. Yau R, Rape M. The Increasing Complexity of the Ubiquitin Code. *Nat Cell Biol* (2016) 18(6):579–86. doi: 10.1038/ncb3358
68. Feng H, Zhang YB, Gui JF, Lemon SM, Yamane D. Interferon Regulatory Factor 1 (IRF1) and Anti-Pathogen Innate Immune Responses. *PloS Pathog* (2021) 17(1):e1009220. doi: 10.1371/journal.ppat.1009220
69. Jiang SY, Wang Y, Zhou L, Chen F, Li Z, Gui JF. Molecular Characteristics, Genomic Structure and Expression Patterns of Diverse *Bmp15* Alleles in Polyploid Gibel Carp Clone F. *Acta Hydrobiol Sin* (2020) 44:518–27. doi: 10.7541/2020.063
70. Zhang QQ, Zhou L, Li Z, Gan RH, Yu ZX, Gui JF, et al. Allelic Diversification, Syntenic Alignment and Expression Patterns of *Nanos2* in Polyploid Gibel Carp. *Acta Hydrobiol Sin* (2020) 44(5):1087–96. doi: 10.7541/2020.126
71. Upadhyay AS, Stehling O, Panayiotou C, Rosser R, Lill R, Overby AK. Cellular Requirements for Iron-Sulfur Cluster Insertion Into the Antiviral Radical SAM Protein Viperin. *J Biol Chem* (2017) 292(33):13879–89. doi: 10.1074/jbc.M117.780122
72. Upadhyay AS, Vonderstein K, Pichlmair A, Stehling O, Bennett KL, Dobler G, et al. Viperin is an Iron-Sulfur Protein That Inhibits Genome Synthesis of Tick-Borne Encephalitis Virus *via* Radical SAM Domain Activity. *Cell Microbiol* (2014) 16(6):834–48. doi: 10.1111/cmi.12241
73. Panayiotou C, Lindqvist R, Kurhade C, Vonderstein K, Pasto J, Edlund K, et al. Viperin Restricts Zika Virus and Tick-Borne Encephalitis Virus Replication by Targeting NS3 for Proteasomal Degradation. *J Virol* (2018) 92(7):e02054–17. doi: 10.1128/JVI.02054-17
74. Dumbrepatil AB, Ghosh S, Zegalia KA, Malec PA, Hoff JD, Kennedy RT, et al. Viperin Interacts With the Kinase IRAK1 and the E3 Ubiquitin Ligase TRAF6, Coupling Innate Immune Signaling to Antiviral Ribonucleotide Synthesis. *J Biol Chem* (2019) 294(17):6888–98. doi: 10.1074/jbc.RA119.007719
75. Zheng Y, Gao CJ. E3 Ubiquitin Ligases, the Powerful Modulator of Innate Antiviral Immunity. *Cell Immunol* (2019) 340:103915. doi: 10.1016/j.cellimm.2019.04.003
76. Cohen-Kaplan V, Livneh I, Avni N, Cohen-Rosenzweig C, Ciechanover A. The Ubiquitin-Proteasome System and Autophagy: Coordinated and Independent Activities. *Int J Biochem Cell Biol* (2016) 79:403–18. doi: 10.1016/j.biocel.2016.07.019
77. Diki K, Ghanmi A. A Quaternionic Analogue of the Segal-Bargmann Transform. *Complex Anal Oper Th* (2017) 11(2):457–73. doi: 10.1007/s11785-016-0609-5

Conflict of Interest: The authors declare that the research was conducted in the absence of any commercial or financial relationships that could be construed as a potential conflict of interest.

Publisher's Note: All claims expressed in this article are solely those of the authors and do not necessarily represent those of their affiliated organizations, or those of the publisher, the editors and the reviewers. Any product that may be evaluated in this article, or claim that may be made by its manufacturer, is not guaranteed or endorsed by the publisher.

frontiers in Immunology

ORIGINAL RESEARCH
published: 21 September 2021
doi: 10.3389/fimmu.2021.705601

Transcriptome Responses of Atlantic Salmon (*Salmo salar* L.) to Viral and Bacterial Pathogens, Inflammation, and Stress

Aleksei Krasnov[1]*, *Lill-Heidi Johansen*[1], *Christian Karlsen*[1], *Lene Sveen*[1], *Elisabeth Ytteborg*[1], *Gerrit Timmerhaus*[1], *Carlo C. Lazado*[1] *and Sergey Afanasyev*[2]

[1] Fish Health Department, Nofima AS, Ås, Norway, [2] Laboratory of Neurophysiology and Behavioral Pathology, I. M. Sechenov Institute of Evolutionary Physiology and Biochemistry, Saint-Petersburg, Russia

Transcriptomics provides valuable data for functional annotations of genes, the discovery of biomarkers, and quantitative assessment of responses to challenges. Meta-analysis of Nofima's Atlantic salmon microarray database was performed for the selection of genes that have shown strong and reproducible expression changes. Using data from 127 experiments including 6440 microarrays, four transcription modules (TM) were identified with a total of 902 annotated genes: 161 virus responsive genes – VRG (activated with five viruses and poly I:C), genes that responded to three pathogenic bacteria (523 up and 33 down-regulated genes), inflammation not caused by infections – wounds, melanized foci in skeletal muscle and exposure to PAMP (180 up and 72 down-regulated genes), and stress by exercise, crowding and cortisol implants (33 genes). To assist the selection of gene markers, genes in each TM were ranked according to the scale of expression changes. In terms of functional annotations, association with diseases and stress was unknown or not reflected in public databases for a large part of genes, including several genes with the highest ranks. A set of multifunctional genes was discovered. Cholesterol 25-hydroxylase was present in all TM and 22 genes, including most differentially expressed matrix metalloproteinases 9 and 13 were assigned to three TMs. The meta-analysis has improved understanding of the defense strategies in Atlantic salmon. VRG have demonstrated equal or similar responses to RNA (SAV, IPNV, PRV, and ISAV), and DNA (gill pox) viruses, injection of bacterial DNA (plasmid) and exposure of cells to PAMP (CpG and gardiquimod) and relatively low sensitivity to inflammation and bacteria. Genes of the highest rank show preferential expression in erythrocytes. This group includes multigene families (gig and several trim families) and many paralogs. Of pathogen recognition receptors, only RNA helicases have shown strong expression changes. Most VRG (82%) are effectors with a preponderance of ubiquitin-related genes, GTPases, and genes of nucleotide metabolism. Many VRG have unknown roles. The identification of TMs makes possible quantification of responses and assessment of their interactions. Based on this, we are able to separate pathogen-specific responses from general inflammation and stress.

Keywords: Atlantic salmon, transcriptome, meta-analysis, virus, bacterial pathogen, inflammation, stress

OPEN ACCESS

Edited by:
Verónica Chico Gras, Universidad Miguel Hernández de Elche, Spain

Reviewed by:
Tor Gjøen, University of Oslo, Norway
Kristina Marie Miller, University of British Columbia, Canada

***Correspondence:**
Aleksei Krasnov
aleksei.krasnov@nofima.no

Specialty section:
This article was submitted to Comparative Immunology, a section of the journal Frontiers in Immunology

Received: *05 May 2021*
Accepted: *03 September 2021*
Published: *21 September 2021*

Citation:
Krasnov A, Johansen L-H, Karlsen C, Sveen L, Ytteborg E, Timmerhaus G, Lazado CC and Afanasyev S (2021) Transcriptome Responses of Atlantic Salmon (Salmo salar L.) to Viral and Bacterial Pathogens, Inflammation, and Stress. Front. Immunol. 12:705601. doi: 10.3389/fimmu.2021.705601

INTRODUCTION

Since its inception at the beginning of the new millennium, transcriptomics has continued to play an essential role in fish biology and aquaculture research. The assembly and publication of the Atlantic salmon (*Salmo salar* L.) genome (1) have enhanced further development by standardizing gene nomenclature and provided a framework for mapping differentially expressed genes, thereby facilitating comparison among experiments. The number of sequenced bony fish genomes is rapidly increasing, and currently, 77 full genome builds are deposited in Ensembl (https://www.ensembl.org/index.html). However, functional annotations lag far behind the genomes sequencing, assembly, and identification of genes. Migrating the annotations of putative homologues is an efficient and straightforward approach, but it comes with limitations and challenges. The roles of many genes remain unknown even in the best-studied species and the presumed homology and structural similarities do not always imply preservation of functions in vertebrate evolution. Many teleost fish-specific genes remain completely unexplored, despite their active participation in various processes and responses. Transcriptome data is a valuable source of functional annotations, which still hasn't realized the potential. The main conditions for the association between a gene and a trait or biological process are the reproducibility of responses and the magnitude of differential expression, and meta-analysis of data obtained with RNA-seq and DNA microarrays is the most appropriate strategy for approaching this problem. In addition to the annotation of genes, such a strategy works for the discovery of marker genes. Despite the rapid development of high-throughput methods, qPCR analyses of single genes or small diagnostic sets remain important. Candidate marker genes are often selected based on general knowledge of their roles without detailed information on the expression profiles. Meta-analyses facilitate the discovery of genes with strong and reproducible responses. Identification of co-regulated genes, which we refer to as transcription modules (TMs) enhances the reliability of diagnostics and reduces the risk of misinterpretation of findings. TMs include genes with various functions co-activated under specific conditions, and their composition adds to the understanding of biological processes, and strategies of adaptation and defense.

This report summarizes our research over the last decade since the launch of Nofima's Atlantic salmon DNA oligonucleotide microarrays (2). Data from a large number of *in vivo* and *in vitro* studies of fish responses to viral and bacterial pathogens, inflammation, wound healing, and stress have reached a critical mass, which makes reliable identifications of TMs possible. The genes were ranked and divided into groups according to the scale of expression changes. Both specialized and multifunctional genes were identified. TMs enable the quantitative assessment of complex transcriptome responses and their separation into biologically meaningful components. Identification and ranking by the stability and magnitude of differential expression aids in selection of candidate marker genes for diagnostics. The first practical outcome of this activity was the development of multi-gene expression assay for assessment of the immune status of Atlantic salmon smolts and growers (3).

MATERIAL AND METHODS

Nofima's bioinformatic pipeline STARS (4) is used to process and manage transcriptome data and functional annotation of fish genes. It currently houses 127 experiments with Atlantic salmon that used 6440 microarrays, mainly SIQ-6 (GPL1655 and 30031) containing probes to 15k genes selected by their expression profiles and the functional roles, and 44k genome-wide Salgeno (GPL28079 and 28080) with probes to all identified protein-coding genes. In each experiment, we save one or several lists of differentially expressed genes that fit the standard criteria (>1.75-fold and $p < 0.05$) and contrasts – expression differences, such as differences between the treatment and control groups, time-points, developmental stages etc. Contrasts from exemplary studies with large gene expression changes served as material for the search for co-regulated genes. Microarray data (signal intensity) were also used for the assessment of tissue distribution of transcripts. We used experiments that were published or submitted to NCBI GEO Omnibus (**Table 1**). These trials are described in detail elsewhere, so here we restrict ourselves with brief summaries. The trials were divided into four groups, and four TMs were compiled.

-Virus responsive genes (VRG). The research included five pathogens (four RNA and one DNA virus): salmonid alphavirus (SAV) causing pancreas disease (PD) (16), piscine orthoreovirus (PRV) causing heart and skeletal muscle inflammation (HSMI) (17), the recently identified salmon gill poxvirus (SGPV) causing gill disease (18), infectious pancreatic necrosis virus (IPNV) causing infectious pancreatic necrosis (IPN) and infectious salmon anaemia virus (ISAV), causing infectious salmon anaemia (ISA). Double-stranded synthetic RNA polyinosinic: polycytidylic acid (poly I:C) is a widely used synthetic analog capable of inducing strong antiviral responses (19).

-Bacteria responsive genes (BACT). We have performed challenges with three bacteria: *Moritella viscosa*, the aetiological agent of winter-ulcer disease (20), *Tenacibaculum finnmarkense* inducing skin lesions and mouth erosions (21, 22), and *Piscirickettsia salmonis* (23), causing piscirickettsiosis, a severe disease with high mortality.

-Inflammation responsive genes (INFL). The main data sets were time-course of wound healing in skin and melanized foci in skeletal muscle. In addition, we included exposures of primary cultures of head kidney leukocytes to PAMP – TLR agonists CpG oligodeoxynucleotides and gardiquimod, and analyses of skeletal muscle injected with bacterial DNA (plasmids).

-Stress responsive genes (STR). A suite of genes was activated in the heart and spleen after acute swimming exercise, in the skin after crowding, and in the skin of salmon with cortisol implants.

The meta analyses were performed in three stages. In trials with bacterial and viral challenges, infected tissues with strong expression changes were selected (tissue that do not harbor pathogens show only weak unspecific responses). The $\log_2$-

TABLE 1 | Summary of studies included in search of transcription modules (TM).

Pathogens, challenges	Cells, tissue*	Time-points	Reference
Virus responsive genes			
Salmonid alphavirus	Heart	21 days	(5), GSE173130, GSE183260
Piscine orthoreovirus	Heart	42, 56, 63 and 77 days	(5), GSE183260
Piscine orthoreovirus	Erythrocytes	35 and 42 days	(6), GSE183005
Salmon gill poxvirus[1]	Gill	8 and 12 days	(7), GSE151463
Infectious pancreatic necrosis virus	Liver, TO cells	4, 6, 8 and 10 days	GSE172862
Infectious salmon anaemia virus	ASK cells	1 and 5 days	GSE183265
Poly I:C	Adipocytes,	1 and 4 days	GSE171562
Poly I:C	ASK cells	1 and 5 days	GSE183265
Bacterial diseases			
Moritella viscosa	Head kidney, skin, spleen	42 days	GSE173130
Moritella viscosa	Skin, spleen	36 days	(8), GSE171693
Moritella viscosa	Skin (epidermis and dermis)	4 and 35 days	GSE171738
Tenacibaculum finnmarkense	Skin, dermis, epidermis	3 days	GSE171699
Piscirickettsia salmonis	Head kidney	60 days	GSE173095
Inflammation			
PAMP (CpG, gardiquimod)	Mononuclear phagocytes	7 days or 6 + 1 day	(9), GSE126993
Wound	Skin	1, 3, 7 14 days	(10, 11), GSE122142
Plasmid DNA	Skeletal muscle	1, 2 weeks	(12, 13), GSE106111
[2] Melanized foci	Skeletal muscle		(14), GSE182962
Stress			
Exhaustive exercise	Heart, spleen	2 hours	GSE173119
Cortisol implant	Skin	18 days	(15), GSE36072
Crowding	Skin	1 day	GSE173229

[1]*Field material from outbreak. All other data on virus and bacteria infected fish are obtained in challenge trials.*
[2]*Field material (slaughter fish).*

expression ratios were first averaged across trials and then between trials with the same pathogen or treatment. In several trials with few contrasts and high variance, medians were calculated instead of means. Genes that showed significant differential expression in several independent trials and higher than 2-fold mean expression changes were included in TMs. To rank the genes, the magnitude of expression changes in each TM was divided into three (VRG, BACT, and INFL) or two (STR) equal intervals. The list of genes with ranks is in **Supplementary File**. Enrichment analysis compared the numbers of genes per functional category (GO) and pathway (KEGG) in TM and on the genome-wide Salgeno platform. Significance was assessed with Yates' corrected chi-square ($p < 0.05$).

RESULTS

An Overview

A total of 902 Atlantic salmon genes were annotated (**Supplementary File 1**). All down-regulated and most of the upregulated genes were assigned to only one TM (**Figure 1A**), suggesting relatively high specificity of responses. However, there

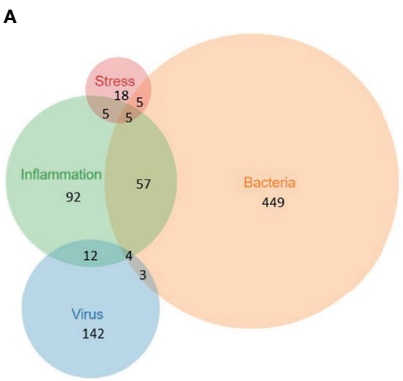

B

Locus	Gene	Virus	Bacteria	Inflam	Stress
c25ha	Cholesterol 25-hydroxylase-like protein A	7.8	2.8	2.1	2.3
mmp13	Matrix metalloproteinase-13	2.1	10.0	4.5	5.9
mmp9	Matrix metalloproteinase-9	1.6	8.1	7.7	3.6
LOC106600447	C-C motif chemokine 4-like	2.4	2.6	7.6	1.4
LOC106585878	C-C motif chemokine 19-4	3.8	4.2	3.2	0.8
LOC106564720	C-X-C motif chemokine 11-like	2.2	4.5	3.1	1.3
LOC106572181	TNF decoy receptor	2.7	5.9	4.3	1.2
junb	Jun B-1	2.8		3.8	3.1
LOC106572480	CCAAT/enhancer binding protein beta	2.3	3.1	3.7	1.5
LOC106607598	NF-kappa-B inhibitor alpha-like	2.0	2.7	2.6	1.1
LOC106562284	Interferon regulatory factor 8	2.1	2.1	2.3	1.2
pdl1	CD274	2.8	3.3	4.9	0.9
saa5	Serum amyloid A	3.1	13.3	7.3	1.4
LOC106566391	Natterin-like protein	1.4	4.1	2.7	2.1
ncf1	Neutrophil cytosolic factor 1	2.1	4.4	3.6	1.5
odc1	Ornithine decarboxylase	2.4	2.4	3.5	1.8
sat1	Diamine acetyltransferase 1	2.2	3.9	3.0	1.6
LOC106577897	Plasminogen activator inhibitor type 1	2.2	4.0	6.1	2.6
LOC106592820	E-selectin-like	2.1	2.1	2.2	1.2
cxb6	Gap junction beta-6 protein	2.1	2.0	2.7	0.8
LOC100380740	Perilipin	4.1	3.1	3.6	1.6
ifi44	Interferon-induced protein 44	2.7	2.5	4.8	1.1
hs90a	Heat shock protein 90 alpha	3.7	2.0	3.2	1.7

FIGURE 1 | Transcription modules. **(A)** numbers of up-regulated genes and overlap between TMs. The down-regulated genes are specific for each TM, no sharing between TMs. **(B)** multifunctional genes assigned to at least three TMs.

was some overlap, smallest for VRG and largest for INFL and a suite of multifunctional genes involved in more than one TM was found (**Figure 1B**). One gene, *cholesterol 25-hydroxylase a*, was included in all TMs, though its responses to viruses were much greater than to other challenges. This enzyme, which is induced with infection and inflammation (24), restricts the propagation of viruses, including ARS-CoV-2 (25). Of 22 genes present in three TMs, the greatest expression changes have been shown by two matrix metalloproteinases, *mmp 9* and *13*, suggesting remodeling of extracellular matrix as an essential strategy of salmon responses to pathogens and stressors. The list includes three *chemokines* and *tnf decoy receptor*, which showed a high correlation with histopathology in SAV infected heart (5). Two pleiotropic transcription factors (*jund1* and *ceb/p beta*) and two immune regulators (*irf8* and *nfkb inhibitor*) can orchestrate expression changes of multiple genes. Of acute phase proteins, the structure and functions of *serum amyloid a* are well conserved in all vertebrates (26), while *natterin-like* proteins are specific for fish (27). The multifunctional genes also included free radicals producing *neutrophil cytosolic factor 1*, two enzymes of polyamine and nitric oxide metabolism (*ornithine decarboxylase* and *diamine transferase*), regulators of cell adhesion *plasminogen activator inhibitor* and *e-selectin* and chaperone *hsp90 alpha*. The immune role of *perilipin*, a protein of lipid droplets, to our knowledge, has not been reported in fish. Enrichment analysis was performed in four TMs. Most part of the enriched GO terms and KEGG pathways are associated with the immune and related systems (e.g. angiogenesis, hemopoiesis), and encompass communication, signal transduction, cell differentiation and migration, humoral and cellular effectors (**Table 2**).

Virus Responsive Genes

The antiviral responses of salmonid fish have been described better than any other functional group of the immune system, for a review, see (28–30). The identification of VRG is facilitated by strong and highly reproducible responses to viruses and dsRNA. Transcriptome analyses performed by our (4) and K. Miller's teams (31, 32) revealed the core set of Atlantic salmon VRG, and the body of knowledge has increased over the past decade. The construction of the genome-wide Salgeno platform expanded the search, while multiple challenge trials with different pathogens provided a more rigorous selection of genes with emphasis on stability of responses. The ranking of 161 VRG by the mean expression changes outlined the core: 19 and 40 genes with correspondingly high and intermediate ranks. This group

TABLE 2 | Enrichment of functional categories (GO) and pathways (KEGG).

Functional group/pathway	VRG	BACT	INFL	Total
Immune responses				
Defense response to virus	43	16	8	522
TNF-mediated signaling pathway	8	NS[1]	NS	293
Toll-like receptor signaling pathway	7	NS	NS	230
Blood coagulation	6	NS	NS	537
Cytokine-mediated signaling pathway	14	41	20	764
Cytokine activity	NS	12	NS	309
Lipoxygenase pathway	NS	7	NS	38
Jak-STAT signaling pathway	8	11	8	288
B cell receptor signaling pathway	NS	9	6	230
Acute-phase response	NS	11	5	90
Complement and coagulation cascades	NS	14	NS	142
Fc gamma R-mediated phagocytosis	NS	NS	10	269
Fc-epsilon receptor signaling pathway	NS	11	9	420
Inflammatory response	NS	63	17	986
Platelet degranulation	NS	15	10	438
Antigen processing and presentation	NS	9	NS	129
Chemotaxis	NS	18	6	310
Leukocyte cell-cell adhesion	NS	14	7	117
Myeloid cell differentiation	NS	5	NS	113
Other systems. Signaling & differentiation				
Cell surface receptor signaling pathway	NS	24	10	746
Insulin receptor signaling pathway	NS	8	NS	289
Integrin-mediated signaling pathway	NS	15	10	400
VEGF receptor signaling pathway	NS	13	11	301
Extracellular matrix organization	NS	21	NS	917
Hematopoietic cell lineage	NS	15	6	132
Angiogenesis	NS	28	14	1203
Myelin sheath	NS	9	NS	227
Cellular processes				
Ubiquitin-dependent protein catabolism	16	NS	NS	854
Ubiquitin protein ligase activity	10	NS	NS	650
Lipid particle	7	NS	NS	296
Histone binding	6	NS	NS	399

[1]*NS, not significant.*

includes two large multi-gene families: *trim-7* and fish-specific *gig-2* (33) and many paralogs (**Figure 2A**), suggesting duplication and diversification of antiviral genes as the main evolutionary scenario in this part of the salmon immune system. VRGs cover three tiers of immune responses: pathogen detection, signal transduction, and effector containing 3%, 15%, and 82% genes, respectively (**Figure 2B**). Although various pathogen recognition receptors have been identified in Atlantic salmon (28), only RNA helicases *rig1* (2 genes), *lgp2*, and *dhx58* have consistently demonstrated strong transcription responses to viruses. Signal transducers include *irf1, irf3, irf7* (2 genes), *stat1* (4 genes), and the lesser-known *srk2*. It should be noted that fewer terms are enriched in VRG than in BACT and INFL (**Table 2**), indicating that most VRGs are highly specialized for antiviral defense. Enrichment analysis indicated the key effector mechanisms associated with ubiquitin metabolism, histone binding, and lipid particles. Further inspection outlined other functional groups: metabolism of nucleotides and RNA and GTPase-mediated activity (**Figure 2C**), the functions of at least twenty salmon VRG are unknown.

The most differentially expressed VRG are in **Figure 3A**. About half of these genes have been investigated and characterized, but the roles of VRG that respond to viruses only in fish are much less known. This is true for *receptor transporting protein 3 (rtp3)*, VRG with the highest rank in Atlantic salmon showing strong responses to viruses in different fish species, including phylogenetically distant sturgeons (34, 35); its mammalian ortholog is involved in olfaction. Gene ranking improves the credibility of diagnostics: up-regulation of highly specialized VRG from the core set strongly suggests a viral infection. Such samples are clearly visible in transcriptome analyses. VRG are active in all tissues, although several highly ranked genes show elevated expression in erythrocytes (**Figure 3B**) in line with the important role of these cells in antiviral defense (6, 36). The increase in their transcripts may happen due to the stimulation of blood circulation, but the scale is much lower in comparison with infections. In theory, diagnostics can also be confounded with responses to bacterial DNA and TLR agonists. However, stimulation was observed in experiments with exposure of cells to PAMP (9) and muscle injection of plasmid DNA (12, 13) at doses that are probably never reached in naturally infected salmon. Several VRG were upregulated in our studies of pathogen-free inflammation but overlap with BACT was minor. RNA and DNA (salpox) viruses and dsRNA induce expression

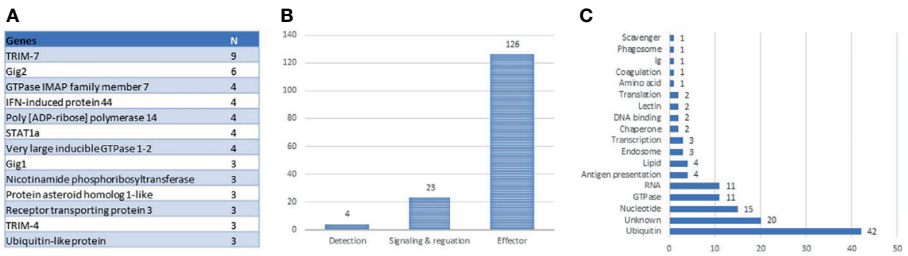

Genes	N
TRIM-7	9
Gig2	6
GTPase IMAP family member 7	4
IFN-induced protein 44	4
Poly [ADP-ribose] polymerase 14	4
STAT1a	4
Very large inducible GTPase 1-2	4
Gig1	3
Nicotinamide phosphoribosyltransferase	3
Protein asteroid homolog 1-like	3
Receptor transporting protein 3	3
TRIM-4	3
Ubiquitin-like protein	3

FIGURE 2 | Composition of antiviral TM (VRG). **(A)** genes with more than two paralogs and multi-gene families. **(B)** tiers of antiviral responses with numbers of genes. **(C)** distribution of antiviral effectors by roles.

A

Locus	Gene	Poly-IC	SAV	PRV	IPNV	Salpox	ISAV	PAMP
	All genes	7.3	7.0	6.0	15.5	5.7	3.1	5.5
LOC106574173	Receptor transporting protein 3	71.5	28.6	28.2	65.8	28.2	20.1	17.5
LOC100136541	ISG15	36.3	24.4	7.8	65.8	24.9	21.9	45.8
LOC106589386	IFIT-5 (2 genes)	37.5	17.9	11.6	39.9	7.8	13.9	16.6
rsad2	Viperin (2 genes)	27.3	14.4	9.5	62.2	18.4	1.5	6.6
LOC106607153	Very large inducible GTPase (2 genes)	20.9	8.8	18.2	47.8	7.0	2.3	16.8
dhx58	ATP-dependent RNA helicase DHX58	13.5	6.1	7.1	20.0	5.7	6.5	9.4
helz2	PPARA-interacting complex 285 kDa-2	7.9	5.4	5.9	13.8	8.0	1.8	6.0
LOC106596088	Suppressor of cytokine signaling 1	9.4	6.7	6.0	35.8	3.2	3.0	16.8
irf1	IRFF	3.1	2.2	6.9	48.8	3.6	2.3	4.6
srk2	SRK2 tyrosine kinase	8.2	5.9	6.5	2.5	3.8	6.1	2.9
LOC106610287	Hect domain and RLD3	15.2	5.9	7.3	15.8	15.5	7.9	11.9
mx	Mx		8.3	6.8	20.4	10.7		
LOC106594559	Barrier-to-autointegration factor 2 genes	17.1	10.2	6.9	13.3	15.8	2.9	9.3
LOC100194720	Gig2	10.9	22.6	9.4	9.2	11.6	2.0	12.6
LOC100196683	Gig2-2	8.4	15.2	8.2	18.3	10.8	1.2	6.7
LOC106583673	NFX1-type zinc finger containing protein	13.5	5.9	7.0	36.3	3.3	4.2	5.4
LOC100196683	Gig2-4	7.6	13.8	7.5	9.6	10.8	1.7	8.1
LOC100194722	Gig1-2	10.4	5.3	5.2	29.9	2.2	7.9	6.6
xaf1	XIAP-associated factor 1	11.4	5.1	4.0	15.9	3.4	5.9	13.0
LOC106573916	Interferon-induced protein 44-1	7.2	6.1	7.3	6.4	10.3	6.6	4.8
LOC106590148	Fish virus induced TRIM-7	5.4	6.9	5.5	22.3	2.9	3.9	6.3
LOC106602317	Ubiquitin protein ligase E3A, hect domain	5.8	6.7	7.8	7.1	10.3	1.5	3.9

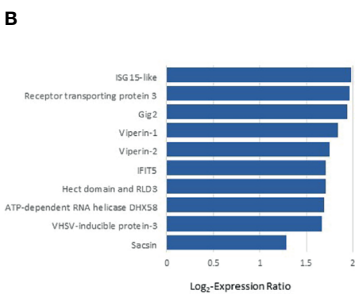

FIGURE 3 | **(A)** Genes with the strongest antiviral responses. Here and in subsequent heat maps, data are the mean folds to intact controls. Information on tissues, cells and time-points is in **Table 1**. For each virus and poly(I:C) all data (contrasts) were averaged. **(B)** highly ranked VRG with preferential expression in erythrocytes (microarray data), log_2-Expression Ratios to means of nine tissues and cell types.

changes that are similar by magnitude (**Figure 3A**). The bias for the two pathogens with smaller (ISAV) and larger (IPNV) changes may be due to small datasets.

Bacterial Diseases and Inflammation

BACT includes genes involved in stable and reproducible responses to bacterial pathogens that are manifested at high infection loads. Expression changes comparable with those induced with *T. finnmarkense* and *P. salmonis* were observed in skin ulcers caused by *M. viscosa*, but not in less severely damaged tissues (**Figure 4**). Responses are similar by scale, or even stronger, than those caused by viruses. Unlike VRG, a suite of genes with the highest ranks either have unknown roles (*saxitoxin and tetrodotoxin-binding protein* and *catechol o-methyltransferase domain* – number one and three in the list) or have not been reported in association with salmon diseases, for example, cell adhesion molecule *ceacam20* (37) and regulator of immune metabolism *irg1* (*aconitate decarboxylase)* (38). Both enrichment analysis and the gene composition of BACT indicate high complexity and diversity of responses to bacteria. TM includes a homolog of bacteria flagellin activated *tlr5* (39), chemokines, cytokines and receptors, and genes involved in the metabolism of lipid mediators, extracellular proteins, such as emblematic markers of inflammation *serum amyloid a* and *cathelicidin* and less investigated *c1q* and *tnf domain* proteins, members of a large multi-gene family, which has been known mainly in association with adipocyte differentiation and obesity (40). *Mmps* and enzymes of the polyamine/nitric oxide metabolism are presented as universal markers in **Figure 1B**. The importance of iron sequestration as an antibacterial defense strategy (41) is supported with strong responses of *hepcidin*, a master regulator of iron metabolism also known for antibacterial activity (42), extracellular iron transporter *transferrin*, and *steap4* – a TNFa-induced regulator of iron and copper homeostasis (43). In addition to immune genes, highly ranked BACT genes include enzymes of amino acid (*l-serine hydratase*) and sugar (*aldolase*) metabolism and regulator of blood pressure *angiotensinogen*. **Figure 4** presents immune genes with decreased expression. Down-regulation of *il-6* and *socs2*, genes with anti-inflammatory action, may enhance inflammation. The similarity of inflammatory responses caused by bacterial infections and non-pathogenic factors is suggested with enrichment of the same functional categories and pathways (**Table 2**). However, slightly more terms were significantly enriched in BACT, mainly due to the larger number of genes. Highly ranked INFL genes (**Figure 1B** and **Figure 5**) include chemokines, cytokines and their receptors, antibacterial and acute phase proteins (*lysozyme*, *cathelicidin* and *serum amyloid a*), *lectins* and *Ig receptor*, ROS producing *neutrophil cytosolic factors*,

Locus	Gene	Tenacibaculum	Piscirickettsia	Moritella ulcer	Moritella
	All up-regulated	6.5	5.5	8.6	1.5
	All down-regulated	-2.4	-2.6	-6.4	-1.4
LOC106604696	Saxitoxin and tetrodotoxin-binding 2	178.5	86.8	247.3	1.4
LOC106578696	Sarcinoembryonic antigen-related 20	21.1	23.1	93.1	9.1
LOC106577197	Catechol O-methyltransferase domain (2 genes)	59.3	12.8	25.1	2.5
saa5	Serum amyloid A	75.1	18.0	14.7	1.6
LOC106571136	C1q and TNF domain	187.4	3.1	14.0	3.7
LOC100136439	Cathelicidin (2 genes)	12.8	80.4	7.5	1.5
tl/lrr	Toll receptor 5	19.0	14.9	5.6	1.0
LOC106575635	IL-8 receptor	14.8	3.5	154.3	5.1
LOC106595660	IL-8	38.9	10.9	20.0	1.0
LOC106604583	Leukocyte cell-derived chemotaxin 2-1	20.8	2.1	10.6	3.1
il1r2	IL-1 receptor type II	19.7	6.1	17.5	1.2
LOC106604000	Arachidonate 5-lipoxygenase-activating protein	8.3	2.8	10.0	2.6
hepc1	Hepcidin-1	17.9	9.8	9.1	1.0
LOC106578511	Ferric-chelate reductase 1	5.2	20.8	11.9	1.4
stea4	Metalloreductase STEAP4 (2 genes)	22.5	10.4	4.8	1.2
trf	Serotransferrin 2	41.1	1.0	24.3	2.6
LOC106580394	L-serine dehydratase/L-threonine deaminase	5.0	81.0	9.4	1.0
gadl1	Aldolase	5.7	2.1	5.2	5.1
ncf1	Neutrophil cytosolic factor 1	10.6	1.0	16.0	2.2
irg1	Immunoresponsive 1 homolog	20.7	104.7	4.9	1.0
mip2a	Macrophage inflammatory protein 2-alpha	49.5	7.0	22.0	1.0
mfap4	Microfibrillar-associated protein 4	37.3	8.4	18.0	1.0
LOC106563105	C1q and TNF domains	12.0	13.1	6.4	2.0
LOC106584298	Polymeric immunoglobulin receptor	13.2	3.5	46.9	1.3
agt	Angiotensinogen (angt)	35.8	3.9	19.6	1.4
LOC106590877	Prostaglandin-H2 D-isomerase (2 genes)	-2.9	-5.0	-13.6	-0.7
ccl21	interleukin-6	-9.6	-1.0	-5.8	-2.0
LOC106599005	Phosphoinositide-3-kinase subunit 2 (2 genes)	-2.7	-2.6	-12.8	-1.2
LOC106576177	Suppressor of cytokine signaling 2	-2.7	-3.5	-9.6	-1.0
ccl21	interleukin-6	-5.4	-1.0	-6.6	-2.3

FIGURE 4 | Responses to pathogenic bacteria: genes ranked by the expression changes with respect to uninfected control. Information on tissues, cells and time-points is in **Table 1**. Responses to *T. finnmarkense* and *M. viscosa* in whole skin and skin layers were averaged, ulcer is presented separately.

Locus	Gene	Melanin foci	Wound	Plasmid	PAMP
	All up-regulated	3.7	4.0	3.4	5.7
	All down-regulated	-3.0	-3.3	-1.9	-1.4
LOC106588482	C-type lectin domain family 4 member E	4.6	4.5	2.1	4.8
LOC106606431	Metalloproteinase inhibitor 2	3.0	4.8	1.5	14.3
LOC106612111	DNA damage-inducible transcript 4 protein	3.6	2.2	2.1	17.3
spd2a	Neutrophil cytosolic factor 4	3.0	4.8	2.9	15.9
LOC100136541	ISG15		3.2	35.5	45.6
LOC100194720	Gig2		2.4	18.4	12.6
rsad2	Viperin		2.7	17.1	6.6
il1r2	IL-1 receptor type II	2.6	8.1	1.4	3.1
LOC106564720	C-X-C motif chemokine 11	3.3	7.1	3.8	
LOC100136439	Cathelicidin (cath)	4.1	16.9		14.2
saa5	Serum amyloid A		13.7	3.6	55.7
LOC100136365	Lysozyme C II	23.4	8.7	2.7	2.0
pdl1	CD274	5.1	4.0	2.1	13.4
mag	Myelin-associated glycoprotein	6.6	8.8	2.3	1.8
cdd	Cytidine deaminase	2.5	21.1	1.8	
LOC100136446	C type lectin receptor A (clec4e)	2.7	8.2	1.8	3.3
ncf1	Neutrophil cytosolic factor 1 (2 genes)		13.5	1.4	8.8
hs90a	Heat shock protein 90, alpha	2.6	3.2	3.7	3.5
LOC106600447	C-C motif chemokine 4	5.0	5.0	6.8	19.2
LOC106580961	High affinity Ig Fc receptor I	6.6	3.6	5.1	24.1
hck	Src-family tyrosine kinase SCK	5.7	3.2	3.6	17.5
LOC106581219	Collagenase 3	15.5	8.8	3.0	
LOC106604553	SAM and SH3 domain-containing protein 3	5.5	4.1	3.1	1.7
odc1	Ornithine decarboxylase	3.4	4.8	2.3	3.9
LOC106572480	CCAAT/enhancer binding protein (C/EBP)_beta	3.3	4.3	2.7	4.6

FIGURE 5 | Responses to inflammation not caused by pathogenic bacteria. Genes are ranked by the expression changes. Information on tissues, cells and time-points is in **Table 1**.

enzymes of polyamine and nitric oxide metabolism, *matrix metalloproteinases* and *mmp inhibitor*. In addition to *mmp 9* and *13*, strong expression changes were shown by the fish-specific *collagenase-3 like* enzyme. Wound up-regulated several VRG (*isg15*, *viperin* and *gig2*). The roles of highly ranked *cytidine deaminase* and *myelin-associated glycoprotein* in inflammation remain unknown. Overall, pathogen-free inflammatory responses included fewer genes than those caused by disease-causing bacteria, but the changes in expression were comparable in scale.

Stress Response

The term "stress" has different meanings depending on the context, and it is hardly possible to find universal stress markers. We have identified a panel of genes activated with pathogens and inflammatory agents, which were also induced with treatments not related to any infectious disease and pathology, such as acute exercise and crowding, and most of these genes also responded to cortisol, the main endocrine mediator of stress in salmonid fish (**Figure 6**). Inspection of these trials found several more consistently up-regulated genes that were added to stress TMs. These TMs make quantitative evaluation of stress components under different conditions possible. Of genes not shown in **Figure 1B**, association with stress was known only for *hsp30*, a chaperone not found in mammals (44), and DNA binding *immediate early response – ier2* [cold-induced in embryos of the kelp grouper, *Epinephelus moara* (45)]. *Butyrate response factor – brf1*, another early response gene, regulates the decay of mRNA (46). Free heme neutralizing *haptoglobins* respond to chemical stress in Atlantic salmon (47). *Angiopoietin-related protein 4* stimulates angiogenesis under hypoxic conditions (48) and the role of *d-aspartate oxidase* in stress responses is unknown.

Separation of the Transcriptome Into Fractions and the Contribution of TMs

Finding thematic associations with the help of functional annotations is probably the most commonly used approach to the analysis and biological interpretation of complex transcriptome responses. Its weakness lies in the implicit assumption of similar expression profiles of functionally related genes. However, this information is not available in public databases. Genes with similar molecular roles can be activated under different conditions (then co-expression is not observed) and many genes generally do not show responses at the transcription level. The identification of TM significantly enhances this approach by providing groups of genes, the responses and co-regulation of which have been confirmed on a large experimental basis. Pure cases are rare, and as a rule, transcriptome responses include several components with different contributions (**Figure 7**). This may help to understand poorly explored problems, such as melanized foci (dark spots) in the skeletal muscle causing heavy economical losses in Atlantic salmon aquaculture, the origin of which has been debated (14, 49). Judging by the minor contribution of antiviral and antibacterial responses, one may think a non-infectious factor probably causing them. STR allows to assess

Symbol	Gene	Exercise spleen	Exercise heart	Crowding stress	Cortisol implant
	All genes	3.5	2.9	2.0	1.8
mmp13	Matrix metalloproteinase-13	1.9	3.7	19.7	8.8
mmp9	Matrix metalloproteinase-9		2.7	7.5	8.0
ier2	Immediate early response 2 (2 genes)	5.2	6.5	1.9	2.2
junb	Jun B-1	7.8	4.0	1.5	2.1
Ssa#S47726557	CCAAT/enhancer-binding protein delta-2	1.9	2.2	1.7	2.3
tisb	Butyrate response factor 1	2.4	2.2	1.8	2.1
LOC106611914	D-aspartate oxidase	3.4	3.8	1.6	5.7
angl4	Angiopoietin-related protein 4	4.7	3.1	2.4	
LOC106598773	Heat shock protein 30		2.2	5.7	
LOC106581595	Haptoglobin	3.5	2.1	3.2	
LOC106611136	Ornithine decarboxylase	1.4	1.5	4.5	2.1

FIGURE 6 | Stress genes. Information on tissues, cells and time-points is in **Table 1**.

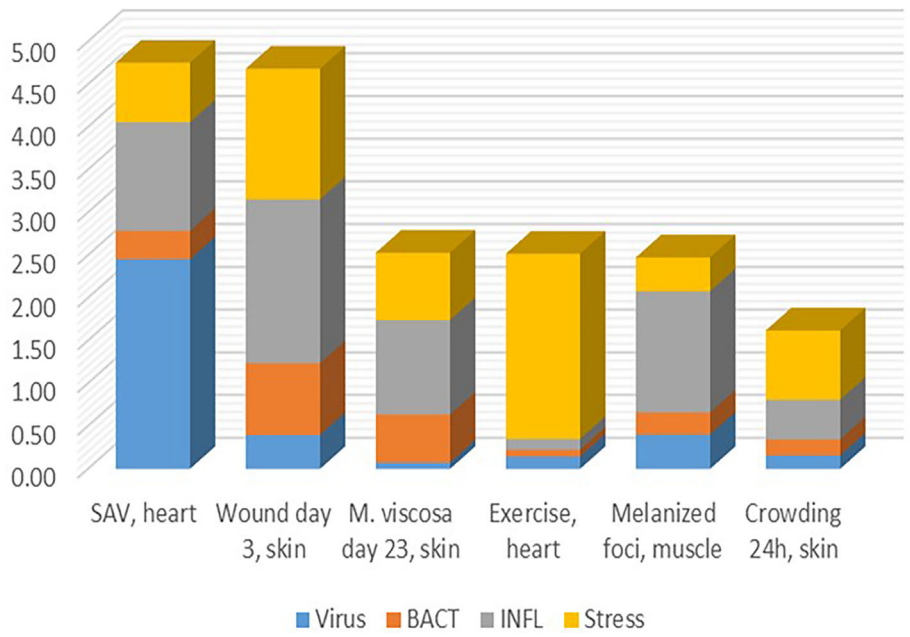

FIGURE 7 | Examples of transcriptome responses (contrast) with contribution of several TM shown as the mean log_2-Expression Ratios.

the degree of stress caused with various disturbances including infection with pathogens, wounds, and other damages. Given that a linear gene expression response to temperature has been shown (50, 51), graded effects of other stressors can be expected.

DISCUSSION

The potential of transcriptome data for the functional annotation of genes and discovery of biomarkers is obvious, and rapid progress in this area can be expected. The reported approach is based on the search of groups of co-regulated Atlantic salmon genes referred to as transcription modules – TMs. Our meta-analyses have revealed two types of TM. The first type includes gene sets showing consistently high correlation of expression profiles most likely due to transcriptional co-regulation, examples are Atlantic salmon myofiber proteins co-regulated with proteins of calcium and glucose metabolism, pituitary hormones, immunoglobulins, and genes involved in steroid biosynthesis (not included in this paper). The number of such groups is small and each gene is

firmly anchored to only one TM. Here, we present genes that have shown differential expression under certain conditions, where each member of the TM can be relatively independent of the rest and belong to several groups. We focused on responses to bacterial and viral pathogens, inflammatory agents, and stress, due to the high importance of these issues for aquaculture and the large amount of data produced by our group. A similar search can be implemented for any biological process and trait, and the only requirement is a set of high-quality transcriptome data. In our approach, the main priority is the consistency of expression changes – each gene in the TM must show differential expression in several independent trials under the standard thresholds. The results of transcriptome analysis in similar studies, as a rule, do not coincide in detail, and even if the main trends are stable, the deviations can be large. This does not mean a weakness in the design of experiments and analysis. The instability is largely determined with the complexity and diversity of transcriptome responses combined with an imbalance between the number of measurements (genes) and the number of animals, known as the multiplicity problem. There can be several different scenarios for responding to a challenge in a population. A small sampling group can highlight genes or groups of genes that are affected in some individuals but will not overcome statistical thresholds of significance in a representative comparison of populations. Deviations between experiments can also be caused by the difference in the genetic background, age and physiological condition of fish, season, the severity of infections and damages and many other factors. Both annotations and diagnostics are based on stable responses and therefore, a meta-analysis of independent studies is essential.

The four presented TMs include many uncharacterized genes and genes whose association with responses to pathogens, inflammation and stress was unknown or not reflected in public databases. In addition, differential expression and its scale can add a new dimension to the functional annotations. The composition of TMs is useful for the understanding of protective strategy in Atlantic salmon. VRG represents a separate branch of innate immunity characterized with relatively high specificity, although they can be activated with abnormally high levels of PAMP. The similarity of responses to bacteria and non-pathogenic inflammation suggests the dominance of proactive defense in Atlantic salmon. The mission of inflammation is the clearance of infection and damaged tissues – cell debris and extracellular matrix. We see that even in the absence of infections, inflammation includes a powerful effector arm targeted at killing microorganisms. In our studies, experimentally inflicted wounds induced inflammatory responses, which were similar to bacteria-caused ulcers being much stronger in comparison with the skin of salmon infected with *M. viscosa.* The stress component is clearly seen in all treatments including the viral and bacterial infections and inflammation caused by non-pathogenic factors. Identification of TM enhances diagnostics. In relation to transcriptomic data, differential expression of genes representing a significant portion of TM substantially increases the confidence of conclusions and ranking of genes provides additional validation: upregulation of the core set is strong evidence. TMs allow quantification and comparison of the magnitude of responses. TMs also serve as a basis for developing biomarkers and diagnostic sets of genes for qPCR or multigene assays, such as our assay of immune competence (3, 8, 8, 52) developed on the Biomark HD platform, which was recently introduced in research with salmonid fish (31, 50, 53). These studies validated differential expression under various conditions and determined the core gene sets for various diagnostic tasks.

TMs are open to changes and improvements and new groups of co-expressed genes will be identified. The core set of VRG has been well established: we have worked with all important viral infections of concern to the Atlantic salmon industry and did not find significant differences in responses. Although no major changes are expected even if new pathogens will emerge, low-ranked VRG can be added or excluded with new experimental data. Some genes can either exceed or fall below the threshold value, but the adjustments are unlikely to go beyond fine-tuning. INFL is mainly based on studies of wound healing with support from melanized foci and exposures to PAMP. New trials with strong inflammation, free of pathogens, would be very useful to verify and strengthen this association. We can expect certain changes in the set of genes activated with pathogenic bacteria. We currently have extensive data sets for *T. finnmarkense* and *M. viscosa* only. High variation has been observed with respect to the disease stage and the severity of lesions, especially for *M. viscosa*. In the future, it may be necessary to split BACT or compile several groups of genes activated or suppressed with bacterial infections. The same is true for STR, because this TM was created to highlight the stress component in the challenge trials and responses that otherwise had little in common. Most genes included in TMs are highly expressed in different organs or in blood cells that infiltrate infected or damaged tissues. Currently, we do not have enough material to search for genes with tissue-specific responses. Related task is discovery of markers discriminating responses to specific stressors and pathogens (31, 50) and differential diagnostics of diseases (54, 55). Here, we report the first step in using transcriptome data for functional annotation of Atlantic salmon genes in order to demonstrate the usefulness and potential of this approach.

DATA AVAILABILITY STATEMENT

Publicly available datasets were analyzed in this study. This data can be found here: https://www.ncbi.nlm.nih.gov/geo/subs/ GSE172862 GSE171562 GSE171693 GSE171738 GSE173130 GSE171699 GSE173095 GSE173119 GSE173229 GSE183005 GSE183260 GSE183265.

AUTHOR CONTRIBUTIONS

AK – conceptualization, methodology, original draft preparation. SA – software, data curation. L-HJ, CK, LS, EY, GT, CL – experiments and laboratory analyses, writing. All authors contributed to the article and approved the submitted version.

FUNDING

The study was funded by the National Research Council of Norway (267644) and Nofima (internal grant). SA was supported with a grant from I. M. Sechenov Institute of Evolutionary Physiology and Biochemistry (IEPHB RAS, research theme No. AAAA-A18-118012290373-7.

ACKNOWLEDGMENTS

Unpublished viral and bacterial challenge trials were performed in collaboration with Nina Santi, Thomas Moen, Vicente Castro, Sverre B. Småge and Erik Burgerhout. We wish to thank all partners who contributed into our transcriptome research during last decade.

SUPPLEMENTARY MATERIAL

The Supplementary Material for this article can be found online at: https://www.frontiersin.org/articles/10.3389/fimmu.2021.705601/full#supplementary-material

Supplementary File | Contains two sheets. List – all annotated genes with ranks in TMs. Data – contrasts used for meta-analyses. Microarrays contain different probes to the same genes; identifiers are in columns C and D. Data are contrasts (log_2-expression ratios of treated to controls). Rows 3 – identifiers, line 4 – source (cells, tissues and origin), line 5 – treatment. Missing and insignificant data (no differential expression) are highlighted with colour.

REFERENCES

1. Lien S, Koop BF, Sandve SR, Miller JR, Kent MP, Nome T, et al. The Atlantic Salmon Genome Provides Insights Into Rediploidization. *Nature* (2016) 533 (7602):200–5. doi: 10.1038/nature17164
2. Krasnov A, Timmerhaus G, Afanasyev S, Jørgensen SM. Development and Assessment of Oligonucleotide Microarrays for Atlantic Salmon (*Salmo Salar* L.). *Comp Biochem Physiol Part D Genomics Proteomics* (2011a) 6(1):31–8. doi: 10.1016/j.cbd.2010.04.006
3. Krasnov A, Afanasyev S, Nylund S, Rebl A. Multigene Expression Assay for Assessment of the Immune Status of Atlantic Salmon. *Genes (Basel)* (2020) 11 (11):1236. doi: 10.3390/genes11111236
4. Krasnov A, Timmerhaus G, Schiotz BL, Torgersen J, Afanasyev S, Iliev D, et al. Genomic Survey of Early Responses to Viruses in Atlantic Salmon, Salmo Salar L. *Mol Immunol* (2011b) 49(1-2):163–74. doi: 10.1016/j.molimm.2011.08.007
5. Johansen LH, Thim HL, Jorgensen SM, Afanasyev S, Strandskog G, Taksdal T, et al. Comparison of Transcriptomic Responses to Pancreas Disease (PD) and Heart and Skeletal Muscle Inflammation (HSMI) in Heart of Atlantic Salmon (Salmo Salar L). *Fish Shellfish Immunol* (2015) 46(2):612–23. doi: 10.1016/j.fsi.2015.07.023
6. Dahle MK, Wessel O, Timmerhaus G, Nyman IB, Jorgensen SM, Rimstad E, et al. Transcriptome Analyses of Atlantic Salmon (Salmo Salar L.) Erythrocytes Infected With Piscine Orthoreovirus (PRV). *Fish Shellfish Immunol* (2015) 45(2):780–90. doi: 10.1016/j.fsi.2015.05.049
7. Gjessing MC, Krasnov A, Timmerhaus G, Brun S, Afanasyev S, Dale OB, et al. The Atlantic Salmon Gill Transcriptome Response in a Natural Outbreak of Salmon Gill Pox Virus Infection Reveals New Biomarkers of Gill Pathology and Suppression of Mucosal Defense. *Front Immunol* (2020) 11:2154. doi: 10.3389/fimmu.2020.02154
8. Krasnov A, Burgerhout E, Johnsen H, Tveiten H, Bakke AF, Lund H, et al. Development of Atlantic Salmon (Salmo Salar L.) Under Hypoxic Conditions Induced Sustained Changes in Expression of Immune Genes and Reduced Resistance to Moritella Viscosa. *Front Ecol Evol* (2021) 505:505. doi: 10.3389/fevo.2021.722218
9. Iliev DB, Hansen T, Jorgensen SM, Krasnov A, Jorgensen JB. CpG- and LPS-Activated MAPK Signaling in *In Vitro* Cultured Salmon (Salmo Salar) Mononuclear Phagocytes. *Fish Shellfish Immunol* (2013) 35(4):1079–85. doi: 10.1016/j.fsi.2013.07.014
10. Sveen LR, Timmerhaus G, Krasnov A, Takle H, Stefansson SO, Handeland SO, et al. High Fish Density Delays Wound Healing in Atlantic Salmon (Salmo Salar). *Sci Rep* (2018) 8(1):16907. doi: 10.1038/s41598-018-35002-5
11. Sveen LR, Timmerhaus G, Krasnov A, Takle H, Handeland S, Ytteborg E. Wound Healing in Post-Smolt Atlantic Salmon (Salmo Salar L.). *Sci Rep* (2019) 9(1):3565. doi: 10.1038/s41598-019-39080-x
12. Sobhkhez M, Krasnov A, Chang CJ, Robertsen B. Transcriptome Analysis of Plasmid-Induced Genes Sheds Light on the Role of Type I IFN as Adjuvant in DNA Vaccine Against Infectious Salmon Anemia Virus. *PloS One* (2017) 12 (11):e0188456. doi: 10.1371/journal.pone.0188456
13. Sobhkhez M, Krasnov A, Robertsen B. Transcriptome Analyses of Atlantic Salmon Muscle Genes Induced by a DNA Vaccine Against Salmonid Alphavirus, the Causative Agent of Salmon Pancreas Disease (PD). *PloS One* (2018) 13(10):e0204924. doi: 10.1371/journal.pone.0204924
14. Krasnov A, Moghadam H, Larsson T, Afanasyev S, Morkore T. Gene Expression Profiling in Melanised Sites of Atlantic Salmon Fillets. *Fish Shellfish Immunol* (2016) 55:56–63. doi: 10.1016/j.fsi.2016.05.012
15. Tadiso TM, Krasnov A, Skugor S, Afanasyev S, Hordvik I, Nilsen F. Gene Expression Analyses of Immune Responses in Atlantic Salmon During Early Stages of Infection by Salmon Louse (Lepeophtheirus Salmonis) Revealed Bi-Phasic Responses Coinciding With the Copepod-Chalimus Transition. *BMC Genomics* (2011) 12:141. doi: 10.1186/1471-2164-12-141
16. Weston JH, Welsh MD, McLoughlin MF, Todd D. Salmon Pancreas Disease Virus, an Alphavirus Infecting Farmed Atlantic Salmon, Salmo Salar L. *Virology* (1999) 256(2):188–95. doi: 10.1006/viro.1999.9654
17. Palacios G, Lovoll M, Tengs T, Hornig M, Hutchison S, Hui J, et al. Heart and Skeletal Muscle Inflammation of Farmed Salmon is Associated With Infection With a Novel Reovirus. *PloS One* (2010) 5(7):e11487. doi: 10.1371/journal.pone.0011487
18. Nylund A, Watanabe K, Nylund S, Karlsen M, Saether PA, Arnesen CE, et al. Morphogenesis of Salmonid Gill Poxvirus Associated With Proliferative Gill Disease in Farmed Atlantic Salmon (Salmo Salar) in Norway. *Arch Virol* (2008) 153(7):1299–309. doi: 10.1007/s00705-008-0117-7
19. Robertsen B, Trobridge G, Leong JA. Molecular Cloning of Double-Stranded RNA Inducible Mx Genes From Atlantic Salmon (Salmo Salar L.). *Dev Comp Immunol* (1997) 21(5):397–412. doi: 10.1016/S0145-305X(97)00019-0
20. Benediktsdóttir E, Verdonck L, Spröer C, Helgason S, Swings J. Characterization of Vibrio Viscosus and Vibrio Wodanis Isolated at Different Geographical Locations: A Proposal for Reclassification of Vibrio Viscosus as Moritella Viscosa Comb. Nov. *Int J Syst Evol Microbiol* (2000) 50 (Pt 2):479–88. doi: 10.1099/00207713-50-2-479
21. Powell M, Carson J, van Gelderen R. Experimental Induction of Gill Disease in Atlantic Salmon Salmo Salar Smolts With Tenacibaculum Maritimum. *Dis Aquat Organ* (2004) 61(3):179–85. doi: 10.3354/dao061179
22. Småge SB, Frisch K, Vold V, Duesund H, Brevik ØJ, Olsen RH, et al. Induction of Tenacibaculosis in Atlantic Salmon Smolts Using Tenacibaculum Finnmarkense and the Evaluation of a Whole Cell Inactivated Vaccine. *Aquaculture* (2018) 495:858–64. doi: 10.1016/j.aquaculture.2018.06.063
23. Fryer JL, Lannan CN, Giovannoni SJ, Wood ND. "Piscirickettsia Salmonis Gen. Nov., Sp. Nov., the Causative Agent of an Epizootic Disease in Salmonid Fishes. *Int J Syst Bacteriol* (1992) 42(1):120–6. doi: 10.1099/00207713-42-1-120
24. Lathe R, Sapronova A, Kotelevtsev Y. Atherosclerosis and Alzheimer–diseases With a Common Cause? Inflammation, Oxysterols, Vasculature. *BMC Geriatr* (2014) 14:36. doi: 10.1186/1471-2318-14-36
25. Wang S, Li W, Hui H, Tiwari SK, Zhang Q, Croker BA, et al. Cholesterol 25-Hydroxylase Inhibits SARS-CoV-2 and Other Coronaviruses by Depleting

Membrane Cholesterol. *EMBO J* (2020) 39(21):e106057. doi: 10.15252/embj.2020106057
26. Sack GHJr. Serum Amyloid A (SAA) Proteins. *Subcell Biochem* (2020) 94:421–36. doi: 10.1007/978-3-030-41769-7_17
27. Rajan B, Patel DM, Kitani Y, Viswanath K, Brinchmann MF. Novel Mannose Binding Natterin-Like Protein in the Skin Mucus of Atlantic Cod (Gadus Morhua). *Fish Shellfish Immunol* (2017) 68:452–7. doi: 10.1016/j.fsi.2017.07.039
28. Langevin C, Aleksejeva E, Passoni G, Palha N, Levraud JP, Boudinot P. The Antiviral Innate Immune Response in Fish: Evolution and Conservation of the IFN System. *J Mol Biol* (2013) 425(24):4904–20. doi: 10.1016/j.jmb.2013.09.033
29. Robertsen B. The Role of Type I Interferons in Innate and Adaptive Immunity Against Viruses in Atlantic Salmon. *Dev Comp Immunol* (2018) 80:41–52. doi: 10.1016/j.dci.2017.02.005
30. Dahle MK, Jørgensen JB. Antiviral Defense in Salmonids - Mission Made Possible? *Fish Shellfish Immunol* (2019) 87:421–37. doi: 10.1016/j.fsi.2019.01.043
31. Miller KM, Günther OP, Li S, Kaukinen KH, Ming TJ. Molecular Indices of Viral Disease Development in Wild Migrating Salmon(†). *Conserv Physiol* (2017) 5(1):cox036. doi: 10.1093/conphys/cox036
32. Mordecai GJ, Di Cicco E, Günther OP, Schulze AD, Kaukinen KH, Li S, et al. Discovery and Surveillance of Viruses From Salmon in British Columbia Using Viral Immune-Response Biomarkers, Metatranscriptomics, and High-Throughput RT-PCR. *Virus Evol* (2021) 7(1):veaa069. doi: 10.1093/ve/veaa069
33. Sun C, Liu Y, Hu Y, Fan Q, Li W, Yu X, et al. Gig1 and Gig2 Homologs (CiGig1 and CiGig2) From Grass Carp (Ctenopharyngodon Idella) Display Good Antiviral Activities in an IFN-Independent Pathway. *Dev Comp Immunol* (2013) 41(4):477–83. doi: 10.1016/j.dci.2013.07.007
34. Liu P, Wang L, Ye BQ, Huang S, Wong SM, Yue GH. Characterization of a Novel Disease Resistance Gene Rtp3 and Its Association With VNN Disease Resistance in Asian Seabass. *Fish Shellfish Immunol* (2017) 61:61–7. doi: 10.1016/j.fsi.2016.12.021
35. Mugue N, Terekhanova N, Afanasyev S, Krasnov A. Transcriptome Sequencing of Hybrid Bester Sturgeon: Responses to Poly (I:C) in the Context of Comparative Immunogenomics. *Fish Shellfish Immunol* (2019) 93:888–94. doi: 10.1016/j.fsi.2019.08.038
36. Wessel O, Krasnov A, Timmerhaus G, Rimstad E, Dahle MK. Antiviral Responses and Biological Concequences of Piscine Orthoreovirus Infection in Salmonid Erythrocytes. *Front Immunol* (2018) 9:3182. doi: 10.3389/fimmu.2018.03182
37. Kitamura Y, Murata Y, Park JH, Kotani T, Imada S, Saito Y, et al. Regulation by Gut Commensal Bacteria of Carcinoembryonic Antigen-Related Cell Adhesion Molecule Expression in the Intestinal Epithelium. *Genes Cells* (2015) 20(7):578–89. doi: 10.1111/gtc.12247
38. Wu R, Chen F, Wang N, Tang D, Kang R. ACOD1 in Immunometabolism and Disease. *Cell Mol Immunol* (2020) 17(8):822–33. doi: 10.1038/s41423-020-0489-5
39. Kirschning CJ, Bauer S. Toll-Like Receptors: Cellular Signal Transducers for Exogenous Molecular Patterns Causing Immune Responses. *Int J Med Microbiol* (2001) 291(4):251–60. doi: 10.1078/1438-4221-00128
40. Shanaki M, Shabani P, Goudarzi A, Omidifar A, Bashash D, Emamgholipour S. The C1q/TNF-Related Proteins (CTRPs) in Pathogenesis of Obesity-Related Metabolic Disorders: Focus on Type 2 Diabetes and Cardiovascular Diseases. *Life Sci* (2020) 256:117913. doi: 10.1016/j.lfs.2020.117913
41. Sunder-Plassmann G, Patruta SI, Hörl WH. Pathobiology of the Role of Iron in Infection. *Am J Kidney Dis* (1999) 34(4 Suppl 2):S25–9. doi: 10.1053/ajkd.1999.v34.aajkd0344b0025
42. Verga Falzacappa MV, Muckenthaler MU. Hepcidin: Iron-Hormone and Anti-Microbial Peptide. *Gene* (2005) 364:37–44. doi: 10.1016/j.gene.2005.07.020
43. Scarl RT, Lawrence CM, Gordon HM, Nunemaker CS. STEAP4: Its Emerging Role in Metabolism and Homeostasis of Cellular Iron and Copper. *J Endocrinol* (2017) 234(3):R123–34. doi: 10.1530/JOE-16-0594
44. Heikkila JJ. The Expression and Function of Hsp30-Like Small Heat Shock Protein Genes in Amphibians, Birds, Fish, and Reptiles. *Comp Biochem Physiol A Mol Integr Physiol* (2017) 203:179–92. doi: 10.1016/j.cbpa.2016.09.011
45. Chen ZF, Tian YS, Ma WH, Zhai JM. Gene Expression Changes in Response to Low Temperatures in Embryos of the Kelp Grouper, Epinephelus Moara. *Cryobiology* (2020) 97:159–67. doi: 10.1016/j.cryobiol.2020.05.013
46. Stoecklin G, Colombi M, Raineri I, Leuenberger S, Mallaun M, Schmidlin M, et al. Functional Cloning of BRF1, a Regulator of ARE-Dependent mRNA Turnover. *EMBO J* (2002) 21(17):4709–18. doi: 10.1093/emboj/cdf444
47. Lazado CC, Haddeland S, Timmerhaus G, Berg RS, Merkin G, Pittman K, et al. Morphomolecular Alterations in the Skin Mucosa of Atlantic Salmon (Salmo Salar) After Exposure to Peracetic Acid-Based Disinfectant. *Aquacult Rep* (2020) 17:100368. doi: 10.1016/j.aqrep.2020.100368
48. Le Jan S, Amy C, Cazes A, Monnot C, Lamandé N, Favier J, et al. Angiopoietin-Like 4 is a Proangiogenic Factor Produced During Ischemia and in Conventional Renal Cell Carcinoma. *Am J Pathol* (2003) 162(5):1521–8. doi: 10.1016/S0002-9440(10)64285-X
49. Bjørgen H, Haldorsen R, Oaland Ø., Kvellestad A, Kannimuthu D, Rimstad E, et al. Melanized Focal Changes in Skeletal Muscle in Farmed Atlantic Salmon After Natural Infection With Piscine Orthoreovirus (PRV). *J Fish Dis* (2019) 42(6):935–45. doi: 10.1111/jfd.12995
50. Houde ALS, Akbarzadeh A, Günther OP, Li S, Patterson DA, Farrell AP, et al. Salmonid Gene Expression Biomarkers Indicative of Physiological Responses to Changes in Salinity and Temperature, But Not Dissolved Oxygen. *J Exp Biol* (2019) 222:13. doi: 10.1242/jeb.198036
51. Akbarzadeh A, Günther OP, Houde AL, Li S, Ming TJ, Jeffries KM, et al. Developing Specific Molecular Biomarkers for Thermal Stress in Salmonids. *BMC Genomics* (2018) 19(1):749. doi: 10.1186/s12864-018-5108-9
52. Bakke A, Rebl A, Frost P, Afanasyev S, Røyset KA, Søfteland T, et al. Effect of Two Constant Light Regimens on Antibody Profiles and Immune Gene Expression in Atlantic Salmon Following Vaccination and Experimental Challenge With Salmonid Alphavirus. *Fish Shellfish Immunol* (2021) 118:188–96. doi: 10.1016/j.fsi.2021.07.002
53. Lennox RJ, Eldøy SH, Vollset KW, Miller KM, Li S, Kaukinen KH, et al. How Pathogens Affect the Marine Habitat Use and Migration of Sea Trout (Salmo Trutta) in Two Norwegian Fjord Systems. *J fish Dis* (2020) 43(7):729–46. doi: 10.1111/jfd.13170
54. Tang BM, Shojaei M, Parnell GP, Huang S, Nalos M, Teoh S, et al. A Novel Immune Biomarker IFI27 Discriminates Between Influenza and Bacteria in Patients With Suspected Respiratory Infection. *Eur Respir J* (2017) 49(6):1602098. doi: 10.1183/13993003.02098-2016
55. Sampson DL, Fox BA, Yager TD, Bhide S, Cermelli S, McHugh LC, et al. A Four-Biomarker Blood Signature Discriminates Systemic Inflammation Due to Viral Infection *Versus* Other Etiologies. *Sci Rep* (2017) 7(1):2914. doi: 10.1038/s41598-017-02325-8

Conflict of Interest: The authors declare that the research was conducted in the absence of any commercial or financial relationships that could be construed as a potential conflict of interest.

Publisher's Note: All claims expressed in this article are solely those of the authors and do not necessarily represent those of their affiliated organizations, or those of the publisher, the editors and the reviewers. Any product that may be evaluated in this article, or claim that may be made by its manufacturer, is not guaranteed or endorsed by the publisher.

frontiers in Immunology

ORIGINAL RESEARCH
published: 10 November 2021
doi: 10.3389/fimmu.2021.767813

MicroRNA-124 Promotes Singapore Grouper Iridovirus Replication and Negatively Regulates Innate Immune Response

Pin-Hong Li[1], Li-Qun Wang[1], Jia-Yang He[1], Xiang-Long Zhu[1], Wei Huang[1], Shao-Wen Wang[1], Qi-Wei Qin[1,2,3]* and Hong-Yan Sun[1]**

[1] University Joint Laboratory of Guangdong Province, Hong Kong and Macao Region on Marine Bioresource Conservation and Exploitation, College of Marine Sciences, South China Agricultural University, Guangzhou, China, [2] Southern Marine Science and Engineering Guangdong Laboratory, Zhuhai, China, [3] Laboratory for Marine Biology and Biotechnology, Qingdao National Laboratory for Marine Science and Technology, Qingdao, China

OPEN ACCESS

Edited by:
Verónica Chico Gras, Universidad Miguel Hernández de Elche, Spain

Reviewed by:
Junfa Yuan, Huazhong Agricultural University, China
Chengyu Hu, Nanchang University, China

***Correspondence:**
Shao-Wen Wang
wangsw@scau.edu.cn
Qi-Wei Qin
qinqw@scau.edu.cn
Hong-Yan Sun
hongyanlucky@scau.edu.cn

Specialty section:
This article was submitted to Comparative Immunology, a section of the journal Frontiers in Immunology

Received: *31 August 2021*
Accepted: *19 October 2021*
Published: *10 November 2021*

Citation:
Li P-H, Wang L-Q, He J-Y, Zhu X-L, Huang W, Wang S-W, Qin Q-W and Sun H-Y (2021) MicroRNA-124 Promotes Singapore Grouper Iridovirus Replication and Negatively Regulates Innate Immune Response. Front. Immunol. 12:767813. doi: 10.3389/fimmu.2021.767813

Viral infections seriously affect the health of organisms including humans. Now, more and more researchers believe that microRNAs (miRNAs), one of the members of the non-coding RNA family, play significant roles in cell biological function, disease occurrence, and immunotherapy. However, the roles of miRNAs in virus infection (entry and replication) and cellular immune response remain poorly understood, especially in low vertebrate fish. In this study, based on the established virus-cell infection model, Singapore grouper iridovirus (SGIV)-infected cells were used to explore the roles of miR-124 of *Epinephelus coioides*, an economically mariculture fish in southern China and Southeast Asia, in viral infection and host immune responses. The expression level of *E. coioides* miR-124 was significantly upregulated after SGIV infection; miR-124 cannot significantly affect the entry of SGIV, but the upregulated miR-124 could significantly promote the SGIV-induced cytopathic effects (CPEs), the viral titer, and the expressions of viral genes. The target genes of miR-124 were JNK3/p38α mitogen-activated protein kinase (MAPK). Overexpression of miR-124 could dramatically inhibit the activation of NF-κB/activating protein-1 (AP-1), the transcription of proinflammatory factors, caspase-9/3, and the cell apoptosis. And opposite results happen when the expression of miR-124 was inhibited. The results suggest that *E. coioides* miR-124 could promote viral replication and negatively regulate host immune response by targeting JNK3/p38α MAPK, which furthers our understanding of virus and host immune interactions.

Keywords: miR-124, *Epinephelus coioides*, SGIV, viral replication, immune response

INTRODUCTION

Viral infections seriously affect the health of organisms including humans. It is important to study the mechanism of viral infection and control the processing of diseases induced by virus. Singapore grouper iridovirus (SGIV) belonging to genus *Ranavirus*, family *Iridoviridae*, is a double-stranded DNA virus with icosahedral symmetry and a diameter of 120–200 nm (1). As a high pathogenic

virus of marine fish, SGIV can induce mortality rates of more than 90% and cause major economic losses of the aquaculture (2–6). It is important to clear the SGIV life cycle and the relationship between viral infection and host immunity for controlling the disease induced by SGIV. In recent years, the researchers found that some non-coding RNA could be involved in SGIV infection and replication (7, 8).

MicroRNAs (miRNAs) are small non-coding RNAs with about 22–25 nucleotides in length (9). Since miRNA was found in the embryonic development of *Caenorhabditis elegans*, multiple roles of miRNA were gradually demonstrated (10–12). By binding to the 3′ untranslated region (UTR) of mRNA, miRNA can regulate the translation and expression of genes to affect the processing of proliferation, metabolism, apoptosis, immunity, growth, and plasticity of neurons, etc. (13–15). MiRNAs can also regulate viral replication by adjusting innate immune response or apoptosis of host (16): miR-214 enhances the expression of the target gene AMPK and promotes Snakehead vesiculovirus (SHVV) replication by reducing the expression of type I interferon regulator (17); miR-731 can increase *Cytomegalovirus* replication in the early stage of infection by inhibiting the expression of IRF7 and p53, IFN-I response, cell apoptosis, and cell cycle arrest (18).

In mammals, miR-124 participates in the development and progression of cancer, nervous system, and host–pathogen: miR-124 inhibits cell proliferation in hepatocellular carcinoma by targeting PIK3CA and plays important roles in many cancers *via* the inhibition of PI3K/Akt pathway (19); miR-124 in the brain plays a key role in neurogenesis, neuronal differentiation, and synaptic plasticity in adults (20, 21); and miR-124 has a broad spectrum antiviral activity against influenza A virus (IAV) and respiratory syncytial virus (RSV) (22). To date, whether miR-124 affects the entry of virus remains unknown. In low vertebrate fish, the roles of miR-124 in the interactions of virus and host immune response need to be explored.

Epinephelus coioides is an economically mariculture fish in southern China and Southeast Asia, and SGIV can kill large numbers of *E. coioides* in a short time (1–6). Based on this information, the aim of this study was to explore the expression pattern of miR-124 response to SGIV infection; the role of miR-124 in the entry of SGIV, viral titers, and the expressions of viral genes; and immune response of host SGIV-induced cell apoptosis.

MATERIALS AND METHODS

Cells, Virus, and MicroRNAs

The *E. coioides* spleen cells (GS cells, College of Marine Sciences, South China Agricultural University, China) were established in culture medium with 10% fetal bovine serum (Gibco, USA) at 28°C in Leibovitz's L-15 medium (Gibco, USA). Because of the source, GS cells are good for studying the functions of *E. coioides* miRNAs (8, 23). Because SGIV cannot induce typical apoptosis in GS cells, the fathead minnow (FHM) cells have been verified to be good for analyzing SGIV-induced apoptosis (8, 23, 24). FHM cells herein were used for apoptosis analysis. FHM cells were cultured in Leibovitz's L-15 medium (Gibco, USA) embodying 10% fetal bovine serum (Gibco, USA) at 28°C (8, 23, 24). SGIV used for viral-infection experiments was originally obtained by our lab as previously described (1). The miRNAs, including control mimics, miR-124 mimics, control inhibitors, and miR-124-specific inhibitors, were purchased from RiboBio (China).

Total RNA Extraction and cDNA Synthesis

The RNA was isolated from *E. coioides* tissues from the liver, spleen, intestine, trunk kidney, gills, head kidney, skin, muscle, brain, and heart using TRIzol reagent (Invitrogen, Canada) and purified with DNase I (Promega, USA). RNA from the GS cells infected by SGIV was isolated using TRIzol reagent according to the manufacturer's instruction. The cDNA was synthesized using ReverTra Ace kit (Toyobo, Japan), and the specific miR-124 reverse transcription was obtained using miRNA RT kit (RiboBio, China). The reverse transcription was performed in a final volume of 20 μl containing 4 μl of 5× RT buffer, 1 μl of RT polymerase, 1 μl of miR-124-specific RT primer, and 14 μl of the denatured RNA. The reverse transcription condition was 42°C for 60 min, followed by 70°C for 10 min and 4°C for 15 min. The products obtained were used as a template in quantitative real-time PCR amplification (qPCR).

Expression Analysis

MiR-124 level was determined using Bulge-Loop™ miRNA qRT-PCR kit (RiboBio, China), and the U6 was used as the reference genes. qPCR was performed with SYBR Green Real-Time PCR Master Mix (Toyobo) at Applied Biosystems QuantStudio 5 Real Time Detection System (Thermo Fisher, USA). The reaction system was 10 μl including 5 μl of SYBR qPCR mix, 0.3 μl of forward and reverse bulge-loop miRNA primer, 3.4 μl of PCR-grade water, and 1 μl of diluted miR-124-specific cDNA. The reaction condition was 95°C for 5 min, followed by 40 cycles of 94°C for 5 s, 56°C for 10 s, and 72°C for 15 s. The expression of the genes was normalized to reference gene and calculated with the $2^{-\Delta\Delta Ct}$ method.

Western Blotting Analysis

Cells were lysed in pierce IP lysis buffer (Thermo Fisher) and separated by 10% sodium dodecyl sulfate–polyacrylamide gel electrophoresis (SDS-PAGE); and after electrophoresis, the proteins were transferred onto polyvinylidene difluoride (PVDF) membranes (Millipore, USA). In our lab, 5% bovine serum albumin (BSA) diluted rabbit anti-MCP antibody (1:1,000 dilution) was prepared, in which the patent number was CN111363758A (8). P-JNK3(1:1,000 dilution), P-p38 mitogen-activated protein kinase (MAPK) (1:1,000 dilution), caspase-3 (1:1,000 dilution), cleaved caspase-3 (1:1,000 dilution), and rabbit anti-β-tubulin antibody (1:2,000 dilution) was purchased from Abcam. Horseradish peroxidase (HRP)-conjugated goat anti-rabbit (1:5,000) was purchased from KPL (USA). And then we used the HRP-DAB Chromogenic Substrate Kit (Tiangen, China) to visualize according to the manufacturer's instructions and took photos.

Confocal Microscopy and Single-Particle Imaging Assay

To explore the effect of miR-124 on the entry of SGIV, we explored the miR-124 on virus entry using confocal imaging. Fluorescence images were observed through ZEISS LSM 7 DUO confocal microscope. The fluorescent label, Alexa Fluor 647 (labelled SGIV), and 4% paraformaldehyde were purchased from Invitrogen. The lipophilic dye, DiO, which indicates the cell boundaries (green), was purchased from Biotium, USA. Fluorescence emission was collected and imaged through a 100× (numerical aperture, 1.4) oil immersion objective. A 488-nm Ar-Kr laser was used to excite DiO signals, and a 500- to 550-nm bandpass filter was used for emission. For quantification analysis, confocal images were obtained by noise filtering, edge detection, and fluorescence signal extraction using a MATLAB program. Approximately 60 cells were randomly analyzed by the MATLAB program to calculate the number of SGIV particles in the cytoplasm.

The Cytopathic Effect

To evaluate the effects of miR-124 on virus infection, control mimics, miR-124 mimics, control inhibitors, or miR-124 inhibitors (100 nM) were transfected into GS cells in 24-well plates using Lipofectamine RNAiMAX (Invitrogen, USA) according to the manufacturer's instructions. Twenty-four hours after transfection, the cells were then infected with SGIV for 12-h point infection, and photos of the cell morphology were taken.

Virus Titer Assay

To detect the effect of miR-124 on SGIV production, the viral titer was evaluated by $TCID_{50}$ analysis. GS cells were transfected with the miR-124 mimics (100 nM) in 24-well plates for 24 h and then infected with SGIV for 24 h. Cells were collected and freeze–thawed three times at −80°C. The cell lysate was then serially diluted and used for GS cell infection in 96-well plates. About 6 days after infection, the viral titer was calculated using $TCID_{50}$ analysis.

Virus Gene Analysis

To evaluate the effects of miR-124 on virus infection, the miRNAs (100 nM) were transfected into GS cells in 12-well plates. Twenty-four hours after transfection, the cells were infected with SGIV for 24 h, and then the expressions of the viral genes (*MCP*, *VP19*, *ICP18*, and *LITAF*) were detected by RT-qPCR with the β-actin as the reference gene. And the Western blotting analysis was used to detect the protein synthesis of SGIV MCP.

Plasmid Construction

According to the transcriptome data and the BLAST information, the GenBank accession numbers of JNK3 and p38α MAPK were KT385696.1 and JN408831.1, respectively. The primers JNK3-3′ UTR-F/JNK3-3′ UTR-R, and p38α-3′ UTR-F/p38α-3′ UTR-R (**Table 1**), were designed to amplify JNK3-3′UTR and p38α-3′UTR cDNA. PCR in a final volume of 25 μl was as follows: 1 μl of template DNA, 1 μl of each primer, 12.5 μl of LA Taq polymerase (Takara), and 9.5 μl of H_2O. The conditions for PCR amplification were as follows: 34 cycles of 94°C, 30 s; 57°C, 30 s; and 72°C, 30 s, followed by 72°C for 5 min. The PCR products were purified and cloned into pmiR-RB-Report™ (RiboBio, China). The restriction sites are *Xho*I and *Not*I. And the recombinant plasmid (pmiR-JNK3 and pmiR-p38α) was confirmed by DNA sequencing. And the primers JNK3-mut-3′UTR-F/JNK3-mut-3′UTR-R and p38α-mut-3′ UTR-F/p38α-mut-3′UTR-R were designed to make mutant plasmid (pmiR-mut-JNK3 and pmiR-mut-p38α).

MicroRNA Target Prediction

The RNAhybrid (https://bibiserv.cebitec.uni-bielefeld.de/rnahybrid), TargetScan (http://www.targetscan.org/cgi-bin/), and miRanda (http://www.microrna.org/microrna/) were used to predict the putative targets of miR-124. And the 3′ UTR regions of the target gene of miR-124 of grouper immune-related genes were collected from the National Center for Biotechnology Information (NCBI) database (https://www.ncbi.nlm.nih.gov/).

To analyze the relationship between miR-124 and the gene JNK3/p38α MAPK, GS cells were co-transfected with miR-124 mimics/control mimics (100 nM), luciferase reporter vector (pmiR-JNK3/pmiR-p38α MAPK, 800 ng), and (pmiR-mut-JNK3/pmiR-mut-p38α MAPK, 800 ng) in 24-well plates for 24 h. Luciferase activity was detected using the Dual-Luciferase Reporter Assay system (Promega, USA). The specificity of target was ascertained by the relative luciferase activity of Firefly/Renilla.

Dual Luciferase Reporter Assays

In order to verify the role of miR-124 in the transcriptional regulation of NF-κB and activating protein-1 (AP-1), control mimics, miR-124 mimics, control inhibitors, or miR-124 inhibitors (100 nM) were co-transfected with 150 ng of NF-κB/AP-1-dependent firefly luciferase reporter plasmid and 40 ng of Renilla luciferase vectors into GS cells at 24-well plates using luciferase reporter assay for 24 h. The cells were infected with SGIV for 12/24 h and harvested using the Dual-Luciferase® Reporter Assay System (Promega, USA) to measure the luciferase activities according to the manufacturer's instructions.

Cell Apoptosis Analysis

It was demonstrated that SGIV can induce the typical apoptosis in FHM cells (24). To explore the function of miR-124 in SGIV-induced cell apoptosis, control mimics, miR-124 mimics, control inhibitors, and miR-124 inhibitors at 100 nM were transfected into FHM cells for 24-well plates by three replicates. After 24 h of SGIV infection, the cells were harvested, and the apoptosis was detected by both the terminal deoxy nucleotidyl transferase (TdT)-mediated dUTP nick-end labeling (TUNEL) assay using fluorescence microscope and flow cytometry using the Annexin V-FITC apoptosis detection kit (Beyotime, China) according to the manufacturer's instructions. Each sample was analyzed in triplicate. Data acquisition and analysis were performed using a flow cytometry system (Beckman Coulter, USA) and FlowJo VX software.

Caspase-9/3 Activity Analysis

To detect the effect of miR-124 in caspase-9/3 activity, the Caspase Fluorometric assay kit (BioVision, USA) was used to

TABLE 1 | The primers of this study.

Primer	Sequence (5′–3′)
β-Actin-F	TGCTGTCCCTGTATGCCTCT
β-Actin-R	CCTTGATGTCACGCACGAT
VP19-RT-F	TCCAAGGGAGAAACTGTAAG
VP19-RT-R	GGGGTAAGCGTGAAGACT
LITAF-RT-F	GATGCTGCCGTGTGAACTG
LITAF-RT-R	GCACATCCTTGGTGGTGTTG
MCP-RT-F	GCACGCTTCTCTCACCTTCA
MCP-RT-R	AACGGCAACGGGAGCACTA
ICP18-RT-F	ATCGGATCTACGTGGTTGG
ICP18-RT-R	CCGTCGTCGGTGTCTATTC
JNK3-RT-F	CCAGGACCGCAGGCACCAGTT
JNK3-RT-R	GTGGCGCACCATTTCTCCCATAA
p38α-RT-F	CCTCAACAACATCGTCAAGTG
p38α-RT-R	GGCTTCAAGTCTCTGTGGAT
JNK3-3′UTR-F	CCCTCGAGCCCCCCCTCCTCCTCCATAA
JNK3-3′UTR-R	TTGCGGCCGCCAGGCAGGCGGCTAGTCACC
p38α-3′UTR-F	CCCTCGAGCAGAACCATGACATTCAAGTG
p38α-3′UTR-R	TTGCGGCCGCCAGAGTAACAAAAACAGCAAA
JNK3-mut-3′UTR-F	AATTCTAGGCGATCGCTCGAGCCCCCC
JNK3-mut-3′UTR-R	TTTTATTGCGGCCAGCGGCCGCCCTTACGCGCCATAGTCACCTGCAACAC
p38α-mut-3′UTR-F	AATTCTAGGCGATCGCTCGAGCAGAACCATGAGTAAGTACACGGAGCCGTC
p38α-mut-3′UTR-R	TTTTATTGCGGCCAGCGGCCGCCAG
TNFα-RT-F	GTGTCCTGCTGTTTGCTTGGTA
TNFα-RT-R	CAGTGTCCGACTTGATTAGTGCTT
IL-6-RT-F	CTCTACACTCAACGCGTACATGC
IL-6-RT-R	TCATCTTCAAACTGCTTTTCGTG
IL-8-RT-F	GCCGTCAGTGAAGGGAGTCTAG
IL-8-RT-R	ATCGCAGTGGGAGTTTGCA
IL-1β-RT-F	AACCTCATCATCGCCACACA
IL-1β-RT-R	AGTTGCCTCACAACCGAACAC

test the activity of caspase-9/3 according to the manufacturer's instructions. FHM cells at 24-well plates transfected with 100 nM of control mimics, miR-124 mimics, control inhibitors, or miR-124 inhibitors were infected by SGIV for 24 h. The cells were lysed in 50 μl of cold lysis buffer on ice for 10 min and centrifuged at 1,800 rpm for 3 min, and the supernatant was retained. The reaction system was prepared: 50 μl of the supernatant, 50 μl of 2× reaction buffer, 5 μl of caspase-9/3 fluorogenic substrate (LEHD-AFC/DEVD-AFC), and 0.5 μl of fresh DTT. After incubation at 37°C for 1 h, fluorescence was measured (excitation 400 nm, excitation 505 nm) by Thermo Scientific™ Varioskan™ LUX (Thermo Fisher, USA).

Statistical Analysis

All of the data expressed as mean ± standard error of the mean (SD) were analyzed with GraphPad Prism 7.0 software using one-way ANOVA followed by Duncan's test. Significance was set at $p < 0.05$.

RESULTS

MiR-124 Is Upregulated by Singapore Grouper Iridovirus Infection

E. coioides miR-124 was obtained by employing the Solexa deep sequencing approach in our lab (7). As shown in **Table 2**, the sequence was the same except for a difference of 2 or 3 bases in the end of 3′ end in the species, indicating that miR-124 is highly conserved between species.

To obtain the tissue-specific distribution profiles of *E. coioides* miR-124, the total RNA of the 10 tissues from healthy *E. coioides* was extracted, and qPCR was used to quantify the expression of *E. coioides* miR-124. MiR-124 was detected in all of the tissues, and the miR-124 was specifically expressed in the brain, followed by the heart, intestine, skin, liver, gills, muscle, spleen, trunk kidney, and head kidney (**Figure 1A**).

In order to characterize the expression profile of miR-124 after SGIV infection, the expression of miR-124 under the stimulation of SGIV was examined by qPCR. The expression of miR-124 was upregulated during the SGIV infection (**Figure 1B**) ($p < 0.05$).

MiR-124 Promoted the Singapore Grouper Iridovirus Replication

To examine the efficiency of miR-124 mimics or inhibitors, the expression of miR-124 of the GS cells transfected with miR-124 mimics (100 nM) or inhibitors (100 nM) for 24 and 48 h was examined. As shown in **Figure 2A**, the significantly higher expression of miR-124 was detected in the cells with the miR-124 mimics for 48 h ($p < 0.05$), and the miR-124 was significantly downregulated in the cells transfected with the miR-124 inhibitor for 48 h (**Figure 2B**) ($p < 0.05$), showing that it is still efficient at 48 h post transfection with miR-124 mimics or inhibitor.

TABLE 2 | Sequence of miR-124 in different species.

MiRNA name	Sequence (5′–3′)	Species	miRBase number
eco-miR-124	UAAGGCACGCGGUGAAUGCCAA	*Epinephelus coioides*	Undetermined
dre-miR-124	UAAGGCACGCGGUGAAUGCCAA	*Danio rerio*	MIMAT0001819
hsa-miR-124-3p	UAAGGCACGCGGUGAAUGCCAA	*Homo sapiens*	MIMAT0000422
bta-miR-124a	UAAGGCACGCGGUGAAUGCCAAG	*Bos taurus*	MIMAT0003811
dme-miR-124-3p	UAAGGCACGCGGUGAAUGCCAAG	*Drosophila melanogaster*	MIMAT0000351
cfa-miR-124	UAAGGCACGCGGUGAAUGCCA	*Canis familiaris*	MIMAT0006657
mmu-miR-124-3p	UAAGGCACGCGGUGAAUGCC	*Mus musculus*	MIMAT0000134
rno-miR-124-3p	UAAGGCACGCGGUGAAUGCC	*Rattus norvegicus*	MIMAT0000828

The red font indicates completely the same sequence.

To explore the effect of miR-124 on the entry of SGIV, virus entry in the cells transfected with miR-124 mimics was analyzed using confocal imaging. Compared with the cells transfected with the control mimics, cells transfected with miR-124 mimics were not significantly different on SGIV entry (**Figures 3A, B**), suggesting that miR-124 might not be involved in the entry of SGIV.

The GS cells transfected with miR-124 mimics were infected with SGIV for 24 h. Subsequently, the SGIV-induced cytopathic effects (CPEs), the SGIV production, and expression of the viral genes were analyzed. And the CPE was increased in the cells transfected with miR-124 mimics and decreased in the cells transfected with miR-124 inhibitor (**Figure 4A**). The viral titer, which was used to evaluate viral production, of the miR-124 overexpression cells was significantly higher than that of the control cells, while that of the miR-124 downregulated cells was significantly lower than that of the control cells (**Figure 4B**) ($p < 0.05$). Furthermore, the transcription levels of SGIV genes (*MCP*, *VP19*, *ICP18*, and *LITAF*) were examined. The expression of viral genes *MCP*, *VP19*, *ICP18*, and *LITAF* were

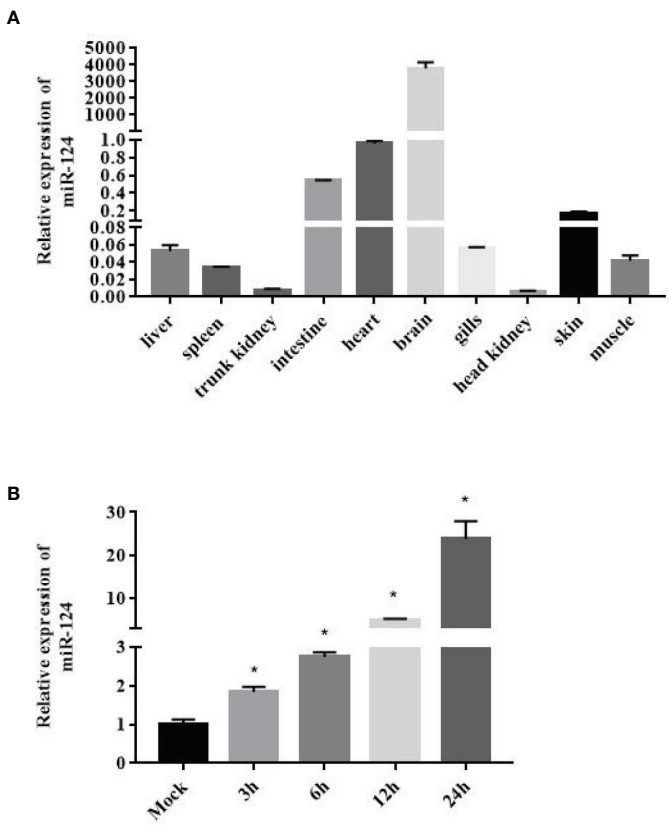

FIGURE 1 | Expression of miR-124 in tissues and in response to Singapore grouper iridovirus (SGIV) infection in the GS cell. **(A)** Expression of miR-124 was detected in the 10 tissues. Data are presented as mean ± SD, N = 3. **(B)** Expression of miR-124 in response to SGIV infection in the GS cell. The GS cells were incubated in 24-well plates and after 24 h were infected by SGIV. U6 was used as internal reference. The control and SGIV infection groups of the miR-124 expression significant differences at each time points are indicated with * ($p < 0.05$). Data are presented as mean ± SD, N = 4.

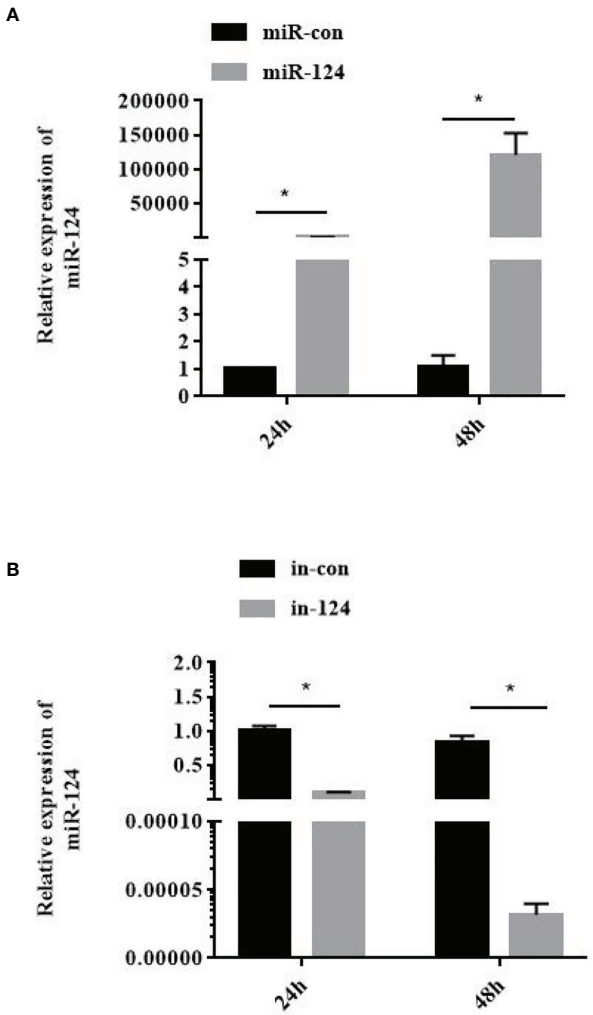

FIGURE 2 | Efficiency detection of miR-124 overexpression. 100nM control mimics **(A)**, miR-124 mimics **(A)**, control inhibitors **(B)**, or miR-124 inhibitors **(B)** were transfected into the GS cells in 12 well plate. The cells at 24 h and 48 h was collected and the expression of miR-124 was detected. U6 was used as internal reference. Control mimics, miR-con; miR-124 mimics, miR-124; control inhibitors, in-con; miR-124 inhibitors, in-124. All data are presented as Mean ± SD, N = 4. Compared with the control group, significant difference of experimental group is indicated with *($P < 0.05$).

significantly upregulated in the cells transfected with miR-124 mimics, which were downregulated in the cells transfected with miR-124 inhibitor (**Figures 4C–F**). By Western blotting, the protein level of MCP in the cells transfected with miR-124 mimics (1.30) was higher than that of the control group (0.94), while the protein level of MCP in the cells transfected with miR-124 inhibitor (0.78) was lower than that of the control group (1.18) (**Figure 4G**), showing that overexpression of miR-124 could enhance the protein synthesis of SGIV MCP and that inhibited miR-124 could decrease the synthesis of MCP.

MiR-124 Regulates Innate Immune Response of *Epinephelus coioides*

By bioinformatics tools, JNK3 and p38α MAPK were the putative target genes of miR-124, and the binding energy value was −27.1 and −24.4 kcal/mol, respectively. The miR-124 sequence contains a conserved sequence matching the JNK3/p38α MAPK binding 3′-UTR (**Figures 5A, B**). To study the role miR-124 on JNK3 and p38α MAPK, the JNK3 and p38α MAPK mRNAs were examined in the overexpression miR-124 cells by qPCR. The expressions of both JNK3 and p38α MAPK in the cells transfected with miR-124 mimics were significantly downregulated than those in the control groups (**Figures 5C, D**) ($p < 0.05$). To verify the relationship of JNK3/p38α MAPK and miR-124, JNK3/p38α MAPK 3′-UTR or JNK3/p38α MAPK mutant 3′-UTR was cloned into a luciferase reporter vector pmiR-RB-Report. The GS cells transfected with the luciferase reporter containing miR-124 mimics and JNK3/p38αMAPK wild 3′-UTR or JNK3/p38α MAPK mutant 3′-UTR were analyzed. The luciferase activities were significantly reduced in

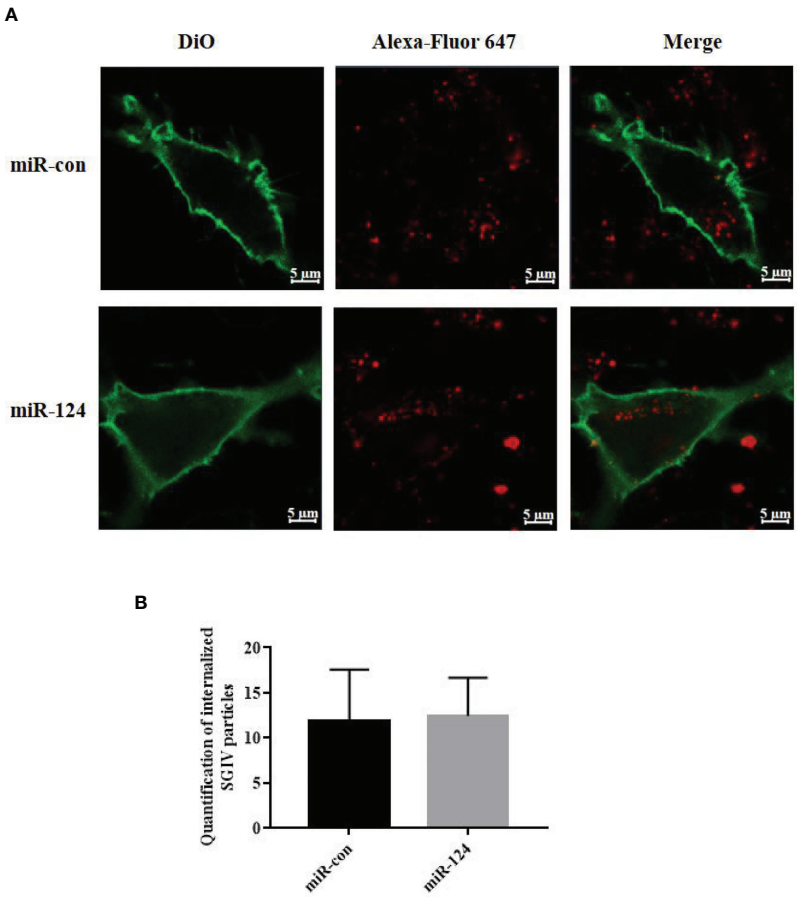

FIGURE 3 | The effect of miR-124 on the entry of Singapore grouper iridovirus (SGIV). **(A)** Three-dimensional confocal images of SGIV attachment in control mimics (miR-con) or miR-124 mimics (miR-124) transfected cells. The samples were stained with DiO to show the cell boundaries (green). The SGIV was labeled Alexa Fluor 647 (red). Scale bars represent 5 μm. **(B)** Quantification of internalized SGIV particles. Over 60 cells were randomly selected and analyzed by MATLAB program. The data are indicated as mean ± SD, N = 60.

the cells containing JNK3/p38α MAPK wild 3′-UTR (**Figures 5E, F**) ($p < 0.05$), and there was no significant change in the cells of JNK3/p38α MAPK mutant 3′-UTR ($p < 0.05$). And the protein level of P-JNK3/P-p38α MAPK in the cells transfected with miR-124 mimics (0.33 and 0.48) was lower than that of the control group (0.49 and 0.71) (**Figures 5G, H**).

To study the effect of miR-124 on the transcriptional activity of NF-κB and AP-1, the control mimics, miR-124 mimics, control inhibitors, and miR-124 inhibitors at 100 nM were transfected into GS cells for 24 h; and then the cells were infected with SGIV and collected at 12 and 24 h post infection. The activations of the NF-κB and AP-1 were significantly reduced in the cells transfected with miR-124 mimics ($p < 0.05$), and those of the NF-κB and AP-1 were significantly upregulated in the cells transfected with miR-124 inhibitor compared with the control group ($p < 0.05$) (**Figures 6A, B**).

To verify the roles of miR-124 in innate immunity, GS cells transfected with control mimics/miR-124 mimics/control inhibitors/miR-124 inhibitors were infected with SGIV, and the expressions of the proinflammatory factors TNF-α, IL-6, IL-8, and IL-1β were detected. The expressions of these factors in the cells transfected with miR-124 mimics were significantly lower than those in the control group; those of the miR-124 inhibitors were significantly higher those of the control inhibitor (**Figure 7**) ($p < 0.05$), suggesting that miR-124 significantly reduced the transcription levels of the *E. coioides* immune-related factors.

MiR-124 Inhibited the Singapore Grouper Iridovirus-Induced Cell Apoptosis

SGIV infection can cause cell apoptosis in FHM cells (8). To explore the influence of miR-124 on SGIV-induced cell apoptosis, miR-124 mimics/control mimics/control inhibitors/miR-124 inhibitors were transfected into FHM cells, and the cells were infected by SGIV for 24 h. Subsequently, the cells were harvested, and the apoptosis was analyzed.

By TUNEL assay, the fractured DNA was labeled using fluorescein isothiocyanate (FITC)-conjugated UTP. The

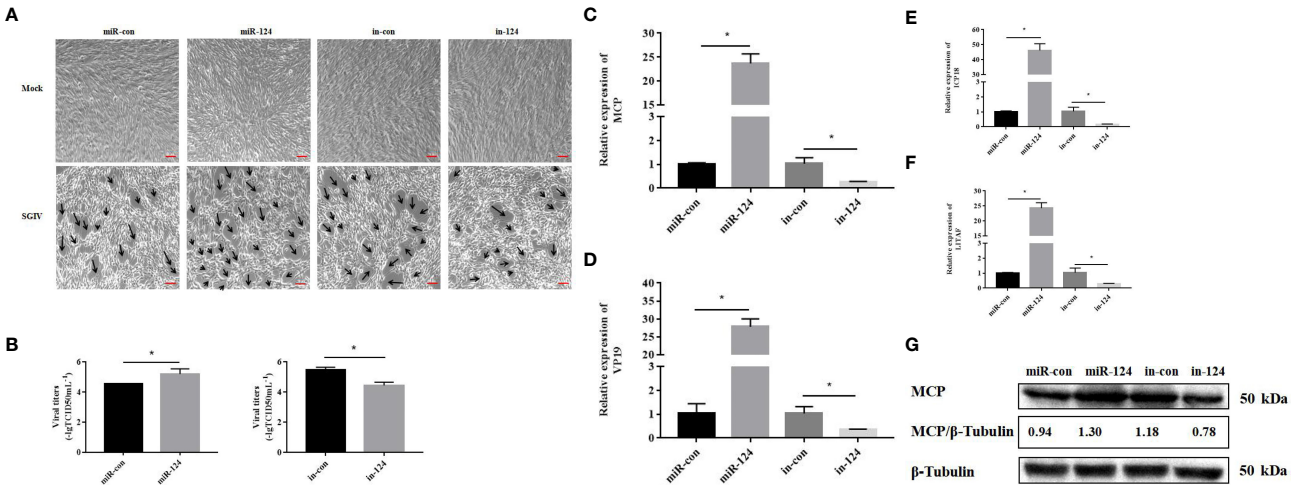

FIGURE 4 | Effect of miR-124 on virus infection and replication. **(A)** The cytopathic effect (CPE) of Singapore grouper iridovirus (SGIV)-infected miRNA-transfected GS cells, and the black arrows indicate the severity of CPE caused by SGIV infection at 24 h.The scale is 50 μm. **(B)** The viral titers in each group were measured using the $TCID_{50}$ method. Data are presented as mean ± SD, N = 3. **(C–F)** The expression levels of SGIV genes (*MCP*, *VP19*, *ICP18*, and *LITAF*). Data are presented as mean ± SD, N = 4. Compared with the control group, significant difference of experimental group is indicated with *($P < 0.05$). **(G)** The level of SGIV MCP proteins was detected by Western blotting, the band intensity was calculated, and ratios of target protein/β-tubulin were assessed by ImageJ software. Control mimics, miR-con; miR-124 mimics, miR-124; control inhibitors, in-con; miR-124 inhibitors, in-124.

apoptotic cells were counted with florescence microscope. As shown in **Figure 8A**, the fractured DNA fragments were decreased in the cells transfected with miR-124 mimics and increased in the cells transfected with miR-124 inhibitor. The apoptosis rates in the cells transfected with control mimics and miR-124 mimics were 27.0% and 12.7%, respectively (**Figure 8B**). The apoptosis rates were 15.7% and 23.3% in the cells transfected with miR-124 inhibitor (**Figure 8B**).

Similar results occurred in the analysis of flow cytometry. By flow cytometry, the apoptosis rate (sum of early apoptosis and late apoptosis) in the cells transfected with control mimics or miR-124 mimics was 74.0% or 55.2%, respectively (**Figures 8C, D**). The apoptosis rate (sum of early apoptosis and late apoptosis) in control cells was 35.8% and 40.2% in the cells transfected with miR-124 inhibitor (**Figures 8C, D**).

By Western blotting, the protein level of caspase-3 in the cells transfected with miR-124 mimics (0.29) was lower than that of the control group (0.68), while the protein level of caspase-3 in the cells transfected with miR-124 inhibitor (0.39) was higher than that of the control group (0.29) (**Figure 8E**); the protein level of cleaved caspase-3 in the cells transfected with miR-124 mimics (0.27) was lower than that of the control group (0.40), while the protein level of cleaved caspase-3 in the cells transfected with miR-124 inhibitor (0.46) was higher than that of the control group (0.45) (**Figure 8F**), showing that overexpression of miR-124 could decrease the protein of caspase-3 and cleaved caspase-3 and that inhibited miR-124 could enhance the protein of caspase-3 and cleaved caspase-3. The activity of caspase-9 and caspase-3 in the cells transfected with miR-124 mimics was significantly inhibited, as compared with that in the control group (**Figures 8G, H**) ($p < 0.05$). The results indicated that miR-124 significantly suppressed SGIV-induced cell apoptosis.

DISCUSSION

It is well known viral infections seriously affect the health of organisms. To date, non-coding RNA as a key factor has been involved in multiple biological processing including its roles in the response to pathogen stimulates. Non-coding RNA and miRNA regulated many functions of cells, including proliferation, metabolism, apoptosis, immunity, growth, and plasticity of neurons (13–15). However, the relationship of miRNA such as miR-124 and the viral entry remains unknown. In this study, the roles of marine fish *E. coioides* miR-124 in the infection and replication of SGIV and the innate immune response of host were explored.

Except for the difference of 2 or 3 bases in the 3′ end, *E. coioides* miR-124 shares the same sequences with other species from worm to humans, suggesting that its roles in these species might be similar (25, 26). In mammals, miR-124 is closely related to brain development, function, and homeostasis (27–29). However, the brain controls the spleen to regulate the function of the immune system from top to bottom; a special brain–spleen connection was recognized, enhancing humoral response autonomously and displaying immune stimulation through physical behavior, which revealed the brain's control of adaptive immunity, and proposes the possibility of improving immune ability through behavioral intervention (30). Similarly, miR-124 here was specifically expressed in *E. coioides* brain.

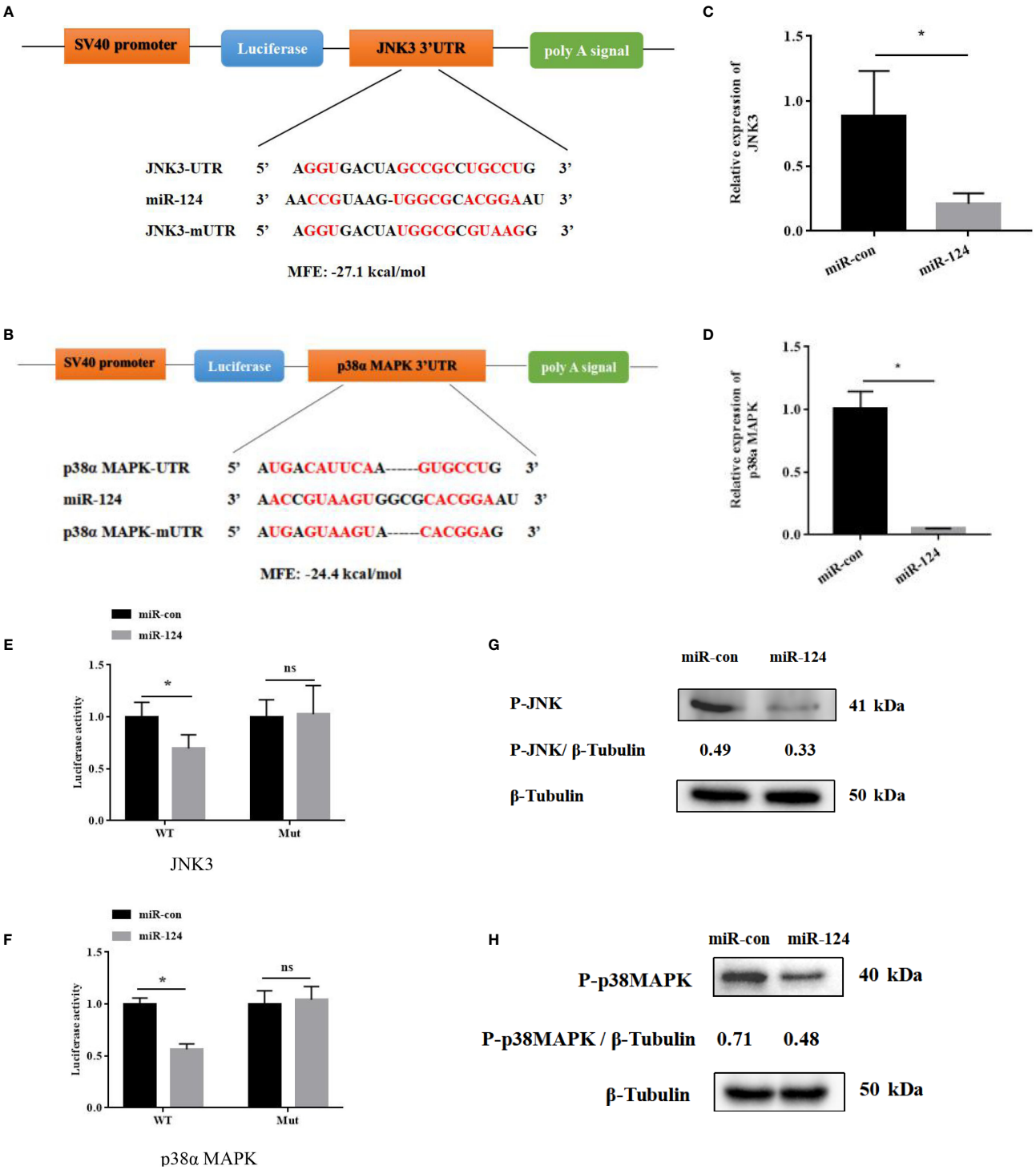

FIGURE 5 | JNK3 and p38α MAPK were identified as the targets of miR-124. **(A)** Diagram of JNK3 3′ UTR-containing reporter constructs. **(B)** Diagram of p38α 3′ UTR-containing reporter constructs. **(C)** The mRNA levels of JNK3 were reduced in GS cells treated with miR-124 mimics for 24 h. Actin was used as internal reference. **(D)** The mRNA levels of p38α were reduced in GS cells treated with miR-124 mimics for 24 h. β-Actin was used as internal reference. **(E)** The 3′ UTR reporter assay was performed in GS cells 24 h after transfection. **(F)** The 3′ UTR reporter assay was performed in GS cells 24 h after transfection. **(G)** The level of P-JNK3 proteins was detected by Western blotting, the band intensity was calculated, and ratios of target protein/β-tubulin were assessed by ImageJ software. **(H)** The level of P-p38 MAPK proteins was detected by Western blotting, the band intensity was calculated, and ratios of target protein/β-tubulin were assessed by ImageJ software. Control mimics, miR-con; miR-124 mimics, miR-124; control inhibitors, in-con; miR-124 inhibitors, in-124. All data are presented as mean ± SD, N = 4. Compared with the control group, significant difference of experimental group is indicated with *($P < 0.05$), and no significant difference is indicated with ns ($P > 0.05$).

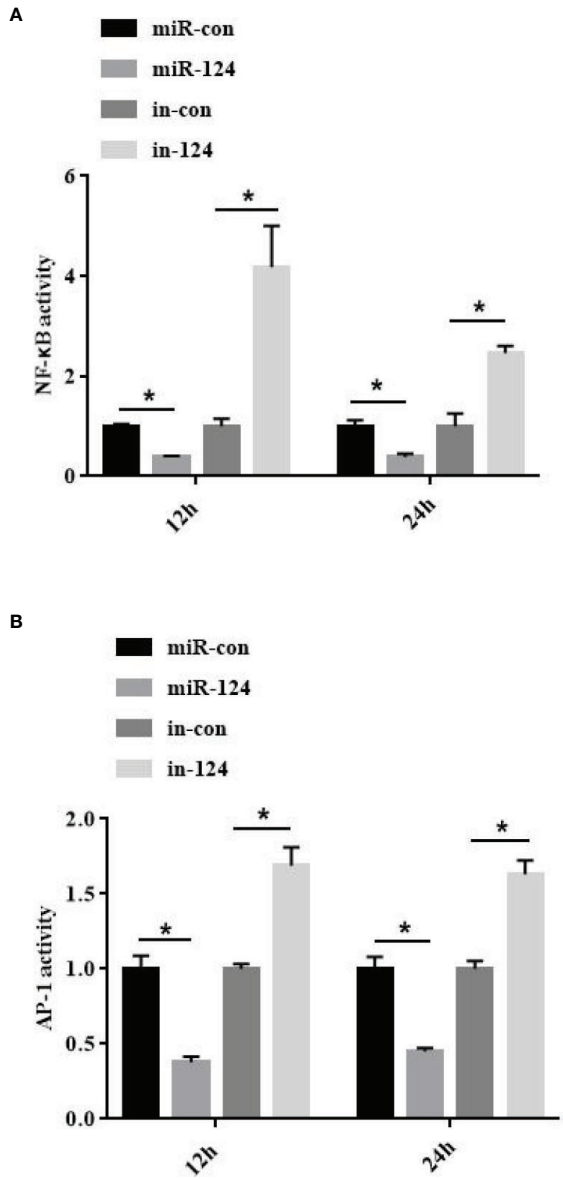

FIGURE 6 | MiR-124 inhibited NF-κB and activating protein-1 (AP-1) activation. The activities of NF-κB **(A)** and AP-1 **(B)** were analyzed by dual luciferase reporter assays. The miRNAs were transfected into the fathead minnow (FHM) cells in 24-well plates. After 24-h transfection, cells were infected with Singapore grouper iridovirus (SGIV) for 12 and 24 h. Relative luciferase activity is measured as a ratio of firefly luciferase activity to Renilla luciferase activity. Control mimics, miR-con; miR-124 mimics, miR-124; control inhibitors, in-con; miR-124 inhibitors, in-124. All data are presented as mean ± SD, N = 4. Compared with the control group, significant difference of experimental group is indicated with *($P < 0.05$).

The pathogenesis of virus is a complex process, which is the dynamic interaction of many host factors, such as miRNAs as the key factors. Viral infection can affect the expression of host miRNA. *Litopenaeus vannamei* miRNAs were differentially expressed after white spot syndrome virus (WSSV) infection, and the different expression of miRNAs could affect host signaling pathway of immune response (31). SGIV is an important virus of marine cultured fish causing huge financial losses, and SGIV infection can cause a series of host immune responses, including the changes of host miRNA expression (23). Previous studies in our lab have shown that the numbers of miRNA of *E. coioides* occurred with different expression responses to SGIV infection, and the expressions of some miRNAs were increased (7). In this study, miR-124 is upregulated during SGIV infection, indicating that miR-124 would be involved in SGIV infection and replication.

MiRNA could regulate viral infection (32). During viral infection, differential expression profiles of host miRNAs may lead to viral replication with feedback or feedforward effects (33). MiR-214 can directly interact with hepatitis E virus (HEV) RNA to enhance the replication and the genome translation of HEV, and the increase of HEV ORF2 level can upregulate the expression of miR-214 (34). MiR-1307 inhibits the replication of foot and mouth disease virus (FMDV) by the degradation of FMDV VP3 through proteasome pathway (35). In this study, SGIV infection can increase the expression of miR-124, and the upregulated miR-124 could not be involved in SGIV entry, but it could increase SGIV-induced CPE, and virus titers, transcription levels of SGIV genes, and the protein level of SGIV MCP, suggesting that miR-124 can be activated by SGIV infection, and the activated miR-124 could promote the replication of SGIV.

To further explore the roles of miR-124 in innate immune response of *E. coioides*, bioinformatics, gene mutants, Western blotting, etc., were used. By miRNA target prediction and the binding sties mutation of targeting genes, JNK3 and p38α MAPK were important target genes of miR-124: the 3′-UTR of JNK3/p38α MAPK contained the matched binding sequence with miR-124; miR-124 can downregulate the mRNA and protein JNK3/p38α MAPK, and JNK3/p38α MAPK 3′-UTR-contained reporter. As members of MAPK family, JNK3 and p38α MAPK can be activated; can convert the extracellular signals into intracellular signals by stress, viral infection, inflammatory cytokines, and mitotic factors (36–39); and can regulate the cell apoptosis and the viral replication (40–42). In mammals, miR-124 regulates the expression of p38α MAPK to participate in the neurons of signal transduction to translation machinery (43), and miR-124 regulates JNK to induce cell death in $CD133^+$ HCC cells (44). Previous studies in our lab demonstrated that SGIV infection can induce the inflammation, and the immune response of host, causing the differential expression of host mRNA such as JNK and p38α MAPK (5, 45). JNK and p38α MAPK were the target genes of miR-124; the high expression of JNK and p38 MAPK would stimulate miR-124; and the expression of miR-124 was upregulated, suggesting that miR-124 could regulate SGIV infection by targeting JNK3 and p38α MAPK.

JNK and p38 MAPK could affect the activity of NF-κB and other transcription factors like AP-1 (3, 5, 8, 45). NF-κB plays key roles in response to various stress stimuli and is the main regulator and initiator of inflammatory response (46–48).

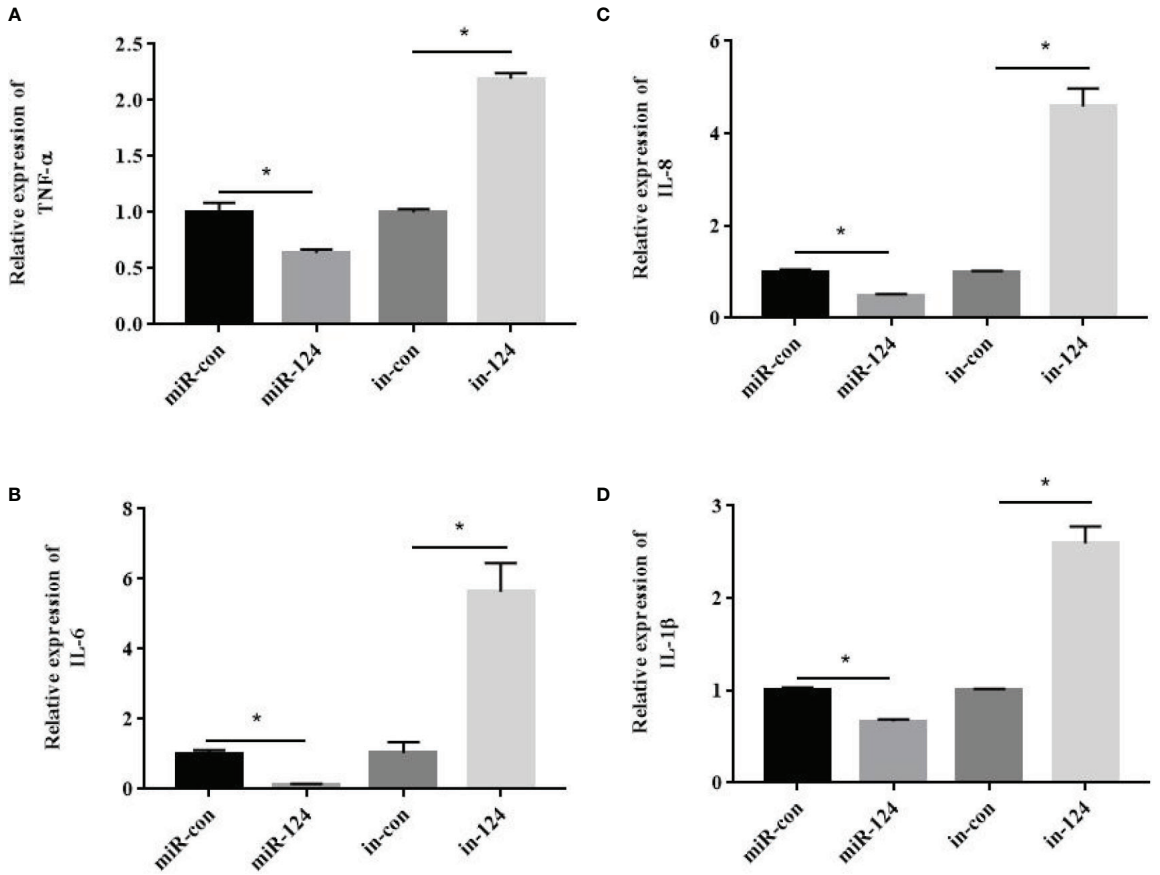

FIGURE 7 | The effect of miR-124 on the transcription of proinflammatory factors. β-Actin was used as internal reference. The transcription of TNF-α **(A)**, IL-6 **(B)**, IL-8 **(C)** and IL-1β **(D)** were analyzed by qRT-PCR. control mimics: miR-con; miR-124 mimics: miR-124; control inhibitors: in-con; miR-124 inhibitors: in-124. All data are presented as Mean ± SD, N = 4. Compared with the control group, significant difference of experimental group is indicated with *($P < 0.05$).

Together with AP-1, the activated NF-κB participated in many cellular processes, including apoptosis, proliferation, and differentiation (49). The factors of TNF-α, IL-1β, IL-6, and IL-8 are in synergy with cytokines, which are messengers of the inflammatory cascade (50, 51). In this study, the activation of NF-κB and AP-1 and the expressions of the factors (TNF-α, IL-6, IL-8, and IL-1β) were significantly inhibited in miR-124-overexpressing cells with SGIV infection, suggesting that miR-124 inhibits the activity of NF-κB and AP-1, and the expressions of the inflammatory factors to regulate the innate immunity.

Apoptosis is an innate cellular response to inflammatory response, transmission, and expression of virus. Virus has acquired the ability to regulate host cell apoptosis, control inflammatory response, and escape immune response (52). The Giant seaperch iridovirus (GSIV) ST kinase can activate caspase-9 and caspase-3 and induce the apoptosis (53). SGIV can induce typical apoptosis and increase the activities of caspase-9 and caspase-3 in FHM cells (2, 3, 5, 8, 24). Both grouper miR-146a and miR-122 can reduce the SGIV-induced cell apoptosis and the activation of caspase-9 and caspase-3 (8, 23). To explore the roles of miR-124 in SGIV-induced apoptosis, apoptosis rates and the activation of caspase-9/3 were analyzed. A significant decrease of the SGIV-induced apoptosis was observed in the cells with overexpression miR-124; the protein levels of caspase-3 and cleaved caspase-3 were reduced; and the activity of caspase-9/3 was significantly inhibited in miR-124-overexpressing cells. It has been demonstrated that p38 MAPK mediates the activity of caspase-8/9/3 in human umbilical vein endothelial cells when apoptosis is induced by PEDF; JNK was independently involved in the upregulation of caspase-3 activity; and p38 MAPK was known to act as an upstream regulator of caspase-3 in apoptotic endothelial cells (54–56). Since JNK and p38 MAPK can active caspase-9/3 and induce the cell apoptosis, and miR-124 here can deregulate the expression of JNK and p38 MAPK by targeting 3′-UTR, we speculate that miR-124 might regulate the cell apoptosis and the activities of caspase-9 and caspase-3 *via* JNK and p38 MAPK.

In conclusion, in low vertebrates *E. coioides*, the roles of miR-124 in SGIV infection and replication, and innate immune response were analyzed in this study. The expression level of

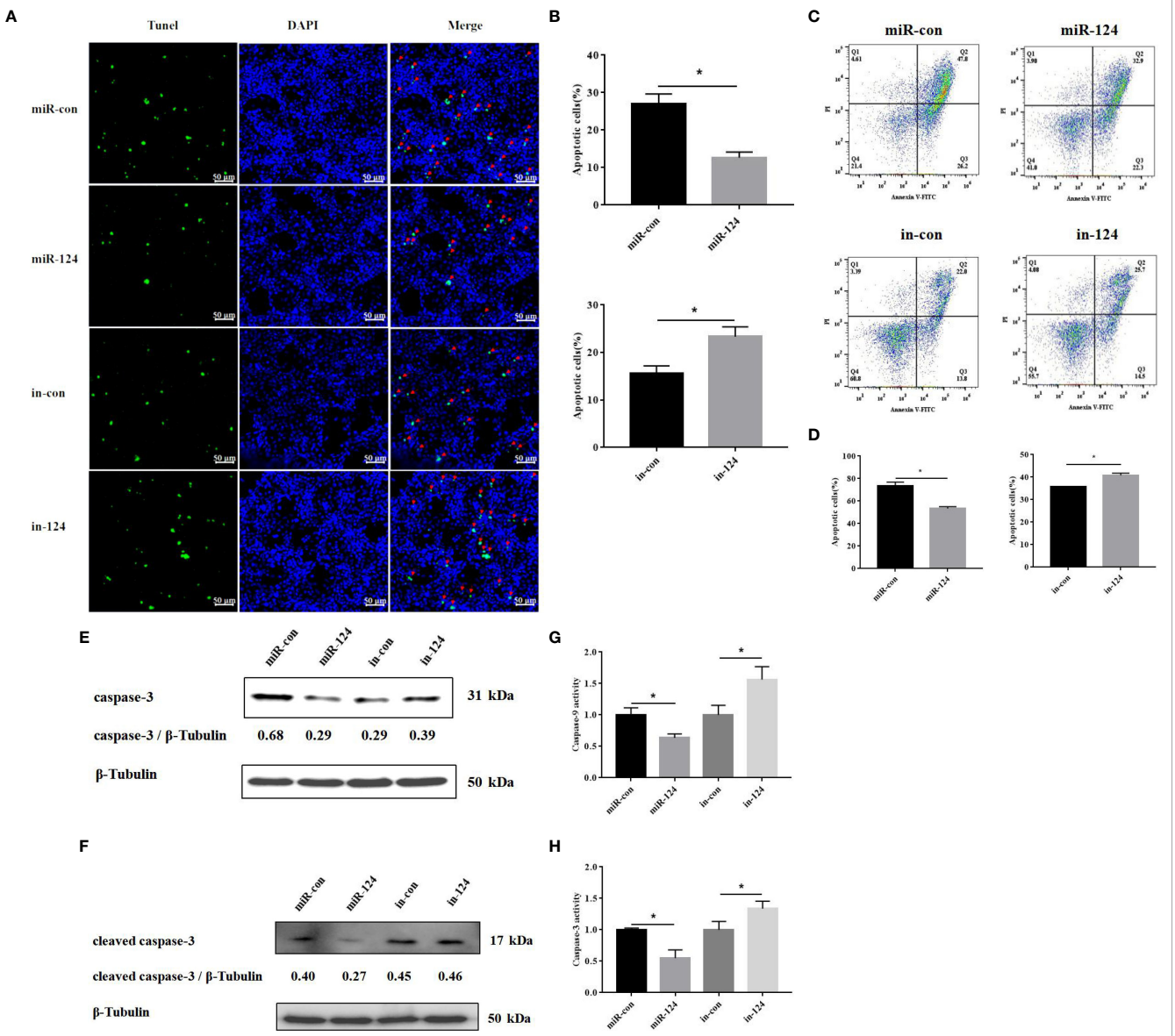

FIGURE 8 | The effect of miR-124 on apoptosis of fathead minnow (FHM) cells. **(A)** Detection of apoptosis by TUNEL assay. The green fluorescent markers indicate fractured DNA fragments, and the blue fluorescent markers represent the nucleus. The red arrows indicate the fractured DNA fragments. Scale bars represent 50 μm. **(B)** Comparison of apoptosis rates of FHM cells in different groups. **(C)** Singapore grouper iridovirus (SGIV)-induced apoptotic bodies in FHM cells. Q1: PI+, Annexin−. Q2: PI+, Annexin+. Q3: PI−, Annexin+. Q4: PI−, Annexin−. Q2 and Q3 represent the percentage of late apoptosis and early apoptosis, respectively. **(D)** The graph is based on the average of three parallel experimental data. **(E, F)** The level of caspase-3 and cleaved caspase-3 proteins was detected by Western blotting, the band intensity was calculated, and ratios of target protein/β-tubulin were assessed by ImageJ software. **(G, H)** The activity of caspase-9 and caspase-3 after SGIV infection. Control mimics, miR-con; miR-124 mimics, miR-124; control inhibitors, in-con; miR-124 inhibitors, in-124. All data are presented as mean ± SD, N = 3. Compared with the control group, significant difference of experimental group is indicated with *($P < 0.05$).

miR-124 was significantly upregulated during SGIV infection. Overexpression of miR-124 cannot affect SGIV entry but significantly increased SGIV-induced CPE, viral replication, and the expressions of SGIV key genes. MiR-124 can inhibit the activities of NF-κB and AP-1, the expressions of inflammatory factors (TNF-α, IL-6, IL-8, and IL-1β), and the SGIV-induced apoptosis by targeting 3′ UTR of JNK3 and p38α MAPK. This study demonstrated that miR-124 was not related to SGIV entry but promotes SGIV replication and negatively regulates the innate immunity, which provides new insights into understanding the roles of fish miRNAs in virus pathogenesis.

DATA AVAILABILITY STATEMENT

The datasets presented in this study can be found in online repositories. The names of the repository/repositories and accession number(s) can be found in the article/supplementary material.

ETHICS STATEMENT

The animal study was reviewed and approved by South China Agricultural University. Written informed consent was obtained from the owners for the participation of their animals in this study.

AUTHOR CONTRIBUTIONS

Q-WQ and H-YS conceived the experiments and reviewed the drafts of the manuscript. S-WW and L-QW contributed the materials/analysis tools. P-HL wrote the manuscript, conducted the experiment, and analyzed the data. All authors contributed to the article and approved the submitted version.

FUNDING

This work was funded by National Natural Science Foundation of China (U20A20102, 31930115), Innovation Group Project of Southern Marine Science and Engineering Guangdong Laboratory (Zhuhai) (311021006), the China Agriculture Research System of MOF and MARA (CARS-47-G16), Marine Fisheries Bureau Key funds and marine projects (GDME-2018C002), the National Key R&D Program of China (2018YFD0900501 and 2018YFC0311302).

REFERENCES

1. Qin QW, Lam TJ, Sin YM, Shen H, Chang SF, Ngoh GH, et al. Electron Microscopic Observations of a Marine Fish Iridovirus Isolated From Brown-Spotted Grouper, *Epinephelus Tauvina*. *J Virol Methods* (2001) 98(1):17–24. doi: 10.1016/S0166-0934(01)00350-0
2. Su YL, Chen JP, Mo ZQ, Zheng JY, Lv SY, Li PH, et al. A Novel MKK Gene (EcMKK6) in *Epinephelus Coioides*: Identification, Characterization and Its Response to *Vibrio Alginolyticus* and SGIV Infection. *Fish Shellfish Immunol* (2019) 92:500–7. doi: 10.1016/j.fsi.2019.06.043
3. Li PH, Liang YL, Su YL, Jiang YF, Chen B, Chen SY, et al. Molecular Characterization and Function Analysis of *Epinephelus Coioides* Hsp22 Response to SGIV and *Vribro Alginolyticus* Infection. *Fish Shellfish Immunol* (2020) 97:125–34. doi: 10.1016/j.fsi.2019.11.069
4. Li C, Yu YP, Zhang X, Wei JG, Qin QW. Grouper Atg12 Negatively Regulates the Antiviral Immune Response Against Singapore Grouper Iridovirus (SGIV) Infection. *Fish Shellfish Immunol* (2019) 93:702–10. doi: 10.1016/j.fsi.2019.08.037
5. Guo M, Wei JG, Zhou YC, Qin QW. C-Jun N-Terminal Kinases 3 (JNK3) From Orange-Spotted Grouper, *Epinephelus Coioides*, Inhibiting the Replication of Singapore Grouper Iridovirus (SGIV) and SGIV-Induced Apoptosis. *Dev Comp Immunol* (2016) 65:169–81. doi: 10.1016/j.dci.2016.06.009
6. Xia LQ, Liang HY, Huang YH, Ou-Yang Z, Qin QW. Identification and Characterization of Singapore Grouper Iridovirus (SGIV) ORF162L, an Immediate-Early Gene Involved in Cell Growth Control and Viral Replication. *Virus Res* (2009) 147(1):30–9. doi: 10.1016/j.virusres.2009.09.015
7. Guo CY, Cui HC, Ni SW, Yan Y, Qin QW. Comprehensive Identification and Profiling of Host miRNAs in Response to Singapore Grouper Iridovirus (SGIV) Infection in Grouper (*Epinephelus Coioides*). *Dev Comp Immunol* (2015) 52(2):226–35. doi: 10.1016/j.dci.2015.05.014
8. Sun HY, Su YL, Li PH, He JY, Qin QW. The Roles of *Epinephelus Coioides* miR-122 in SGIV Infection and Replication. *Mar Biotechnol* (2021) 23:294–307. doi: 10.1007/s10126-021-10023-w
9. Fabian MR, Sonenberg N, Filipowicz W. Regulation of mRNA Translation and Stability by microRNAs. *Annu Rev Biochem* (2010) 79:351–79. doi: 10.1146/annurev-biochem-060308-103103
10. Lee RC, Feinbaum RL, Ambros V. The *C. Elegans* Heterochronic Gene Lin-4 Encodes Small RNAs With Antisense Complementarity to Lin-14. *Cell* (1993) 75(5):843–54. doi: 10.1016/0092-8674(93)90529-y
11. Wightman B, Ha I, Ruvkun G. Posttranscriptional Regulation of the Heterochronic Gene Lin-14 by Lin-4 Mediates Temporal Pattern Formation in *C. Elegans*. *Cell* (1993) 75(5):855–62. doi: 10.1016/0092-8674(93)90530-4
12. Reinhart BJ, Slack FJ, Basson M, Pasquinelli AE, Bettinger JC, Rougvie AE, et al. The 21-Nucleotide Let-7 RNA Regulates Developmental Timing in *Caenorhabditis Elegans*. *Nature* (2000) 403(6772):901–6. doi: 10.1038/35002607
13. Lagos-Quintana M, Rauhut R, Lendeckel W, Tuschl T. Identification of Novel Genes Coding for Small Expressed RNAs. *Science* (2001) 294:853–8. doi: 10.1126/science.1064921
14. Lau NC, Lim LP, Weinstein EG, Bartel DP. An Abundant Class of Tiny RNAs With Probable Regulatory Roles in *Caenorhabditis Elegans*. *Science* (2001) 294:858–62. doi: 10.1126/science.1065062
15. Lee RC, Ambros V. An Extensive Class of Small RNAs in *Caenorhabditis Elegans*. *Science* (2001) 294:862–4. doi: 10.1126/science.1065329
16. Zhang C, Tu JG, Zhang YA. MicroRNA Regulation of Viral Replication in Teleost Fish: A Review. *Rev Aquacult* (2021) 13:1367–78. doi: 10.1111/raq.12526
17. Zhang C, Feng S, Zhang W, Chen N, Hegazy AM, Chen W, et al. MicroRNA miR-214 Inhibits Snakehead Vesiculovirus Replication by Promoting IFN-A Expression *via* Targeting Host Adenosine 5'-Monophosphate-Activated Protein Kinase. *Front Immunol* (2017) 8:1775. doi: 10.3389/fimmu.2017.01775
18. Zhang B, Zhou Z, Sun L. pol-miR-731, a Teleost miRNA Upregulated by Megalocytivirus, Negatively Regulates Virus-Induced Type I Interferon Response, Apoptosis, and Cell Cycle Arrest. *Sci Rep* (2016) 6:28354. doi: 10.1038/srep28354
19. Lang Q, Ling C. MiR-124 Suppresses Cell Proliferation in Hepatocellular Carcinoma by Targeting PIK3CA. *Biochem Biophys Res Commun* (2012) 426(2):247–52. doi: 10.1016/j.bbrc.2012.08.075
20. Cheng LC, Pastrana E, Tavazoie M, Doetsch F. miR-124 Regulates Adult Neurogenesis in the Subventricular Zone Stem Cell Niche. *Nat Neurosci* (2009) 12(4):399–408. doi: 10.1038/nn.2294
21. Makeyev EV, Zhang JW, Carrasco MA, Maniatis T. The MicroRNA miR-124 Promotes Neuronal Differentiation by Triggering Brain-Specific Alternative Pre-mRNA Splicing. *J Mol Cell* (2007) 27(3):435–48. doi: 10.1016/j.molcel.2007.07.015
22. Mccaskill JL, Ressel S, Alber A, Redford J, Power UF, Schwarze J, et al. Broad-Spectrum Inhibition of Respiratory Virus Infection by MicroRNA Mimics Targeting P38 MAPK Signaling. *Mol Ther Nucleic Acids* (2017) 7:256–66. doi: 10.1016/j.omtn.2017.03.008
23. Ni S, Yan Y, Cui H, Yu Y, Qin Q. Fish miR-146a Promotes Singapore Grouper Iridovirus Infection by Regulating Cell Apoptosis and NF-kB Activation. *J Gen Virol* (2017) 98:1489. doi: 10.1099/jgv.0.000811
24. Huang XH, Huang YH, Ouyang ZL, Xu LX, Yang Y, Cui HC, et al. Singapore Grouper Iridovirus, a Large DNA Virus, Induces Nonapoptotic Cell Death by a Cell Type Dependent Fashion and Evokes ERK Signaling. *Apoptosis* (2011) 16:831–45. doi: 10.1007/s10495-011-0616-y
25. Guo L, Sun B, Sang F, Wang W, Lu Z. Haplotype Distribution and Evolutionary Pattern of miR-17 and miR-124 Families Based on Population Analysis. *PloS One* (2009) 4(11):e7944. doi: 10.1371/journal.pone.0007944

26. Weng R, Cohen SM. Drosophila miR-124 Regulates Neuroblast Proliferation Through Its Target Anachronism. *Development* (2012) 139:1427–34. doi: 10.1371/journal.pone.0007944
27. Aksoy-Aksel A, Zampa F, Schratt G. MicroRNAs and Synaptic Plasticity-a Mutual Relationship. *Philos Trans R Soc Lond Ser B Biol Sci* (2014) 369(1652): 20130515. doi: 10.1098/rstb.2013.0515
28. Follert P, Cremer H, Beclin C. MicroRNAs in Brain Development and Function: A Matter of Flexibility and Stability. *Front Mol Neurosci* (2014) 7:5. doi: 10.3389/fnmol.2014.00005
29. Krichevsky AM, King KS, Donahue CP, Khrapko K, Kosik KS. A microRNA Array Reveals Extensive Regulation of microRNAs During Brain Development. *RNA* (2003) 9:1274–81. doi: 10.1261/rna.5980303
30. Zhang X, Lei B, Yuan Y, Zhang L, Qi H. Brain Control of Humoral Immune Responses Amenable to Behavioural Modulation. *Nature* (2020) 581:204–8. doi: 10.1038/s41586-020-2235-7
31. Wu WL, Dai CJ, Duan XW, Wang CF, Lin XS, Ke JY, et al. MiRNAs Induced by White Spot Syndrome Virus Involve in Immunity Pathways in Shrimp Litopenaeus Vannamei. *Fish Shellfish Immunol* (2019) 93:743–51. doi: 10.1016/j.fsi.2019.08.009
32. Trobaugh DW, Klimstra WB. MicroRNA Regulation of RNA Virus Replication and Pathogenesis. *Trends Mol Med* (2017) 23:80–93. doi: 10.1016/j.molmed.2016.11.003
33. Mehinto AC, Martyniuk CJ, Spade DJ, Denslow ND. Applications for Next-Generation Sequencing in Fish Ecotoxicogenomics. *Front Genet* (2012) 3:62. doi: 10.3389/fgene.2012.00062
34. Rajashree NP, Yogesh AK. Uncovering the Roles of miR-214 in Hepatitis E Virus Replication. *J Mol Biol* (2020) 432(19):5322–42. doi: 10.1016/j.jmb.2020.07.015
35. Qi LL, Wang KL, Chen HT, Liu XS, Lv JL, Hou ST, et al. Host microRNA miR-1307 Suppresses Foot-and-Mouth Disease Virus Replication by Promoting VP3 Degradation and Enhancing Innate Immune Response. *J Virol* (2019) 535:162–70. doi: 10.1016/j.virol.2019.07.009
36. Cargnello M, Roux PP. Activation and Function of the MAPKs and Their Substrates, the MAPK-Activated Protein Kinases. *Microbiol Mol Biol Rev* (2011) 75(1):50–83. doi: 10.1128/MMBR.00031-10
37. Du Y, Taylor CG, Aukema HM, Zahradka P. Regulation of Docosahexaenoic Acid-Induced Apoptosis of Confluent Endothelial Cells: Contributions of Mapks and Caspases. *BBA-Mol Cell Biol L* (2021) 1866(5):158902. doi: 10.1016/j.bbalip.2021.158902
38. Kyriakis JM, Avruch J. Mammalian Mitogen-Activated Protein Kinase Signal Transduction Pathways Activated by Stress and Inflammation. *Physiol Rev* (2001) 81:807–69. doi: 10.1007/s004240100541
39. Raingeaud J, Gupta S, Rogers JS, Dickens M, Han J, Ulevitch RJ, et al. Pro-Inflammatory Cytokines and Environmental Stress Cause P38 Mitogen-Activated Protein Kinase Activation by Dual Phosphorylation on Tyrosine and Threonine. *J Biol Chem* (1995) 270:7420–6. doi: 10.1074/jbc.270.13.7420
40. Clarke P, Meintzer SM, Wang Y, Moffitt LA, Richardson-Burns SM, Johnson GL, et al. JNK Regulates the Release of Proapoptotic Mitochondrial Factors in Reovirus-Infected Cells. *J Virol* (2004) 78(23):13132–8. doi: 10.1128/JVI.78.23.13132-13138.2004
41. Hirasawa K, Kim A, Han HS, Han J, Jun HS, Yoon JW. Effect of P38 Mitogen-Activated Protein Kinase on the Replication of Encephalomyocarditis Virus. *J Virol* (2003) 77(10):5649. doi: 10.1128/JVI.77.10.5649-5656.2003
42. Holloway G, Coulson BS. Rotavirus Activates JNK and P38 Signaling Pathways in Intestinal Cells, Leading to AP-1-Driven Transcriptional Responses and Enhanced Virus Replication. *J Virol* (2006) 80:10624–33. doi: 10.1128/JVI.00390-06
43. Lawson SK, Dobrikova EY, Shveygert M, Gromeier M. P38α Mitogen-Activated Protein Kinase Depletion and Repression of Signal Transduction to Translation Machinery by miR-124 and -128 in Neurons. *Cell Mol Biol* (2013) 33(1):127–35. doi: 10.1128/MCB.00695-12
44. Xu Y, Lai Y, Weng H, Tan L, Ye Y. Mir-124 Sensitizes Cisplatin-Induced Cytotoxicity Against Cd133+ Hepatocellular Carcinoma Cells by Targeting Sirt1/Ros/Jnk Pathway. *Aging* (2019) 11(9):2551–64. doi: 10.18632/aging.101876
45. Huang X, Huang Y, Ou-Yang Z, Cai J, Qin QW. Roles of Stress-Activated Protein Kinases in the Replication of Singapore Grouper Iridovirus and Regulation of the Inflammatory Responses in Grouper Cells. *J Gen Virol* (2011) 92(6):1292. doi: 10.1099/vir.0.029173-0
46. Pasporakis M. Regulation of Tissue Homeostasis by NF-kB Signalling: Implications for Inflammatory Disease. *Nat Rev Immunol* (2009) 9(11):778–88. doi: 10.1038/nri2655
47. Bonizzi G, Karin M. The Two NF-Kb Activation Pathways and Their Role in Innate and Adaptive Immunity. *Trends Immunol* (2004) 25:280–8. doi: 10.1016/j.it.2004.03.008
48. Ghosh S, Hayden MS. New Regulators of NF-kappaB in Inflammation. *J Immunol* (2008) 8:837–48. doi: 10.1038/nri2423
49. Yue J, Chang S, Xiao Z, Qi YJ. The Protective Effect of Puerarin on Angiotensin II-Induced Aortic Aneurysm Formation by the Inhibition of NADPH Oxidase Activation and Oxidative Stress-Triggered AP-1 Signaling Pathways. *Oncol Lett* (2018) 16:3327–32. doi: 10.3892/ol.2018.9021
50. Merviel P, Carbillon L, Challier JC, Rabreau M, Beaufils M, Uzan S. Pathophysiology of Preeclampsia: Links With Implantation Disorders. *Euro J Obstet Gynecol* (2004) 115:134–47. doi: 10.1016/j.ejogrb.2003.12.030
51. Jonsson Y, Ruber M, Matthienssen L, Berg G, Nieminen K, Sharma S, et al. Cytokine Mapping of Sera From Women With Preeclampsia and Normal Pregnancies. *J Reprod Immunol* (2006) 70:83–91. doi: 10.1016/j.jri.2005.10.007
52. Galluzzi L, Brenner C, Morselli E, Touat Z, Kroemer G. Viral Control of Mitochondrial Apoptosis. *PloS Pathog* (2008) 4:1000018. doi: 10.1371/journal.ppat.1000018
53. Reshi L, Wu HC, Wu JL, Wang HV, Hong JR. GSIV Serine/Threonine Kinase can Induce Apoptotic Cell Death *via* P53 and Pro-Apoptotic Gene Bax Upregulation in Fish Cells. *Apoptosis* (2016) 21:443–58. doi: 10.1007/s10495-016-1219-4
54. Chen L, Zhang SS, Barnstable CJ, Tombran-Tink J. PEDF Induces Apoptosis in Human Endothelial Cells by Activating P38 MAP Kinase Dependent Cleavage of Multiple Caspases Biochem. *Biophys Res Commun* (2006) 348:1288–95. doi: 10.1016/j.bbrc.2006.07.188
55. Chaudhury H, Zakkar M, Boyle J, Cuhlmann S, van der Heiden K, Luong le A, et al. C-Jun N-Terminal Kinase Primes Endothelial Cells at Atheroprone Sites for Apoptosis. *Arterioscler Thromb Vasc Biol* (2010) 30:546–53. doi: 10.1161/ATVBAHA.109.201368
56. Jiang DJ, Jia SJ, Dai Z, Li YJ. Asymmetric Dimethylarginine Induces Apoptosis *via* P38 MAPK/caspase-3-Dependent Signaling Pathway in Endothelial Cells. *J Mol Cell Cardiol* (2006) 40:529–39. doi: 10.1016/j.yjmcc.2006.01.021

Conflict of Interest: The authors declare that the research was conducted in the absence of any commercial or financial relationships that could be construed as a potential conflict of interest.

Publisher's Note: All claims expressed in this article are solely those of the authors and do not necessarily represent those of their affiliated organizations, or those of the publisher, the editors and the reviewers. Any product that may be evaluated in this article, or claim that may be made by its manufacturer, is not guaranteed or endorsed by the publisher.

frontiers in Immunology

ORIGINAL RESEARCH
published: 09 December 2021
doi: 10.3389/fimmu.2021.734520

MicroRNA-181b-2 and MicroRNA-21-1 Negatively Regulate NF-κB and IRF3-Mediated Innate Immune Responses *via* Targeting TRIF in Teleost

Yuena Sun[1,2], *Lei Zhang*[1], *Ling Hong*[3*], *Weiwei Zheng*[1], *Junxia Cui*[1], *Xuezhu Liu*[4] *and Tianjun Xu*[1,2,5,6*]

[1] Laboratory of Fish Molecular Immunology, College of Fisheries and Life Science, Shanghai Ocean University, Shanghai, China, [2] Laboratory of Marine Biology and Biotechnology, Qingdao National Laboratory for Marine Science and Technology, Qingdao, China, [3] School of Medicine, Tongji University, Shanghai, China, [4] Laboratory of Fish Biogenetics & Immune Evolution, College of Marine Science, Zhejiang Ocean University, Zhoushan, China, [5] Key Laboratory of Exploration and Utilization of Aquatic Genetic Resources (Shanghai Ocean University), Ministry of Education, Shanghai, China, [6] National Pathogen Collection Center for Aquatic Animals, Shanghai Ocean University, Shanghai, China

Upon recognition of bacterial or viral components by Toll-like receptors (TLRs), cells could be activated to induce a series of reactions to produce inflammatory cytokines, type I interferon (IFN), and IFN stimulating genes (ISG). MicroRNAs (miRNAs) are an important regulatory molecules that are widely involved in the regulatory networks of mammalian inflammation and immune responses; however, in lower vertebrates, the regulatory network of miRNA-mediated immune responses is poorly understood. Here, we report two miRNAs form *Miichthys miiuy*, namely, miR-181b-2 and miR-21-1, that play a negative role in host antiviral and antibacterial immunity. We found that miR-181b-2 and miR-21-1 are abundantly expressed in gram-negative bacteria, as well as RNA rhabdovirus infection. Inducible miR-181b-2 and miR-21-1 suppress the production of inflammatory cytokines and type I IFN by targeting TRIF, thereby avoiding excessive inflammation. We further revealed that miR-181b-2 and miR-21-1 modulate antibacterial and antiviral immunity through the TRIF-mediated NF-κB and IRF3 signaling pathways. The overall results indicate that miR-181b-2 and miR-21-1 act as negative feedback regulators and participate in host antibacterial and antiviral immune responses; this finding could provide information for a deeper understanding of the resistance of lower vertebrates to the invasion of pathogens and to avoidance of excessive immunity.

Keywords: microRNA, TRIF, gene regulation, immune response, innate immune

OPEN ACCESS

Edited by:
Maria Del Mar Ortega-Villaizan, Miguel Hernández University of Elche, Spain

Reviewed by:
Ivan Nombela, Charité University Medicine Berlin, Germany
Patricia Diaz-Rosales, Centro de Investigación en Sanidad Animal (CISA), Spain

****Correspondence:***
Ling Hong
hongling789@163.com
Tianjun Xu
tianjunxu@163.com

Specialty section:
This article was submitted to Comparative Immunology, a section of the journal Frontiers in Immunology

Received: *01 July 2021*
Accepted: *22 November 2021*
Published: *09 December 2021*

Citation:
Sun Y, Zhang L, Hong L, Zheng W, Cui J, Liu X and Xu T (2021) MicroRNA-181b-2 and MicroRNA-21-1 Negatively Regulate NF-κB and IRF3-Mediated Innate Immune Responses via Targeting TRIF in Teleost. Front. Immunol. 12:734520. doi: 10.3389/fimmu.2021.734520

INTRODUCTION

Toll-like receptors (TLRs) play an important role in the activation of innate immunity by recognizing specific patterns of microbial components; the related signaling pathways consist of the MyD88-dependent pathway and the MyD88-independent pathway. In the MyD88-dependent pathway, MyD88 binds to TLRs through their C-terminal TIR domain as a connector molecule, after which its N-terminal dead domain activates the downstream IRAKs family. Following a series of transductions, it transmits TLRs-mediated signals to the cells, which ultimately leads to the activation and translocation of nuclear factor κB (NF-κB) (1, 2). Some studies have found that lipopolysaccharide (LPS) can activate TLR4 and NF-κB (3) in MyD88 knockout mice. Therefore, a MyD88-independent pathway may be involved in the process of TLR4 signal transduction. Subsequent studies found that LPS stimulation could activate interferon (INF) regulatory factor 3 (IRF3) in MyD88 knockout cells through the TLR4 pathway and promote IFN-induced gene expression. DsRNA could also activate NF-κB and IRF3 *via* the TLR3 pathway, which may follow the same MyD88-independent pathway as TLR4 for signal transduction (4). How TLR4 mediates the expression of type I IFN was previously unknown until TIR-domain-containing adapter-inducing interferon-β (TRIF) was discovered. According to the results of studies on TRIF-deficient mice induced by gene targeting or *N*-ethyl-*N*-nitrosourea mutagenesis, TRIF is essential for TLR4-mediated IFN expression (5). In fact, researchers had previously identified a TRIF in the TLR3 pathway by using yeast two-hybrid technology and named it TICAM-1; TICAM-1 is a TLR that contains the TIR domain and induces INF-β (interleukin 1) linker molecule (6, 7). Other studies have proven that no activation of NF-κB or up-regulation of inflammation-related genes occurs in TRIF and MyD88-deficient MBrC cells after LPS stimulation (8). Such studies confirm that TRIF plays an important role in the TLR4-mediated MyD88-independent pathway.

The signaling pathway connected by the TRIF is called the TRIF-dependent pathway (9). In mammals, the TRIF gene is composed of an N-terminal region, a TIR domain, a C-terminal region, an N-terminal region, and a tumor necrosis factor receptor-related factor (TRAF) family protein binding activator TBK1 (TANK-binding kinase-1), which mainly activates IFNs (10, 11). The C-terminal region of TRIF recruits receptor protein 1 and induces NF-κB activation (12). The TRIF gene has been cloned and identified in zebrafish, *Takifugu rubripes*, and *Ctenopharyngodon idella* (13–15). Studies have also revealed that the TRIF gene is involved in the antiviral immune response (15, 16). The TLR3 and TLR22 genes could recognize double-stranded RNA viruses and stimulate MBrC to trigger the transduction of the TRIF gene signaling pathway and activate MAPK, NF-κB, and IRF3/7, eventually inducing the production and release of inflammatory cytokines and IFN (17, 18). At present, an increasing body of evidence indicates that TRIF and its signaling pathways play an important role in the immune response and disease regulation. For example, researchers have found that the LPS-induced TLR4/TRIF pathway can activate the NLRP3 gene and that NLRP3 can activate caspase-1, which prompts cells to secrete IL-18 to the extracellular, thereby up-regulating Fasl and TNF-α and causing liver damage (19). Other studies have confirmed that damaged tissues can recruit myeloid cells for tissue repair through TLR3/TRIF-mediated cytokine secretion (20). Given the role of TRIF in disease, this protein has become a research focus in attempts to provide new insights and ideas for understanding the etiology of various diseases. The important role of TRIF in the immune response highlights the need to study the regulation and function of this protein. TRIF can be negatively regulated to suppress an organism's immune response, prevent the organism from producing an excessive immune response, and maintain the immune system's homeostasis. For example, studies have reported that IRF3 can negatively regulate TRIF-mediated NF-κB signaling pathways (21). Another study found that ADAM15 acts as a negative regulator of TRIF-mediated NF-κB and IFN-β reporter gene activity and acts as an anti-inflammatory molecule by disrupting TRIF-mediated TLR signaling (22). The present article focuses on the roles of miR-181b-2 and miR-21-1 in miiuy croaker (*Miichthys miiuy*) in regulating TRIF and the immune response.

MicroRNAs (miRNAs) are a type of endogenous single-stranded small-molecule RNAs with a length of approximately 21-23 bases. Single-stranded RNA precursors with a hairpin structure of approximately 70-90 bases pass through Dicer. It is produced after enzyme processing, which is different from siRNA (double-stranded) but closely related to siRNA. MiRNAs present a variety of essential regulatory functions in cells, such as cell proliferation, differentiation, and apoptosis (23, 24). The complex regulatory networks connected to miRNAs can either regulate the expression of multiple genes through one miRNA or finely regulate the expression of a gene through the combination of several miRNAs. For example, miR-8159-5p and miR-217-5p can target and regulate TLR1 expression in miiuy croaker (25). In addition, miR-3570 and miR-214 may negatively regulate the expression of the MyD88 gene in mackerel, thereby inhibiting the activation of NF-κB and the production of inflammatory cytokines (26, 27). Researchers speculate that one-third of all human genes are regulated by miRNAs. Mature miRNAs are not only conserved in various gene positions in different species but also show high homology in their sequences (28–30). Recent studies have found that miRNAs in some species exhibit transboundary regulation, which presents new ideas for miRNA research. For example, studies have found that miRNAs from *Cuscuta campestris* can target host mRNAs across species to regulate their gene expression, thereby indicating that these miRNAs could function as pathogenic factors and play a role in the process of *C. campestris* parasitism (31). In addition, plant miR-159 can inhibit the development of breast cancer, exogenous plant miR-168a can specifically target mammalian LDLRAP1, and the atypical microRNA2911 of honeysuckle directly targets influenza a virus (32–34). These studies demonstrated that the transboundary regulation of microRNAs. MiRNAs can be partially paired with the 3'untranslated region (UTR) of their target gene to regulate the expression of the target gene at the post-transcriptional level. Although the number of miRNAs

involved in regulating the immune response in fish is increasing, they are still rare when compared with the miRNAs of two mammals. In this study, we found that miR-21-1 and miR-181b-2 can inhibit the activation of NF-κB, IRF3, and IFN by targeting TRIF, thereby suppressing the expression of inflammatory cytokines. Double luciferase reporter experiment confirmed this conclusion for the first time, that miR-21-1 and miR-181b-2 can target TRIF-3'UTR and inhibit its expression. We then demonstrated that miR-21-1 and miR-181b-2 can inhibit TRIF mRNA expression *via* qRT-PCR. Our findings were confirmed by Western blotting. MiR-21-1 and miR-181b-2 can inhibit the activation of NF-κB, IRF3, IFNα, and other reporter genes by targeting TRIF, which has been verified in EPC cells. Thus, studying its evolutionary history can help improve the understand of its mechanism and function.

MATERIALS AND METHODS

Sample and Challenge

Miiuy croaker (~50 g) was obtained from Zhoushan Fisheries Research Institute, Zhejiang Province, China. Fish was acclimated in aerated seawater tanks at 25°C for six weeks before experiments. The challenge experiments were conducted as follows. Briefly, fish was respectively challenged with 100 μl of *V. anguillarum* (1.5×10^8 CFU/ml), SCRV at a multiplicity of infection (MOI) of 5 or poly(I:C) (*In vivo*Gen, 1mg/ml) through intraperitoneal. Afterward, fishes were respectively sacrificed at different time points and the liver and spleen tissues were collected for RNA extraction. All animal experimental procedures were performed in accordance with the National Institutes of Health's Guide for the Care and Use of Laboratory Animals, and the experimental protocols were approved by the Research Ethics Committee of Shanghai Ocean University (No. SHOU-DW-2018-047.

Cell Culture and LPS/Poly(I:C) Stimulate

Miiuy croaker brain cell line (MBrC) were cultured in L-15 medium (HyClone) supplemented with 10% fetal bovine serum (FBS; Gibco), 100 U/ml penicillin, and 100μg/ml streptomycin at 26°C. MBrC line were prepared from the brain tissue of the miiuy croaker, and the isolation process is the same as previously reported (35). HEK293 cells were cultured in DMEM high glucose medium (HyClone) containing 10%FBS, 100 U/ml penicillin, and 100 μg/ml streptomycin at 37°C in 5% CO_2. Epithelioma papulosum cyprini (EPC) cells were cultured in medium 199 (Invitrogen) supplemented with 10% FBS, 100 U/ml penicillin, and 100 mg/ml streptomycin at 28°C in 5% CO_2. 24 hours after miR-21-1 and miR-181b-2 were transfected into MBrC cells, LPS/poly(I: C) was added to the cell culture medium by changing the medium. After 12 hours, cells were collected and total RNA was extracted and stored in -80°C standby.

Prediction of MiR-21-1 and MiR-181b-2 Targeting Sites and Plasmid Construction

The miR-21-1 and miR-181b-2 targets were predicted using Targetscan (36), miRanda (37), and miRInspector (38) algorithms. To construct the TRIF-3'UTR reporter plasmid, miiuy croaker TRIF-3'UTR sequence was amplified using PCR and cloned into pmirGLO luciferase reporter plasmid, and the TRIF-3'UTR-MT mutant plasmid was constructed by using Mut Express II Rapid Mutagenesis Kit v2 (Vazyme Biotech). In order to construct TRIF expression plasmid, full-length coding sequence (CDS) and 3'UTR of TRIF gene in miiuy croaker were amplified by PCR with specific primers and inserted into pcDNA3.1 vector. The TAK1 3'UTR sequence was inserted into the mVenus-C1 vector to construct the green fluorescent protein (GFP) report plasmid. The pre-miR-21-1 and pre-miR-181b-2 sequence was amplified by PCR with specific primers and cloned into pcDNA3.1 vector. All plasmids were extracted by endotoxin-free plasmid DNA Miniprep kit (Tiangen) and confirmed by Sanger sequencing before using plasmids. The expression of protein was confirmed by Western blot analysis of full-length plasmid.

Transfection and Virus Infection

Cells were seeded into 24-well plates and incubated overnight. Subsequently, MBrC cells were transfected with miR-21-1 or miR-181b-2 by using Lipofectamine 3000 (Invitrogen) according to the manufacturer's protocols. 24 h after transfection, the MBrC were washed, the cells were infected with SCRV, and incubated at different times as indicated. Total RNA was extracted for quantitative real-time PCR (qPCR) analysis.

MiRNA Mimic and Inhibitors

miR-21-1 or miR-181b-2 mimic (dsRNA oligonucleotides) and miR-21-1 or miR-181b-2 inhibitors (single stranded, chemically modified oligonucleotides), and control oligonucleotides were ordered from GenePharma (Shanghai, China). Sequences are as follows: miR-21-1 mimic, 5'-CAACAGCAGUCUGUAAGCUGGC-3'

(sense) and 5'-CAGCUUACAGACUGCUGUUGUU-3' (antisense); miR-181b-2 mimic, 5'-AACAUUCAUUGC UGUCGCUGGG-3'

(sense) and 5'-CAGCGACAGCAAUGAAUGUUUU-3' (antisense); negative control mimic, 5'-UUCUCCGAACGUGUCACGUTT-3' (sense) and 5'-ACGUGACACGUUCGGAGAATT-3' (antisense); miR-21-1 inhibitors, 5'-GCCAGCUUACAGACUGCUGUUG-3' (chemically modified by 29-Ome) and miR-181b-2 inhibitors, 5'-CCCAGCGACAGCAAUGAAUGUU-3' (chemically modified by 29-Ome) and negative control inhibitors, 5'-CAGUAC UUUUGUGUAGUACAA- 3'. MBrC, EPC or HEK293 cells were transfected with 50-100 nM of each oligonucleotide.

RNA Interference

The TRIF-specific small interfering RNA (si-TRIF) sequence were 5'-GAGACAACUACCUUGCUAGTT-3'(sense) and 5'-CUAG CAAGGUAGUUGUCUCTT-3' (antisense). The scrambled control RNA sequences were 5'-UUCUCCGAACGUGUCA CGUTT-3' (sense) and 5'-ACGUGACACGUUCGGAGAATT-3' (antisense). 100nM of each small interfering RNA (siRNA) were transfected into MBrC for up to 48 h and then stimulated with poly(I:C) or SCRV.

Real-Time Quantitative PCR

We have used Lipofectamine™ RNAiMAX (Invitrogen) transfect miR-21-1 and miR-181b-2 mimics or miR-21-1 and miR-181b-2 inhibitors, NC mimic and NC inhibitor as negative control into MBrC cells. 24 hours after transfection, the MBrC cells were stimulated with LPS or poly(I:C) or SCRV, and then cells were collected with Trizol. Total RNA was isolated with Trizol reagent (Invitrogen) by following the Ultrapure RNA kit (CWBIO) instructions, and it was reverse transcribed into cDNA according to the HiScript II Q RT SuperMix (Vazyme Biotech) instructions. Then we designed specific RT primers to detect the expression of TRIF, TNF-α, Mx1 and IFN-2 genes, and β-actin was used as endogenous control to normalize the expression. The triple fluorescence intensity of each gene experimental group and control group was measured by Super Real PreMix Plus (Tian Gen) reagent and 7500 qRT-PCR system (Applied Biosystems, USA). At the end of the determination, the results of curve analysis were analyzed to determine the specificity of the target. For each sample, all amplification reactions were performed in triplicate. The sequences of all mRNA primers are listed in **Supplementary Table 1**.

Dual-Luciferase Reporter Assays

The wild-type or mutant-type of the TRIF-3'UTR luciferase reporters were cotransfected with miR-21-1 or miR-181b-2 mimics or inhibitors, pre-miR-21-1 or pre-miR-181b-2 plasmid into EPC cells as well as HEK293 cells. Then TRIF-3'UTR luciferase activities were measured using the Dual-Luciferase Reporter Assay System (Promega). In order to exam TRIF functional regulation, EPC cells were cotransfected with NF-κB, IFN-2, IRF3, and IL-1β luciferase reporter gene, TRIF full-length expression plasmid, and phRL-TK Renilla luciferase plasmid, together with miR-21-1 or miR-181b-2, or pre-miR-21-1 and pre-miR-181b-2 for dual-luciferase reporter assays. Transfected 24 or 48 h later, cells were lysed for reporter activity testing using the Dual-Luciferase Reporter Assay System (Promega). All the results were obtained by three repeated independent experiments.

Western Blotting

The miR-21-1 and miR-181b-2 mimics or pre-miR-21-1 and pre-miR-181b-2 plasmids and the TRIF full-length expression plasmid were cotransfected into HEK293 cells using Lipofectamine 3000 (Invitrogen) transfection reagent. After 48 h of transfection, the medium was aspirated, HEK293 cells were washed three times with cold phosphate-buffered saline (PBS), and the cellular lysates were generated by using 1×SDS-PAGE (10%) loading buffer. The disrupted cells were heated in a 95°C metal bath for 5 minutes, and the same number of samples were taken for SDS-PAGE electrophoresis and the protein was transferred to a PVDF membrane (Millipore) by semidry blotting (Bio-Rad Trans Blot Turbo System). The membranes were blocked with 5% BSA. Protein was blotted with different Abs. The Ab against anti-Flag and anti-Tubulin mAb were diluted at 1:2000 (Sigma-Aldrich), and HRP-conjugated anti-mouse IgG (Abbkine) was diluted at 1:5000. The results were representative of three independent experiments. Proteins were detected by using BeyoECL Plus (Beyotime) and digital imaging was performed using a cold CCD camera.

Statistical Analysis

Data are expressed as the mean ± SD from at least three independent triplicated experiments. Student's t-test was used to evaluate the data. The relative gene expression data was acquired using the $2^{-\Delta\Delta CT}$ method and comparisons between groups were analyzed by one-way analysis of variance (ANOVA) followed by Duncan's multiple comparison tests (39). A value of $p< 0.05$ was considered significant.

RESULTS

LPS, *V. anguillarum* or Poly(I:C) Stimulation and SCRV Infection Significantly Upregulated miR-21-1 and miR-181b-2 Expression

Hundreds of miRNAs were expressed in poly(I:C)-treated miiuy croaker liver (40, 41) to investigate the host-encoded miRNAs that may potentially be involved in regulating TRIF and its signaling pathways in fish upon virus injection. A miRNA target prediction program was then used to predict candidate miRNAs that bind to TRIF by using the 3'-UTR of miiuy croaker TRIF (**Supplementary Table 2**). Combining our present findings with those reported in our previous work, we found that two miRNAs, namely, miR-21-1 and miR-181b-2, were upregulated under the stimulation of poly(I:C) (40, 41). We examined the expression levels of miR-21-1and miR-181b-2 in miiuy croaker brain and liver tissue samples after LPS (a gram-negative endotoxin) or *V. anguillarum* stimulation by using qRT-PCR. The results showed that the expression levels of miR-21-1 and miR-181b-2 peak after 12 h in brain samples stimulated by LPS (**Figure 1A**) and after 24 h in liver tissues stimulated by *V. anguillarum* (**Figure 1B**). We used poly(I:C) or SCRV as pathogens to stimulate miiuy croaker and MBrC cells to detect changes in miR-21-1 and miR-181b-2 expression levels. As shown in **Figures 1C, D**, the expression of miR-21-1 and miR-181b-2 peaked after 24 h in SCRV-injected MBrC cells. In addition, and the expression of miR-181b-2 peaked after 24 h while the expression of miR-21-1 peaked after 36 h in poly(I:C)-stimulated MBrC cells. Finally, we examined the expression of miR-21-1 in SCRV-stimulated spleen tissue. The results showed that the expression of miR-21-1 peaks after 36h while the expression of miR-181b-2 peaks after 24h (**Figure 1E**). These results indicate that miR-21-1 and miR-181b-2 are involved in the immune response induced by miiuy croaker-infected pathogens.

MiR-21-1 and MiR-181b-2 Negatively Regulate the Expression of Inflammatory Response

To investigate the role of miR-21-1 and miR-181b-2 in the regulation of bacterium-induced inflammation, we examined the effect of miR-21-1 and miR-181b-2 mimics or inhibitors

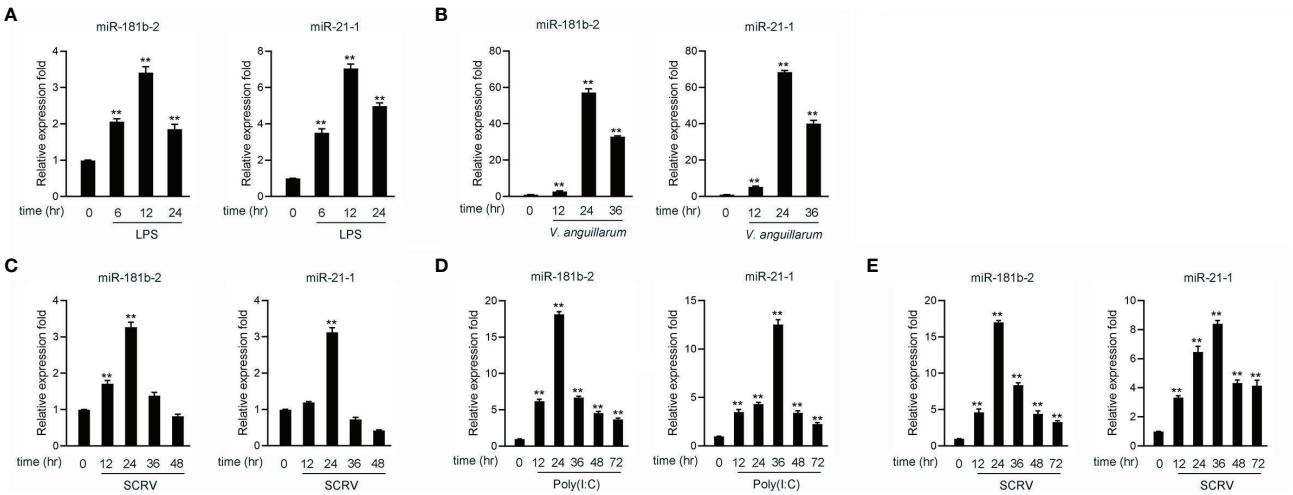

FIGURE 1 | The expression analysis of miR-21-1 and miR-181b-2 following bacterial infection and virus injection. **(A)** The expression of miR-21-1 and miR-181b-2 in LPS-stimulation MBrC cells. **(B)** The expression of miR-21-1 and miR-181b-2 in miiuy croaker liver samples after *V. anguillarum* infection. **(C)** The expression of miR-21-1 and miR-181b-2 in the MBrC cells of SCRV injection. **(D)** The expression of miR-21-1 and miR-181b-2 in miiuy croaker spleen after poly(I:C) stimulation. **(E)** The expression of miR-181b-2 and miR-21-1 in miiuy croaker spleen after SCRV injection. The expression of miR-181b-2 and miR-21-1 were measured by qRT-PCR and normalized to 5.8S rRNA. All data are presented as the means ± SE from three independent triplicate experiments. $^{**}p < 0.01$, versus the controls.

on the expression of inflammatory cytokines or antiviral effectors, such as IL-8, Mx1, and TNF-α, following LPS or poly (I:C) stimulation or SCRV injection. First, we examined the effects of synthetic miR-21-1 and miR-181b-2 mimics and inhibitors on the expression of the miRNAs. As shown in **Figures 2A, B**, after the transfection of synthetic miR-21-1 and miR-181b-2 mimics, the expression of miR-21-1 and miR-181b-2 significantly increased (**Figure 2A**). After the transfection of synthetic miR-21-1 and miR-181b-2 inhibitors, the expression of miR-21-1 and miR-181b-2 significantly decreased (**Figure 2B**). Next, we explored whether the overexpression of miR-21-1 and miR-181b-2 can affects the expression of inflammatory cytokines after LPS or poly(I:C) treatment, or SCRV injection. NC, the miR-21-1 and miR-181b-2 mimics, or miR-217 inhibitor were

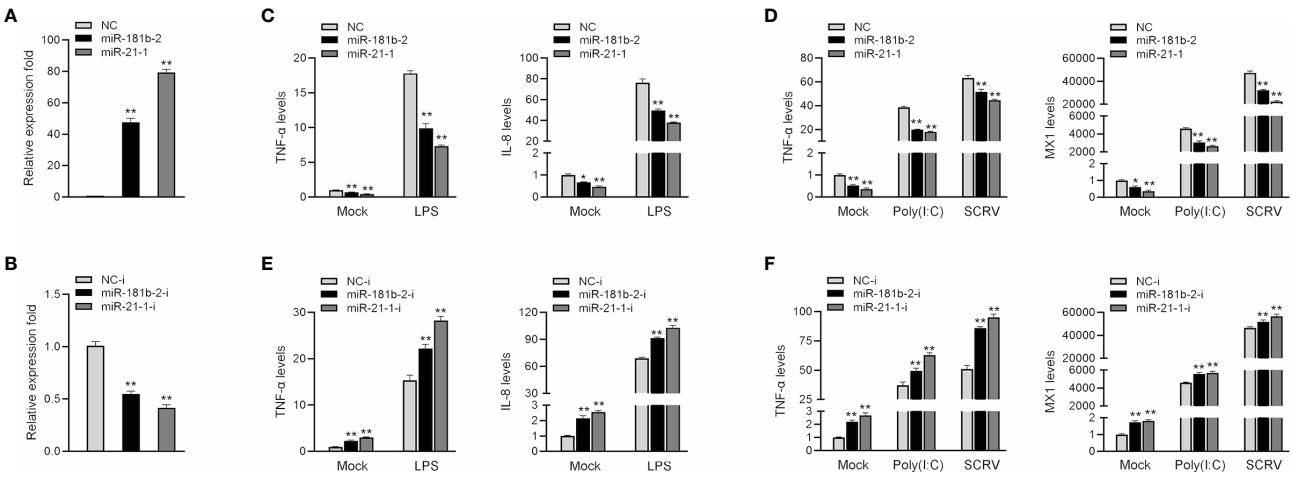

FIGURE 2 | MiR-181b-2 and miR-21-1 inhibit LPS, poly(I:C) or SCRV induce inflammatory response. **(A, B)** We transfected miR-21-1 and miR-181b-2 mimic **(A)** and miR-21-1 and miR-181b-2 inhibitors or NC, inhibitor NC into macrophage. **(C, D)** We transfected miR-21-1 and miR-181b-2 mimic into MBrC cells, and NC was used as a negative control. 24 h after transfection, the cells of the experimental group were stimulated with LPS, or poly (I:C) stimulation or SCRV injection, and then total RNA was extracted from the cells. The mRNA expression of TNF-α, IL-8 and Mx1 were detected by qRT-PCR. **(E, F)** miR-21-1 or miR-181b-2 inhibitors were transfected into MBrC cells, and inhibitor NC was used as a negative control. 24 h after transfection, the cells were stimulated with LPS, poly (I:C) and SCRV stimulation, total RNA was extracted by trizol. The mRNA expression of TNF-α, IL-8 and Mx1 were analyzed by qRT-PCR. All data are presented as the means ± SE from three independent triplicate experiments. $^{**}p < 0.01$, $^{*}p < 0.05$ versus the controls.

transfected into miiuy croaker MBrC cells prior to LPS or poly(I:C) stimulation or SCRV injection and analysis was performed 24 h later. The results showed that the overexpression of miR-21-1 or miR-181b-2 significantly inhibits the expression of TNF-α and IL-8 cytokines after LPS stimulation compared with NC (compared with NC; **Figure 2C**). The expression of TNF-α and MX1 was also inhibited after poly(I:C) and SCRV treatment (compared with NC; **Figure 2D**). On the contrary, the expression of TNF-α and IL-8 cytokines increased after transfection of miR-21-1 or miR-181b-2 inhibitor after LPS stimulation (compared with NC; **Figure 2E**), and the expression of TNF-α and MX1 were also increased after poly(I:C) or SCRV treatment (compared with NC; **Figure 2F**). The above data suggest that miR-21-1 and miR-181b-2 and their inhibitors can significantly increase or decrease, respectively, the expression levels of these proteins. Additionally, miR-21-1 and miR-181b-2 inhibited the production of inflammatory cytokines such as TNF-α, IL-8, and MX1 in response to LPS, poly(I:C), or SCRV stimulation, thus confirming the regulatory effect of miR-21-1 and miR-181b-2 on the immune system of miiuy croaker.

TRIF Is a Direct Target Gene of MiR-21-1 and MiR-181b-2

To prove that TRIF is a potential target of miR-21-1 and miR-181b-2, we performed predictive analysis. TRIF appeared to harbor a target sequence for miR-181b-2 at nucleotides 231-253 of its 3'UTRs and another target sequence for miR-21-1 at nucleotides 333-355 of its 3'UTRs (**Figure 3A**). To obtain direct evidence that TRIF-3'UTR is a target of miR-181b-2 and miR-21-1, we cloned the miiuy croaker TRIF-3'UTR sequence into the pmri-GLO luciferase report vector and changed the miR-21-1 and miR-181b-2 binding sites to construct a TRIF-3'UTR mutant. Then, we co-transfected miR-21-1 and miR-181b-2 mimics with TRIF-3'UTR or the TRIF-3'UTR mutant into HEK293 cells; here, NC was used as the negative control. After 48 hours later, the luciferase activity was detected in the collected cells. The results showed that the miR-21-1 and miR-181b-2 mimics could decrease the luciferase activity of TRIF-3'UTR-WT, but had no such effect on the mutant TRIF-3'UTR-MT (**Figure 3B**). When HEK293 cells were cotransfected with the same amount of miR-21-1 and miR-181b-2 mimics and miR-21-1 and miR-181b-2 inhibitors, the downregulation of TRIF-3'UTR was inhibited by the mimics (**Figure 3C**). In addition, the combined effect of miR-21-1 and miR-181b-2 was better than that of either miRNA alone (**Figure 3D**). We also found that the miR-21-1 and miR-181b-2 mimics could inhibit TRIF-3'UTR luciferase activity in a dose-dependent and time-dependent manner (**Figure 3E**). When we cloned the TRIF-3'UTR into the mVenus-C1 vector and cotransfected it into HEK293 cells with the miR-21-1 and miR-181b-2 mimic, miR-21-1 and miR-181b-2 mimic down-regulated the expression of TRIF-3'UTR-GFP (WT), did not change the expression of TRIF-3'UTR-GFP (MT) (**Figure 3F**).

The pre-miR-21-1 and pre-miR-181b-2 sequences of miiuy croaker were cloned into the pcDNA3.1 vector to construct pre-miR-21-1 and pre-miR-181b-2 plasmids (**Figure 3G**). We cotransfected pre-miR-21-1 and pre-miR-181b-2 plasmids with TRIF-3'UTR or the TRIF-3'UTR mutant into HEK293 cells, and used pcDNA3.1 as the negative control. The results showed that pre-miR-21-1 and pre-miR-181b-2 plasmids could decrease the luciferase activity of TRIF-3'UTR-WT but had no effect on the mutant TRIF-3'UTR-MT (**Figure 3H**). In addition, we found that the miR-21-1 and miR-181b-2 mimics inhibited TRIF-3'UTR luciferase activity in a dose- and time-dependent manner (**Figure 3I**). When HEK293 cells were cotransfected with the same amount of pre-miR-21-1 or pre-miR-181b-2 plasmids and miR-21-1 or miR-181b-2 inhibitors, the downregulation of TRIF-3'UTR was inhibited. Moreover, the combined effect of pre-miR-21-1 and pre-miR-181b-2 was better than that of either pre-miRNA alone (**Figure 3J**). These results show that exogenous miR-21-1 and miR-181b-2 mimics could inhibit the expression of TRIF-3'UTR, and that TRIF is a new target of miR-21-1 and miR-181b-2.

MiR-21-1 and MiR-181b-2 Regulate TRIF Expression at the Post-Transcriptional Level

MicroRNAs function by binding to the 3'UTR of target mRNAs to regulate gene expression at the posttranslational level. To verify whether miR-21-1 and miR-181b-2 inhibit TRIF protein expression at the posttranslational level, we designed and synthesized CDS region and 3'UTR region-specific primers of miiuy croaker TRIF and then cloned them into pcDNA3-Flag vector plasmids by PCR amplification to construct a TRIF expression plasmid. Then, we transfected miR-21-1 and miR-181b-2 with the TRIF expression plasmid into HEK293 cells and used qPCR and Western blotting to detect changes in TRIF expression after 48 h transfection. The results showed that miR-21-1 and miR-181b-2 significantly inhibit TRIF mRNA and protein expression and that the combined effect of the two miRNAs is more significant than that of either miRNA alone (**Figure 4A**). The TRIF expression plasmid was cotransfected with pre-miR-21-1 and miR-181b-2 into HEK293 cells, and results showed that the combined effect of pre-miR-21-1 and pre-miR-181b-2 was stronger than that of either pre-miRNA alone (**Figure 4B**). This finding further shows that endogenous miR-21-1 and miR-181b-2 coregulate the expression of TRIF. We found that miR-21-1 and miR-181b-2 mimics inhibit TRIF mRNA and protein expression in a dose-dependent manner (**Figures 4C, D**).

To assess whether miR-181b-2 and miR-21-1 could also regulate the expression of TRIF at the mRNA level, we transfected the miRNA mimic, inhibitors, or NC into MBrC cells for 48 h and then stimulated the cells with LPS. The results shown in **Figures 4E, F** indicated that miR-181b-2 and miR-21-1 mimics could reduce the mRNA expression of TRIF following LPS stimulation; by contrast, miR-181b-2 and miR-21-1 inhibitors increased the mRNA expression of TRIF. The miRNA mimics, inhibitors, or NC were transfected into MBrC cells for 48 h, after which the cells were stimulated with poly(I:C) or SCRV. The results shown in **Figures 4G, H** indicate that miR-181b-2 and miR-21-1 mimics could reduce the mRNA expression of TRIF following poly(I:C) and SCRV treatment;

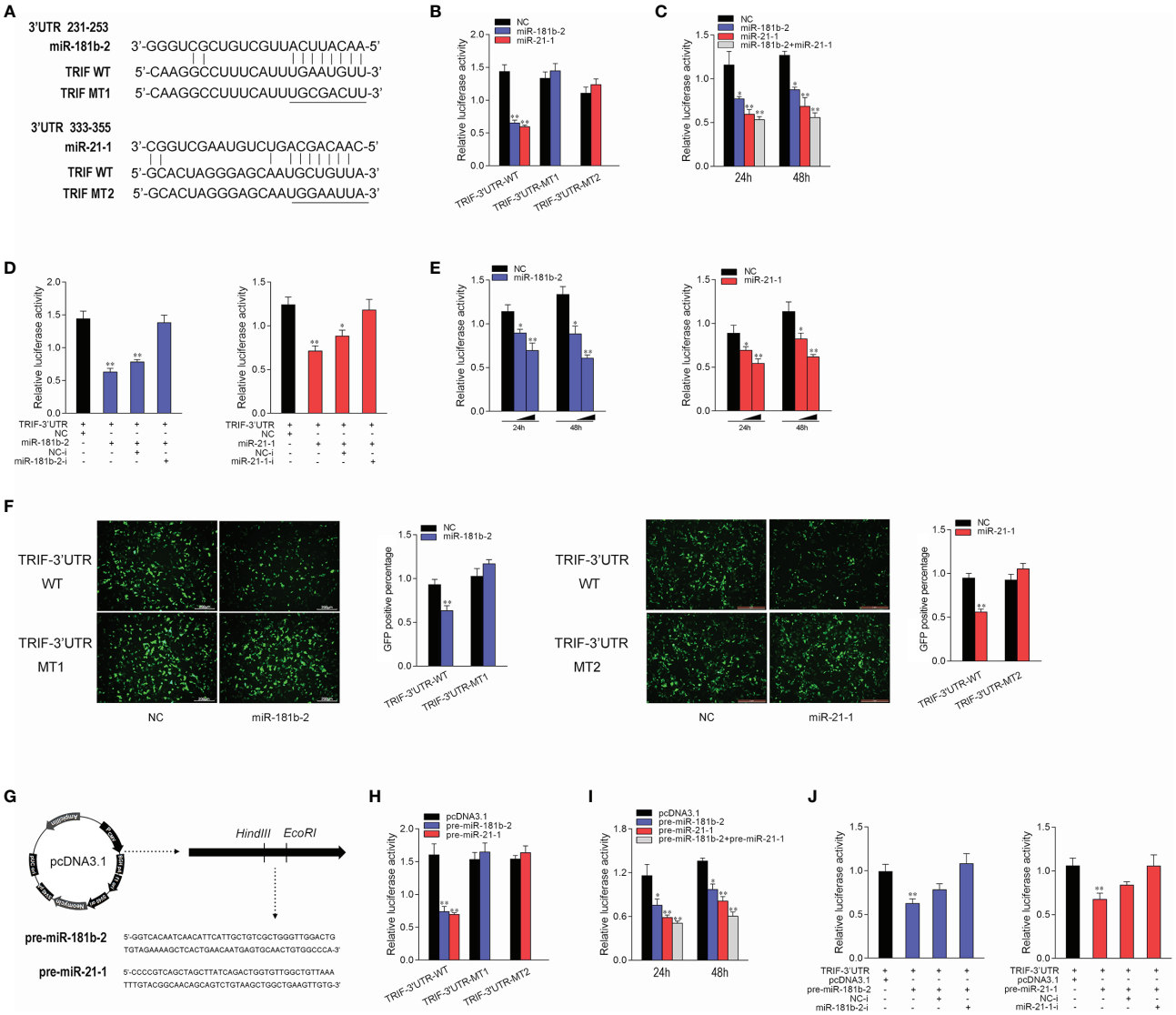

FIGURE 3 | Miiuy croaker TRIF is a directly target of miR-21-1 and miR-181b-2. **(A)** Sequence alignment of the 3'UTR of TRIF and its binding sites. **(B)** TRIF-3'UTR-WT or TRIF-3'UTR–MT1, TRIF-3'UTR–MT2 was cotransfected with miR-21-1 or miR-181b-2 into HEK293 cells with NC as a negative control, and cells were harvested after 24 h to detect luciferase activity. **(C)** MiR-21-1 and miR-181b-2 was transfection with TRIF-3'UTR into HEK293 cells, 24 h later, to detect and normalize luciferase activity to *Renilla* luciferase activity. **(D)** Cotransfect TRIF-3'UTR with miR-21-1 or miR-181b-2 mimics or inhibitors into HEK293 cells, NC or NC inhibitors as negative control, and harvest cells 24 h later, to detect and normalize luciferase activity to *Renilla* luciferase activity. **(E)** TRIF-3'UTR was cotransfected with miR-21-1 or miR-181b-2 into HEK293 cells, with NC as negative control, and concentration gradients and time gradients were set respectively. **(F)** The wild-type or mutant mVenus-TRIF-3'UTR and miR-21-1 or miR-181b-2 were cotransfected into HEK293 cells. The right histogram is the percentage of GFP positive under excitation light. **(G)** Pre-miR-21-1 and pre-miR-181b-2 sequence was inserted into pcDNA3.1 vector using HindIII and EcoRI restriction sites to construct a pre-miR-21-1 or miR-181b-2 expression plasmid. **(H)** TRIF-3'UTR-WT or TRIF-3'UTR-MT1, TRIF-3'UTR-MT2 was cotransfected with pre-miR-21-1 or pre-miR-181b-2 plasmids into HEK293 cells with pcDNA3.1 as a negative control, and cells were harvested after 24 h to detect luciferase activity. **(I)** Pre-miR-21-1 and pre-miR-181b-2 was transfection with TRIF-3'UTR into HEK293 cells, 24 h later, to detect and normalize luciferase activity to *Renilla* luciferase activity. **(J)** Cotransfect TRIF-3'UTR with pre-miR-21-1 or pre-miR-181b-2 and miR-21-1 and miR-181b-2 inhibitors into HEK293 cells, pcDNA3.1 and NC inhibitors as negative control, and harvest cells 24 h later, to detect and normalize luciferase activity to *Renilla* luciferase activity. All data are presented as the means ± SE from three independent triplicate experiments. $^{**}p < 0.01$, $^{*}p < 0.05$ versus the controls.

by contrast, miR-181b-2 and miR-21-1 inhibitors increased the mRNA expression of TRIF. These results demonstrate that miR-181b-2 and miR-21-1 directly target TRIF during LPS or poly(I:C) stimulation or SCRV injection.

MiR-21-1 and MiR-181b-2 Regulate the TRIF-Activated NF-κb Signaling Pathway

Given that miR-144 and miR-217 modulate the expression of inflammatory cytokines (42), we examined whether TRIF can

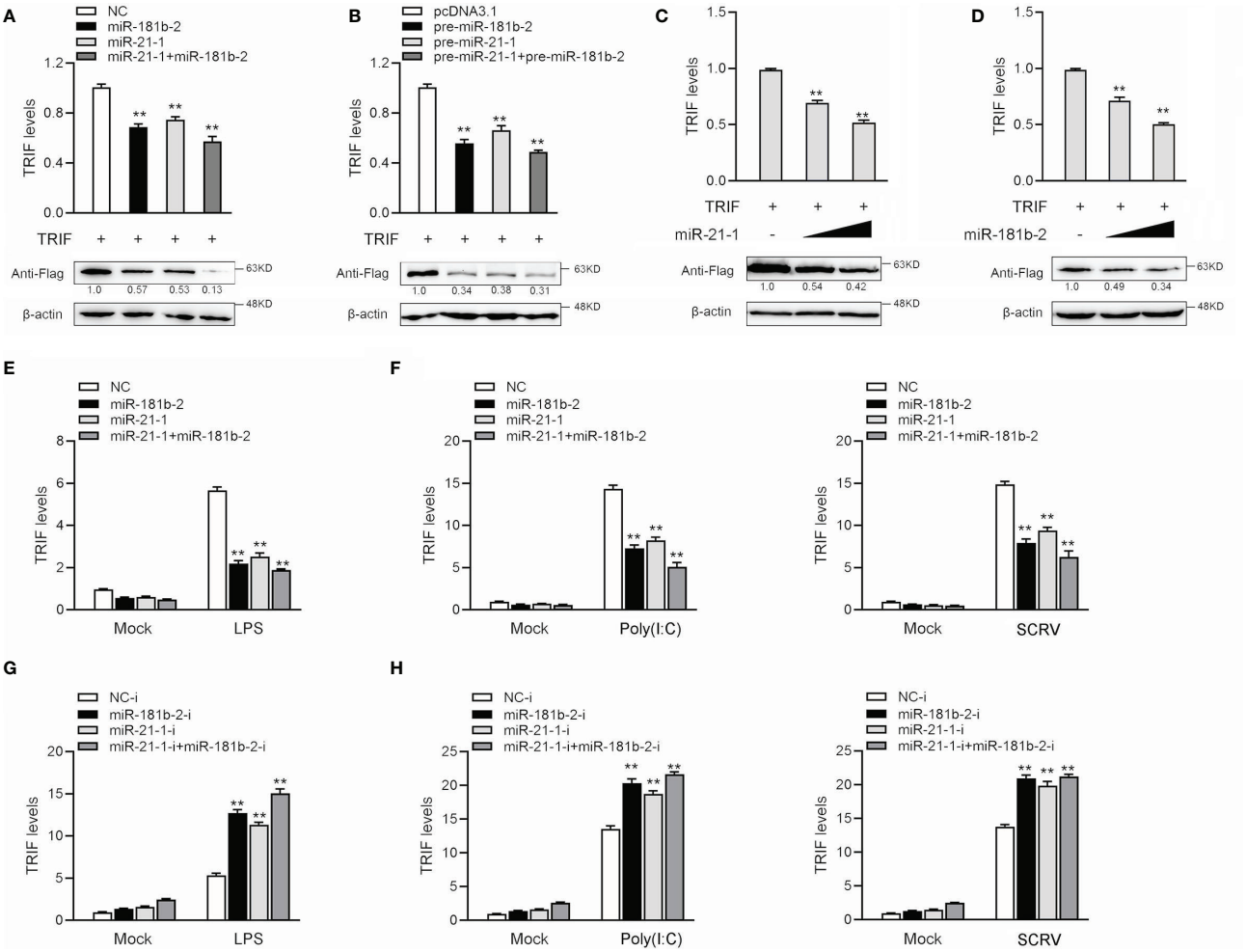

FIGURE 4 | MiR-21-1and miR-181b-2 inhibits the expression of TRIF at post-transcriptional level. **(A)** HEK293 cells were cotransfected with TRIF expression plasmid with NC, miR-21-1 or miR-181b-2. After 48 h, TRIF protein and mRNA levels were determined by Western blotting and qRT-PCR, respectively. **(B)** HEK293 cells were cotransfected with TRIF expression plasmid with pcDNA3.1, pre-miR-21-1 or pre-miR-181b-2. After 48 h, TRIF protein and mRNA levels were determined by Western blotting and qRT-PCR, respectively. **(C, D)** HEK293 cells were cotransfected with TRIF expression plasmid, along with NC, miR-21-1 **(C)** (0, 50, and 100 nM) or miR-181b-2 **(D)** (0, 50, and 100 nM) in a concentration gradient manner, and NC was used to control the same amounts of molecules for transfections. After 48 h, TRIF protein and mRNA levels were determined by western blotting and qRT-PCR, respectively. **(E)** We transfected miR-21-1 and miR-181b-2 into MBrC cells, NC as negative control, and stimulated with LPS for 6 h, and the TRIF mRNA expression were determined by qRT-PCR. **(F)** miR-21-1 and miR-181b-2 were transfected into MBrC cells, NC as negative control, and stimulated with poly(I:C) for 12 h or SCRV injection for 12 h, and the TRIF mRNA expression were determined by qRT-PCR. **(G)** We transfected miR-21-1-i and miR-181b-2-i into MBrC cells, NC-i as negative control, and stimulated with LPS for 6 h, and the TRIF mRNA expression were determined by qRT-PCR. **(H)** miR-21-1-i and miR-181b-2-i were transfected into MBrC cells, NC-i as negative control, and stimulated with poly(I:C) for 12 h or SCRV injection for 12 h, and the TRIF mRNA expression were determined by qRT-PCR. All data are presented as the means ± SE from three independent triplicate experiments. $^{**}p < 0.01$, versus the controls.

activate NF-κB and other signaling pathway genes. We co-transfected TRIF; NF-κB, IL-8, IL1β, IRF3 and IFN-2 reporter genes; and phRL-TK *Renilla* luciferase reporter genes into EPC cells. As shown in **Figure 5A**, TRIF could significantly activate the luciferase activity of reporter genes such as NF-κB, IL-8, IL1β, IRF3, and IFN-2. We cotransfected miR-21-1 and miR-181b-2 with TRIF and the reporter genes into EPC cells to verify whether the miRNAs can inhibit the activation of TRIF on these genes. The results showed that miR-21-1 and miR-181b-2 could significantly inhibit the expression of some TRIF-activated reporter genes, such as NF-κB, IRF3, and IFN-2, and that the combined effect of miR-21-1 and miR-181b-2 was better than that of either miRNA alone (**Figure 5B**). In addition, we found that miR-21-1 and miR-181b-2 mimics inhibit TRIF-activated reporter genes in a dose-dependent manner 24 and 48 h posttransfection (**Figures 5C, D**). We further verified the regulation of TRIF by miR-21-1 and miR-181b-2. Specifically, miR-21-1 and miR-181b-2 could regulate TRIF-activated NF-κB or IRF3 signaling pathway genes.

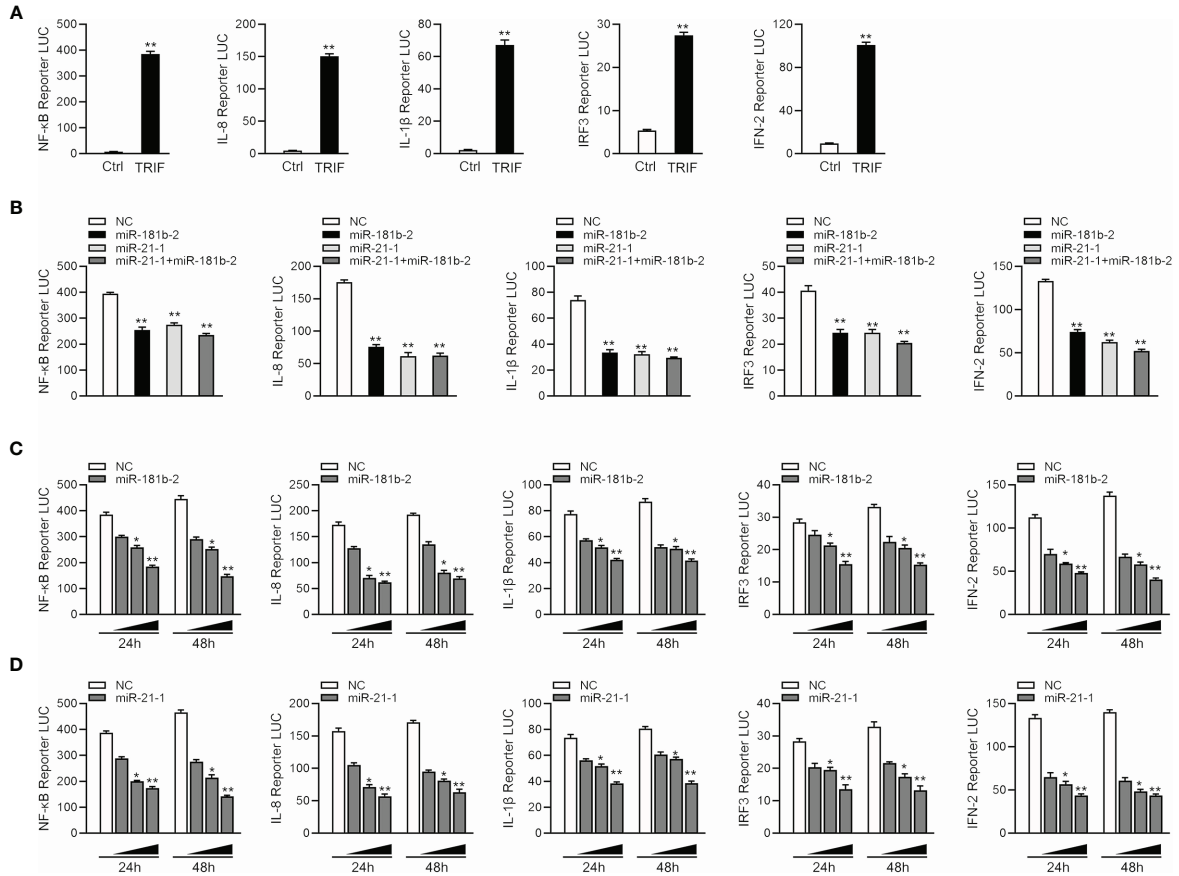

FIGURE 5 | MiR-21-1 or miR-181b-2 regulates NF-κB signaling pathway by regulating TRIF. **(A)** TRIF expression plasmid and NF-κB, IL-8, IL1β, IFN-2, IRF3 with PhRL-TK luciferase reporter gene vector were cotransfection into EPC cells, mock is TRIF negative control, 48 h later detection of luciferase activity. **(B)** We cotransfect miR-21-1 and miR-181b-2 and TRIF expression plasmid with NF-κB, IL-8, IL1β, IFN-2 and IRF3 reporter gene and PhRL-TK luciferase reporter vector into EPC cells. After 24 h, cells were collected, and the firefly fluorescence intensity was measured. **(C, D)** miR-181b-2 (0, 25, 50, and 100 nM) **(C)** and miR-21-1 (0, 25, 50, and 100 nM) **(D)** along with NC (100, 75, 50, and 0 nM) and TRIF expression plasmid with NF-κB, IL-8, IL1β, IFN-2 and IFN-3 reporter gene and PhRL-TK luciferase reporter vector were transfected into EPC cells, and designed concentration-gradient. After 24 or 48 h, cells were collected and the firefly fluorescence intensity was measured, and normalization was performed according to the fluorescence activity of the *Renilla*. All data are presented as the means ± SE from three independent triplicate experiments. $^{**}p < 0.01$, $^{*}p < 0.05$ versus the controls.

TRIF Knockdown Inhibits Antiviral and Bacterial Inflammation Responses

To confirm the effect of TRIF on antiviral and antibacterial inflammatory responses, we examined changes in inflammatory cytokine and antiviral gene expression after poly(I: C), SCRV, or LPS treatment. We designed a specific miiuy croaker TRIF siRNA (si-TRIF) and then transfected this molecule into MBrC cells. Results showed that si-TRIF could knock-down the expression of TRIF mRNA (**Figure 6A**). We cotransfected the TRIF expression plasmid and si-TRIF into HEK293 cells to verify the knockdown effect of si-TRIF. As shown in **Figure 6B**, si-TRIF inhibited the expression of TRIF protein. We transfected si-TRIF into miiuy croaker MBrC cells and used qRT-PCR to verify that whether TRIF regulates inflammatory cytokines. The results showed that after normal or LPS stimulation, siRNA could knock down the expression level of TRIF and suppress the expression of TRIF and its downstream TRAF6 gene (**Figure 6C**), thereby further downregulating the expression of TNF-α and IL-8 (**Figure 6D**). We verified whether knockdown TRIF under poly (I:C) stimulation and SCRV injection shows the same effect. Si-TRIF was transfected into MBrC cells and then treated with poly(I:C) or SCRV 24 h later. The results showed that si-TRIF consistently reduces the expression of TRIF mRNA, thereby inhibiting the expression of TRAF6 (**Figure 6E**), and inhibits the expression of TNF-α and MX1 (**Figure 6F**). This finding indicates that TRIF plays an important role in upstream and downstream genes. SiRNA can reduce the expression of TRIF, and miR-21-1 and miR-181b-2 have the same function as si-TRIF.

MiR-21-1 and MiR-181b-2 Regulate the Expression of Some Components of the TRIF Signaling Cascade

To study the TRIF-induced signaling pathway in fish and examine whether miR-21-1 and miR-181b-2 participate in

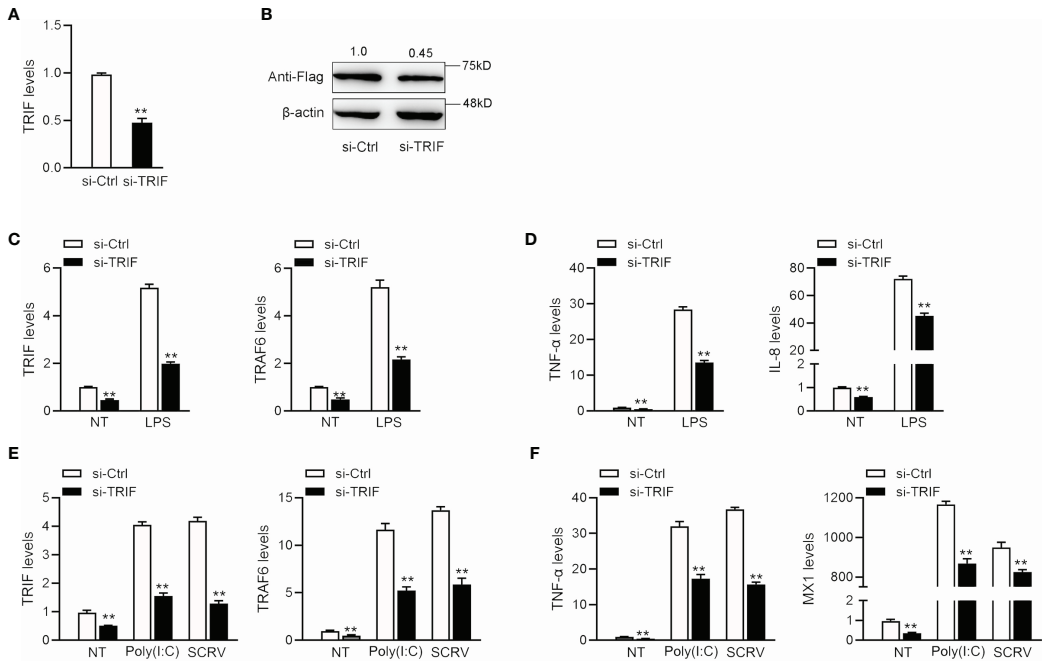

FIGURE 6 | The expression levels of inflammatory cytokines after TRIF interference. **(A)** si-TRIF or si-NC were transfected into miiuy croaker MBrC cells, after 48 h, TRIF mRNA expression was measured. **(B)** TRIF expression plasmids, si-TRIF and si-NC were transfected into HEK293 cells, after 48 h, TRIF protein expression was measured by western blotting. **(C)** si-TRIF or si-NC were transfected into MBrC cells with LPS stimulation, after 48 h, TRIF and TRAF6 mRNA expression were measured by qRT-PCR. **(D)** si-TRIF or si-NC were transfected into MBrC cells with LPS stimulation, after 48 h, TNF-α and IL-8 mRNA expression were measured by qRT-PCR. **(E)** We transfected si-TRIF or si-NC into miiuy croaker MBrC cells with poly(I:C) stimulation or SCRV injection, TRIF and TRAF6 mRNA expression were tested by qRT-PCR. **(F)** We transfected si-TRIF or si-NC into miiuy croaker MBrC cells with poly(I:C) stimulation or SCRV injection, TNF-α and IL-8 mRNA expression were tested by qRT-PCR. All data are presented as the means ± SE from three independent triplicate experiments. $^{**}p < 0.01$ versus the controls.

modulating TRIF-induced NF-κB signaling pathways, we transfected miR-21-1 or miR-181b-2 mimics or the NC mimic into MBrC cells, and then challenged the cells with LPS, poly(I:C), or SCRV. We harvested the cells 48 h later, extracted their RNA, and detected the expression of tumor necrosis factor-related factors 3 (TRAF3) and 6 (TRAF6) by qRT-PCR. As shown in **Figures 7A, B**, miR-21-1 and miR-181b-2 significantly inhibited TRAF3 and TRAF6 expression under mock, LPS stimulation. Moreover, the expressions of TRAF3 and TRAF6 were obviously decreased following miR-21-1 and miR-181b-2 mimic overexpression. We transfected miR-21-1 or miR-181b-2 inhibitors or NC-inhibitors into MBrC cells, and then challenged the cells with poly(I:C) or SCRV. Whereas they were significantly increased by miR-21-1 and miR-181b-2 inhibitors treatment in MBrC cells upon poly(I:C) or SCRV treatment (**Figures 7C, D**). MiR-21-1 and miR-181b-2 inhibited the expression of TRIF and its pathway gene TRAF6 under poly(I:C) stimulation. The combination of miR-21-1 and miR-181b-2 demonstrated more significant effects than either miRNA alone.

DISCUSSION

The innate immune system enables the body to produce a rapid and effective immune response to invading microorganisms. The key to ensuring this rapid response is that the body has a good recognition system. TLR recognition proteins are found in invading microorganisms; they stimulate intracellular signal transduction pathways and eventually produce a variety of immune responses. After a pathogen stimulates the body, all TLRs in the body stimulate the secretion of cytokines in the cells to initiate and promote the occurrence and development of inflammation. The stimulation of TLR3 and TLR4 causes the secretion of IFN-β through a single signal. This protein finally activates a series of genes, and its products help clear the pathogen. TLR3 can recognize double-stranded RNA and other molecules with similar structures, so it plays an important role in virus clearance. TLR4 is activated by the specific bacterial wall component LPS. The study of this pathway has been very clear, but it cannot explain all of the body's responses to bacteria and viruses, especially IFN-2 production. A TRIF protein was recently reported to be a key component of this pathway (43, 44). TRIF is a new member of the TLRs signal transduction pathway. Research on this protein has gradually deepened, and the importance of TRIF-dependent signaling pathways to the body's immunity is now better understood. Recent studies have found that TRAF3 and TRAF6 interact with the binding motif present in the N-terminal portion of TRIF through its region. Disrupting the TRAF9-binding motif of TRIF prevents it from connecting to TRAF6, resulting in the reduced activation of the

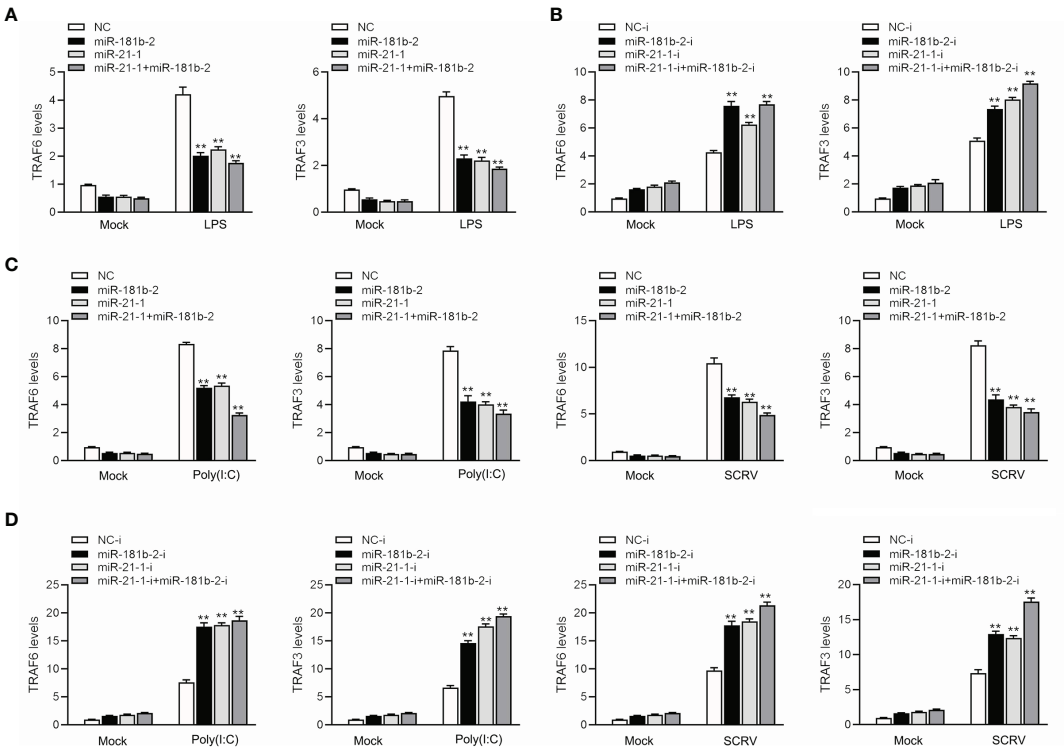

FIGURE 7 | MiR-181b-2 and miR-21-1 regulates the expression of components of the TRIF signaling cascade. **(A, B)** We transfected NC, miR-181b-2 and miR-21-1 or NC-i, miR-181b-2-i and miR-21-1-i into MBrC cells for 48 h, then stimulated LPS for 6 h. Afterwards, the expression levels TRAF6 and TRAF3 were determined and normalized to β-actin. **(C, D)** We transfected NC, miR-181b-2 and miR-21-1 or NC-i, miR-181b-2-i and miR-21-1-i into MBrC cells for 48 h, then poly(I:C) stimulated and SCRV injection. Afterwards, the expression levels TRAF6 and TRAF3 were determined and normalized to β-actin. All data are presented as the means ± SE from three independent triplicate experiments. $^{**}p < 0.01$, versus the controls.

NF-κB-dependent pathway induced by TRIF without affecting the IFN-β promoter. TBK1 is also connected to the N-terminal region of TRIF, and this link requires TBK1 kinase activation and TRIF phosphorylation. Because the binding sites of TRIF6 and TBK1 on TRIF are close to each other, TRAF6 may be able to physically prevent the connection of TBK1 and TRIF physically. Studies have found that IκB kinase I and TRAFs-related NF-κB activating molecule-binding kinase 1can be used as IRF3 kinases that are linked not only to IRF3 but also to TRIF (45, 46). The above results indicate that TRIF, TRAF6 and TBK1 are linked to activating two different transcription factors, NF-κB, and IRF3, respectively.

TRIF, as an important linker molecule, plays an extremely important role in the bacterial and viral immune pathways. Recent research on the function and mechanism of TRIF has deepened our understanding of this molecule. We can speculate on the TRIF signal transduction pathways on the basis of previous experience (**Figure 8**). The virus invades cells and is recognized by TLRs. TLRs transduce signals to the linker molecule TRIF, which is divided into two pathways for the next level of transmission. One signal is transmitted to TBK1 and eventually triggers IRF3 activation. Another signal is transmitted to TRAF3 or TRAF6, which, in turn, triggers downstream NF-κB activation. These two pathways eventually promote the release of inflammatory cytokines. Research on the regulation of TRIF is important. For example, as the fifth identified TIR domain-containing adaptor protein SARM, it can specifically block the TRIF-mediated activation of transcription factors but has no effect on the MyD88 or non-TLR signaling pathways, such as the TNF and RIG-I pathways (47). At present, the regulatory mechanism of SARM is not very clear. The combination of SARM and TRIF is believed to block the recruitment of downstream signaling proteins by TRIF or recruit other unknown proteins that inhibit the TRIF pathway through the SAM domain. A series of studies have shown that certain proteins have a negative regulatory effect on TRIF. The SRC homology2 (SH2)-domain-containing protein tyrosine phosphatase 2 can also negatively regulate the production of cytokines and IFNs induced by the TRIF pathway of TLR3 and TLR4 without affecting the MyD88 pathway. The binding of TBK1 prevents it from affecting the activation of downstream pathways (48). The recently discovered TRIF negative regulatory protein TAG plays a role in the TLR4-mediated TRIF pathway (49). TAG, as a splicing mutant of TRAM, can replace the binding of TRIF and TRAM, and, therefore, specifically inhibits the TRIF pathway activated by TLR4. In addition, several studies have reported the involvement of miRNAs in TRIF-mediated signaling. The overexpression of cardiac miR-

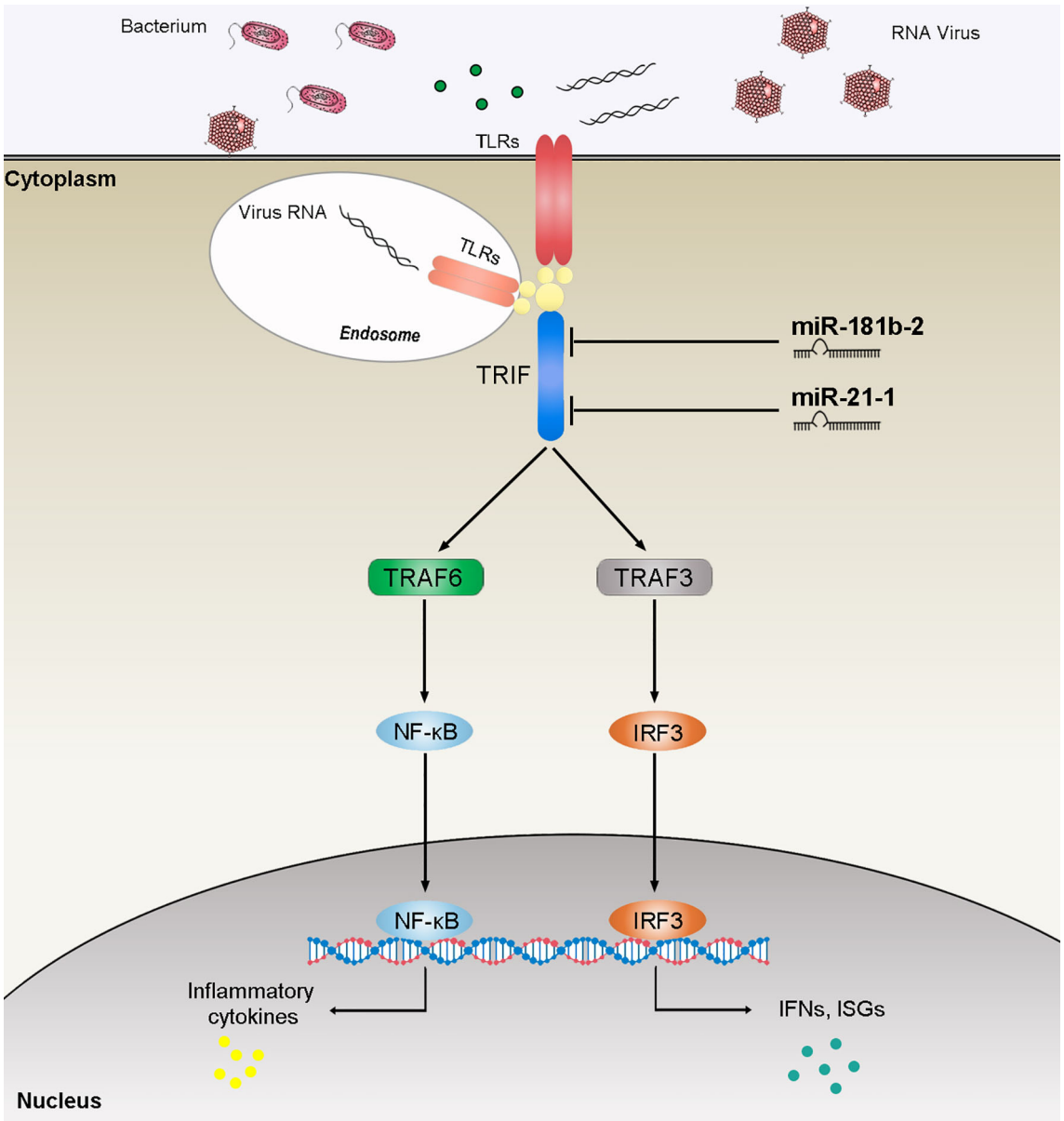

FIGURE 8 | The speculated mechanism model miR-21-1 and miR-181b-2 negatively regulates NF-κB and IRF3 pathway by targeting TRIF. MiR-21-1 and miR-181b-2 target TRIF and represses TRIF-mediated innate immune responses.

34a modulates TRIF-mediated cardiac remodeling in aldosterone-treated mice (50). In this article, we studied miR-21-1 and miR-181b-2 as negative regulators that together negatively regulate TRIF expression, thereby clarifying the role of miRNAs in regulating the host-pathogen interaction networks and providing new insights for future research.

MiRNA inhibits target genes translation or induces mRNA degradation at the posttranscriptional level to achieve the negative regulation of the target protein. Since let-7 was first identified as a miRNA, an increasing number of miRNAs have been discovered. It can inhibit the translation and further inhibit protein expression in nematodes by complementing the 3'UTR region of the target gene, thereby regulating the function of organisms (51). Studies have shown that Stat3 and C/EBPβ synergistically induce miR-21 and miR-181b expression during sepsis (52). Later studies found that STAT3 activates miR-21 and miR-181b-1 through PTEN and CYLD as part of an epigenetic switch that links inflammation to cancer (53). MiR-181b can be targeted in the human cancer cell lines BCL2 (to regulate multidrug resistance) (54). Another study demonstrated the

prognostic significance of miR-181b and miR-21 in patients with gastric cancer treated with S-1/oxaliplatin or doxfluridine/oxaliplatin (55). Given the important role of miR-21-1 and miR-181b-2 in human research, we attempted to determine the functions of miR-21-1 and miR-181b-2. We first verified that miR-21-1 and miR-181b-2 inhibit the fluorescent activity of TRIF-3'UTR by using double-fluorescence experiments. Thus, we believe that TRIF may be a new target of miR-21-1 and miR-181b-2. Then, we transfected miiuy croaker MBrC cells with miR-21-1 or miR-181b-2 mimics or inhibitors and then detected TRIF and the expression of cytokines used by qRT-PCR. In this study, we first determined the up-regulation of miR-21-1 and miR-181b-2 expression after LPS stimulation, *V. anguillarum*, or poly(I:C) stimulation or SCRV infection of miiuy croaker. We then predicted the target gene for miR-21-1 and miR-181b-2 and presumed that TRIF is a direct target of these miRNAs. Then we transfected miR-21-1 and miR-181b-2 mimics or inhibitors into miiuy croaker MBrC cells and detected changes in the expression levels of a number of inflammatory cytokines such as IL-8, TNF-α, and Mx1. We found that the expression of inflammatory cytokines was significantly decreased after transfection of miR-21-1 and miR-181b-2, and the expression of inflammatory cytokines was up-regulated after transfection with miR-21-1 and miR-181b-2 inhibitor. We also examined the expression levels of inflammatory cytokines. We verified that miR-21-1 and miR-181b-2 can inhibit the expression of TRIF protein at the translation level and inhibit reporter genes, such as NF-κB, activated by TRIF. The results of this study will improve the understanding on the innate immune response mechanism of fish and provide new insights into the study of mammalian TRIF.

DATA AVAILABILITY STATEMENT

The original contributions presented in the study are included in the article/**Supplementary Material**. Further inquiries can be directed to the corresponding authors.

AUTHOR CONTRIBUTIONS

Conceived and designed the experiments: TX and LH. Performed the experiments: YS, LZ, and WZ. Analyzed the data: YS, LZ, WZ, and JC. Contributed reagents/materials/analysis tools: TX, LH, and XL. Wrote the paper: YS, LZ, WZ, and JC. All authors contributed to the article and approved the submitted version.

FUNDING

This study was supported by the National Natural Science Foundation of China (31802325 and 31822057) and Open Fund of CAS Key Laboratory of Experimental Marine Biology, Institute of Oceanology, Chinese Academy of Sciences (KF2019NO1).

SUPPLEMENTARY MATERIAL

The Supplementary Material for this article can be found online at: https://www.frontiersin.org/articles/10.3389/fimmu.2021.734520/full#supplementary-material

REFERENCES

1. Akira S, Takeda K. Toll-Like Receptor Signalling. *Nat Rev Immunol* (2004) 4:499–511. doi: 10.1038/nri1391
2. West AP, Koblansky AA, Ghosh S. Recognition and Signaling by Toll-Like Receptors. *Annu Rev Cell Dev Biol* (2006) 22:409–37. doi: 10.1146/annurev.cellbio.21.122303.115827
3. Kawai T, Adachi O, Ogawa T, Takeda K, Akira S. Unresponsiveness of MyD88-Deficient Mice to Endotoxin. *Immunity* (1999) 11:115–22. doi: 10.1016/S1074-7613(00)80086-2
4. Takeda K, Akira S. TLR Signaling Pathways. *Semin Immunol* (2004) 16:3–9. doi: 10.1016/j.smim.2003.10.003
5. Yamamoto M, Sato S, Hemmi H, Hoshino K, Kaisho T, Sanjo H, et al. Role of Adaptor TRIF in the MyD88-Independent Toll-Like Receptor Signaling Pathway. *Science* (2003) 301:640–3. doi: 10.1126/science.1087262
6. Oshiumi H, Matsumoto M, Funami K, Akazawa T, Seya T. TICAM-1, an Adaptor Molecule That Participates in Toll-Like Receptor 3-Mediated Interferon Beta Induction. *Nat Immunol* (2003) 4:161–7. doi: 10.1038/ni886
7. Rautap R, Samanta M, Dash HR, Nayak B, Das S. Toll-Like Receptors (TLRs) in Aquatic Animals: Signaling Pathways, Expressions and Immune Responses. *Immunol Lett* (2014) 158:14–24. doi: 10.1016/j.imlet.2013.11.013
8. Hirotani T, Yamamoto M, Kumagai Y, Uematsu S, Kawase I, Takeuchi O, et al. Regulation of Lipopolysaccharide-Inducible Genes by MyD88 and Toll/IL-1 Domain Containing Adaptor Inducing IFN-Beta. *Biochem Biophys Res Commun* (2005) 328:383–92. doi: 10.1016/j.bbrc.2004.12.184
9. Liu Q, Ding JL. The Molecular Mechanisms of TLR-Signaling Cooperation in Cytokine Regulation. *Immunol Cell Biol* (2016) 94:538–42. doi: 10.1038/icb.2016.18
10. Huang B, Zhang LL, Du YS, Li L, Qu T, Meng J, et al. Alternative Splicing and Immune Response of Crassostrea Gigas Tumor Necrosis Factor Receptor-Associated Factor 3. *Mol Biol Rep* (2014) 41:6481–91. doi: 10.1007/s11033-014-3531-9
11. Bakshi S, Taylor J, Strickson S, Mccartney T, Cohen P. Identification of TBK1 Complexes Required for the Phosphorylation of IRF3 and the Production of Interferon β. *Biochem J* (2017) 474:1163–74. doi: 10.1042/BCJ20160992
12. Meylan E, Burns K, Hofmann K, Blancheteau V, Martinon F, Kelliher M, et al. Rip1 Is an Essential Mediator of Toll-Like Receptor 3–Induced NF-κb Activation. *Nat Immunol* (2004) 5:503–7. doi: 10.1038/ni1061
13. Fan S, Chen S, Liu Y, Lin Y, Liu H, Guo L, et al. Zebrafish TRIF, a Golgi-Localized Protein, Participates in IFN Induction and NF-Kappa B Activation. *J Immunol* (2008) 180:5373–83. doi: 10.4049/jimmunol.180.8.5373
14. Matsuo A, Oshiumi H, Tsujita T, Mitani H, Kasai H, Yoshimizu M, et al. Teleost TLR22 Recognizes RNA Duplex to Induce IFN and Protect Cells From Birna Viruses. *J Immunol* (2008) 181:3474–85. doi: 10.4049/jimmunol.181.5.3474
15. Yang C, Li Q, Su J, Chen X, Wang Y, Peng L. Identification and Functional Characterizations of a Novel TRIF Gene From Grass Carp (*Ctenopharyngodon Idella*). *Dev Comp Immunol* (2013) 41:222–9. doi: 10.1016/j.dci.2013.05.018
16. Fan S, Chen S, Liu Y, Lin Y, Xu A. Zebrafish TRIF, a Golgi-Localized Protein, Participates in IFN Induction and NF-κb Activation. *J Immunol* (2008) 180:5373–83. doi: 10.4049/jimmunol.180.8.5373
17. Tartey S, Takeuchi O. Pathogen Recognition and Toll-Like Receptor Targeted Therapeutics in Innate Immune Cells. *Int Rev Immunol* (2017) 36:1–17. doi: 10.1080/08830185.2016.1261318
18. Takeuchi O, Akira S. Pattern Recognition Receptors and Inflammation. *Cell* (2010) 140:810–20. doi: 10.1016/j.cell.2010.01.022
19. Tsutsui H, Imamura M, Fujimoto J, Nakanishi K. The TLR4/TRIF-Mediated Activation of NLRP3 Inflammasome Underlies Endotoxin-Induced Liver

Injury in Mice. *Gastroenterol Res Pract* (2010) 10:1–11. doi: 10.1155/2010/641865
20. Lin Q, Fang D, Fang J, Ren X, Yang X, Wen F, et al. Impaired Wound Healing With Defective Expression of Chemokines and Recruitment of Myeloid Cells in TLR3-Deficient Mice. *J Immunol* (2011) 186:3710–7. doi: 10.4049/jimmunol.1003007
21. Zhao XY, Huo RX, Yan XL, Xu TJ. IRF3 Negatively Regulates Toll-Like Receptor-Mediated NF-κb Signaling by Targeting TRIF for Degradation in Teleost Fish. *Front Immunol* (2018) 9:867. doi: 10.3389/fimmu.2018.00867
22. Ahmed S, Maratha A, Butt AQ, Shevlin E, Miggin ASM. TRIF-Mediated TLR3 and TLR4 Signaling Is Negatively Regulated by Adam15. *J Immunol* (2013) 190:2217–28. doi: 10.4049/jimmunol.1201630
23. O'Connell RM, Rao DS, Chaudhuri AA, Baltimore D. Physiological and Pathological Roles for microRNAs in the Immune System. *Nat Rev Immunol* (2010) 10:111–22. doi: 10.1038/nri2708
24. Bartel DP. MicroRNAs: Genomics, Biogenesis, Mechanism, and Function. *Cell* (2004) 116:281–97. doi: 10.1016/S0092-8674(04)00045-5
25. Chu Q, Sun YN, Bi DK, Cui JX, Xu TJ. Up-Regulated of miR-8159-5p and miR-217-5p by LPS Stimulation Negatively Co-Regulate TLR1 in Miiuy Croaker. *Dev Comp Immunol* (2017) 67:117–25. doi: 10.1016/j.dci.2016.11.004
26. Chu Q, Sun YN, Cui JX, Xu TJ. Inducible microRNA-214 Contributes to the Suppression of NF-κb Mediated Inflammatory Response *via* Targeting MyD88 in Fish. *J Biol Chem* (2017) 292:5282–90. doi: 10.1074/jbc.M117.777078
27. Zhang K, Zhang Y, Liu C, Ying X, Zhang JQ. MicroRNAs in the Diagnosis and Prognosis of Breast Cancer and Their Therapeutic Potential (Review). *Int J Oncol* (2014) 45:950–8. doi: 10.3892/ijo.2014.2487
28. Lee RC, Ambros V. An extensive class of small RNAs in *Caenorhabditis elegans*. *Science* (2001) 294:862–4. doi: 10.1126/science.1065329
29. Pasquinelli AE, Reinhart BJ, Slack F, Martindale MQ, Ruvkun G. Conservation of the Sequence and Temporal Expression of Let-7 Heterochronic Regulatory RNA. *Nature* (2000) 408:86–9. doi: 10.1038/35040556
30. Ruvkun G. Glimpses of a Tiny RNA World. *Science* (2001) 294:797–9. doi: 10.1126/science.1066315
31. Shahid S, Kim GJ, Johnson NR, Wafula E, Wang F, Coruh C, et al. MicroRNAs From the Parasitic Plant *Cuscuta Campestris* Target Host Messenger RNAs. *Nature* (2018) 553:82–5. doi: 10.1038/nature25027
32. Zhang L, Hou DX, Chen X, Li DH, Zhu LV, Zhang YJ, et al. Exogenous Plant MIR168a Specifically Targets Mammalian LDLRAP1: Evidence of Cross-Kingdom Regulation by microRNA. *Cell Res* (2012) 22:107–26. doi: 10.1038/cr.2011.158
33. Zhou Z, Li JX, Dong L, Chen Q, Liu JL, Kong HH, et al. Honeysuckle-Encoded Atypical Microrna2911 Directly Targets Influenza A Viruses. *Cell Res* (2015) 25:39–49. doi: 10.1038/cr.2014.130
34. Chin AR, Fong MY, Somlo G, Wu J, Swiderski P, Wu XW, et al. Cross-Kingdom Inhibition of Breast Cancer Growth by Plant Mir159. *Cell Res* (2016) 26:217–28. doi: 10.1038/cr.2016.13
35. Chu Q, Sun YN, Cui JX, Xu TJ. MicroRNA-3570 Modulates the NF-κb Pathway in Teleost Fish by Targeting Myd88. *J Immunol* (2017) 198:3274–82. doi: 10.4049/jimmunol.1602064
36. Lewis BP, Shih IH, Jones-Rhoades MW, Bartel DP, Burge CB. Prediction of Mammalian microRNA Targets. *Cell* (2003) 115:787–98. doi: 10.1016/S0092-8674(03)01018-3
37. John B, Enright AJ, Aravin A, Tuschl T, Sander C, Marks DS. Human microRNA Targets. *PloS Biol* (2004) 2:e363. doi: 10.1371/journal.pbio.0020363
38. Rusinov V, Baev V, Minkov IN, Tabler M. MicroInspector: A Web Tool for Detection of miRNA Binding Sites in an RNA Sequence. *Nucleic Acids Res* (2005) 33:W696–700. doi: 10.1093/nar/gki364
39. Livak KJ, Schmittgen TD. Analysis of Relative Gene Expression Data Using Real-Time Quantitative PCR and the $2^{-\Delta\Delta CT}$ Method. *Methods* (2001) 25:402–8. doi: 10.1006/meth.2001.1262
40. Han J, Xu G, Xu T. The Miiuy Croaker microRNA Transcriptome and microRNA Regulation of RIG-I Like Receptor Signaling Pathway After Poly (I:C) Stimulation. *Fish Shellfish Immunol* (2016) 54:419–26. doi: 10.1016/j.fsi.2016.04.126
41. Bi D, Cui J, Chu Q, Xu T. MicroRNA-21 Contributes to Suppress Cytokines Production by Targeting TLR28 in Teleost Fish. *Mol Immunol* (2017) 83:107–14. doi: 10.1016/j.molimm.2017.01.016
42. Chu Q, Bi D, Zheng W, Xu T. MicroRNA Negatively Regulates NF-κb-Mediated Immune Responses by Targeting NOD1 in the Teleost Fish *Miichthys Miiuy*. *Sci China Life Sci* (2021) 64:803–15. doi: 10.1007/s11427-020-1777-y
43. Hoebe K, Du X, Georgel P, Janssen E, Tabeta K, Kim SO, et al. Identification of LPS2 as a Key Transducer of MyD88-Independent TIR Signaling. *Nature* (2003) 424:743–8. doi: 10.1038/nature01889
44. Yamamoto M, Sato S, Hemmi H, Sanjo H, Uematsu S, Kaisho T, et al. Essential Role for TIRAP in Activation of the Signaling Cascade Shared by TLR2 and TLR4. *Nature* (2002) 420:324–9. doi: 10.1038/nature01182
45. Sato S, Sugiyama M, Yamamoto M, Watanabe Y, Kawai T, Takeda K, et al. Toll / IL1 Receptor Domain Containing Adaptor Inducing IFN Beta (TRIF) Associates With TNF Receptor Associated Factor 6 and TANK Binding Kinas E 1, and Activates Two Distinct Transcription Factors, NF Kappa B and IFN β Regulatory Factor 3, in the Toll Like Receptor Signaling. *J Immunol* (2003) 171:4304–10. doi: 10.4049/jimmunol.171.8.4304
46. Sharma S, Tenoever BR, Grandvaux H, Zhou GP, Lin RT, Hiscott J. Triggering the Interferon Antiviral Response Through an IKK Related Pathway. *Science* (2003) 300:1148. doi: 10.1126/science.1081315
47. Carty M, Goodbody R, Schrder M, Stack J, Moynagh PN, Bowie AG. The Human Adaptor SARM Negatively Regulates Adaptor Protein TRIF-Dependent Toll-Like Receptor Signaling. *Nat Immunol* (2006) 7:1074–81. doi: 10.1038/ni1382
48. An HZ, Zhao W, Hou J, Zhang Y, Xie Y, Zheng YJ, et al. SHP-2 Phosphatase Negatively Regulates the TRIF Adaptor Protein-Dependent Type I Interferon and Proinflammatory Cytokine Production. *Immunity* (2006) 25:919–28. doi: 10.1016/j.immuni.2006.10.014
49. Palsson-McDermott EM, Doyle SL, McGettrick AF, Hardy M, Husebye H, Banahan K, et al. TAG, a Splice Variant of the Adaptor TRAM, negatively Regulates the Adaptor MyD88-Independent TLR4 Pathway. *Nat Immunol* (2009) 10:579–86. doi: 10.1038/ni.1727
50. Li S, Cao W, Wang B, Zhan E, Xu J, Li S. TRIF/miR-34a Mediates Aldosterone-Induced Cardiac Inflammation and Remodeling. *Clin Sci* (2020) 134:1319–31. doi: 10.1042/CS20200249
51. Lee RC, Feinbaum RL, Ambros V. The *C. Elegan* Sheterochronic Gene Lin-4 Encodes Small RNAs With Antisense Complementarity to Lin-14. *Cell* (1993) 75:843–54. doi: 10.1016/0092-8674(93)90529-Y
52. Mcclure C, Mcpeak MB, Youssef D, Yao ZQ, EMcall CE, ElGazzar M. Stat3 and C/Ebpβ Synergize to Induce miR-21 and miR-181b Expression During Sepsis. *Immunol Cell Biol* (2016) 85:42–55. doi: 10.1038/icb.2016.63
53. Iliopoulos D, Jaeger SA, Hirsch HA, Bulyk ML, Struhl K. STAT3 Activation of miR-21 and miR-181b-1 *via* PTEN and CYLD Are Part of the Epigenetic Switch Linking Inflammation to Cancer. *Mol Cell* (2010) 39:493–506. doi: 10.1016/j.molcel.2010.07.023
54. Zhu W, Shan X, Wang T, Shu Y, Liu P. miR-181b Modulates Multidrug Resistance by Targeting BCL2 in Human Cancer Cell Lines. *Int J Cancer* (2010) 127:2520–9. doi: 10.1002/ijc.25260
55. Jiang J, Zheng X, Xu X, Zhou Q, Yan H, Zhang X, et al. Prognostic Significance of miR-181b and miR-21 in Gastric Cancer Patients Treated With S-1/Oxaliplatin or 8Doxifluridine/Oxaliplatin. *PloS One* (2011) 6:e23271. doi: 10.1371/journal.pone.0023271

Conflict of Interest: The authors declare that the research was conducted in the absence of any commercial or financial relationships that could be construed as a potential conflict of interest.

Publisher's Note: All claims expressed in this article are solely those of the authors and do not necessarily represent those of their affiliated organizations, or those of the publisher, the editors and the reviewers. Any product that may be evaluated in this article, or claim that may be made by its manufacturer, is not guaranteed or endorsed by the publisher.

frontiers | Frontiers in Immunology

REVIEW
published: 06 April 2022
doi: 10.3389/fimmu.2022.768621

Sleeping With the Enemy? The Current Knowledge of Piscine Orthoreovirus (PRV) Immune Response Elicited to Counteract Infection

Eva Vallejos-Vidal[1,2*], *Felipe E. Reyes-López*[1,3], *Ana María Sandino*[1,4] *and Mónica Imarai*[1,4]

[1] Centro de Biotecnología Acuícola, Facultad de Química y Biología, Universidad de Santiago de Chile, Santiago, Chile, [2] Facultad de Medicina Veterinaria y Agronomía, Universidad de Las Américas, Santiago, Chile, [3] Department of Cell Biology, Physiology, and Immunology, Universitat Autònoma de Barcelona, Barcelona, Spain, [4] Departamento de Biología, Facultad de Química y Biología, Universidad de Santiago de Chile, Santiago, Chile

OPEN ACCESS

Edited by:
Maria Del Mar Ortega-Villaizan, Miguel Hernández University of Elche, Spain

Reviewed by:
Espen Rimstad, Norwegian University of Life Sciences, Norway
Francisca Samsing, The University of Sydney, Australia

***Correspondence:**
Eva Vallejos-Vidal
Eva.vallejosv@usach.cl

Specialty section:
This article was submitted to Comparative Immunology, a section of the journal Frontiers in Immunology

Received: 31 August 2021
Accepted: 25 February 2022
Published: 06 April 2022

Citation:
Vallejos-Vidal E, Reyes-López FE, Sandino AM and Imarai M (2022) Sleeping With the Enemy? The Current Knowledge of Piscine Orthoreovirus (PRV) Immune Response Elicited to Counteract Infection. Front. Immunol. 13:768621. doi: 10.3389/fimmu.2022.768621

Piscine orthoreovirus (PRV) is a virus in the genus Orthoreovirus of the Reoviridae family, first described in 2010 associated with Heart and Skeletal Muscle Inflammation (HSMI) in Atlantic salmon (*Salmo salar*). Three phases of PRV infection have been described, the early entry and dissemination, the acute dissemination phase, and the persistence phase. Depending on the PRV genotype and the host, infection can last for life. Mechanisms of immune response to PRV infection have been just beginning to be studied and the knowledge in this matter is here revised. PRV induces a classical antiviral immune response in experimental infection of salmonid erythrocytes, including transcriptional upregulation of *ifn-α*, *rig-i*, *mx*, and *pkr*. In addition, transcript upregulation of *tcra, tcrb, cd2, il-2, cd4-1, ifn-γ, il-12, and il-18* has been observed in Atlantic salmon infected with PRV, indicating that PRV elicited a Th1 type response probably as a host defense strategy. The high expression levels of *cd8a*, *cd8b*, and *granzyme-A* in PRV-infected fish suggest a positive modulatory effect on the CTL-mediated immune response. This is consistent with PRV-dependent upregulation of the genes involved in antigen presentation, including MHC class I, transporters, and proteasome components. We also review the potential immune mechanisms associated with the persistence phenotype of PRV-infected fish and its consequence for the development of a secondary infection. In this scenario, the application of a vaccination strategy is an urgent and challenging task due to the emergence of this viral infection that threatens salmon farming.

Keywords: piscine orthoreovirus, double strand RNA (dsRNA) virus, heart and skeletal muscle inflammation (HSMI), antiviral immune response, pro-inflammatory cytokines, fish vaccines, aquaculture, emerging diseases

INTRODUCTION

Piscine orthoreovirus (PRV) is a virus that belongs to the *Reoviridae* family, *Spinareovirinae* subfamily, and genus *Orthoreovirus*. PRV was firstly described in 2010 (1), as it was associated with Heart and Skeletal Muscle Inflammation (HSMI) in Atlantic salmon (*Salmo salar*) (2). The disease was described in 1999 in fish farms in Norway (3). In Chile, the first report of PRV was published in 2016. Authors found PRV strains in HSMI lesions of farmed Atlantic salmon, and Coho salmon (*Oncorhynchus kisutch*) (4). HSMI has been diagnosed all the years over the last decade in more than 100 farm centers in Norway (excepting 2017 and 2019) (5), resulting in economic losses estimated at €9 million annually (6). In Chile, 3.7% of the infectious disease mortality of Atlantic salmon, and 14.9% of the infectious disease mortality of Coho salmon were associated with HSMI during 2020 (7). Because of the epidemiological evolution observed in the sanitary surveillance, HSMI was categorized as an emerging disease in Chilean salmon farming (7). The economic impact of PRV infection is associated with mortality and melanized spots in salmon filets (8) that correlate with a pro-inflammatory environment (9). Another concern is that its etiological agent, the PRV, is reportedly spreading from farmed to wild Atlantic salmon with yet undetermined impacts (10). In seawater Atlantic salmon farms, the infection prevalence can reach up to 97% (11), and the etiological agent, PRV, is also present in freshwater Atlantic salmon presmolts with high frequency, found in parr between 30 and 60 grams (4).

PRV AND HEART AND SKELETAL MUSCLE INFLAMMATION

PRV is a dsRNA virus that has a genome composed of 10 RNA segments that can be classified into three different groups according to sizes: small segments (S1, S2, S3, S4) between 1040 and 1329 bp, medium (M1, M2, M3) between 2179 and 2403 bp, and large (L1, L2, L3) between 3911 and 3935 bp (1, 12, 13). The genome has at least 13 ORFs that encode for at least 11 proteins (14, 15). Eight of these proteins are structural components of the virus particle: segments L1, L3, M1, and S2 encode the inner capsid proteins λ1, λ3, μ2, and σ2, respectively; segments L2, M2, S1, and S4 encode for the outer capsid proteins λ2, μ1, σ3, and σ1, respectively; and segments S3, M3 and S1 encode for the three non-structural proteins σNS, μNS, and p13, respectively (**Figure 1**) (16, 17). PRV is a non-enveloped virus with an icosahedral structure (13).

Three different subtypes of PRV have been described using the coding sequence of PRV segments, denominated as PRV-1, PRV-2 and PRV-3 (18, 19). Phylogenetic analysis focused on the PRV genomic segments S1, differentiates this virus into two major genotypes, I and II, and each of them into two subgenotypes designated as Ia and Ib, and IIa and IIb, respectively. Subgenotypes Ia and Ib make up the PRV-1 subtype and subgenotypes IIb and IIa correspond to the PRV-2 and PRV-3 subtypes, respectively (20).

Recently, with all Gen Bank available PRV sequences (May 2020) and using new PRV S1 and M2 segment sequences was determined that a significant number of the publicly available sequences belong to the PRV-1 subtype (subgenotypes Ia and Ib), less belong to the PRV-3 subtype (subgenotype IIa) and there are few sequences of PRV-2 subtype (subgenotype IIb) (15). PRV is the etiological agent of HSMI in Norway, Canada, Germany, Scotland, Iceland, and Chile. Recently, it was suggested that PRV-1 subgenotype Ib can be responsible for HSMI in Atlantic salmon (15) while the subgenotype Ia was associated with low virulence (12, 15). PRV-2 is a virus found only in Coho salmon in Japan (not associated with HSMI symptoms); while PRV-3 induces a disease similar to HSMI in rainbow trout and salmon coho in Norway, Germany and Chile (12, 15, 21, 22).

Although it is necessary to complement the study using methodologies based on complete genome sequencing, besides segments S1 and M2 of PRV a lower resolution and representativeness of the remaining eight genomic segments for classifications of subgenotypes or subtypes have been observed. Phylogenetic trees support the original classification using the PRV genomic segment S1 (15).

Three phases have been described for PRV infection: *i)* the early entry and dissemination, *ii)* the acute phase and *iii)* persistence (14). Two to three weeks after the host entry, the replication and dissemination of the virus occurs into blood cells (23, 24). In this phase no infection *via* cohabitation has been described so far (24). To this date, there is no clarity about the mechanism of entry of the virus (14). The acute phase appears after 4 to 6 weeks of exposure to the virus and is characterized by the development of acute inflammation of the heart muscle and skeletal muscle, and substantial PRV replication in the erythrocyte occurs (14, 17, 24, 25). The duration of this phase depends on several factors related to the host immunity and on the PRV genotype causing the infection (26, 27). Cohabitation challenges show a successful infection at this point. This phase lasts between 1 to 2 weeks and then, the load of viral proteins drops dramatically in the erythrocytes, the clinical signs of the disease disappear, and the virus becomes persistent (17, 25). In the persistence phase, the viral RNA is found in erythroid progenitor cells, erythrocytes, macrophages, melano-macrophages, and other uncharacterized cells in the kidney (28). At this phase, poor viral infection is produced by cohabitation, but i.p. injected PRV inoculum prepared from clarified lysed blood cells from persistence phase Atlantic salmon accomplishes successful infection into naive fish (24). The extent of this phase depends on the PRV genotype and the host, but experimental trials have shown that this phase probably can last for life. The early entry and dissemination and acute phases have only been described under laboratory conditions.

Heart and skeletal muscle inflammation was first described in farmed Atlantic salmon in 1999 (3). The disease appears mainly between 5 to 9 months after salmon are transferred to marine water (2) but has also been described even earlier at 14 days of the seawater transfer (3). The clinical signs of the disease may emerge during the peak of the acute phase, but the clinical signs are found usually in the early stages of the persistent phase

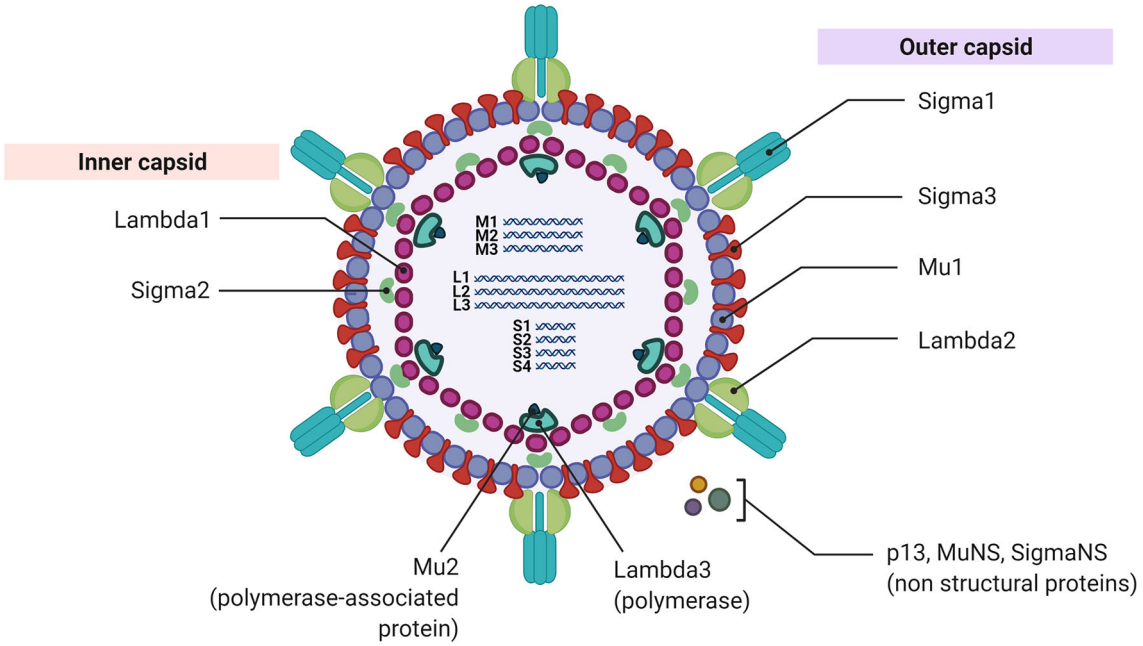

FIGURE 1 | Schematic representation of Piscine orthoreovirus: Structural proteins, dsRNA segments and non-structural proteins are represented.

(24, 29, 30). In the field, the mortality of infected fish is usually low but can also go up to 20% of the infected cages (3). Macroscopic signs are pale heart, pericardial bleeding, ascites, and a pale or stained liver, but hematocrit levels are usually normal. Lesions can occasionally be found in the liver, spleen, gills, and kidney. The main histopathological lesions are in the heart and skeletal muscle. In the heart, necrosis of myocytes, infiltration with mononuclear cells (mainly lymphocytes and macrophages), and a massive inflammatory response are observed associated with myocardial degeneration (26). Pericarditis is usually found in association with myocarditis (2), also, perivasculitis is found in myocardial blood vessels, coronary veins, and grooves. In severe cases, an infiltrative pattern is also found (26). Red muscle inflammation follows the same pattern as seen in the heart but is not a consistent finding (2) and it has been proposed to be attributed to seasonal variation being most prevalent in autumn and winter (26). In experimental conditions, the production of cardiac lesions consistent with HSMI is related to the virulence of the isolate (24, 26, 31). At the same time, the highest virulent isolates correlated with higher plasma viremia, while the low virulent isolates showed a lower amount of virus detected by qPCR (31). There was no correlation between any specific viral gene, protein, or amino acid differences with the virulence of the distinct PRV-1 isolates analyzed although the virus strain and host specific factors are necessary to initiate HSMI (31). For example, in Canada, Pacific-adapted Mowi-McConnell Atlantic salmon infected with PRV shows only mild or non-heart inflammation, even though these fish show high blood viremia (24). A review of the biology, geographic distribution, and host range of PRV has been recently published and is recommended for deeper details of the knowledge on this virus and HSMI (14).

IMMUNE RESPONSE AGAINST PRV INFECTION

PRV generates in *ex vivo* infected erythrocytes of Atlantic salmon upregulation of Interferon-a (*ifn-a)*, Retinoic acid-inducible gene I *(rig-i)*, Protein kinase R (*pkr)*, and Myxovirus resistance gene (*mx)*, all genes of the innate antiviral immune response (32, 33). In Atlantic salmon, intraperitoneal injected with PRV, *ifn-a* and *mx-α* were up-regulated in blood at 4 and 25 days post-challenge (dpc) and in heart, four dpc (34). The peak was in both tissues at four dpc, corresponding to the early infection stage, then the expression decreased to the control level (34). Similar results were reported in seawater adapted post-smolt salmon challenged with PRV by cohabitation. In these fish an increased expression of *ifn-a*, *rig-i, pkr, mx-α, viperin*, and *Interferon-stimulated gene 15 (isg15)* was observed in blood, heart, and in the spleen (35). In addition, a significant upregulation of both β-defensin and hepcidin genes in blood cells was reported at 4 weeks post challenge compared to day 0 (35). These studies show that PRV induces a strong innate immune response in Atlantic

salmon, which may induce protection because the induced genes encode a dsRNA receptor like *rig-i* (35), interferon and interferon induced antiviral proteins such as *pkr, mx-α*, and *viperin*, and antiviral peptides like β-defensin and hepcidin (35). However, at this stage, it is unknown whether this response indeed results in protection because viruses have numerous evasion mechanisms against the IFN type I response (36). In fact, immune evasion mechanisms for IFN type I response have been reported for fish viruses such as IPNV, where preVP2, VP3, VP4, and VP5 viral proteins inhibit IFNa1 activation (37). Similarly, s7ORF1 of ISAV inhibits IFN and Mx transcription, while s8ORF2, acting as RNA silencing suppressor, inhibits IFN production (38–40). Therefore, further studies are required to understand whether PRV displays mechanisms to antagonize the IFN type I responses and antiviral peptides observed in infected fish.

Regarding adaptive immunity, transcript upregulation of T lymphocyte related genes such as T cell receptor-a (*tcra)*, *tcrb*, cluster of differentiation 2 (*cd2)*, and interleukin-2 (*il-2)* was reported in the head kidney of parr salmon challenged with PRV (41). In addition, *cd4-1*, the gene encoding the T cell co-receptor, was also upregulated in infected salmon (34), all indicating that PRV elicited the adaptive immune response in Atlantic salmon, which probably involves T cell proliferation. $CD4^+$ $CD3^+$ T cells (T helper) have been in fact identified, isolated and characterized in some fish species, including Japanese Pufferfish (*Takifugu rubripes*), ginbuna crucian carp (*Carassius auratus langsdorfii*), zebrafish (*Danio rerio*), rainbow trout (*Oncorhynchus mykiss*) (42–47); and rohu (*Labeo rohita*) (48). Although in Atlantic salmon, T cell isolation and characterization awaits further studies, transcriptional data and the studies in rainbow trout (44, 49–52) support the presence of T lymphocytes in this fish species and its role in response to the pathogens or model antigens. Furthermore, *ifn-γ* (41) and *il-12* were also upregulated in PRV infected salmon (34), indicating that a T helper type-1 response can take place as a host defense strategy. In teleost fish, the differentiation of naive $CD4^+$ T cells into Th1 cells appears to be possible because these cells express both the *T-bet* master transcription factor and *ifn-γ* during differentiation (44, 45, 47). Other studies suggest that the differentiation of the $CD4^+$ T cell into Th1, Th2, Th17, Treg lymphocytes can occur in fish, mostly based on the fact that many Th-type cytokine genes have been identified in fish (53) and are upregulated in lymphoid tissues and isolated T cells after antigen stimulation (53). A Th1 response could induce PRV clearance, as in the presence of IFN-γ and IL-12, cellular-mediated immune response can eradicate intracellular pathogens like viruses (54). Furthermore, in HSMI-sick Atlantic salmon hearts, a strong signal of MHC-II in the lesion areas and a moderate signal of CD3+ (55) by immunohistochemistry was detected, suggesting the activation of CD4+ T cells in response to PRV infection.

Following interaction with various bacterial and viral pathogens, macrophages become activated and secrete a wide range of antiviral, pro-inflammatory, and immunomodulatory cytokines (56). Mirroring the Th type differentiation, the macrophages are classified as M1-like or M2-like cells (57, 58) and they reflect the bidirectional macrophage–lymphocyte interaction. Using *in situ* hybridization to identify double MCSFR and PRV positive cells, it has been found that macrophage-like cells of spleen and kidney, and in melano-macrophages of kidney contain PRV-1, indicating that macrophages might be targets of infections (28). In PRV-infected salmon of a commercial farm, lesions of the white muscle, known as red spots, show abundant iNOS (inducible nitric oxide synthase) in positive M1-polarized macrophages infected with PRV-1. Transformation of red spots into black spots was associated with the presence of arginase-2 expressing M2 melano-macrophages and the reduction of the relative number of PRV-1 in the white skeletal muscle (9). Interestingly, in experimental PRV infection, M1 macrophages does not appear related to the infection damage of the heart in HSMI, although M2 macrophages in heart tissue suggested a role in HSMI recovery (59). Since PRV upregulates IFN-γ and IL-12 during viral infection of Atlantic salmon, it seems plausible that an efficient well-regulated response induces M1 macrophage differentiation for virus clearance in the heart. Furthermore, as IFN-γ can also increase CD80/86, CD83, and MHC-II levels in salmon immune cells, an efficient clearance can also be due to antigen presentation and recognition improvement leading to a rapid immune response (60).

Regarding cellular immunity, recent studies shed light on the potential role of the cytotoxic T lymphocytes (CTL) during PRV infection. First, the high expression levels of *cd8a, cd8b*, and *granzyme-A* in the head kidney of PRV-infected fish suggest a positive modulatory effect on the CTL-mediated immune response (34) because fish CTLs express CD8 co-receptor and enzymes able to induce apoptosis of the target cells (61). Recently, a study has shown that Atlantic salmon CD8+ cells appear abundant in areas of the heart that contain PRV-1 infected cells after experimental challenge. Moreover, upregulation of CD8α correlated in time with a moderate decline in PRV-1 RNA levels (59). Interestingly, these results suggest a role of CD8+ cells in virus clearance but direct evidence for the role of functional CTLs (CD8+ T cells) during PRV infection is not available yet. The evaluation of PRV-specific CTL function will require haplotype-matched between the effector and target cells, which can be achieved using clonal teleost fish (62, 63) or infected autologous cells (64, 65). The potential role of CTL in PRV infection of fish is consistent with the Th1 type response observed in salmon because IFN-γ can stimulate the development of CD8+ T cells during viral infection (66). It is also consistent with the fact that PRV infection of salmon erythrocytes induced upregulation of the genes involved in antigen presentation *via* MHC class I, including transporters like *tapasin* (*tapbp*) and proteasome components like *proteasome subunit beta type 9* (*psmb9a*) and *proteasome subunit beta type 6* (*psmb11*) (33), which will positively impact the activation of CD8+ T cells. Activating the antigen-presenting machinery may also be a consequence of IFN-γ upregulation during PRV infection because, in turn, this cytokine upregulates many genes involved in antigen presentation (67).

Finally, regarding humoral immune response against PRV, production of IgM against the PRV μ1 and μNS proteins has been detected in plasma of PRV-1-infected Atlantic Salmon (68). Using a bead based multiplex immunoassays, anti-s1 IgM was also detected in salmon seven weeks after the exposure of PRV shedders. A reduction in HSMI lesions was observed when the specific IgM production reached a maximum level, suggesting a protective effect, even though this humoral immune response has been insufficient to eradicate PRV as viral RNA persisted in the blood of fish with PRV-specific IgM in challenge trials (68). Similarly, in PRV-3-infected rainbow trout a significant increase in -specific IgM in plasma is reported 8 weeks after the exposure (29). Notably, no studies are measuring neutralizing antibodies.

The current knowledge of the innate and adaptive immune response elicited by PRV infection is summarized in **Figure 2**.

WHEN THE FISH DECIDES TO LIVE WITH THE ENEMY: THE PHENOTYPE OF PERSISTENT VIRAL INFECTION IN ATLANTIC SALMON

The persistence is a complex meta-stability exercise involving the overall outcome that favors the coexistence of the viral infection on the host, being considered one of the most successful surveillance strategies in the host-pathogen repertoire (69). In mammals, the phenotype of viral persistence is directly associated with the activity of inhibitory/immunosuppressive cytokines (70). In this process, the modulation of anti-inflammatory cytokines helps establish chronic viral infection (71–73). One of these anti-inflammatory cytokines of the viral persistence phenotype is IL-10, which impairs different immune mechanisms, including antigen recognition, cytokine production, antibody production, and cell proliferation processes, all vital processes for the success of immune response activation and resolution of infection (74). Consistently, viral persistence phenotype in Atlantic salmon infected with the infectious pancreatic necrosis virus (IPNV) is characterized by the upregulation of *il-10*, the low expression levels of *il-1b* and *il-8* and low levels of total IgM (75). In PRV-infected Atlantic salmon, the persistence phenotype has been recently reported (28). The description of this persistence phenotype is associated with a high level of viral RNA (28) and low levels of viral proteins in the erythrocytes (17), in which an antiviral innate immune response is observed at the transcriptional level (33). Not the cellular or molecular immune mechanisms responsible for or associated with the persistence phenotype of PRV-infected fish are known.

Thus, it seems reasonable that several regulatory mechanisms associated with the recognition and activation of the immune response are activated in the PRV persistence phenotype. They can contribute to establishing a weakened immune status, helping to develop secondary infections with highly prevalent pathogens in salmon farming. Only one study has evaluated the potential effect of PRV on the development of secondary infections, thus centering on the co-occurrence of PRV and salmonid alphavirus (SAV) (35). In co-infected Atlantic salmon (PRV- and then SAV-infected), lower SAV neutralizing titers were observed compared with the controls infected with SAV only (35) suggesting a detrimental effect for immunity. Moreover, a positive correlation between PRV and SAV was observed in moribund or dead salmon (35). These data suggest that PRV infection may affect the infection and susceptibility to other pathogens present in farmed fish. For instance, as far as we know, no articles are reporting the consequences of PRV on the development of secondary bacterial infections of high prevalence in salmon farming. Taking together, it is urgent from the sanitary point of view to elucidating the consequence of the high PRV prevalence upon the risk for the development of a secondary infection that the infection by PRV might produce by itself.

PRV VACCINES

At present, there are no commercially available vaccines against HSMI in the market, and research and evaluation of PRV vaccines are still incipient. Only four studies performed on Atlantic salmon and Coho salmon have been reported (76–79). Wessel et al. (76) evaluated the protective effect of an inactivated vaccine using PRV purified from infected erythrocytes in a vaccination trial against HSMI.

Those immunized fish challenged with PRV by intraperitoneal injection showed a lower PRV load in blood cells and plasma compared both to PBS control group and vaccine control group (vaccinated with ALPHA JECT micro-6; PHARMAQ AS). Differences were observed for all the time-points assessed, i.e., 2-, 4-, 7-, and 10-weeks post-challenge (wpc). However, the PRV load was estimated based on the quantification cycle (Cq) value instead of absolute quantification. Beyond this methodological concern, only differences at 4wpc were registered between the PRV-inactivated vaccine group and the PBS-vaccinated group (76). Furthermore, the same trend was observed from the histopathological evidence on the heart. Thus, data indicate that PRV vaccination substantially reduced the severity of HSMI specific lesions, mainly in the experimental group following an unnatural way of infection (i.e., following an intraperitoneal injection), but did not prevent PRV infection and virus replication. Notably, a different study reported that the inactivated PRV-1 vaccine does not prevent PRV-1 infection and only partially protects against HSMI (78). Regrettably, the applicability of these vaccines is minimal because there are currently no reports of a cell line capable of producing PRV-1 viral progeny (80).

One common and ancient strategy for successful immunization is the cross-protection induced by related low virulent virus variants to cause low-grade disease (78). Particularly for HSMI, the cross-protection has been assessed using PRV-2 and PRV-3 genotypes not associated with disease development in Atlantic salmon. The cross-protection assay showed that the primary infection with intraperitoneally injected PRV-3 genotype completely blocked the infection

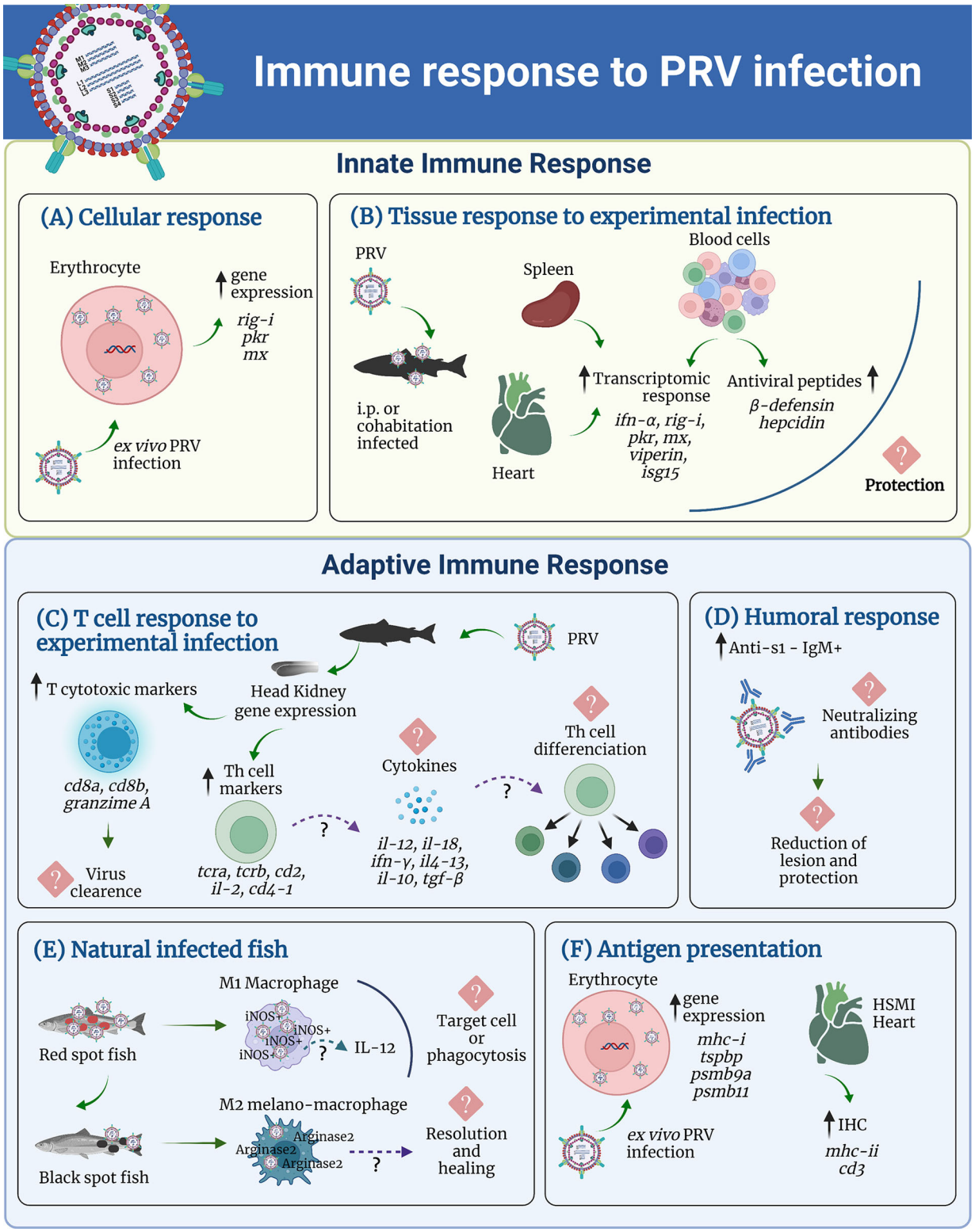

FIGURE 2 | Summary of the current knowledge of the innate and adaptive immune response elicited by PRV infection. In the innate immune response panel, the transcriptome for **(A)** Cellular response, and **(B)** Tissue response to experimental infection is represented. For the adaptive immune response panel are shown, **(C)** T cell response to experimental infection, **(D)** humoral response, **(E)** macrophages response in naturally infected fish, and **(F)** Antigen presentation.

against PRV-1 and the development of HSMI in Atlantic salmon ten weeks later the immunization with PRV-3 (78), which is in agreement with the fact that PRV-3 induces a disease similar to HSMI in rainbow trout and salmon coho (12, 15, 18, 21, 22, 78). The mechanisms of protection induced by PRV-3 are not known. In fact, the gene expression analysis of cellular immunity indicators (*cd8α*, *ifn-γ*, and *granzyme-a*) indicated that PRV-3 did not trigger spleen upregulation of these genes beyond ten weeks (78). The authors also state that antiviral immune genes *viperin, myxovirus resistance gene* (Mx), and *interferon-stimulated gene* (ISG-15) did not change their expression pattern (78).

By contrast, PRV-2 infection did not prevent PRV-1 infection, reducing only the severity of HSMI pathology punctually in some few individuals (78). Since PRV-2 is the etiological agent of a different disease in coho salmon (*Oncorhynchus kisutch*), named erythrocytic inclusion body syndrome (EIBS) (18), this results may have been expected. Perhaps the protection is associated with the higher amino acid identity of PRV-1 with PRV-3 (90%) than PRV-2 (80%) (81). Importantly, the high identity between PRV-3 and PRV-1 is present in proteins probably involved in the pathogenic effects (82, 83), such as the outer clamp protein σ3 (79.1%) and the non-structural protein p13 (78.2%) (81). Beyond these unknowns, one critical concern on the use of PRV-3 in immunizing Atlantic salmon is the possibility that the RNA segmented of PRV-3 and PRV-1 could reassort if they infect the same cell (84), in which case the consequences are unpredictable. Therefore, the side-effects and potential consequences of this type of immunizing strategy must be carefully analyzed.

In aquaculture, there are DNA vaccines licensed for commercial use for protecting Atlantic salmon against viruses including Infectious Hematopoietic Necrosis Virus (IHNV) (APEX-IHN; Novartis/Elanco) (85), and Salmon Pancreas Disease Virus (SPDV) (86). In this scenario, the vaccine efficacy against HSMI following intramuscular-injected immunization was assessed using pSAV-based replicon vaccines and pcDNA3.1-based expression vaccines. The Atlantic salmon vaccinated with pcDNA3.1 vector expressing μNS, σNS, and σ1 controlled by a CMV promoter showed a substantial reduction in the viral RNA load and the HSMI histopathological changes in epicardium and ventricle (77). By contrast, the pSAV cocktail replicons containing μNS + μ1 + σNS + σ1 + σ3 + λ2, slightly reduced the cardiac histopathological score, but did not reduce the PRV RNA levels in the blood after infection compared to the control, suggesting that the type and number of different expression vectors may influence on such differences (77). The secretion of specific antibodies as an inducer of protection through DNA vaccines (87) was not evaluated. Based on the study of Haatveit et al. (77) it seems that μNS and σ1 are the most promising PRV antigens for a DNA vaccine against HSMI in Atlantic salmon. However, the mechanism of action of these proteins activating the immune response remains to be elucidated. Consequently, the application of DNA vaccine as prophylactic treatment against aquaculture-related viruses, including PRV, must be further assessed.

CONCLUSIONS AND PERSPECTIVE

This article revised the current knowledge regarding the immune mechanisms activated in response to PVR infection. There is evidence that PRV activates the antiviral immunity in salmonid erythrocytes, one of its cellular infection targets. Currently, it is unclear whether activating an antiviral environment is enough to induce host protection. Because viruses, including aquatic viruses, show numerous immune evasion mechanisms against the IFN type I host response, understanding PRV-host interaction, which may antagonize the IFN type I response, needs to be addressed. The scope of other immune mechanisms against the PRV and its actual contribution to the resolution of infection, including the role of neutralizing antibodies, still need to be elucidated. Nonetheless, the eradication of virus does not always occur during infection in nature. In fact, for PRV, there are reports of persistent infection promoting host-pathogen coexistence. PRV persistence is characterized by immune modulators´ upregulation mainly associated with anti-inflammatory molecules. Consequently, this lower immune capacity to respond against a threat aggregates complexity to the mechanisms developed by the host for ensuring survival. Importantly, as far as we know, there is a gap in the knowledge concerning the cellular and molecular mechanisms responsible for the promotion of the persistence phenotype on PRV-infected fish.

The generation of further knowledge to understand the immune mechanisms in response to and for protection against PRV will make possible the development of strategies capable of effectively and efficiently facing this viral infection and the negative impact produced in the fish farming industry and the environment. Within the sustainable aquaculture industry framework, all the above is committed to the environment.

AUTHOR CONTRIBUTIONS

All the authors wrote, read and approved the original draft.

FUNDING

This work has been supported by DICYT-USACH Postdoctoral fellowship (Nb. 022043IB) and Fondecyt iniciación (Proyect number 11221308).

ACKNOWLEDGMENTS

The authors thank the Fondecyt regular (project number 1201664 (MI), and 1211841 (FR-L)), Fondecyt iniciación (project number 11221308; EV-V) grants (ANID, Government of Chile), and DICYT-USACH Postdoctoral fellowship (Nb. 022043IB (MI; EV-V).

REFERENCES

1. Palacios G, Lovoll M, Tengs T, Hornig M, Hutchison S, Hui J, et al. Heart and Skeletal Muscle Inflammation of Farmed Salmon Is Associated With Infection With a Novel Reovirus. *PloS One* (2010) 5:3–9. doi: 10.1371/journal.pone.0011487
2. Kongtorp RT, Taksdal T, Lyngøy A. Pathology of Heart and Skeletal Muscle Inflammation (HSMI) in Farmed Atlantic Salmon Salmo Salar. *Dis Aquat Organisms* (2004) 59:217–24. doi: 10.3354/dao059217
3. Kongtorp RT, Kjerstad A, Taksdal T, Guttvik A, Falk K. Heart and Skeletal Muscle Inflammation in Atlantic Salmon, Salmo Salar L.: A New Infectious Disease. *J Fish Dis* (2004) 27:351–8. doi: 10.1111/j.1365-2761.2004.00549.x
4. Godoy MG, Kibenge MJT, Wang Y, Suarez R, Leiva C, Vallejos F, et al. First Description of Clinical Presentation of Piscine Orthoreovirus (PRV) Infections in Salmonid Aquaculture in Chile and Identification of a Second Genotype (Genotype II) of PRV. *Virol J* (2016) 13:98. doi: 10.1186/s12985-016-0554-y
5. Sommerset I, Bang Jensen B, Borno B, Haukaas A, Brun E. *The Health Situation in Norwegian Aquaculture 2020* (2021). Available at: www.vetinst.no.
6. Kristoffersen AB, Bang Jensen B, Jansen PA. Risk Mapping of Heart and Skeletal Muscle Inflammation in Salmon Farming. *Prev Vet Med* (2013) 109:136–43. doi: 10.1016/j.prevetmed.2012.08.012
7. SERNAPESCA. *Informe Sanitario De La Salmonicultura En Centros Marinos Año*, 2020. Servicio Nacional de Pesca y Acuicultura, Ministerio de Economía, Fomento y Turismo, Gobierno de Chile. Valparaíso (V Región), Chile. (2021).
8. Färber F. *Melanin Spots in Atlantic Salmon Fillets-an Investigation of the General Problem, the Frequency and the Economic Implication Based on an Online Survey*. Ås, Norway: Norwegian University of Life Sciences. (2017).
9. Malik MS, Bjørgen H, Nyman IB, Wessel Ø, Koppang EO, Dahle MK, et al. PRV-1 Infected Macrophages in Melanized Focal Changes in White Muscle of Atlantic Salmon (Salmo Salar) Correlates With a Pro-Inflammatory Environment. *Front Immunol* (2021) 12:664624. doi: 10.3389/fimmu.2021.664624
10. Morton A, Routledge R, Hrushowy S, Kibenge M, Kibenge F. The Effect of Exposure to Farmed Salmon on Piscine Orthoreovirus Infection and Fitness in Wild Pacific Salmon in British Columbia, Canada. *PloS One* (2017) 12:1–18. doi: 10.1371/journal.pone.0188793
11. Mordecai GJ, Miller KM, Bass AL, Bateman AW, Teffer AK, Caleta JM, et al. *Aquaculture Mediates Global Transmission of a Viral Pathogen to Wild Salmon* (2021). Available at: http://advances.sciencemag.org/.
12. Dhamotharan K, Tengs T, Wessel Ø, Braaen S, Nyman IB, Hansen EF, et al. Evolution of the Piscine Orthoreovirus Genome Linked to Emergence of Heart and Skeletal Muscle Inflammation in Farmed Atlantic Salmon (Salmo Salar). *Viruses* (2019) 11(5):465. doi: 10.3390/v11050465
13. Markussen T, Dahle MK, Tengs T, Løvoll M, Finstad ØW, Wiik-Nielsen CR, et al. Sequence Analysis of the Genome of Piscine Orthoreovirus (PRV) Associated With Heart and Skeletal Muscle Inflammation (HSMI) in Atlantic Salmon (Salmo Salar). *PloS One* (2013) 8(7):e70075. doi: 10.1371/journal.pone.0070075
14. Polinski MP, Vendramin N, Cuenca A, Garver KA. Piscine Orthoreovirus: Biology and Distribution in Farmed and Wild Fish. *J Fish Dis* (2020) 43:1331–52. doi: 10.1111/jfd.13228
15. Godoy M, Medina DA, Suarez R, Valenzuela S, Romero J, Kibenge M, et al. Extensive Phylogenetic Analysis of Piscine Orthoreovirus Genomic Sequences Shows the Robustness of Subgenotype Classification. *Pathogens* (2021) 10:1–12. doi: 10.3390/pathogens10010041
16. Dryden KA, Wang G, Yeager M, Nibert ML, Coombs KM, Furlong DB, et al. Early Steps in Reovirus Infection Are Associated With Dramatic Changes in Supramolecular Structure and Protein Conformation: Analysis of Virions and Subviral Particles by Cryoelectron Microscopy and Image Reconstruction. *J Cell Biol* (1993) 122:1023–41. doi: 10.1083/jcb.122.5.1023
17. Haatveit HM, Wessel Ø, Markussen T, Lund M, Thiede B, Nyman IB, et al. Viral Protein Kinetics of Piscine Orthoreovirus Infection in Atlantic Salmon Blood Cells. *Viruses* (2017) 9(3):49. doi: 10.3390/v9030049
18. Takano T, Nawata A, Sakai T, Matsuyama T, Ito T, Kurita J, et al. Full-Genome Sequencing and Confirmation of the Causative Agent of Erythrocytic Inclusion Body Syndrome in Coho Salmon Identifies a New Type of Piscine Orthoreovirus. *PloS One* (2016) 11:1–20. doi: 10.1371/journal.pone.0165424
19. Kuehn R, Stoeckle BC, Young M, Popp L, Taeubert JE, Pfaffl MW, et al. Identification of a Piscine Reovirus-Related Pathogen in Proliferative Darkening Syndrome (PDS) Infected Brown Trout (Salmo Trutta Fario) Using a Next-Generation Technology Detection Pipeline. *PloS One* (2018) 13(10):e0206164. doi: 10.1371/journal.pone.0206164
20. Kibenge FS. Emerging Viruses in Aquaculture. *Curr Opin Virol* (2019) 34:97–103. doi: 10.1016/j.coviro.2018.12.008
21. Adamek M, Hellmann J, Flamm A, Teitge F, Vendramin N, Fey D, et al. Detection of Piscine Orthoreoviruses (PRV-1 and PRV-3) in Atlantic Salmon and Rainbow Trout Farmed in Germany. *Transbound Emerging Dis* (2019) 66:14–21. doi: 10.1111/tbed.13018
22. Cartagena J, Tambley C, Sandino AM, Spencer E, Tello M. Detection of Piscine Orthoreovirus in Farmed Rainbow Trout From Chile. *Aquaculture* (2018) 493:79–84. doi: 10.1016/j.aquaculture.2018.04.044
23. Hauge H, Vendramin N, Taksdal T, Olsen AB, Wessel Ø, Mikkelsen SS, et al. Infection Experiments With Novel Piscine Orthoreovirus From Rainbow Trout (Oncorhynchus Mykiss) in Salmonids. *PloS One* (2017) 12:1–24. doi: 10.1371/journal.pone.0180293
24. Polinski MP, Marty GD, Snyman HN, Garver KA. Piscine Orthoreovirus Demonstrates High Infectivity But Low Virulence in Atlantic Salmon of Pacific Canada. *Sci Rep* (2019) 9:1–22. doi: 10.1038/s41598-019-40025-7
25. Finstad ØW, Dahle MK, Lindholm TH, Nyman IB, Løvoll M, Wallace C, et al. Piscine Orthoreovirus (PRV) Infects Atlantic Salmon Erythrocytes. *Vet Res* (2014) 45:1–13. doi: 10.1186/1297-9716-45-35
26. Di Cicco E, Ferguson HW, Schulze AD, Kaukinen KH, Li S, Vanderstichel R, et al. Heart and Skeletal Muscle Inflammation (HSMI) Disease Diagnosed on a British Columbia Salmon Farm Through a Longitudinal Farm Study. *PLoS One* (2017) 12(2):e0171471. doi: 10.1371/journal.pone.0171471
27. Lund M, Røsæg MV, Krasnov A, Timmerhaus G, Nyman IB, Aspehaug V, et al. Experimental Piscine Orthoreovirus Infection Mediates Protection Against Pancreas Disease in Atlantic Salmon (Salmo Salar). *Vet Res* (2016) 47:1–16. doi: 10.1186/s13567-016-0389-y
28. Malik MS, Bjørgen H, Dhamotharan K, Wessel Ø, Koppang EO, di Cicco E, et al. Erythroid Progenitor Cells in Atlantic Salmon (Salmo Salar) may be Persistently and Productively Infected With Piscine Orthoreovirus (PRV). *Viruses* (2019) 11:824. doi: 10.3390/v11090824
29. Vendramin N, Kannimuthu D, Olsen AB, Cuenca A, Teige LH, Wessel Ø, et al. Piscine Orthoreovirus Subtype 3 (PRV-3) Causes Heart Inflammation in Rainbow Trout (Oncorhynchus Mykiss). *Vet Res* (2019) 50:1–13. doi: 10.1186/s13567-019-0632-4
30. Wessel Ø, Braaen S, Alarcon M, Haatveit H, Roos N, Markussen T, et al. Infection With Purified Piscine Orthoreovirus Demonstrates a Causal Relationship With Heart and Skeletal Muscle Inflammation in Atlantic Salmon. *PloS One* (2017) 12:1–24. doi: 10.1371/journal.pone.0183781
31. Wessel Ø, Hansen EF, Dahle MK, Alarcon M, Vatne NA, Nyman IB, et al. Piscine Orthoreovirus-1 Isolates Differ in Their Ability to Induce Heart and Skeletal Muscle Inflammation in Atlantic Salmon (Salmo Salar). *Pathogens* (2020) 9:1–22. doi: 10.3390/pathogens9121050
32. Wessel Ø, Olsen CM, Rimstad E, Dahle MK. Piscine Orthoreovirus (PRV) Replicates in Atlantic Salmon (Salmo Salar L.) Erythrocytes *Ex Vivo*. *Vet Res* (2015) 46:1–11. doi: 10.1186/s13567-015-0154-7
33. Dahle MK, Wessel Ø, Timmerhaus G, Nyman IB, Jørgensen SM, Rimstad E, et al. Transcriptome Analyses of Atlantic Salmon (Salmo Salar L.) Erythrocytes Infected With Piscine Orthoreovirus (PRV). *Fish Shellfish Immunol* (2015) 45:780–90. doi: 10.1016/j.fsi.2015.05.049
34. Zhang Y, Polinski MP, Morrison PR, Brauner CJ, Farrell AP, Garver KA. High-Load Reovirus Infections do Not Imply Physiological Impairment in Salmon. *Front Physiol* (2019) 10:114. doi: 10.3389/fphys.2019.00114
35. Røsæg MV, Lund M, Nyman IB, Markussen T, Aspehaug V, Sindre H, et al. Immunological Interactions Between Piscine Orthoreovirus and Salmonid Alphavirus Infections in Atlantic Salmon. *Fish Shellfish Immunol* (2017) 64:308–19. doi: 10.1016/j.fsi.2017.03.036
36. Beachboard DC, Horner SM. Innate Immune Evasion Strategies of DNA and RNA Viruses. *Curr Opin Microbiol* (2016) 32:113–9. doi: 10.1016/j.mib.2016.05.015
37. Lauksund S, Greiner-Tollersrud L, Chang CJ, Robertsen B. Infectious Pancreatic Necrosis Virus Proteins VP2, VP3, VP4 and VP5 Antagonize Ifna1 Promoter Activation While VP1 Induces Ifna1. *Virus Res* (2015) 196:113–21. doi: 10.1016/j.virusres.2014.11.018

38. García-Rosado E, Markussen T, Kileng Ø, Baekkevold ES, Robertsen B, Mjaaland S, et al. Molecular and Functional Characterization of Two Infectious Salmon Anaemia Virus (ISAV) Proteins With Type I Interferon Antagonizing Activity. *Virus Res* (2008) 133:228–38. doi: 10.1016/j.virusres.2008.01.008
39. McBeath AJA, Collet B, Paley R, Duraffour S, Aspehaug V, Biering E, et al. Identification of an Interferon Antagonist Protein Encoded by Segment 7 of Infectious Salmon Anaemia Virus. *Virus Res* (2006) 115:176–84. doi: 10.1016/j.virusres.2005.08.005
40. Thukral V, Varshney B, Ramly RB, Ponia SS, Mishra SK, Olsen CM, et al. S8orf2 Protein of Infectious Salmon Anaemia Virus Is a RNA-Silencing Suppressor and Interacts With Salmon Salar Mov10 (Ssmov10) of the Host Rnai Machinery. *Virus Genes* (2018) 54:199–214. doi: 10.1007/s11262-017-1526-z
41. Johansen LH, Dahle MK, Wessel Ø, Timmerhaus G, Løvoll M, Røsæg M, et al. Differences in Gene Expression in Atlantic Salmon Parr and Smolt After Challenge With Piscine Orthoreovirus (PRV). *Mol Immunol* (2016) 73:138–50. doi: 10.1016/j.molimm.2016.04.007
42. Toda H, Saito Y, Koike T, Takizawa F, Araki K, Yabu T, et al. Conservation of Characteristics and Functions of CD4 Positive Lymphocytes in a Teleost Fish. *Dev Comp Immunol* (2011) 35:650–60. doi: 10.1016/j.dci.2011.01.013
43. Bird S, Zou J, Savan R, Kono T, Sakai M, Woo J, et al. Characterisation and Expression Analysis of an Interleukin 6 Homologue in the Japanese Pufferfish, Fugu Rubripes. *Dev Comp Immunol* (2005) 29:775–89. doi: 10.1016/j.dci.2005.01.002
44. Maisey K, Montero R, Corripio-Miyar Y, Toro-Ascuy D, Valenzuela B, Reyes-Cerpa S, et al. Isolation and Characterization of Salmonid CD4 + T Cells. *J Immunol* (2016) 196:4150–63. doi: 10.4049/jimmunol.1500439
45. Takizawa F, Magadan S, Parra D, Xu Z, Korytář T, Boudinot P, et al. Novel Teleost CD4-Bearing Cell Populations Provide Insights Into the Evolutionary Origins and Primordial Roles of CD4 Lymphocytes and CD4 Macrophages. *J Immunol* (2016) 196:4522–35. doi: 10.4049/jimmunol.1600222.Novel
46. Kono T, Korenaga H. Cytokine Gene Expression in CD4 Positive Cells of the Japanese Pufferfish, Takifugu Rubripes. *PloS One* (2013) 8(6):e66364. doi: 10.1371/journal.pone.0066364
47. Yoon S, Mitra S, Wyse C, Alnabulsi A, Zou J, Weerdenburg EM, et al. First Demonstration of Antigen Induced Cytokine Expression by CD4-1+ Lymphocytes in a Poikilotherm: Studies in Zebrafish (Danio Rerio). *PloS One* (2015) 10:1–26. doi: 10.1371/journal.pone.0126378
48. Rebello SC, Rathore G, Punia P, Sood N. Development and Characterization of a Monoclonal Antibody Against the Putative T Cells of Labeo Rohita. *Cytotechnology* (2016) 68:469–80. doi: 10.1007/s10616-014-9800-6
49. Hu Y, Maisey K, Subramani PA, Liu F, Flores-Kossack C, Imarai M, et al. Characterisation of Rainbow Trout Peripheral Blood Leucocytes Prepared by Hypotonic Lysis of Erythrocytes, and Analysis of Their Phagocytic Activity, Proliferation and Response to Pamps and Proinflammatory Cytokines. *Dev Comp Immunol* (2018) 88:104–13. doi: 10.1016/j.dci.2018.07.010
50. Zhang Y-A, Salinas I, Oriol Sunyer J. Recent Findings on the Structure and Function of Teleost Igt. *Fish shellfish Immunol* (2011) 31:627–34. doi: 10.1016/j.fsi.2011.03.021
51. Nakanishi T, Shibasaki Y. Matsuura Y. T Cells in Fish. *Biol (Basel)* (2015) 4:640–63. doi: 10.3390/biology4040640
52. Partula S. Surface Markers of Fish T-Cells(1999) (Accessed February 20, 2013).
53. Zou J, Secombes CJ. The Function of Fish Cytokines. *Biology* (2016) 5(2):23. doi: 10.3390/biology5020023
54. Zhou L, Chong MMW, Littman DR. Plasticity of CD4+ T Cell Lineage Differentiation. *Immunity* (2009) 30:646–55. doi: 10.1016/j.immuni.2009.05.001
55. Yousaf MN, Koppang EO, Skjødt K, Hordvik I, Zou J, Secombes C, et al. Comparative Cardiac Pathological Changes of Atlantic Salmon (Salmo Salar L.) Affected With Heart and Skeletal Muscle Inflammation (HSMI), Cardiomyopathy Syndrome (CMS) and Pancreas Disease (PD). *Vet Immunol Immunopathol* (2013) 151:49–62. doi: 10.1016/j.vetimm.2012.10.004
56. Porcheray F, Viaud S, Rimaniol AC, Léone C, Samah B, Dereuddre-Bosquet N, et al. Macrophage Activation Switching: An Asset for the Resolution of Inflammation. *Clin Exp Immunol* (2005) 142:481–9. doi: 10.1111/j.1365-2249.2005.02934.x
57. Biswas SK, Mantovani A. Macrophage Plasticity and Interaction With Lymphocyte Subsets: Cancer as a Paradigm. *Nat Immunol* (2010) 11:889–96. doi: 10.1038/ni.1937
58. Nikonova A, Khaitov M, Jackson DJ, Traub S, Trujillo-Torralbo MB, Kudlay DA, et al. M1-Like Macrophages Are Potent Producers of Anti-Viral Interferons and M1-Associated Marker-Positive Lung Macrophages Are Decreased During Rhinovirus-Induced Asthma Exacerbations. *EBioMedicine* (2020) 54:102734. doi: 10.1016/j.ebiom.2020.102734
59. Malik MS, Nyman IB, Wessel Ø, Dahle MK, Rimstad E. Dynamics of Polarized Macrophages and Activated CD8+ Cells in Heart Tissue of Atlantic Salmon Infected With Piscine Orthoreovirus-1. *Front Immunol* (2021) 12:729017. doi: 10.3389/fimmu.2021.729017
60. Morales-Lange B, Ramírez-Cepeda F, Schmitt P, Guzmán F, Lagos L, Øverland M, et al. Interferon Gamma Induces the Increase of Cell-Surface Markers (CD80/86, CD83 and MHC-II) in Splenocytes From Atlantic Salmon. *Front Immunol* (2021) 12:666356. doi: 10.3389/fimmu.2021.666356
61. Somamoto T, Koppang EO, Fischer U. Antiviral Functions of CD8+ Cytotoxic T Cells in Teleost Fish. *Dev Comp Immunol* (2014) 43:197–204. doi: 10.1016/j.dci.2013.07.014
62. Somamoto T, Nakanishi T, Okamoto N. Specific Cell-Mediated Cytotoxicity Against a Virus-Infected Syngeneic Cell Line in Isogeneic Ginbuna Crucian Carp. *Dev Comp Immunol* (2000) 24:633–40. doi: 10.1016/S0145-305X(00)00018-5
63. Dijkstra JM, Fischer U, Sawamoto Y, Ototake M, Nakanishi T. Exogenous Antigens and the Stimulation of MHC Class I Restricted Cell-Mediated Cytotoxicity: Possible Strategies for Fish Vaccines. *Fish Shellfish Immunol* (2001) 11:437–58. doi: 10.1006/fsim.2001.0351
64. Hogan RJ, Stuge TB, Clem LW, Miller NW, Chinchar VG. Anti-Viral Cytotoxic Cells in the Channel Catfish (Ictalurus Punctatus). *Dev Comp Immunol* (1996) 20:115–27. doi: 10.1016/0145-305X(95)00043-S
65. Chang Y-T, Kai Y-H, Chi S-C, Song Y-L. Cytotoxic CD8α+ Leucocytes Have Heterogeneous Features in Antigen Recognition and Class I MHC Restriction in Grouper. *Fish Shellfish Immunol* (2011) 30:1283–93. doi: 10.1016/j.fsi.2011.03.018
66. Whitmire JK, Tan JT, Whitton JL. Interferon-γ Acts Directly on CD8+ T Cells to Increase Their Abundance During Virus Infection. *J Exp Med* (2005) 201:1053–9. doi: 10.1084/jem.20041463
67. Pereiro P, Figueras A, Novoa B. Insights Into Teleost Interferon-Gamma Biology: An Update. *Fish Shellfish Immunol* (2019) 90:150–64. doi: 10.1016/j.fsi.2019.04.002
68. Teige LH, Lund M, Haatveit HM, Røsæg MV, Wessel Ø, Dahle MK, et al. A Bead Based Multiplex Immunoassay Detects Piscine Orthoreovirus Specific Antibodies in Atlantic Salmon (Salmo Salar). *Fish Shellfish Immunol* (2017) 63:491–9. doi: 10.1016/j.fsi.2017.02.043
69. Goic B, Saleh MC. Living With the Enemy: Viral Persistent Infections From a Friendly Viewpoint. *Curr Opin Microbiol* (2012) 15:531–7. doi: 10.1016/j.mib.2012.06.002
70. Alcami A, Koszinowski UH. Viral Mechanisms of Immune Evasion. *Trends Microbiol* (2000) 8:410–8. doi: 10.1016/S0966-842X(00)01830-8
71. MacDonald AJ, Duffy M, Brady MT, McKiernan S, Hall W, Hegarty J, et al. CD4 T Helper Type 1 and Regulatory T Cells Induced Against the Same Epitopes on the Core Protein in Hepatitis C Virus–Infected Persons. *J Infect Dis* (2002) 185:720–7. doi: 10.1086/339340
72. Blackburn SD, Wherry EJ. IL-10, T Cell Exhaustion and Viral Persistence. *Trends Microbiol* (2007) 15:143–6. doi: 10.1016/j.tim.2007.02.006
73. Redpath S, Angulo A, Gascoigne NRJ, Ghazal P. Murine Cytomegalovirus Infection Down-Regulates MHC Class II Expression on Macrophages by Induction of IL-10. *J Immunol* (1999) 162:6701–7.
74. Ouyang W, O'Garra A. IL-10 Family Cytokines IL-10 and IL-22: From Basic Science to Clinical Translation. *Immunity* (2019) 50:871–91. doi: 10.1016/j.immuni.2019.03.020
75. Reyes-Cerpa S, Reyes-López F, Toro-Ascuy D, Montero R, Maisey K, Acuña-Castillo C, et al. Induction of Anti-Inflammatory Cytokine Expression by IPNV in Persistent Infection. *Fish Shellfish Immunol* (2014) 41:172–82. doi: 10.1016/j.fsi.2014.08.029

76. Wessel Ø, Haugland Ø, Rode M, Fredriksen BN, Dahle MK, Rimstad E. Inactivated Piscine Orthoreovirus Vaccine Protects Against Heart and Skeletal Muscle Inflammation in Atlantic Salmon. *J Fish Dis* (2018) 41:1411–9. doi: 10.1111/jfd.12835
77. Haatveit HM, Hodneland K, Braaen S, Hansen EF, Nyman IB, Dahle MK, et al. DNA Vaccine Expressing the Non-Structural Proteins of Piscine Orthoreovirus Delay the Kinetics of PRV Infection and Induces Moderate Protection Against Heart -and Skeletal Muscle Inflammation in Atlantic Salmon (Salmo Salar). *Vaccine* (2018) 36:7599–608. doi: 10.1016/j.vaccine.2018.10.094
78. Malik MS, Teige LH, Braaen S, Olsen AB, Nordberg M, Amundsen MM, et al. Piscine Orthoreovirus (Prv)-3, But Not Prv-2, Cross-Protects Against Prv-1 and Heart and Skeletal Muscle Inflammation in Atlantic Salmon. *Vaccines* (2021) 9:1–20. doi: 10.3390/vaccines9030230
79. Matsuyama T, Takano T, Honjo M, Kikuta T, Nawata A, Kumagai A, et al. Enhancement of Piscine Orthoreovirus-2 DNA Vaccine Potency by Linkage of Antigen Gene to a Trigger Factor Gene or Signal Peptide Genes. *Aquaculture* (2021) 533:736163. doi: 10.1016/j.aquaculture.2020.736163
80. Pham PH, Misk E, Papazotos F, Jones G, Polinski MP, Contador E, et al. Screening of Fish Cell Lines for Piscine Orthoreovirus-1 (PRV-1) Amplification: Identification of the Non-Supportive PRV-1 Invitrome. *Pathogens* (2020) 9:1–25. doi: 10.3390/pathogens9100833
81. Dhamotharan K, Vendramin N, Markussen T, Wessel Ø, Cuenca A, Nyman IB, et al. Molecular and Antigenic Characterization of Piscine Orthoreovirus (PRV) From Rainbow Trout (Oncorhynchus Orthoreovirumykiss). *Viruses* (2018) 10:1–16. doi: 10.3390/v10040170
82. Key T, Read J, Nibert ML, Duncan R. Piscine Reovirus Encodes a Cytotoxic, Non-Fusogenic, Integral Membrane Protein and Previously Unrecognized Virion Outer-Capsid Proteins. *J Gen Virol* (2013) 94:1039–50. doi: 10.1099/vir.0.048637-0
83. Yue Z, Shatkin AJ. Double-Stranded RNA-Dependent Protein Kinase (PKR) Is Regulated by Reovirus Structural Proteins. *Virology* (1997) 234:364–71. doi: 10.1006/viro.1997.8664
84. Mcdonald SM, Nelson MI, Turner PE, Patton JT. Reassortment in Segmented RNA Viruses: Mechanisms and Outcomes Outcomes. *Nat Rev Microbiol* (2016) 14:448–60. doi: 10.1038/nrmicro.2016.46
85. Salonius K, Simard N, Harland R, Ulmer JB. The Road to Licensure of a DNA Vaccine. *Curr Opin Invest Drugs* (2007) 8:635–41.
86. Collins C, Lorenzen N, Collet B. DNA Vaccination for Finfish Aquaculture. *Fish Shellfish Immunol* (2019) 85:106–25. doi: 10.1016/j.fsi.2018.07.012
87. Tang DC, DeVit M, Johnston SA. Genetic Immunization Is a Simple Method for Eliciting an Immune Response. *Nature* (1992) 356:152–4. doi: 10.1038/356152a0

Conflict of Interest: The authors declare that the research was conducted in the absence of any commercial or financial relationships that could be construed as a potential conflict of interest.

Advantages of publishing in Frontiers

OPEN ACCESS
Articles are free to read for greatest visibility and readership

FAST PUBLICATION
Around 90 days from submission to decision

HIGH QUALITY PEER-REVIEW
Rigorous, collaborative, and constructive peer-review

TRANSPARENT PEER-REVIEW
Editors and reviewers acknowledged by name on published articles

Frontiers
Avenue du Tribunal-Fédéral 34
1005 Lausanne | Switzerland

Visit us: www.frontiersin.org
Contact us: frontiersin.org/about/contact.

REPRODUCIBILITY OF RESEARCH
Support open data and methods to enhance research reproducibility

DIGITAL PUBLISHING
Articles designed for optimal readership across devices

FOLLOW US
@frontiersin

IMPACT METRICS
Advanced article metrics track visibility across digital media

EXTENSIVE PROMOTION
Marketing and promotion of impactful research

LOOP RESEARCH NETWORK
Our network increases your article's readership